frontiers | Research Topics

Non-coding RNAs as potential therapeutics and biomarkers for human diseases

Edited by
Alice Conigliaro, Margarida Gama-Carvalho and Chiara De Santi

Published in
Frontiers in Pharmacology



FRONTIERS EBOOK COPYRIGHT STATEMENT

The copyright in the text of individual articles in this ebook is the property of their respective authors or their respective institutions or funders. The copyright in graphics and images within each article may be subject to copyright of other parties. In both cases this is subject to a license granted to Frontiers.

The compilation of articles constituting this ebook is the property of Frontiers.

Each article within this ebook, and the ebook itself, are published under the most recent version of the Creative Commons CC-BY licence. The version current at the date of publication of this ebook is CC-BY 4.0. If the CC-BY licence is updated, the licence granted by Frontiers is automatically updated to the new version.

When exercising any right under the CC-BY licence, Frontiers must be attributed as the original publisher of the article or ebook, as applicable.

Authors have the responsibility of ensuring that any graphics or other materials which are the property of others may be included in the CC-BY licence, but this should be checked before relying on the CC-BY licence to reproduce those materials. Any copyright notices relating to those materials must be complied with.

Copyright and source acknowledgement notices may not be removed and must be displayed in any copy, derivative work or partial copy which includes the elements in question.

All copyright, and all rights therein, are protected by national and international copyright laws. The above represents a summary only. For further information please read Frontiers' Conditions for Website Use and Copyright Statement, and the applicable CC-BY licence.

ISSN 1664-8714
ISBN 978-2-8325-7340-2
DOI 10.3389/978-2-8325-7340-2

Generative AI statement
Any alternative text (Alt text) provided alongside figures in the articles in this ebook has been generated by Frontiers with the support of artificial intelligence and reasonable efforts have been made to ensure accuracy, including review by the authors wherever possible. If you identify any issues, please contact us.

About Frontiers

Frontiers is more than just an open access publisher of scholarly articles: it is a pioneering approach to the world of academia, radically improving the way scholarly research is managed. The grand vision of Frontiers is a world where all people have an equal opportunity to seek, share and generate knowledge. Frontiers provides immediate and permanent online open access to all its publications, but this alone is not enough to realize our grand goals.

Frontiers journal series

The Frontiers journal series is a multi-tier and interdisciplinary set of open-access, online journals, promising a paradigm shift from the current review, selection and dissemination processes in academic publishing. All Frontiers journals are driven by researchers for researchers; therefore, they constitute a service to the scholarly community. At the same time, the *Frontiers journal series* operates on a revolutionary invention, the tiered publishing system, initially addressing specific communities of scholars, and gradually climbing up to broader public understanding, thus serving the interests of the lay society, too.

Dedication to quality

Each Frontiers article is a landmark of the highest quality, thanks to genuinely collaborative interactions between authors and review editors, who include some of the world's best academicians. Research must be certified by peers before entering a stream of knowledge that may eventually reach the public - and shape society; therefore, Frontiers only applies the most rigorous and unbiased reviews. Frontiers revolutionizes research publishing by freely delivering the most outstanding research, evaluated with no bias from both the academic and social point of view. By applying the most advanced information technologies, Frontiers is catapulting scholarly publishing into a new generation.

What are Frontiers Research Topics?

Frontiers Research Topics are very popular trademarks of the *Frontiers journals series*: they are collections of at least ten articles, all centered on a particular subject. With their unique mix of varied contributions from Original Research to Review Articles, Frontiers Research Topics unify the most influential researchers, the latest key findings and historical advances in a hot research area.

Find out more on how to host your own Frontiers Research Topic or contribute to one as an author by contacting the Frontiers editorial office: frontiersin.org/about/contact

Non-coding RNAs as potential therapeutics and biomarkers for human diseases

Topic editors

Alice Conigliaro — University of Palermo, Italy

Margarida Gama-Carvalho — University of Lisbon, Portugal

Chiara De Santi — Royal College of Surgeons in Ireland, Ireland

Citation

Conigliaro, A., Gama-Carvalho, M., De Santi, C., eds. (2026). *Non-coding RNAs as potential therapeutics and biomarkers for human diseases*. Lausanne: Frontiers Media SA. doi: 10.3389/978-2-8325-7340-2

Table of contents

05 Editorial: Non-coding RNAs as potential therapeutics and biomarkers for human diseases
Margarida Gama-Carvalho, Alice Conigliaro and Chiara De Santi

09 Current concepts of the crosstalk between lncRNA and E2F1: shedding light on the cancer therapy
Peng Huang, Feng Wen and Qiu Li

28 FOXO1-mediated autophagy regulation by miR-223 in sepsis-induced immunosuppression
Guoan Xiang, Qi Li, Di Lian, Chengcheng Su, Xin Li, Shoulong Deng and Lixin Xie

40 The long non-coding RNA GAS5 contributes to the suppression of inflammatory responses by inhibiting NF-κB activity
Debora Curci, Biljana Stankovic, Nikola Kotur, Letizia Pugnetti, Vladimir Gasic, Maurizio Romano, Branka Zukic, Giuliana Decorti, Gabriele Stocco, Marianna Lucafò and Sonja Pavlovic

51 A prognostic signature of Glutathione metabolism-associated long non-coding RNAs for lung adenocarcinoma with immune microenvironment insights
Junxi Hu, Shuyu Tian, Qingwen Liu, Jiaqi Hou, Jun wu, Xiaolin Wang and Yusheng Shu

69 Deciphering the role of Wnt/β-catenin and miR-214 in knee osteoarthritis: molecular and clinical insights
Waad A. Samman, Esraa M. Mosalam, Dalia S. Saif, Mahmoud S. Abdallah, Abdel-Aziz A. Zidan, Amany Said Sallam, Shimaa Abdelsattar, Fatma Omar Khalil, Amany E. Elashkar, Somia Mokabel Mohamed, Mohamed Al-Ghannam and Hend E. Abo Mansour

82 Exosomes enriched with miR-124-3p show therapeutic potential in a new microfluidic triculture model that recapitulates neuron–glia crosstalk in Alzheimer's disease
Artemizia Évora, Gonçalo Garcia, Ana Rubi, Eleonora De Vitis, Ana Teresa Matos, Ana Rita Vaz, Francesca Gervaso, Giuseppe Gigli, Alessandro Polini and Dora Brites

110 The prognostic value of miR-34 family in ovarian cancer: a systematic review and meta-analysis
Xiulan Luo, Xiaolu Li, Chaolin Chen, Jing Yang and Hong Zheng

119 Exploring the roles of ncRNAs in prostate cancer via the PI3K/AKT/mTOR signaling pathway
Rongwang Guo, Liji Shi, Yonghui Chen, Canling Lin and Weihua Yin

138 Prognostic and clinicopathological roles of circular RNA expression in chemoresistance in head and neck squamous cell carcinoma: a systematic review
Sayan Kumar Das, Sameer Khasbage, Ashim Mishra and Babban Jee

153 A novel cancer-associated lncRNA, LINC01123, participates in tumor progression, metabolism, immune escape, and resistance
Qiang Liu, He Huang, Shuwen Zhang, Fangteng Liu and Ting Lou

163 Long non-coding rnas as key modulators of the immune microenvironment in hepatocellular carcinoma: implications for Immunotherapy
Siqi Zhao, Fei Chen, Lingyu Hu, Xiaoping Li, Zhaofeng Gao, Minjie Chen, Xiaoguang Wang and Zhengwei Song

183 Circular RNAs as disease modifiers of complex neurologic disorders
Veronica Galli, Sara Vinciguerra, Marta Biagioli and Jasmin Morandell

198 A review of circular RNAs in colorectal cancer: insights into biomarker discovery and therapeutic targeting
Sibin Nambidi, Karunakaran Bhuvaneswari Shruthi, Sujatha Padmanaban Kanimozhe, Antara Banerjee, Suresh Babu Kondaveeti, Asim K. Duttaroy and Surajit Pathak

212 A migrasome-related lncRNA signature predicts prognosis and immune response in hepatocellular carcinoma: Implications for biomarker discovery and therapeutic targeting
Haotian Qin, Tiantian Qi, Min Liu, Weibei Sheng, Junyu Qian, Jian Weng, Qi Yang and Jun Yang

frontiers | Frontiers in Pharmacology

TYPE Editorial
PUBLISHED 18 December 2025
DOI 10.3389/fphar.2025.1753536

Check for updates

OPEN ACCESS

EDITED AND REVIEWED BY
John M. Seubert,
University of Alberta, Canada

*CORRESPONDENCE
Chiara De Santi,
chiaradesanti@rcsi.ie

RECEIVED 24 November 2025
REVISED 04 December 2025
ACCEPTED 08 December 2025
PUBLISHED 18 December 2025

CITATION
Gama-Carvalho M, Conigliaro A and De Santi C (2025) Editorial: Non-coding RNAs as potential therapeutics and biomarkers for human diseases.
Front. Pharmacol. 16:1753536.
doi: 10.3389/fphar.2025.1753536

COPYRIGHT
© 2025 Gama-Carvalho, Conigliaro and De Santi. This is an open-access article distributed under the terms of the Creative Commons Attribution License (CC BY). The use, distribution or reproduction in other forums is permitted, provided the original author(s) and the copyright owner(s) are credited and that the original publication in this journal is cited, in accordance with accepted academic practice. No use, distribution or reproduction is permitted which does not comply with these terms.

Editorial: Non-coding RNAs as potential therapeutics and biomarkers for human diseases

Margarida Gama-Carvalho[1], Alice Conigliaro[2] and Chiara De Santi[3]*

[1]BioISI – Biosystems and Integrative Sciences Institute, Faculty of Sciences, University of Lisbon, Lisbon, Portugal, [2]Department of Biomedicine Neuroscience and Advanced Diagnostic, University of Palermo, Palermo, Italy, [3]School of Pharmacy and Biomolecular Sciences, Royal College of Surgeons in Ireland, Dublin, Ireland

KEYWORDS

biomarkers, CircRNAs, lncRNAs, miRNAs, ncRNA, RNA therapeutics

Editorial on the Research Topic
Non-coding RNAs as potential therapeutics and biomarkers for human diseases

NcRNAs in health and disease

Once considered "junk DNA", non-coding genomic regions have gained substantial attention over the past 2 decades (Pennisi, 2012). A very rich and diverse set of non-coding RNA (ncRNA) transcripts has been revealed thanks to technological advances in transcriptomics and bioinformatic annotation methods. In the current GENCODE release, 7,563 small non-coding RNA (sncRNA) genes and 35,899 long non-coding RNA genes (lncRNAs) are annotated in the human genome, exceeding the number of protein-coding genes by more than two-fold (Mudge et al., 2024).

The catalogue of sncRNA continues to expand, with families defined by their biogenesis, associated protein complexes and cellular functions (Shi et al., 2022). microRNAs (miRs) remain the most extensively characterized, regulating mRNA stability and translation, and influencing key biological processes, including proliferation, metabolism, differentiation, and organ development (Shang et al., 2023). Other sncRNA classes, like piRNAs, are central to genome stability and antiviral defense, or participate in RNA biogenesis and modification pathways (e.g., snoRNAs in rRNA biogenesis). Additional groups, such as tRNA-derived fragments, illustrate the increasing complexity of this regulatory layer.

LncRNAs have only recently begun to be characterized systematically (Mattick et al., 2023). Their capacity to form diverse ribonucleoprotein assemblies and act across multiple regulatory levels complicates efforts to classify them or predict function, although many operate as modulators of chromatin and transcription. A third major class – circular RNAs (circRNAs) – initially considered "splicing noise", has emerged as a distinct group with covalently closed structures and regulatory functions increasingly recognized across physiological and pathological contexts. Predominantly generated by head-to-tail back-splicing events from "parental" gene transcripts, most circRNAs regulate gene expression by

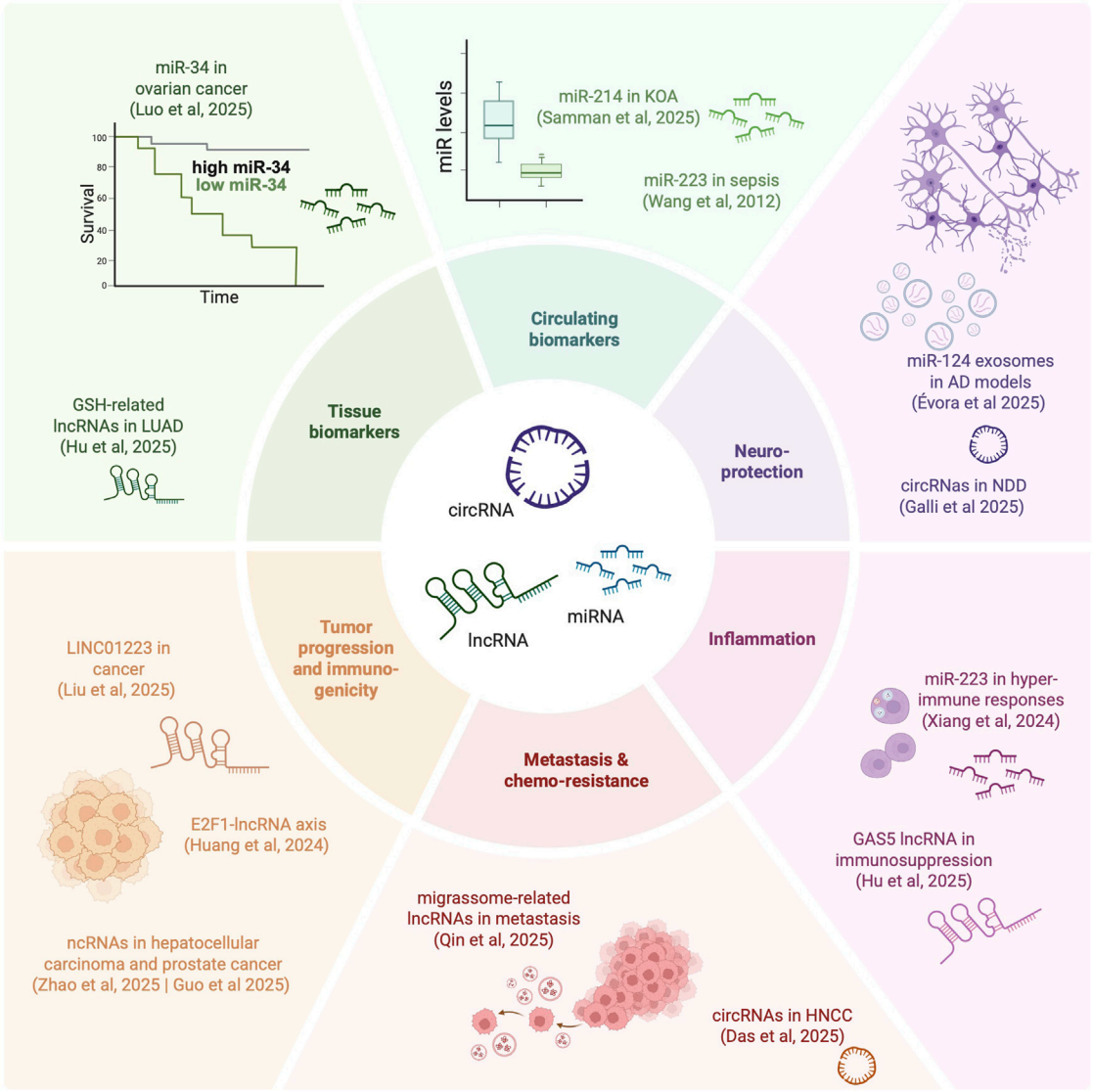


FIGURE 1
Non-coding RNAs as Potential Therapeutics and Biomarkers for Human Diseases. Different areas of impact of ncRNAs covered in this Research Topic. AD – Alzheimer's Disease. HNCC – head and neck carcinoma. KOA – knee osteoarthritis. LUAD – lung adenocarcinoma. NDD – neurodegenerative disorders. Created in BioRender. Gama-Carvalho, M. (2025) https://BioRender.com/vdnbyzf.

acting as sponges for proteins and miRs, although other functions have been reported (Yang et al., 2022).

Of relevance for pharmacology, specific ncRNAs show altered expression across diverse pathological contexts, and have been proposed as diagnostic or prognostic biomarkers, particularly in neurological diseases and cancer. Their presence in circulation–either freely or within extracellular vesicles - enhances their potential as minimally invasive disease monitors. Beyond biomarker applications, ncRNA actively modulate pathological processes, making them attractive therapeutic targets or agents. In cancer, for instance, ncRNAs influence oncogenic signaling and tumor-immune interactions, highlighting translational opportunities. The associate review by Guo et al. on ncRNA regulation of the PI3K/AKT/mTOR pathway in prostate cancer showcases this potential. Collectively, the articles assembled in this Research Topic provide a high-level view of a rapidly evolving field with direct relevance to disease monitoring and therapeutic development (Figure 1).

MiRNAs take the lead

The Research Topic includes a set of original studies on miRs that illustrate their clinical and translational relevance across diverse pathological contexts. Several miRs have been proposed as biomarkers for disease severity and prognosis. A meta-analysis of tumor expression levels of the onco-suppressor miR-34 family from seven studies involving 672 women, revealed that higher expression is associated with significantly improved overall survival and progression-free survival, supporting a possible prognostic value for these miRs (Luo et al.) (Samman et al.) explore the correlation of serum levels of miR-214, a known regulator of the Wnt-signalling pathway, in patients with knee

osteoarthritis (KOA), proving evidence for decreased levels compared to healthy controls. Their observations proof that this miR is functionally linked to a pathogenic signalling axis (Wnt/β-catenin) in KOA, being quantitatively associated with disease severity and structural damage, suggesting that, beyond a promising biomarker, it may be of value as a therapeutic agent too. Circulating levels of miR-223 were found to be altered in the context of sepsis (Wang et al., 2012). In a continuation of this study published as part of this Research Topic, authors now show that miR-223 participates in the regulation of autophagy in $CD4^+$ T lymphocytes and potentially limits cytokine-driven hyperimmune responses, supporting its relevance as both biomarker and therapeutic target for sepsis (Xiang et al.). Finally, the work of Évora et al. explores the potential of miR-124-3p loaded exosomes, showing they exert neuro- and immune-protective effects across neurons, microglia, and astrocytes in a microfluidic Alzheimer's disease triculture model characterized by neurodegeneration and glia-driven neuroinflammation.

Collectively, the miR studies featured in this Research Topic underscore the capacity of sncRNAs to link molecular regulation with clinically observable phenotypes. They exemplify how miRs can serve as accessible biomarkers, inform disease mechanisms and support the development of targeted therapeutic strategies across inflammatory and degenerative conditions.

LncRNAs in tumor progression and immunogenicity

LncRNAs offer substantial opportunities in disease definition and treatment. Research in this area focuses on two main fronts: identifying novel lncRNAs within the genome and characterizing their functional mechanisms. The latter is particularly challenging, as lncRNAs can exert contrasting effects depending on cellular context and cofactors.

In this Research Topic, Curci et al. investigated lncRNA GAS5 in inflammation, showing that it influences the NF-κB pathway in a context-depending manner. GAS5 directly binds to p65, boosting NF-κB ability to bind to DNA. Notably, when glucocorticoids (GCs) are present, GAS5 reverses its role: it inhibits NF-κB DNA binding and strengthens the anti-inflammatory effects of GCs. These results identify GAS5 as an important modulator of inflammation and immune responses. as both a biomarker for GC therapy response and a potential target to improve efficacy or overcome resistance.

Another study reports original work on the use of lncRNA-based signatures in cancer prognosis and therapy. Hu et al. developed prognostic model based on glutathione (GSH) metabolism-related lncRNAs in lung adenocarcinoma. By linking GSH metabolism, lncRNA expression, and immune contexture, the model predicts patient outcomes and correlates with immune infiltration, tumour mutation burden, and drug sensitivity - supporting personalized treatment strategies.

LncRNAs have been extensively studied as regulators of cancer progression. In this Research Topic, Huang et al. reviewed the current literature on the effect of the bidirectional regulation of several lncRNAs towards the (largely) pro-oncogenic transcription factor E2F1 in different cancer types, suggesting that targeting the E2F1-lncRNA network could represent a viable therapeutic option. Liu and colleagues summarised the current literature around a novel lncRNA called LINC01123 in tumour progression, metabolism, immune escape, and resistance (Liu et al.). The function of lncRNAs in tumour immunogenicity and response to immunotherapy in hepatocellular carcinoma is the focus of another review (Zhao et al.), highlighting once again that lncRNAs do not only modulate the biology of the cancer cells their selves but also the overall tumour microenvironment, with important consequences on immune responses to tumour development and treatment outcomes.

A significant advancement in lncRNA biomarker research is their presence in extracellular vesicles (EVs), which facilitate intercellular communication. However, identifying the origin of EVs in biological fluids remains a challenge. The discovery of migrasomes - EVs formed during cell migration - helps narrow this uncertainty. Migrasomes released by cancer cells influence the tumour microenvironment, promoting migration and invasion. In hepatocellular carcinoma (HCC), researchers (Qin et al.) characterized migrasome-related lncRNAs (MRlncRNAs), revealing a new regulatory axis involving lncRNAs, migrasomes, and immune signalling. Their validated signature offers insights into tumour biology and supports MRlncRNA-targeted therapies and refined patient stratification in HCC.

Overall, studies in this Research Topic explore lncRNAs as biomarkers, prognostic tools, and therapeutic targets, emphasizing their context-dependent functions and emerging significance in extracellular vesicle-mediated communication and tumor microenvironment regulation.

The promise of circular RNAs

CircRNAs are one of the most recent additions to the world of regulatory ncRNAs. In this Research Topic, three reviews were published highlighting their emerging potential as disease modifiers of complex neurologic disorders (Galli et al.), as therapeutic targets and biomarkers for colorectal cancer (Nambidi et al.), and as modulators of chemoresistance in head and neck squamous cell carcinoma (Das et al.). All three papers converge on the idea that while circRNAs are promising, moving from bench to bedside requires: (i) better mechanistic understanding; (ii) robust validation in clinical samples; and (iii) scalable and safe delivery platforms.

Conclusion and future directions

Our Research Topic contribute to building knowledge around the role of ncRNAs in human disease in the hope that with increased understanding of the biology behind these fascinating molecules we will finally increase the chances of finding a therapeutic strategy for not-yet curable diseases.

The articles assembled in this Research Topic highlight the expanding roles of ncRNAs in biomarker development and therapeutic exploration. Together, they illustrate how diverse ncRNA families act at multiple regulatory levels and how these functions can be leveraged to improve diagnosis, stratification and intervention across pathological contexts. As the field advances, several priorities are emerging, namely, improving mechanistic understanding of ncRNA regulatory networks and developing standards for clinical-grade biomarker validation. Progress in delivery technologies and chemical modification strategies is also accelerating the translation of ncRNA-based therapeutics. The recently reported success of a small

clinical trial using miRNA-based therapeutics to slow progression of Huntington's disease (Dolgin, 2025) is an encouraging prospect for the future of the field. The contributions in this Research Topic exemplify the breadth of ongoing efforts and point to a growing set of opportunities for ncRNAs to inform future diagnostics and treatments.

Author contributions

MG-C: Writing – review and editing, Visualization. AC: Writing – review and editing. CD: Writing – original draft, Writing – review and editing.

Funding

The author(s) declared that financial support was received for this work and/or its publication. MG-C is supported by UID/04046/2023 - Biosystems and Integrative Sciences Institute Centre grant from FCT, Portugal.

Acknowledgements

We thank the submitting authors, the reviewers and editorial team for support in developing this Research Topic.

Conflict of interest

The author(s) declared that this work was conducted in the absence of any commercial or financial relationships that could be construed as a potential conflict of interest.

Generative AI statement

The author(s) declared that generative AI was not used in the creation of this manuscript.

Any alternative text (alt text) provided alongside figures in this article has been generated by Frontiers with the support of artificial intelligence and reasonable efforts have been made to ensure accuracy, including review by the authors wherever possible. If you identify any issues, please contact us.

Publisher's note

All claims expressed in this article are solely those of the authors and do not necessarily represent those of their affiliated organizations, or those of the publisher, the editors and the reviewers. Any product that may be evaluated in this article, or claim that may be made by its manufacturer, is not guaranteed or endorsed by the publisher.

References

Dolgin, E. (2025). Huntington's disease treated for first time using gene therapy. *Nature* 646, 15. doi:10.1038/d41586-025-03139-9

Mattick, J. S., Amaral, P. P., Carninci, P., Carpenter, S., Chang, H. Y., Chen, L.-L., et al. (2023). Long non-coding RNAs: definitions, functions, challenges and recommendations. *Nat. Rev. Mol. Cell Bio* 24, 1–17. doi:10.1038/s41580-022-00566-8

Mudge, J. M., Carbonell-Sala, S., Diekhans, M., Martinez, J. G., Hunt, T., Jungreis, I., et al. (2024). GENCODE 2025: reference gene annotation for human and mouse. *Nucleic Acids Res.* 53, D966–D975. doi:10.1093/nar/gkae1078

Pennisi, E. (2012). ENCODE Project writes eulogy for junk DNA. *Science* 337, 1159–1161. doi:10.1126/science.337.6099.1159

Shang, R., Lee, S., Senavirathne, G., and Lai, E. C. (2023). microRNAs in action: biogenesis, function and regulation. *Nat. Rev. Genet.* 24, 816–833. doi:10.1038/s41576-023-00611-y

Shi, J., Zhou, T., and Chen, Q. (2022). Exploring the expanding universe of small RNAs. *Nat. Cell Biol.* 24, 415–423. doi:10.1038/s41556-022-00880-5

Wang, H., Zhang, P., Chen, W., Feng, D., Jia, Y., and Xie, L. (2012). Serum MicroRNA signatures identified by solexa sequencing predict sepsis patients' mortality: a prospective observational Study. *PLoS ONE* 7, e38885. doi:10.1371/journal.pone.0038885

Yang, L., Wilusz, J. E., and Chen, L.-L. (2022). Biogenesis and regulatory roles of circular RNAs. *Annu. Rev. Cell Dev. Biol.* 38, 263–289. doi:10.1146/annurev-cellbio-120420-125117

frontiers | Frontiers in Pharmacology

TYPE Review
PUBLISHED 25 July 2024
DOI 10.3389/fphar.2024.1432490

Check for updates

OPEN ACCESS

EDITED BY
Chiara De Santi,
Royal College of Surgeons in Ireland, Ireland

REVIEWED BY
Lei Huang,
University of Massachusetts Medical School, United States
Sutapa Mukherjee,
Chittaranjan National Cancer Institute (CNCI), India

*CORRESPONDENCE
Qiu Li,
liqiu@scu.edu.cn

RECEIVED 14 May 2024
ACCEPTED 08 July 2024
PUBLISHED 25 July 2024

CITATION
Huang P, Wen F and Li Q (2024), Current concepts of the crosstalk between lncRNA and E2F1: shedding light on the cancer therapy. *Front. Pharmacol.* 15:1432490. doi: 10.3389/fphar.2024.1432490

COPYRIGHT
© 2024 Huang, Wen and Li. This is an open-access article distributed under the terms of the Creative Commons Attribution License (CC BY). The use, distribution or reproduction in other forums is permitted, provided the original author(s) and the copyright owner(s) are credited and that the original publication in this journal is cited, in accordance with accepted academic practice. No use, distribution or reproduction is permitted which does not comply with these terms.

Current concepts of the crosstalk between lncRNA and E2F1: shedding light on the cancer therapy

Peng Huang[1,2], Feng Wen[1,3] and Qiu Li[1,2]*

[1]Division of Abdominal Tumor Multimodality Treatment, Cancer Center, West China Hospital, Sichuan University, Chengdu, Sichuan, China, [2]Department of Medical Oncology, Cancer Center, West China Hospital, Sichuan University, Chengdu, Sichuan, China, [3]Department of Radiation Oncology, Cancer Center, West China Hospital, Sichuan University, Chengdu, Sichuan, China

Long noncoding RNAs (lncRNAs) constitute a distinctive subset of RNA molecules with limited protein-coding potential, which exert crucial impacts on various biological activities. In the context of cancer, dysregulated lncRNAs function as essential regulators that affect tumor initiation and malignant progression. These lncRNAs serve as competitive endogenous RNAs (ceRNAs) through sponging microRNAs and regulating the expression of targeted genes. Moreover, they also directly bind to RNA-binding proteins, which can be integrated into a complex mechanistic network. E2F1, an extensively studied transcription factor, mediates multiple malignant behaviors by regulating cell cycle progression, tumor metastasis, and therapeutic response. Emerging evidence suggests that lncRNAs play a pivotal role in regulating the E2F1 pathway. This review aims to elucidate the intricate gene regulatory programs between lncRNAs and E2F1 in cancer progression. We elaborate on distinct mechanistic networks involved in cancer progression, emphasizing the potential of the lncRNAs/E2F1 axes as promising targets for cancer therapy. Additionally, we provide novel perspectives on current evidence, limitations, and future directions for targeting lncRNAs in human cancers. Fully deciphering the intricate network of lncRNA/E2F1-mediated regulatory mechanisms in cancer could facilitate the translation of current findings into clinical course, such efforts ultimately significantly improve the clinical prognosis of cancer patients.

KEYWORDS

lncRNA, E2F1, cancer progression, immune response, gene therapy

1 Introduction

Cancer is a major global health concern, posing significant life-threatening risks in both developed and developing countries (Zhou et al., 2024). Despite advancements in improving clinical prognosis in the past few decades, cancer still presents an immense clinical challenge due to its high mortality rates, posing heavy burdens for public health and global medical expenses (Torre et al., 2016; Cao et al., 2024). The crucial treatment modalities for cancer patients including surgical resection, systematic chemotherapy, radiotherapy, immunotherapy, and molecular targeted therapy, which are associated with systemic toxicity and therapeutic resistance, impeding therapeutic efficacies and their clinical application (Khan et al., 2024; Murthy and Are, 2024). Therefore, developing feasible strategies for cancer is essential, but the intricate pathological

mechanisms underlying cancer progression pose a formidable challenge, underscored by multi-faceted considerations of therapeutic efficacies and adverse events (Doostmohammadi et al., 2024; Galluzzi et al., 2024).

Cancer is perceived as a malignant disease characterized by various genetic dysregulations and epigenetic irregularities, leading to elevated expression of oncogenes, which mechanistically promote carcinogenesis by multiple molecular mechanisms including activating the mRNA transcription and augmenting the downstream protein translation (Gong and Li, 2024; Ju et al., 2024). However, protein-coding genes only account for 2%, even though approximately 85% of the human genes are transcribed (Sherman and Salzberg, 2020). Emerging evidence has uncovered that these non-coding genes participate in transcribing a group of noncoding RNAs (ncRNAs) that exert an essential role in the epigenetic modulation of downstream genes (Xu et al., 2023; Yang et al., 2023). They can be classified into two groups based on size: small ncRNAs, such as microRNAs (miRNAs), which are approximately 22 nucleotides in length, and long non-coding RNAs (lncRNAs), which are longer than 200 nucleotides with limited coding potential (Thapa et al., 2024). Numerous studies have indicated a crucial role for lncRNAs in modulating gene expression at transcriptional and translational levels (Siddique et al., 2024). A growing interest in the realm of carcinogenesis has demonstrated that lncRNAs drive tumor initiation and prompt malignant progression by regulating chromatin structure, mRNA stabilization, and protein translation, and acting as competitive endogenous RNAs (ceRNAs) for influencing target gene expression (Huang P. et al., 2024; Saranya et al., 2024; Song et al., 2024; Xiang et al., 2024).

Transcription factors (TFs) are acknowledged as a collection of regulatory proteins that exert significant impacts on gene expression and protein synthesis by binding to certain DNA sequences (Bushweller, 2019; Kant et al., 2022). These changes result in a variety of outcomes such as tissue maintenance, inflammation regulation, and determining cell phenotype (Kant et al., 2022; Li et al., 2022). In the setting of malignant disease, dysregulated TFs are pivotal in the survival and proliferation of tumor cells, and are evident across numerous cancer types (Ahmad et al., 2023). Existing experimental studies have associated functional alterations and expression patterns of TFs with cancer initiation and progression, including SOX2 (Novak et al., 2020), NF-κB (Yu H. et al., 2020), c-Myc (Gao et al., 2023), Snail (Kielbik et al., 2023), signal transducer and activator of transcription (STAT) (Li YJ. et al., 2023), and E2F (Kent and Leone, 2019), which are considered essential TFs influencing cellular homeostasis.

Regarding E2Fs specifically, there have identified eight members, out of which E2F1 has been extensively studied (Fang et al., 2020a; Chun et al., 2020; Kassab et al., 2023). E2F1 significantly contributes to cell cycle regulation and apoptosis induction in human cancer cells (Meng and Ghosh, 2014). Moreover, there is ample evidence uncovering a direct regulation of E2F1 by lncRNAs, which further promotes malignant behaviors including cell proliferation, metastasis, stemness, and therapeutic response (Priyanka et al., 2022; Barczak et al., 2023; Yu et al., 2023). Notably, dysregulation of the lncRNA-E2F1 axis can be affected by certain signaling pathways, which provide novel insights into drug development for cancer therapy (Logotheti et al., 2020; Xiao et al., 2022). In this review, we emphasize current evidence of lncRNA-E2F1 interaction in the context of malignancies and highlight the feasible preclinical therapeutic modalities for targeting lncRNAs or E2F1, aiming to facilitate the translation of molecular crosstalk into clinical application, which holds immense promises for tumor eradication and ameliorating prognosis (Figure 1).

2 Deregulation of E2F1 in cancer progression

The E2F1 gene is situated within the human chromosome 20 region 11 zone 2 (20 q11.2), spanning approximately 11 kilobases in length, which encodes the E2F1 protein that plays a crucial role in various biological processes (Fouad et al., 2020). E2F1 predominantly performs its biological roles through enhancing the expression of numerous downstream genes related to cell cycle regulation, DNA damage response, cellular self-renewal, and tissue development (Ertosun et al., 2016; Denechaud et al., 2017; Manickavinayaham et al., 2020).

E2F1 is deregulated in the setting of human cancers including breast, colorectal, lung, prostate, ovarian, and bladder cancer (Chun et al., 2020; Logotheti et al., 2020; Jing et al., 2022; Priyanka et al., 2022; Yu et al., 2023). Existing evidence has indicated that E2F1 was an essential predictor of prognosis in cancer patients. E2F1 was highly expressed in esophageal squamous cell carcinoma (ESCC) cases and associated lymph node metastasis (Mega et al., 2005). Furthermore, overexpression of E2F1 significantly shortened overall survival (OS) in lung cancer patients observed over 200 months, while this trend was also noted in hepatocellular carcinoma (HCC) patients (Gao et al., 2016; Liu Y. et al., 2022). Indeed, E2F1 plays a critical role in cancer progression. For example, E2F1 expression was upregulated by non-SMC Condensin II Complex Subunit D3 (NCAPD3) in colorectal cancer (CRC) cells, which in turn promoted the transcription of pyruvate dehydrogenase kinase 1 (PDK1) and PDK3 genes, significantly enhancing Warburg effect and leading to advanced disease (Jing et al., 2022). E2F1 directly stimulated protease, serine S1 family member 22 (PRSS22) transcription, which facilitated efficient cleavage of Annexin A1 (ANXA1), producing an N-terminal peptide to activate formyl-peptide receptor-2 (FPR2)/ERK cascade, thus favoring the invasive phenotype in breast cancer (Song et al., 2022). In line with this, Zafar et al. reported that E2F1 enhanced the expression of kinesin superfamily 26A (KIF26A), abolishing p21 expression, consequently favoring cell cycle progression, resulting in tumor growth in the mouse model of breast cancer (Xu J. et al., 2020). In lung cancer, elevated E2F1 was associated with invasion and metastasis of cancer cells (Wang T. et al., 2017; Zhang and Shi, 2023). Mechanistically, E2F1 dampened Zinc finger E-box binding homeobox 2 (ZEB2) expression and promoted the epithelial-mesenchymal transformation (EMT) (Wang T. et al., 2017), which revealed the potential for suppressing distant metastasis by targeting E2F1.

In addition to influencing malignant transformation, E2F1 significantly regulates therapeutic response to cancer cells. E2F1 was reported to orchestrate ABCG2 expression and drive chemotherapeutic drug efflux by targeting ABCG2, which could

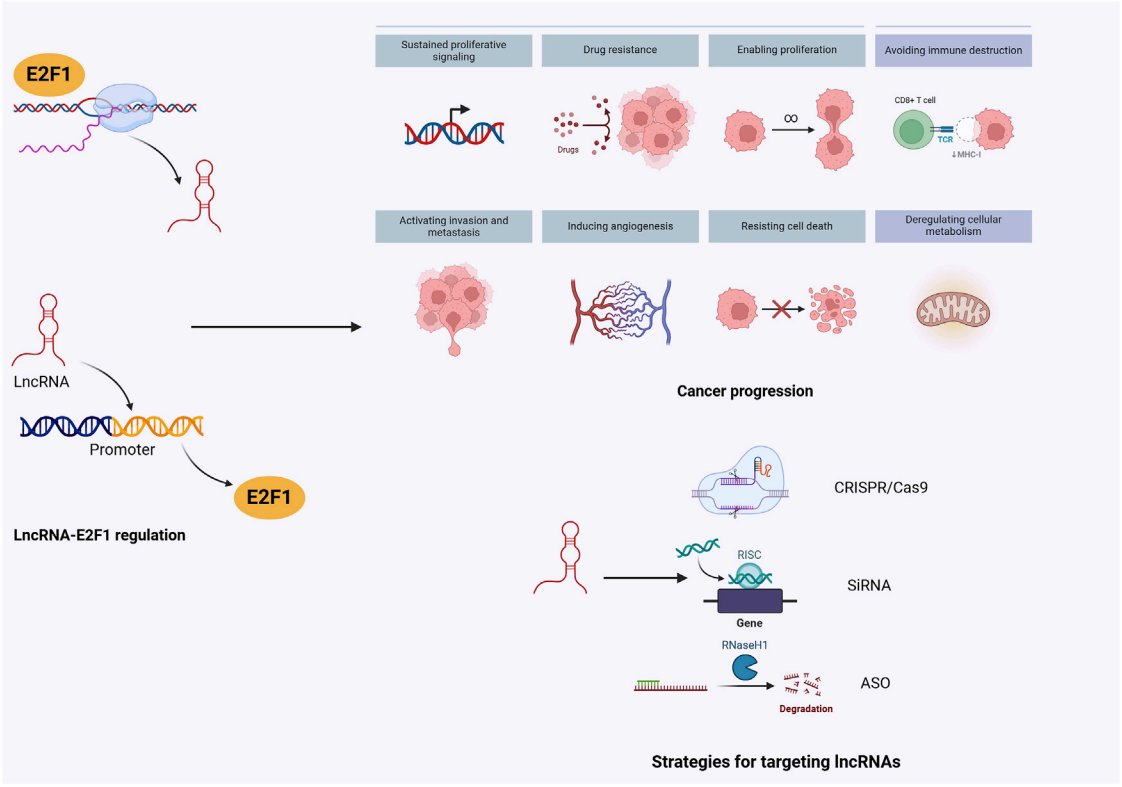


FIGURE 1
The concise overview of lncRNA/E2F1 crosstalk in cancer.

be restored by inhibiting ABCG2 (Rosenfeldt et al., 2014). Moreover, E2F1/insulin-like growth factor receptor (IGF-1R) axis mediated the activation of phosphoinositide 3-kinase (PI3K)/AKT pathway, promoting BRAF inhibitor resistance in melanoma (Liu et al., 2020). These findings uncover novel pathways in multidrug resistance and reveal previously unrecognized functions of E2F1 that are pertinent to cancer therapy.

3 Deregulated lncRNAs in cancer progression

A myriad of well-defined lncRNAs have undergone extensive research, leading to the elucidation of their functional mechanisms. Within the nucleus, lncRNAs modulate gene transcription and mediate epigenetic alterations via interactions with chromatin and remodeling chromatin (Bridges et al., 2021). In the cytoplasm, lncRNAs contribute to signaling transduction, mRNA stabilization, and translational regulation (Bridges et al., 2021). Notably, some lncRNAs act as ceRNAs, sequestering miRNAs to modulate the activities and abundance of RNA-binding proteins, thereby influencing post-translational modifications (Yang et al., 2023). Moreover, lncRNAs serve as scaffolds to assemble intricate protein networks involved in tightly modulated signaling pathways (Schmitz et al., 2016). Through diverse mechanisms, lncRNAs exert crucial roles in numerous biological processes (Figure 2).

An emerging focus of lncRNA research revolves around gaining deeper insights into the molecular networks of tumorigenesis (Sakurai and Ito, 2024; Thapa et al., 2024). Recognizing the pivotal control of lncRNAs on various facets of malignant transformation including cell proliferation, growth, metastasis, metabolism, and drug resistance, the interest in elucidating its modulation is significantly reasoned (Hashemi et al., 2022; Wang S. et al., 2023). Metastasis-associated lung adenocarcinoma transcript-1 (MALAT-1) is deregulated in various human cancers (Yan H. et al., 2023; Li GZ. et al., 2023). MALAT1 was found to sponge miR-1-3p, upregulating B-related factor 2 expression, which in turn promoted cell viability and growth in HCC (Li GZ. et al., 2023). In multiple myeloma (MM), MALAT1 acted as ceRNA of miR-15a and miR-16 to upregulate the expression of vascular endothelial growth factor A (VEGFA), which significantly facilitated angiogenesis and led to tumor growth in a MM mouse model (Yan H. et al., 2023). Min et al. (2024) reported that lncRNA MIR100HG exhibited elevated expression levels in lung cancer cells. Further mechanistic studies have disclosed that MIR100HG directly targeted the miRNA-5590-3p/DCBLD2 cascade, which facilitated cell proliferation, invasion, and migration (Min et al., 2024). In contrast with this, lncRNA TINCR was downregulated in pancreatic cancer tissues and dampened EMT by suppressing the Wnt/β-catenin signaling pathway (Wei and Zhu, 2024), which serves as an essential activator of tumor metastasis (Zhan et al., 2017). Moreover, Liu and colleagues reported that CCAT5 was transactivated by the Wnt/β-catenin/transcription factor 3 (TCF3) cascade in gastric cancer cells (Liu et al., 2024). Mechanistic studies have uncovered that CCAT5 directly disturbed the Src homology 2 domain-containing protein

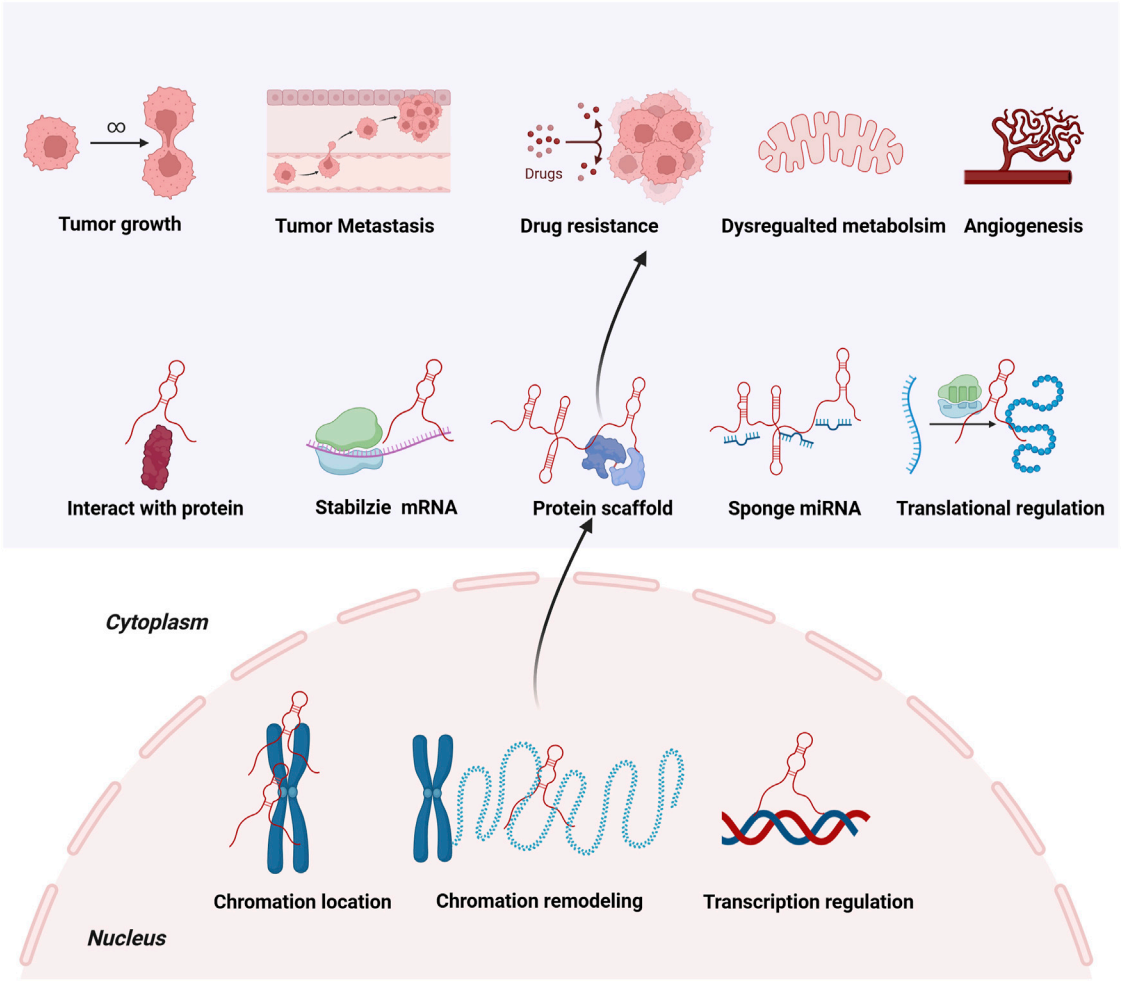


FIGURE 2
Molecular mechanisms of lncRNAs in the regulation of cancer progression.

TABLE 1 Deregulated lncRNAs in cancer progression.

LncRNA	LncRNA expression	Cancer	Mechanism	Function	References
MALAT1	Up	HCC	Sponged miR-1-3p, upregulating B-related factor 2 expression	Promoted cell viability and growth	Li et al. (2023b)
MALAT1	Up	Multiple myeloma	Acted as a ceRNA of miR-15a and miR-16 to upregulate the expression of VEGFA	Facilitated angiogenesis and tumor growth	Yan et al. (2023a)
MIR100HG	Up	Lung cancer	MIR100HG targeted the miRNA-5590-3p/DCBLD2 cascade	Facilitated cell proliferation, invasion, and migration	Min et al. (2024)
TINCR	Down	Pancreatic cancer	Suppressed the Wnt/β-catenin signaling pathway	Inhibited EMT	Wei and Zhu (2024)
CCAT5	Up	Gastric cancer	CCAT5 was transactivated by the Wnt/β-catenin/TCF3 cascade	Accelerated tumor growth, metastasis and resistance to oxaliplatin	Liu et al. (2024)
Linc01056	Down	HCC	Knockdown of linc01056 activated PPARα, leading to elevated fatty acid metabolism and abrogated glycolysis	resensitizing cancer cell to sorafenib	Chan et al. (2024)

TABLE 2 The molecular mechanisms of lncRNA/E2F1 crosstalk in human cancers.

LncRNA	LncRNA expression	Upstream regulator	Cancer	Mechanism	Function	References
MNX1-AS1	Up	MNX1-AS1	NSCLC	MNX1-AS1 directly triggers the phase separation of IGF2BP1, maintaining E2F1 and c-Myc mRNA stability	Promotes cell proliferation and tumor growth	Zhu et al. (2022)
TAZ-AS202	Up	TAZ-AS202	NSCLC	TAZ-AS202 upregulates E2F1 expression, enhancing EPHB2 and activating EPH-Ephrin pathway	Promotes tumor growth and metastasis	Gobbi et al. (2023)
HIT	Up	HIT	NSCLC	Upregulates E2F1 expression	Promotes cancer porgression	Park et al. (2018)
EPEL	Up	EPEL	NSCLC	Upregulates E2F1 expression	Promotes cancer porgression	Yu et al. (2017)
SVIL-AS1	Down	SVIL-AS1	LUAD	SVIL-AS1 is induced by METTL3, which facilitates E2F1 degradation	Promotes cell apoptosis	Hu et al. (2022)
GAS5	Down	GAS5	NSCLC	GAS5 inhibits E2F1 expression	Promotes cell apoptosis	Shi et al. (2015)
GAS6-AS1	Down	GAS6-AS1	NSCLC	Suppresses GLUT1 expression by interacting with E2F1	Inhibits glycolysis and tumor growth	Luo et al. (2021)
SBF2-AS1	Up	SBF2-AS1	LUAD	Sponges miR-338-3p and miR-362-3p to upregulate E2F1 expression	Promotes cancer progression	Chen et al. (2019)
PTTG3P	Up	E2F1	NSCLC	E2F1 transcriptionally activates PTTG3P, which interactes with ILF3 to stabilize MAP2K6 mRNA.	Promotes cancer progression	Wang et al. (2023b)
SNHG3	Up	E2F1	NSCLC	E2F1 induces SNHG3 expression, thus activating TGF-β and IL-6/JAK2/STAT3 pathways	Promotes tumor EMT and metastasis	Shi et al. (2020)
SBF2-AS1	Up	E2F1	NSCLC	E2F1 induces SBF2-AS1 expression, which upregulates GRB2 through sequestering miR-362-3p	Promotes tumor metastasis	Wang and Wang (2020)
MCF2L-AS1	up	E2F1	NSCLC	E2F1 induces MCF2L-AS1 expression, which binds to ELAVL1 and stabilizes CCND1 mRNA	Promotes gefitinib resistance	Shan et al. (2022)
FTH1P3	Up	E2F1	NSCLC	Recruits LSD1 and epigenetically suppresses TIMP3 expression	Promotes gefitinib resistance	Zheng et al. (2020)
LINC00847	Up	E2F1	NSCLC	LINC00847 is transcriptionally activated by E2F1 and modulates miR-147a/IFITM1 axis	Promotes cancer progression	Li et al. (2021a)
LINC00662	Up	LINC00662	NSCLC	Sponges miR-320d to enhance E2F1 expression	Promotes cancer progression	Lv et al. (2021)
LINC00511	Up	LINC00662	Breast cancer	LINC00511 sponges miR-185-3p, recovering E2F1 expression and promoting Nanog transcription	Aggravates the sphere-formation ability and stemness of cancer	Lu et al. (2018)
MALAT1	UP	MALAT1	Breast cancer	Targets miR-124/CDK4/E2F1 signaling pathway	Promotes cancer progression	Feng et al. (2016)
DANCR	UP	E2F1	Breast cancer	E2F1-responsive DANCR Sequesteres miR-34c-5p to aggravate E2F1 transcription	Promotes cancer progression	Yan et al. (2024)
RP11-19E11.1	Up	E2F1	Breast cancer	E2F1 promotes RP11-19E11.1 transcription	Promotes enzastaurin resistance	Giro-Perafita et al. (2020)
AGPG	Up	AGPG	Breast cancer	AGPG physically activates E2F1 via interacting with PURα and blocking the binding of E2F1 to PURα	Promotes tumor growth and endocrine resistance	Yu et al. (2023)
ERINA	Up	ERINA	Breast cancer	ERINA is directly transactivated by the ER binding site and interfers with the interaction between E2F1 and RB1	Promotes tamoxifen and palbociclib resistance	Fang et al. (2020b)

(Continued on following page)

TABLE 2 (*Continued*) The molecular mechanisms of lncRNA/E2F1 crosstalk in human cancers.

LncRNA	LncRNA expression	Upstream regulator	Cancer	Mechanism	Function	References
CDKN2B-AS1	Up	CDKN2B-AS1	HCC	CDKN2B-AS1 interacts with E2F1 and exacerbates the transcription of GNAZ	Promotes cancer progression	Tao et al. (2023)
LINC01089	Up	E2F1	HCC	E2F1-induced LINC01089 binds to hnRNPM, which undermines N6-methyladenosine-mediated DIAPH3 mRNA stability and elicits ERK/Snail signaling pathway	Promotes EMT and metastasis	Su et al. (2023)
LINC01004	Up	E2F1	HCC	E2F1 activates the transcription of LINC01004	Promotes EMT and metastasis	Li et al. (2023c)
KDM4A-AS1	Up	E2F1	HCC	Elevated KDM4A-AS1 expression mediated by E2F1 stabilizes AURKA via recruiting ILF3, provoking PI3K/AKT pathway	Promotes cancer progression	Shen et al. (2023)
lnc-APUE	Up	lnc-APUE	HCC	lnc-APUE sequesteres miR-20b and ameliorates the repression of E2F1 expression	Promotes cancer progression	Li et al. (2021b)
SNHG6	Up	SNHG6	HCC	Sponges miR-204-5p to upregulate E2F1	Promotes cancer progression	Chen et al. (2021)
LINC00852	Up	LINC00852	HCC	Sponges miR-625 to upregulate E2F1	Promotes cancer progression	Chen (2022)
ZEB1-AS1	Up	ZEB1-AS1	HCC	Sponges miR-299-3p to upregulate E2F1	Promotes cancer progression	Mu et al. (2021)
DUBR	Up	DUBR	HCC	SP1-transcribed lncRNA DUBR recruited E2F1 and enhanced CIP2A expression, whereas DUBR also sequesteres miR-520d-5p to enhance the stability of E2F1 mRNA and elicits Notch1 signaling pathway	Promotes cancer stemness and oxaliplatin resistance	Liu et al. (2022b)
H19	Up	H19	CRC	H19 activates E2F1 signaling pathway	Promotes cell proliferation and tumor growth	Ohtsuka et al. (2016)
NEAT1	Up	NEAT1	CRC	NEAT1 abrogates KDM5A expression via interacting with E2F1, which suppressed the KDM5A/H3K4me3-mediated repression of Cul4A expression, resulting in activated Wnt signaling pathway	Promotes cancer progression	Shen et al. (2021)
LINC01703	Up	LINC01703	CRC	LINC01703 promotes PI3K/AKT signaling pathway via miR-205-5p/E2F1 axis	Promotes cell proliferation and migration	Xu et al. (2024)
CRNDE	Up	CRNDE	CRC	CRNDE sponges miR-136 and indirectly targets E2F1	Promotes cancer metastasis and oxaliplatin resistance	Gao et al. (2017)
DLGAP1-AS2	Up	DLGAP1-AS2	rectal cancer	DLGAP1-AS2 enhances the radiotherapy resistance of rectal cancer cells by interacting with E2F1 to increase CD151 expression through activating the AKT/mTOR/cyclinD1 signaling pathway	Promotes radiotherapy resistance	Xiao et al. (2022)
EGFR-AS1	Up	EGFR-AS1	Gastric cancer	EGFR-AS1 promotes TUBA1C expression, which aggravates E2F1 expression and facilitates the G1 phase to the S phase transition	Promotes tumor growth and metastasis	Wang et al. (2023c)
NNT-AS1	Up	NNT-AS1	Gastric cancer	NNT-AS1 sponges miR-424 and elevates E2F1 expression	Promotes cancer progression	Chen et al. (2018)

(Continued on following page)

TABLE 2 (*Continued*) The molecular mechanisms of lncRNA/E2F1 crosstalk in human cancers.

LncRNA	LncRNA expression	Upstream regulator	Cancer	Mechanism	Function	References
GAS5	Down	GAS5	Gastric cancer	GAS5 disturbs E2F1 expression, and modulates miR-34c expression, which leads to the repressed p38MAPK signaling pathway	Inhibits cancer progression	Sun et al. (2014), Gupta et al. (2022)
PIN1P1	Up	PIN1P1	Gastric cancer	CREB1 activates PIN1P1 transcription, which upregulates YBX1 expression, resulting in enhanced E2F1 and PIN1 expression	Promotes cancer progression	Wang et al. (2024)
HOXA11-AS	Up	E2F1	Gastric cancer	E2F1 mediates the transcription of HOXA11-AS, which establishes a mechanistic model comprising the crosstalk between E2F1/HOXA11-AS/miR-1297/EZH2 axis and LSD1/HOXA11-AS/EZH2 complex	Promotes cancer progression	Sun et al. (2016)
LSINCT5	Up	E2F1	Gastric cancer	E2F1 induces LSINCT5 expression	Promotes cell proliferation, growth, and EMT	Niu et al. (2020)
HCG18	Up	E2F1	Gastric cancer	E2F1 induces HCG18 expression	Promotes cell proliferation, growth, and EMT	Qi et al. (2018)
SLC16A1-AS1	Up	SLC16A1-AS1	Bladder cancer	SLC16A1-AS1 interacts with E2F1 to enhance the expression of SLC16A1/MCT1 and PPARA.	Promotes aerobic glycolysis and exacerbates fatty acid β-oxidation, favoring an invasive phenotype	Logotheti et al. (2020)
TMPO-AS1	Up	E2F1	Bladder cancer	E2F1-induced TMPO-AS1 fuels the binding of E2F1 to OTUB1, enhances the deubiquitination and stability of E2F1, which unveils a novel TMPO-AS1/E2F1/OTUB1 regulatory program	Promotes cell proliferation and aggressiveness	Zhang et al. (2021)
GAS5	Down	GAS5	Prostate cancer	GAS5 facilitates the transcription of $P27^{Kip1}$ by recruiting E2F1 to its promoter	Inhibits cell proliferation and tumor growth	Luo et al. (2017)

tyrosine phosphatase 1 (SHP-1)-mediated dephosphorylation process of STAT3, resulting in accelerating tumor growth, metastasis and resistance to oxaliplatin (Liu et al., 2024). Linc01056 has been identified as a key regulator of sorafenib resistance in HCC (Chan et al., 2024). Knockdown of linc01056 activated peroxisome proliferator-activated receptor alpha (PPARα), leading to elevated fatty acid metabolism and abrogated glycolysis, while aggravating cell resistance to sorafenib (Chan et al., 2024). These findings uncover that deregulated lncRNAs hold great potential as appealing targets for cancer therapy, which awaits further investigations (Table 1).

4 The lncRNA and E2F1 regulatory networks

Emerging evidence has revealed that lncRNAs and E2F1 appear to establish a feedback loop because lncRNA could encourage E2F1 transcription, which in turn upregulates lncRNA expression. For example, lncRNA SNHG15 was upregulated in gastric cancer (GC) and E2F1 could interact with the promoter of SNHG15, leading to an increase in its expression (Duan et al., 2024). Concurrently, SNHG15 sponged miR-24-3p to upregulate the mRNA expression of E2F1, which suppressed ferroptosis and promoted cancer progression (Duan et al., 2024). These findings presented a promising therapeutic avenue for GC treatment. DANCR was another lncRNA that upregulated the expression of E2F1 (Yan et al., 2024). Mechanistically, DANCR sequestering miR-34c-5p in breast cancer cells and enhanced cell proliferation and migration (Yan et al., 2024). Additionally, E2F1 enhanced DANCR transcription by directly binding to its promoter in breast cancer cells (Yan et al., 2024). Based on these facts, blocking E2F1-lncRNA interaction may provide a potential therapeutic approach for tackling cancer.

5 LncRNAs-E2F1 crosstalk in cancer progression

Evidence continually emerges supporting the link between lncRNAs and E2F1 in regulating tumorigenesis in different cancers. Although previous sections have touched upon the involvement of lncRNAs in cancer progression, we will delve into current investigations demonstrating the molecular actions of these lncRNAs regulated by specifically TF, namely, E2F1 in different cancers. Additionally, evidence supporting lncRNA-mediated E2F1 modulation will also be expounded (Table 2).

5.1 Lung cancer

GLOBOCAN 2023 data indicates that lung cancer contributes to the most cancer-related fatalities globally, and this trend is consistent across all ethnic groups, posing a significant public health challenge worldwide (LoPiccolo et al., 2024). Lung cancer cases are categorized into non-small cell lung cancer (NSCLC) and small-cell lung cancer (SCLC), out of which NSCLC accounts for approximately 85% (LoPiccolo et al., 2024). Although great advancements have been made in early diagnosis and systemic therapy, the 5-year survival rates of lung cancer patients remain dismal, emphasizing the urgent requirement for novel therapeutic modalities (LoPiccolo et al., 2024).

By overlapping the differentially expressed lncRNAs from the GENCODE database and NSCLC-related microarray, which contented 42 paired NSCLC and normal lung tissues, Zhu and his colleagues found that lncRNA MNX1-AS1 was upregulated and associated with advanced tumor stage (Zhu et al., 2022). Elevated MNX1-AS1 directly triggered the phase separation of insulin-like growth factor 2 mRNA-binding protein 1 (IGF2BP1), maintaining E2F1 and c-Myc mRNA stability by binding to their untranslated regions, which remarkably increased c-Myc and E2F1 protein levels (Zhu et al., 2022). The MNX1-AS1/IGF2BP1/c-Myc/E2F1 cascade activated cell-cycle regulatory signals to facilitate cell colony formation and tumor growth both *in vitro* and *in vivo*, providing fresh perspectives on the control of c-Myc and E2F1 signaling in the malignant transformation of NSCLC, indicating that the MNX1-AS1/IGF2BP1 axis could potentially function as a promising target for NSCLC therapy (Zhu et al., 2022). In line with this, lncRNA TAZ-AS202 was identified as a TAZ-transcribed RNA molecule that supported the activation of EPH-Ephrin signaling pathways (Gobbi et al., 2023). Further investigations demonstrated that dysregulated TAZ-AS202 upregulated E2F1 expression, which accelerated NSCLC growth and metastasis by transcriptionally activating a myriad of oncogenes including Eph receptor B2 (EPHB2), a key component of EPH-Ephrin pathway (Gobbi et al., 2023). Similarly, several studies have identified that lncRNA HIT and EPEL directly targeted E2F1, prompting cell proliferation, invasion, and migration in NSCLC models (Yu et al., 2017; Park et al., 2018). LncRNA SVIL antisense RNA 1 (SVIL-AS1) was decreased in lung adenocarcinoma (LUAD) cells, abolished cell-cycle progression, and restrained cell proliferation (Hu et al., 2022). Mechanistically, SVIL-AS1 could be induced by methyltransferase-like 3 (METTL3), which facilitated E2F1 ubiquitination and proteasomal degradation, which could be reversed by E2F1 overexpression (Hu et al., 2022). GAS5 was another lncRNA that was downregulated in NSCLC and promoted cell apoptosis by interacting with E2F1 (Shi et al., 2015). In LUAD, GAS6-AS1 was downregulated and suppressed the expression of glucose transporter protein-1 (GLUT1), a pivotal regulator of glycolysis. Overexpression of GLUT1 reversed the inhibitory impact of GAS6-AS1 on the aggressive nature and the metabolic reprogramming. Subsequent explorations revealed that GAS6-AS1 directly bound to E2F1, thereby abolishing GUT1 transcription (Luo et al., 2021). Moreover, lncRNA SBF2-AS1 formed a novel gene regulatory model in the early-stage LUAD by sponging miR-338-3p and miR-362-3p to regulate E2F1 expression, which might function as a promising diagnostic marker (Chen et al., 2019).

E2F1 could act as the upstream regulator of lncRNAs by inducing their transcription. For example, lncRNA PTTG3P interacted with interleukin enhancer-binding factor 3 (ILF3) to stabilize the mRNAs of MAP2K6 and E2F1, which induced malignant transformation in the mouse model of NSCLC (Wang J. et al., 2023). Interestingly, increased E2F1 in turn transcriptionally activated PTTG3P, establishing a reciprocal regulatory loop (Wang J. et al., 2023). Moreover, E2F1-induced lncRNA SNHG3 enhanced NSCLC cell proliferation, invasion, and EMT by activating transforming growth factor-β (TGF-β) and IL-6/JAK2/STAT3 signaling pathway (Shi et al., 2020). SBF2-AS1 was associated with distant metastasis of NSCLC patients (Chen et al., 2020; Wang and Wang, 2020). E2F1 contributed to the overexpression of SBF2-AS1, which led to the upregulated expression of GRB2 through sequestering miR-362-3p, ultimately facilitating tumor metastasis (Wang and Wang, 2020). Gefitinib, the orally administered tyrosine kinase inhibitor for lung cancer patients harboring the epidermal growth factor receptor (EGFR) mutations across therapy lines (Wu and Shih, 2018). Acquired resistance to gefitinib significantly impedes its therapeutic efficiencies, with a myriad of studies exploring its potential mechanisms (Wu and Shih, 2018). Shan et al. (2022) reported that the upregulation of MCF2L-AS1 induced by E2F1 directly bound to ELAVL1, which stabilized Cyclin D1 (CCND1) mRNA, inducing cell resistance to gefitinib. Notably, ferritin heavy chain 1 pseudogene 3 (FTH1P3) was also induced by E2F1 and facilitated gefitinib resistance through recruiting lysine-specific demethylase 1 (LSD1) and epigenetically suppressing the tissue inhibitors of metalloproteinases 3 (TIMP3) (Zheng et al., 2020). These findings indicate that targeting E2F1-lncRNA interactions and their downstream molecules might be feasible strategies for overcoming gefitinib resistance, which provides fresh insights into the treatment of advanced NSCLC patients.

CeRNA is an emerging regulatory mechanism focusing on the crosstalk among lncRNA, miRNA, and target genes (Chen et al., 2020; Li H. et al., 2021). Exosomal lncRNA LINC00662 functioned as a molecular sponge for miR-320d and indirectly regulated E2F1 expression, thus accelerating cell proliferation, metastasis, and repressing cell cycle arrest of NSCLC *in vitro* (Lv et al., 2021). Notably, LINC00847 was transcriptionally activated by E2F1 and contributed to NSCLC progression through targeting modulating miR-147a/IFITM1 axis (Li H. et al., 2021).

As research technologies advance, there is immense potential to delve into the relationship between E2F1 and lncRNAs in lung cancer, leading to a more detailed understanding of lncRNA mechanisms. Interfering with the E2F1-lncRNA network could emerge as a pivotal approach for precise lung cancer therapy (Figure 3).

5.2 Breast cancer

Breast cancer stands out as the most common malignancy among women, featuring highly heterogeneous and various intrinsic molecular subtypes, harboring distinct therapeutic responses (Xu X. et al., 2020). Recent studies have considered lncRNAs as key regulators in breast cancer progression. For example, overexpressed LINC00511 aggravated the sphere-formation ability and stemness of

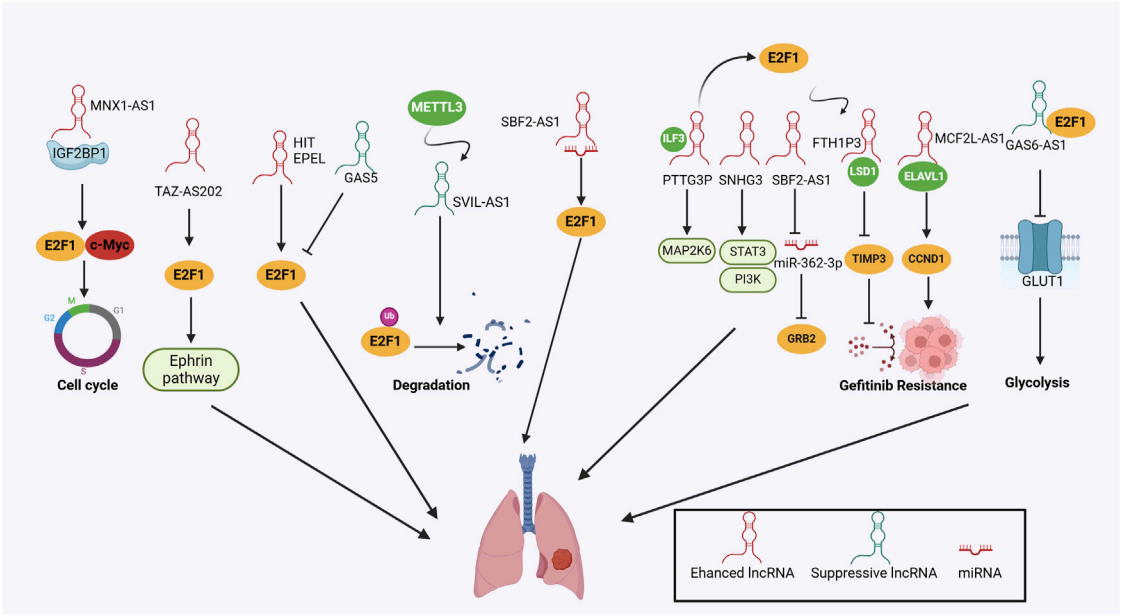


FIGURE 3
The mechanisms of the lncRNA/E2F1 crosstalk in lung cancer.

breast cancer. Mechanically, LINC00511 acted as a ceRNA for miR-185-3p, thereby recovering E2F1 expression and promoting the transcription of Nanog, an essential stemness factor (Lu et al., 2018). MALAT1 played an essential role in breast cancer development by targeting miR-124/CDK4/E2F1 signaling pathway (Feng et al., 2016). DANCR sequestered miR-34c-5p to aggravate E2F1 transcription, leading to enhanced malignant behaviors (Yan et al., 2024). Furthermore, E2F1 also activated DANCR transcription, forming an E2F1/DANCR/miR-34c-5p positive feedback loop (Yan et al., 2024), presenting novel approaches for tackling cancer progression.

Ensuring optimal therapeutic efficacy while minimizing adverse effects is essential for effective breast cancer treatment, aiming to maintain a high quality of life for patients (Xu X. et al., 2020). Drug resistance still presents a remarkable challenge for breast cancer, contributing to tumor recurrence and metastasis (Herzog and Fuqua, 2022). By using RNA-sequencing data derived from the TCGA database, Giro-Perafita, and his colleagues focused on RP11-19E11.1, a chromatin-associated lncRNA targeted by E2F1, which was essential for cell survival, cell cycle progression and associated with decreased sensitivity to enzastaurin of breast cancer cells (Giro-Perafita et al., 2020). AGPG was measured to be upregulated in endocrine-resistant breast cancer specimens and related to poor prognosis in ERα+ breast cancer patients (Yu et al., 2023). Mechanistically, AGPG physically activated E2F1 via interacting with PURα and blocking the binding of E2F1 to PURα, while AGPG inhibition significantly repressed tumor growth in the endocrine-resistant mouse model (Yu et al., 2023). Notably, nuclear lncRNA ERINA was directly transactivated by the ER binding site and aggravated cell cycle progression through interfering with the interaction between E2F1 and RB1, which remarkably promoted tamoxifen and palbociclib resistance, demonstrating that targeting lncRNAs holds great potential for combating endocrine-resistant tumors (Fang et al., 2020b) (Figure 4).

5.3 Hepatocellular carcinoma

HCC represents a significant public health challenge globally, being the most prevalent type of primary liver cancer (Vogel et al., 2022). Studies have shown that epigenetic changes are closely associated with HCC progression (Ganesan and Kulik, 2023). In recent years, researchers have taken an interest in exploring the functional role of lncRNAs in hepatocarcinogenesis (Ganesan and Kulik, 2023). Tao et al. (2023) revealed that upregulation of lncRNA CDKN2B-AS1 was observed in HCC samples. CDKN2B-AS1 exerted a pro-oncogenic role by interacting with E2F1 and exacerbating the transcription of G protein subunit alpha Z (GNAZ), thereby aggravating cell proliferation, and growth, and repressing cell apoptosis. LINC01089 was identified as a super-enhancer lncRNA that was induced by E2F1 (Su et al., 2023). Highly expressed LINC01089 acted as a promoter of HCC cell EMT and metastasis through binding to heterogeneous nuclear ribonucleoprotein M (hnRNPM), which undermined N6-methyladenosine (m6A)-mediated DIAPH3 mRNA stability and elicited ERK/Snail signaling pathway (Su et al., 2023). LINC01004 was another SE-lncRNA transcribed by E2F1, significantly exacerbating cell growth and metastasis, providing mechanistic perspectives on hepatocarcinogenesis and the HCC treatment (Li J. et al., 2023). Elevated KDM4A-AS1 expression mediated by E2F1 significantly stabilized Aurora kinase A (AURKA) mRNA via recruiting interleukin enhancer-binding factor 3 (ILF3), which provoked PI3K/AKT pathway and augmented tumorigenicity in HCC experimental models (Shen et al., 2023).

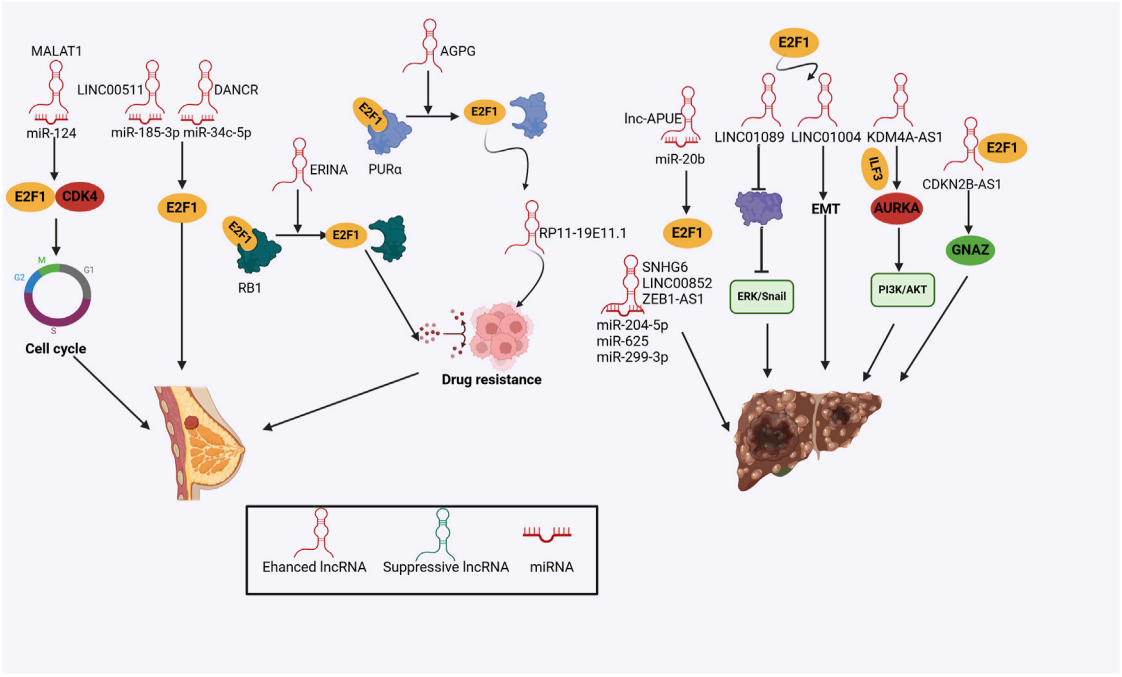


FIGURE 4
The mechanisms of the lncRNA/E2F1 crosstalk in breast cancer and hepatocellular carcinoma.

A bioinformatics study performed by Dong and Zhan (2022) has annotated several distinct lncRNA/miRNA/E2F1 regulatory loops in the tumor formation of HCC, although lacking experimental evidence. Li S. Y et al. (2021) annotated the oncogenic role of lncRNA accelerating proliferation by upregulating E2F1 (lnc-APUE) by loss-of-function analyses. Mechanistic evidence disclosed that lnc-APUE sequestered miR-20b and ameliorated the repression of E2F1 expression, facilitating cell cycle progression and cell proliferation. However, the upregulation of lnc-APUE could be antagonized by hepatocyte nuclear factor 4 alpha (HNF4α), while its downregulation supported HCC development (Li SY. et al., 2021). Additionally, SNHG6, LINC00852, and ZEB1-AS1 worked as the sponges for miR-204-5p, miR-625, and miR-299-3p respectively, relieving the suppression of E2F1 expression, leading to exacerbated G1-S phase transition, tumor growth and metastasis (Chen et al., 2021; Mu et al., 2021; Chen, 2022). These findings identified several distinct regulatory axes and represented appealing candidates for novel drug development of HCC.

Oxaliplatin is commonly utilized as a therapeutic option for advanced HCC, but chemotherapy resistance worsens clinical prognosis and provokes tumor recurrence (Liu S. et al., 2022). Current theoretical investigations have identified a novel SP1/DUBR/E2F1-miR-520d-5p/CIP2A regulatory axis and deciphered its molecular actions, that was, SP1-transcribed lncRNA DUBR recruited E2F1 and enhanced CIP2A expression in HCC, whereas DUBR also sequestered miR-520d-5p to stabilize CIP2A protein, which in turn enhanced the stability of E2F1 mRNA and elicited Notch1 signaling pathway, thus accelerating cancer stemness and promoted HCC cell resistance to oxaliplatin (Liu S. et al., 2022), supporting a novel molecular candidate for therapeutic intervention against oxaliplatin resistance and awaiting further verifications in the clinical setting (Figure 4).

5.4 Colorectal cancer

CRC is the third most commonly diagnosed cancer and ranks second in terms of mortality globally (Jiang et al., 2024). Previous studies have reported that lncRNA H19 was involved in CRC tumorigenicity, whereas Ohtsuka et al. underscored the H19-E2F1 cascade in CRC, that was, H19 activated E2F1 signaling pathway to promote cell proliferation and tumor growth (Ohtsuka et al., 2016). In line with this, NEAT1 was found to abrogate KDM5A expression via interacting with E2F1, which suppressed the KDM5A/H3K4me3-mediated repression of Cul4A expression, resulting in activated Wnt signaling pathway and augmented tumor formation (Shen et al., 2021). Notably, the PI3K/AKT pathway could also be regulated in CRC cell proliferation and migration by lncRNA LINC01703 via the miR-205-5p/E2F1 axis (Xu et al., 2024). CRNDE was recently recognized as a key regulator in the metastasis and oxaliplatin resistance of CRC by working as a ceRNA for miR-136 and indirectly targeting E2F1 (Gao et al., 2017). Radioresistance stands as a primary contributor to the failure of cancer treatment (Xiao et al., 2022). LncRNA DLGAP1-AS2 enhanced the radiotherapy resistance of rectal cancer cells by interacting with E2F1 to increase CD151 expression through activating the AKT/mTOR/cyclinD1 signaling pathway (Xiao et al., 2022). These findings deciphered the molecular mechanisms of lncRNA-E2F1 interplay in CRC and emphasized the clinical prospects of targeting lncRNAs or E2F1 (Figure 5A).

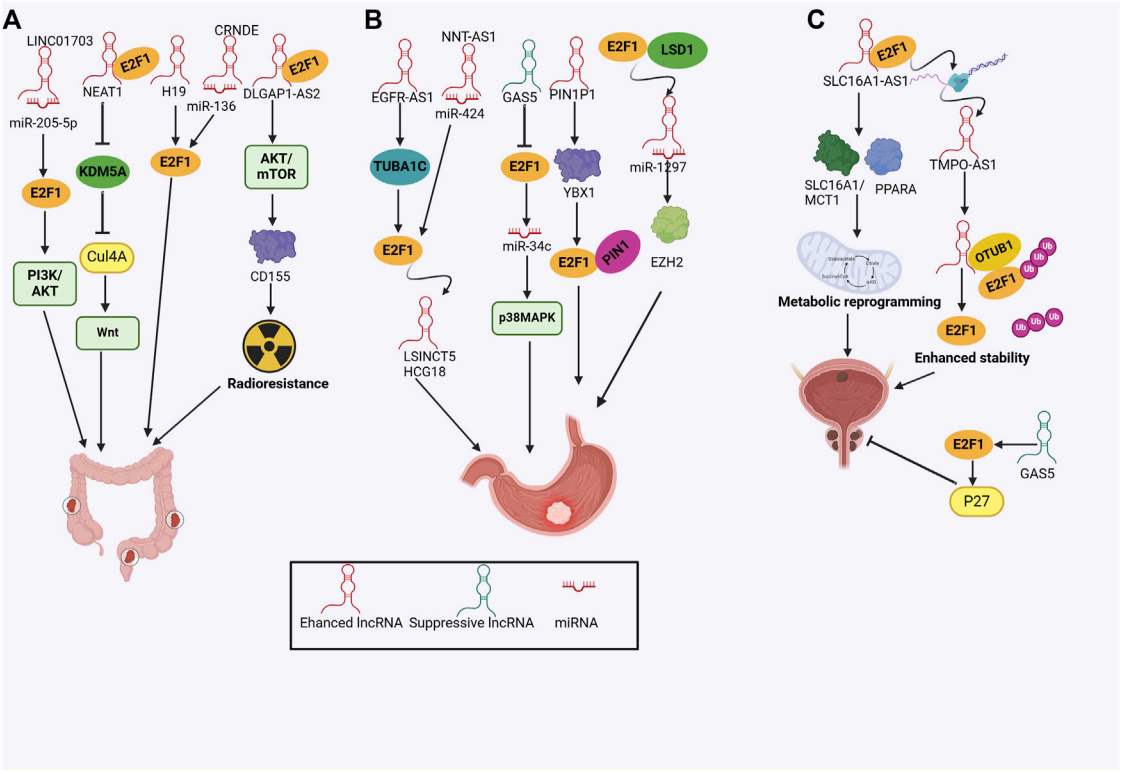


FIGURE 5
(A) The mechanisms of the lncRNA/E2F1 crosstalk in colorectal cancer; **(B)** The mechanisms of the lncRNA/E2F1 crosstalk in gastric cancer; **(C)** The mechanisms of the lncRNA/E2F1 crosstalk in prostate and bladder cancer.

5.5 Gastric cancer

GC is perceived as one of the most common gastrointestinal malignancies globally and poses a high burden on public health owing to hight morbidity and lethality (Smyth et al., 2020). By global transcriptomic analyses, Sun et al. (2023) reported that E2F1 was the essential TF in GC progression by interacting with a plethora of dysregulated lncRNAs and forming specific regulatory axes. Consistent evidence has also been annotated in the case of lncRNA EGFR-AS1/TUBA1C/E2F1 (Wang H. et al., 2023). Elevated EGFR-AS1 promoted GC growth and metastasis by targeting TUBA1C, which aggravated E2F1 expression and facilitated the G1 phase to the S phase transition (Wang H. et al., 2023). Moreover, lncRNA might sponge miRNA to rescue the E2F1 inhibition, thus promoting disease development. E2F1 functioned as the downstream target of the NNT-AS1/miR-424 axis, leading to enhanced tumorigenesis (Chen et al., 2018). GAS5 was perceived as a tumor suppressor that has been dysregulated in multiple cancers, including GC. In the preclinical evidence, GAS5 could directly disturb E2F1 expression, suppressing GC cell proliferation and growth (Sun et al., 2014). The GAS5-E2F1 interaction also modulated miR-34c expression, which led to the repressed p38MAPK signaling pathway (Gupta et al., 2022), fully elaborating on the molecular crosstalk of GAS5 in GC. In another mechanistic model, the CAMP response element binding protein (CREB1) activated lncRNA PIN1P1 transcription, which upregulated YBX1 expression, resulting in enhanced E2F1 and PIN1 expression, ultimately boosting GC tumorigenicity (Wang et al., 2024).

In the realm of GC models, E2F1 mediated the transcription of HOXA11-AS, which severed as a molecular scaffold by recruiting LSD1 and EZH2 (Sun et al., 2016). Additionally, HOXA11-AS also sponged miR-1297 to antagonize its inhibitory effects on the protein translation process of EZH2, establishing a mechanistic model comprising the crosstalk between E2F1/HOXA11-AS/miR-1297/EZH2 axis and LSD1/HOXA11-AS/EZH2 complex, which supported that HOXA11-AS and E2F1 severed as engaging therapeutic targets against the aggressive growth of GC (Sun et al., 2016). Similarly, E2F1 induced lncRNA LSINCT5 and HCG18 transcriptional activity, leading to increased expression of lncRNAs, which stimulated proliferation, growth, and EMT in GC (Qi et al., 2018; Niu et al., 2020) (Figure 5B).

5.6 Urinary tract tumors

As one of the most prevalent urinary tract tumors, the role of lncRNA in bladder cancer has not been fully deciphered. Logotheti and colleagues presented the holistic evidence that lncRNA SLC16A1-AS1 interacted with E2F1 to form an RNA-protein complex, enhancing the expression of SLC16A1/MCT1 and PPARA, which accelerated aerobic glycolysis and exacerbating fatty acid β-oxidation, favoring an invasive phenotype (Logotheti et al., 2020). Through functional assays, Zhang et al. (2021)

demonstrated that TMPO-AS1 fueled cell proliferation and aggressiveness of bladder cancer. Mechanistic evidence underscored the upregulation of TMPO-AS1 was attributed to the activity of E2F1. Additionally, TMPO-AS1 fueled the binding of E2F1 to OTU domain-containing ubiquitin aldehyde binding 1 (OTUB1), enhancing the deubiquitination and stability of E2F1, which unveiled a novel TMPO-AS1/E2F1/OTUB1 regulatory program (Zhang et al., 2021). In prostate cancer, GAS5 facilitated the transcription of $P27^{Kip1}$ by recruiting E2F1 to its promoter, repressing cell proliferation and growth (Luo et al., 2017) (Figure 5C).

6 E2F1-related lncRNAs in cancer immunotherapy

LncRNA genes represent a diverse group of genes with heterogeneous expression patterns, particularly evident in the context of cancer (Song et al., 2024). LncRNAs, previously thought to be non-coding, may indeed have the capability to encode biological peptides that are shorter than 100 amino acids, which are involved in the modulation of multiple malignant tumor phenotypes (Wu et al., 2020; Zhang et al., 2023). Additionally, lncRNA-derived peptides have been found to regulate immune response. It is worth noting that lncRNA-derived peptides are self-antigens, which should be obliterated during the development of organisms (Reinhard et al., 2020). Intriguingly, the immunogenic peptides showed a tendency towards upregulation in normal thymocytes, indicating that these peptides may evade central tolerance mechanisms in the thymus, such as clonal negative selection, owing to their low expression patterns, and instead, they might be affected by peripheral tolerance mechanisms (Reinhard et al., 2020). Cumulative evidence has reported immunization protocols that delivered lncRNA-derived peptides as a cancer vaccine into cancer models, generating a remarkable immune response against tumor progression (Zhang et al., 2023). By RNA sequencing analysis, Wojciech et al. unveiled that protein arginine methyltransferase (PRMT) 5 and E2F1 exerted striking effects on the expression of various human lncRNA genes including MALAT1, DANCR, TTC28-AS1, LINC00963, and LNCOC1 (Barczak et al., 2023). Notably, E2F1 was highly presented at the promoters of numerous lncRNA genes encoding peptides; approximately 44% of lncRNAs seemed to be targets of E2F1 (Barczak et al., 2023). These lncRNAs produced small peptides that interacted with ribosomes and underwent translation into polypeptides, which were subsequently processed, likely resulting in the generation of peptides that bound to the MHC class I complex (Barczak et al., 2023). Then, they designed two cancer vaccines (ChAdOx1-PepLnc and MVA-PepLnc) that were delivered to the immune system in mice either by loading onto dendritic cells *ex vivo* or by expression from a viral vector, which elicited a robust production of interferon (IFN) γ, reflecting the activated immune response of CD8 T lymphocytes along with significantly hindered tumor growth (Barczak et al., 2023). These findings underscore that E2F1-responsive lncRNAs-derived immunogenic peptides can bind to MHC class I complex and be engineered as cancer vaccines that trigger the CD8 T cell-mediated adaptive immune response, providing remarkably therapeutic benefits.

Programmed cell death ligand 1 (PD-L1) functions as a pivotal immune checkpoint commonly expressed in multiple types of human cancers, exerting a crucial role in immune evasion by repressing activated T lymphocytes via binding to PD-1 (Yi et al., 2022). Understanding the molecular mechanisms governing PD-L1 expression significantly promotes comprehension of the functions of the tumor immunosuppressive microenvironment and augmenting antitumor immune responses (Yi et al., 2022). In the experimental investigation performed by Lin et al. (2023) lncRNA HIF-1α inhibitor at translation level (HITT) was induced by E2F1 upon IFN-γ stimulation. HITT cooperated with the regulator of G protein signaling 2 (RGS2) to bind to the promoter of PD-L1, leading to decreased PD-L1 translation, which augmented T lymphocyte-mediated cytotoxicity and significantly impeded tumor growth in mouse models, emphasizing the activation of HITT as a promising therapeutic avenue to boost cancer immunotherapy (Lin et al., 2023). In line with this, Song and his colleagues expanded the regulatory associations of lncRNA/E2F1 in the immune response to HCC. It revealed that lncRNA CASC11 regulated by YY1 recruited EIF4A3 and stabilized E2F1, activating the NF-κB and PI3K/AKT/mTOR signaling pathway, which further enhanced PD-L1 expression, emphasizing that CASC11/E2F1 might promote HCC progression via PD-L1-mediated immune evasion (Song et al., 2020). One recent pan-cancer analysis has identified a novel lncRNA ribonucleotide reductase small subunit M2 (RRM2) that was overexpressed in thirty types of human cancers. Further mechanistic investigations identified that E2F1 regulated RRM2 expression, which impacted resistance to ICIs via the PI3K/AKT pathway (Wu et al., 2022). These studies provide preclinical evidence that targeting lncRNA functions as a potent avenue to enhance the responsiveness of ICIs.

7 Targeting lncRNAs as potent strategies for cancer therapy

Given the prominent roles of lncRNAs in driving cancer progression and their impact on the fundamental characteristics of nearly all malignancies, as well as their involvement in the immune response to tumors, multiple therapeutic strategies have been deployed to target lncRNAs and attenuate their oncogenic functions. So far, the disruption of lncRNA networks has been undertaken through several approaches. LncRNAs possess distinct characteristics from mRNAs and proteins, which enhance their potential as therapeutic targets against cancer.

7.1 RNA interference

RNA interference (RNAi) has traditionally served as the standard method for functional screening, contributing to the identification of notable cancer-associated lncRNAs such as MALAT1, LINC00152, and DGCR5 (Wang R. et al., 2017; Nötzold et al., 2017; Li Y. et al., 2023). RNAi applications include using chemically synthesized small interfering RNAs (siRNAs) or deploying short hairpin RNAs (shRNAs) delivered by lentiviral vectors (Gagnon et al., 2014; Booth et al., 2023). Numerous siRNAs have been assessed for their efficacy in silencing

lncRNAs within cancer cell lines. MALAT1, an oncogenic lncRNA implicated in cancer metastasis (Feng et al., 2016; Li GZ. et al., 2023), was silenced by a specific siRNA, resulting in reduced tumor growth and metastasis in prostate cancer (Wang R. et al., 2017). DANCR plays a crucial role in the development of multiple types of human cancers, while the invasion phenotype and growth of lung tumors were repressed by shRNA treatment (Yu J. E. et al., 2020). Despite acclimating evidence demonstrating the effective silencing of oncogenic lncRNAs, the functions of RNAi in targeting lncRNAs remain a controversial topic. Some researchers have indicated suboptimal performance, particularly for targets enriched in the nucleus, where many lncRNAs reside, may be attributed to diminished RNAi activity (Gagnon et al., 2014). Furthermore, *in vivo* studies of siRNAs have been challenging to conduct, likely due to the limited bioactivity of siRNAs in living organisms and difficulties in drug delivery (Dowdy, 2017).

7.2 Antisense oligonucleotides

Antisense oligonucleotides (ASOs) are short, single-stranded oligonucleotides consisting of 12–25 nucleotides, which undergo chemical modifications to degrade target RNAs through the action of ribonuclease H (RNAse H) that is an enzyme found ubiquitously to cleave RNAs (Booth et al., 2023). The subcutaneous administration of ASO targeting ITGB8-AS1 in CRC-bearing mice markedly delayed tumor growth and reduced the number of liver metastases (Lin et al., 2022). Moreover, utilizing ASO against hypoxia-induced lncRNA LUCAT1 promoted cell apoptosis and re-sensitized CRC cells to chemotherapeutic drugs, indicating a novel therapeutic target for chemotherapy-refractory hypoxic tumors (Huan et al., 2020). When deploying ASO treatments against oncogenic lncRNAs, it's essential to consider the distinct molecular actions inherent to lncRNAs.

Optimal candidates necessitate optimization for both great therapeutic efficiencies and less untoward effects. Due to their high repetitive contents, lncRNAs could be especially susceptible to off-target toxicities, as this enhances the chances of targeting ASOs containing partial complementarity to multiple off-target lncRNAs with the same repeat sequences (Shen et al., 2019). These instances can be prevented through meticulous experimental validation employing multiple, distinct ASO sequences.

Equally daunting is the task of identifying accessible and potent ASO target sites on the desired lncRNA, which may be obscured by secondary structures or molecular binding partners (Doxtader Lacy et al., 2022). Currently, there are limited publicly available methods for ASO prediction, and the majority of studies depend on costly and time-consuming ASO optimization, which entails synthesizing and testing numerous sequences *in vitro* (Ramasamy et al., 2022). Consequently, ASO prediction stands out as a promising area within RNA therapeutics that is highly conducive to innovation.

7.3 CRISPR–Cas9 system

Remarkable advancements in gene editing techniques, including CRISPR–Cas9, offer an innovative therapeutic approach against lncRNAs (Xie et al., 2015). The inactivated Cas9 is paired with transcriptional inhibitors and guided RNAs, guiding this fusion protein toward the targets to trigger silencing (Xie et al., 2015). In this regard, CRISPR/Cas9-mediated silencing of LINC00511, significantly enhanced cell apoptosis by downregulating the expression of anti-apoptotic genes in breast cancer (Azadbakht et al., 2022). Under hypoxic conditions, LUCAT1 was induced by HIF1α in glioma stem-like cells. Functionally, LUCAT1 directly targeted HIF1α, facilitating tumor growth, which could be reversed by CRISPR–Cas9-mediated depletion of LUCAT1 (Huang H. et al., 2024).

It is worth noting that the artificial intelligence technique has reached a point where it can provide predictions and identifications of the single guide RNAs (sgRNAs) within the CRISPR-Cas9 platform, which may provide fresh perspectives on anti-cancer drug development and cancer therapy (Chan et al., 2022). Although CRISPR-Cas9-based gene editing exhibits high efficiency, its broad adoption in clinical studies is hindered by the unforeseen off-target effects (Kozovska et al., 2021; Vicente et al., 2021). Feasible approaches aimed at mitigating undesired editing involve the targeted delivery of the CRISPR system and chemical modification of Cas9, which partially prevent the adverse events of the clinical application (Vicente et al., 2021; Chan et al., 2022). More technological innovations are required to balance the potency and safety of this technology, such efforts ultimately effectively treating cancers.

7.4 Current clinical course on lncRNA-mediated therapy strategies

Following the approval by the FDA, the first RNA-based drug was Macugen, a siRNA medication authorized for the treatment of macular degeneration (Nagpal et al., 2007; Starita et al., 2007). Following this milestone, different ASO therapies are currently under clinical trials for conditions like cystic fibrosis (Allaire et al., 2023) and retinitis pigmentosa (Schellens et al., 2023). Another type of RNA therapy includes mRNA, which can be utilized to lower protein levels using Cas9 cleavage methods, or to correct protein mutations at the DNA level through base editing (Gillmore et al., 2021).

While several miRNA mimics and anti-miRNA-based RNA therapies are advancing through phases II or III of clinical development (Ma et al., 2023; Traber and Yu, 2023), treatments utilizing lncRNAs have not yet been integrated into clinical practice. However, promising progress in fields such as molecular biology, immunology, pharmacology, and nanotechnology suggests the potential future adoption of these therapies (Winkle et al., 2021; Entezari et al., 2022). Targeting lncRNAs and their associated RNA-binding proteins in medical treatments is a critical goal for the scientific and medical communities, requiring significant efforts to enhance prospects for patients (Yao et al., 2022). Concerns may arise regarding the importance and consequences of these interactions in comparison to protein-protein, mRNA-protein, and miRNA-protein interactions (Shaath et al., 2022).

Developing strategies to shield therapeutic molecules, allowing for immune evasion and effective uptake, could greatly enhance the efficacy and longevity of administered treatments (Sparmann and Vogel, 2023). Cutting-edge methods, such as administering anti-miRNAs through ultrasound and microbubble-targeted systems for cardiovascular conditions, offer promising opportunities for

advancing efficient and feasible RNA-based therapeutics (Pham et al., 2020). The specific therapeutic benefits of lncRNAs are still being uncovered, and in-depth research using experimental and machine learning-based approaches to better understand these interactions will pave the way for the utilization of lncRNA-based treatments in the fight against cancer (Mehmandar-Oskuie et al., 2024; Nemeth et al., 2024).

8 Current knowledge for targeting E2F1 in cancer therapy

As discussed above, E2F1 impacts malignant behaviors in various types of human cancers, thus it serves as a candidate for anti-cancer treatment. Multiple peptides were deployed to hinder the DNA-binding ability of E2Fs, exhibiting efficacies in curtailing cell proliferation and tumor growth. A small peptide containing seven-amino acid that were identified by Xie et al. (2013). This peptide, when conjugated with penetratin (PEP), elicited cellular uptake and has been demonstrated to bind to the E2F1 promoter to abrogate its transcription and downregulated E2F-responsive enzymes, leading to notable cytotoxicities in cell lines of lung cancer and prostate cancer (Xie et al., 2013; Xie et al., 2014). Additionally, PEP encapsulation within PEGylated liposomes improved its stability *in vivo* in xenograft models, thereby effectively suppressing tumor growth (Xie et al., 2013). Subsequent studies by Shaik and his colleagues confirmed the efficacy of a functional structure, D-Arg penetratin peptide (D-Arg PEP), as a transcriptional inhibitor of E2F1 (Shaik et al., 2018). This novel compound has demonstrated comparable stability and heightened efficacy for eliminating lung cancer and prostate cancer cells, positioning it as a potent candidate for developing targeted therapy against E2F1-induced tumors (Shaik et al., 2018).

Fungi serve as a rich reservoir of pharmaceutical compounds, including those with anti-tumor properties (Han et al., 2022). Among them, the anti-tumor function of Neurospora crassa has been evaluated in breast cancer models (Han et al., 2022). The Neurospora crassa mixture markedly blocked E2F1 transcription and downregulated lncRNA HOTAIR, thus exhibiting the anti-tumor impacts on cancer invasiveness and growth *in vivo*, while it had less effects on normal mammary cells (Han et al., 2022). Notably, Actinidia chinensis Planch Root extracts (acRoots), bioactive components derived from Chinese medicine, have been shown to suppress cancer cell proliferation, invasion, and metastasis (Wang et al., 2020; Gan et al., 2021). In the setting of hypopharyngeal carcinoma, administration of acRoots repressed tumor growth through decreasing E2F1 expression and inhibiting lncRNA MNX1-AS1 activity (Zheng et al., 2022), which holds immense potential for medical interventions treating E2F1 dysregulated cancers, although more holistic evidence should be presented in the clinical settings.

9 Challenges in targeting lncRNA in cancer therapy

Cancer stands as the primary cause of mortality worldwide, commonly diagnosed in advanced stages due to mild symptoms and lacking reliable biomarkers (Zhan et al., 2017). Among the extensively studied genes in the realm of carcinogenesis, E2F1 emerges as a crucial regulator, which functions as an oncogenic TF to provoke tumorigenesis by inducing cell cycle progression and inhibiting apoptosis through modulating target genes (Fang et al., 2020a; Chun et al., 2020).

E2F1 represents a central node interconnected with various signaling pathways implicated in human cancers (Fang et al., 2020a). Emerging evidence has demonstrated that lncRNAs contribute to E2F1 pathway regulation and play multifaceted roles in the disease progression in diverse tumor types (Song et al., 2022; Shen et al., 2023; Zhang and Shi, 2023). By influencing cellular processes like cell proliferation and metastasis in cancer, lncRNAs become integral components of the E2F1 regulatory networks. Moreover, the dysregulated lncRNAs hint at their potential applications in cancer therapy.

Despite considerable advancements in recent years, lncRNA-based gene therapy still faces several challenges (Figure 6). 1) Numerous unidentified lncRNAs remain to be discovered and characterized. Despite the establishment of several databases for predicting potential functions and investigating mechanistic modes of lncRNAs, the number of lncRNAs cataloged in these databases remains limited (Iwakiri et al., 2016; Yan J. et al., 2023). Additionally, a myriad of lncRNAs newly detected through high-throughput sequencing technology await to be annotated. Consequently, there is a pressing need to develop a high-coverage database and integrate it into emerging sequencing techniques to decipher the role of tumor-specific lncRNAs. 2) The sluggish pace of preclinical and clinical development. LncRNAs are functional molecules with limited evolutionary conservation, which presents a challenge in evaluating off-target toxicities and therapeutic efficacies in experimental models. To address the cost and time delays associated with poor-quality targets, one strategy is to anchor structural conservation for orthologue identification. While these orthologues can not share the same sequences, they demonstrate similarity in their 3D structures (Seemann et al., 2017). Additionally, advancements in human organoids, offer opportunities to boost clinical development in the realm of lncRNA research (Diermeier and Spector, 2017). 3) An effective lncRNA delivery system is required for effective cancer treatment. Researchers have explored various biological materials to facilitate the delivery of lncRNAs. Exosomes, a subset of cell-derived extracellular vesicles (EVs), have shown excellent biocompatibility for cellular uptake (Kalluri and LeBleu, 2020). Their membrane can be engineered, and their small size makes them promising carriers for delivering lncRNAs (Kalluri and LeBleu, 2020). However, the high cost associated with exosome purification and membrane engineering technologies poses challenges for mass production (Liang et al., 2021). Further research into various types of nanoparticles could significantly reduce the costs associated with lncRNA-based drug development. Lipid nanoparticles (LNPs), widely used as gene therapy carriers in clinical trials, have demonstrated success in delivering ASOs for targeting mRNAs (Kon et al., 2023). The emergence of mRNA-contained LNP vaccines during the COVID-19 pandemic underscores the potential advantages of utilizing LNPs for drug delivery (Wilson and Geetha, 2022). Considering the structural similarities between lncRNAs and mRNAs, it is conceivable that lncRNA-contained LNP drugs could become feasible and provide clinical benefits.

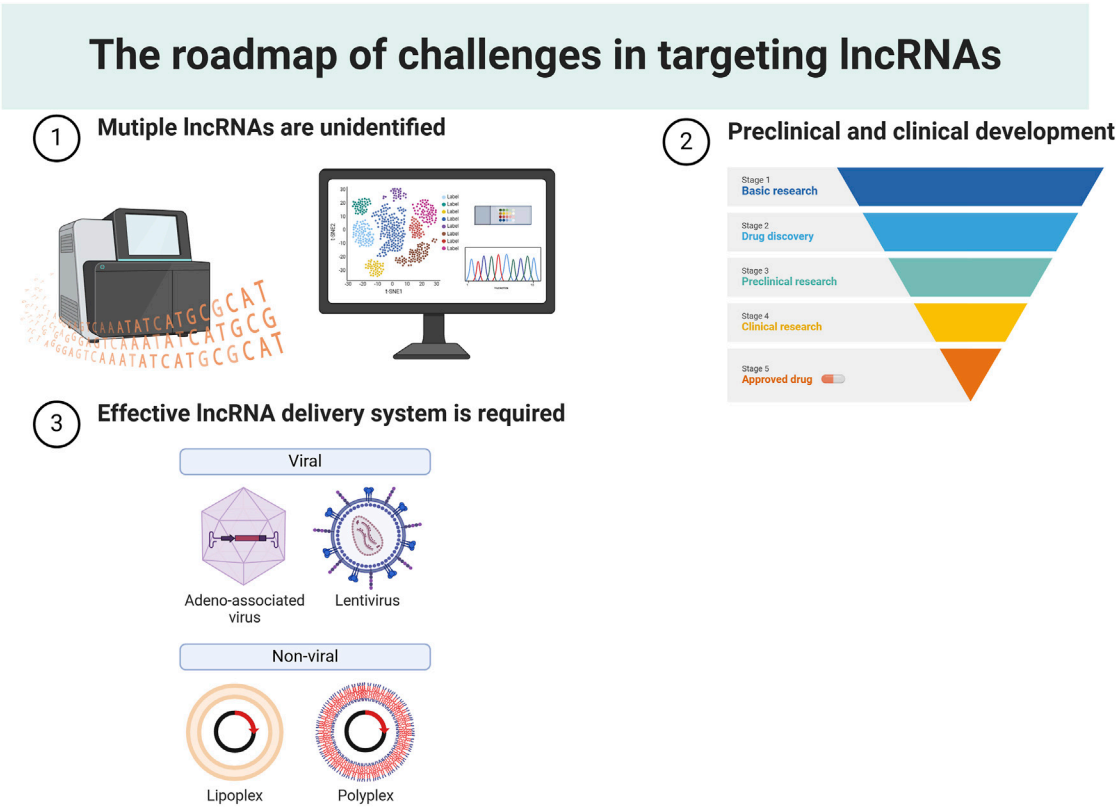


FIGURE 6
The roadmap of challenges in targeting lncRNAs.

While the progression of Andes-1537 into phase 1 clinical trials is promising, the clinical applications of lncRNA-based drugs are largely unexplored, akin to the tip of an iceberg. As a nascent field, lncRNAs hold promising potential in tumor research, offering novel avenues and opportunities for efficiently treating cancers and ultimately eliminating tumors.

10 Conclusion

Throughout this review, we have emphasized the critical role of lncRNAs and E2F1 in oncogenesis and the progression of various cancer types by regulating diverse cellular processes and signaling networks. LncRNAs, which have recently been identified as a subset of non-coding RNAs, have attracted considerable attention due to their potential to advance the development of next-generation RNA therapeutics. Their specificity, low toxicity, and ability to interact with other regulatory molecules make them advantageous for targeting complex pathways involved in diseases, particularly cancer. By delving into the interactions between E2F1 and lncRNAs, researchers may uncover the molecular mechanisms underlying malignant transformation and disease advancement, potentially leading to innovative therapeutic approaches for treating cancer. But the potential manipulation of these interactions as a therapeutic strategy for cancer awaits validation through animal models and human clinical trials.

Author contributions

PH: Conceptualization, Data curation, Formal Analysis, Methodology, Project administration, Resources, Writing–original draft, Writing–review and editing. FW: Conceptualization, Funding acquisition, Methodology, Project administration, Visualization, Writing–original draft. QL: Funding acquisition, Supervision, Validation, Visualization, Writing–review and editing.

Funding

The author(s) declare that financial support was received for the research, authorship, and/or publication of this article. This research was supported by Science and Technology Department of Sichuan Province Funding Project (2022YFSY0027) and Science and Technology Department of Sichuan Province Funding Project (2022NSFSC1564).

Acknowledgments

We thank the BioRender drawing software (https://www.biorender.com/).

Conflict of interest

The authors declare that the research was conducted in the absence of any commercial or financial relationships that could be construed as a potential conflict of interest.

Publisher's note

All claims expressed in this article are solely those of the authors and do not necessarily represent those of their affiliated organizations, or those of the publisher, the editors and the reviewers. Any product that may be evaluated in this article, or claim that may be made by its manufacturer, is not guaranteed or endorsed by the publisher.

References

Ahmad, A., Rashid, S., Chaudhary, A. A., Alawam, A. S., Alghonaim, M. I., Raza, S. S., et al. (2023). Nanomedicine as potential cancer therapy via targeting dysregulated transcription factors. *Semin. Cancer Biol.* 89, 38–60. doi:10.1016/j.semcancer.2023.01.002

Allaire, N. E., Griesenbach, U., Kerem, B., Lueck, J. D., Stanleigh, N., and Oren, Y. S. (2023). Gene, RNA, and ASO-based therapeutic approaches in cystic fibrosis. *J. Cyst. Fibros.* 22 (Suppl. 1), S39–s44. doi:10.1016/j.jcf.2022.12.016

Azadbakht, N., Doosti, A., and Jami, M. S. (2022). CRISPR/Cas9-mediated LINC00511 knockout strategies, increased apoptosis of breast cancer cells via suppressing antiapoptotic genes. *Biol. Proced. Online* 24 (1), 8. doi:10.1186/s12575-022-00171-1

Barczak, W., Carr, S. M., Liu, G., Munro, S., Nicastri, A., Lee, L. N., et al. (2023). Long non-coding RNA-derived peptides are immunogenic and drive a potent anti-tumour response. *Nat. Commun.* 14 (1), 1078. doi:10.1038/s41467-023-36826-0

Booth, B. J., Nourreddine, S., Katrekar, D., Savva, Y., Bose, D., Long, T. J., et al. (2023). RNA editing: expanding the potential of RNA therapeutics. *Mol. Ther.* 31 (6), 1533–1549. doi:10.1016/j.ymthe.2023.01.005

Bridges, M. C., Daulagala, A. C., and Kourtidis, A. (2021). LNCcation: lncRNA localization and function. *J. Cell Biol.* 220 (2), e202009045. doi:10.1083/jcb.202009045

Bushweller, J. H. (2019). Targeting transcription factors in cancer - from undruggable to reality. *Nat. Rev. Cancer* 19 (11), 611–624. doi:10.1038/s41568-019-0196-7

Cao, M., Tang, Y., Luo, Y., Gu, F., Zhu, Y., Liu, X., et al. (2024). Natural compounds modulating mitophagy: implications for cancer therapy. *Cancer Lett.* 582, 216590. doi:10.1016/j.canlet.2023.216590

Chan, Y. T., Lu, Y., Wu, J., Zhang, C., Tan, H. Y., Bian, Z. X., et al. (2022). CRISPR-Cas9 library screening approach for anti-cancer drug discovery: overview and perspectives. *Theranostics* 12 (7), 3329–3344. doi:10.7150/thno.71144

Chan, Y. T., Wu, J., Lu, Y., Li, Q., Feng, Z., Xu, L., et al. (2024). Loss of lncRNA LINC01056 leads to sorafenib resistance in HCC. *Mol. Cancer* 23 (1), 74. doi:10.1186/s12943-024-01988-y

Chen, B., Zhao, Q., Guan, L., Lv, H., Bie, L., Huang, J., et al. (2018). Long non-coding RNA NNT-AS1 sponges miR-424/E2F1 to promote the tumorigenesis and cell cycle progression of gastric cancer. *J. Cell Mol. Med.* 22 (10), 4751–4759. doi:10.1111/jcmm.13726

Chen, K., Hou, Y., Liao, R., Yang, H., and Gong, J. (2021). LncRNA SNHG6 promotes G1/S-phase transition in hepatocellular carcinoma by impairing miR-204-5p-mediated inhibition of E2F1. *Oncogene* 40 (18), 3217–3230. doi:10.1038/s41388-021-01671-2

Chen, Q., Guo, S. M., Huang, H. Q., Huang, G. P., Li, Y., Li, Z. H., et al. (2020). Long noncoding RNA SBF2-AS1 contributes to the growth and metastatic phenotypes of NSCLC via regulating miR-338-3p/ADAM17 axis. *Aging (Albany NY)* 12 (18), 17902–17920. doi:10.18632/aging.103332

Chen, R., Xia, W., Wang, S., Xu, Y., Ma, Z., Xu, W., et al. (2019). Long noncoding RNA SBF2-AS1 is critical for tumorigenesis of early-stage lung adenocarcinoma. *Mol. Ther. Nucleic Acids* 16, 543–553. doi:10.1016/j.omtn.2019.04.004

Chen, S. (2022). LINC00852 regulates cell proliferation, invasion, migration and apoptosis in hepatocellular carcinoma via the miR-625/E2F1 Axis. *Cell Mol. Bioeng.* 15 (2), 207–217. doi:10.1007/s12195-021-00714-8

Chun, J. N., Cho, M., Park, S., So, I., and Jeon, J. H. (2020). The conflicting role of E2F1 in prostate cancer: a matter of cell context or interpretational flexibility? *Biochim. Biophys. Acta Rev. Cancer* 1873 (1), 188336. doi:10.1016/j.bbcan.2019.188336

Denechaud, P. D., Fajas, L., and Giralt, A. (2017). E2F1, a novel regulator of metabolism. *Front. Endocrinol. (Lausanne)* 8, 311. doi:10.3389/fendo.2017.00311

Diermeier, S. D., and Spector, D. L. (2017). Antisense oligonucleotide-mediated knockdown in mammary tumor organoids. *Bio Protoc.* 7 (16), e2511. doi:10.21769/BioProtoc.2511

Dong, W., and Zhan, C. (2022). Bioinformatic-based mechanism identification of E2F1-related ceRNA and E2F1 immunoassays in hepatocellular carcinoma. *J. Gastrointest. Oncol.* 13 (4), 1915–1926. doi:10.21037/jgo-22-674

Doostmohammadi, A., Jooya, H., Ghorbanian, K., Gohari, S., and Dadashpour, M. (2024). Potentials and future perspectives of multi-target drugs in cancer treatment: the next generation anti-cancer agents. *Cell Commun. Signal* 22 (1), 228. doi:10.1186/s12964-024-01607-9

Dowdy, S. F. (2017). Overcoming cellular barriers for RNA therapeutics. *Nat. Biotechnol.* 35 (3), 222–229. doi:10.1038/nbt.3802

Doxtader Lacy, K. A., Liang, X. H., Zhang, L., and Crooke, S. T. (2022). RNA modifications can affect RNase H1-mediated PS-ASO activity. *Mol. Ther. Nucleic Acids* 28, 814–828. doi:10.1016/j.omtn.2022.05.024

Duan, Y., Yan, Y., Fu, H., Dong, Y., Li, K., Ye, Z., et al. (2024). SNHG15-mediated feedback loop interplays with HNRNPA1/SLC7A11/GPX4 pathway to promote gastric cancer progression. *Cancer Sci.* doi:10.1111/cas.16181

Entezari, M., Taheriazam, A., Orouei, S., Fallah, S., Sanaei, A., Hejazi, E. S., et al. (2022). LncRNA-miRNA axis in tumor progression and therapy response: an emphasis on molecular interactions and therapeutic interventions. *Biomed. Pharmacother.* 154, 113609. doi:10.1016/j.biopha.2022.113609

Ertosun, M. G., Hapil, F. Z., and Osman Nidai, O. (2016). E2F1 transcription factor and its impact on growth factor and cytokine signaling. *Cytokine Growth Factor Rev.* 31, 17–25. doi:10.1016/j.cytogfr.2016.02.001

Fang, Z., Lin, M., Li, C., Liu, H., and Gong, C. (2020a). A comprehensive review of the roles of E2F1 in colon cancer. *Am. J. Cancer Res.* 10 (3), 757–768.

Fang, Z., Wang, Y., Wang, Z., Xu, M., Ren, S., Yang, D., et al. (2020b). ERINA is an estrogen-responsive LncRNA that drives breast cancer through the E2F1/RB1 pathway. *Cancer Res.* 80 (20), 4399–4413. doi:10.1158/0008-5472.Can-20-1031

Feng, T., Shao, F., Wu, Q., Zhang, X., Xu, D., Qian, K., et al. (2016). miR-124 downregulation leads to breast cancer progression via LncRNA-MALAT1 regulation and CDK4/E2F1 signal activation. *Oncotarget* 7 (13), 16205–16216. doi:10.18632/oncotarget.7578

Fouad, S., Hauton, D., and D'Angiolella, V. (2020). E2F1: cause and consequence of DNA replication stress. *Front. Mol. Biosci.* 7, 599332. doi:10.3389/fmolb.2020.599332

Gagnon, K. T., Li, L., Chu, Y., Janowski, B. A., and Corey, D. R. (2014). RNAi factors are present and active in human cell nuclei. *Cell Rep.* 6 (1), 211–221. doi:10.1016/j.celrep.2013.12.013

Galluzzi, L., Guilbaud, E., Schmidt, D., Kroemer, G., and Marincola, F. M. (2024). Targeting immunogenic cell stress and death for cancer therapy. *Nat. Rev. Drug Discov.* 23, 445–460. doi:10.1038/s41573-024-00920-9

Gan, C., Jin, Z., Wei, X., and Jin, M. (2021). Actinidia chinensis Planch. root extract inhibits the proliferation, migration and invasion of breast cancer cells via the AKT/GSK-3β signaling pathway. *Folia Histochem Cytobiol.* 59 (4), 226–235. doi:10.5603/FHC.a2021.0023

Ganesan, P., and Kulik, L. M. (2023). Hepatocellular carcinoma: new developments. *Clin. Liver Dis.* 27 (1), 85–102. doi:10.1016/j.cld.2022.08.004

Gao, F. Y., Li, X. T., Xu, K., Wang, R. T., and Guan, X. X. (2023). c-MYC mediates the crosstalk between breast cancer cells and tumor microenvironment. *Cell Commun. Signal* 21 (1), 28. doi:10.1186/s12964-023-01043-1

Gao, H., Song, X., Kang, T., Yan, B., Feng, L., Gao, L., et al. (2017). Long noncoding RNA CRNDE functions as a competing endogenous RNA to promote metastasis and oxaliplatin resistance by sponging miR-136 in colorectal cancer. *Onco Targets Ther.* 10, 205–216. doi:10.2147/ott.S116178

Gao, Z., Shi, R., Yuan, K., and Wang, Y. (2016). Expression and prognostic value of E2F activators in NSCLC and subtypes: a research based on bioinformatics analysis. *Tumour Biol.* 37 (11), 14979–14987. doi:10.1007/s13277-016-5389-z

Gillmore, J. D., Gane, E., Taubel, J., Kao, J., Fontana, M., Maitland, M. L., et al. (2021). CRISPR-Cas9 *in vivo* gene editing for transthyretin amyloidosis. *N. Engl. J. Med.* 385 (6), 493–502. doi:10.1056/NEJMoa2107454

Giro-Perafita, A., Luo, L., Khodadadi-Jamayran, A., Thompson, M., Akgol Oksuz, B., Tsirigos, A., et al. (2020). LncRNA RP11-19E11 is an E2F1 target required for proliferation and survival of basal breast cancer. *NPJ Breast Cancer* 6, 1. doi:10.1038/s41523-019-0144-4

Gobbi, G., Grieco, A., Torricelli, F., Sauta, E., Santandrea, G., Zanetti, E., et al. (2023). The long non-coding RNA TAZ-AS202 promotes lung cancer progression via regulation of the E2F1 transcription factor and activation of Ephrin signaling. *Cell Death Dis.* 14 (11), 752. doi:10.1038/s41419-023-06277-y

Gong, Y., and Li, H. (2024). CDK7 in breast cancer: mechanisms of action and therapeutic potential. *Cell Commun. Signal* 22 (1), 226. doi:10.1186/s12964-024-01577-y

Gupta, S., Panda, P. K., Luo, W., Hashimoto, R. F., and Ahuja, R. (2022). Network analysis reveals that the tumor suppressor lncRNA GAS5 acts as a double-edged sword in response to DNA damage in gastric cancer. *Sci. Rep.* 12 (1), 18312. doi:10.1038/s41598-022-21492-x

Han, R., Yang, H., Ling, C., and Lu, L. (2022). Neurospora crassa is a potential source of anti-cancer agents against breast cancer. *Breast Cancer* 29 (6), 1032–1041. doi:10.1007/s12282-022-01383-9

Hashemi, M., Moosavi, M. S., Abed, H. M., Dehghani, M., Aalipour, M., Heydari, E. A., et al. (2022). Long non-coding RNA (lncRNA) H19 in human cancer: from proliferation and metastasis to therapy. *Pharmacol. Res.* 184, 106418. doi:10.1016/j.phrs.2022.106418

Herzog, S. K., and Fuqua, S. A. W. (2022). ESR1 mutations and therapeutic resistance in metastatic breast cancer: progress and remaining challenges. *Br. J. Cancer* 126 (2), 174–186. doi:10.1038/s41416-021-01564-x

Hu, Z., Zhu, L., Zhang, Y., and Chen, B. (2022). N6-methyladenosine-induced SVIL antisense RNA 1 restrains lung adenocarcinoma cell proliferation by destabilizing E2F1. *Bioengineered* 13 (2), 3093–3107. doi:10.1080/21655979.2022.2025697

Huan, L., Guo, T., Wu, Y., Xu, L., Huang, S., Xu, Y., et al. (2020). Hypoxia induced LUCAT1/PTBP1 axis modulates cancer cell viability and chemotherapy response. *Mol. Cancer* 19 (1), 11. doi:10.1186/s12943-019-1122-z

Huang, H., Shah, H., Hao, J., Lin, J., Prayson, R. A., Xie, L., et al. (2024b). LncRNA LUCAT1 promotes glioblastoma progression by enhancing HIF1α activity. *Neuro Oncol.*, noae036. doi:10.1093/neuonc/noae036

Huang, P., Wen, F., Li, Y., and Li, Q. (2024a). The tale of SOX2: focusing on lncRNA regulation in cancer progression and therapy. *Life Sci.* 344, 122576. doi:10.1016/j.lfs.2024.122576

Iwakiri, J., Hamada, M., and Asai, K. (2016). Bioinformatics tools for lncRNA research. *Biochim. Biophys. Acta* 1859 (1), 23–30. doi:10.1016/j.bbagrm.2015.07.014

Jiang, C., Zhou, Q., Yi, K., Yuan, Y., and Xie, X. (2024). Colorectal cancer initiation: understanding early-stage disease for intervention. *Cancer Lett.* 589, 216831. doi:10.1016/j.canlet.2024.216831

Jing, Z., Liu, Q., He, X., Jia, Z., Xu, Z., Yang, B., et al. (2022). NCAPD3 enhances Warburg effect through c-myc and E2F1 and promotes the occurrence and progression of colorectal cancer. *J. Exp. Clin. Cancer Res.* 41 (1), 198. doi:10.1186/s13046-022-02412-3

Ju, Y., Fang, S., Liu, L., Ma, H., and Zheng, L. (2024). The function of the ELF3 gene and its mechanism in cancers. *Life Sci.* 346, 122637. doi:10.1016/j.lfs.2024.122637

Kalluri, R., and LeBleu, V. S. (2020). The biology, function, and biomedical applications of exosomes. *Science* 367 (6478), eaau6977. doi:10.1126/science.aau6977

Kant, R., Manne, R. K., Anas, M., Penugurti, V., Chen, T., Pan, B. S., et al. (2022). Deregulated transcription factors in cancer cell metabolisms and reprogramming. *Semin. Cancer Biol.* 86 (Pt 3), 1158–1174. doi:10.1016/j.semcancer.2022.10.001

Kassab, A., Gupta, I., and Moustafa, A. A. (2023). Role of E2F transcription factor in oral cancer: recent insight and advancements. *Semin. Cancer Biol.* 92, 28–41. doi:10.1016/j.semcancer.2023.03.004

Kent, L. N., and Leone, G. (2019). The broken cycle: E2F dysfunction in cancer. *Nat. Rev. Cancer* 19 (6), 326–338. doi:10.1038/s41568-019-0143-7

Khan, M. M., Yalamarty, S. S. K., Rajmalani, B. A., Filipczak, N., and Torchilin, V. P. (2024). Recent strategies to overcome breast cancer resistance. *Crit. Rev. Oncol. Hematol.* 197, 104351. doi:10.1016/j.critrevonc.2024.104351

Kielbik, M., Przygodzka, P., Szulc-Kielbik, I., and Klink, M. (2023). Snail transcription factors as key regulators of chemoresistance, stemness and metastasis of ovarian cancer cells. *Biochim. Biophys. Acta Rev. Cancer* 1878 (6), 189003. doi:10.1016/j.bbcan.2023.189003

Kon, E., Ad-El, N., Hazan-Halevy, I., Stotsky-Oterin, L., and Peer, D. (2023). Targeting cancer with mRNA-lipid nanoparticles: key considerations and future prospects. *Nat. Rev. Clin. Oncol.* 20 (11), 739–754. doi:10.1038/s41571-023-00811-9

Kozovska, Z., Rajcaniova, S., Munteanu, P., Dzacovska, S., and Demkova, L. (2021). CRISPR: history and perspectives to the future. *Biomed. Pharmacother.* 141, 111917. doi:10.1016/j.biopha.2021.111917

Li, G. Z., Meng, G. X., Pan, G. Q., Zhang, X., Yan, L. J., Li, R. Z., et al. (2023b). MALAT1/mir-1-3p mediated BRF2 expression promotes HCC progression via inhibiting the LKB1/AMPK signaling pathway. *Cancer Cell Int.* 23 (1), 188. doi:10.1186/s12935-023-03034-1

Li, H., Chen, Y. K., Wan, Q., Shi, A. Q., Wang, M., He, P., et al. (2021a). Long non-coding RNA LINC00847 induced by E2F1 accelerates non-small cell lung cancer progression through targeting miR-147a/IFITM1 Axis. *Front. Med. (Lausanne)* 8, 663558. doi:10.3389/fmed.2021.663558

Li, J., Wang, J., Wang, Y., Zhao, X., and Su, T. (2023c). E2F1 combined with LINC01004 super-enhancer to promote hepatocellular carcinoma cell proliferation and metastasis. *Clin. Epigenetics* 15 (1), 17. doi:10.1186/s13148-023-01428-6

Li, S. Y., Zhu, Y., Li, R. N., Huang, J. H., You, K., Yuan, Y. F., et al. (2021b). LncRNA lnc-APUE is repressed by HNF4α and promotes G1/S phase transition and tumor growth by regulating MiR-20b/E2F1 Axis. *Adv. Sci. (Weinh)* 8 (7), 2003094. doi:10.1002/advs.202003094

Li, Y., Azmi, A. S., and Mohammad, R. M. (2022). Deregulated transcription factors and poor clinical outcomes in cancer patients. *Semin. Cancer Biol.* 86 (Pt 3), 122–134. doi:10.1016/j.semcancer.2022.08.001

Li, Y., Chen, B., Jiang, X., Wang, X., Huang, S., Wu, X, et al. (2023d). A Wnt-induced lncRNA-DGCR5 splicing switch drives tumor-promoting inflammation in esophageal squamous cell carcinoma. *Cell Rep.* 42 (6), 112542. doi:10.1016/j.celrep.2023.112542

Li, Y. J., Zhang, C., Martincuks, A., Herrmann, A., and Yu, H. (2023a). STAT proteins in cancer: orchestration of metabolism. *Nat. Rev. Cancer* 23 (3), 115–134. doi:10.1038/s41568-022-00537-3

Liang, Y., Duan, L., Lu, J., and Xia, J. (2021). Engineering exosomes for targeted drug delivery. *Theranostics* 11 (7), 3183–3195. doi:10.7150/thno.52570

Lin, Q., Liu, T., Wang, X., Hou, G., Xiang, Z., Zhang, W., et al. (2023). Long noncoding RNA HITT coordinates with RGS2 to inhibit PD-L1 translation in T cell immunity. *J. Clin. Invest.* 133 (11), e162951. doi:10.1172/jci162951

Lin, X., Zhuang, S., Chen, X., Du, J., Zhong, L., Ding, J., et al. (2022). lncRNA ITGB8-AS1 functions as a ceRNA to promote colorectal cancer growth and migration through integrin-mediated focal adhesion signaling. *Mol. Ther.* 30 (2), 688–702. doi:10.1016/j.ymthe.2021.08.011

Liu, C., Shen, A., Song, J., Cheng, L., Zhang, M., Wang, Y., et al. (2024). LncRNA-CCAT5-mediated crosstalk between Wnt/β-Catenin and STAT3 signaling suggests novel therapeutic approaches for metastatic gastric cancer with high Wnt activity. *Cancer Commun. (Lond)* 44 (1), 76–100. doi:10.1002/cac2.12507

Liu, S., Bu, X., Kan, A., Luo, L., Xu, Y., Chen, H., et al. (2022b). SP1-induced lncRNA DUBR promotes stemness and oxaliplatin resistance of hepatocellular carcinoma via E2F1-CIP2A feedback. *Cancer Lett.* 528, 16–30. doi:10.1016/j.canlet.2021.12.026

Liu, X., Mi, J., Qin, H., Li, Z., Chai, J., Li, M., et al. (2020). E2F1/IGF-1R loop contributes to BRAF inhibitor resistance in melanoma. *J. Invest. Dermatol* 140 (6), 1295–1299. doi:10.1016/j.jid.2019.09.025

Liu, Y., Yao, Y., Liao, B., Zhang, H., Yang, Z., Xia, P., et al. (2022a). A positive feedback loop of CENPU/E2F6/E2F1 facilitates proliferation and metastasis via ubiquitination of E2F6 in hepatocellular carcinoma. *Int. J. Biol. Sci.* 18 (10), 4071–4087. doi:10.7150/ijbs.69495

Logotheti, S., Marquardt, S., Gupta, S. K., Richter, C., Edelhäuser, B. A. H., Engelmann, D., et al. (2020). LncRNA-SLC16A1-AS1 induces metabolic reprogramming during Bladder Cancer progression as target and co-activator of E2F1. *Theranostics* 10 (21), 9620–9643. doi:10.7150/thno.44176

LoPiccolo, J., Gusev, A., Christiani, D. C., and Jänne, P. A. (2024). Lung cancer in patients who have never smoked - an emerging disease. *Nat. Rev. Clin. Oncol.* 21 (2), 121–146. doi:10.1038/s41571-023-00844-0

Lu, G., Li, Y., Ma, Y., Lu, J., Chen, Y., Jiang, Q., et al. (2018). Long noncoding RNA LINC00511 contributes to breast cancer tumourigenesis and stemness by inducing the miR-185-3p/E2F1/Nanog axis. *J. Exp. Clin. Cancer Res.* 37 (1), 289. doi:10.1186/s13046-018-0945-6

Luo, G., Liu, D., Huang, C., Wang, M., Xiao, X., Zeng, F., et al. (2017). LncRNA GAS5 inhibits cellular proliferation by targeting P27(kip1). *Mol. Cancer Res.* 15 (7), 789–799. doi:10.1158/1541-7786.Mcr-16-0331

Luo, J., Wang, H., Wang, L., Yao, Y., Xie, K., Li, X., et al. (2021). lncRNA GAS6-AS1 inhibits progression and glucose metabolism reprogramming in LUAD via repressing E2F1-mediated transcription of GLUT1. *Mol. Ther. Nucleic Acids* 25, 11–24. doi:10.1016/j.omtn.2021.04.022

Lv, X., Lian, Y., Liu, Z., Xiao, J., Zhang, D., and Yin, X. (2021). Exosomal long non-coding RNA LINC00662 promotes non-small cell lung cancer progression by miR-320d/E2F1 axis. *Aging (Albany NY)* 13 (4), 6010–6024. doi:10.18632/aging.202522

Ma, Y., Lin, H., Wang, P., Yang, H., Yu, J., Tian, H., et al. (2023). A miRNA-based gene therapy nanodrug synergistically enhances pro-inflammatory antitumor immunity against melanoma. *Acta Biomater.* 155, 538–553. doi:10.1016/j.actbio.2022.11.016

Manickavinayaham, S., Velez-Cruz, R., Biswas, A. K., Chen, J., Guo, R., and Johnson, D. G. (2020). The E2F1 transcription factor and RB tumor suppressor moonlight as DNA repair factors. *Cell Cycle* 19 (18), 2260–2269. doi:10.1080/15384101.2020.1801190

Mega, S., Miyamoto, M., Ebihara, Y., Takahashi, R., Hase, R., Li, L., et al. (2005). Cyclin D1, E2F1 expression levels are associated with characteristics and prognosis of esophageal squamous cell carcinoma. *Dis. Esophagus* 18 (2), 109–113. doi:10.1111/j.1442-2050.2005.00463.x

Mehmandar-Oskuie, A., Jahankhani, K., Rostamlou, A., Mardafkan, N., Karamali, N., Razavi, Z. S., et al. (2024). Molecular mechanism of lncRNAs in pathogenesis and diagnosis of auto-immune diseases, with a special focus on lncRNA-based therapeutic approaches. *Life Sci.* 336, 122322. doi:10.1016/j.lfs.2023.122322

Meng, P., and Ghosh, R. (2014). Transcription addiction: can we garner the Yin and Yang functions of E2F1 for cancer therapy? *Cell Death Dis.* 5 (8), e1360. doi:10.1038/cddis.2014.326

Min, S., Zhang, L., Zhang, L., Liu, F., and Liu, M. (2024). LncRNA MIR100HG affects the proliferation and metastasis of lung cancer cells through mediating the microRNA-5590-3p/DCBLD2 axis. *Immun. Inflamm. Dis.* 12 (4), e1223. doi:10.1002/iid3.1223

Mu, B., Lv, C., Liu, Q., and Yang, H. (2021). Long non-coding RNA ZEB1-AS1 promotes proliferation and metastasis of hepatocellular carcinoma cells by targeting miR-299-3p/E2F1 axis. *J. Biochem.* 170 (1), 41–50. doi:10.1093/jb/mvab042

Murthy, S. S., and Are, C. (2024). Cancer surgery on the global stage: updates and progress. *J. Surg. Oncol.* 129 (1), 145–149. doi:10.1002/jso.27548

Nagpal, M., Nagpal, K., and Nagpal, P. N. (2007). A comparative debate on the various anti-vascular endothelial growth factor drugs: pegaptanib sodium (Macugen), ranibizumab (Lucentis) and bevacizumab (Avastin). *Indian J. Ophthalmol.* 55 (6), 437–439. doi:10.4103/0301-4738.36478

Nemeth, K., Bayraktar, R., Ferracin, M., and Calin, G. A. (2024). Non-coding RNAs in disease: from mechanisms to therapeutics. *Nat. Rev. Genet.* 25 (3), 211–232. doi:10.1038/s41576-023-00662-1

Niu, W., Guo, L. Y., Zhang, J. Y., Ji, T., Mao, D., Li, X. F., et al. (2020). E2F1-induced upregulation of lncRNA HCG18 stimulates proliferation and migration in gastric cancer by binding to miR-197-3p. *Eur. Rev. Med. Pharmacol. Sci.* 24 (19), 9949–9956. doi:10.26355/eurrev_202010_23207

Nötzold, L., Frank, L., Gandhi, M., Polycarpou-Schwarz, M., Groß, M., Gunkel, M., et al. (2017). The long non-coding RNA LINC00152 is essential for cell cycle progression through mitosis in HeLa cells. *Sci. Rep.* 7 (1), 2265. doi:10.1038/s41598-017-02357-0

Novak, D., Hüser, L., Elton, J. J., Umansky, V., Altevogt, P., and Utikal, J. (2020). SOX2 in development and cancer biology. *Semin. Cancer Biol.* 67 (Pt 1), 74–82. doi:10.1016/j.semcancer.2019.08.007

Ohtsuka, M., Ling, H., Ivan, C., Pichler, M., Matsushita, D., Goblirsch, M., et al. (2016). H19 noncoding RNA, an independent prognostic factor, regulates essential Rb-E2F and CDK8-β-catenin signaling in colorectal cancer. *EBioMedicine* 13, 113–124. doi:10.1016/j.ebiom.2016.10.026

Park, S. M., Choi, E. Y., Bae, D. H., Sohn, H. A., Kim, S. Y., and Kim, Y. J. (2018). The LncRNA EPEL promotes lung cancer cell proliferation through E2F target activation. *Cell Physiol. Biochem.* 45 (3), 1270–1283. doi:10.1159/000487460

Pham, T. P., Kremer, V., and Boon, R. A. (2020). RNA-based therapeutics in cardiovascular disease. *Curr. Opin. Cardiol.* 35 (3), 191–198. doi:10.1097/hco.0000000000000724

Priyanka, P., Sharma, M., Das, S., and Saxena, S. (2022). E2F1-induced lncRNA, EMSLR regulates lncRNA LncPRESS1. *Sci. Rep.* 12 (1), 2548. doi:10.1038/s41598-022-06154-2

Qi, P., Lin, W. R., Zhang, M., Huang, D., Ni, S. J., Zhu, X. L., et al. (2018). E2F1 induces LSINCT5 transcriptional activity and promotes gastric cancer progression by affecting the epithelial-mesenchymal transition. *Cancer Manag. Res.* 10, 2563–2571. doi:10.2147/cmar.S171652

Ramasamy, T., Ruttala, H. B., Munusamy, S., Chakraborty, N., and Kim, J. O. (2022). Nano drug delivery systems for antisense oligonucleotides (ASO) therapeutics. *J. Control Release* 352, 861–878. doi:10.1016/j.jconrel.2022.10.050

Reinhard, K., Rengstl, B., Oehm, P., Michel, K., Billmeier, A., Hayduk, N., et al. (2020). An RNA vaccine drives expansion and efficacy of claudin-CAR-T cells against solid tumors. *Science* 367 (6476), 446–453. doi:10.1126/science.aay5967

Rosenfeldt, M. T., Bell, L. A., Long, J. S., O'Prey, J., Nixon, C., Roberts, F., et al. (2014). E2F1 drives chemotherapeutic drug resistance via ABCG2. *Oncogene* 33 (32), 4164–4172. doi:10.1038/onc.2013.470

Sakurai, K., and Ito, H. (2024). Multifaced roles of the long non-coding RNA DRAIC in cancer progression. *Life Sci.* 343, 122544. doi:10.1016/j.lfs.2024.122544

Saranya, I., Dharshini, V. S., Akshaya, R. L., Subhashini, P. S., and Selvamurugan, N. (2024). Regulatory and therapeutic implications of competing endogenous RNA network in breast cancer progression and metastasis: a review. *Int. J. Biol. Macromol.* 266 (Pt 2), 131075. doi:10.1016/j.ijbiomac.2024.131075

Schellens, R. T. W., Broekman, S., Peters, T., Graave, P., Malinar, L., Venselaar, H., et al. (2023). A protein domain-oriented approach to expand the opportunities of therapeutic exon skipping for USH2A-associated retinitis pigmentosa. *Mol. Ther. Nucleic Acids* 32, 980–994. doi:10.1016/j.omtn.2023.05.020

Schmitz, S. U., Grote, P., and Herrmann, B. G. (2016). Mechanisms of long noncoding RNA function in development and disease. *Cell Mol. Life Sci.* 73 (13), 2491–2509. doi:10.1007/s00018-016-2174-5

Seemann, S. E., Mirza, A. H., Hansen, C., Bang-Berthelsen, C. H., Garde, C., Christensen-Dalsgaard, M., et al. (2017). The identification and functional annotation of RNA structures conserved in vertebrates. *Genome Res.* 27 (8), 1371–1383. doi:10.1101/gr.208652.116

Shaath, H., Vishnubalaji, R., Elango, R., Kardousha, A., Islam, Z., Qureshi, R., et al. (2022). Long non-coding RNA and RNA-binding protein interactions in cancer: experimental and machine learning approaches. *Semin. Cancer Biol.* 86 (Pt 3), 325–345. doi:10.1016/j.semcancer.2022.05.013

Shaik, T., Rather, G. M., Bansal, N., Minko, T., Garbuzenko, O., Szekely, Z., et al. (2018). Modeling and antitumor studies of a modified L-penetratin peptide targeting E2F in lung cancer and prostate cancer. *Oncotarget* 9 (70), 33249–33257. doi:10.18632/oncotarget.26064

Shan, K. Z., Yang, S. F., Deng, Y. J., Yue, P. Y., and Du, Z. Q. (2022). E2F1-induced long non-coding RNA MCF2L-AS1 modulates Cyclin D1 mRNA stability through ELAVL1 to induce Gefitinib resistance in non-small cell lung cancer. *Acta Biochim. Pol.* 69 (4), 795–804. doi:10.18388/abp.2020_6118

Shen, H. M., Zhang, D., Xiao, P., Qu, B., and Sun, Y. F. (2023). E2F1-mediated KDM4A-AS1 up-regulation promotes EMT of hepatocellular carcinoma cells by recruiting ILF3 to stabilize AURKA mRNA. *Cancer Gene Ther.* 30 (7), 1007–1017. doi:10.1038/s41417-023-00607-0

Shen, W., De Hoyos, C. L., Migawa, M. T., Vickers, T. A., Sun, H., Low, A., et al. (2019). Chemical modification of PS-ASO therapeutics reduces cellular protein-binding and improves the therapeutic index. *Nat. Biotechnol.* 37 (6), 640–650. doi:10.1038/s41587-019-0106-2

Shen, X., Ye, Z., Wu, W., Zhao, K., Cheng, G., Xu, L., et al. (2021). lncRNA NEAT1 facilitates the progression of colorectal cancer via the KDM5A/Cul4A and Wnt signaling pathway. *Int. J. Oncol.* 59 (1), 51. doi:10.3892/ijo.2021.5231

Sherman, R. M., and Salzberg, S. L. (2020). Pan-genomics in the human genome era. *Nat. Rev. Genet.* 21 (4), 243–254. doi:10.1038/s41576-020-0210-7

Shi, J., Li, J., Yang, S., Hu, X., Chen, J., Feng, J., et al. (2020). LncRNA SNHG3 is activated by E2F1 and promotes proliferation and migration of non-small-cell lung cancer cells through activating TGF-β pathway and IL-6/JAK2/STAT3 pathway. *J. Cell Physiol.* 235 (3), 2891–2900. doi:10.1002/jcp.29194

Shi, X., Sun, M., Liu, H., Yao, Y., Kong, R., Chen, F., et al. (2015). A critical role for the long non-coding RNA GAS5 in proliferation and apoptosis in non-small-cell lung cancer. *Mol. Carcinog.* 54 (Suppl. 1), E1–E12. doi:10.1002/mc.22120

Siddique, R., Gupta, G., Mgm, J., Kumar, A., Kaur, H., Ariffin, I. A., et al. (2024). Targeting notch-related lncRNAs in cancer: insights into molecular regulation and therapeutic potential. *Pathol. Res. Pract.* 257, 155282. doi:10.1016/j.prp.2024.155282

Smyth, E. C., Nilsson, M., Grabsch, H. I., van Grieken, N. C., and Lordick, F. (2020). Gastric cancer. *Lancet* 396 (10251), 635–648. doi:10.1016/s0140-6736(20)31288-5

Song, H., Liu, Y., Li, X., Chen, S., Xie, R., Chen, D., et al. (2020). Long noncoding RNA CASC11 promotes hepatocarcinogenesis and HCC progression through EIF4A3-mediated E2F1 activation. *Clin. Transl. Med.* 10 (7), e220. doi:10.1002/ctm2.220

Song, L., Li, H., Ma, R. R., Liu, S., Zhang, G. H., Guo, X. Y., et al. (2022). E2F1-initiated transcription of PRSS22 promotes breast cancer metastasis by cleaving ANXA1 and activating FPR2/ERK signaling pathway. *Cell Death Dis.* 13 (11), 982. doi:10.1038/s41419-022-05414-3

Song, P., Han, R., and Yang, F. (2024). Super enhancer lncRNAs: a novel hallmark in cancer. *Cell Commun. Signal* 22 (1), 207. doi:10.1186/s12964-024-01599-6

Sparmann, A., and Vogel, J. (2023). RNA-based medicine: from molecular mechanisms to therapy. *Embo J.* 42 (21), e114760. doi:10.15252/embj.2023114760

Starita, C., Patel, M., Katz, B., and Adamis, A. P. (2007). Vascular endothelial growth factor and the potential therapeutic use of pegaptanib (macugen) in diabetic retinopathy. *Dev. Ophthalmol.* 39, 122–148. doi:10.1159/000098504

Su, T., Zhang, N., Wang, T., Zeng, J., Li, W., Han, L., et al. (2023). Super enhancer-regulated LncRNA LINC01089 induces alternative splicing of DIAPH3 to drive hepatocellular carcinoma metastasis. *Cancer Res.* 83 (24), 4080–4094. doi:10.1158/0008-5472.Can-23-0544

Sun, K. K., Zu, C., Wu, X. Y., Wang, Q. H., Hua, P., Zhang, Y. F., et al. (2023). Identification of lncRNA and mRNA regulatory networks associated with gastric cancer progression. *Front. Oncol.* 13, 1140460. doi:10.3389/fonc.2023.1140460

Sun, M., Jin, F. Y., Xia, R., Kong, R., Li, J. h., Xu, T. p., et al. (2014). Decreased expression of long noncoding RNA GAS5 indicates a poor prognosis and promotes cell proliferation in gastric cancer. *BMC Cancer* 14, 319. doi:10.1186/1471-2407-14-319

Sun, M., Nie, F., Wang, Y., Zhang, Z., Hou, J., He, D., et al. (2016). LncRNA HOXA11-AS promotes proliferation and invasion of gastric cancer by scaffolding the chromatin modification factors PRC2, LSD1, and DNMT1. *Cancer Res.* 76 (21), 6299–6310. doi:10.1158/0008-5472.Can-16-0356

Tao, Z. G., Yuan, Y. X., and Wang, G. W. (2023). Long non-coding RNA CDKN2B-AS1 promotes hepatocellular carcinoma progression via E2F transcription factor 1/G protein subunit alpha Z axis. *World J. Gastrointest. Oncol.* 15 (11), 1974–1987. doi:10.4251/wjgo.v15.i11.1974

Thapa, R., Afzal, M., Goyal, A., Gupta, G., Bhat, A. A., Almalki, W. H., et al. (2024). Exploring ncRNA-mediated regulation of EGFR signalling in glioblastoma: from mechanisms to therapeutics. *Life Sci.* 345, 122613. doi:10.1016/j.lfs.2024.122613

Torre, L. A., Siegel, R. L., Ward, E. M., and Jemal, A. (2016). Global cancer incidence and mortality rates and trends--an update. *Cancer Epidemiol. Biomarkers Prev.* 25 (1), 16–27. doi:10.1158/1055-9965.Epi-15-0578

Traber, G. M., and Yu, A. M. (2023). RNAi-based therapeutics and novel RNA bioengineering technologies. *J. Pharmacol. Exp. Ther.* 384 (1), 133–154. doi:10.1124/jpet.122.001234

Vicente, M. M., Chaves-Ferreira, M., Jorge, J. M. P., Proença, J. T., and Barreto, V. M. (2021). The off-targets of clustered regularly interspaced short palindromic repeats gene editing. *Front. Cell Dev. Biol.* 9, 718466. doi:10.3389/fcell.2021.718466

Vogel, A., Meyer, T., Sapisochin, G., Salem, R., and Saborowski, A. (2022). Hepatocellular carcinoma. *Lancet* 400 (10360), 1345–1362. doi:10.1016/s0140-6736(22)01200-4

Wang, A., and Wang, J. (2020). E2F1-Induced overexpression of long noncoding RNA SBF2-AS1 promotes non-small-cell lung cancer metastasis through regulating miR-362-3p/GRB2 Axis. *DNA Cell Biol.* 39 (7), 1290–1298. doi:10.1089/dna.2020.5426

Wang, H., Cui, H., Yang, X., and Peng, L. (2023c). TUBA1C: a new potential target of LncRNA EGFR-AS1 promotes gastric cancer progression. *BMC Cancer* 23 (1), 258. doi:10.1186/s12885-023-10707-7

Wang, J., He, X., Yao, Q., Wang, C., Lu, X., Wang, R., et al. (2023b). LncRNA PTTG3P promotes tumorigenesis and metastasis of NSCLC by binding with ILF3 to maintain mRNA stability and form a positive feedback loop with E2F1. *Int. J. Biol. Sci.* 19 (13), 4291–4310. doi:10.7150/ijbs.81738

Wang, L., Hou, J., Wang, J., Zhu, Z., Zhang, W., Zhang, X., et al. (2020). Regulatory roles of HSPA6 in Actinidia chinensis Planch. root extract (acRoots)-inhibited lung cancer proliferation. *Clin. Transl. Med.* 10 (2), e46. doi:10.1002/ctm2.46

Wang, R., Sun, Y., Li, L., Niu, Y., Lin, W., Lin, C., et al. (2017b). Preclinical study using Malat1 small interfering RNA or androgen receptor splicing variant 7 degradation enhancer ASC-J9(®) to suppress enzalutamide-resistant prostate cancer progression. *Eur. Urol.* 72 (5), 835–844. doi:10.1016/j.eururo.2017.04.005

Wang, S., Qiao, C., Fang, R., Yang, S., Zhao, G., Liu, S., et al. (2023a). LncRNA CASC19: a novel oncogene involved in human cancer. *Clin. Transl. Oncol.* 25 (10), 2841–2851. doi:10.1007/s12094-023-03165-x

Wang, T., Chen, X., Qiao, W., Kong, L., Sun, D., and Li, Z. (2017a). Transcription factor E2F1 promotes EMT by regulating ZEB2 in small cell lung cancer. *BMC Cancer* 17 (1), 719. doi:10.1186/s12885-017-3701-y

Wang, Y. W., Zhu, W. J., Ma, R. R., Tian, Y. R., Chen, X., and Gao, P. (2024). PIN1P1 is activated by CREB1 and promotes gastric cancer progression via interacting with YBX1 and upregulating PIN1. *J. Cell Mol. Med.* 28 (1), e18022. doi:10.1111/jcmm.18022

Wei, Y., and Zhu, P. (2024). Long non-coding RNA TINCR suppresses growth and epithelial-mesenchymal transition by inhibiting Wnt/β-catenin signaling pathway in human pancreatic cancer PANC-1 cells: insights from *in vitro* and *in vivo* studies. *Acta Pharm.* 74 (1), 131–147. doi:10.2478/acph-2024-0009

Wilson, B., and Geetha, K. M. (2022). Lipid nanoparticles in the development of mRNA vaccines for COVID-19. *J. Drug Deliv. Sci. Technol.* 74, 103553. doi:10.1016/j.jddst.2022.103553

Winkle, M., El-Daly, S. M., Fabbri, M., and Calin, G. A. (2021). Noncoding RNA therapeutics - challenges and potential solutions. *Nat. Rev. Drug Discov.* 20 (8), 629–651. doi:10.1038/s41573-021-00219-z

Wu, L., Yin, L., Ma, L., Yang, J., Yang, F., Sun, B., et al. (2022). Comprehensive bioinformatics analysis of ribonucleoside diphosphate reductase subunit M2(RRM2) gene correlates with prognosis and tumor immunotherapy in pan-cancer. *Aging (Albany NY)* 14 (19), 7890–7905. doi:10.18632/aging.204315

Wu, P., Mo, Y., Peng, M., Tang, T., Zhong, Y., Deng, X., et al. (2020). Emerging role of tumor-related functional peptides encoded by lncRNA and circRNA. *Mol. Cancer* 19 (1), 22. doi:10.1186/s12943-020-1147-3

Wu, S. G., and Shih, J. Y. (2018). Management of acquired resistance to EGFR TKI-targeted therapy in advanced non-small cell lung cancer. *Mol. Cancer* 17 (1), 38. doi:10.1186/s12943-018-0777-1

Xiang, S., Yan, W., Ren, X., Feng, J., and Zu, X. (2024). Role of ferroptosis and ferroptosis-related long non'coding RNA in breast cancer. *Cell Mol. Biol. Lett.* 29 (1), 40. doi:10.1186/s11658-024-00560-2

Xiao, S. Y., Yan, Z. G., Zhu, X. D., Qiu, J., Lu, Y. C., and Zeng, F. R. (2022). LncRNA DLGAP1-AS2 promotes the radioresistance of rectal cancer stem cells by upregulating CD151 expression via E2F1. *Transl. Oncol.* 18, 101304. doi:10.1016/j.tranon.2021.101304

Xie, K., Minkenberg, B., and Yang, Y. (2015). Boosting CRISPR/Cas9 multiplex editing capability with the endogenous tRNA-processing system. *Proc. Natl. Acad. Sci. U. S. A.* 112 (11), 3570–3575. doi:10.1073/pnas.1420294112

Xie, X., Bansal, N., Shaik, T., Kerrigan, J. E., Minko, T., Garbuzenko, O., et al. (2014). A novel peptide that inhibits E2F transcription and regresses prostate tumor xenografts. *Oncotarget* 5 (4), 901–907. doi:10.18632/oncotarget.1809

Xie, X., Kerrigan, J. E., Minko, T., Garbuzenko, O., Lee, K. C., Scarborough, A., et al. (2013). Antitumor and modeling studies of a penetratin-peptide that targets E2F-1 in small cell lung cancer. *Cancer Biol. Ther.* 14 (8), 742–751. doi:10.4161/cbt.25184

Xu, J., Liu, L., Ma, R., Wang, Y., Chen, X., Liu, H., et al. (2020a). E2F1 induces KIF26A transcription and promotes cell cycle progression via CDK-RB-E2Fs feedback loop in breast cancer. *Front. Oncol.* 10, 530933. doi:10.3389/fonc.2020.530933

Xu, K., Xia, P., Chen, X., Ma, W., and Yuan, Y. (2023). ncRNA-mediated fatty acid metabolism reprogramming in HCC. *Trends Endocrinol. Metab.* 34 (5), 278–291. doi:10.1016/j.tem.2023.02.007

Xu, X., Zhang, M., Xu, F., and Jiang, S. (2020b). Wnt signaling in breast cancer: biological mechanisms, challenges and opportunities. *Mol. Cancer* 19 (1), 165. doi:10.1186/s12943-020-01276-5

Xu, Y., Jia, K., Zhao, X., Li, Y., and Zhang, Z. (2024). LncRNA LINC01703 promotes the proliferation, migration, and invasion of colorectal cancer by activating PI3K/AKT pathway. *J. Biochem. Mol. Toxicol.* 38 (1), e23594. doi:10.1002/jbt.23594

Yan, H., Gao, S., Xu, A., Zuo, L., Zhang, J., Zhao, Y., et al. (2023a). MALAT1 regulates network of microRNA-15a/16-VEGFA to promote tumorigenesis and angiogenesis in multiple myeloma. *Carcinogenesis* 44 (10-11), 760–772. doi:10.1093/carcin/bgad053

Yan, J., Wang, R., and Tan, J. (2023b). Recent advances in predicting lncRNA-disease associations based on computational methods. *Drug Discov. Today* 28 (2), 103432. doi:10.1016/j.drudis.2022.103432

Yan, S., Teng, L., Du, J., Ji, L., Xu, P., Zhao, W., et al. (2024). Long non-coding RNA DANCR aggravates breast cancer through the miR-34c/E2F1 feedback loop. *Mol. Med. Rep.* 29 (6), 93. doi:10.3892/mmr.2024.13217

Yang, S., Wang, X., Zhou, X., Hou, L., Wu, J., Zhang, W., et al. (2023). ncRNA-mediated ceRNA regulatory network: transcriptomic insights into breast cancer progression and treatment strategies. *Biomed. Pharmacother.* 162, 114698. doi:10.1016/j.biopha.2023.114698

Yao, Z. T., Yang, Y. M., Sun, M. M., He, Y., Liao, L., Chen, K. S., et al. (2022). New insights into the interplay between long non-coding RNAs and RNA-binding proteins in cancer. *Cancer Commun. (Lond)* 42 (2), 117–140. doi:10.1002/cac2.12254

Yi, M., Zheng, X., Niu, M., Zhu, S., Ge, H., and Wu, K. (2022). Combination strategies with PD-1/PD-L1 blockade: current advances and future directions. *Mol. Cancer* 21 (1), 28. doi:10.1186/s12943-021-01489-2

Yu, H., Lin, L., Zhang, Z., Zhang, H., and Hu, H. (2020a). Targeting NF-κB pathway for the therapy of diseases: mechanism and clinical study. *Signal Transduct. Target Ther.* 5 (1), 209. doi:10.1038/s41392-020-00312-6

Yu, J. E., Ju, J. A., Musacchio, N., Mathias, T. J., and Vitolo, M. I. (2020b). Long noncoding RNA DANCR activates wnt/β-catenin signaling through MiR-216a inhibition in non-small cell lung cancer. *Biomolecules* 10 (12), 1646. doi:10.3390/biom10121646

Yu, L., Fang, F., Lu, S., Li, X., Yang, Y., and Wang, Z. (2017). lncRNA-HIT promotes cell proliferation of non-small cell lung cancer by association with E2F1. *Cancer Gene Ther.* 24 (5), 221–226. doi:10.1038/cgt.2017.10

Yu, S., Wang, Y., Gong, X., Fan, Z., Wang, Z., Liang, Z., et al. (2023). LncRNA AGPG confers endocrine resistance in breast cancer by promoting E2F1 activity. *Cancer Res.* 83 (19), 3220–3236. doi:10.1158/0008-5472.Can-23-0015

Zhan, T., Rindtorff, N., and Boutros, M. (2017). Wnt signaling in cancer. *Oncogene* 36 (11), 1461–1473. doi:10.1038/onc.2016.304

Zhang, L., and Shi, L. (2023). The E2F1/MELTF axis fosters the progression of lung adenocarcinoma by regulating the Notch signaling pathway. *Mutat. Res.* 827, 111837. doi:10.1016/j.mrfmmm.2023.111837

Zhang, Y., Wang, X., Hu, C., and Yi, H. (2023). Shiny transcriptional junk: lncRNA-derived peptides in cancers and immune responses. *Life Sci.* 316, 121434. doi:10.1016/j.lfs.2023.121434

Zhang, Y., Zhu, Y., Xiao, M., Cheng, Y., He, D., Liu, J., et al. (2021). The long non-coding RNA TMPO-AS1 promotes bladder cancer growth and progression via OTUB1-induced E2F1 deubiquitination. *Front. Oncol.* 11, 643163. doi:10.3389/fonc.2021.643163

Zheng, G., Chen, W., Li, W., Ding, Y., and Tu, P. (2020). E2F1-induced ferritin heavy chain 1 pseudogene 3 (FTH1P3) accelerates non-small cell lung cancer gefitinib resistance. *Biochem. Biophys. Res. Commun.* 530 (4), 624–631. doi:10.1016/j.bbrc.2020.07.044

Zheng, Y., Su, L., Tan, J., and Dong, F. (2022). Actinidia chinensis Planch Root extract suppresses the growth and metastasis of hypopharyngeal carcinoma by inhibiting E2F Transcription Factor 1-mediated MNX1 antisense RNA 1. *Bioengineered* 13 (3), 4911–4922. doi:10.1080/21655979.2022.2037226

Zhou, M., He, X., Zhang, J., Mei, C., Zhong, B., and Ou, C. (2024). tRNA-derived small RNAs in human cancers: roles, mechanisms, and clinical application. *Mol. Cancer* 23 (1), 76. doi:10.1186/s12943-024-01992-2

Zhu, Q., Zhang, C., Qu, T., Lu, X., He, X., Li, W., et al. (2022). MNX1-AS1 promotes phase separation of IGF2BP1 to drive c-myc-mediated cell-cycle progression and proliferation in lung cancer. *Cancer Res.* 82 (23), 4340–4358. doi:10.1158/0008-5472.Can-22-1289

frontiers | Frontiers in Pharmacology

TYPE Original Research
PUBLISHED 08 October 2024
DOI 10.3389/fphar.2024.1469286

Check for updates

OPEN ACCESS

EDITED BY
Alice Conigliaro,
University of Palermo, Italy

REVIEWED BY
Shenglan Shang,
General Hospital of Central Theater Command, China
Aarti Sharma,
Mayo Clinic Arizona, United States

*CORRESPONDENCE
Xin Li,
lixin9207@163.com
Shoulong Deng,
dengshoulong@cnilas.org
Lixin Xie,
xielx301@126.com

†These authors have contributed equally to this work

RECEIVED 23 July 2024
ACCEPTED 25 September 2024
PUBLISHED 08 October 2024

CITATION
Xiang G, Li Q, Lian D, Su C, Li X, Deng S and Xie L (2024) FOXO1-mediated autophagy regulation by miR-223 in sepsis-induced immunosuppression.
Front. Pharmacol. 15:1469286.
doi: 10.3389/fphar.2024.1469286

COPYRIGHT
© 2024 Xiang, Li, Lian, Su, Li, Deng and Xie. This is an open-access article distributed under the terms of the Creative Commons Attribution License (CC BY). The use, distribution or reproduction in other forums is permitted, provided the original author(s) and the copyright owner(s) are credited and that the original publication in this journal is cited, in accordance with accepted academic practice. No use, distribution or reproduction is permitted which does not comply with these terms.

FOXO1-mediated autophagy regulation by miR-223 in sepsis-induced immunosuppression

Guoan Xiang[1,2†], Qi Li[3†], Di Lian[1†], Chengcheng Su[4], Xin Li[5*], Shoulong Deng[6*] and Lixin Xie[1,2*]

[1]College of Pulmonary and Critical Care Medicine, Chinese PLA General Hospital, Beijing, China, [2]Chinese PLA Medical School, Beijing, China, [3]Department of Tuberculosis, Beijing Chest Hospital, Capital Medical University, Beijing, China, [4]Department of Respiratory and Critical Care Medicine, Pingjin Hospital, Characteristic Medical Center of the Chinese People's Armed Police Force, Tianjin, China, [5]Department of Emergency, Third Medical Center of Chinese PLA General Hospital, Beijing, China, [6]National Center of Technology Innovation for Animal Model, National Human Diseases Animal Model Resource Center, National Health Commission of China (NHC) Key Laboratory of Comparative Medicine, Institute of Laboratory Animal Sciences, Chinese Academy of Medical Sciences and Comparative Medicine Center, Peking Union Medical College, Beijing, China

Introduction: Immunosuppression is the main cause of the high mortality rate in patients with sepsis. The decrease in the number and dysfunction of $CD4^+$ T lymphocytes is crucial to the immunosuppressed state of sepsis, in turn affecting the development and prognosis of sepsis. Autophagy has been shown to play an important role in the immune imbalance exhibited during sepsis.

Methods: In this study, we modulate the expression of miR-223 in $CD4^+$ T lymphocytes, via the transfection of a mimic or an inhibitor of miR-223 to establish cell models of miR-223 overexpression and knockdown, respectively. Levels of autophagy were monitored using a double-labeled lentivirus (mRFP-GFP-LC3) and electron microscopy, and western blot analysis was used to estimate the levels of autophagy-related proteins and FOXO1 in the two cell models after co-treatment with lipopolysaccharide (LPS) and siRNA against FOXO1.

Results: We found that when the expression of miR-223 increased, FOXO1 expression decreased and autophagy decreased; whereas, when FOXO1 expression was inhibited, autophagy decreased significantly in different cell models after LPS induction.

Conclusion: Thus, this study proved that miR-223 participate in the regulation of LPS-induced autophagy via the regulation of FOXO1 expression in $CD4^+$ T lymphocytes which shed a new light for the diagnosis and treatment of sepsis.

KEYWORDS

sepsis, miR-223, $CD4^+$ T lymphocytes, autophagy, FOXO1, immunosuppression

1 Introduction

Sepsis refers to severe organ dysfunction due to an infection (Seymour et al., 2016). It has an acute onset and leads to a high mortality rate; it is a particularly difficult problem in the field of critical respiratory illnesses. In recent years, the incidence of sepsis is on the rise, and the lack of an effective treatment has become one of the leading causes of human death, as sepsis is one of the leading factors contributing to the immediate death of hospitalized patients (Stevenson et al., 2014; Walkey et al., 2015). Thus, there is an urgent need to find effective solutions for the treatment of sepsis (Hotchkiss et al., 2013b; Franks et al., 2015; Shankar-Hari et al., 2015). Previous studies have shown that an immune imbalance plays a key role in the development of sepsis. During immune dysfunction, immunosuppression, and immune paralysis, the innate and adaptive immune systems cannot eliminate pathogens and harmful substances from the body and any additional stressors can lead to aggravation of the existing condition and even death of the patient. T lymphocyte dysfunction is the most important aspect of immune dysfunction during sepsis; however, the underlying mechanism remains unknown (Stieglitz et al., 2015; Bermejo-Martin et al., 2016; Delano and Ward, 2016). Decreased numbers, reduced function, exhaustion, and apoptotic clearance of T lymphocytes are directly related to the poor prognosis of sepsis, and these findings are consistent with our previous study, wherein septic patients exhibited a lower proportion of $CD4^+$ T lymphocytes than that in healthy patients. Thus, health of patients with sepsis may worsen, develop multiple organ dysfunction, and even die (Hotchkiss et al., 2013a; Boomer et al., 2014; Hotchkiss and Sherwood, 2015; Luan et al., 2015). $CD4^+$ T lymphocytes act as early biomarkers of sepsis and impact the prognosis (Li J. et al., 2015). Further, autophagy of T lymphocytes leads to the expression of abnormal or aged proteins and organelles and excessive peroxide-mediated degradation of proteins. Thus, programmed cell death during immunosuppression might be the key to solving the immune imbalance exhibited during sepsis.

In patients with HIV, nearly 10 micro RNAs (miRs) were found to regulate $CD4^+$ T lymphocyte numbers and affect the replication and infection ability of the virus. In a previous study, we used Solexa sequencing to analyze circulating microRNAs in the early stages of sepsis to determine whether there were any microRNAs that functioned as biomarkers of sepsis. Thus, we identified microRNAs differentially expressed between septic and healthy patients, and among them, miR-223, which is known to have a profound impact on the differentiation of blood cells and on granulocytes and T lymphocytes, was found to exhibit higher sensitivity and specificity in predicting the prognosis of septic patients (Wang et al., 2012; Wang et al., 2014). High expression of miR-223 has also been detected in the peripheral blood and synovial T lymphocytes of patients with rheumatoid arthritis, and miR-223 possibly impacts the development of arthritis and inflammatory bowel disease (IBD) by affecting the activity of immune cells (Fasseu et al., 2010). Although many studies have found that some miRNAs regulate autophagy levels in cells and in turn affect the prognosis in animal disease models, its role in regulating autophagy levels of immune cells in patients of sepsis is still unknown.

In our previous study, we used TargetScan and miRanda, in conjunction with the Kyoto Encyclopedia of Genes and Genomes pathway and the gene ontology enrichment analysis, and predicted the gene encoding the forkhead box protein O1 (FOXO1) as one of the target genes of miR-223, and studies have also shown that FOXO1, as a miR-223 downstream target, plays a role in cancer development (Haneklaus et al., 2013). As a member of the FOX transcription gene family, subtype O, FOXO1 is widely expressed in eukaryotes and is located on human chromosome 13q14.1. FOXO1 is also known to participate in the PI3K/AKT pathway, and its downstream targets are involved in many important cellular biological processes, such as apoptosis (Fu and Tindall, 2008), cell cycle inhibition, oxidative stress tolerance, anabolism, and catabolism (Du et al., 2020).

In this study, we modulated miR-223 expression in $CD4^+$ T lymphocytes using chemically synthesized miRs and estimated the autophagy levels after lipopolysaccharide (LPS) treatment. We also inhibited the expression of FOXO1 using small interfering (si) RNA technology, and subsequently detected changes in the level of autophagy after LPS treatment, in order to explore the possible pathways by which miR-223 regulates the levels of autophagy during sepsis and find a potential treatment for sepsis.

2 Materials and methods

2.1 Reagents and materials

CD4 (L3T4) MicroBeads, LS columns with pre-separation filters (70 μm) were purchased from Miltenyi Biotec, United States. Two milliliters of CD4 (L3T4) MicroBeads were conjugated to monoclonal anti-mouse CD4 antibody (L3T4; isotype: rat IgG2b). IFN gamma Mono-clonal Antibody (XMG1.2), APC, eBioscience™ was purchased from Thermo Fisher, and Anti-IL-4 antibody [11B11] (PE) (ab93503), recombinant Anti-Annexin V/ANXA5 anti-body [EPR3980] (ab108194) purchased from Abcam. The miR-223 mimic (chemically synthesized double-stranded mature miRNA), and miR-223 inhibitor (Chemically synthesized mature miRNA complementary single-stranded) were purchased from Biomics Biotechnology Co., Ltd. The study design was approved by the appropriate ethics review board. Synthesized microRNAs were purchased from Biomics, China. siRNA-FOXO1 was purchased from Shenggong Bioengineering Co., Ltd., China. The primer sequences used in this experiment are including miR-223 (F: 5′-ACACTCCAGCTGGGACCCCATAAACTGTTT-3′, R: 5′-TGG TGTCGTGGAGTCG-3′), U6 (F: 5′-CTCGCTTCGGCAGCACA-3′, R: 5′-AACGCTTCACGAATTTGCGT-3′), FOXO1 (F: 5′-GAG CGTGCCCTACTTCAA-3′, R: 5′-CCATCTCCCAGGTCATCC-3′), P62(F: 5′-CAGATGCCAGAATCGGAAG-3′, R: 5′-GGTCTG TAGGAGCCTGGTGAG-3′), LC3B (F: 5′-CCCCACCAAGATCCC AGT-3′, R: 5′- CGCTCATGTTCACGTGGT-3), β-actin (F: 5′-AAGGAGCCCCACGAGAAAAAT-3′, R: 5′- ACCGAACTTGCA TTGATTCCAG-3′). The miRcute miRNA extraction and separation kit (spin column type) and the miRcute enhanced miRNA cDNA first strand synthesis kit were purchased from Tiangen Bio-chemical Technology Co., Ltd., China. Lipofectamine 2000 was purchased from Thermo Fisher, United States, and LPS was purchased from Sigma-Aldrich, United States. Double-labeled lentivirus (mRFP-GFP-LC3) was purchased from Hanbio Biotechnology Co., Ltd., China. CD3 antibody and CD28 antibody were purchased from Thermo Fisher, United States.

2.2 Mice housing and sample tissue collection

Specific pathogen-free healthy 10-weeks old C57BL/6J male or female mice SPF grade, weighing about 20 g, were purchased from the Sbefu (Beijing) Biotechnology Co., Ltd. (license number: SCXK-(jing) 2019-0010). The experiment comply with the ARRIVE guidelines and be carried out in accordance with the National Institutes of Health guide for the care and use of Laboratory animals (NIH Publications No. 8023, revised 1978). We obtained ethical approval from the Research Ethics Committee of the Institute of Microbiology, Chinese Academy of Sciences, with the approval number APIMCAS2022143. The mice were euthanized by cervical dislocation, and subsequently, spleen tissues were collected for the isolation of $CD4^+$ T lymphocytes.

2.3 Isolation of $CD4^+$ T lymphocytes and TCR activation

Magnetic bead sorting was used to sort $CD4^+$ T lymphocytes from the spleen of C57BL/6J mice, and flow cytometry was used to detect the proportion of $CD4^+$ T lymphocytes and the number of viable cells. The whole process was performed under sterile conditions. The cells were put into the well plate coated with CD3e and CD28 antibody for 72 h, and $CD4^+$ T lymphocytes were cultured at 5% CO2 and 37°C. Roswell Park Memorial Institute (RPMI) 1640 medium with 10% fetal bovine serum (FBS), density, and the number of cells were estimated using a Nikon E600POL polarized light microscope.

2.4 Transfection of $CD4^+$ T lymphocytes

To manipulate miR-223 expression levels in $CD4^+$ T lymphocytes, we employed synthetic miR-223 mimics and inhibitors, following the product instructions and adhering to the recommended dosage concentrations. Specifically, the experimental groups were divided into two cohorts: one subjected to the miR-223 mimic treatment, which involved the transfection of a 50 nM final concentration of miR-223-5p mimic to augment miR-223 levels; and the other to the miR-223 inhibitor treatment, characterized by the administration of a 100 nM final concentration of miR-223-5p inhibitor to attenuate miR-223 expression. Parallel control groups were established for both the miR-223 mimic and inhibitor treatments. The success of transfection was estimated using real-time polymerase chain reaction to quantify miR-223 expression in each group 48 h post-transfection. Subsequently, the cells were treated with 20 nM Bafilomycin A1 (BafA1) for 4 h, centrifuged at 1,000 rpm for 5 min at room temperature, followed by the addition of RPMI 1640, containing 10% fetal bovine serum (FBS), and incubation with 1 μg/mL LPS for 18 h.

2.5 Estimation of autophagy levels and differentiation in LPS-treated $CD4^+$ T lymphocytes

Observation of the number of autophagosomes in different groups of cells under electron microscopy. Double-labeled lentivirus (mRFP-GFP-LC3) and Nikon ECLIPSE 80i fluorescence microscope and image acquisition and analysis system were used to estimate the changes in autophagy levels in LPS-treated $CD4^+$ T lymphocytes. Fluorescence microscopy were used to observe the green fluorescent protein (GFP), red fluorescent protein (RFP), and estimate the fluorescence intensity at × 400. Antibodies against IFN- γ and IL-4 markers were used to detect the T helper type 1 (Th1) and T helper type 2 (Th2) per-centage in the LPS-treated cells using flow cytometry.

2.6 siRNA-FOXO1 transfection

Cells transfected with synthetic miRs and siRNA-FOXO1. After 48 h, the cells were incubated with 20 nM BafA1 for 4 h, centrifuged at 1,000 rpm for 5 min at room temperature, followed by addition of RPMI 1640 medium, containing 10% FBS, and incubation with 1 μg/mL LPS for 18 h.

2.7 Western-blotting

The western blotting technique was used to detect the differences in the protein expression levels of FOXO1, P62, IL3B between the cells in each group treated with LPS 1 ug/ml for 18 h. In brief, total protein was extracted from each group using a RIPA lysis buffer. Protein concentration was then detected using a BCA (bicinchoninic acid) protein assay kit. SDS-PAGE was conducted, and the protein was electrotransferred to a polyvinylidene fluoride (PVDF) membrane. It was blocked with 5% skim milk and incubated for 2 h at room temperature, followed by overnight incubation at 4°C with primary antibody. After washing with TBST, HRP-labeled protein bands were visualized using an ECL kit. The bands were analyzed using ImageJ software with β-actin as an internal reference.

2.8 Statistical analysis

A two-tailed Student's t-test or a one-way analysis of variance (ANOVA) was per-formed when comparing two groups or more than two groups, respectively. The normality test was checked by the Shapiro–Wilk test and equal variance was checked by Levene's test. Statistical analysis was performed using Microsoft Excel LTSC 2021 and Prism 9.0 (GraphPad). Data are expressed as means ± SEM. Difference was considered to be significant if $p < 0.05$ ($^*p < 0.05$, $^{**}p < 0.01$, $^{***}p < 0.001$, unless otherwise indicated).

3 Results

3.1 $CD4^+$ T lymphocytes capture

The surviving $CD4^+$ T lymphocytes were screened from mouse spleen cell suspension by magnetic bead sorting technique (Figure 1A). Annexin revealed that 95% of $CD4^+$ T cells, sorted using flow cytometry, were living (Figure 1B).

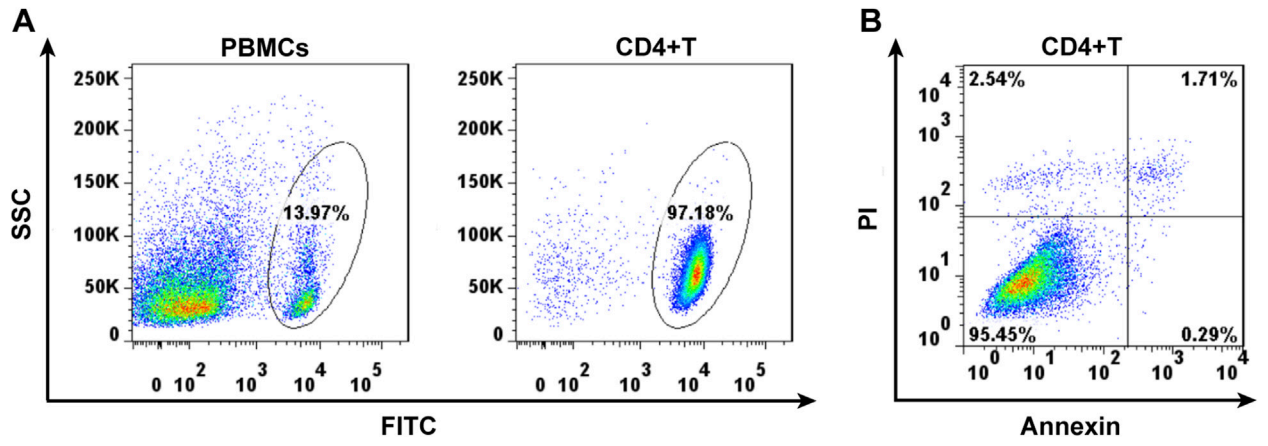


FIGURE 1
Cell separation of the CD4⁺ lymphocytes by magnetic cell sorting **(A)** and cell viability detected by Annexin using flow cytometry **(B)**.

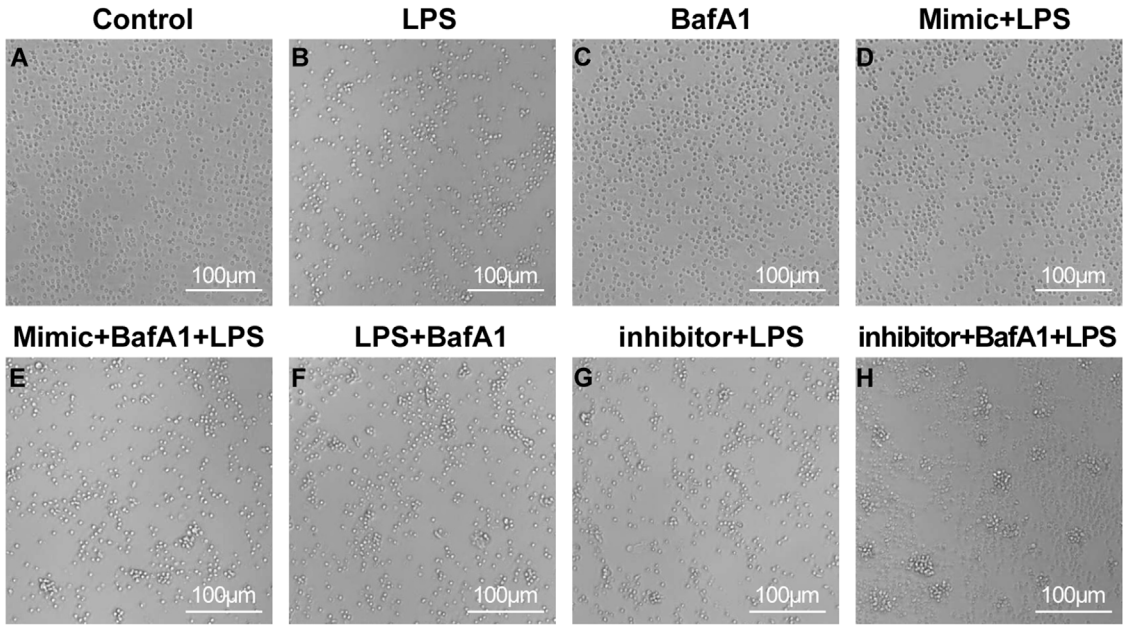


FIGURE 2
The survival state of CD4 + T lymphocytes after various interventions under the micro-scope. **(A–H)** The cell morphology was control group, LPS group, BafA1 group, mimic + LPS group, mimic + BafA1 + LPS group, LPS + BafA1 group, inhibitor + LPS group and inhibitor + BafA1 + LPS group, respectively.

3.2 miR-223 affects the health of LPS-treated CD4⁺ T lymphocytes

The sorted CD4⁺ T cells were cultured for 24 h and given different interventions respectively. The cells of different groups could be observed to present different cell states through microscopy (Figure 2). In the control group, the cell count filled the entire field of view, with cells exhibiting a plump morphology and no evidence of cell clumping. In the control group, the cell count filled the entire field of view, with cells exhibiting a plump morphology and no evidence of clumping cells. The cells in the BafA1 group showed a similar state to the control. In contrast, in the remaining groups, under LPS stimulation, cells exhibited aggregation and a significant reduction in number. However, the miR-223 mimic corrected the effects induced by LPS, with the cell state resembling that of the control group, while the miR-223 inhibitor exacerbated the damage to the cells caused by LPS.

3.3 miR-223 affects the autophagosome formation in LPS-treated CD4⁺ T lymphocytes

To investigate the regulatory role of miR-223 on autophagy activity, we employed electron microscopy to observe and assess the

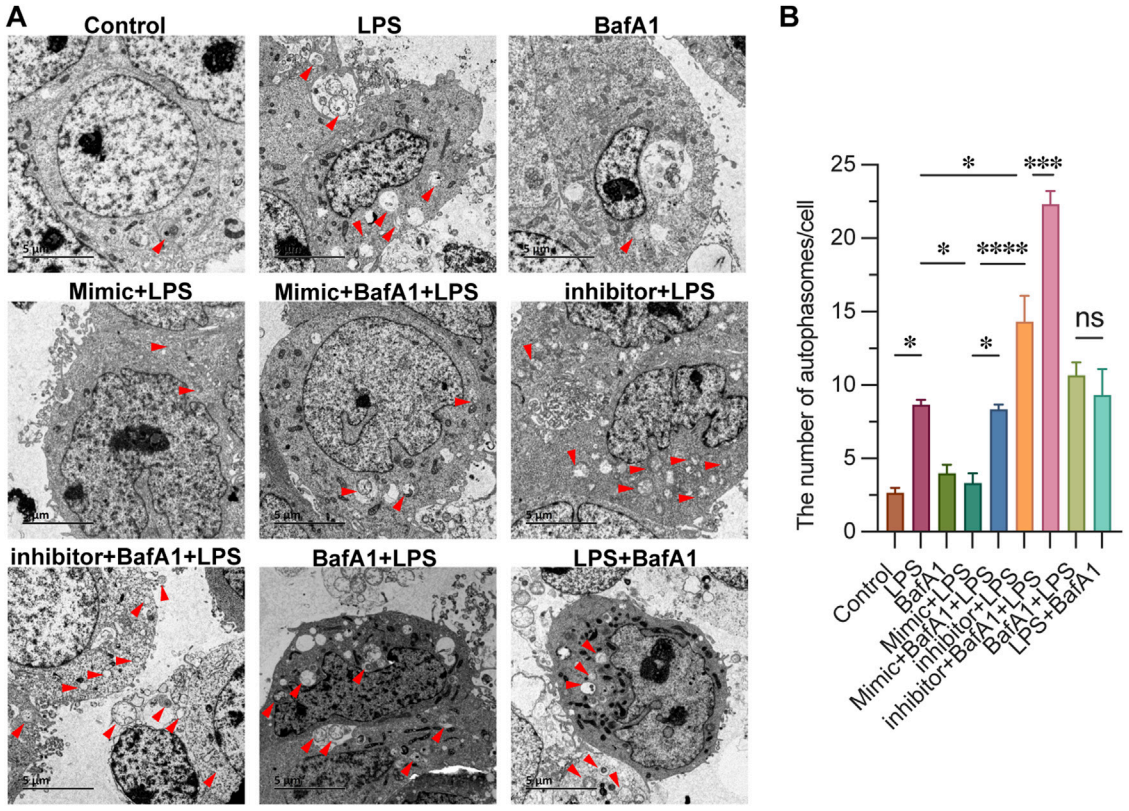


FIGURE 3
miR-223 affects the autophagosome formation in LPS-treated CD4⁺ T lymphocytes. **(A)** Representative images of autophagosomes, observed under an electron microscope, in cells of each group (red arrow). Scale bars: 5 μm. **(B)** The quantitation data were represented with 3 replicates. *$p < 0.05$, ***$p < 0.001$, ****$p < 0.0001$. error bars represent mean ± SEM.

levels of autophagy in each group, and quantified the number of autophagosomes within individual cells. As shown in Figure 3, The typical phenotype of CD4⁺ T lymphocytes, characterized by a large nucleus and rare autophagosome structures, was observed in the Control group. In the LPS group, we observed abundant accumulation of autophagosomes in CD4⁺ T lymphocytes, confirming the activation of autophagy. This accumulation was also evident in both the BafA1 + LPS group (where BafA1 was treated first) and the LPS + BafA1 group (where LPS was treated first), regardless of the order of BafA1 treatment. Following treatment with the miR-223 mimic in mimic + LPS group, the absence of autophagosome accumulation suggested an impairment of autophagy. Conversely, the inhibitor + LPS group showed the opposite effect. Here, we document that the miR-223 mimic inhibits LPS-induced autophagosome formation in CD4⁺ T lymphocytes.

3.4 Cell transfected with the miR-223 mimic showed lower levels of autophagy

We evaluated the impact of miR-223 mimic or inhibitor on autophagy by transfecting CD4⁺ T lymphocytes with an mRFP-GFP-LC3 expression construct. To confirm the efficacy of transfection, we quantified the relative expression levels of miR-223 mRNA. Fluorescence microscopy was utilized to assess the fluorescence intensity of cells exhibiting mRFP-GFP-LC3 punctae across different groups. The merging of GFP and RFP fluorescence channels revealed that orange-red punctae are indicative of active autophagy within the cells (Figure 4). Upon LPS stimulation, an increased fluorescence intensity of mRFP-GFP-LC3 punctae was observed compared to the control group, suggesting that LPS triggers autophagy. Notably, the miR-223 mimic treatment significantly diminished the intensity of the orange-red fluorescence in cells with mRFP-GFP-LC3 punctae. Conversely, the inhibition of miR-223 exacerbated the effects of LPS, as evidenced by the increased accumulation of orange-red punctae. Collectively, these findings indicate that the miR-223 mimic inhibits LPS-induced autophagy in CD4⁺ T lymphocytes.

3.5 miR-223 affects Th1/Th2 differentiation in LPS-treated CD4⁺ T lymphocytes

IFN- γ, IL-4 labeled the Th1 and Th2 ratio of cells in each group, evaluating the effect of miR-223 on the Th2/Th1 differentiation of CD4+ T cells in each group. The percentage of Th1 cells labeled with IFN-γ showed that the proportion of control group and BafA1 group was the lowest, followed by mimic + LPS group and mimic + BafA1 + LPS group, and the ratio of Th1 cells was the highest in inhibitor + BafA1 + LPS group, followed by BafA1 + LPS group and inhibitor + LPS group. The results showed that the proportion of Th2 cells in BafA1 group and control group were the highest, followed by mimic

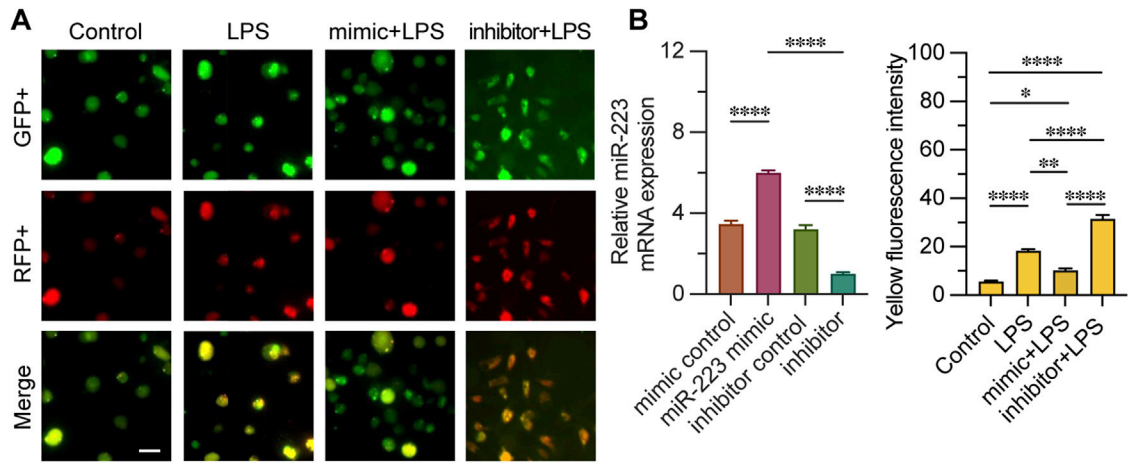


FIGURE 4
Quantitative analysis of mRFP-GFP-LC3 fluorescence monitoring autophagy process fluorescence intensity. **(A)** observation of mRFP-GFP-LC3 autophagy by fluorescence microscope in groups mimic + LPS, inhibitor + LPS, LPS and control. **(B)** Relative miR-223 mRNA expression was examined to verify whether transfection was effective, the fluorescence intensity of both GFP+ and RFP+ was measured in each group; n = 3. Scale bar represents 10 μm. *, **$p < 0.05$, ***$p < 0.001$, ****$p < 0.0001$, ns $p > 0.05$.

+ LPS and mimic + BafA1 + LPS group, and the ratio of Th2 cells in inhibitor + BafA1 + LPS group was the lowest, followed by the group of BafA1 + LPS, inhibitor + LPS and LPS. It is considered that the increased miR-223-expression makes CD4 + T lymphocytes more likely to differentiate into Th2 cells. It is suggested that the change of miR-223 expression affects the Th2/Th1 differentiation ratio of LPS-affected CD4 + T lymphocytes (Figure 5).

3.6 miR-223 affects mRNA levels of FOXO1 and P62

The mRNA expression levels of FOXO1 and p62 were assessed using real-time quantitative PCR, and the activation level of autophagy was evaluated at the mRNA level. p62 is a crucial autophagy substrate, and its expression level can directly reflect the intensity of autophagy activity. In this study, the results indicated that the expression of FOXO1 in the control and BafA1 groups was significantly lower compared to other groups, with the mimic + LPS group showing an intermediate level. Notably, the highest expression of FOXO1 was observed in the inhibitor + BafA1 + LPS group. These findings suggest that FOXO1 expression decreases as miR-223 expression increases (Figure 6A). Conversely, p62 expression was highest in the control group, with the mimic + BafA1 + LPS group exhibiting a higher level than the mimic + LPS group, and the lowest level found in the inhibitor + LPS group. This suggests that following LPS intervention, p62 mRNA expression increases with the upregulation of miR-223 (Figure 6B).

3.7 miR-223 regulates the expression of FOXO1 and autophagy-related proteins

To evaluate the impact of miR-223 on FOXO1-mediated autophagy in $CD4^+$ T lymphocytes, we conducted Western blot analysis to examine the expression levels of FOXO1 and p62, as well as the conversion of LC3, which are proteins associated with autophagy (Figure 7A). The results revealed that the expression level of FOXO1 in the inhibitor + LPS group was significantly higher compared to both the mimic + LPS group and the Control group (Figure 7B). This observation suggests that miR-223 expression indeed regulates FOXO1 expression, which is consistent with previous studies identifying FOXO1 as a target gene of miR-223. In the context of autophagy induction, protein aggregate removal, and autophagy inhibition, p62 labeling serves as a highly informative method. The LC3B label enables the tracking of p62 binding and the subsequent replenishment of autophagosomes. Typically, a decrease in LC3BII and an increase in p62 expression are indicative of autophagy activation (Yoshii and Mizushima, 2017). Our results demonstrated that in the presence of BafA1, LC3-II accumulated under all conditions, including in untreated and LPS-treated cells. Furthermore, we observed that p62 expression was lowest in the inhibitor + LPS group, followed by the inhibitor + BafA1 + LPS group, with the highest levels detected in the control group and the mimic + BafA1 + LPS group (Figures 7C, D). The expression of autophagy-related proteins was influenced by the levels of miR-223, suggesting that increased miR-223 expression leads to weakened autophagy activity, while decreased miR-223 expression enhances autophagy activity.

3.8 FOXO1 regulates autophagy in $CD4^+$ T lymphocytes

To determine whether miR-223 regulates autophagy by regulating FOXO1 in LPS-treated cells. The autophagy activity of cells in each group were detected by autophagy related proteins after blocking the expression of FOXO1. Transfection of cells with siRNA-FOXO1 lead to the death of a large number of cells and the remaining cells were collected to estimate the expression of autophagy-related proteins. Western blot analysis indicated that, in the absence of LPS and inhibitor, the expression levels of

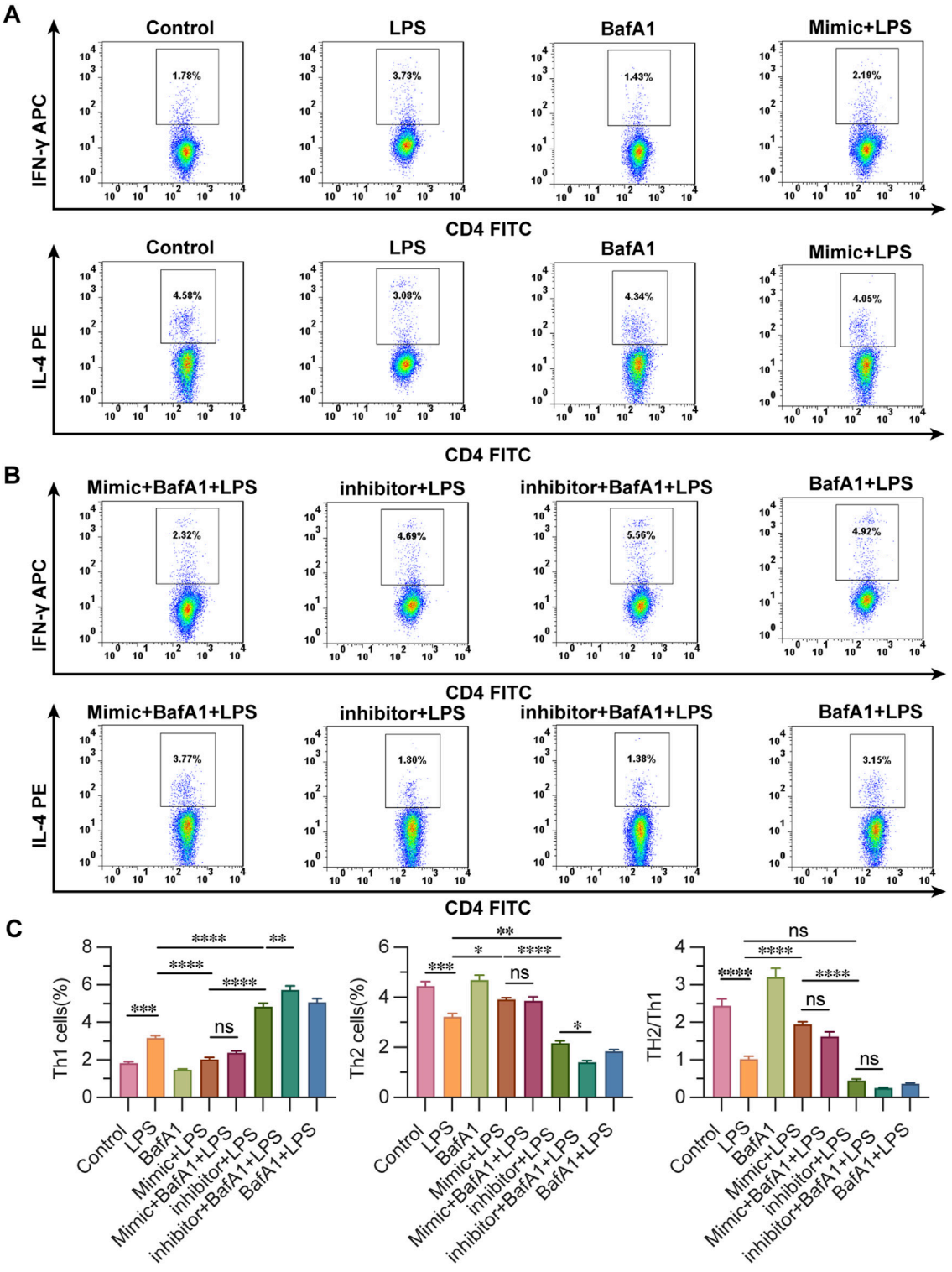


FIGURE 5
Detection of the ratio of Th2/Th1 differentiation of CD4⁺ T lymphocytes using flow cytometry. **(A, B)** observation of the ratio of Th2/Th1 differentiation of CD4⁺ T lymphocytes by flow cytometry in groups. **(C)** The ratio of Th1 cells and Th2 cells by flow cytometry in groups. Results are represented as mean ± SEM, n = 3. *, **$p < 0.05$, ***$p < 0.001$, ****$p < 0.0001$, ns $p > 0.05$.

FOXO1 and LC3BII proteins were significantly elevated in transfected cells, while the expression of P62 protein was reduced, compared to untransfected cells (Figures 8A–D). The silencing of FOXO1 disrupted the formation of the autophagic flux. Following siRNA-FOXO1 transfection, the expression of P62 protein in the miR-223 mimic group was lower than that in the inhibitor group, although this difference did not reach statistical significance. These findings suggest that FOXO1 is a primary

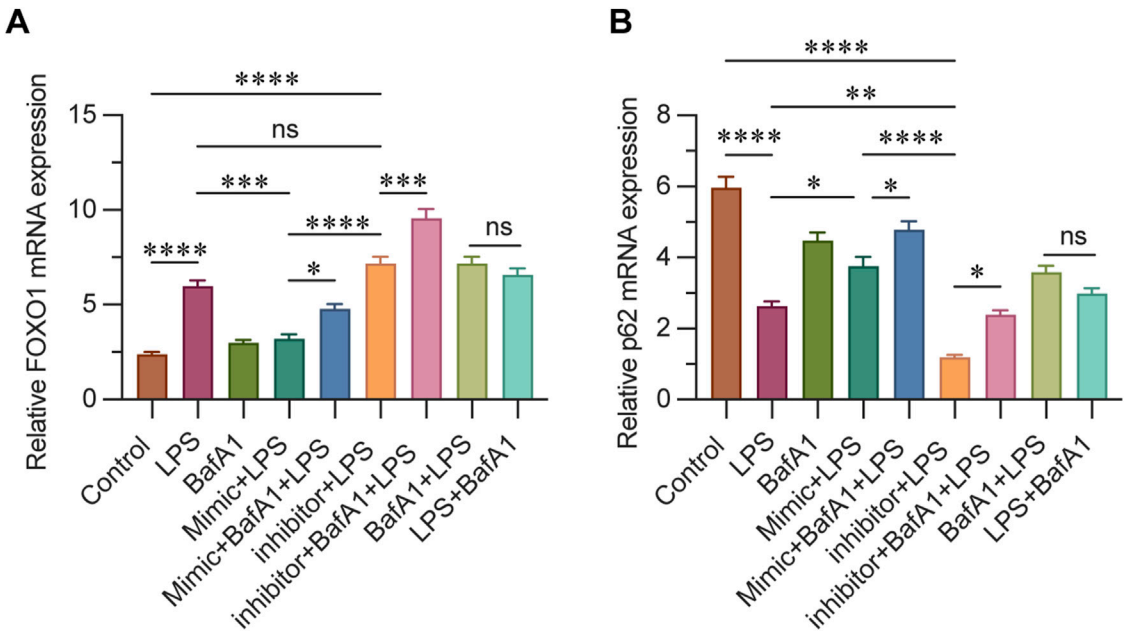


FIGURE 6
(A) Relative mRNA levels of FOXO1 in each group were determined using qPCR. **(B)** Relative mRNA levels of P62 in each group were determined using qPCR. β-actin was used as the loading control. Results are represented as mean ± SEM, n = 3. *, $^{**}p < 0.05$, $^{**}p < 0.01$, $^{***}p < 0.001$, $^{****}p < 0.0001$, ns $p > 0.05$.

pathway through which miR-223 regulates autophagy in CD4$^+$ T lymphocytes.

4 Discussion

The objective of this study was to investigate the role of miR-223 in regulating autophagy and immune function in CD4$^+$ T lymphocytes during sepsis, and to elucidate the mechanisms through which miR-223 contributes to the pathophysiology of sepsis. Our goal was to identify potential novel strategies for the diagnosis and treatment of this condition. We discovered a significant correlation between miR-223 and FOXO1, with FOXO1 being a downstream target of miR-223. Specifically, we observed that the expression of FOXO1 decreases with an increase in miR-223 expression, and *vice versa*, at both the protein and mRNA levels. Further, we also demonstrate that with an increase in expression of miR-223, autophagy levels also significantly reduced in CD4$^+$ T lymphocytes. When FOXO1 expression was inhibited in CD4$^+$ T lymphocytes, autophagy was found to be significantly reduced, indicating that the miR-223-mediated regulation of FOXO1 expression is one of the main pathways through which miR-223 regulates autophagy of CD4$^+$ T lymphocytes. We also report that miR-223 mediates the differentiation of CD4$^+$ T lymphocytes treated with LPS into Th2 rather than Th1-type cells, indicating that high levels of miR-223 expression plays a role in regulating the Th1/Th2 balance and consequently reducing the incidence of cytokine-mediated hyperimmune responses associated with Th1 in sepsis. The molecular mechanisms by which miR-223 regulates FOXO1-mediated autophagy in LPS-induced sepsis in CD4$^+$ T lymphocytes, and its effects on autophagy-related proteins, are summarized in Figure 9.

Sepsis is a life-threatening condition characterized by organ dysfunction and high mortality rates, resulting from the body's dysregulated response to infection. An exaggerated immune reaction to bacterial pathogens can precipitate sepsis. In this context, sepsis biomarkers play an extremely crucial role in diagnostics, therapeutic monitoring, and prognostic assessment. Our previous work has showed that miR-223 can be used as an early biomarker of sepsis. However, other potential functions and roles of miR-223 in sepsis have not been fully revealed. At the same time, our preliminary literature research found that autophagy is a biological phenomenon whereby components of cells can self-degrade using autophagosomes, the regulation of autophagy defects may potentially be used to treat some diseases (Wang et al., 2023).

The miR-223 has been previously demonstrated to play a role in a variety of biological processes, including development, differentiation, hematopoiesis, and immune system regulation. Recent studies, including those by Li Y. et al., have shed new light on autophagy. They confirmed that in mice, miR-223 deficiency leads to increased ATG16L1 and LC3-II protein expression in bone marrow-derived macrophages. Conversely, ATG16L1 levels were found to decrease in BV2 cells with miR-223 overexpression but increase with antagomir treatment. This suggests that miR-223 regulates autophagy by targeting the 3′UTR of ATG16L1, and that autophagy levels can be restored to normal by overexpressing ATG16L1, even in the presence of miR-223 mimics (Li et al., 2019b). Another study suggests that miR-223-3p expression and related cytokine levels could serve as predictors of response to ECT in individuals with treatment-resistant depressive

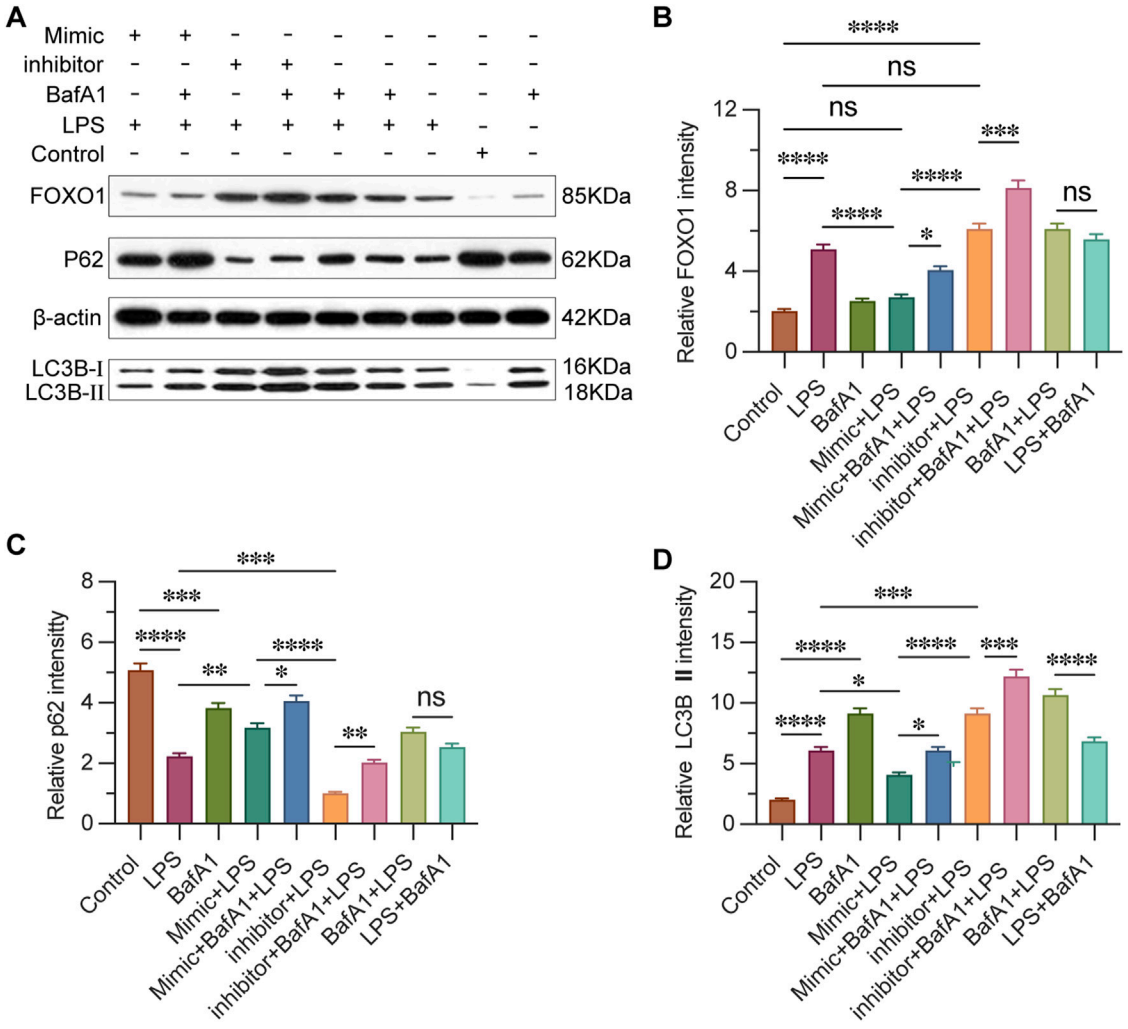


FIGURE 7
miR-223 affects the expression of FOXO1, autophagy-related proteins. **(A)** Western blot analysis of the expression of FOXO1 and autophagy-related proteins. **(B)** Results are reported as relative intensity values of FOXO1 in each group. **(C)** Results are reported as relative intensity values of p62 in each group. **(D)** Results are reported as relative intensity values of LC3B II in each group. β-actin was used as the loading control. Results are represented as mean ± SEM, n = 3. *, **$p < 0.05$, **$p < 0.01$, ***$p < 0.001$, ****$p < 0.0001$, ns $p > 0.05$.

disorders. They confirm that ROC analysis of confirmed the diagnostic power of miR-223-3p demarcating ECT-responders from non-responder subjects (AUC = 0.76, $p = 0.0031$) (Kaurani et al., 2023). As gene therapy technology advances, the clinical value of miR-223 is expected to become increasingly apparent. Despite the absence of current clinical trials examining the clinical value of miR-223, its therapeutic potential to target inflammatory pathways is emphasized as a means to counteract excessive innate immune responses during mucosal inflammation.

Transgenic miR-223-/Y mice administrated intraperitoneal or intravenous LPS, in order to establish sepsis, exhibited a larger extent of tissue damage compared to that of the controls (Johnnidis et al., 2008). It is interesting to note that miR-223 is expressed at low levels during sepsis. The negative correlation between miR-223 expression and the incidence of sepsis suggests miR-223 downregulation is vital to the development of inflammation and infection in sepsis (Wang et al., 2010). A similar link between miR-223 expression and autophagy levels are seen in patients with atherosclerosis obliterans. As the expression of miR-223 decreases, vascular smooth muscle cells lose the ability to induce cellular autophagy and evolve into foam cells. However, the underlying mechanism of miR-223-mediated regulation of autophagy in $CD4^+$ T lymphocytes autophagy and its impact on the prognosis of the disease remains unknown.

LPS is the main pathogenic component of gram-negative bacilli, and it often causes systemic inflammation, blood hypercoagulation, hypothermia, and other fatal complications. Intraperitoneal injection of LPS is a classical method to induce sepsis in mice (Doi et al., 2009; Dejager et al., 2011). The classic pathogenic mechanism of LPS involves the activation of innate immune cells, like macrophages, to secrete inflammatory cytokines through activation of the toll-like receptor 4 (TLR4), including TNF-α, IL-1 β, IL-6, IL-12, and IFN-γ (Li C. C. et al., 2015). Additionally, LPS has pro-inflammatory effects, triggering pulmonary inflammatory responses through nitrogen oxide-dependent redox signaling in pulmonary endothelial cells

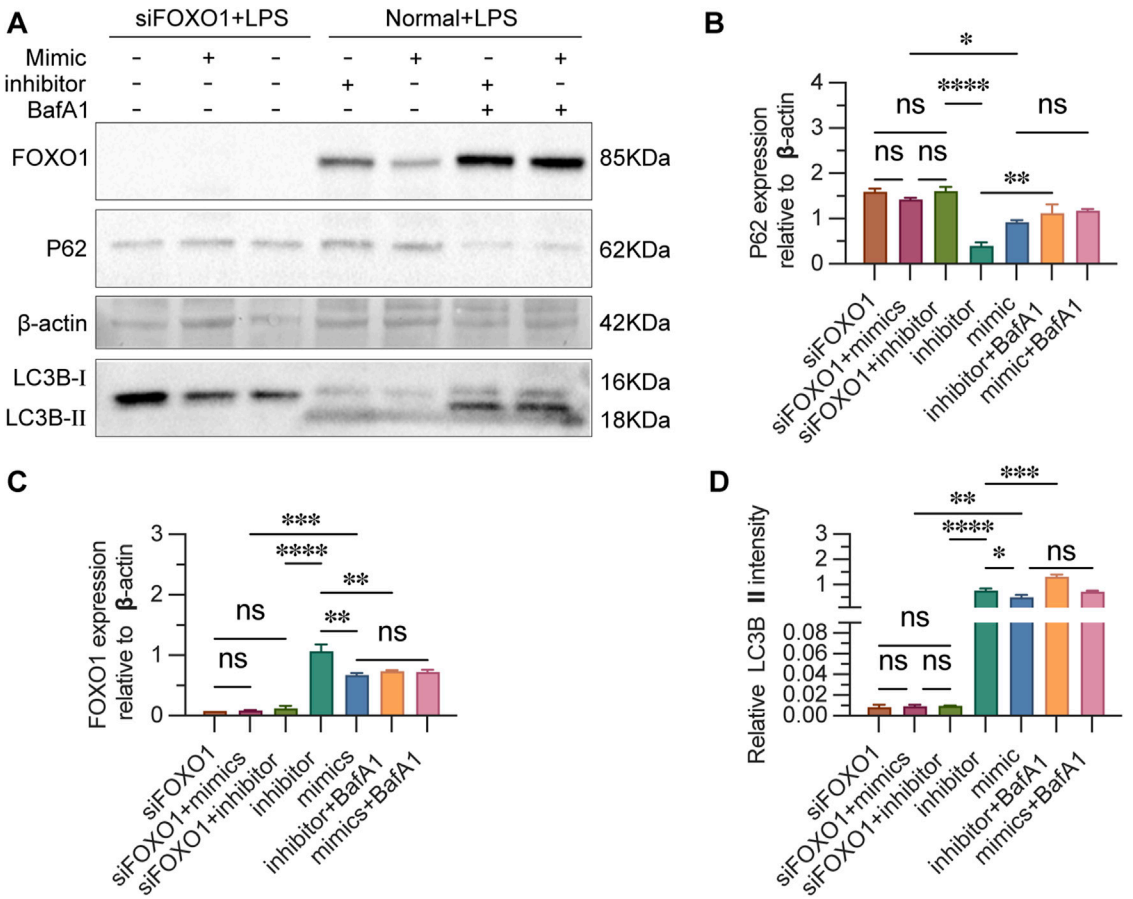


FIGURE 8
Estimation of FOXO1 and autophagy-related proteins after si-FOXO1 transfection. **(A)** Western blot analysis of the expression of FOXO1 and autophagy-related proteins. **(B)** The results are reported as the relative intensity values of p62in each group. **(C)** The ratios are reported as the intensity values of FOXO1 in each group. **(D)** The results are reported as the relative intensity values of LC3B II in each group. β-actin was used as the loading control. Results are represented as mean ± SEM, n = 3. *$p < 0.05$, **$p < 0.01$, ***$p < 0.001$, ****$p < 0.0001$, ns $p > 0.05$.

(Menden et al., 2013), perturbing airway function, and pulmonary circulation in mice (Ni et al., 2012; Lin et al., 2015). Thus, LPS is widely used to induce systemic inflammation in animal models. Of note, the effect of LPS on cell viability is double-sided. Not only proliferation inhibition from LPS is well known, but also promotion of LPS on cellular proliferation and survival was also reported. It was because that LPS could play a role in the cell pyroptosis, which has a close relationship with acute lung injury, therefore LPS is investigated as a therapy of cancer with its inhibition of cellular proliferation and apoptosis promotion through the caspase-11/NLRP3 inflammasome pathway (Li et al., 2019a). Similarly, Shigetoshi Yokoyama etc,. raised that LPS-triggered acute inflammation decreases the proliferative ability of T cells (Hsiung et al., 2020). On the other hand, a study focused on *helicobacter* pylori-induced human gastric mucosa diseases revealed that LPS could induce more intense cell proliferation in chronic inflection (4 weeks) than that in acute inflammation (1 week) (Massarrat et al., 2016). Overall, LPS, indeed, has the ability to induce the cellular proliferation especially for chronic infection and the cellular inhibition of LPS are easily observed in acute pathological changes. Furthermore, in our study, the CD4+ T cells were analyzed after 18 h 1 μg/mL LPS challenge, and the inhibition of cells proliferation was observed consequently, which agrees with the outcome observed in acute inflammatory models.

FOXO1, a key transcription factor in apoptosis, induces the expression of membrane-associated proteins like the FAS ligand and the TNF-related apoptosis-inducing ligand (TRAIL), which activate the death receptor and subsequently caspase 8, thereby initiating the extrinsic apoptosis pathway. Furthermore, FOXO1 can indirectly inhibit the pro-survival protein Bcl-XL, a member of the BCL-2 family, leading to increased mitochondrial permeability and the activation of the intrinsic apoptosis pathway. Notably, Beclin-1, a protein that promotes autophagy, can interact with BCL-2, thereby inhibiting Beclin-1-mediated autophagy. Additionally, FOXO1 indirectly regulates other proteins of the BCL-2 family, influencing the balance between autophagy and apoptosis (Fu and Tindall, 2008). In addition, studies have reported the regulation of cell apoptosis by the PI3K/AKT/FOXO1 pathway, thereby affecting the pathology of many diseases (Du et al., 2020).

Thus, we are the first study to report the effect of different expression levels of miR-223 on the level of autophagy in $CD4^+$ T lymphocytes. Regulation of the autophagy in $CD4^+$ T lymphocytes by miR-223 establishes a potential target for treating sepsis. However, our study suffers from a few limitations, including the fact that the results of this experiment are from an *in vitro* system

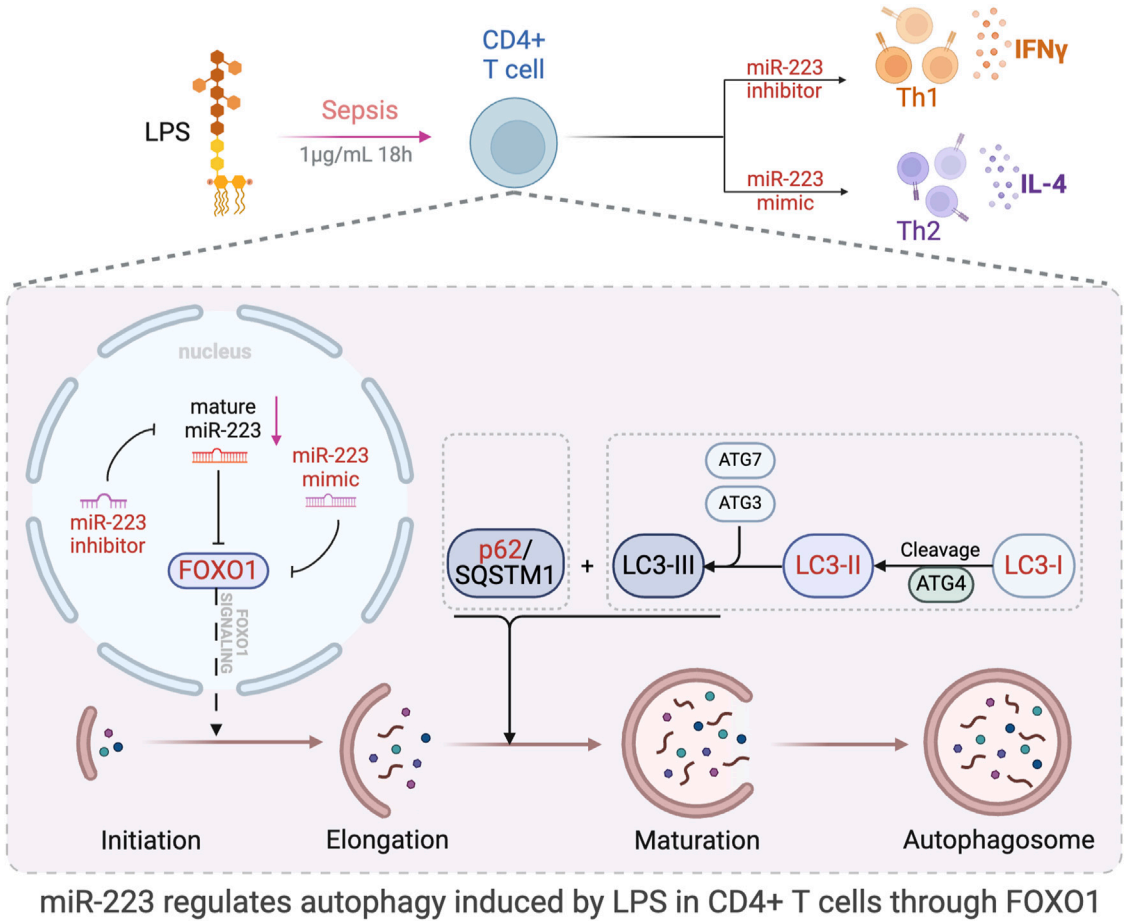


FIGURE 9
Schematic representation of the study and results. The figure was created in part using BioRender.com. Model of the effect of miR-223 regulation of autophagy through direct targeting of FOXO1. This study proved that miR-223 participate in the regulation of LPS-induced autophagy via the regulation of FOXO1 expression in CD4⁺ T lymphocytes.

and should be verified *in vivo*. Further, we have only suggested a linear mechanism for the miR-223-mediated regulation of CD4⁺ T lymphocyte function. Further investigations are required to uncover the nuances of this regulation. Therefore, we demonstrate that miR-223 affects the level of autophagy in CD4⁺ T lymphocytes via the regulation of FOXO1, thereby affecting the development of sepsis.

5 Conclusion

This study proves that miR-223 participate in the regulation of LPS-induced autophagy via the regulation of FOXO1 expression in CD4⁺ T lymphocytes which shed a new light for the diagnosis and treatment of sepsis.

Data availability statement

The original contributions presented in the study are included in the article/Supplementary Material, further inquiries can be directed to the corresponding authors.

Ethics statement

The animal study was approved by Research Ethics Committee of the Institute of Microbiology, Chinese Academy of Sciences. The study was conducted in accordance with the local legislation and institutional requirements.

Author contributions

GX: Writing–original draft, Validation, Methodology, Investigation, Formal Analysis, Data curation, Conceptualization. QL: Writing–original draft, Project administration, Methodology, Investigation, Funding acquisition, Formal Analysis, Data curation. DL: Writing–review and editing, Formal Analysis. CS: Writing–original draft, Investigation, Data curation. XL: Writing–review and editing, Investigation, Formal Analysis. SD: Writing–review and editing, Conceptualization. LX: Writing–review and editing, Validation, Project administration, Funding acquisition, Data curation, Conceptualization.

Funding

The author(s) declare that financial support was received for the research, authorship, and/or publication of this article. This work was supported by the National Natural Science Foundation of China (82172109) and Beijing Tongzhou District Science and Technology Plan (KJ2023CX052).

Conflict of interest

The authors declare that the research was conducted in the absence of any commercial or financial relationships that could be construed as a potential conflict of interest.

Publisher's note

All claims expressed in this article are solely those of the authors and do not necessarily represent those of their affiliated organizations, or those of the publisher, the editors and the reviewers. Any product that may be evaluated in this article, or claim that may be made by its manufacturer, is not guaranteed or endorsed by the publisher.

Supplementary material

The Supplementary Material for this article can be found online at: https://www.frontiersin.org/articles/10.3389/fphar.2024.1469286/full#supplementary-material

References

Bermejo-Martin, J. F., Andaluz-Ojeda, D., Almansa, R., Gandia, F., Gomez-Herreras, J. I., Gomez-Sanchez, E., et al. (2016). Defining immunological dysfunction in sepsis: a requisite tool for precision medicine. *J. Infect.* 72 (5), 525–536. doi:10.1016/j.jinf.2016.01.010

Boomer, J. S., Green, J. M., and Hotchkiss, R. S. (2014). The changing immune system in sepsis: is individualized immuno-modulatory therapy the answer?. *Virulence* 5 (1), 45–56. doi:10.4161/viru.26516

Dejager, L., Pinheiro, I., Dejonckheere, E., and Libert, C. (2011). Cecal ligation and puncture: the gold standard model for polymicrobial sepsis?. *Trends Microbiol.* 19 (4), 198–208. doi:10.1016/j.tim.2011.01.001

Delano, M. J., and Ward, P. A. (2016). Sepsis-induced immune dysfunction: can immune therapies reduce mortality?. *J. Clin. Invest* 126 (1), 23–31. doi:10.1172/JCI82224

Doi, K., Leelahavanichkul, A., Yuen, P. S., and Star, R. A. (2009). Animal models of sepsis and sepsis-induced kidney injury. *J. Clin. Invest* 119 (10), 2868–2878. doi:10.1172/JCI39421

Du, L. J., Pang, B., Tan, Y. M., Yang, Y. N., Zhang, M. Z., Pang, Q., et al. (2020). Banxia xiexin decoction ameliorates t-BHP-induced apoptosis in pancreatic beta cells by activating the PI3K/AKT/FOXO1 signaling pathway. *J. Diabetes Res.* 2020, 3695689. doi:10.1155/2020/3695689

Fasseu, M., Treton, X., Guichard, C., Pedruzzi, E., Cazals-Hatem, D., Richard, C., et al. (2010). Identification of restricted subsets of mature microRNA abnormally expressed in inactive colonic mucosa of patients with inflammatory bowel disease. *PLoS One* 5 (10), e13160. doi:10.1371/journal.pone.0013160

Franks, Z., Carlisle, M., and Rondina, M. T. (2015). Current challenges in understanding immune cell functions during septic syndromes. *BMC Immunol.* 16, 11. doi:10.1186/s12865-015-0073-4

Fu, Z., and Tindall, D. J. (2008). FOXOs, cancer and regulation of apoptosis. *Oncogene* 27 (16), 2312–2319. doi:10.1038/onc.2008.24

Haneklaus, M., Gerlic, M., O'Neill, L. A., and Masters, S. L. (2013). miR-223: infection, inflammation and cancer. *J. Intern Med.* 274 (3), 215–226. doi:10.1111/joim.12099

Hotchkiss, R. S., Monneret, G., and Payen, D. (2013a). Immunosuppression in sepsis: a novel understanding of the disorder and a new therapeutic approach. *Lancet Infect. Dis.* 13 (3), 260–268. doi:10.1016/S1473-3099(13)70001-X

Hotchkiss, R. S., Monneret, G., and Payen, D. (2013b). Sepsis-induced immunosuppression: from cellular dysfunctions to immunotherapy. *Nat. Rev. Immunol.* 13 (12), 862–874. doi:10.1038/nri3552

Hotchkiss, R. S., and Sherwood, E. R. (2015). Immunology. Getting sepsis therapy right. *Science* 347 (6227), 1201–1202. doi:10.1126/science.aaa8334

Hsiung, S., Moro, A., Ban, Y., Chen, X., Savio, A. S., Hernandez, R., et al. (2020). Acute lipopolysaccharide-induced inflammation lowers IL-2R signaling and the proliferative potential of regulatory T cells. *Immunohorizons* 4 (12), 809–824. doi:10.4049/immunohorizons.2000099

Johnnidis, J. B., Harris, M. H., Wheeler, R. T., Stehling-Sun, S., Lam, M. H., Kirak, O., et al. (2008). Regulation of progenitor cell proliferation and granulocyte function by microRNA-223. *Nature* 451 (7182), 1125–1129. doi:10.1038/nature06607

Kaurani, L., Besse, M., Methfessel, I., Methi, A., Zhou, J., Pradhan, R., et al. (2023). Baseline levels of miR-223-3p correlate with the effectiveness of electroconvulsive therapy in patients with major depression. *Transl. Psychiatry* 13 (1), 294. doi:10.1038/s41398-023-02582-4

Li, C. C., Munitic, I., Mittelstadt, P. R., Castro, E., and Ashwell, J. D. (2015). Suppression of dendritic cell-derived IL-12 by endogenous glucocorticoids is protective in LPS-induced sepsis. *PLoS Biol.* 13 (10), e1002269. doi:10.1371/journal.pbio.1002269

Li, J., Li, M., Su, L., Wang, H., Xiao, K., Deng, J., et al. (2015). Alterations of T helper lymphocyte subpopulations in sepsis, severe sepsis, and septic shock: a prospective observational study. *Inflammation* 38 (3), 995–1002. doi:10.1007/s10753-014-0063-3

Li, Y., Song, D., Bo, F., Deng, M., and Tang, X. (2019a). Diazepam inhibited lipopolysaccharide (LPS)-induced pyroptotic cell death and alleviated pulmonary fibrosis in mice by specifically activating GABAA receptor α4-subunit. *Biomed. Pharmacother.* 118, 109239. doi:10.1016/j.biopha.2019.109239

Li, Y., Zhou, D., Ren, Y., Zhang, Z., Guo, X., Ma, M., et al. (2019b). Mir223 restrains autophagy and promotes CNS inflammation by targeting ATG16L1. *Autophagy* 15 (3), 478–492. doi:10.1080/15548627.2018.1522467

Lin, M. H., Chen, M. C., Chen, T. H., Chang, H. Y., and Chou, T. C. (2015). Magnolol ameliorates lipopolysaccharide-induced acute lung injury in rats through PPAR-gamma-dependent inhibition of NF-kB activation. *Int. Immunopharmacol.* 28 (1), 270–278. doi:10.1016/j.intimp.2015.05.051

Luan, Y. Y., Yao, Y. M., Xiao, X. Z., and Sheng, Z. Y. (2015). Insights into the apoptotic death of immune cells in sepsis. *J. Interferon Cytokine Res.* 35 (1), 17–22. doi:10.1089/jir.2014.0069

Massarrat, S., Saniee, P., Siavoshi, F., Mokhtari, R., Mansour-Ghanaei, F., and Khalili-Samani, S. (2016). The effect of helicobacter pylori infection, aging, and consumption of proton pump inhibitor on fungal colonization in the stomach of dyspeptic patients. *Front. Microbiol.* 7, 801. doi:10.3389/fmicb.2016.00801

Menden, H., Tate, E., Hogg, N., and Sampath, V. (2013). LPS-mediated endothelial activation in pulmonary endothelial cells: role of Nox2-dependent IKK-β phosphorylation. *Am. J. Physiol. Lung Cell Mol. Physiol.* 304 (6), L445–L455. doi:10.1152/ajplung.00261.2012

Ni, Y. F., Jiang, T., Cheng, Q. S., Gu, Z. P., Zhu, Y. F., Zhang, Z. P., et al. (2012). Protective effect of magnolol on lipopolysaccharide-induced acute lung injury in mice. *Inflammation* 35 (6), 1860–1866. doi:10.1007/s10753-012-9507-9

Seymour, C. W., Liu, V. X., Iwashyna, T. J., Brunkhorst, F. M., Rea, T. D., Scherag, A., et al. (2016). Assessment of clinical criteria for sepsis: for the third international consensus definitions for sepsis and septic shock (Sepsis-3). *JAMA* 315 (8), 762–774. doi:10.1001/jama.2016.0288

Shankar-Hari, M., Bertolini, G., Brunkhorst, F. M., Bellomo, R., Annane, D., Deutschman, C. S., et al. (2015). Judging quality of current septic shock definitions and criteria. *Crit. Care* 19, 445. doi:10.1186/s13054-015-1164-6

Stevenson, E. K., Rubenstein, A. R., Radin, G. T., Wiener, R. S., and Walkey, A. J. (2014). Two decades of mortality trends among patients with severe sepsis: a comparative meta-analysis. *Crit. Care Med.* 42 (3), 625–631. doi:10.1097/CCM.0000000000000026

Stieglitz, D., Schmid, T., Chhabra, N. F., Echtenacher, B., Mannel, D. N., and Mostbock, S. (2015). TNF and regulatory T cells are critical for sepsis-induced suppression of T cells. *Immun. Inflamm. Dis.* 3 (4), 374–385. doi:10.1002/iid3.75

Walkey, A. J., Lagu, T., and Lindenauer, P. K. (2015). Trends in sepsis and infection sources in the United States. A population-based study. *Ann. Am. Thorac. Soc.* 12 (2), 216–220. doi:10.1513/AnnalsATS.201411-498BC

Wang, H., Li, X., Zhang, Q., Fu, C., Jiang, W., Xue, J., et al. (2023). Autophagy in disease onset and progression. *Aging Dis.* 15, 1646–1671. doi:10.14336/AD.2023.0815

Wang, H., Zhang, P., Chen, W., Feng, D., Jia, Y., and Xie, L. (2012). Serum microRNA signatures identified by Solexa sequencing predict sepsis patients' mortality: a prospective observational study. *PLoS One* 7 (6), e38885. doi:10.1371/journal.pone.0038885

Wang, H. J., Wang, B. Z., Zhang, P. J., Deng, J., Zhao, Z. R., Zhang, X., et al. (2014). Identification of four novel serum protein biomarkers in sepsis patients encoded by target genes of sepsis-related miRNAs. *Clin. Sci. (Lond)* 126 (12), 857–867. doi:10.1042/CS20130301

Wang, J. F., Yu, M. L., Yu, G., Bian, J. J., Deng, X. M., Wan, X. J., et al. (2010). Serum miR-146a and miR-223 as potential new biomarkers for sepsis. *Biochem. Biophys. Res. Commun.* 394 (1), 184–188. doi:10.1016/j.bbrc.2010.02.145

Yoshii, S. R., and Mizushima, N. (2017). Monitoring and measuring autophagy. *Int. J. Mol. Sci.* 18 (9), 1865. doi:10.3390/ijms18091865

frontiers | Frontiers in Pharmacology

TYPE Original Research
PUBLISHED 09 October 2024
DOI 10.3389/fphar.2024.1448136

Check for updates

OPEN ACCESS

EDITED BY
Alice Conigliaro,
University of Palermo, Italy

REVIEWED BY
Ana Fernanda Castillo,
University of Buenos Aires, Argentina
Simona Ronchetti,
University of Perugia, Italy

*CORRESPONDENCE
Marianna Lucafò,
mlucafo@units.it

†These authors have contributed equally to this work and share first authorship

RECEIVED 12 June 2024
ACCEPTED 25 September 2024
PUBLISHED 09 October 2024

CITATION
Curci D, Stankovic B, Kotur N, Pugnetti L, Gasic V, Romano M, Zukic B, Decorti G, Stocco G, Lucafò M and Pavlovic S (2024) The long non-coding RNA GAS5 contributes to the suppression of inflammatory responses by inhibiting NF-κB activity.
Front. Pharmacol. 15:1448136.
doi: 10.3389/fphar.2024.1448136

COPYRIGHT
© 2024 Curci, Stankovic, Kotur, Pugnetti, Gasic, Romano, Zukic, Decorti, Stocco, Lucafò and Pavlovic. This is an open-access article distributed under the terms of the Creative Commons Attribution License (CC BY). The use, distribution or reproduction in other forums is permitted, provided the original author(s) and the copyright owner(s) are credited and that the original publication in this journal is cited, in accordance with accepted academic practice. No use, distribution or reproduction is permitted which does not comply with these terms.

The long non-coding RNA GAS5 contributes to the suppression of inflammatory responses by inhibiting NF-κB activity

Debora Curci[1†], Biljana Stankovic[2†], Nikola Kotur[2], Letizia Pugnetti[1], Vladimir Gasic[2], Maurizio Romano[3], Branka Zukic[2], Giuliana Decorti[4], Gabriele Stocco[1,4], Marianna Lucafò[3]* and Sonja Pavlovic[2]

[1]Laboratory of Advanced Translational Diagnostics, Institute for Maternal and Child Health IRCCS "Burlo Garofolo", Trieste, Italy, [2]Group for Molecular Biomedicine, Department of Human Molecular Genetics and Genomics, Institute of Molecular Genetics and Genetic Engineering, University of Belgrade, Belgrade, Serbia, [3]Department of Life Sciences, University of Trieste, Trieste, Italy, [4]Department of Medicine Surgery and Health Sciences, University of Trieste, Trieste, Italy

Introduction: Nuclear factor kappa B (NF-κB) is a key regulator of immune and inflammatory responses. Glucocorticoid drugs (GC) act through the glucocorticoid receptor (GR) as immunosuppressant also in pediatric patients inhibiting NF-κB activity. The long non-coding RNA GAS5 interacts with the GR, influencing GC activity. No data on the role of GAS5 on GR-dependent inhibition of NF-κB activity have been published.

Methods: This study investigated the impact of GAS5 on NF-κB activity in HeLa cells overexpressing GAS5, both under basal conditions and during GC treatment. The study used EMSA, RNA-immunoprecipitation (RIP), Western blotting, and bioinformatic analyses to assess NF-κB DNA binding, GAS5-p65 interaction, and NF-κB signaling pathway modulation.

Results: GAS5 overexpression increased NF-κB DNA binding activity in untreated cells. RNA-IP confirmed a direct interaction between GAS5 and the NF-κB subunit p65, suggesting a potential regulatory mechanism. GAS5 overexpression led to downregulation of NF-κB target genes, TNF-α, and NR3C1. GC treatment reduced NF-κB DNA binding activity in GAS5-overexpressing cells, indicating a potential synergistic effect. Furthermore, GAS5 overexpression increased IκB levels and reduced p-p65/pan-p65 levels during GC treatment.

Discussion: GAS5 appears to modulate NF-κB activity in a complex manner, influencing both basal and GC-induced signaling. The interaction between GAS5, GCs, and NF-κB is multi-faceted, and further research is needed to fully elucidate the underlying mechanisms. These findings suggest that GAS5 could be a potential target for personalized therapy, particularly in pediatric patients with inflammatory conditions.

KEYWORDS

lncRNA, Gas5, NF-κB, glucocorticoids, inflammation

1 Introduction

Nuclear factor kappa B (NF-κB) plays a central role in regulating immune and inflammatory responses. NF-κB is involved in the development and progression of health conditions associated with chronic inflammation, including type 2 diabetes, obesity, autoimmune disorders, and cancer (Capece et al., 2022). Proinflammatory signals, often conveyed via cytokines, such as tumor necrosis factor (TNF), lead to activation of NF-kB, which is typically a heterodimer of p50 and p65 subunits. In particular, upon receiving proinflammatory signals, IkappaB kinase (IKK) complex phosphorylates IkappaB (IkB), leading to its degradation. NF-κB is released from its inhibitor IkB and translocates to the nucleus, where it binds to DNA, and modulates the expression of target genes (Mulero et al., 2019). In addition, phosphorylation of the NF-κB p-65 subunit by IKK complex and other specific kinases is also essential for activation and fine-tuning of the NF-κB pathway (Christian et al., 2016; Kwon et al., 2016).

Treatment of many inflammatory and malignant diseases relies on glucocorticoid drugs (GC), which act through the glucocorticoid receptor (GR) as anti-inflammatory agents. When activated by GCs, the GR translocates from the cytoplasm into the nucleus and binds, through its DNA binding domain, the GC responsive elements in the regulatory regions of GC responsive genes. The activated GR can also suppress inflammatory signals by directly binding the NF-κB transcription factor, inhibiting its activity (Hudson et al., 2018). In addition to direct binding, the crosstalk between GR and NF-κB can manifest at various levels. This includes competing for binding to specific response element sequences within the promoters of target genes, or competition for a limited pool of coregulators, which may result in the repression of one of these transcription factors (Hudson et al., 2018; Gerber et al., 2021; Giridharan and Srinivasan, 2018).

Long non-coding RNAs (lncRNAs) have emerged as significant regulators of gene expression and hold promise as potential biomarkers for clinical applications. They possess modular domains enabling direct interaction with proteins, including transcription factors like NF-κB, thereby modulating inflammatory responses (Chew et al., 2018), immunity, cell proliferation, and survival (Ruland, 2011). The growth arrest-specific 5 (GAS5) gene encodes a lncRNA that functions as a riborepressor of the GR. Acting as a decoy, GAS5 binds to the GR, inhibiting its ability to recognize binding sites on the DNA of target genes (Kino et al., 2010), thus influencing GC activity and clinical drug response (Ruland, 2011; Gasic et al., 2018; Lucafo et al., 2015; Lucafò et al., 2016). Additionally, GAS5 has been demonstrated to interact with the NF-κB signaling pathway (Ji et al., 2022; Yang et al., 2022; Zhang et al., 2019). However, the precise mechanism of this interaction remains unclear.

Several studies have suggested that GAS5 is implicated in numerous types of cancer, such as leukemia, breast cancer, liver cancer, and lung cancer, as well as autoimmune diseases such as pediatric patients affected by inflammatory bowel disease (IBD) (Ji et al., 2022; Yang et al., 2022; Zhang et al., 2019; Lucafò et al., 2019). Indeed, this lncRNA may play a role in regulating inflammation, but the exact details of this mechanism are not yet fully understood (Lucafò et al., 2019; Xiao and Wang, 2023; Curci et al., 2024). To date, it is unknown if GAS5 has an impact on the GR-dependent repression of NF-κB activity and understanding its role in regulating the GAS5-GR-NF-κB network is of great significance. By understanding the mechanisms involved in this pathway, potential therapeutic targets can be identified and utilized in various diseases associated with inflammation.

The current study explored the influence of lncRNA GAS5 on NF-κB activity in HeLa cell line treated or not with GCs. The aim was to advance current understanding of the complex interplay between these molecular regulators and its role in inflammation.

2 Materials and methods

2.1 Cell line

The HeLa human cervical carcinoma (ATCC, CCL-2) cell line was grown in DMEM medium (Sigma-Aldrich, Milwaukee, WI, United States) supplemented with 10% FBS, 1% L-glutamine 200 mM, 1% penicillin 10,000 UI/mL and streptomycin 10 mg/mL. Cell culture was maintained according to standard procedures in a humidified incubator at 37 °C and with 5% CO_2.

2.2 Expression studies

Total RNA was extracted from HeLa cells in TRI reagent solution (Ambion Inc., Austin, TX, United States), following the manufacturer's instructions. The concentration and purity of RNA were measured spectrophotometrically at 260 and 280 nm. cDNA was synthesized from RNA using the RevertAid Reverse Transcriptase (Thermo Fisher Scientific, Waltham, MA, United States), following the manufacturer's instructions. GAS5 expression levels were quantified by real-time PCR (Applied Biosystems 7,900, Foster city, CA, United States) using the TaqMan gene expression assay kit (Thermo Fisher Scientific, Waltham, MA, United States). To normalize the obtained values, GAPDH gene expression was used as an internal control, using the TaqMan gene expression assay kit (Thermo Fisher Scientific, Waltham, MA, United States). The relative expression levels of GAS5 were calculated using the ΔΔCT method.

2.3 Transfection

For GAS5 plasmid transient transfection, Hela cells were seeded in 6-well plates at 3.5×10^5 per well. Twenty-four hours later, cells were transfected with the empty vector or the pcDNA3.1_GAS5 plasmid using Lipofectamine®2000 Transfection Reagent (Thermo Fisher Scientific, Waltham, MA, United States) according to the provided protocol. The amount of the plasmid DNA (pcDNA3.1_GAS5 construct and pcDNA3.1 empty) was 4 μg per well. The medium was replaced 5 h after the transfection.

2.4 Preparation of total and nuclear extracts

Total and nuclear extracts were prepared using HeLa cells transfected with the empty vector (pcDNA3.1) or the pcDNA3.1_GAS5 plasmid and treated with dexamethasone (DEXA) at the final concentration of 100 nM and 1 μM for 4 and 24 h at 37°C and 5% of CO_2 on the basis of the data published by Kino T. and colleagues

(Kino et al., 2010). To prepare the total lysate 100 µL of a lysis buffer with protease inhibitor cocktail 1× (Thermo Fisher Scientific, Waltham, MA, United States) was used, followed by sonication for 30 s and centrifugation at 10,000 ×g for 10 min. The supernatant contains the whole protein lysate.

To isolate nuclear proteins, cells were collected and resuspended on ice in 400 µL of cold buffer A: 10 mM HEPES [pH 7.9], 10 mM KCl, 0.1 mM EDTA, 0.1 mM EGTA, 1 mM DTT, and 0.5 mM PMSF. Cells were left on ice for 15 min and then 25 µL of 10% NP-40 was added. Samples were vortexed and centrifuged at maximum speed for 30 s. After that, the pellet, which contained cells' nuclei, was resuspended in 50 µL of cold buffer B (20 mM HEPES [pH 7.9], 0.4 M NaCl, 1 mM EDTA, 1 mM EGTA, 1 mM DTT, and 1 mM PMSF) and left on the shaking platform for 15 min at 4 °C.

The nuclei were collected by centrifugation at 13,000 rpm for 5 min at 4 °C. Concentration of the total and nuclear extract proteins was measured using the Bradford method (Bio-Rad Laboratories, Hercules, CA, United States), following the manufacturer's recommendations. Nuclear protein extracts were further used for electrophoretic mobility shift assay, while total protein extracts were used for Western blot analysis.

2.5 Electrophoretic mobility shift assay (EMSA)

DNA binding activity of NF-κB was analyzed using EMSA. In this method, a radioactively labeled double-stranded probe that contained NF-κB consensus sequence was incubated with nuclear extracts from HeLa cells. After incubation, formed DNA-protein complexes were analyzed using polyacrylamide gel electrophoresis (PAGE) and then their presence was detected by autography.

In EMSA experiments, 21bp length NF-κB probe was used after hybridization of sense and antisense oligonucleotides, from which sense oligonucleotide was previously radioactively labeled. The sequences of the oligonucleotides used for preparing the NF-κB probe were as follows.

- NF-kB_sense 5′- AGTTGAGGGGACTTTCCCAGG - 3′
- NF-kB_antisense 5' - CCTGGGAAAGTCCCCTCAACT - 3′

Ten pmol of NF-κB sense oligonucleotide was labelled at the 5′ end with 1.6 pmol of [γ-32^P] dATP (32^P, radioisotope phosphorus-32) using T4 polynucleotide kinase (Thermo Fisher Scientific, Waltham, MA, United States) at 37 °C for 45 min, according to the manufacturer's instructions. Afterwards, the excess of free radioactive nucleotides was eliminated using Sephadex G-50 columns (Sigma-Aldrich, Milwaukee, WI, United States). Labelled NF-kB_sense oligonucleotide was then completely dried in the vacuum centrifuge and dissolved in 25 µL of the annealing buffer (10 mM Tris-Cl pH 7.5, 50 mM NaCl, 10 mM $MgCl_2$, 1 mM EDTA, 1 mM DTT). Fifty pmol of the NF-kB_antisense oligonucleotide was added to the annealing mixture to ensure complete hybridization of the radioactively labelled sense oligonucleotide. Hybridization of the sense and antisense oligonucleotides was acquired after short denaturation at 90 °C for 3 min and renaturation at room temperature.

To enable DNA-protein binding, 3 µg of HeLa nuclear extract were incubated at 37°C for 30 min with 10,000 cpm of NF-κB probe in the presence of 50 ng of double-stranded nonspecific competitor Poly (dI-dC) (Sigma-Aldrich, Milwaukee, WI, United States). The binding reaction was performed in a 25 µL final volume with the 1× binding buffer (5 mM Tris-Cl pH 8.0, 25 mM NaCl, 0.5 mM DTT, 0.5 mM EDTA, 5% glycerol).

The EMSA reaction's specificity was shown through the addition of a specific competitor (a 10-fold molar excess of cold, unlabeled NF-κB probe) or by using 2 µg of anti-p65 antibody (Santa Cruz Biotechnologies, Dallas, TX, United States).

After incubation, the binding reaction was loaded on the 4% polyacrylamide gel, and electrophoresis was run using 250 V and 65 mA at 16°C for 1 h with 0.5% TBE. After PAGE, gel was dried and DNA-protein complexes were analyzed using Cyclone Phosphor Imager (Perkin Elmer, Waltham, MA, United States) and autoradiography (X-ray-sensitive films were exposed to the dried gels in the cassettes at −80°C for 24 h). Films were scanned in high resolution using transmission scanning and intensities of the formed complexes were quantified densitometrically with ImageJ software (Schneider et al., 2012).

2.6 RNA immunoprecipitation (RNA-IP)

HeLa cells lysates were obtained using the RIP buffer, composed of 20 mM HEPES pH 7.7 (Euroclone®, Pero (Mi), Italy), 150 mM NaCl, 0.5 mM EDTA, 1 mM DTT, 10% glycerol, 0.1% TritonX (Sigma-Aldrich, Milwaukee, WI, United States) with protease inhibitor cocktail (Thermo Fisher Scientific, Waltham, MA, United States). After an incubation of 30 min in ice, samples were centrifuged at 10,000 ×g for 20 min at 4°C to remove cell debris. The supernatant containing the whole protein lysate was incubated with Sepharose G Beads (1:1) (Sigma-Aldrich, Milwaukee, WI, United States) for 20 min at 4°C, for sample pre-clearing. After, beads were pelleted at 200 ×g for 30 min, and the supernatants were incubated overnight at 4°C in a solution with RIP buffer, 5 µg/mL heparin and the primary antibodies anti-P65 (Santa Cruz Biotechnologies, Dallas, TX, United States), and anti-IgG (Sigma-Aldrich, Milwaukee, WI, United States), as negative control. Sepharose G Beads were added to the samples and incubated for 4 h at 4 °C. At the end, samples were divided in two aliquots and then centrifuged at 1,000 rpm for 30 s. For the first aliquot, used for RNA isolation, the supernatant was removed, and beads were resuspended in 500 µL of RNA wash buffer (HGEN buffer with DOC 0.2% and urea 5 mM), incubated 10 min at 4°C with gentle rotation, then centrifuged for at 5,000 xg for 30 s, and repeated for a total of four washes. Beads were resuspended in TRIzol® reagent (Thermo Fisher Scientific, Waltham, MA, United States). Co-precipitated RNAs were isolated and quantitative reverse transcription PCR (real-time PCR) for GAS5 was performed. The second aliquot was used for Western blot to verify the immunoprecipitation of the protein of interest. Beads were washed three times in the Wash buffer (PBS 0.2% TritonX, all from Sigma-Aldrich, Milwaukee, WI, United States). Beads were then resuspended in Loading Buffer 4X (Thermo Fisher Scientific, Waltham, MA, United States) and protein (P65) was detected by Western blot analysis. The relative enrichment of one RNA-IP experiment was calculated by the ratio between IP mRNA levels and total lysate (INPUT) mRNA and normalized to negative control (anti-IgG).

2.7 Western blotting

Total cell extracts were prepared in RIPA buffer without SDS (150 mM NaCl, 50 mM Tris-HCl pH 8.0, 1 mM EDTA, 1% NP-40, 0.5% Na-deoxycholate) supplemented with protease inhibitor cocktail 1X (Thermo Fisher, Waltham, MA, United States). After sonication, protein concentrations were determined by BCA assay using bovine serum albumin as standard. Twenty μg of lysates were loaded on Sodium Dodecyl Sulphate–Polyacrylamide Gel Electrophoresis (SDS-PAGE) 4–12% gradient gels (NUPAGE 4%–12%, Bis-Tris Plus Gels, Thermo Fisher, Waltham, MA, United States) and transferred, in wet condition, onto a nitrocellulose membrane.

Afterwards, each sample was incubated with 5% milk solution in T-TBS (10 mM Tris-HCl pH 8, 150 mM NaCl; 0.1% Tween 20) for 1 h at 4°C on a rocking platform. After blocking, incubation with the following primary antibodies was performed overnight, at 4 C: anti p65 mouse 1:500 (Santa Cruz Biotechnologies, Dallas, TX, United States), anti-phospho p65 rabbit 1:1,000 (Ser536) (Cell Signaling Technologies, Danvers, MA, United States), anti-IKB rabbit 1:3,000 (Abcam, Cambridge, United Kingdom) anti-β-actin mouse 1:3,000 (Abcam). Anti-mouse (Cell Signaling Technologies, Danvers, MA, United States) and anti-rabbit HRP conjugated (OriGene Technologies, Rockville, MD, United States and Sigma-Aldrich, Milwaukee, WI, United States) secondary antibodies were incubated for 1 h at 4 °C. Proteins were detected by chemiluminescence using a ChemiDoc system (Bio-Rad Laboratories, Hercules, CA, United States) and the band's density was analyzed using the ImageJ program. All data were normalized on β-actin.

2.8 Bioinformatics analysis

To investigate the potential interactions between GAS5 and RELA (p65), the NPInter database (http://bigdata.ibp.ac.cn/npinter5/) (Zheng et al., 2023), which integrates RNA-protein interactions derived from various high-throughput data sources, was used. This analysis allowed us to explore the functional interaction between GAS5 and p65, providing evidence for a direct binding interaction between these molecules.

Additionally, to explore the role of RNA-binding proteins (RBPs) in facilitating the interaction between GAS5 and RELA, the ENCORI database (https://rnasysu.com/encori/) (Li et al., 2014), which offers comprehensive data on RNA-binding protein interactions based on CLIP-seq data was used. We retrieved the RBPs interacting with GAS5 from this database. To complement this analysis, the IntAct database (https://www.ebi.ac.uk/intact/) (Del Toro et al., 2022), a repository and analysis platform for molecular interaction data was used. We specifically interrogated this database to identify proteins interacting with p65. By overlapping the sets of RBPs interacting with GAS5 and p65, we identified shared RBPs that may mediate or stabilize the GAS5-p65 interaction.

2.9 Statistical analysis

Statistical analyses were performed using Graph-Pad Prism version 4.00 (GraphPad, La Jolla, CA, United States). Wilcoxon sign rank test was used for the EMSA analysis. T-test was used to analyze Western blot assay results and gene expression. p-values <0.05 were considered statistically significant.

3 Results

3.1 Effect of GAS5 on NF-κB DNA binding activity

We examined the effect of overexpressed GAS5 on NF-κB DNA binding activity in transfected HeLa cells using EMSA. The efficiency of the overexpression of the lncRNA in HeLa cells was assessed by real-time PCR after 4 and 24 h (Supplementary Figure S1). Additionally, we stimulated non-transfected HeLa cells with the proinflammatory cytokine TNF-α as a positive control for NF-κB signaling activation. EMSA showed nuclear protein:DNA complexes whose specificity was confirmed with competitive and supershift (anti-p65) assays (Supplementary Figure S2).

In HeLa cells transfected with pcDNA3.1_GAS5, we observed increased binding of NF-κB to DNA consensus probe compared to HeLa cells transfected with empty pcDNA3.1 (Figures 1A, B). A similar effect was observed in TNF-α-induced NF-κB activation in non-transfected HeLa cells. Our findings suggested GAS5 involvement in regulating the NF-κB pathway, enhancing the binding of this transcriptional factor to DNA.

3.2 Analysis of GAS5 and NF-κB interaction

The potential interaction between the lncRNA GAS5 and the NF-κB subunit p65 was further investigated using an RNA immunoprecipitation (RNA-IP) experiment in HeLa cells. The specificity of the immunoprecipitation assay was confirmed by the observation that the p65 protein was successfully isolated using a specific antibody (anti-p65) (Figure 2A, lane IP) but not using an IgG control antibody (anti-IgG) (Figure 2A, lane IgG). Subsequently, the presence of GAS5/p65 interaction was tested by RNA-IP followed by Real-Time PCR targeting GAS5 or the housekeeping gene GAPDH, to confirm the specific enrichment of the assay. The result clearly showed that GAS5 was present in the protein complex with p65, indicating a potential direct physical bond (Figure 2B).

3.3 In silico analysis of GAS5-p65 interaction

To explore the interaction between GAS5 and the NF-κB subunit p65/RELA, we carried out a series of bioinformatic analyses. Utilizing the NPInter database, which compiles RNA-protein interaction data from high-throughput sequencing techniques such as CLIP-seq, we identified a significant RNA-protein interaction between GAS5 and p65. This interaction, classified as a binding event (ID: ncRI-50112523), was detected in a CLIP-seq dataset (GSE197707), suggesting that GAS5 directly binds to p65. The functional annotation of this interaction indicates that GAS5 may play a role in the positive regulation of I-kappaB kinase/NF-kappaB signaling, implying a potential regulatory influence of GAS5 on NF-κB pathways through its interaction with p65.

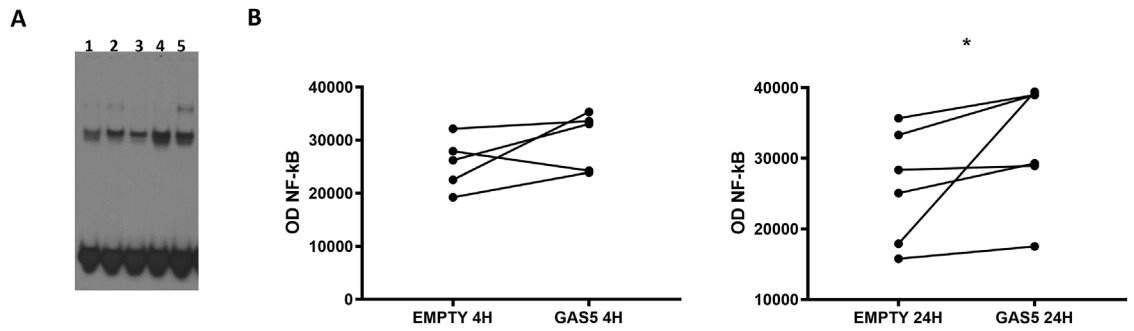


FIGURE 1
(A) Representative NF-κB EMSA analyses in HeLa cells transfected with empty pcDNA3.1 (lanes 1, 3) and pcDNA3.1_GAS5 (lanes 2, 4), after 4 (lanes 1, 2) and 24 h (lanes 3, 4) from transfection or treated with TNF-α (lane 5). EMSA experiments were performed in five to six replicates. **(B)** The optical density (OD) of the shifted bands was measured in all samples. Wilcoxon signed rank test, GAS5 vs. EMPTY 4H p-value = 0.187; GAS5 vs. EMPTY 24H p-value = 0.031.

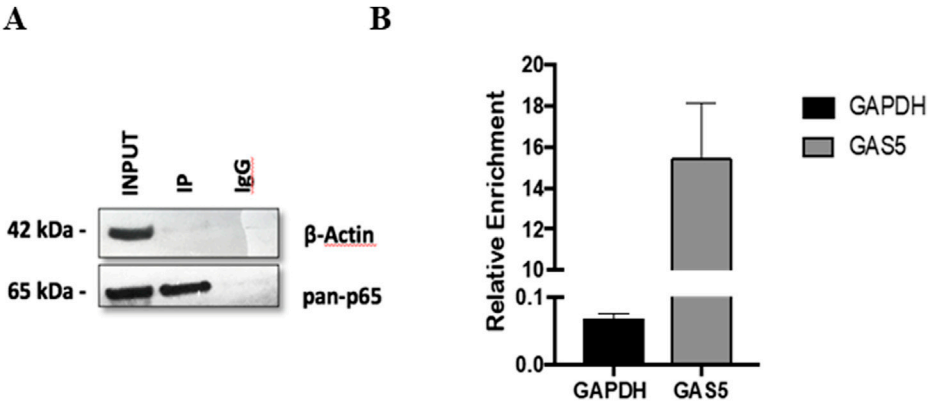


FIGURE 2
The protein-mRNA immune-complex with either anti-p65 or the control anti-IgG complexes were processed for immunoblotting **(A)** and for Real Time-PCR **(B)**. Total lysate (INPUT) was not subjected to immunoprecipitation. GAPDH mRNA was used as a control for RNA-IP specificity. The relative enrichment for GAS5 or GAPDH mRNA, reported in the graph, was calculated by the ratio between IP anti-p65 mRNA and INPUT mRNA (ΔCt = Ct_IP - Ct_Input), and normalized to negative control (IP anti-IgG) mRNA (ΔΔCt = ΔCT_IP - ΔCt_IgG. Relative enrichment, RE = $2^{-\Delta\Delta CT}$. Three experiments were conducted in total. WB image was from one representative experiment.

Given that RNA-protein interactions can be mediated or stabilized by RNA-binding proteins (RBPs), we further investigated the potential involvement of RBPs in the GAS5-p65 interaction. From the ENCORI database, we retrieved 222 RBPs that interact with GAS5. Similarly, the IntAct database provided a list of 89 RBPs that interact with RELA. Venn analysis identified 11 RBPs that are common interactors of both GAS5 and RELA, including AIFM1, DDX21, DHX9, FBL, HNRNPM, HNRNPU, NPM1, PARP1, RPS3, SFPQ, and VIM (Figure 3).

3.4 Effects of GAS5 on NF-κB target genes' expression

To further test the ability of GAS5 to modulate NF-κB activity, we compared the gene expression levels of several NF-κB target genes in GAS5-overexpressed cells (Figure 4). As shown in Figure 4A, no mRNA level changes were observed after 4 h in GAS5-overexpressing cells. After 24 h of transfection, NR3C1 and TNF were significantly downregulated when GAS5 was overexpressed in HeLa cells (Figure 4B).

3.5 Effects of GAS5 on GC-induced modulation of NF-κB DNA binding activity

Using EMSA, we evaluated the effect of overexpressed GAS5 on NF-κB DNA binding activity in transfected HeLa cells during the treatment with the GC dexamethasone (DEXA) at 100 nM and 1 μM for 4 and 24 h. We observed differences in the level of NF-κB DNA binding activity within samples measured at 4 h under control, 100 nM and 1 μM conditions in HeLa cells transfected both with empty and pcDNA3.1_GAS5 vector (p = 0.049 and p = 0.038, respectively), however, after *post hoc* pairwise comparisons, we found no differences between these conditions (Supplementary Figure S3). However, when observed relative to the cells

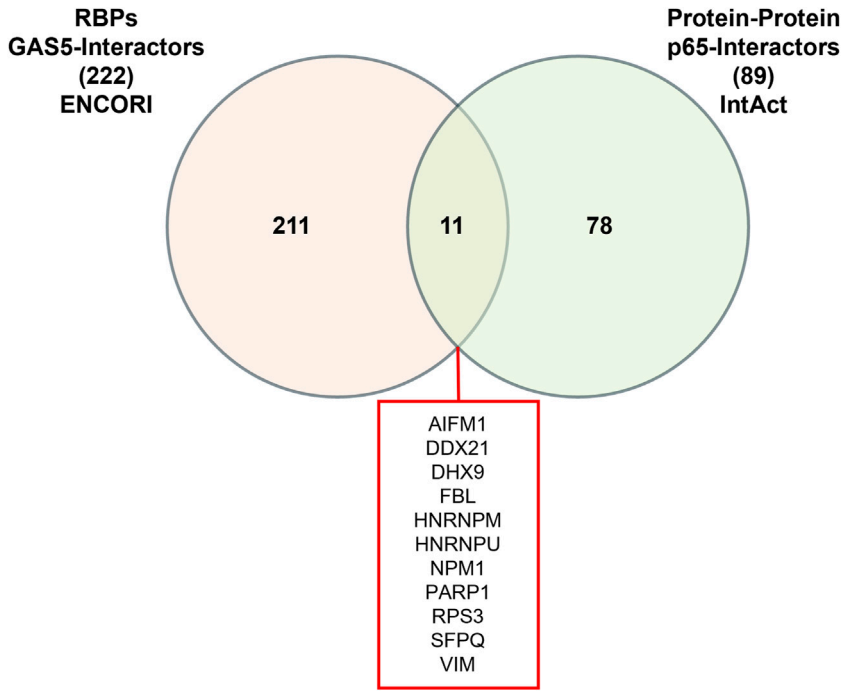


FIGURE 3
Venn Diagram of RNA-binding proteins (RBPs) interacting with GAS5 and p65.

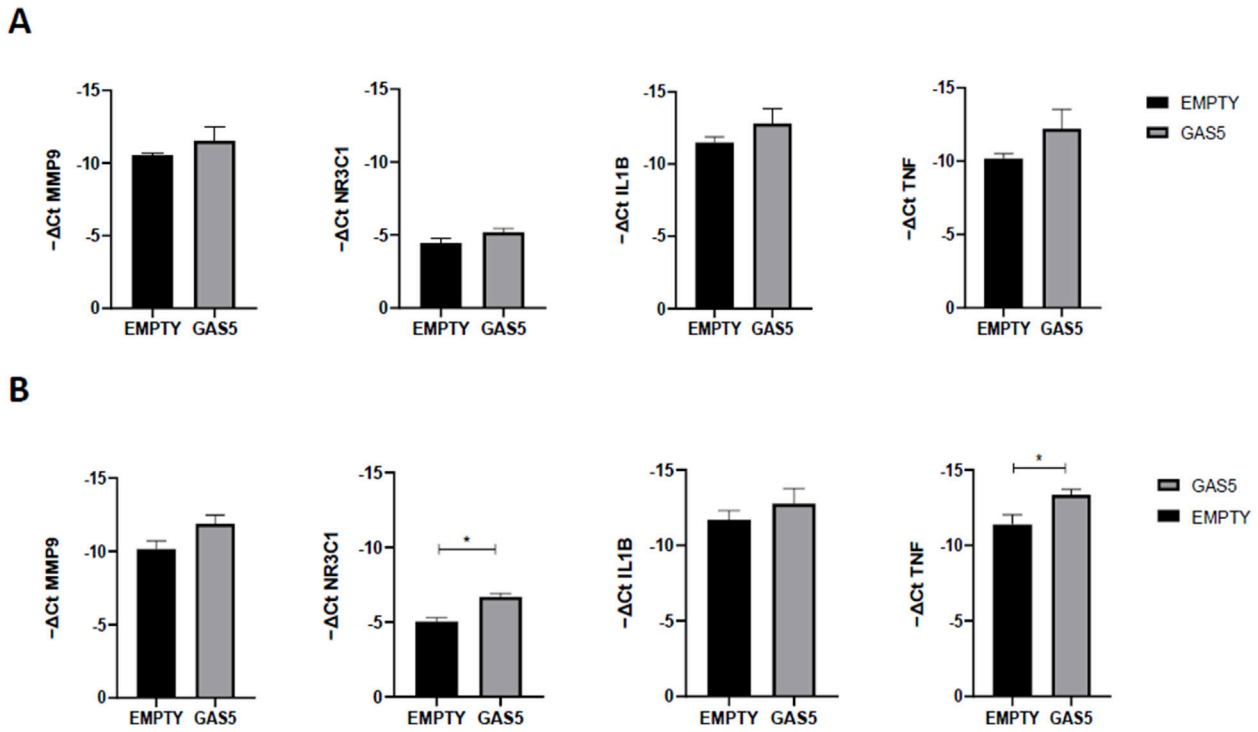


FIGURE 4
MMP9, NR3C1, IL1B, and TNF gene expression (-ΔCt) in HeLa cells transfected with pcDNA3.1_GAS5 (GAS5) or the empty pcDNA3.1 vector (EMPTY), after 4 **(A)** and 24 **(B)** hours. Gene expression was normalized using the expression of GAPDH gene. Unpaired t-test GAS5 vs. EMPTY at 4h and 24 h *$p < 0.05$, **$p < 0.01$. The data are reported as means ± SD of three independent experiments performed in triplicate.

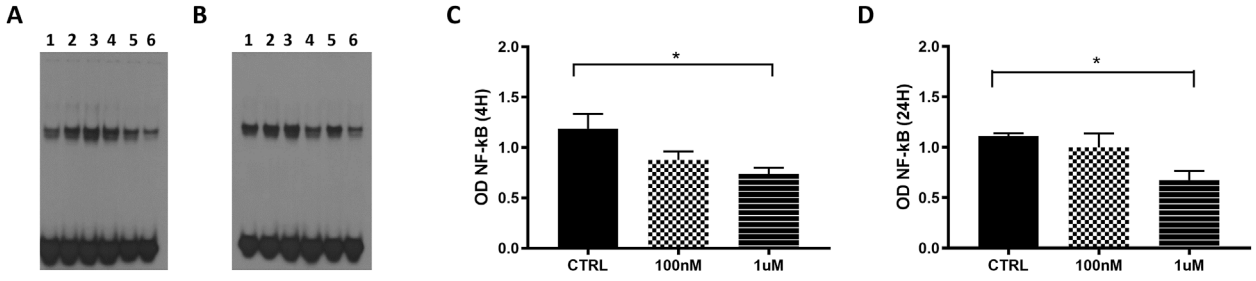


FIGURE 5
NF-κB EMSA analyses in HeLa cells transfected with empty pcDNA3.1 (lanes 1, 3 and 5) and pcDNA3.1_GAS5 (lanes 2, 4 and 6), treated with DEXA 100 nM (lanes 3 and 4), DEXA 1 μM (lanes 5 and 6) and untreated (CTRL, lines 1 and 2) after 4 h **(A)** and 24 h **(B)**. Nuclear extracts were prepared in triplicate. The EMSA produced optical densities (OD) of the shifted NF-κB bands were measured in all samples after 4 **(C)** and 24 h **(D)**. OD values of pcDNA3.1_GAS5 CTRL, DEXA 100 nM and DEXA 1 μM have been normalized by the OD value of corresponding empty pcDNA3.1. Kruskal–Wallis test, 4 h p-value = 0.036; 24 h p-value = 0.041; Dunn's Multiple Comparison Test *$p < 0.05$.

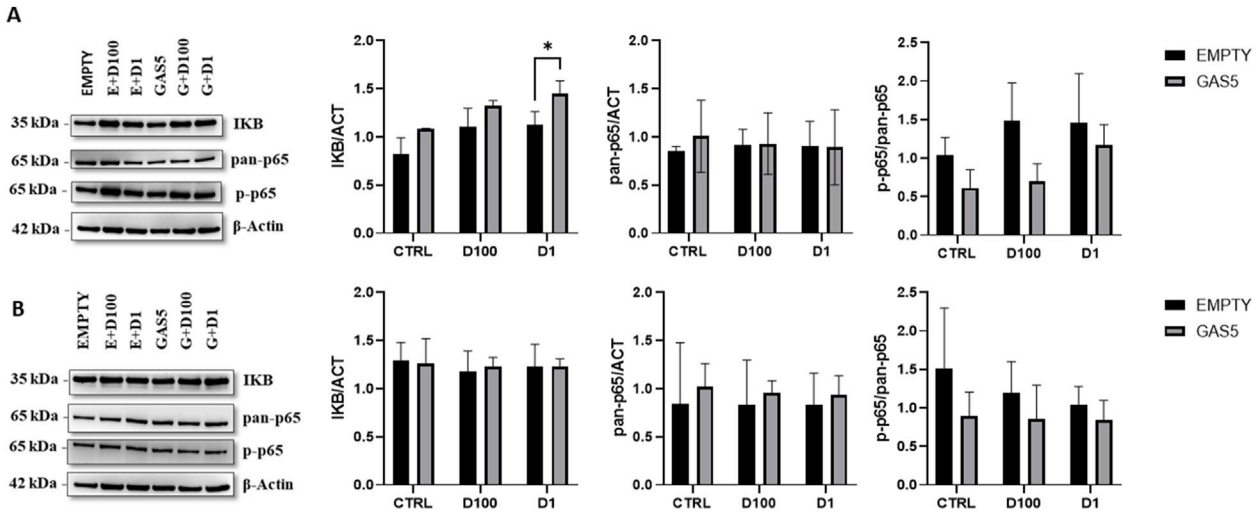


FIGURE 6
Representative Western blot and quantification histogram for protein levels of IKB, pan-p65, and p-p65 in untreated cells (CTRL) after 4 panel **(A)** and 24 h Panel **(B)** of treatment with 100nM and 1 μM of dexamethasone (D100 and D1). β-actin was used as internal control. The levels of p-p65 expression were expressed as p-p65/pan-p65 ratio. Panel A, 2-way ANOVA IKB/ACT: Row Factor (Treatment condition): $p = 0.002$, Column Factor (Empty and GAS): $p = 0.001$. Sidak's multiple comparisons test: *$p < 0.05$; pan-p65/ACT: Row Factor (Treatment condition): p = ns, Column Factor (Empty and GAS): p = ns, p-p65/pan-p65: Row Factor (Treatment condition): p = ns, Column Factor (Empty and GAS): $p = 0.017$. Panel B, 2-way ANOVA IKB/ACT: Row Factor (Treatment condition): p = ns, Column Factor (Empty and GAS): p = ns; pan-p65/ACT: Row Factor (Treatment condition): p = ns, Column Factor (Empty and GAS): p = ns, p-p65/pan-p65: Row Factor (Treatment condition): p = ns, Column Factor (Empty and GAS): p = ns. The data are reported as means ± SD of three independent experiments performed in triplicate.

transfected with the empty plasmid, in the cells transfected with pcDNA3.1_GAS5 construct, NF-κB DNA binding activity was decreased in response to DEXA treatment: statistically significant for 1 μM, but not for 100 nM DEXA treatment. The same trend was observed after both 4 and 24 h of DEXA treatment (Figure 5).

3.6 Effect of GAS5 on the p65 activation during GC treatment

To evaluate whether the effect of overexpressed GAS5 during GC treatment could alter p65 activation, we measured IKB levels, total p65 (pan-p65), and phospho-p65 (p-p65) levels in HeLa cells by Western blot. Levels of IKB protein increased significantly after 4 h of DEXA treatment in HeLa cells, particularly in GAS5-overexpressing cells (Figure 6A). Total p65 (pan-p65) did not change in cells after 4 h of GC incubation (Figure 6A). Furthermore, overexpression of GAS5 seems to reduce p-p65/pan-p65 ratio when compared to cells transfected with empty plasmid (Figure 6A). No significant change in protein levels after 24 h of DEXA treatment was observed for all proteins analyzed (Figure 6B).

4 Discussion

Dysregulation of NF-κB has been implicated in various inflammatory and autoimmune diseases, as well as cancer (Mao

et al., 2017). Activity of NF-κB signaling pathway is regulated by several factors including lncRNAs. For instance, NKILA and Lethe are lncRNAs known to impact NF-κB activity by inhibiting its DNA binding ability (Ghafouri-Fard et al., 2021; Liu et al., 2015). While several studies have investigated the interplay between the lncRNA GAS5 and NF-κB-related pathways, the precise regulatory mechanisms by which GAS5 affects NF-κB remain unclear. Our study, for the first time, showed increased DNA binding activity of NF-κB in HeLa cells overexpressing GAS5, confirming its involvement in regulating the NF-κB pathway. Moreover, the RNA-IP result highlighted the ability of GAS5 to bind p65 subunit and the identification of this interaction through the NPInter database, along with its classification as a binding interaction in CLIP-seq datasets, reinforces the hypothesis that GAS5 plays a regulatory role in the NF-κB signaling cascade. To gain deeper insights into the mechanisms underlying this interaction, our study also investigated the structural aspects of both GAS5 and p65. The Rel Homology Domain (RHD) of p65, known for its DNA-binding capability, may also have RNA-binding potential. The structural features of the RHD, particularly the immunoglobulin-like beta barrel subdomains, suggest a possible role in RNA recognition (Kaur et al., 2022; Lecoq et al., 2017). Although direct experimental evidence for p65's RNA-binding domain specifically recognizing GAS5 remains to be confirmed, there is substantial evidence supporting the interaction of NF-κB and its subunits with other lncRNAs (Shin et al., 2024). Future studies focusing on mutagenesis of the RHD will be essential to map the specific regions involved in RNA binding.

Moreover, our *in silico* identification of 11 RBPs that interact with both GAS5 and p65 opens new avenues for understanding the potential indirect interaction mechanisms. These RBPs could act as molecular bridges, facilitating or stabilizing the GAS5-p65 complex, thereby enhancing the regulatory effects of GAS5 on NF-κB signaling. Experimental validation through RBP knockdown or pull-down assays will be critical in determining the roles these proteins play in the GAS5-p65 interaction.

GAS5 is known to have a modular structure, with distinct regions that form specific secondary structures, which may be crucial for its interaction with proteins (Frank et al., 2020). Based on the available secondary structure of GAS5, considering that the 5′ end has low secondary structure content, both the core module (which is highly structured and mediates the effects of mammalian target of rapamycin inhibition on cell growth) and the 3′ end (which contains the steroid receptor binding module) are more likely to interact with proteins other than those already described (Frank et al., 2020).To elucidate the consequence of GAS5-p65 interaction, we tested gene expression of NF-κB target genes in overexpressing GAS5 cells and found downregulation of TNF-α, and NR3C1 after 24 h. These results could be in line with previous data published by Yang and colleagues, in which overexpression of GAS5 led to a reduction in the expression level of proinflammatory genes IL1β, IL6, and IL8 (Yang et al., 2022). Moreover, previous data have also shown that GAS5 overexpression is associated with a lower expression of TNFα, IL-1, IL-6, and IL-8 (Li et al., 2018). Interestingly, in our study NR3C1 is downregulated in overexpressing GAS5 cells. Even in the absence of GC, cytosolic GR has been shown to interact with p65, p50, and IκB, and inhibit nuclear translocation of NF-κB (Widén et al., 2003). Therefore, the observed decrease in GR mRNA upon GAS5 overexpression suggests that GAS5 may influence the mutual antagonism between GR and NF-κB and may be an important basis for GC resistance. These findings highlight the need for further investigation into the mechanisms by which GAS5 affects GR and NF-kB activity and its broader implications in therapeutics (Schaaf and Cidlowski, 2002).

Although the increased DNA binding of NF-kB should theoretically promote its transcriptional activity, the complexity and lack of knowledge about the mechanism of action of GAS5 and its interaction with NF-kB, cannot exclude the possibility that several co-regulators may influence the effects observed. The NF-κB family comprises five activating and repressive subunits that form functional homo- and heterodimers. In particular, the dimers containing the C-terminal transactivation domain (TAD) are capable of recruiting transcriptional co-activators, which promote gene expression; dimers without TADs act as transcriptional repressors (de Jesús and Ramakrishnan, 2020). The interaction between GAS5 and p65 could influence the dimer composition inhibiting the NF-kB transcriptional activity and further investigation should evaluate this possibility. Analyzing total protein extracts in GAS5 overexpressed compared to control HeLa cells, we showed diminished p-p65/pan-p65 levels and increased IκB expression. It has been reported that high levels of GAS5 reduced p-p65 expression, enhanced the level of IκB, and inhibited the entry of p65 into the nucleus within the TNF-α activated NF-κB pathway in periodontal ligament stem cells (Yang et al., 2022). Specific phosphatases could reduce p-p65 levels in GAS5 overexpressed cells (Cai et al., 2002; Tsuchiya et al., 2017), although the role of GAS5 in the regulation of phosphatases such as serine/threonine phosphatase (Protein phosphatase 2A) or Protein phosphatase one is currently unknown.

Interestingly, GAS5 was found bound to IKK and was positively related to IKK and negatively related to NF-κB activity in mouse mesangial cells (Zhang et al., 2019). These results could partly explain the mechanisms underlying the increase in IκB in GAS5-overexpressing cells: the inhibition of IKK activation by the lncRNA could favour the IκB accumulation by limiting its ubiquitin-mediated proteasomal degradation. It will therefore be important to assess the IKK levels and the ability of p65 to enter into the nucleus in our experimental model. We can hypothesise that the decrease in phosphorylation of p65 and its increase in DNA binding are independent and sequential events: GAS5 may rapidly inhibit the phosphorylation of p65, thereby affecting its activation and nuclear translocation, and subsequently alter its DNA-binding capacity. Future studies should focus on determining their temporal dynamics to fully understand how GAS5 modulates NF-κB signaling.

We further analyzed the effects of GAS5 on the NF-κB activity under GC treatment. In our EMSA, DEXA treatment reduced the ability of the transcription factor NF-κB to bind DNA in HeLa cells overexpressing GAS5. Downregulation of NF-κB DNA binding activity by GCs has been described in various studies (Auphan et al., 1995; He et al., 2017; Mukaida et al., 1994; Scheinman et al., 1995). To date, it is unknown if GAS5 could impact the GR-dependent repression of NF-κB activity, but it is already known that GAS5 binds to GR at the same domain, of which GR could interact with NF-κB (De Bosscher et al., 2003). Since GAS5 acts as a regulatory repressor of the GR, one would expect diminished

negative regulation of NF-κB-mediated transcription by DEXA in our model system. However, we observed a decrease in NF-κB DNA binding activity, suggesting the existence of possible alternative regulatory mechanisms. Decrease of NF-κB DNA binding activity in GAS5 overexpressed conditions during DEXA treatment could reflect displacement of NF-κB from its response elements or decreased activation of NF-κB in cytoplasm and its translocation to the nucleus. However, additional experiments should be performed to explain and confirm this mechanism.

Next, we explored whether GAS5 could modulate the protein expression of IκB and p65 during treatment with GCs. At 4 h of DEXA treatment, a significant increment of IκB protein after GC treatment in HeLa cells was found, as already reported in other studies (Auphan et al., 1995; Scheinman et al., 1995; He et al., 2020) where the increased expression of IκB has been proposed as the principal mechanism for the immunosuppressive GC effect (Newton et al., 1998). In our study, GC-related increase of IκB levels was higher in HeLa cells overexpressing GAS5 following treatment with DEXA, which implies that GAS5 may play a regulatory role in modulating the interaction between GCs and NF-κB. It is possible that GAS5 promotes the effects of GCs on IκB by reducing NF-κB activity. Additionally, the active form of p65 was lower in GAS5-overexpressing cells respect to the control. The phosphorylation of p65 subunit is necessary for cytoplasmic to nuclear localization of NF-κB/p65 and downstream target genes transcription (Christian et al., 2016). When inactive, NF-κB is bound to IκBα, which masks the nuclear localization signal of p65 reducing the rate of shuttling of NF-κB between the nucleus and cytoplasm. Interestingly, it has been shown that the exposure to GCs can increase NF-κB translocation to the nucleus, indicating that the effects of GCs on NF-κB pathway are environment-dependent and not related strictly to inhibition of NF-κB activation (Feng et al., 2019; Jong-Hun et al., 2019). In this context, the IκB and p-p65 levels during GAS5 overexpression in HeLa cells could not explain the decrease in DNA binding activity of NF-κB under GC treatment. Therefore, we hypothesize that mechanisms of GAS5 interference with the NF-κB pathway could be orchestrated independently of the GC pathway through potential direct interaction with p65, as demonstrated from the RIP experiments. However, further analysis of cells transfected with GAS5 in presence of a steroid treatment and after an inflammatory stimulation, such as TNF-α, should be performed to better understand the implication of NF-κB interaction.

In conclusion, our study showed that GAS5 presents distinct modulatory roles on the NF-κB pathway under basal and GC treatment conditions. GAS5 increases NF-κB DNA binding activity in non-treated cells, while decreasing it in GC-treated cells. The lncRNA GAS5 seems to physically interact with a member of the NF-κB family, p65, and influences the expression pattern of NF-κB-target genes. These results indicate that GAS5 could be considered a regulator of the NF-κB signaling pathway. Interaction between GAS5, GCs, and NF-κB is complex and probably involves more than one regulatory mechanism and further studies are therefore necessary. These regulatory mechanisms are most probably cell specific and should be examined in different conditions, such as models of diseases associated with dysregulated inflammatory responses, cell survival and apoptosis or poor GC therapeutic effects. These results could be useful for developing strategies to personalise therapy, particularly for pediatric patients.

Data availability statement

The original contributions presented in the study are included in the article/Supplementary Material, further inquiries can be directed to the corresponding author.

Author contributions

DC: Data curation, Formal Analysis, Investigation, Writing–original draft, Writing–review and editing, Conceptualization. BS: Conceptualization, Data curation, Formal Analysis, Investigation, Writing–original draft, Writing–review and editing. NK: Conceptualization, Data curation, Formal Analysis, Investigation, Writing–original draft, Writing–review and editing. LP: Data curation, Formal Analysis, Writing–original draft. VG: Data curation, Formal Analysis, Writing–original draft. MR: Data curation, Formal Analysis, Writing–original draft, Writing–review and editing, Supervision. BZ: Data curation, Writing–review and editing, Investigation. GD: Investigation, Writing–review and editing, Funding acquisition, Resources, Supervision. GS: Investigation, Writing–review and editing, Formal Analysis, Funding acquisition, Resources, Supervision. ML: Investigation, Writing–review and editing, Conceptualization, Data curation, Formal Analysis, Writing–original draft, Resources, Supervision. SP: Investigation, Writing–review and editing, Conceptualization, Funding acquisition, Project administration, Resources, Supervision.

Funding

The author(s) declare that financial support was received for the research, authorship, and/or publication of this article. This work was supported by the Italian Ministry of Health, through the contribution given to the Institute for Maternal and Child Health IRCCS Burlo Garofolo, Trieste, Italy (RC 15/23) and by the Ministry of Science and Technological Development, Republic of Serbia (III41004) and The Ministry of Science, Technological Development and Innovation of the Republic of Serbia (451-03-66/2024-03/200042).

Conflict of interest

The authors declare that the research was conducted in the absence of any commercial or financial relationships that could be construed as a potential conflict of interest.

Publisher's note

All claims expressed in this article are solely those of the authors and do not necessarily represent those of their

affiliated organizations, or those of the publisher, the editors and the reviewers. Any product that may be evaluated in this article, or claim that may be made by its manufacturer, is not guaranteed or endorsed by the publisher.

Supplementary material

The Supplementary Material for this article can be found online at: https://www.frontiersin.org/articles/10.3389/fphar.2024.1448136/full#supplementary-material

References

Auphan, N., DiDonato, J. A., Rosette, C., Helmberg, A., and Karin, M. (1995). Immunosuppression by glucocorticoids: inhibition of NF-kappa B activity through induction of I kappa B synthesis. *Science* 270, 286–290. doi:10.1126/science.270.5234.286

Cai, Y., Lechner, M. S., Nihalani, D., Prindle, M. J., Holzman, L. B., and Dressler, G. R. (2002). Phosphorylation of Pax2 by the c-Jun N-terminal kinase and enhanced Pax2-dependent transcription activation. *J. Biol. Chem.* 277, 1217–1222. doi:10.1074/jbc.M109663200

Capece, D., Verzella, D., Flati, I., Arboretto, P., Cornice, J., and Franzoso, G. (2022). NF-κB: blending metabolism, immunity, and inflammation. *Trends Immunol.* 43, 757–775. doi:10.1016/j.it.2022.07.004

Chew, C. L., Conos, S. A., Unal, B., and Tergaonkar, V. (2018). Noncoding RNAs: master regulators of inflammatory signaling. *Trends Mol. Med.* 24, 66–84. doi:10.1016/j.molmed.2017.11.003

Christian, F., Smith, E. L., and Carmody, R. J. (2016). The regulation of NF-κB subunits by phosphorylation. *Cells* 5, 12. doi:10.3390/cells5010012

Curci, D., Franzin, M., Zudeh, G., Bramuzzo, M., Lega, S., Decorti, G., et al. (2024). Expression profiles of the lncRNA antisense GAS5-AS1 in colon biopsies from pediatric inflammatory bowel disease patients and its role in regulating sense transcript GAS5. *Eur. J. Pediatr.* 183, 1657–1665. doi:10.1007/s00431-023-05403-4

De Bosscher, K., Vanden Berghe, W., and Haegeman, G. (2003). The interplay between the glucocorticoid receptor and nuclear factor-kappaB or activator protein-1: molecular mechanisms for gene repression. *Endocr. Rev.* 24, 488–522. doi:10.1210/er.2002-0006

de Jesús, T. J., and Ramakrishnan, P. (2020). NF-κB c-rel dictates the inflammatory threshold by acting as a transcriptional repressor. *iScience* 23, 100876. doi:10.1016/j.isci.2020.100876

Del Toro, N., Shrivastava, A., Ragueneau, E., Meldal, B., Combe, C., Barrera, E., et al. (2022). The IntAct database: efficient access to fine-grained molecular interaction data. *Nucleic Acids Res.* 50, D648–d653. doi:10.1093/nar/gkab1006

Feng, X., Zhao, Y., Yang, T., Song, M., Wang, C., Yao, Y., et al. (2019). Glucocorticoid-driven NLRP3 inflammasome activation in hippocampal microglia mediates chronic stress-induced depressive-like behaviors. *Front. Mol. Neurosci.* 12, 210. doi:10.3389/fnmol.2019.00210

Frank, F., Kavousi, N., Bountali, A., Dammer, E. B., Mourtada-Maarabouni, M., and Ortlund, E. A. (2020). The lncRNA growth arrest specific 5 regulates cell survival via distinct structural modules with independent functions. *Cell Rep.* 32, 107933. doi:10.1016/j.celrep.2020.107933

Gasic, V., Zukic, B., Stankovic, B., Janic, D., Dokmanovic, L., Lazic, J., et al. (2018). Pharmacogenomic markers of glucocorticoid response in the initial phase of remission induction therapy in childhood acute lymphoblastic leukemia. *Radiol. Oncol.* 52, 296–306. doi:10.2478/raon-2018-0034

Gerber, A. N., Newton, R., and Sasse, S. K. (2021). Repression of transcription by the glucocorticoid receptor: a parsimonious model for the genomics era. *J. Biol. Chem.* 296, 100687. doi:10.1016/j.jbc.2021.100687

Ghafouri-Fard, S., Abak, A., Fattahi, F., Hussen, B. M., Bahroudi, Z., Shoorei, H., et al. (2021). The interaction between miRNAs/lncRNAs and nuclear factor-κB (NF-κB) in human disorders. *Biomed. Pharmacother.* 138, 111519. doi:10.1016/j.biopha.2021.111519

Giridharan, S., and Srinivasan, M. (2018). Mechanisms of NF-κB p65 and strategies for therapeutic manipulation. *J. Inflamm. Res.* 11, 407–419. doi:10.2147/jir.S140188

He, J., Zhou, J., Yang, W., Zhou, Q., Liang, X., Pang, X., et al. (2017). Dexamethasone affects cell growth/apoptosis/chemosensitivity of colon cancer via glucocorticoid receptor α/NF-κB. *Oncotarget* 8, 67670–67683. doi:10.18632/oncotarget.18802

He, R. Z., Jiang, J., and Luo, D. X. (2020). The functions of N6-methyladenosine modification in lncRNAs. *Genes Dis.* 7, 598–605. doi:10.1016/j.gendis.2020.03.005

Hudson, W. H., Vera, I. M. S., Nwachukwu, J. C., Weikum, E. R., Herbst, A. G., Yang, Q., et al. (2018). Cryptic glucocorticoid receptor-binding sites pervade genomic NF-κB response elements. *Nat. Commun.* 9, 1337. doi:10.1038/s41467-018-03780-1

Ji, J., Song, L., Hong, F., Zhang, W., Zhu, M., Yang, X., et al. (2022). Highly expressed lncRNA GAS5 in the serum of children with mycoplasma pneumoniae pneumonia and its effect on LAMPs-induced apoptosis and inflammation. *Contrast Media Mol. Imaging* 2022, 7872107. doi:10.1155/2022/7872107

Jong-Hun, J., lt, sup, gt, lt, sup, gt, Young-Yul, K., lt, sup, et al. (2019). Dexamethasone facilitates NF-κB signal pathway in TNF-α stimulated rotator cuff tenocytes. *J. Microbiol. Biotechnol.* 29, 297–303. doi:10.4014/jmb.1810.10051

Kaur, J., Salehen, N., Norazit, A., Rahman, A. A., Murad, N. A. A., Rahman, N., et al. (2022). Tumor suppressive effects of GAS5 in cancer cells. *Noncoding RNA* 8, 39. doi:10.3390/ncrna8030039

Kino, T., Hurt, D. E., Ichijo, T., Nader, N., and Chrousos, G. P. (2010). Noncoding RNA gas5 is a growth arrest- and starvation-associated repressor of the glucocorticoid receptor. *Sci. Signal* 3, ra8. doi:10.1126/scisignal.2000568

Kwon, H. J., Choi, G. E., Ryu, S., Kwon, S. J., Kim, S. C., Booth, C., et al. (2016). Stepwise phosphorylation of p65 promotes NF-κB activation and NK cell responses during target cell recognition. *Nat. Commun.* 7, 11686. doi:10.1038/ncomms11686

Lecoq, L., Raiola, L., Chabot, P. R., Cyr, N., Arseneault, G., Legault, P., et al. (2017). Structural characterization of interactions between transactivation domain 1 of the p65 subunit of NF-κB and transcription regulatory factors. *Nucleic Acids Res.* 45, 5564–5576. doi:10.1093/nar/gkx146

Li, F., Sun, J., Huang, S., Su, G., and Pi, G. (2018). LncRNA GAS5 overexpression reverses LPS-induced inflammatory injury and apoptosis through up-regulating KLF2 expression in ATDC5 chondrocytes. *Cell Physiol. Biochem.* 45, 1241–1251. doi:10.1159/000487455

Li, J. H., Liu, S., Zhou, H., Qu, L. H., and Yang, J. H. (2014). starBase v2.0: decoding miRNA-ceRNA, miRNA-ncRNA and protein-RNA interaction networks from large-scale CLIP-Seq data. *Nucleic Acids Res.* 42, D92–D97. doi:10.1093/nar/gkt1248

Liu, B., Sun, L., Liu, Q., Gong, C., Yao, Y., Lv, X., et al. (2015). A cytoplasmic NF-κB interacting long noncoding RNA blocks IκB phosphorylation and suppresses breast cancer metastasis. *Cancer Cell* 27, 370–381. doi:10.1016/j.ccell.2015.02.004

Lucafo, M., De Iudicibus, S., Di Silvestre, A., Pelin, M., Candussio, L., Martelossi, S., et al. (2015). Long noncoding RNA GAS5: a novel marker involved in glucocorticoid response. *Curr. Mol. Med.* 15, 94–99. doi:10.2174/1566524015666150114122354

Lucafò, M., Pugnetti, L., Bramuzzo, M., Curci, D., Di Silvestre, A., Marcuzzi, A., et al. (2019). Long non-coding RNA GAS5 and intestinal MMP2 and MMP9 expression: a translational study in pediatric patients with IBD. *Int. J. Mol. Sci.* 20, 5280. doi:10.3390/ijms20215280

Lucafò, M., Stocco, G., and Decorti, G. (2016). Emerging molecular mechanisms underlying cancer metastasis: the rising role of the long non-coding RNA GAS5. *Transl. Cancer Res.* 5, S827–S830. doi:10.21037/tcr.2016.10.01

Mao, X., Su, Z., and Mookhtiar, A. K. (2017). Long non-coding RNA: a versatile regulator of the nuclear factor-κB signalling circuit. *Immunology* 150, 379–388. doi:10.1111/imm.12698

Mukaida, N., Okamoto, S., Ishikawa, Y., and Matsushima, K. (1994). Molecular mechanism of interleukin-8 gene expression. *J. Leukoc. Biol.* 56, 554–558. doi:10.1002/jlb.56.5.554

Mulero, M. C., Huxford, T., and Ghosh, G. (2019). NF-κB, IκB, and IKK: integral components of immune system signaling. *Adv. Exp. Med. Biol.* 1172, 207–226. doi:10.1007/978-981-13-9367-9_10

Newton, R., Hart, L. A., Stevens, D. A., Bergmann, M., Donnelly, L. E., Adcock, I. M., et al. (1998). Effect of dexamethasone on interleukin-1beta-(IL-1beta)-induced nuclear factor-kappaB (NF-kappaB) and kappaB-dependent transcription in epithelial cells. *Eur. J. Biochem.* 254, 81–89. doi:10.1046/j.1432-1327.1998.2540081.x

Ruland, J. (2011). Return to homeostasis: downregulation of NF-κB responses. *Nat. Immunol.* 12, 709–714. doi:10.1038/ni.2055

Schaaf, M. J., and Cidlowski, J. A. (2002). Molecular mechanisms of glucocorticoid action and resistance. *J. Steroid Biochem. Mol. Biol.* 83, 37–48. doi:10.1016/s0960-0760(02)00263-7

Scheinman, R. I., Cogswell, P. C., Lofquist, A. K., and Baldwin, A. S., Jr. (1995). Role of transcriptional activation of I kappa B alpha in mediation of immunosuppression by glucocorticoids. *Science* 270, 283–286. doi:10.1126/science.270.5234.283

Schneider, C. A., Rasband, W. S., and Eliceiri, K. W. (2012). NIH Image to ImageJ: 25 years of image analysis. *Nat. Methods* 9, 671–675. doi:10.1038/nmeth.2089

Shin, J. J., Park, J., Shin, H. S., Arab, I., Suk, K., and Lee, W. H. (2024). Roles of lncRNAs in NF-κB-Mediated macrophage inflammation and their implications in the pathogenesis of human diseases. *Int. J. Mol. Sci.* 25, 2670. doi:10.3390/ijms25052670

Tsuchiya, Y., Osaki, K., Kanamoto, M., Nakao, Y., Takahashi, E., Higuchi, T., et al. (2017). Distinct B subunits of PP2A regulate the NF-κB signalling pathway through dephosphorylation of IKKβ, IκBα and RelA. *FEBS Lett.* 591, 4083–4094. doi:10.1002/1873-3468.12912

Widén, C., Gustafsson, J. A., and Wikström, A. C. (2003). Cytosolic glucocorticoid receptor interaction with nuclear factor-kappa B proteins in rat liver cells. *Biochem. J.* 373, 211–220. doi:10.1042/bj20030175

Xiao, J., and Wang, D. (2023). LncRNA GAS5 as an inflammatory regulator acting through pathway in human lupus. *Curr. Pharm. Des.* 29, 1293–1299. doi:10.2174/1381612829666230517102205

Yang, Q., Liu, P., Han, Y., Wang, C., Huang, Y., Li, X., et al. (2022). Long noncoding RNA GAS5 alleviates the inflammatory response of human periodontal ligament stem cells by regulating the NF-κB signalling pathway. *Eur. J. Orthod.* 44, 669–678. doi:10.1093/ejo/cjac030

Zhang, R., Han, X., Huang, T., and Wang, X. (2019). Danggui buxue tang inhibited mesangial cell proliferation and extracellular matrix accumulation through GAS5/NF-κB pathway. *Biosci. Rep.* 39. doi:10.1042/bsr20181740

Zheng, Y., Luo, H., Teng, X., Hao, X., Yan, X., Tang, Y., et al. (2023). NPInter v5.0: ncRNA interaction database in a new era. *Nucleic Acids Res.* 51, D232–d239. doi:10.1093/nar/gkac1002

frontiers | Frontiers in Immunology

TYPE Original Research
PUBLISHED 10 February 2025
DOI 10.3389/fimmu.2025.1477437

Check for updates

OPEN ACCESS

EDITED BY
Nejat Dalay,
Istanbul University, Türkiye

REVIEWED BY
Junwei Luo,
Henan Polytechnic University, China
Mario Perez-Medina,
Instituto Nacional de Enfermedades Respiratorias Ismael Cosio Villegas, Mexico

*CORRESPONDENCE
Xiaolin Wang
18051063909@yzu.edu.cn
Yusheng Shu
dz120220059@stu.yzu.edu.cn

RECEIVED 07 August 2024
ACCEPTED 20 January 2025
PUBLISHED 10 February 2025

CITATION
Hu J, Tian S, Liu Q, Hou J, wu J, Wang X and Shu Y (2025) A prognostic signature of Glutathione metabolism-associated long non-coding RNAs for lung adenocarcinoma with immune microenvironment insights. *Front. Immunol.* 16:1477437. doi: 10.3389/fimmu.2025.1477437

COPYRIGHT
© 2025 Hu, Tian, Liu, Hou, wu, Wang and Shu. This is an open-access article distributed under the terms of the Creative Commons Attribution License (CC BY). The use, distribution or reproduction in other forums is permitted, provided the original author(s) and the copyright owner(s) are credited and that the original publication in this journal is cited, in accordance with accepted academic practice. No use, distribution or reproduction is permitted which does not comply with these terms.

A prognostic signature of Glutathione metabolism-associated long non-coding RNAs for lung adenocarcinoma with immune microenvironment insights

Junxi Hu[1,2], Shuyu Tian[2,3], Qingwen Liu[2,3], Jiaqi Hou[2,3], Jun wu[1,2], Xiaolin Wang[1,2]* and Yusheng Shu[1,2]*

[1]Clinical Medical College, Yangzhou University, Yangzhou, China, [2]Department of Thoracic Surgery, Northern Jiangsu People's Hospital, Yangzhou, China, [3]Dalian Medical University, Dalian, China

Background: Glutathione (GSH) metabolism supports tumor redox balance and drug resistance, while long non-coding RNAs (lncRNAs) influence lung adenocarcinoma (LUAD) progression. This study developed a prognostic model using GSH-related lncRNAs to predict LUAD outcomes and assess tumor immunity.

Methods: This study analyzed survival data from The Cancer Genome Atlas (TCGA) and identified GSH metabolism-related lncRNAs using Pearson correlation. A prognostic model was built with Cox and Least Absolute Shrinkage and Selection Operator (LASSO) methods and validated by Kaplan-Meier analysis, Receiver Operating Characteristic (ROC) curves, and Principal Component Analysis (PCA). Functional analysis revealed immune infiltration and drug sensitivity differences. Quantitative PCR and experimental studies confirmed the role of lnc-AL162632.3 in LUAD.

Results: Our model included a total of nine lncRNAs, namely AL162632.3, AL360270.1, LINC00707, DEPDC1-AS1, GSEC, LINC01711, AL078590.2, AC026355.2, and AL096701.4. The model effectively forecasted patient survival, and the nomogram, incorporating additional clinical risk factors, satisfied clinical needs adequately. Patient stratification based on model scores revealed significant disparities in immune cell composition, functionality, and mutations between groups. Additionally, variations were noted in the IC50 values for key lung cancer medications such as Cisplatin, Docetaxel, and Paclitaxel. *In vitro* cell experiment results showed that AL162632.3 was markedly upregulated, while AC026355.2 tended to be downregulated across these cell lines. Ultimately, suppressing lnc-AL162632.3 markedly reduced the growth, mobility, and invasiveness of lung cancer cells.

Conclusion: This study identified GSH metabolism-related lncRNAs as key prognostic factors in LUAD and developed a model for risk stratification. High-risk patients showed increased tumor mutation burden (TMB) and stemness, emphasizing the potential of personalized immunotherapy to improve survival outcomes.

KEYWORDS

lung adenocarcinoma, Glutathione metabolism, lncRNA, prognostic prediction, immune microenvironment

1 Introduction

Lung cancer is among the most prevalent and lethal cancers worldwide, accounting for a significant proportion of all cancer-related deaths (1). Non-small cell lung cancer (NSCLC) comprises the majority of lung cancer cases, with LUAD as the primary subtype, and is more frequently observed in non-smokers and women (2). Despite the numerous existing treatment options, only about 20% of lung adenocarcinoma patients benefit from them, and the majority of patients still experience poor survival outcomes (3). Conventional treatments have limited effects on advanced LUAD, and although targeted therapies and immunotherapy are effective, resistance and tumor heterogeneity still significantly impact treatment outcomes and patient survival rates (4). Recent advances in molecular biology and genomics have revealed complex mechanisms of tumor development, increasingly highlighting the importance of molecular markers in the diagnosis, prognostic assessment, and treatment decision-making (5). The lncRNA, as an emerging molecular marker, exhibits unique functions in regulating gene expression and affecting the tumor microenvironment (6). Exploring new lncRNA molecular markers and related prognostic models can facilitate early cancer screening, precise diagnosis, and the formulation of personalized treatment plans, thereby improving therapeutic effectiveness.

lncRNAs are RNA molecules exceeding 200 nucleotides in length and do not code for proteins (7). Although lncRNAs do not encode proteins, they are critical in gene expression regulation, chromatin modification, and post-transcriptional control. Recently, research on lncRNAs has greatly expanded their applications in the biomedical field, particularly in cancer research (8). For example, MALAT1 (Metastasis Associated Lung Adenocarcinoma Transcript 1) is highly expressed in lung cancer and is closely associated with poor prognosis, promoting tumor metastasis by regulating gene transcription and RNA splicing (9). In breast cancer, high HOTAIR expression promotes chromatin changes, enhancing tumor invasion and metastasis, and correlates with lower survival rates (10). Additionally, H19, a significant lncRNA, regulates multiple signaling pathways in liver and colorectal cancer, affecting tumor cell proliferation and survival (11). Importantly, lncRNAs not only regulate the onset and progression of tumors but also serve as potential therapeutic targets and prognostic markers. For instance, studies have shown that lncRNA-ATB can alter the growth characteristics of liver cancer cells by enhancing the TGF-β signal to promote their metastasis (12). Currently, the specific roles of lncRNAs in the tumor microenvironment and their potential clinical applications still require further exploration.

GSH is a crucial intracellular antioxidant composed of glutamic acid, cysteine, and glycine (13). GSH plays a significant role in maintaining cellular redox balance by reducing hydrogen peroxide and lipid peroxides, thus protecting cells from oxidative stress damage (14). In tumor cells, GSH metabolism pathways are often remodeled to cope with oxidative stress and metabolic demands brought about by rapid proliferation (15). Tumor cells resist the toxicity of chemotherapy drugs by enhancing GSH synthesis or reducing its consumption, leading to chemotherapy resistance (16). Furthermore, it has been found that inhibiting GSH synthesis can enhance the efficacy of immunotherapy, boosting the anti-tumor immune response (17). Investigating the metabolic functions of GSH in tumors aids in the creation of novel therapeutic approaches for tackling tumor resistance and immune escape, ultimately enhancing patient treatment outcomes and survival rates (18).

Through the analysis of TCGA dataset, this research has identified long lncRNAs related to GSH metabolism and has developed a new type of risk assessment model accordingly. We developed and validated a nomogram model that integrates features of GSH metabolism-related lncRNAs with clinical factors. Additionally, based on functional analysis of model differential genes, we also explored whether the model could preliminarily predict drug treatment outcomes for LUAD patients. Finally, we performed preliminary validation of the lncRNAs in the model in both normal and tumor cell lines.

2 Materials and methods

2.1 Data acquisition

By May 9, 2024, our research had retrieved 600 files from the TCGA official site (https://cancergenome.nih.gov/), encompassing RNA-seq expression matrices and clinical data for 517 LUAD

patients. This study utilized Active Perl software for preprocessing the raw files, creating a consolidated table of gene and clinical information. Using the metadata gene annotation file downloaded from the official website, this study converted Ensembl IDs to common official gene names using Active Perl. Before analyzing the expression data, all data were normalized using log2 transformation. Somatic mutation information for all LUAD patients was downloaded from the TCGA official website. After excluding 10 patients with incomplete clinical information, further analysis included 507 patients. This study used the createDataPortion package to randomly split patients into training (355 individuals) and test (152 individuals) groups. Additionally, the grouped data passed clinical statistical difference testing. Based on the annotation files from the Ensembl human genome browser GRCh38, this study performed iterative processing on all genes using Active Perl, extracting the expression matrices for mRNA and lncRNA. Integrating published papers and data from the GSEA official site, this study identified 87 crucial genes. Since all data in this study came from publicly accessible databases and followed TCGA database publication guidelines, ethics committee approval was omitted. This study adhered to the 2013 revised Declaration of Helsinki.

2.2 Identification of lncRNAs related to GSH metabolism

Based on the research by Shi et al. (19) and MSigDB, we identified 78 genes associated with GSH metabolism. From the obtained gene list, we extracted expression data for GSH-related genes. The limma software package was utilized for co-expression analysis. Using filters with a Pearson correlation coefficient greater than 0.4 and a *p*-value below 0.001, we identified 1748 lncRNAs associated with GSH metabolism. These thresholds were chosen to balance biological relevance, statistical significance, and clinical translational feasibility. Based on the identified lncRNA gene names, we extracted the corresponding expression matrix for GSH metabolism-related lncRNAs.

2.3 Construction and validation of a prognostic model for GSH-related lncRNA characteristics

Employing the Survival software, COX univariate regression analysis was conducted on lncRNA expression and survival data for the training cohort, with a filter threshold of $p < 0.001$. Subsequently, feature lncRNAs in the prognostic model were selected using a combined LASSO-COX model (20). Additionally, the independent correlation of the key lncRNAs selected in the model must meet the requirements of multiple linear stepwise regression analysis. Concurrently, the minimum Akaike Information Criterion (AIC) is calculated to obtain optimal simulation effects (21). Ultimately, the prognostic model includes 9 lncRNAs, with the risk scoring formula as:

$$\text{Risk score} = \sum_{i}^{n} \alpha i \times \beta i$$

where α i represents the regression coefficient of the ith lncRNA obtained from the multivariate Cox regression analysis, and β i represents the expression value of each GSH metabolism-related lncRNAs.These coefficients are fixed values derived from the training dataset.The expression levels of the selected lncRNAs, which vary with each patient sample, were then multiplied by their respective coefficients to compute the individualized Risk score. Using the "survival" and "survminer" packages, KM curves for OS and PFS were plotted, with statistical differences assessed via the log-rank test. The "timeROC" package was utilized for receiver operating characteristic (ROC) analysis, computing the AUC value. The C-index value was derived through the Hmisc package in conjunction with patient survival information analysis. The "scatterplot3d" package was used for PCA principal component analysis and visualization of model-related lncRNAs, all genes, and GSH-related genes and lncRNAs.

2.4 Construction and calibration of predictive nomograms

In this study, we used the median risk score as the cutoff value for grouping, evenly distributing patients into high-risk and low-risk groups. By integrating routine clinical data with model risk assessments, this study utilizes the rms, regplot, and Survival packages to construct clinically relevant nomograms. These nomograms aim to accurately predict patients' overall survival (OS) rates. Furthermore, we meticulously generated the corresponding calibration curves to validate the predictive accuracy.

2.5 Functional enrichment analysis

Using the limma software package, we identified differentially expressed genes between high and low risk groups of LUAD patients (log2FC>1,FDR<0.05). According to the descending order of p-values, we selected the top ten significant and meaningful results. These results were visualized using different packages like ggplot2, circlize, and ComplexHeatmap (21, 22). The GSEA software package was used for gene set enrichment analysis, comparing pathway gene sets in the KEGG database to evaluate the association of lncRNAs involved in model construction with these gene sets. Finally, we visualized the top five results using the clusterProfiler (23) and enrichplot packages.

2.6 Analysis of tumor mutational burden and tumor immune microenvironment

Through the CIBERSORT package, the immune infiltration results in tumor samples of LUAD patients were obtained. The study comprehensively assessed how model risk scores correlate with various immune cell types using multiple algorithms (24–30). The

GSVA package evaluated the correlation between 13 immune function genes and LUAD transcriptome expression (31). The Maftools software package (32) is used to process and analyze the proportions of missense mutations, nonsense mutations, frameshift deletions, frameshift insertions, inframe deletions, and multiple mutations in high-frequency mutated genes and tumor-related genes.

2.7 Prediction of immunotherapy efficacy and potential chemotherapeutic drug screening

The limma package integrated the immunotherapy data with patient risk group information, and the ggpubr package generated violin plots for cohorts. Screening of potential chemotherapeutic drugs is conducted using the oncoPredict package (33). Obtain the GDSC2 training dataset (https://www.cancerrxgene.org/) containing 198 chemotherapy drugs from the oncoRespond section on the OSF site. Conduct drug sensitivity analysis using the calcPhenotype function to calculate IC50. Set the significance filtering threshold to a *p*-value less than 0.001.

2.8 cell line culture

HBE cells and NSCLC cell lines were acquired from the Chinese Cell Resource Center. Cells were cultured in complete medium with 10% fetal bovine serum (FBS, Gibco brand), under incubator conditions of 5% CO2, 37°C, and 95% humidity.

2.9 Cell transfection

RNAi reagents and transfection aids were supplied by genepharma, with detailed interference sequences available in Supplementary Table 1. Cells were plated a day before transfection, ensuring that cell density reached approximately 50%-60% confluency on the day of transfection. RNAi reagents were preincubated with transfection enhancers and subsequently allowed to equilibrate at room temperature for 20 minutes to optimize complex formation. During the resting period, medium exchange was conducted, and the settled transfection complex was introduced to the culture plates, with timely replenishment or replacement of the medium depending on cell growth conditions. Transfection efficiency was assessed 48 hours after the procedure.

2.10 Real-time quantitative PCR

Total RNA was extracted from cells using TRIzol reagent as per the protocol outlined in the manual (Vazyme, Cat No. R701-01). The RNA concentration and purity were then assessed using the Nanodrop 2000 spectrophotometer. By adhering to the cDNA synthesis kit's instructions (Vazyme, Cat No. Q141-02/03), reverse-transcribed cDNA was generated through RT-PCR amplification. The quantitative results of gene expression were collected and analyzed on the StepOne Plus system. The data were analyzed using the 2^(-ΔΔCt) method. GAPDH was used as an internal reference gene to normalize the target genes.

2.11 colony formation assays

Cells in good condition 48 hours post-transfection were selected for counting. Both experimental and control plates were prefilled with serum-free medium. Based on the calculations, 500 cells were evenly seeded per well and incubated for two weeks. After culturing, cells were washed twice with PBS and fixed in 4% paraformaldehyde for 10 minutes. After a PBS wash, cells were stained with crystal violet for 10 minutes, rinsed under running water for 5 minutes, and the plates were dried and photographed.

2.12 CCK8 proliferation assays

Digest and count cells in good condition and in the logarithmic growth phase after transfection, adjusting the cell density to 5×10^3 cells/ml with blank medium. Add 200 μl of the adjusted cell suspension to each well of a 96-well plate, and measure the optical density (OD) at 24, 48, 72, and 96 hours post cell adherence. Subsequently, 10 μl of CCK8 reagent was meticulously added to each well, followed by an incubation period of 2 hours. Absorbance was then precisely measured at 450 nm using a spectrophotometer.

2.13 Cell invasion assay

Prior to the experiment, evenly distribute the matrix gel at the bottom of the Transwell chambers and incubate until the gel completely solidifies. On the experiment day, select well-conditioned and logarithmically growing post-transfection cells for trypsin digestion and counting. Resuspend the cells in serum-free medium, adjusting the density to 2.5×10^5 cells/ml. Extract the Transwell chambers, aspirate excess medium or liquid from the upper compartment, and add 200 μl of adjusted cell suspension to it, along with 500 μl of complete medium to the lower compartment. Continue culturing the Transwell chambers in the incubator for 48 hours, then proceed with further processing. Remove the old medium, wash the chambers twice with PBS, and fix the cells in 4% paraformaldehyde for 10 minutes. After removing the fixative, apply 0.1% crystal violet stain for 10 minutes. Next, remove the staining solution and wash the Transwell chambers three times with deionized water to eliminate excess dye. Lastly, use

a damp cotton ball to gently wipe the upper surface of the chamber, removing cells that have not penetrated the matrix gel. Allow the chambers to air dry at room temperature, then examine and photograph the results under a microscope.

2.14 Wound healing test

Prior to the experiment, each well of the culture plate is prefilled with 2 ml of blank medium. Digest and count cells in good condition and in the logarithmic phase after transfection, resuspending them in blank medium. Add 400,000 cells evenly to each well. Once cells adhere, remove them using a 200 μl pipette tip and wash once with PBS. Add blank medium and incubate for 48 hours. Remove the plate, wash with PBS, and use a microscope to photograph and document the scratch healing process.

2.15 Xenograft model

Ten genetically defined, 5-week-old female nude mice were procured from the Jiangsu Jicui official website and randomly assigned into two groups. Prior to the experiment, target cells and empty vector control cells, both in optimal condition and the logarithmic growth phase, were precultured. Cells were trypsinized, resuspended in sterile Phosphate-Buffered Saline (PBS), and the concentration was adjusted to 4×10^3 cells/μl. Each mouse received a subcutaneous injection of 200 μl of this suspension into the right axillary region. Tumor dimensions were measured every three days with calipers. After one month, the mice were euthanized, and the tumors were excised, weighed, and measured for volume. The study was approved by the Yangzhou University Animal Experiment Ethics Review Committee, adhering strictly to ethical guidelines.

2.16 Statistical analysis

Statistical analysis was conducted in R (version 4.3.0). For evaluating the differences between pairs of groups, the Wilcoxon rank-sum test was employed. In contrast, differences across multiple groups were determined using the Kruskal-Wallis test. Results were deemed statistically significant at a *p*-value below 0.05.

3 Results

3.1 Identification of GSH metabolism-related lncRNAs

Figure 1 showed the flowchart of this study. This study included samples from 541 cancer patients, identifying 16,876 lncRNAs from 59,427 genes in the transcripts. The GSH-related gene set used in this study included 87 genes such as ABCC1, ABCC4, ABCC5. A comprehensive analysis revealed 1,748 lncRNAs associated with GSH metabolism, characterized by a correlation coefficient exceeding 0.4 and a *p*-value below 0.001 (Figure 2A).

3.2 Development and assessment of the prognostic GSH-based risk model

This study included 507 samples for the construction of a GSH-related lncRNA risk model. Using the createDataPartition package, we randomly assigned all samples into a training set (355 persons) and a testing set (152 persons), without statistical differences in clinical data between the two groups (Supplementary Table 2). Through LASSO-COX analysis (P<0.05), we identified 9 lncRNAs significantly associated with prognosis (Figures 2B, C; Supplementary Table 3). Risk scores for patients in both the training and testing groups were calculated using the formula, and patients were divided into high and low risk groups based on the median value (Supplementary Table 4). The correlation heatmap in Figure 2D showed the relationship between the GSH metabolism gene set and the model-building lncRNAs. The K-M analysis demonstrated that high-risk patients have significantly lower overall survival (OS) than low-risk patients in both the training and testing groups (Figures 3A–C). The PFS analysis results were consistent with the aforementioned OS results, P<0.05 (Figure 3D). The risk curves indicated a positive correlation between rising risk scores and increasing patient mortality. The correlation heatmap showed that the expression of lncRNAs such as AL162632.3, AL360270.1, LINC00707, DEPDC1-AS1, GSEC, and LINC01711 increases with rising risk scores, while the expression of AL078590.2, AC026355.2, and AL096701.4 decreases (Figures 3E–G).

3.3 Validate the independence of the constructed model in LUAD

Independent prognostic evaluation consistently showed that the model yielded hazard ratios (HRs) exceeding 1, with highly significant *p*-values observed across univariate and multivariate Cox regression analyses (Figures 4A, B). We conducted ROC curve analyses to explore the model's predictive capability on patient prognosis (Figure 4C). The prognostic model demonstrated the highest AUC and C-index values compared to clinical factors (e.g., age and stage) (Figures 4D, E). To investigate the model's applicability across different cancer stages, we divided patients into early and late stages and conducted OS analysis; the results demonstrated that, in both early and late stages, the high and low-risk scores clearly distinguished between patients' survival durations (Figures 5C, D).

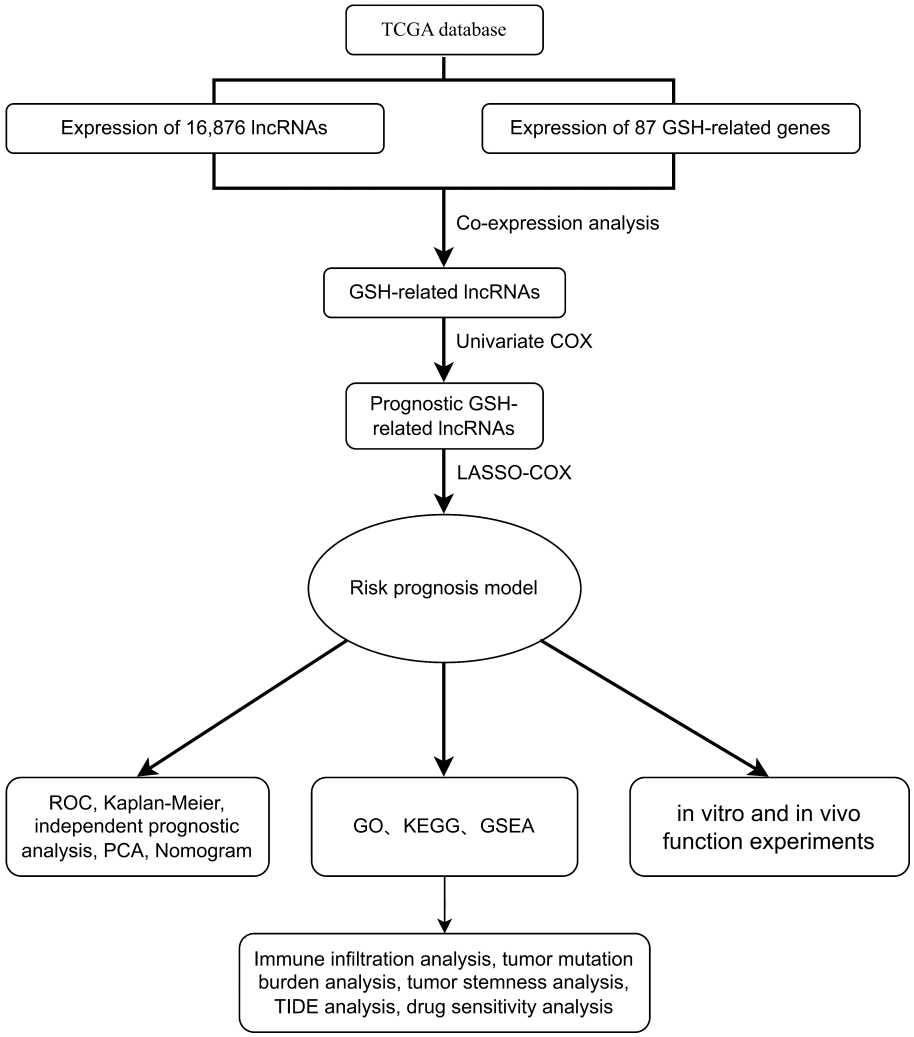


FIGURE 1
Flow diagram.

3.4 PCA and nomogram

PCA presented in Figures 4F–I showed that the lncRNA model we developed could best distinguish patients. Figures 5A, B showed the clinical nomogram, where each clinical factor is scored, and the sum of all factors' scores was the total composite score. According to the scale for the composite score, one can estimate the survival probabilities for 1 year, 3 years, and 5 years for patients. For instance, a patient with a total score of 146 exhibited survival probabilities of 0.961 at 1 year, 0.853 at 3 years, and 0.708 at 5 years, respectively.

3.5 Functional enrichment analysis

We conducted a detailed investigation into the prognostic influence of critical lncRNAs on LUAD survival by differentially analyzing high and low risk groups (logFC > 1, FDR < 0.05), identifying 447 significant genes (Supplementary Table 5). GO functional analysis indicated that the differentially expressed genes primarily cluster in immune cell infiltration (like chemotaxis induction, migration of myeloid cells), immune activation (such as antimicrobial humoral response (GO:0019730), humoral immune response (GO:0006959), and antimicrobial peptide-driven humoral immunity (GO:0061844)), extracellular matrix (ECM) remodeling (including collagen-rich ECM, cytoplasmic vesicles, lamellar bodies), and cytokine-cytokine receptor interactions (such as regulation of endopeptidase activity) (Figures 6A, B).The results of the KEGG pathway analysis, represented through bubble charts and histograms, demonstrated an enrichment of these different genes in pathways that regulate immune cells, including the ras signaling pathway, the pi3k-akt signaling pathway, and cytokine-cytokine receptor interactions (Figure 6C). GSEA analyses were conducted for each gene within the model, such as AL360270.1, which showed that most lncRNAs are linked to pathways involved in cancer, immunity, and metabolism (Figure 6D).

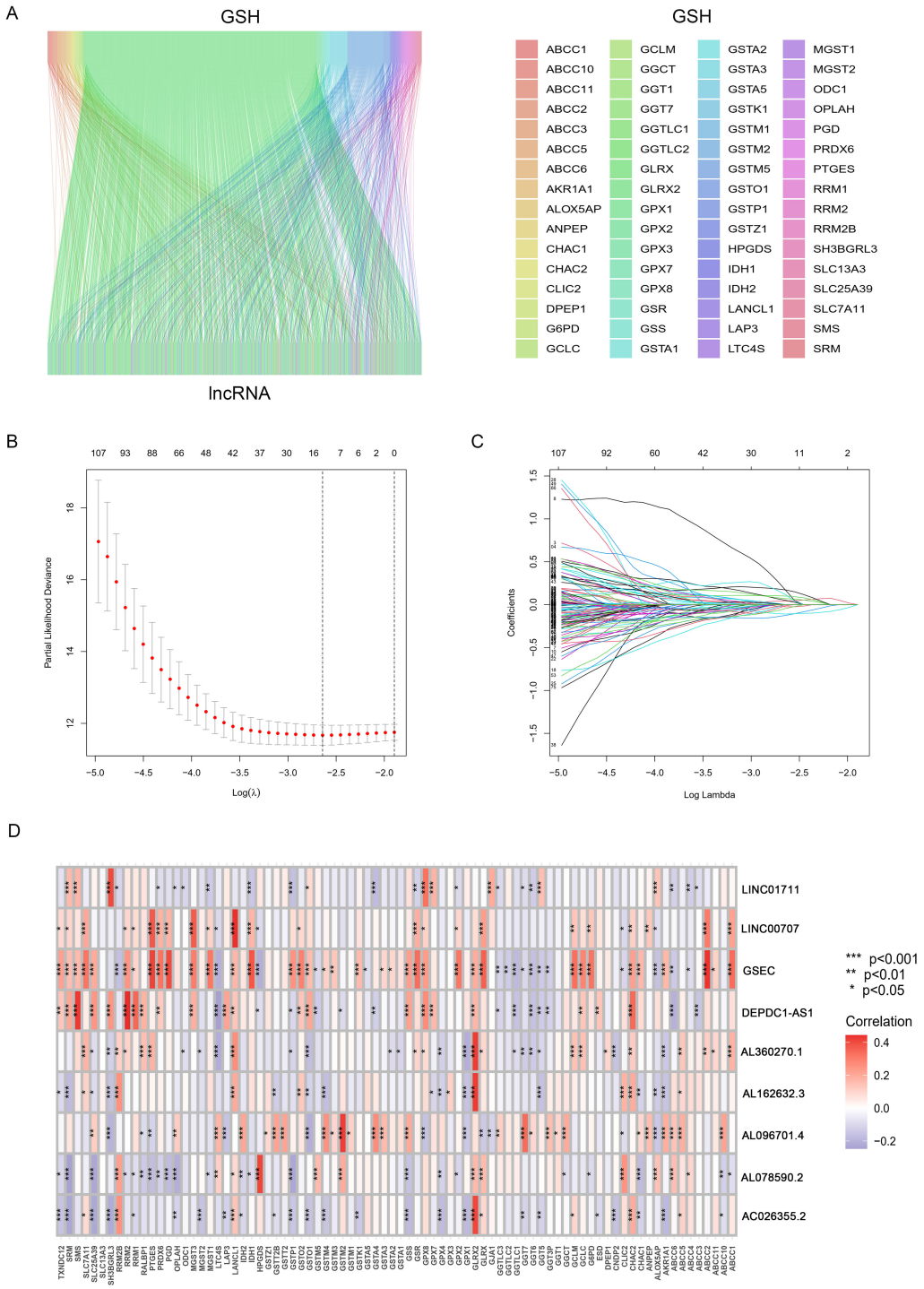


FIGURE 2
Identification and Prognostic Model Construction of GSH Metabolism-related lncRNAs. **(A)** The Sankey diagram shows the co-expressed GSH metabolism-related genes and lncRNAs. **(B)** ten-fold cross-validation. **(C)** LASSO coefficient curves. **(D)** Correlation heatmap between lncRNAs and gene sets.

3.6 Evaluation of tumor-immune landscape and analysis of immune related function

Figure 7A showed the proportions of typical immune cells in LUAD patient samples from the TCGA database. Figure 7E demonstrated that while there were no significant differences in stromal cell scores, patients classified as high-risk exhibited notably lower immune cell scores within TME and overall estimation scores compared to those at low risk. We employed tools like XCELL, TIMER, QUANTISEQ, and MCPCOUNTER for correlation

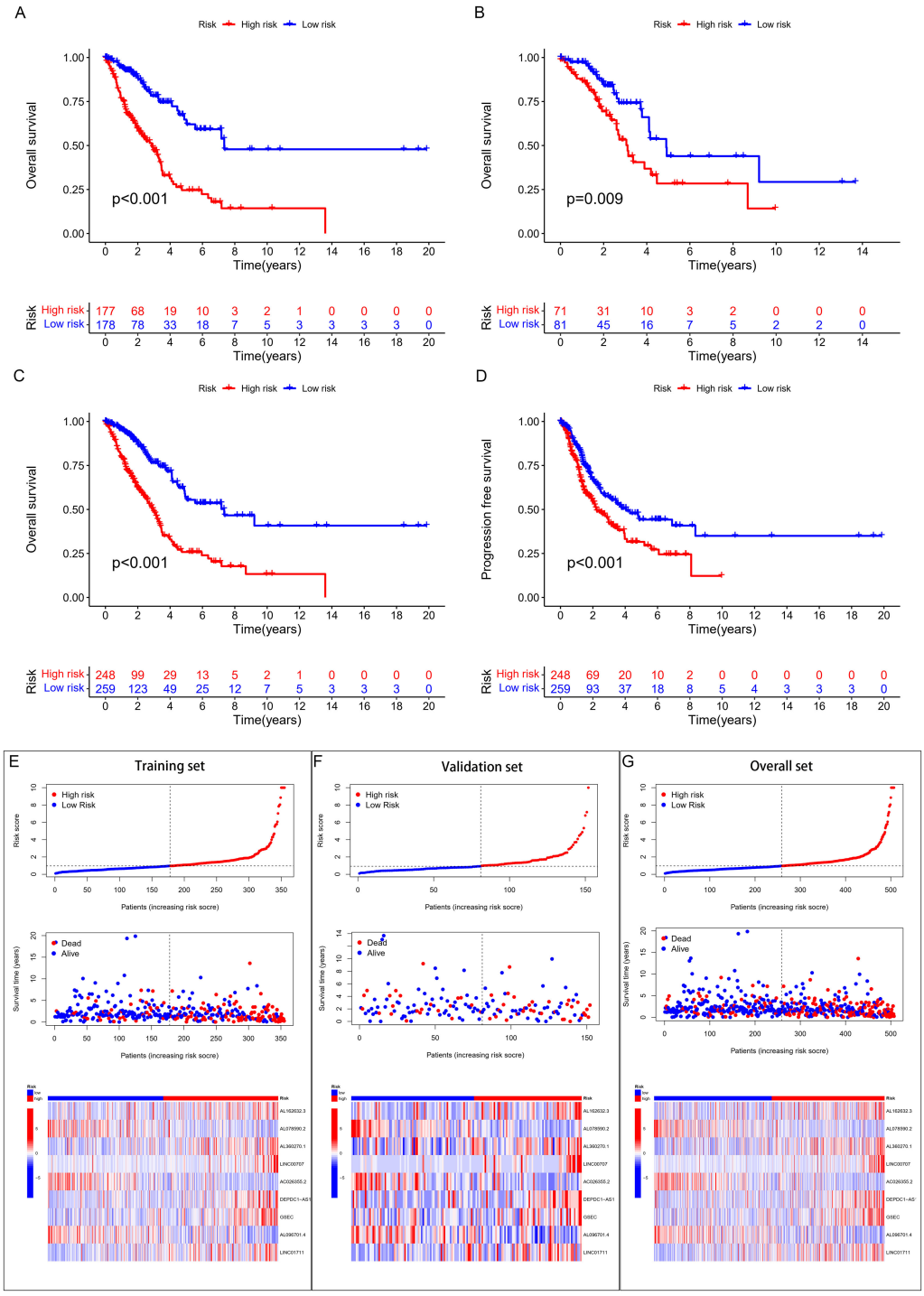


FIGURE 3
Survival analysis and validation. **(A)** K-M curves for OS in the training set, **(B)** validation set, **(C)** overall cohort. **(D)** K-M curves for PFS in the overall cohort. **(E)** (training set), **(F)** (validation set), **(G)** (overall set) risk score plots, survival status graphs, and heatmaps.

analysis, as depicted in the bubble chart of Figure 7B. We further explored the interactions between these immune cells. Figure 7D depicted the correlations between immune cells in the tumors of these patients. Figure 7C showed the heatmap of correlations between LUAD samples and immune functions, indicating significant differences between the high and low risk groups in classical immune functions such as Type II IFN Response, Type I IFN Response, HLA, etc.

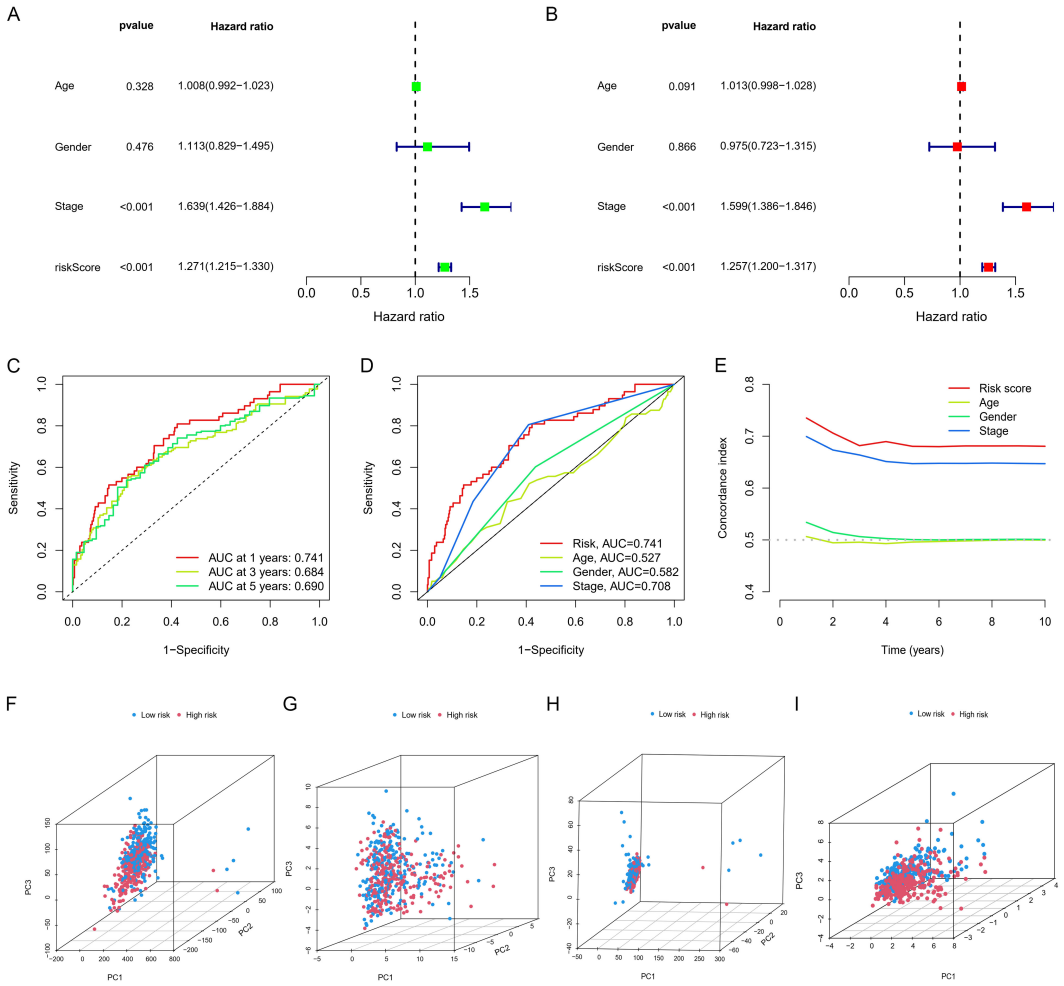


FIGURE 4
Independent prognostic analysis and PCA analysis. **(A, B)** Cox regression analysis. **(C)** Time-dependent ROC curves for overall survival (OS). **(D)** ROC curves and **(E)** C-index for risk scores and other clinical risk factors. **(F)** PCA for the whole genome, **(I)** GSH metabolism genes, **(G)** all GSH metabolism-related lncRNAs, and **(H)** model-related lncRNAs.

3.7 TMB

Tumor mutational burden analysis revealed higher mutation rates in key genes including TP53, KRAS, and COL11A1 in the high-risk group. Waterfall and violin plots demonstrated that the tumor mutational burden in the high-risk group is significantly higher than that in the low-risk group (Figures 8A–C). Kaplan-Meier analysis showed significantly longer survival in patients with high TMB compared to those with low burden (Figure 8D). Finally, we divided all patients into four groups based on risk scores and levels of tumor mutational burden to analyze differences in survival. The results showed that high TMB and low-risk groups had the longest survival time, while those in the low TMB and high-risk groups had the shortest survival time, with statistically significant differences in survival among the four groups (Figure 8E).

3.8 Immunotherapy for risk signature and prediction of potential drugs.

Based on the discovery that risk scores were closely related to immunity, we further used existing TIDE data to predict patient drug response. The findings reveal markedly reduced TIDE scores in the high-risk cohort relative to the comparison group (Figure 8F). Furthermore, analysis of tumor stem cell indices demonstrated a positive correlation with risk scores, indicating increased tumor stemness (Figure 7F). Subsequently, we used the oncoPredict package to screen for potential sensitivity drugs. The results indicated that drugs like Cisplatin, Docetaxel, Gemcitabine, Vinorelbine, and Paclitaxel significantly differed in IC50 values (Figure 9). Detailed results were presented in the Supplementary Files.

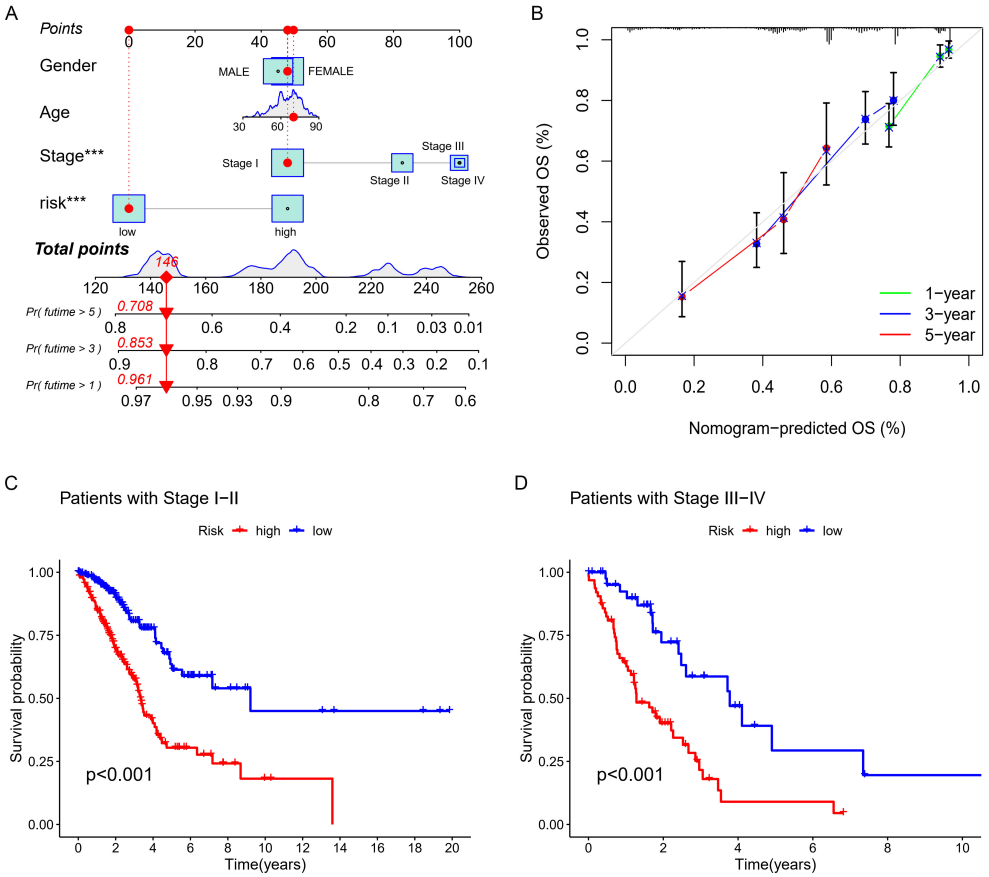


FIGURE 5
Nomogram Development and Validation **(A)** Nomogram. **(B)** Corresponding calibration curve. **(C, D)** K-M analysis of OS.

3.9 Expression confirmed through *in vitro* experiments

We used qPCR to verify the expression levels of lncRNAs with independent prognostic significance to validate the importance of lncRNAs in the model. Compared to the normal cell line HBE, the expression of AL162632.3 significantly increased in the selected cancer cell lines PC9, H1299, A549, and H1975, particularly in H1299 cells. Expression of LINC01711 rose in lung cancer cell lines including PC9, H1299, and H1975 but fell in A549.GSEC showed no significant changes in expression in these cancer cell lines (Figure 10A). AC026355.2 was significantly downregulated in all four cancer cell lines. Conversely, expression of AL096701.4 declined in the PC9, H1299, and A549 cell lines, while it increased in H1975 (Figure 10B).

3.10 Decreased lnc-AL162632.3 expression inhibited LUAD proliferation, migration and invasion

Using RNAi technology, we effectively knocked down the highly expressed lnc-AL162632.3 in H1299 and A549 lung cancer cell lines. The RNAi efficiency was validated through qPCR, identifying RNA3 as the most effective. Consequently, we selected siRNA3 for all subsequent experiments. CCK8 proliferation and colony formation assays showed that knocking down lnc-AL162632.3 significantly reduced cell growth compared to the control group. Wound healing and invasion assays further demonstrated that suppression of lnc-AL162632.3 markedly weakened the motility of the cancer cells (Figure 11). *In vivo*, tumors in the lnc-AL162632.3 knockdown mice were noticeably smaller and lighter than the controls (Figure 12).

4 Discussion

Lung cancer is one of the most common malignancies worldwide and is a leading cause of cancer-related deaths (1). In China, LUAD represents the predominant subtype of non-small cell lung cancer (34). The majority of patients are diagnosed at advanced stages, at which point surgery is often no longer viable. Despite some effectiveness of targeted and immunotherapies, the issue of resistance persists, resulting in poor long-term survival rates. Hence, the investigation and detection of molecular markers are crucial for identifying patients suitable for specific therapies and monitoring resistance, thereby enhancing treatment strategies and prognoses. GSH metabolism is pivotal in the onset, progression,

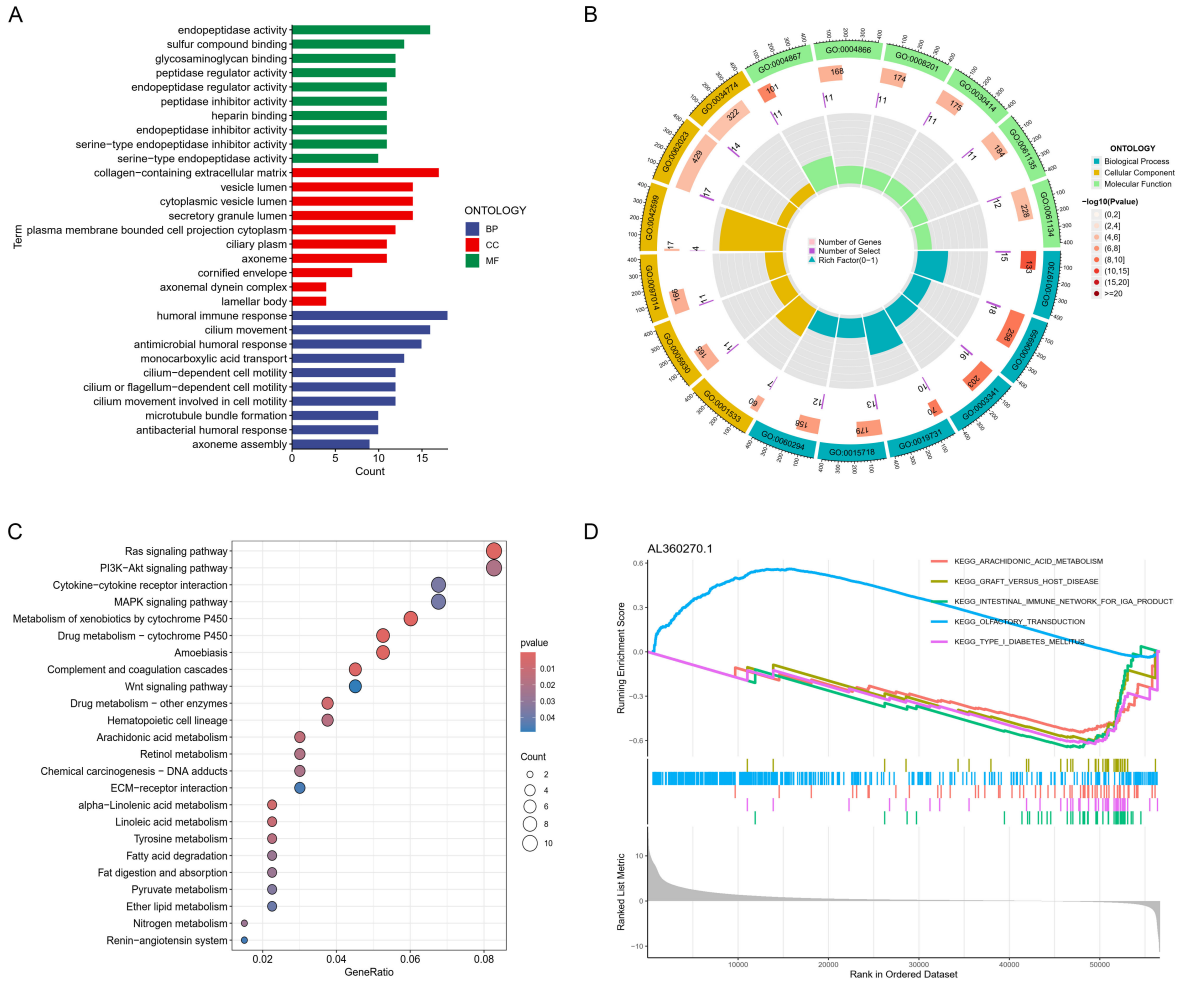


FIGURE 6
Gene function enrichment analysis. **(A)** Bar graphs and **(B)** chord diagrams displaying significant GO enrichment outcomes. **(C)** Bubble charts illustrating significant KEGG enrichment findings. **(D)** GSVA analysis for lncRNA (AL360270.1).

and immune response of tumors (35, 36). GSH regulates cell proliferation, apoptosis, and immune function (37). Novel therapeutic approaches targeting GSH metabolism could enhance treatment efficacy and address drug resistance. LncRNAs have been reported to play an irreplaceable role in many cancers, particularly in lung cancer research, with examples including MALAT1 and LINC00707 (9, 36). This study aims to investigate and validate GSH metabolism-related lncRNAs in LUAD, to assess their role in prognosis and immune response, and to enhance personalized treatment outcomes.

Initially, lncRNAs related to GSH metabolism were identified through co-expression analysis, and prognostically significant lncRNAs were selected using LASSO-Cox analysis. The criteria for lncRNA selection (Pearson correlation > 0.4, $p < 0.001$) were established to balance biological relevance, statistical significance, and clinical feasibility. This ensured the identification of highly relevant lncRNA features, enhancing model interpretability and predictive accuracy and avoiding unnecessary complexity. Six risk factors (AL162632.3, AL360270.1, LINC00707, DEPDC1-AS1, GSEC, and LINC01711) and three protective factors (AL078590.2, AC026355.2, and AL096701.4) were included. LINC00707 has been shown to play significant biological roles in various cancers by interacting with Smad proteins to regulate TGFβ signaling and promote cancer cell invasion (38). Its oncogenic function is further supported by studies in breast and gastric cancers, where elevated LINC00707 expression is associated with reduced patient survival (39). DEPDC1-AS1, an antisense RNA of DEPDC1, promotes proliferation and migration of human gastric cancer cells HGC-27 via the R-F11R pathway (40). LINC01711 can also promote hepatic fibrosis cell proliferation and migration by regulating XYLT1 (41). Moreover, this study is the first to report that AL162632.3, AL360270.1, GSEC, AL078590.2, AC026355.2, and AL096701.4 may be related to the prognosis of LUAD. Although not previously associated with tumor prognosis, these lncRNAs provide new insights into LUAD pathogenesis and warrant further investigation.

Samples were randomly divided into training and validation sets at a 7:3 ratio, and patients were stratified into high- and low-

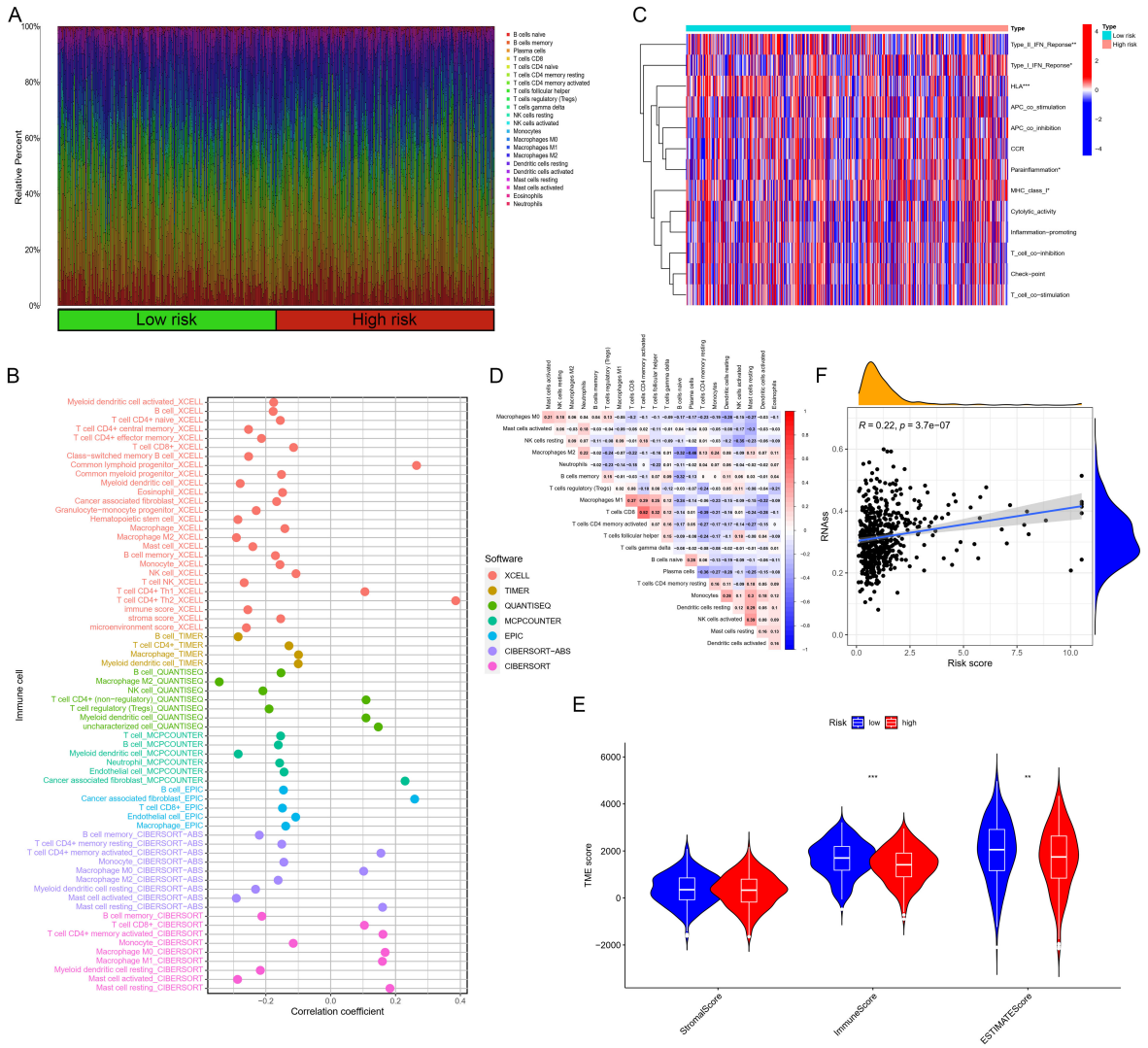


FIGURE 7
Immunological relevance analysis. **(A)** Stacked bar charts showing the composition ratios of classic immune cells in LUAD patient samples. **(B)** Bubble charts showing immune cell infiltration. **(C)** Analysis of the correlation between risk scores and immune pathways. **(D)** Correlation heatmap. **(E)** Violin plots showing the stroma, immune, and estimated scores. **(F)** Correlation analysis between risk scores and tumor stemness.

risk groups using the median risk score. Kaplan-Meier analysis showed significantly worse prognosis for the high-risk group, which was consistent across different cohorts, with DFS and risk curves aligning with OS results. The model outperformed clinical factors in predicting LUAD prognosis, as confirmed by ROC and C-index analyses. PCA demonstrated that the lncRNAs in the model effectively differentiated risk groups. The nomogram integrating clinical features enabled personalized prognostic stratification for post-surgical LUAD patients. High-risk individuals may benefit from additional treatments, such as immunotherapy or adjuvant chemotherapy. Enhanced follow-up strategies could further aid in early recurrence detection.

Functional analysis of differentially expressed genes revealed enrichment in immune-related pathways, including cytokine-cytokine receptor interactions and hematopoietic lineage. These findings highlight their critical role in immune regulation. CIBERSORT analysis showed increased immunosuppressive Tregs and M2 macrophages in the high-risk group, alongside reduced CD8+ T cells and M1 macrophages, indicating an immunosuppressive microenvironment conducive to tumor progression. Furthermore, the high-risk group exhibited impaired immune functions, including reduced Type II interferon responses. In contrast, the low-risk group demonstrated enhanced MHC class I expression and cytotoxic activity, underscoring the importance of immune modulation in prognosis and therapy.

Mutation analysis revealed significantly higher TMB in the high-risk group, primarily driven by mutations in key genes such as TP53, KRAS, and MUC16 (42–44). High TMB correlated with

10.3389/fimmu.2025.1477437

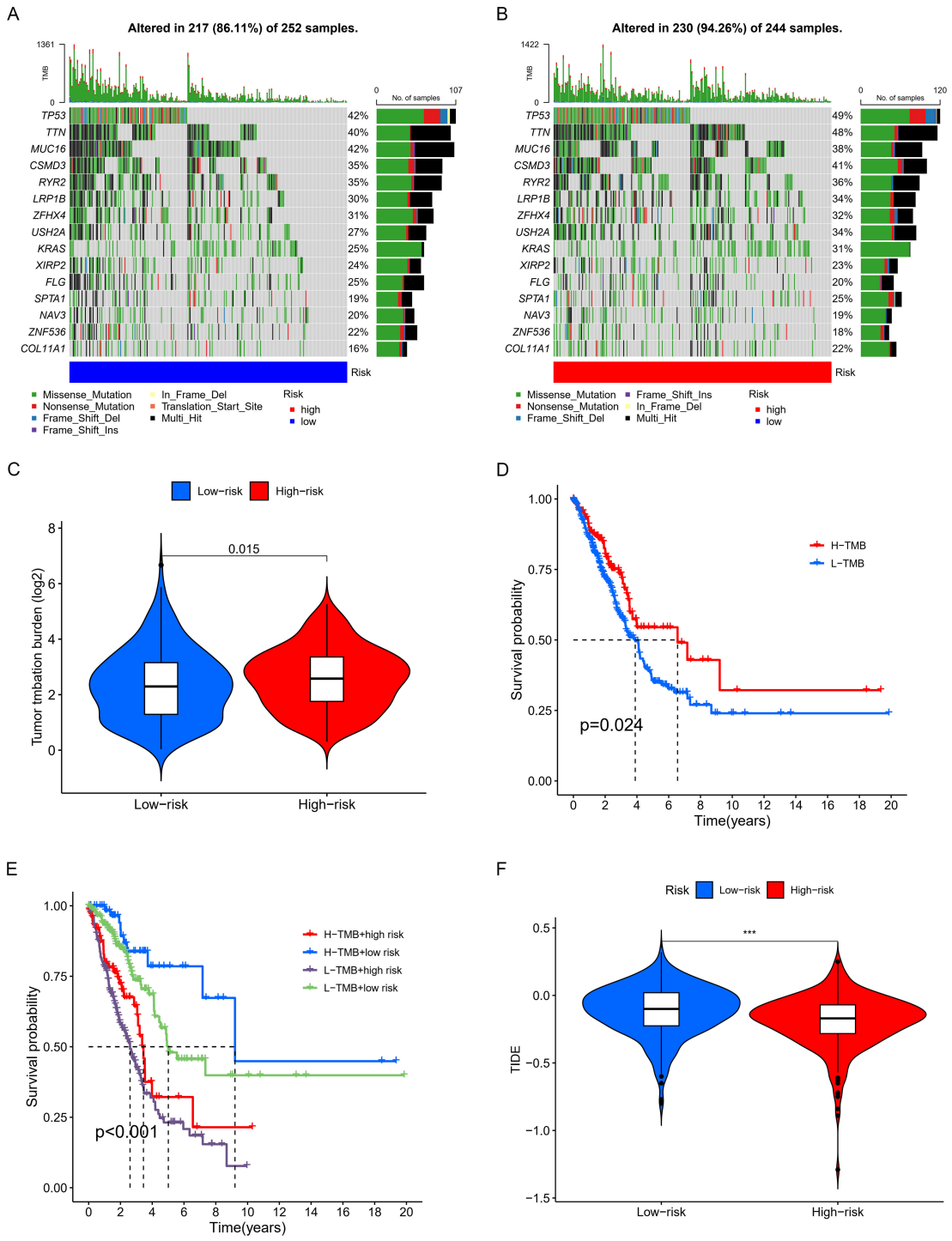


FIGURE 8
Examination of TMB. **(A, B)** Waterfall plots displaying notable gene mutations. **(C)** Comparative analysis of TMB. **(D)** K-M curve analysis evaluating the effect of high and low TMB on overall survival (OS). **(E)** K-M curve analysis of patient overall survival (OS) according to TMB and risk scores. **(F)** Analysis of the relationship between risk scores and immunotherapy responses. *** $p < 0.001$.

better survival rates (p=0.024), but patients in the high-risk group with low TMB had the worst outcomes, which is likely attributable to reduced immunogenicity and increased tumor aggressiveness. Conversely, patients with high TMB and low-risk scores had the best survival, suggesting a favorable response to immunotherapy. Tumor stemness analysis showed that higher RNAss correlated with increased risk scores (R = 0.22, p = 3.7e−07). This finding indicates that high-risk tumors possess stronger stemness traits

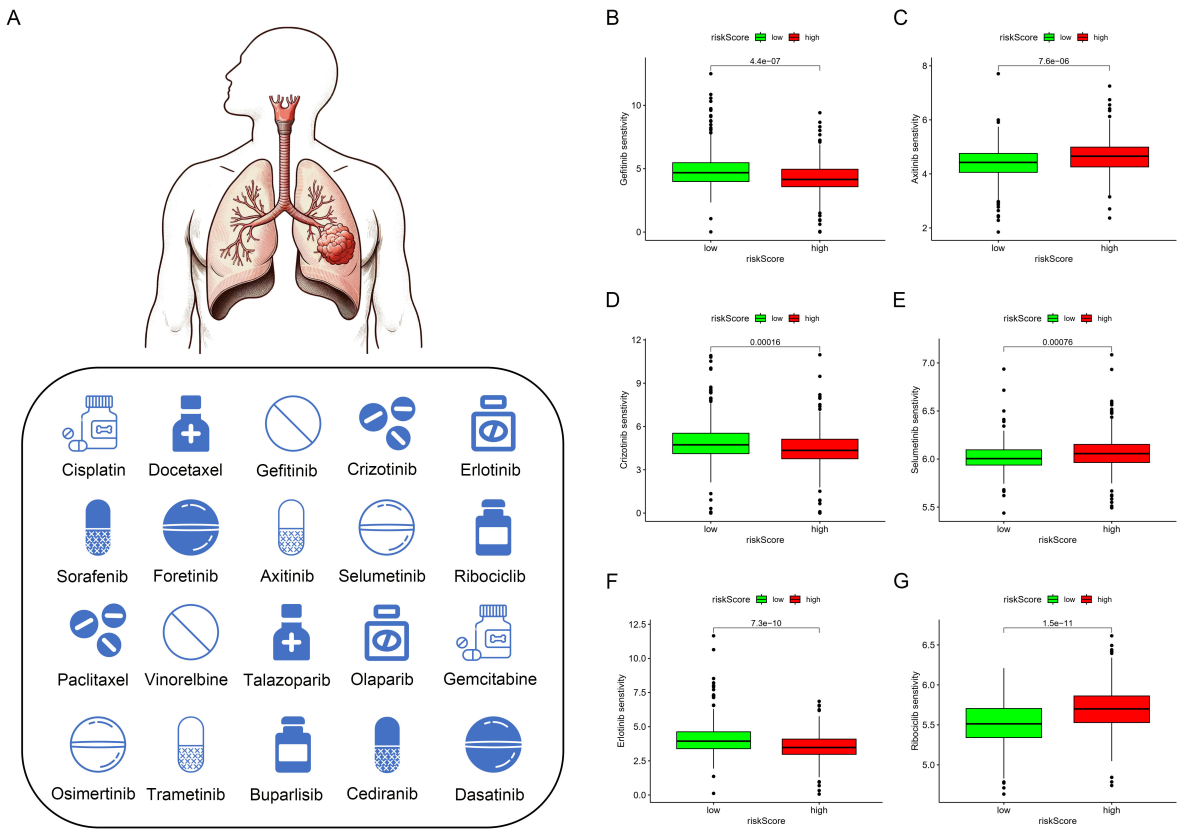


FIGURE 9
Drug sensitivity analysis. **(A–G)** Currently Approved and Investigational Sensitive Drugs for Lung Cancer Based on Model Predictions.

linked to aggressiveness and treatment resistance. Clinically, targeting tumor stemness could improve patient outcomes. TIDE analysis revealed that low-risk tumors, despite their better prognosis, exhibited strong immune evasion features, highlighting the importance of developing personalized immunotherapy strategies. Chemotherapy sensitivity analysis showed reduced efficacy of standard agents in the high-risk group but increased sensitivity to targeted therapies like Selumetinib, Ribociclib, and Axitinib. These findings highlight the reliance of high-risk tumors on specific pathways, providing guidance for future therapeutic strategies.

Additionally, we conducted independent prognostic analyses on 9 lncRNAs involved in the model construction and identified 5 statistically significant lncRNAs: 3 risk factors (AL162632.3, LINC01711, and GSEC) and 2 protective factors (AC026355.2 and AL096701.4). ts showed close alignment with prior bioinformatics analysis. In particular, AL162632.3 was upregulated in all selected lung cancer cell lines, with the most

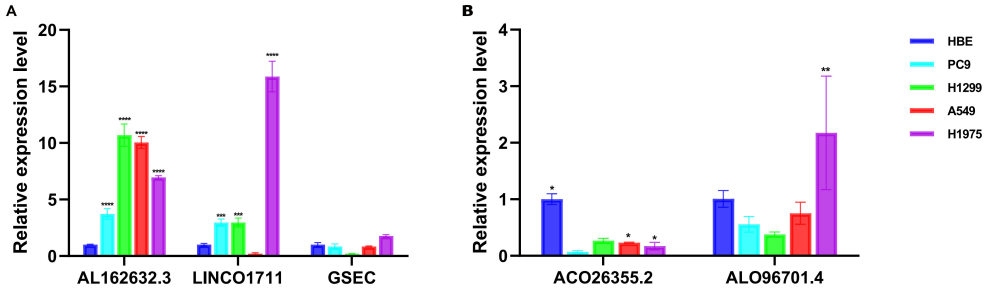


FIGURE 10
Validation of the expression of lncRNAs *in vitro* cell experiments. Analysis of expression levels of lncRNAs associated with **(A)** risk factors and **(B)** protective factors in HBE, PC9, H1299, A549, and H1975. * $p < 0.05$, ** $p < 0.01$, *** $p < 0.001$, **** $p < 0.0001$.

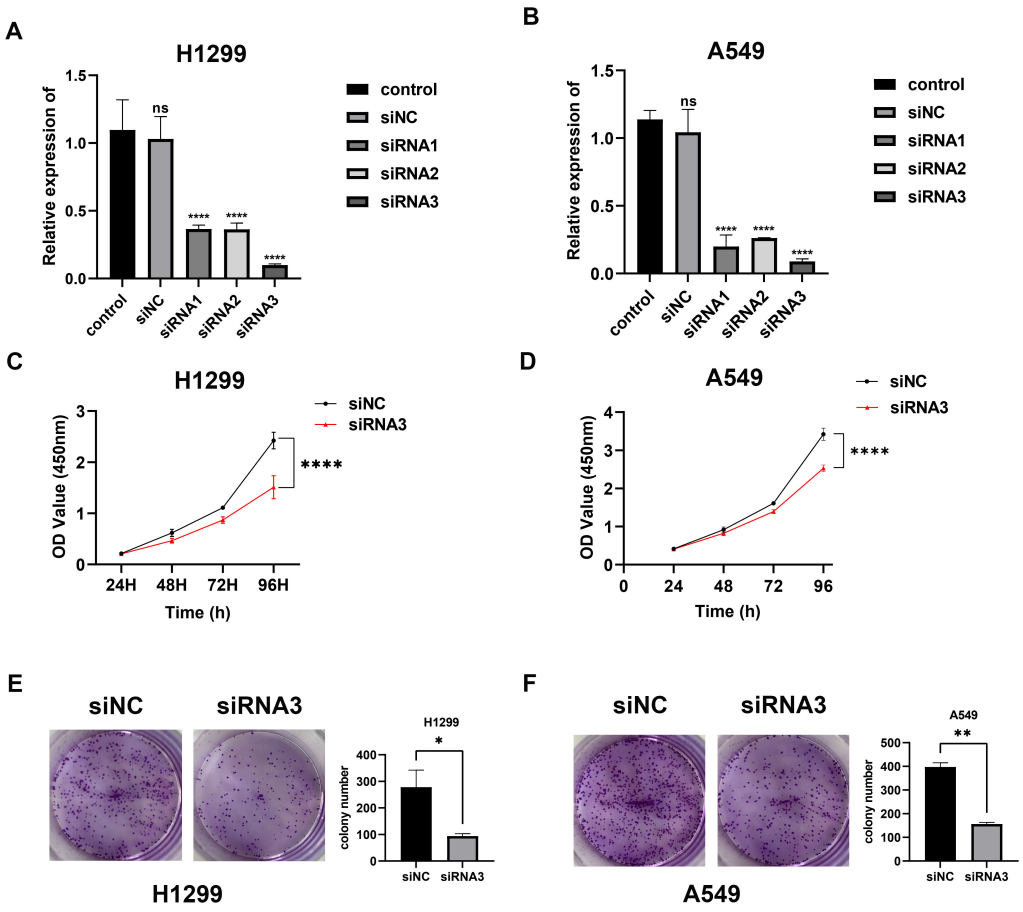


FIGURE 11
Downregulation of lnc-AL162632.3 inhibits LUAD growth. **(A, B)** Verification of interference efficiency. **(C, D)** CCK8 proliferation curves. **(E, F)** Colony formation assay. * $p < 0.05$, ** $p < 0.01$, *** $p < 0.001$, **** $p < 0.0001$.

notable expression in the H1299 cell line. The high expression of AL162632.3 may promote malignant behaviors in lung cancer cells. In contrast, AC026355.2 showed marked downregulation in the selected lung cancer cell lines, suggesting its potential anticancer activity. The downregulation of AC026355.2 may lead to a weakened response to growth-inhibiting signals in lung cancer cells, thereby aiding the progression of lung cancer. Hence, reinstating the expression of AC026355.2 could suppress lung cancer cells, providing a potential therapeutic target for lung cancer.

RT-qPCR analysis confirmed significant overexpression of lnc-AL162632.3 in lung cancer cell lines. To investigate its biological role, we transiently knocked down lnc-AL162632.3 in H1299 and A549 cells using RNAi technology. Knockdown significantly reduced cell proliferation, as shown by CCK8 and colony formation assays, and impaired migration and invasion in wound healing and invasion assays. *In vivo*, subcutaneous tumor models in nude mice revealed that tumors in the knockdown group were significantly smaller in volume and weight compared to controls. These findings indicate that lnc-AL162632.3 overexpression promotes lung cancer progression. To elucidate its regulatory mechanisms, future research will employ transcriptome sequencing to identify potential targets, such as GSH metabolism-related enzymes (e.g., GCLC, GSS) or signaling pathways influencing the tumor immune microenvironment. Additionally, RNA immunoprecipitation (RIP), chromatin immunoprecipitation (ChIP), and luciferase reporter assays will be used to validate these regulatory mechanisms.

This study highlights the role of GSH metabolism-related lncRNAs in LUAD while acknowledging certain limitations. The mechanisms by which lncRNAs regulate GSH metabolism remain unclear. The lack of suitable lncRNA probes has limited external validation, which we plan to address with RNA-seq in clinical samples. While LASSO-Cox was used for feature selection, future studies with larger samples should compare other methods like random forests. The nomogram predicts LUAD prognosis effectively but faces challenges such as individual variability in treatment response and lncRNA detection feasibility in clinical settings.

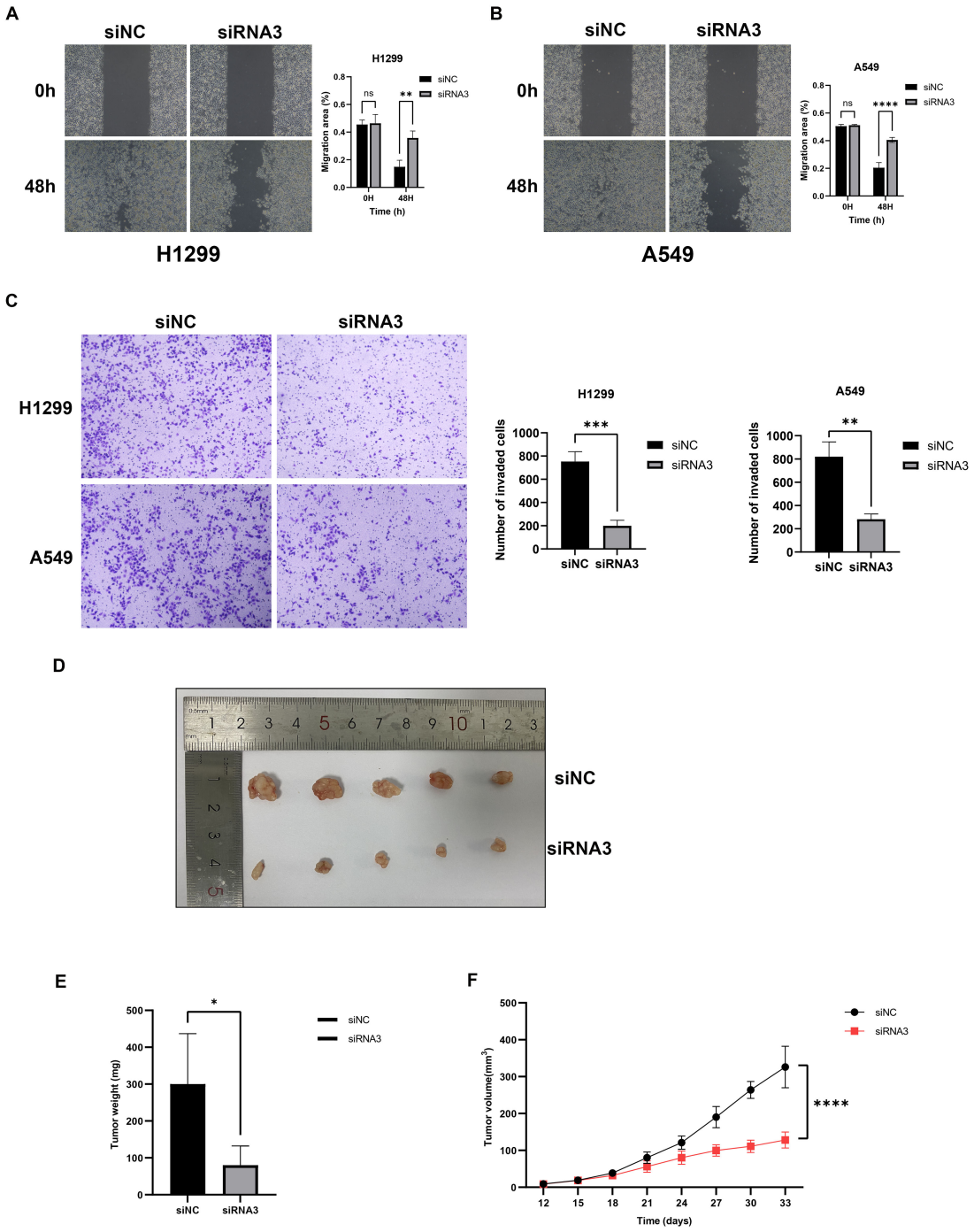


FIGURE 12
Downregulation of lnc-AL162632.3 inhibits migration and invasion in LUAD. **(A, B)** Wound healing assay. **(C)** Invasion assay. **(D-F)** Xenograft tumor model in nude mice. * $p < 0.05$, ** $p < 0.01$, *** $p < 0.001$, **** $p < 0.0001$.

5 Conclusions

This study demonstrated the prognostic importance of GSH metabolism-related lncRNAs in lung adenocarcinoma and developed a risk stratification model, which was further integrated into a nomogram for enhanced clinical applicability. High-risk patients were characterized by increased TMB and stemness, suggesting a strong link between gene mutations and patient outcomes. These findings underscore the potential of the model and nomogram to guide personalized immunotherapy strategies and improve survival in lung adenocarcinoma.

Data availability statement

The original contributions presented in the study are included in the article/Supplementary Material. Further inquiries can be directed to the corresponding author/s.

Ethics statement

The animal study was approved by The Laboratory Animal Ethics Committee of Yangzhou University. The study was conducted in accordance with the local legislation and institutional requirements.

Author contributions

JuH: Conceptualization, Data curation, Formal analysis, Investigation, Software, Supervision, Visualization, Writing – original draft, Writing – review & editing. ST: Methodology, Writing – review & editing. QL: Writing – review & editing, Methodology. JiH: Writing – review & editing, Supervision. JW: Supervision, Writing – review & editing, Visualization. XW: Funding acquisition, Methodology, Project administration, Resources, Validation, Writing – review & editing. YS: Funding acquisition, Methodology, Project administration, Resources, Validation, Writing – review & editing.

Funding

The author(s) declare financial support was received for the research, authorship, and/or publication of this article. This study was supported by the Jiangsu Provincial Health Commission Research Project on Elderly Health (LKZ2022019), Yangzhou Social Development and Clinical Frontier Technology Project (YZ2023084), Yangzhou Innovation Capability Building Design Plan Project (YZ2022168) and Yangzhou Social Development and Clinical Frontier Technology Project (YZ2021078).

Conflict of interest

The authors declare that the research was conducted in the absence of any commercial or financial relationships that could be construed as a potential conflict of interest.

Publisher's note

All claims expressed in this article are solely those of the authors and do not necessarily represent those of their affiliated organizations, or those of the publisher, the editors and the reviewers. Any product that may be evaluated in this article, or claim that may be made by its manufacturer, is not guaranteed or endorsed by the publisher.

Supplementary material

The Supplementary Material for this article can be found online at: https://www.frontiersin.org/articles/10.3389/fimmu.2025.1477437/full#supplementary-material

References

1. Sung H, Ferlay J, Siegel RL, Laversanne M, Soerjomataram I, Jemal A, et al. Global cancer statistics 2020: GLOBOCAN estimates of incidence and mortality worldwide for 36 cancers in 185 countries. *CA Cancer J Clin*. (2021) 71:209–49. doi: 10.3322/caac.21660

2. Planchard D, Popat S, Kerr K, Novello S, Smit EF, Faivre-Finn C, et al. Correction to: "Metastatic non-small cell lung cancer: ESMO clinical practice guidelines for diagnosis, treatment and follow-up. *Ann Oncol*. (2019) 30:863–70. doi: 10.1093/annonc/mdy474

3. Hirsch FR, Scagliotti GV, Mulshine JL, Kwon R, Curran WJ, Wu YL, et al. Lung cancer: current therapies and new targeted treatments. *Lancet*. (2017) 389:299–311. doi: 10.1016/S0140-6736(16)30958-8

4. Mamdani H, Matosevic S, Khalid AB, Durm G, Jalal SI. Immunotherapy in lung cancer: current landscape and future directions. *Front Immunol*. (2022) 13:823618. doi: 10.3389/fimmu.2022.823618

5. Raoof S, Mulford IJ, Frisco-Cabanos H, Nangia V, Timonina D, Labrot E, et al. Targeting FGFR overcomes EMT-mediated resistance in EGFR mutant non-small cell lung cancer. *Oncogene*. (2019) 38:6399–413. doi: 10.1038/s41388-019-0887-2

6. Xiong XD, Ren X, Cai MY, Yang JW, Liu X, Yang JM. Long non-coding RNAs: an emerging powerhouse in the battle between life and death of tumor cells. *Drug Resist Update*. (2016) 26:28–42. doi: 10.1016/j.drup.2016.04.001

7. Volders PJ, Anckaert J, Verheggen K, Nuytens J, Martens L, Mestdagh P, et al. LNCipedia 5: towards a reference set of human long non-coding RNAs. *Nucleic Acids Res*. (2019) 47:D135–9. doi: 10.1093/nar/gky1031

8. Chandra Gupta SC, Nandan Tripathi Y. Potential of long non-coding RNAs in cancer patients: from biomarkers to therapeutic targets. *Int J Cancer*. (2017) 140:1955–67. doi: 10.1002/ijc.30546

9. Martinez-Terroba E, Plasek-Hegde LM, Chiotakakos I, Li V, de Miguel FJ, Robles-Oteiza C, et al. Overexpression of malat1 drives metastasis through inflammatory reprogramming of the tumor microenvironment. *Sci Immunol*. (2024) 9:96. doi: 10.1126/sciimmunol.adh5462

10. Raju GS, Pavitra E, Bandaru SS, Varaprasad GL, Nagaraju GP, Malla RR, et al. HOTAIR: A potential metastatic, drug-resistant and prognostic regulator of breast cancer. *Mol Cancer*. (2023) 22:65. doi: 10.1186/s12943-023-01765-3

11. Sun Y, Zhao Y, Ni X, Yang Y, Fu Z, Liu R, et al. *In vivo* self-assembled small RNA targets H19 lncRNA for the treatment of colorectal cancer. *J Control Release*. (2023) 358:142–60. doi: 10.1016/j.jconrel.2023.04.026

12. Tang F, Wang H, Chen E, Bian E, Xu Y, Ji X, et al. LncRNA-ATB promotes TGF-β-induced glioma cells invasion through NF-κB and P38/MAPK pathway. *J Cell Physiol*. (2019) 234:23302–14. doi: 10.1002/jcp.28898

13. Xiao Z, La Fontaine S, Bush AI, Wedd AG. Molecular mechanisms of glutaredoxin enzymes: versatile hubs for thiol-disulfide exchange between protein thiols and glutathione. *J Mol Biol*. (2019) 431:158–77. doi: 10.1016/j.jmb.2018.12.006

14. Diaz-Vivancos P, de Simone A, Kiddle G, Foyer CH. Glutathione–linking cell proliferation to oxidative stress. *Free Radic Biol Med*. (2015) 89:1154–64. doi: 10.1016/j.freeradbiomed.2015.09.023

15. Kennedy L, Sandhu JK, Harper ME, Cuperlovic-Culf M. Role of glutathione in cancer: from mechanisms to therapies. *Biomolecules*. (2020) 10:1429. doi: 10.3390/biom10101429

16. Mirzaei S, Mohammadi AT, Gholami MH, Hashemi F, Zarrabi A, Zabolian A, et al. Nrf2 signaling pathway in cisplatin chemotherapy: potential involvement in organ protection and chemoresistance. *Pharmacol Res*. (2021) 167:105575. doi: 10.1016/j.phrs.2021.105575

17. Townsend DM, Tew KD. The role of glutathione-S-transferase in anti-cancer drug resistance. *Oncogene*. (2003) 22:7369–75. doi: 10.1038/sj.onc.1206940

18. Marini HR, Facchini BA, di Francia R, Freni J, Puzzolo D, Montella L, et al. Glutathione: lights and shadows in cancer patients. *Biomedicines*. (2023) 11:2226. doi: 10.3390/biomedicines11082226

19. Shi H, Yuan X, Yang X, Huang R, Fan W, Liu G. A novel diabetic foot ulcer diagnostic model: identification and analysis of genes related to glutamine metabolism and immune infiltration. *BMC Genomics*. (2024) 25:125. doi: 10.1186/s12864-024-10038-2

20. Tibshirani R. The lasso method for variable selection in the cox model. *Stat Med*. (1997) 16:385–95. doi: 10.1002/(sici)1097-0258(19970228)16:4<385::aid-sim380>3.0.co;2-3

21. Zeidan AM, Sekeres MA, Garcia-Manero G, Steensma DP, Zell K, Barnard J, et al. Comparison of risk stratification tools in predicting outcomes of patients with higher-risk myelodysplastic syndromes treated with azanucleosides. *Leukemia*. (2016) 30:649–57. doi: 10.1038/leu.2015.283

22. Gu Z, Gu L, Eils R, Schlesner M, Brors B. Circlize implements and enhances circular visualization in R. *Bioinformatics*. (2014) 30:2811–2. doi: 10.1093/bioinformatics/btu393

23. Wu T, Hu E, Xu S, Chen M, Guo P, Dai Z, et al. ClusterProfiler 4.0: A universal enrichment tool for interpreting omics data. *Innovation*. (2021) 2:100141. doi: 10.1016/j.xinn.2021.100141

24. Aran D, Hu Z, Butte AJ. xCell: digitally portraying the tissue cellular heterogeneity landscape. *Genome Biol*. (2017) 18:220. doi: 10.1186/s13059-017-1349-1

25. Li T, Fu J, Zeng Z, Cohen D, Li J, Chen Q, et al. TIMER2.0 for analysis of tumor-infiltrating immune cells. *Nucleic Acids Res*. (2020) 48:W509–14. doi: 10.1093/nar/gkaa407

26. Finotello F, Mayer C, Plattner C, Laschober G, Rieder D, Hackl H, et al. Correction to: molecular and pharmacological modulators of the tumor immune contexture revealed by deconvolution of RNA-seq data. *Genome Med*. (2019) 11:50. doi: 10.1186/s13073-019-0655-5

27. Becht E, Giraldo NA, Lacroix L, Buttard B, Elarouci N, Petitprez F, et al. Estimating the population abundance of tissue-infiltrating immune and stromal cell populations using gene expression. *Genome Biol*. (2016) 17:249. doi: 10.1186/s13059-016-1113-y

28. Racle J, Gfeller D. EPIC: A tool to estimate the proportions of different cell types from bulk gene expression data. *Methods Mol Biol*. (2020) 2120:233–48. doi: 10.1007/978-1-0716-0327-7_17

29. Newman AM, Liu CL, Green MR, Gentles AJ, Feng W, Xu Y, et al. Robust enumeration of cell subsets from tissue expression profiles. *Nat Methods*. (2015) 12:453–7. doi: 10.1038/nmeth.3337

30. Yoshihara K, Shahmoradgoli M, Martínez E, Vegesna R, Kim H, Torres-Garcia W, et al. Inferring tumour purity and stromal and immune cell admixture from expression data. *Nat Commun*. (2013) 4:2612. doi: 10.1038/ncomms3612

31. Hänzelmann S, Castelo R, Guinney J. GSVA: gene set variation analysis for microarray and RNA-seq data. *BMC Bioinf*. (2013) 14:7. doi: 10.1186/1471-2105-14-7

32. Mayakonda A, Lin DC, Assenov Y, Plass C, Koeffler HP. Maftools: efficient and comprehensive analysis of somatic variants in cancer. *Genome Res*. (2018) 28:1747–56. doi: 10.1101/gr.239244.118

33. Maeser D, Gruener RF, Huang RS. OncoPredict: an R package for predicting *in vivo* or cancer patient drug response and biomarkers from cell line screening data. *Briefings Bioinform*. (2021) 22:6. doi: 10.1093/bib/bbab260

34. Zhang Y, Vaccarella S, Morgan E, Li M, Etxeberria J, Chokunonga E, et al. Global variations in lung cancer incidence by histological subtype in 2020: A population-based study. *Lancet Oncol*. (2023) 24:1206–18. doi: 10.1016/S1470-2045(23)00444-8

35. Lo M, Wang YZ, Gout PW. The x(c)- cystine/glutamate antiporter: A potential target for therapy of cancer and other diseases. *J Cell Physiol*. (2008) 215:593–602. doi: 10.1002/jcp.21366

36. Lewerenz J, Hewett SJ, Huang Y, Lambros M, Gout PW, Kalivas PW, et al. The cystine/glutamate antiporter system x(c)(-) in health and disease: from molecular mechanisms to novel therapeutic opportunities. *Antioxid Redox Signal*. (2013) 18:522–55. doi: 10.1089/ars.2011.4391

37. Guo W, Li K, Sun B, Xu D, Tong L, Yin H, et al. Dysregulated glutamate transporter SLC1A1 propels cystine uptake via xc- for glutathione synthesis in lung cancer. *Cancer Res*. (2021) 81:552–66. doi: 10.1158/0008-5472.CAN-20-0617

38. Gélabert C, Papoutsoglou P, Golán I, Ahlström E, Ameur A, Heldin CH, et al. The long non-coding RNA LINC00707 interacts with smad proteins to regulate TGFβ Signaling and cancer cell invasion. *Cell Commun Signal*. (2023) 21:271. doi: 10.1186/s12964-023-01273-3

39. Li H, Liu Q, Hu Y, Yin C, Zhang Y, Gao P. Linc00707 regulates autophagy and promotes the progression of triple negative breast cancer by activation of PI3K/AKT/mTOR pathway. *Cell Death Discovery*. (2024) 10:138. doi: 10.1038/s41420-024-01906-7

40. Xu W, Wang J, Xu J, Li S, Zhang R, Shen C, et al. Long non-coding RNA DEPDC1-AS1 promotes proliferation and migration of human gastric cancer cells HGC-27 via the human antigen R-F11R pathway. *J Int Med Res*. (2022) 50:3000605221093135. doi: 10.1177/03000605221093135

41. Bao L, Chu Y, Kang H. SNAI1-activated long non-coding RNA LINC01711 promotes hepatic fibrosis cell proliferation and migration by regulating XYLT1. *Genomics*. (2023) 115:110597. doi: 10.1016/j.ygeno.2023.110597

42. Voskarides K, Giannopoulou N. The role of TP53 in adaptation and evolution. *Cells*. (2023) 12:512. doi: 10.3390/cells12030512

43. Singhal A, Li BT, O'Reilly EM. Targeting KRAS in cancer. *Nat Med*. (2024) 30:969–83. doi: 10.1038/s41591-024-02903-0

44. Song Y, Yuan M, Wang G. Update value and clinical application of MUC16 (Cancer antigen 125). *Expert Opin Ther Targets*. (2023) 27:745–56. doi: 10.1080/14728222.2023.2248376

frontiers | Frontiers in Pharmacology

TYPE Original Research
PUBLISHED 25 February 2025
DOI 10.3389/fphar.2025.1507693

Check for updates

OPEN ACCESS

EDITED BY
Alice Conigliaro,
University of Palermo, Italy

REVIEWED BY
Omer Faruk Hatipoglu,
Kindai University Hospital, Japan
Basveshwar Gawali,
Upstate Medical University, United States

*CORRESPONDENCE
Esraa M. Mosalam,
esraa.mosalam@phrm.menofia.edu.eg

RECEIVED 08 October 2024
ACCEPTED 20 January 2025
PUBLISHED 25 February 2025

CITATION
Samman WA, Mosalam EM, Saif DS, Abdallah MS, Zidan A-AA, Sallam AS, Abdelsattar S, Khalil FO, Elashkar AE, Mohamed SM, Al-Ghannam M and Abo Mansour HE (2025) Deciphering the role of Wnt/β-catenin and miR-214 in knee osteoarthritis: molecular and clinical insights. *Front. Pharmacol.* 16:1507693. doi: 10.3389/fphar.2025.1507693

COPYRIGHT
© 2025 Samman, Mosalam, Saif, Abdallah, Zidan, Sallam, Abdelsattar, Khalil, Elashkar, Mohamed, Al-Ghannam and Abo Mansour. This is an open-access article distributed under the terms of the Creative Commons Attribution License (CC BY). The use, distribution or reproduction in other forums is permitted, provided the original author(s) and the copyright owner(s) are credited and that the original publication in this journal is cited, in accordance with accepted academic practice. No use, distribution or reproduction is permitted which does not comply with these terms.

Deciphering the role of Wnt/β-catenin and miR-214 in knee osteoarthritis: molecular and clinical insights

Waad A. Samman[1], Esraa M. Mosalam [2,3]*, Dalia S. Saif[4], Mahmoud S. Abdallah[3,5], Abdel-Aziz A. Zidan[6], Amany Said Sallam[7], Shimaa Abdelsattar[8], Fatma Omar Khalil[9], Amany E. Elashkar[10], Somia Mokabel Mohamed[11], Mohamed Al-Ghannam[12] and Hend E. Abo Mansour[2,13]

[1]Department of Pharmacology and Toxicology, College of Pharmacy, Taibah University, Medina, Saudi Arabia, [2]Department of Biochemistry, Faculty of Pharmacy, Menoufia University, Shebin EL-Kom, Menoufia, Egypt, [3]Department of Pharm D, Faculty of Pharmacy, Jadara University, Irbid, Jordan, [4]Department of Rheumatology, Physical Medicine, and Rehabilitation Department Faculty of Medicine, Menoufia University, Shebin EL-Kom, Menoufia, Egypt, [5]Department of Clinical Pharmacy, Faculty of Pharmacy, University of Sadat City, Sadat City, Menoufia, Egypt, [6]Zoology Department, Faculty of Science, Damanhur University, Damanhour, Egypt, [7]Department of Pharmacology and Toxicology, Faculty of Pharmacy, Menoufia University, Shebin EL-Kom, Menoufia, Egypt, [8]Department of Clinical Biochemistry and Molecular Diagnostics, National Liver Institute, Menoufia University, Shebin EL-Kom, Menoufia, Egypt, [9]Clinical Microbiology and Immunology Department, National Liver Institute, Menoufia University, Shebin EL-Kom, Menoufia, Egypt, [10]Clinical Pathology Department, National Liver Institute, Menoufia University, Shebin EL-Kom, Menoufia, Egypt, [11]Department of Physiology, Faculty of Medicine for Girls, Al-Azhar University, Cairo, Egypt, [12]Department of Radiology, Faculty of Medicine, Menoufia University, Shebin EL-Kom, Menoufia, Egypt, [13]Biochemistry Department, Faculty of Pharmacy, Menoufia National University, Birket El-Sab, Egypt

Introduction: Understanding the molecular mechanism underlying the pathogenesis of knee osteoarthritis (KOA) may be beneficial in fetching new therapeutics. Our study aims to investigate the implication of Wnt/ β-catenin pathway in development of KOA by detection of the downstream target genes and their crosstalk with miR-214 in patients with KOA and to correlate that with the clinical findings.

Methods: Sixty participants were involved in the study. The levels of miR-214, β-catenin, Wnt4, matrix metalloproteinase 3 (MMP3), Bax, caspase 3, and phosphorylated glycogen synthase kinase-3 beta (pGSK3β) were determined. All participants were assessed clinically and radiologically regarding knee joint pain, stiffness, range of motion, and knee medial cartilage thickness. Besides, a correlation between Western Ontario and McMaster Universities (WOMAC) score, clinical, and radiological data, and the measured parameters was conducted.

Results and discussion: Patients with KOA showed downregulated miR-214 with upregulated β-catenin, Wnt4, MMP3, Bax, caspase 3, and pGSK3β compared to healthy individuals. Statistically significant positive correlation between WOMAC score, knee joint pain regarding Visual Analogue Scale (VAS) with β-catenin, pGSK3β, Wnt4, MMP3, Bax, and caspase 3, and significant negative relationship between them and knee joint medial cartilage thickness; while there was a statistically significant negative correlation between WOMAC, and clinical findings of osteoarthritis and miR-214 and significant positive relationship between it and knee joint medial cartilage thickness. This study provides

valuable insights into involvement of the Wnt/β-catenin and miR-214 in KOA pathogenesis. By targeting these molecular components, future therapeutics may modulate their activity and mitigate chondrocyte apoptosis and matrix degradation, potentially halting KOA progression.

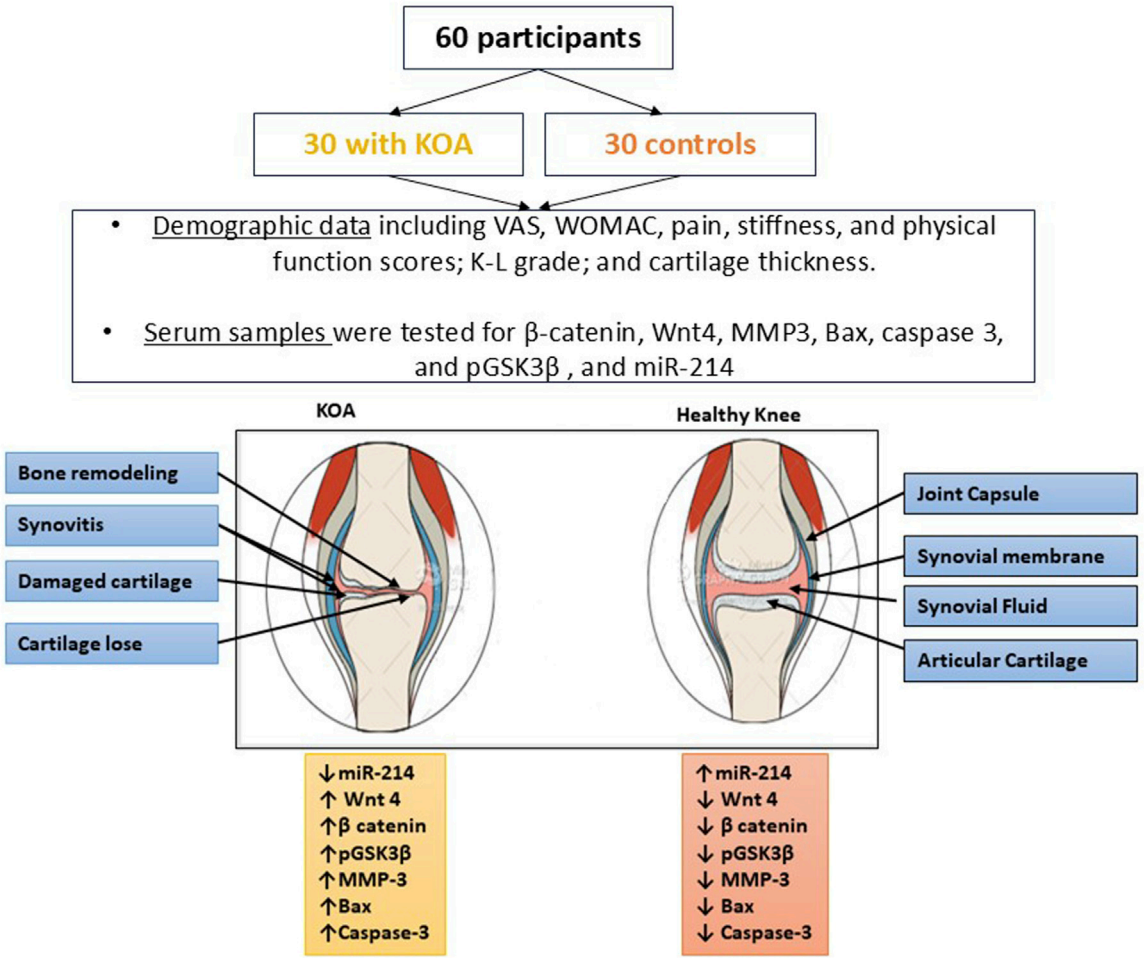
KEYWORDS

knee osteoarthritis, miR-214, Wnt/β-catenin, PGSK3β, WOMAC score

1 Introduction

Osteoarthritis (OA) is the most widespread form of long-lasting musculoskeletal diseases. Hip and knee OA are affecting about 300 million worldwide and they represent the 11th cause of global disability as measured by years lived with disabilities (YLDs). knee osteoarthritis (KOA) is characterized by the progressive breakdown of cartilage, which is mediated by inflammatory cytokines and other molecules (Liang et al., 2019). The stress on the knee increases as the KOA progresses because it gradually impairs the function of the knee, hurts and weakens the muscles. Also, it causes joint discomfort that develops gradually, gets worse with movement, spreads after extended periods of sitting or sleeping, and gets worse over time with stiffness, edema, restricted range of motion, and crepitus in the affected joint (Fang et al., 2021). Despite the progressive degenerative nature of the disease with aging, factors such as obesity, previous knee injuries, and regular crouching and kneeling increase the risk of early onset of knee osteoarthritis (KOA) (Blagojevic et al., 2010). Numerous studies have validated the use of ultrasonography for knee osteophytes, medial meniscal protrusion, and morphological alterations in the medial femoral condyle cartilage assessment and grading of KOA (Serban et al., 2016). When conservative treatment fails, surgical alternatives are considered as a next step in the management of KOA.

Depending on the etiology, KOA is classified as either primary or secondary. Primary KOA is caused by unidentified articular cartilage degeneration. This is frequently referred to as age-related degradation and wear and tear. Secondary KOA is caused by articular cartilage degeneration due to a known cause, such as



GRAPHICAL ABSTRACT

post-traumatic reasons (Manlapaz et al., 2019). Chondrocytes and extracellular matrix (ECM) components make up articular cartilage, an avascular tissue with a restricted potential for regeneration. The sole cell type in articular cartilage is the chondrocytes which control the anabolic to catabolic ratio to preserve the healthy function of the ECM (Moo et al., 2014). Chondrocyte death throughout the OA process is linked to degradation and calcification of ECM; suggesting a role for cell death in the OA pathogenesis. It might be able to boost chondrocyte proliferation to postpone OA development and progression (Gao et al., 2014). Understanding the pathophysiology of the developmental process of OA is depending on exploring the molecular mechanisms underlying the symptoms, which include articular cartilage deterioration, formation of bone spurs, subchondral sclerosis, and synovial hyperplasia (Chen et al., 2017).

Preceding studies have linked Wnt/β-catenin signaling trajectory in the development of OA (Appleton et al., 2010; Yuasa et al., 2008). Wnt is a glycoprotein that secreted outside of the cells with ninteen Wnt genes and many Wnt receptors that govern both canonical and non-canonical-catenin-dependent signaling pathways. Various activities involving cell division, polarization, proliferation, and fate of the cells throughout embryogenesis and later stages of development, are linked to both downstream pathways (Liu S. et al., 2017); as well as the development and progression of various diseases, with growing evidence of their pathogenic involvement in OA. The attachment of Wnt proteins to their receptors inhibits the phosphorylation of β-catenin and glycogen synthase kinase 3 beta (GSK3β). Non-phosphorylated catenin accumulates in the cytoplasm and travels to the nucleus to regulate the expression of target genes, accelerate the cell cycle, and encourage proliferation of cells (Fensterle, 2006).

MicroRNAs (miRNAs) are a subclass of non-protein-coding RNA molecules, with an approximate length of 22 nucleotides. They can mediate the post-transcriptional expression of various genes for the controlling of several physiological and pathological events. However, the degree of sequence similarity between their regulatory activities and the 3′-UTR of target mRNAs varies. It has been shown that miRNA expression controls bone and cartilage growth and preserves homeostasis in the latter (Borgonio et al., 2014; Duan et al., 2020). Previous studies have examined the distinct functions of several miRNAs in KOA, concluding that the expression of miR-214 controls crucial signaling pathways throughout the development of OA, such as the Wnt/β-catenin signaling (Cao et al., 2017). In this work, we aim to explore the possible role of miR-214 in KOA pathogenesis and diagnosis and also to establish a correlation between miR-214 expression and Wnt/β-catenin, clinical and radiological findings in patients with KOA in an attempt to provide molecular basis for developing novel miRNA-based targeted treatment modalities.

2 Patients and methods

2.1 Patients

A case-control study was conducted at Menoufia University Hospital's Department of, Rheumatology, Rehabilitation, and Physical Medicine with 30 KOA cases with average age of 57.57 years and 30 controls with matched sex. Patients were diagnosed using the American College of Rheumatology criteria, which included primary KOA with Kellgren-Lawrence grade (K-L grade) ≥ 1 (Mahmoudian et al., 2021).

One consultant, blind to the clinical data, performed knee ultrasonography within the same day as the clinical and radiographic, and laboratory tests. The physician used a (LOGIQ- E10) fitted with a high frequency broadband linear array transducer at 10–12 MHz. The medial cartilage thickness was assessed: When the patients were supine, their knees were in maximum flexion and the probe was put in an axial plane on the suprapatellar region then femoral cartilage was measured. The cartilage degeneration was categorized semi-quantitatively as follows: 0: normal, grade-1 (mild OA): loss of normal sharpness of cartilage interfaces and/or increased echogenicity of the cartilage, grade-2A (moderate OA): strong local thinning (less than 50%) of the cartilage, grade-2B (moderate OA): local thinning of the cartilage more than 50% but less than 100%, and grade-3 (marked OA): 100% local loss of the cartilage (Schiphof et al., 2008; Østergaard and Wiell, 2004; Boonstra et al., 2008).

The following criteria were excluded: gouty arthritis, post-traumatic arthralgia, autoimmune or connective tissue diseases, metabolic disorders, inflammatory arthritis, endocrine abnormalities, and developmental dysplasia. Healthy controls with similar age and gender were selected among hospital employees and individuals receiving routine medical examinations. Based on the medical record, no control ever experienced any clinical symptoms or signs (pain, swelling, tenderness, or restriction of movement) of OA, other arthritis, or joint illnesses at any site. No controls were related to the patients or the OA history in their family. Furthermore, they did not have any risk factors for KOA that could confound results, such as body mass index (BMI) equal to or more than 30 according to the WHO criteria, menopausal status, estrogen therapy, and type II diabetes mellitus.

Every participant's demographic, lifestyle, and clinical information—including age, gender, BMI, and K-L grading were documented. In the case of OA, the pain was measured using the Visual Analogue Scale (VAS) with ten scale bars (0–10) on one side (Boonstra et al., 2008; Alexander, 2007). As a measure of the severity of a condition, the Western Ontario and McMaster Universities (WOMAC) Osteoarthritis Index scale was used and each patient who was enrolled completed the validated Arabic version of the WOMAC score questionnaire (Faik et al., 2008), which includes 24 items measuring 3 subscales including: the primary factors used to assess the alterations in the structure and function of the knee joint regarding: pain (5 items) with pain ranging from 0 to 20 points, stiffness (2 items) that ranged from 0 to 8 points, and physical function (17 items) ranged from 0 to 68 points. Scores can be calculated for each subscale and a total WOMAC score is calculated by adding all 3 subscale scores that ranged from 0–96 points where 0 represents the best health status and 96 the worst possible status.

All participants provided written informed consent before participation. The Ethical Committee of the Faculty of Medicine Hospital at Menoufia University, under IRB number 12/2022RAD18, accepted the research protocol. The ethical approval complied with the Declaration of Helsinki's requirements.

2.2 Sample size calculation

Based on a review of past literature by Cao et al. (2021a) who reported that miR-214-3p expression was downregulated in inflamed chondrocytes and KOA cartilage. A minimum of sixty participants was determined to be the sample size. G Power software was used to divide them equally into two main groups, each with thirty participants at 80% power and 95% confidence intervals.

2.3 Measurements

All patients' blood was collected and put in vacuum-sealed containers for centrifugation at 4500 g for 15 min. Serum samples were placed into Eppendorf tubes and stored at −80°C for analyses. Specific commercial ELISA kits (MyBioSource, Inc.) were used to determine β-catenin, Wnt4, matrix metalloproteinase 3 (MMP3), Bax, and caspase 3 according to the manufacturer's instructions with catalogue number MBS8291331, MBS8802754, MBS045298, MBS2701194, MBS2513810; respectively. The level of pGSK3β (Ser9) was also measured using a commercially available ELISA kit (Cat No. PEL-GSK3b-S9, RayBiotech, Inc., United States) according to the supplier's instructions.

2.4 miRNA assay

miRNeasy serum/plasma kit (QIAGEN, Germany, Cat. No. 217184) was used to extract total RNAs, including miRNAs, from serum samples in accordance with the manufacturer's instructions. The quantity of RNA present was quantified using a Multiskan Sky High Microplate Spectrophotometer from Thermo Fisher Scientific (United States). By using qRT-PCR, the expression of miR-214 was detected. Thermo Fisher Scientific's TaqMan® microRNA reverse transcriptase kit (Cat. No. 4366596) and the TaqMan assays for hsa- miR-214 and RNU6B (Assay IDs: 002293 and 001093, respectively) were used to convert RNA to cDNA. miR-214 expression was compared to RNU6B, an endogenous control. The PCR reactions were carried out by using TaqMan® Universal Master Mix II (Applied Biosystems ™, United States, Cat. No. 4440043) in 20 µL total volume, including 10 µL TaqMan® Universal Master Mix II, 1 µL TaqMan® assay 20X, and 9 µL cDNA + RNase-free water. The following were the PCR settings: 1 min at 95°C, forty cycles of 95°C for 15 s, 1 min at 60°C, and 5 min at 72°C as the last extension. Real-time PCR was carried out using the StepOnePlus™ Real-Time PCR system (Thermo Fisher Scientific, United States) and the fold change and Ct were computed.

2.5 Protein-protein interaction (PPI) network analysis

This was created by using Cytoscape v3.10.2 and string online database; https://string-db.org/. Wnt protein was chosen as a central protein to create the network. String protein query was used in the setting of the software with a medium confidence score of 0.4, average local clustering coefficient equal to 0.878, PPI enrichment p-value <1.0e^{-16}, and with no more than 5 interactions in the first and the second shells.

2.6 Statistical analysis

The mean and standard deviation (SD) for all data is displayed. Using an independent sample t-test, differences across groups were evaluated. For categorical data, the chi-square test or Fisher's exact test was used as appropriate. The link between the measured parameters was evaluated by calculating Pearson's correlation. A p value of less than 0.05 was used to determine statistical significance. The diagnostic cutoff points were chosen from the receiver operating characteristic (ROC) curve with the maximum accuracy. The computations were completed using IBM's SPSS 21.0 statistical program (IBM, United States).

3 Results

3.1 Demographic and clinical features

The demographic and clinical characteristics of the study participants, categorized by groups and grades, are outlined in Table 1.

3.2 Effect on biological markers

We looked at the expression of miR-214 in serum samples either from KOA patients or healthy donors without any joint conditions to probe the potential function of miR-214 in human KOA. Comparing with healthy donors, the expressional level of miR-214 was significantly reduced in KOA patients by 75.79% ($p < 0.001$) as presented in Figure 1.

The protein levels of Wnt/β-catenin mediators were then examined in both healthy donors and KOA patients. Serum from KOA patients had significantly higher protein levels of β-catenin, Wnt4, MMP3, Bax, caspase 3, and pGSK3β than serum from healthy donors by 1.69, $p = 0.0001$; 1.45, $p = 0.0001$; 2.91, $p = 0.0001$; 2.88, $p < 0.0001$; 4.41 folds, $p < 0.0001$; respectively, and by 86.81%, $p = 0.0001$ for pGSK3β as shown in Figure 2.

3.3 Correlation study

Our results showed a statistically significant positive correlation between WOMAC scores (regarding pain, stiffness, and physical function) and β-catenin, pGSK3β, Wnt4, MMP3, Bax, and caspase 3, while there was a statistically significant negative correlation between WOMAC scores and miR-214 as shown in Figure 3. miR-214 showed a statistically significant negative correlation with β-catenin, pGSK3β, Wnt4, MMP3, Bax, and caspase 3 ($r = −0.819$, $p < 0.001$, $r = −0.780$, $p < 0.001$, $r = −0.766$, $p < 0.001$, $r = −0.791$, $p < 0.001$, $r = −0.831$, $p < 0.001$, and $r = −0.822$, $p < 0.001$, respectively).

As shown in Table 2, there was a significant negative correlation between the serum concentration of miR-214 and the clinical

TABLE 1 Demographic and clinical features of study groups. Sixty participants were involved; 30 with KOA and 30 matched controls.

Laboratory parameters	Group 1 (KOA patients) n = 30	Group 2 (healthy control) n = 30	Statistical values
Age (years)	57.57 ± 4.38	29 ± 4.5	$P = 0.295$
Sex			$P = 1$
Male (n)	7	7	
Female (n)	23	23	
Weight (kg)	82.067 ± 3.35	70.1 ± 4.9	$P = 0.125$
Height (cm)	167.93 ± 3.3	169.66 ± 4.4	$P = 0.072$
BMI (Kg/m^2)	29.1 ± 1.03	24.35 ± 1.65	$P = 0.666$
K–L grade	G1, G2	G0	
Medial cartilage thickness	0.746 ± 0.123	2.49 ± 0.257	$P < 0.001$
VAS score	6.6 ± 1.19	1.1 ± 0.31	$P < 0.001$
WOMAC score	57.57 ± 4.38	1.07 ± 0.37	$P < 0.001$
Pain score	7.73 ± 0.98	1.5 ± 0.5	$P < 0.001$
Stiffness score	7.167 ± 0.53	1.33 ± 0.48	$P < 0.001$
Physical function score	33 ± 2.12	8.47 ± 1.25	$P < 0.001$

KOA: Knee osteoarthritis, WOMAC, score: Western Ontario and McMaster Universities score, VAS:Visual analogue scale, BMI: Body mass index.

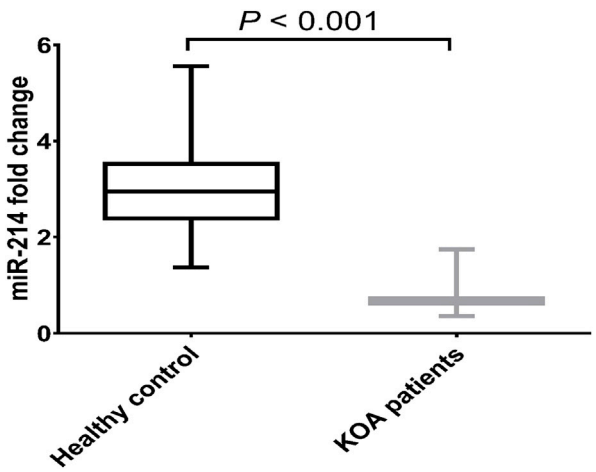


FIGURE 1
Expression pattern of miR-214 in health donors and patients with KOA. Data are presented as mean ± SD, $p < 0.001$, n = 30. miR-214 was found to be downregulated in KOA patients compared to the healthy controls.

finding of KOA regarding the grade of knee joint pain according to VAS, as its serum concentration was low among patients with high grades of knee joint pain, while β-catenin, pGSK3β, Wnt4, MMP3, Bax, and caspases3 concentration were positively correlated with the grade of knee joint pain regarding VAS. On another side there was a significant negative correlation between β-catenin, Wnt4, MMP3, Bax, Caspases3, and pGSK3β with the radiological data of KOA as regards to the medial cartilage thickness of the knee joint as their serum concentration was high among patients with advanced grades of OA (with lower cartilage thickness), while miR-214 serum concentration was low among patients with advanced grades of KOA and low cartilage thickness, as its serum concentration was positively correlated to medial cartilage thickness of the knee joint.

3.4 ROC curve analysis for miR-214

A ROC curve showed the best cutoff value of miR-214 among KOA patients to be less than 1.4832, with a sensitivity of 96.7% and a specificity of 93.3% (area under the curve = 0.997; Figure 4.

3.5 Protein-Protein interaction network analysis

The network created by Cytoscape revealed 17 molecular target protein that are crossly connected with Wnt/β-catenin. These protein can be further investigated in KOA to establish novel diagnostic and therapeutic avenues (Figure 5).

4 Discussion

KOA is the most prevalent joint condition in the world and a chief contributor to disability. KOA can have a detrimental effect on a person's physical and mental health because it is characterized by articular cartilage loss, juxta-articular inflammation, and alterations in periarticular and subchondral bone (Stampella et al., 2017). KOA patients frequently exhibit signs of knee joint swelling, discomfort, and restriction of mobility. Hence, their quality of life is negatively impacted, and cellular inflammatory factors contribute significantly to the development of KOA (He et al., 2021). However, there are currently no efficient strategies for cartilage healing; therefore,

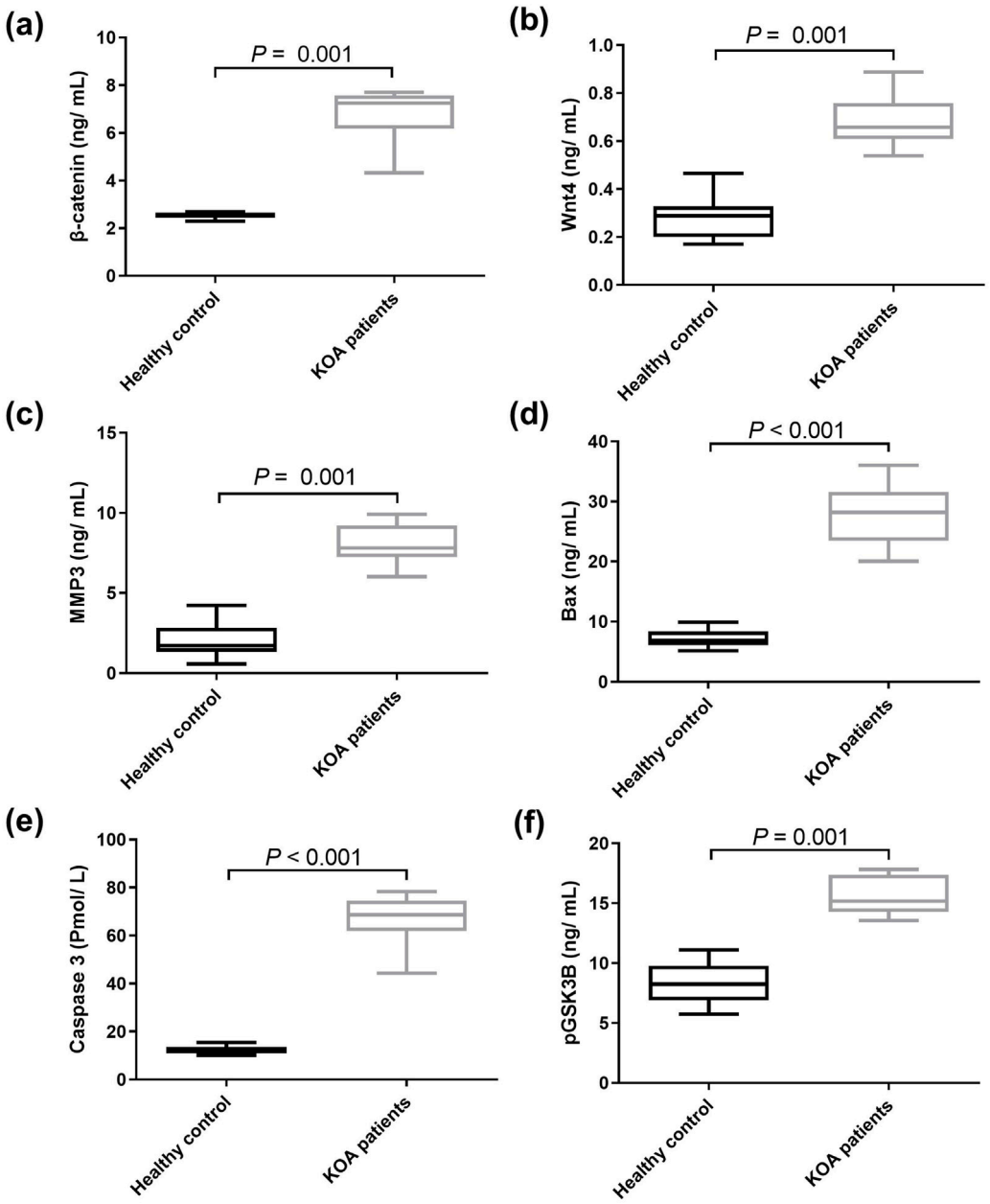


FIGURE 2
Serum levels of downstream genes of Wnt/β-catenin signaling pathway in health donors and patients with KOA. **(A)** β-catenin, **(B)** Wnt4, **(C)** MMP3, **(D)** Bax, **(E)** caspase 3, and **(F)** pGSK3β. Data are presented as mean ± SD, $P < 0.01$, n = 30. Wnt4: wingless-type mmtv integration site family member 4, MMP3: matrix metalloproteinase 3, pGSK3β: phosphorylated glycogen synthase kinase 3 beta. The detected genes were found to be upregulated in KOA patients compared to the healthy controls.

patients with severe KOA typically require joint replacement. Understanding the pathophysiology of KOA may lead to transformative therapeutics (Wu et al., 2022). Our study is the first to establish the relationship between the expression of miR-214 and the Wnt/β-catenin signaling-related proteins and also with the clinical findings in patients with KOA; the issue which could help in better knowledge of the pathophysiology of the disease and developing novel miRNA-based treatment avenues.

In the present study and in KOA patients, we noticed a decline in miR-214 and an increase of β-catenin. This finding suggests that low miR-214 and high β-catenin levels may be linked to the pathophysiology of cartilage degeneration. Additionally, we observed a notable inverse correlation between the concentration of miR-214 in the bloodstream and the WOMAC scores, which assess pain, stiffness, and physical function in patients with KOA. Furthermore, we found that the serum concentration of miR-214 was lower in patients with higher grades of knee joint pain, as indicated by the VAS, and conversely, higher in patients with lower levels of knee joint pain. Moreover, there was a positive relationship between miR-214 concentration and the thickness of

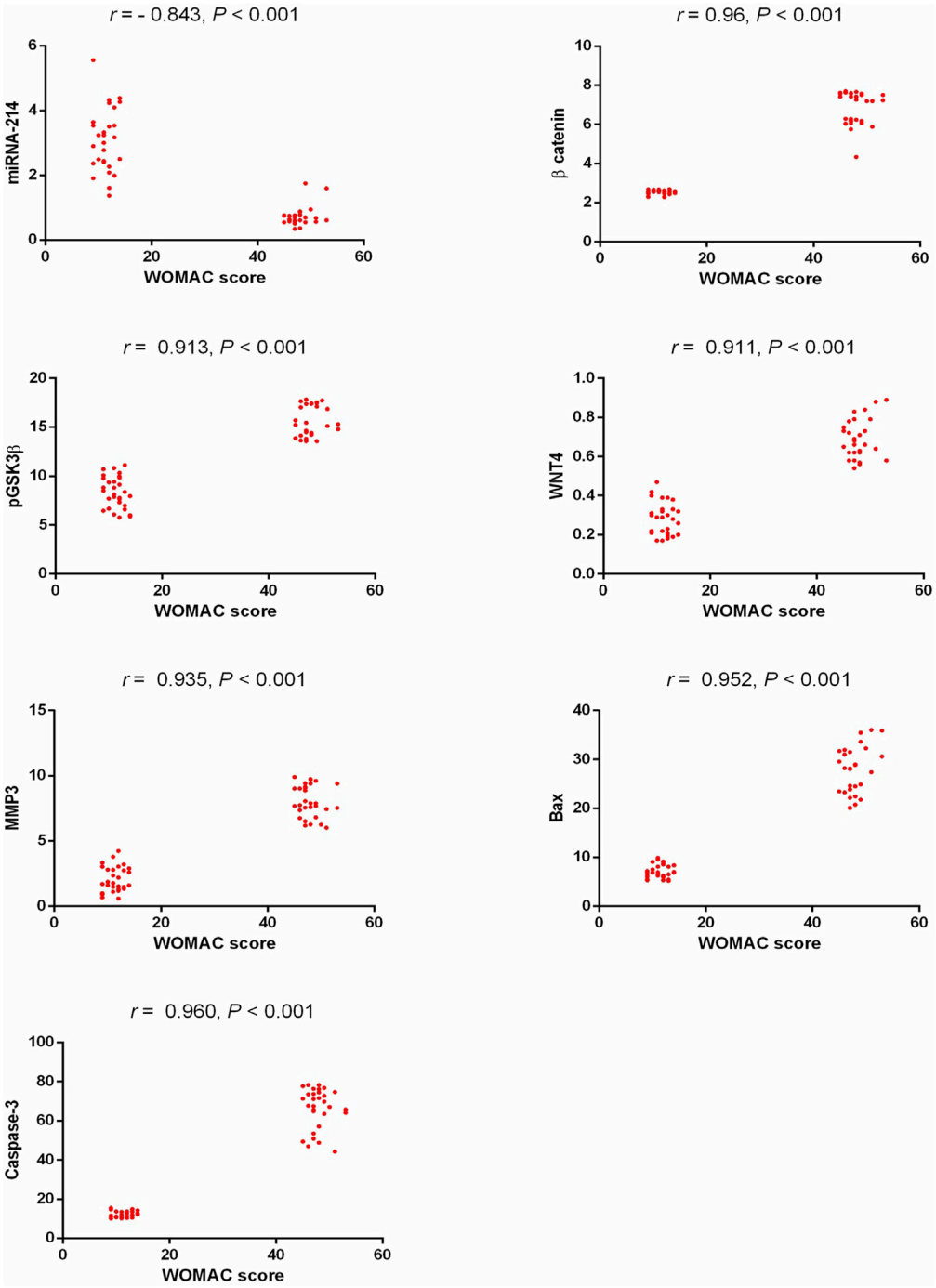


FIGURE 3
Correlation study between the detected biomarkers and WOMAC score in patients with KOA. WOMAC: Western Ontario and McMaster Universities, pGSK3β: phosphorylated glycogen synthase kinase 3 beta, Wnt4: wingless-type mmtv integration site family member 4, MMP3: matrix metalloproteinase 3, Bax: Bcl2-associated X protein.

the medial knee cartilage, as determined by musculoskeletal ultrasound. Specifically, patients in advanced stages of OA with low cartilage thickness exhibited reduced levels of miR-214 in their serum, while those with higher cartilage thickness displayed elevated miR-214 levels. These findings contradict those of He et al. (2021) who suggested that miR-214 may contribute to cartilage and subchondral bone degradation, and contribute to the progression of KOA.

We could explain the controversy between the results of a study conducted by He et al. (2021) and our findings; as the study performed by He et al. (2021) was performed on patients with KOA with no healthy volunteers. It also aimed to study the effect of etoricoxib on miR-214 and inflammatory responses in those patients. This former study showed that etoricoxib has a lowering effect on miR-214 and on the synthesis of prostaglandins, with a

TABLE 2 Correlation between clinical findings regarding visual analogue scale and radiological data regarding medial cartilage thickness and lab parameters among participants of the study groups.

	VAS		Medial cartilage thickness	
	r	*P*	*r*	*p*
miR-214	−0.83	<0.001	0.47	<0.001
β-catenin	0.93	<0.001	−0.55	<0.001
Wnt4	0.88	<0.0013	−0.39	0.002
MMP3	0.93	<0.001	−0.47	<0.001
Bax	0.89	<0.001	−0.43	<0.001
Caspases3	0.94	<0.001	−0.49	<0.001
pGSK3β	0.92	<0.001	−0.56	<0.001

Wnt4: wingless-type mmtv integration site family member 4, MMP3: matrix metalloproteinase 3, Bax: Bcl2-associated X protein, pGSK3β: phosphorylated glycogen synthase kinase 3 beta.

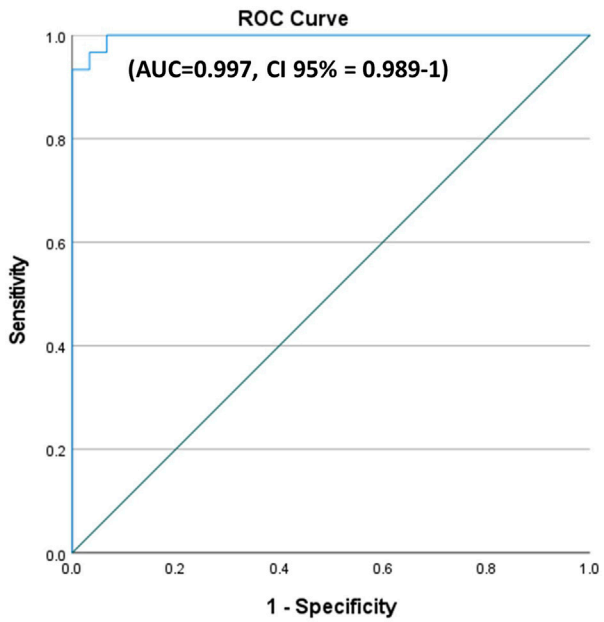


FIGURE 4
ROC curves for miR-214 in KOA patients versus healthy control. A ROC curve showed the best cutoff value of miR-214 among KOA patients to be less than 1.4832, with a sensitivity of 96.7% and a specificity of 93.3%.

subsequent reduction in the level of serum inflammatory biomarkers, and inhibition of some enzymes involved in the deterioration of the cartilages. They also concluded that etoricoxib has a satisfactory therapeutic effect on patients with KOA, and can notably reduce the expression of serum miR-214, which is worthy of clinical application.

On the other hand, Yuan et al. (2019) demonstrated that miR-214 prevented KOA in rats and exerted chondroprotective effects by stimulating the mitogen-activated protein kinase (MAPK) signaling pathway and as its high levels was associated with high cartilage thickness. Furthermore, Cao et al. (2021a) found that reduced miR-214 stimulates nuclear factor kappa-light-chain-enhancer of activated B cells (NF-κB) pathway and aggravates osteoarthritis progression through targeting inhibitory kappa B kinase subunit beta (IKKβ) with subsequent progression of clinical signs and symptoms of OA regarding joint pain, swelling, limited range of motion. These outcomes suggested that targeting miR-214 could be a promising new treatment approach for treating KOA patients. However, the specific functions of miR-214 in osteoarthritis and the molecular mechanisms driving its effects remain to be fully understood.

Lai et al. (2023) also, shown in their research that exosomes produced from synovial fluid that target the miR-214 anti-inflammatory pathway may inhibit the release of inflammatory cytokines that are implicated in the development of osteoarthritis, with subsequent improvement of its clinical manifestations regarding pain, swelling and limited range of motion. Also, they documented that treatment with miR-214 significantly alleviated the loss of proteoglycans, surface irregularities, synovial joint inflammation, and suppressed cartilage tissue degeneration in OA mice. It can also significantly prevent the degeneration of cartilage tissue. It was established that mice with deteriorated cartilage had lower levels of miR-214 expression in their articular cartilage, and that mice with high levels of miR-214 expression in their articular cartilage had a chondroprotective effect against the development of OA (Cao et al., 2022).

It is also noteworthy to discuss the controversial protective effect of miR-214 for the cartilage but inhibitory effect on the bone. In OA, miR-214-3p has been identified as a protective agent against cartilage degeneration. Studies indicated that miR-214-3p expression is reduced in OA chondrocytes (Fioravanti et al., 2021). Overexpression of miR-214-3p counteracts interleukin-1β (IL-1β)-induced apoptosis and matrix degradation in chondrocytes (Fioravanti et al., 2021; Cao et al., 2021b). *In vivo* studies showed that administering miR-214-3p agomir *via* intra-articular injection in OA mice reduced cartilage degeneration and synovial inflammation (Cao et al., 2021b). These results indicate that miR-214-3p has a protective function in cartilage metabolism and may halts the progression of OA. Conversely, miR-214 acts as an inhibitor of bone formation. Research shows that miR-214 inhibits osteoblast activity and deposition of the minerals in the bone matrix by targeting activating transcription factor 4 (ATF4) (Wang et al., 2013).In mouse models, upregulation of miR-214 led to reduced rates of bone formation; revealing its role in defeating osteoblast activity. Additionally, osteoclast-derived exosomal miR-214-3p has been found to inhibit osteoblastic bone formation (Li et al., 2016).

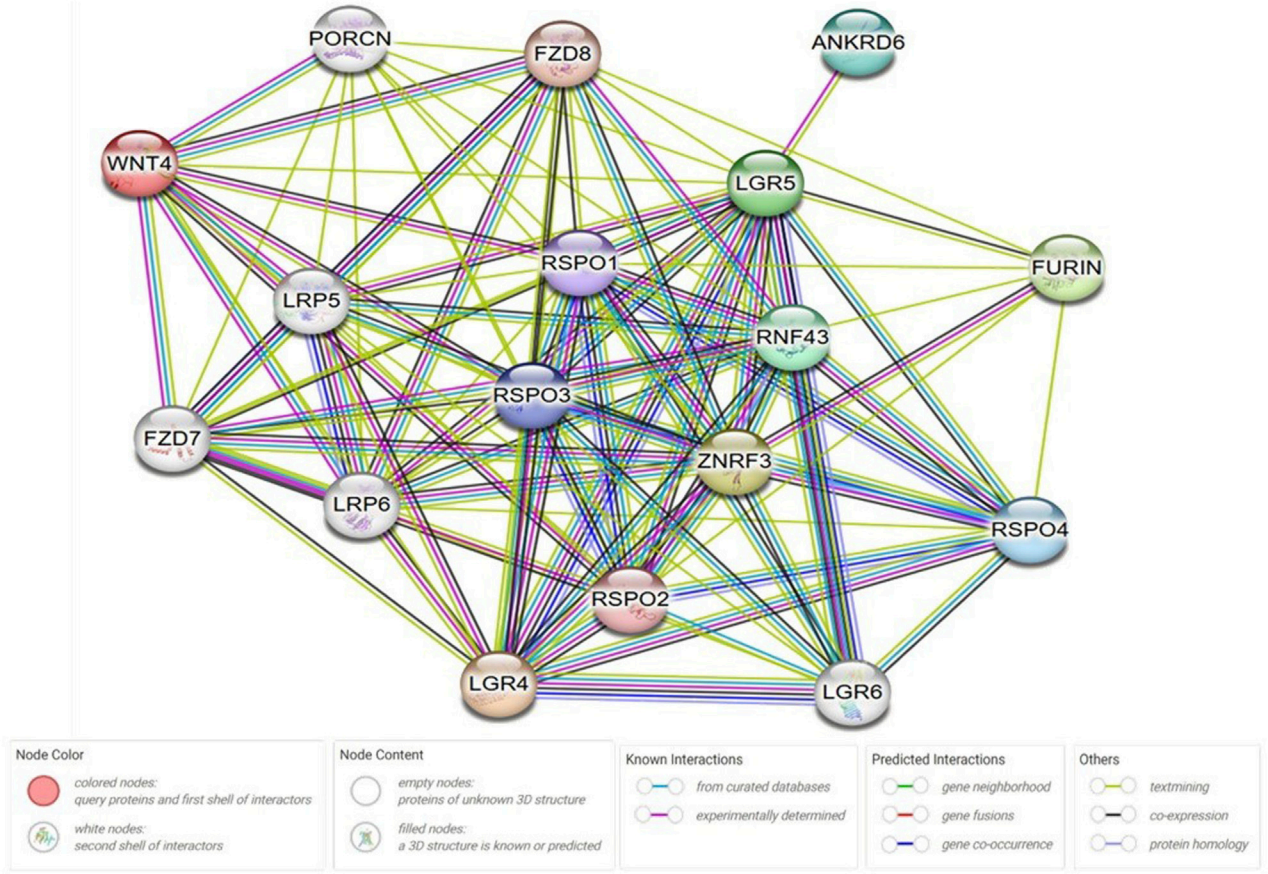


FIGURE 5
Protein-protein interaction (PPI) network analysis. The network was created by using Cytoscape v3.10.2 and string online database; https://string-db.org/. Wnt protein was chosen as a central protein to create the network. String protein query was used in the setting of the software with a medium confidence score of 0.4, average local clustering coefficient equal to 0.878, PPI enrichment p-value <1.0e^{-16}, and with no more than 5 interactions in the first and the second shells. ANKRD6: Ankyrin Repeat Domain 6, RNF43: Ring Finger Protein 43, RSPO: R-spondin, LGR: Leucine-rich repeat-containing G-protein coupled receptor, ZNRF3: Zinc And Ring Finger 3, PORCN: porcupine O-acyltransferase, FZD: Frizzled Class Receptor.

Former studies suggested that miR-214-3p transfers from osteoclasts to osteoblasts, resulting in decreased bone development (Li et al., 2016; Liu J. et al., 2017). These contrasting roles of miR-214 highlight its tissue-specific functions, offering insights into potential therapeutic targets for conditions like osteoarthritis and osteoporosis.

Turning to the value of miR-214 as a diagnostic tool in KOA, the optimal cutoff value for miR-214 in the ROC curve analysis was determined to be below 1.4832, showing an impressive sensitivity of 96.7%, specificity of 93.3%, and an AUC of 0.997. Although research regarding the role of miR-214 in KOA is limited, our findings are in harmony with previous studies investigated the diagnostic potential of plasma levels of miR-200c-3p, miR-100-5p, and miR-1826 in osteoarthritis. The plasma miR-200c-3p had an AUC of 0.755, with sensitivity and specificity both at 82.00%. For miR-100-5p, the AUC was 0.845, sensitivity was 82.00%, and specificity was 86.00%. Likewise, plasma level of miR-1826 showed an AUC of 0.749, with sensitivity at 82.00% and specificity at 86.00% (Lai and Cao, 2019; Ghafouri-Fard et al., 2021).

Generally, the Wnt/β-catenin trajectory controls chondrocyte differentiation and development, and aberrant expression of components of this pathway is significantly associated to KOA (Shi et al., 2021), which suggests that Wnt signaling plays a key role in the disease pathogenesis. Consequently, the Wnt signaling is thought to be a possible target to regulate KOA (Stampella et al., 2017). It has been found that miRNAs have a role in regulating Wnt/β-catenin signaling (Cao et al., 2017). The canonical Wnt pathway starts its signaling within cells by adjusting the intracellular concentration and subcellular location of β-catenin (Chen et al., 2017). Moreover, miR-214 has been shown to regulate β-catenin (Čermák et al., 2021). Furthermore β-catenin gene was confirmed to be a direct target of miR-214 (Cao et al., 2017). In humans, at least 10 frizzled (Fzd) receptors and 19 Wnt proteins have been found. Among these, Wnt4 is expressed in growing joints and contributes to the synovial joint's interzone growth (Corr, 2008). Wnt4 is a canonical Wnt ligand, and it has been considered to be an activator of the canonical Wnt signaling pathway (Zhu et al., 2009). Wnt ligands bind to their trans-membrane receptor Fzd and co-receptors low-density lipoprotein receptor-related protein (LRP)-5/6, which inhibit GSK3β. This boosts the amount of β-catenin, which then translocates into the nucleus to interact with the transcription factor family T-cell factor/lymphoid enhancer-binding factor (TCF/LEF),

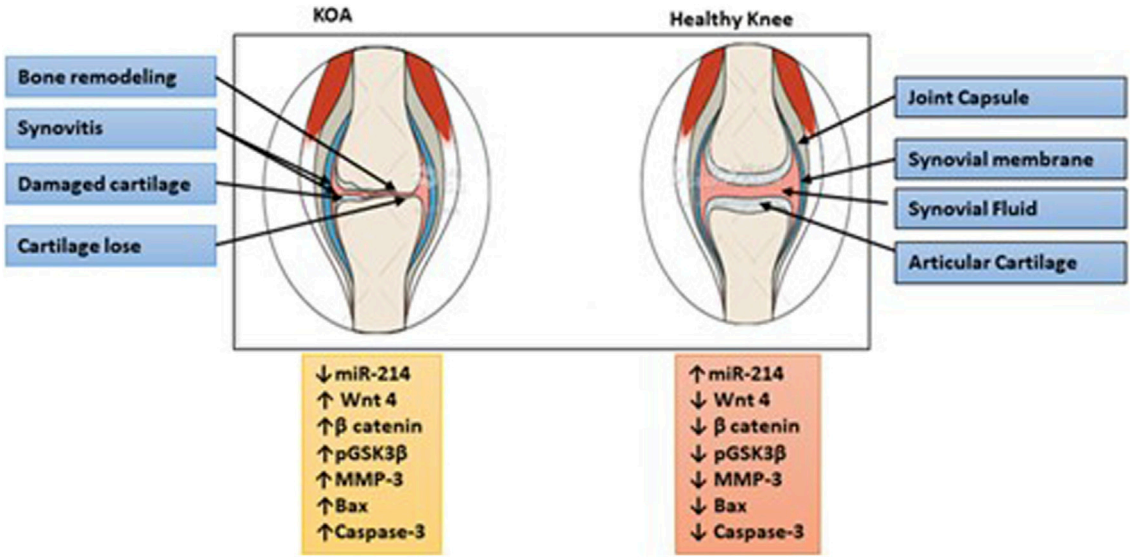


FIGURE 6
Illustration of the summary of the study. The downregulation of miR-214 is involved in the deterioration of cartilage and subchondral bone in the advancement of KOA by activating the Wnt/β-catenin signaling pathway. Individuals diagnosed with KOA experienced symptoms such as pain and stiffness in the joints, along with a reduction in the thickness of their cartilage. Conversely, elevated levels of miR-214 expression have a protective effect on cartilage and help prevent the onset of KOA.

which in turn promotes the expression of particular genes (Stampella et al., 2017; Liu et al., 2019; Lietman et al., 2018). Consistent with the previous studies, our study, found that the expression of Wnt4 and β-catenin was obviously higher in KOA patients than normal ones; also, their levels were higher among patients with high WOMAC scores (regarding pain, stiffness, and physical function), high grades of pain regarding VAS, and among those with low cartilage thickness regarding ultrasonography (as their serum concentration was positively correlated to WOMAC scores, clinical finding as regards to pain, and negatively correlated to radiological findings as regard to medial cartilage thickness). These results indicated that Wnt/β-catenin signaling pathway might be activated. Besides, correlation between miR-214 and Wnt4 as well as β-catenin was analyzed; the expression of Wnt4 and β-catenin in KOA patients was shown to be adversely correlated with the expression of miR-214. This is consistent with that miR-214 inhibits human mesenchymal stem cells differentiation into osteoblasts through targeting β-catenin (Li et al., 2017). Also, miR-214 negatively regulates Wnt/β-catenin signaling in breast cancer (Yi et al., 2016).

A former study documented that throughout the process of osteogenesis, miR-214 prevented the differentiation of mesenchymal stem cells into osteoblasts through targeting β-catenin (Li et al., 2017). Buchtova et al. suggested that the Wnt/β-catenin cascade could regulate the differentiation of chondrocytes. Moreover, overactivated Wnt/β-catenin pathway causes OA-similar alterations in chondrocytes, which are principally revealed by upregulation of MMP-13 and high apoptotic rate of chondrocytes (Cao et al., 2017). Consequently, the miR-214 may have a protective effect for the cartilage *via* targeting β-catenin.

GSK3 plays a vital role in the Wnt/β-catenin signaling pathway. Under normal conditions without Wnt signaling, GSK3β has the ability to phosphorylate β-catenin. Subsequently, the phosphorylated β-catenin can be realized through E3 ubiquitin ligase, resulting in β-catenin destruction by the proteasome. As a result, the β-catenin transcriptional targets are not activated (Chen et al., 2014). Nevertheless, GSK3β′s activity is decreased by phosphorylation following Wnt signal activation, which decreases its capacity to degrade β-catenin (Gu et al., 2019). In our study, we observed an increase in the level of pGSK3β in KOA patients following the inhibition of miR-214, as compared to the control group. Moreover, the serum concentration of pGSK3β showed a positive correlation with WOMAC scores and clinical findings related to pain in KOA, while exhibiting a negative correlation with radiological findings concerning the thickness of the medial cartilage.

The Wnt/β-catenin signaling pathway was also discovered to play an important role in exacerbating KOA by overproduction of MMPs, which resulted in proteoglycan matrix breakdown. It has been demonstrated that β-catenin overexpression in mature chondrocytes can exacerbate cartilage degradation, promote chondrocyte hypertrophy, and upregulate the production of MMPs (Xu et al., 2016). MMP-3, MMP-13, MMP-7, and MMP-9 genes are among the downstream target genes for transcription that are activated when β-catenin is carried to the nucleus and attaches to TCF/LEF. All of these genes are abnormally activated in KOA and play a role in the onset and progression of the disease (Zhu et al., 2009). MMP-3 is the most important MMP family member implicated in cartilage breakdown, and it was assumed to have wide substrate specificity, allowing it to be active against collagen types II, III, and IV, as well as proteoglycans and fibronectin. Furthermore, MMP-3 can activate MMP-1, MMP-2, MMP-9, and MMP-13 (Tong et al., 2017). Therefore, one of the most important ways to prevent the development of MMP-3 and

prevent chondrocyte destruction is through the efficient control of the Wnt/β-catenin signaling pathway. In this study, with the decrease of miR-214, the expression of MMP-3 was increased in KOA patients, and its serum concentration was higher among patients with higher grades of pain regarding VAS, higher WOMAC scores, and among those with lower cartilage thickness.

Chondrocytes are the sole cellular type seen in articular cartilage, and their death has been considered a potential pathological etiology. Apoptosis was more prevalent in KOA cartilage than in normal cartilage (Miao et al., 2019). Bax is a pro-apoptotic protein of Bcl-2 family that plays a critical role in the execution of the apoptotic cascade (Uren et al., 2017). Caspase-3 was thought to be involved in several types of chondrocyte apoptosis by initiating and carrying out cell death (Xia et al., 2020). In the current work, miR-214 diminished while Bax increased, resulting in caspase-3 protein activation and, eventually, chondrocyte apoptosis. The serum concentrations of Bax, and caspase-3 protein were positively correlated to WOMAC scores, clinical findings of KOA as regards to pain and negatively correlated to radiological findings as regards to medial cartilage thickness. These findings in consistent with previous study that revealed the necessity of miR-214 for the homeostasis of chondrocytes and the ECM. miR-214 overexpression was associated with lower expression of apoptosis-promoting genes such as Bax and caspase-3.

To highlight the importance of our study, this work focuses on the molecular mechanism of KOA. miR-214 was identified as a downregulated molecule, clearing up its role in the disease progression and its restoration may counteract the dysregulated Wnt/β-catenin pathway, which contributes to chondrocyte apoptosis and cartilage damage. This illustrates a crosstalk between the miR-214 and Wnt/β-catenin trajectory and explaining how molecular imbalances drive cellular and articular changes in KOA. Consequently, the current study supports developing miRNA-based treatment strategies particularly for upregulation of miR-214.

5 Limitations of the study

The small sample size of the present study and the recruitment of OA patients from a single medical center could be the two main limitations of this study. These limitations can also be attributed to the high cost of laboratory tests used in the study. However, we recommend conducting similar research with a larger number of patients from different medical centers. Moreover, conducting further advanced molecular techniques will be an added value to the work.

6 Conclusion

This research contributes to understanding the complex molecular networks involved in KOA pathogenesis. Identification of miR-214 as a downregulated molecule in KOA patients suggests its potential as a promising therapeutic target for the development of novel treatment strategies. Restoring or increasing miR-214 expression may assist to overcome abnormal Wnt/-catenin pathway activation, thereby mitigating chondrocyte apoptosis and matrix degradation. Wnt/β-Catenin- related proteins were also significant in the development of KOA as summarized in Figure 6.

Data availability statement

The raw data supporting the conclusions of this article will be made available by the authors, without undue reservation.

Ethics statement

The studies involving humans were approved by The Ethics Committee of the Faculty of Medicine Hospital at Menoufia University, under IRB number 12/2022RAD18, accepted the research protocol. The ethical approval complied with the Declaration of Helsinki's requirements. The studies were conducted in accordance with the local legislation and institutional requirements. The participants provided their written informed consent to participate in this study.

Author contributions

WS: Methodology, Software, Resources, Data curation, Writing–review and editing. EM: Methodology, Software, Formal analysis, Investigation, Writing–original draft, Visualization, Project administration, Funding acquisition. DS: Conceptualization, Methodology, Formal analysis, Investigation, Writing–original draft, Visualization, Supervision. MA: Conceptualization, Methodology, Software, Formal analysis, Investigation, Writing–original draft. A-AZ: Methodology, Formal analysis, Investigation, Writing–review and editing. AS: Methodology, Formal analysis, Investigation, Writing–original draft. SA: Methodology, Software, Resources, Data curation, Writing–review and editing. FK: Formal analysis, Validation, Data curation, Resources, Writing–review and editing. AE: Methodology, Formal analysis, Validation, Data curation, Resources, Writing–review and editing. SM: Formal analysis, Validation, Data curation, Resources, Writing–review and editing. MA-G: Methodology, Formal analysis, Investigation, Writing–review and editing. HA: Conceptualization, Methodology, Software, Formal analysis, Investigation, Writing–original draft, Visualization.

Funding

The author(s) declare that no financial support was received for the research, authorship, and/or publication of this article.

Conflict of interest

The authors declare that the research was conducted in the absence of any commercial or financial relationships that could be construed as a potential conflict of interest.

Generative AI statement

The author(s) declare that no Generative AI was used in the creation of this manuscript.

Publisher's note

All claims expressed in this article are solely those of the authors and do not necessarily represent those of their affiliated organizations, or those of the publisher, the editors and the reviewers. Any product that may be evaluated in this article, or claim that may be made by its manufacturer, is not guaranteed or endorsed by the publisher.

References

Alexander, I. (2007). Electronic medical records for the orthopaedic practice. *Clin. Orthop. Relat. Res.* 457, 114–119. doi:10.1097/BLO.0b013e3180342802

Appleton, C. T. G., Usmani, S. E., Mort, J. S., and Beier, F. (2010). Rho/ROCK and MEK/ERK activation by transforming growth factor-alpha induces articular cartilage degradation. *Lab. Investig.* 90 (1), 20–30. doi:10.1038/labinvest.2009.111

Blagojevic, M., Jinks, C., Jeffery, A., and Jordan, K. P. (2010). Risk factors for onset of osteoarthritis of the knee in older adults: a systematic review and meta-analysis. *Osteoarthr. Cartil.* 18 (1), 24–33. doi:10.1016/j.joca.2009.08.010

Boonstra, A. M., Schiphorst Preuper, H. R., Reneman, M. F., Posthumus, J. B., and Stewart, R. E. (2008). Reliability and validity of the visual analogue scale for disability in patients with chronic musculoskeletal pain. *Int. J. rehabilitation Res. Int. Zeitschrift fur Rehabilitationsforschung Revue Int. de recherches de readaptation* 31 (2), 165–169. doi:10.1097/MRR.0b013e3282fc0f93

Borgonio, C. V. M., González-Huerta, N. C., Romero-Córdoba, S., Hidalgo-Miranda, A., and Miranda-Duarte, A. (2014). Altered expression of circulating MicroRNA in plasma of patients with primary osteoarthritis and *in silico* analysis of their pathways. *PLOS ONE* 9 (6), e97690. doi:10.1371/journal.pone.0097690

Cao, F., Zhan, J., Chen, X., Zhang, K., Lai, R., and Feng, Z. (2017). miR-214 promotes periodontal ligament stem cell osteoblastic differentiation by modulating Wnt/β-catenin signaling. *Mol. Med. Rep.* 16 (6), 9301–9308. doi:10.3892/mmr.2017.7821

Cao, H., Zhou, X., Li, H., Wang, M., Wu, W., and Zou, J. (2022). Study on the role of MicroRNA-214 in the rehabilitation of cartilage in mice with exercise-induced traumatic osteoarthritis. *Curr. Issues Mol. Biol.* 44 (9), 4100–4117. doi:10.3390/cimb44090281

Cao, Y., Tang, S., Nie, X., Zhou, Z., Ruan, G., Han, W., et al. (2021a). Decreased miR-214-3p activates NF-κB pathway and aggravates osteoarthritis progression. *EBioMedicine* 65, 103283. doi:10.1016/j.ebiom.2021.103283

Cao, Y., Tang, Sa, Nie, X., Zhou, Z., Ruan, G., Han, W., et al. (2021b). Decreased miR-214–3p activates NF-κB pathway and aggravates osteoarthritis progression. *EBioMedicine* 65, 103283. doi:10.1016/j.ebiom.2021.103283

Čermák, V., Škarková, A., Merta, L., Kolomazníková, V., Palušová, V., Uldrijan, S., et al. (2021). RNA-Seq characterization of melanoma phenotype switch in 3D collagen after p38 MAPK inhibitor treatment. *Biomolecules* 11 (3), 449. doi:10.3390/biom11030449

Chen, D., Shen, J., Zhao, W., Wang, T., Han, L., Hamilton, J. L., et al. (2017). Osteoarthritis: toward a comprehensive understanding of pathological mechanism. *Bone Res.* 5 (1), 16044. doi:10.1038/boneres.2016.44

Chen, H., Wang, S., Chen, L., Chen, Y., Wu, M., Zhang, Y., et al. (2014). MicroRNA-344 inhibits 3T3-L1 cell differentiation via targeting GSK3β of Wnt/β-catenin signaling pathway. *FEBS Lett.* 588 (3), 429–435. doi:10.1016/j.febslet.2013.12.002

Corr, M. (2008). Wnt–β-catenin signaling in the pathogenesis of osteoarthritis. *Nat. Clin. Pract. Rheumatol.* 4, 550–556. doi:10.1038/ncprheum0904

Duan, L., Liang, Y., Xu, X., Xiao, Y., and Wang, D. (2020). Recent progress on the role of miR-140 in cartilage matrix remodelling and its implications for osteoarthritis treatment. *Arthritis Res. and Ther.* 22 (1), 194. doi:10.1186/s13075-020-02290-0

Faik, A., Benbouazza, K., Amine, B., Maaroufi, H., Bahiri, R., Lazrak, N., et al. (2008). Translation and validation of Moroccan Western Ontario and Mc Master Universities (WOMAC) osteoarthritis index in knee osteoarthritis. *Rheumatol. Int.* 28 (7), 677–683. doi:10.1007/s00296-007-0498-z

Fang, T., Zhou, X., Jin, M., Nie, J., and Li, X. (2021). Molecular mechanisms of mechanical load-induced osteoarthritis. *Int. Orthop.* 45 (5), 1125–1136. doi:10.1007/s00264-021-04938-1

Fensterle, J. (2006). A trip through the signaling pathways of melanoma. *JDDG J. der Deutschen Dermatologischen Gesellschaft.* 4 (3), 205–216. doi:10.1111/j.1610-0387.2006.05925.x

Fioravanti, A., Tenti, S., and Cheleschi, S. (2021). MiR-214-3p, a novel possible therapeutic target for the pathogenesis of osteoarthritis. *EBioMedicine* 66, 103300. doi:10.1016/j.ebiom.2021.103300

Gao, Y., Liu, S., Huang, J., Guo, W., Chen, J., Zhang, L., et al. (2014). The ECM-cell interaction of cartilage extracellular matrix on chondrocytes. *BioMed Res. Int.* 2014, 648459. doi:10.1155/2014/648459

Ghafouri-Fard, S., Poulet, C., Malaise, M., Abak, A., Mahmud Hussen, B., Taheriazam, A., et al. (2021). The emerging role of non-coding RNAs in osteoarthritis. *Front. Immunol.* 12, 773171. doi:10.3389/fimmu.2021.773171

Gu, Y., Ren, K., Wang, L., and Yao, Q. (2019). Loss of Klotho contributes to cartilage damage by derepression of canonical Wnt/β-catenin signaling in osteoarthritis mice. *Aging (Albany NY)* 11 (24), 12793–12809. doi:10.18632/aging.102603

He, W., Wu, Y., Liu, Q., Cheng, X., Wu, J., Han, X., et al. (2021). Effect of Etoricoxib on miR-214 and inflammatory reaction in knee osteoarthritis patients. *Am. J. Transl. Res.* 13 (8), 9586–9592.

Lai, C., Liao, B., Peng, S., Fang, P., Bao, N., and Zhang, L. (2023). Synovial fibroblast-miR-214-3p-derived exosomes inhibit inflammation and degeneration of cartilage tissues of osteoarthritis rats. *Mol. Cell. Biochem.* 478 (3), 637–649. doi:10.1007/s11010-022-04535-9

Lai, Z., and Cao, Y. (2019). Plasma miR-200c-3p, miR-100-5p, and miR-1826 serve as potential diagnostic biomarkers for knee osteoarthritis: randomized controlled trials. *Medicine* 98 (51), e18110. doi:10.1097/MD.0000000000018110

Li, D., Liu, J., Guo, B., Liang, C., Dang, L., Lu, C., et al. (2016). Osteoclast-derived exosomal miR-214-3p inhibits osteoblastic bone formation. *Nat. Commun.* 7, 10872. doi:10.1038/ncomms10872

Li, J. P., Zhuang, H. T., Xin, M. Y., and Zhou, Y. L. (2017). MiR-214 inhibits human mesenchymal stem cells differentiating into osteoblasts through targeting β-catenin. *Eur. Rev. Med. Pharmacol. Sci.* 21 (21), 4777–4783. doi:10.3892/etm.2017.5165

Liang, J., Lang, S., Zheng, Y., Wang, Y., Chen, H., Yang, J., et al. (2019). The effect of anti-gravity treadmill training for knee osteoarthritis rehabilitation on joint pain, gait, and EMG: case report. *Medicine* 98 (18), e15386. doi:10.1097/MD.0000000000015386

Lietman, C., Wu, B., Lechner, S., Shinar, A., Sehgal, M., Rossomacha, E., et al. (2018). Inhibition of Wnt/β-catenin signaling ameliorates osteoarthritis in a murine model of experimental osteoarthritis. *JCI Insight* 3 (3), e96308. doi:10.1172/jci.insight.96308

Liu, J., Li, D., Dang, L., Liang, C., Guo, B., Lu, C., et al. (2017b). Osteoclastic miR-214 targets TRAF3 to contribute to osteolytic bone metastasis of breast cancer. *Sci. Rep.* 7, 40487. doi:10.1038/srep40487

Liu, S., Yang, H., Hu, B., and Zhang, M. (2017a). Sirt1 regulates apoptosis and extracellular matrix degradation in resveratrol-treated osteoarthritis chondrocytes via the Wnt/β-catenin signaling pathways. *Exp. Ther. Med.* 14 (5), 5057–5062. doi:10.3892/etm.2017.5165

Liu, X., Wang, L., Ma, C., Wang, G., Zhang, Y., and Sun, S. (2019). Exosomes derived from platelet-rich plasma present a novel potential in alleviating knee osteoarthritis by promoting proliferation and inhibiting apoptosis of chondrocyte via Wnt/β-catenin signaling pathway. *J. Orthop. Surg. Res.* 14 (1), 470. doi:10.1186/s13018-019-1529-7

Mahmoudian, A., Lohmander, L. S., Jafari, H., and Luyten, F. P. (2021). Towards classification criteria for early-stage knee osteoarthritis: a population-based study to enrich for progressors. *Seminars arthritis rheumatism* 51 (1), 285–291. doi:10.1016/j.semarthrit.2020.11.002

Manlapaz, D. G., Sole, G., Jayakaran, P., and Chapple, C. M. (2019). Risk factors for falls in adults with knee osteoarthritis: a systematic review. *Pm R.* 11 (7), 745–757. doi:10.1002/pmrj.12066

Miao, G., Zang, X., Hou, H., Sun, H., Wang, L., Zhang, T., et al. (2019). Bax targeted by miR-29a regulates chondrocyte apoptosis in osteoarthritis. *Biomed. Res. Int.* 2019, 1434538. doi:10.1155/2019/1434538

Moo, E. K., Han, S. K., Federico, S., Sibole, S. C., Jinha, A., Abu Osman, N. A., et al. (2014). Extracellular matrix integrity affects the mechanical behaviour of *in-situ* chondrocytes under compression. *J. Biomechanics* 47 (5), 1004–1013. doi:10.1016/j.jbiomech.2014.01.003

Østergaard, M., and Wiell, C. (2004). Ultrasonography in rheumatoid arthritis: a very promising method still needing more validation. *Curr. Opin. Rheumatol.* 16 (3), 223–230. doi:10.1097/00002281-200405000-00010

Schiphof, D., Boers, M., and Bierma-Zeinstra, S. M. A. (2008). Differences in descriptions of Kellgren and Lawrence grades of knee osteoarthritis. *Ann. Rheumatic Dis.* 67 (7), 1034–1036. doi:10.1136/ard.2007.079020

Serban, O., Porojan, M., Deac, M., Cozma, F., Solomon, C., Lenghel, M., et al. (2016). Pain in bilateral knee osteoarthritis - correlations between clinical examination, radiological, and ultrasonographical findings. *Med. Ultrason.* 18 (3), 318–325. doi:10.11152/mu.2013.2066.183.pin

Shi, T., Fu, X., Wang, F., Zhang, X., Cai, Y., Wu, X., et al. (2021). The WNT/β-catenin signalling pathway induces chondrocyte apoptosis in the cartilage injury caused by T-2 toxin in rats. *Toxicon* 204, 14–20. doi:10.1016/j.toxicon.2021.11.003

Stampella, A., Monteagudo, S., and Lories, R. (2017). Wnt signaling as target for the treatment of osteoarthritis. *Best Pract. and Res. Clin. Rheumatology* 31 (5), 721–729. doi:10.1016/j.berh.2018.03.004

Tong, Z., Liu, Y., Chen, B., Yan, L., and Hao, D. (2017). Association between MMP3 and TIMP3 polymorphisms and risk of osteoarthritis. *Oncotarget* 8 (48), 83563–83569. doi:10.18632/oncotarget.18745

Uren, R. T., Iyer, S., and Kluck, R. M. (2017). Pore formation by dimeric Bak and Bax: an unusual pore? *Philos. Trans. R. Soc. Lond B Biol. Sci.* 372 (1726), 20160218. doi:10.1098/rstb.2016.0218

Wang, X., Guo, B., Li, Q., Peng, J., Yang, Z., Wang, A., et al. (2013). miR-214 targets ATF4 to inhibit bone formation. *Nat. Med.* 19 (1), 93–100. doi:10.1038/nm.3026

Wu, Y., Li, J., Zeng, Y., Pu, W., Mu, X., Sun, K., et al. (2022). Exosomes rewire the cartilage microenvironment in osteoarthritis: from intercellular communication to therapeutic strategies. *Int. J. Oral Sci.* 14 (1), 40. doi:10.1038/s41368-022-00187-z

Xia, H., Cao, D., Yang, F., Yang, W., Li, W., Liu, P., et al. (2020). Jiawei Yanghe decoction ameliorates cartilage degradation *in vitro* and vivo via Wnt/β-catenin signaling pathway. *Biomed. and Pharmacother.* 122, 109708. doi:10.1016/j.biopha.2019.109708

Xu, Q., Gai, P. Y., Lv, H. L., Li, G. R., and Liu, X. Y. (2016). Association of MMP3 genotype with susceptibility to frozen shoulder: a case-control study in a Chinese Han population. *Genet. Mol. Res.* 15 (1). doi:10.4238/gmr.15017228

Yi, S. J., Li, L. L., and Tu, W. B. (2016). MiR-214 negatively regulates proliferation and WNT/β-catenin signaling in breast cancer. *Eur. Rev. Med. Pharmacol. Sci.* 20 (24), 5148–5154.

Yuan, L., Chang, X., Yao, W., He, H., Tang, Z., and Wu, J. (2019). MiR-214 inhibits knee osteoarthritis in rats through MAPK signaling pathway. *Panminerva medica*. doi:10.23736/S0031-0808.19.03716-9

Yuasa, T., Otani, T., Koike, T., Iwamoto, M., and Enomoto-Iwamoto, M. (2008). Wnt/beta-catenin signaling stimulates matrix catabolic genes and activity in articular chondrocytes: its possible role in joint degeneration. *Lab. Investig.* 88 (3), 264–274. doi:10.1038/labinvest.3700747

Zhu, M., Tang, D., Wu, Q., Hao, S., Chen, M., Xie, C., et al. (2009). Activation of beta-catenin signaling in articular chondrocytes leads to osteoarthritis-like phenotype in adult beta-catenin conditional activation mice. *J. Bone Mineral Res.* 24 (1), 12–21. doi:10.1359/jbmr.080901

frontiers | Frontiers in Pharmacology

TYPE Original Research
PUBLISHED 12 March 2025
DOI 10.3389/fphar.2025.1474012

Check for updates

OPEN ACCESS

EDITED BY
Alice Conigliaro,
University of Palermo, Italy

REVIEWED BY
Yang Yang,
Chinese PLA General Hospital, China
Sidharth Mehan,
Indo-Soviet Friendship College of Pharmacy, India
Moorthi Ponnusamy,
University of South Florida, United States

*CORRESPONDENCE
Dora Brites,
dbrites@ff.ulisboa.pt

†These authors have contributed equally to this work and share first authorship

RECEIVED 31 July 2024
ACCEPTED 03 January 2025
PUBLISHED 12 March 2025

CITATION
Évora A, Garcia G, Rubi A, De Vitis E, Matos AT, Vaz AR, Gervaso F, Gigli G, Polini A and Brites D (2025) Exosomes enriched with miR-124-3p show therapeutic potential in a new microfluidic triculture model that recapitulates neuron–glia crosstalk in Alzheimer's disease. *Front. Pharmacol.* 16:1474012. doi: 10.3389/fphar.2025.1474012

COPYRIGHT
© 2025 Évora, Garcia, Rubi, De Vitis, Matos, Vaz, Gervaso, Gigli, Polini and Brites. This is an open-access article distributed under the terms of the Creative Commons Attribution License (CC BY). The use, distribution or reproduction in other forums is permitted, provided the original author(s) and the copyright owner(s) are credited and that the original publication in this journal is cited, in accordance with accepted academic practice. No use, distribution or reproduction is permitted which does not comply with these terms.

Exosomes enriched with miR-124-3p show therapeutic potential in a new microfluidic triculture model that recapitulates neuron–glia crosstalk in Alzheimer's disease

Artemizia Évora[1†], Gonçalo Garcia[1,2†], Ana Rubi[1], Eleonora De Vitis[3], Ana Teresa Matos[1], Ana Rita Vaz[1,2], Francesca Gervaso[3], Giuseppe Gigli[3,4], Alessandro Polini[3] and Dora Brites[1,2*]

[1]Neuroinflammation, Signaling and Neuroregeneration, Research Institute for Medicines (iMed.ULisboa), Faculty of Pharmacy, Universidade de Lisboa, Lisbon, Portugal, [2]Department of Pharmaceutical Sciences and Medicines, Faculty of Pharmacy, Universidade de Lisboa, Lisbon, Portugal, [3]Institute of Nanotechnology, National Research Council (CNR Nanotec), Lecce, Italy, [4]Dipartimento di Medicina Sperimentale, Università Del Salento, Lecce, Italy

Background: Alzheimer's disease (AD), a complex neurodegenerative disease associated with ageing, is the leading cause of dementia. Few people with early AD are eligible for the novel Food and Drug Administration (FDA)-approved drug treatments. Accordingly, new tools and early diagnosis markers are required to predict subtypes, individual stages, and the most suitable personalized treatment. We previously demonstrated that the regulation of microRNA (miR)-124 is crucial for proper neuronal function and microglia reshaping in human AD cell models.

Objective: The aim of this study was to develop an efficient miR-124-3p-loaded exosome strategy and validate its therapeutic potential in using a multi-compartment microfluidic device of neuron–glia that recapitulates age-AD pathological features.

Methods and results: Using cortical microglia from mouse pups, separated from glial mixed cultures and maintained for 2 days *in vitro* (stressed microglia), we tested the effects of SH-SY5Y-derived exosomes loaded with miR-124-3p mimic either by their direct transfection with Exo-Fect™ (ET124) or by their isolation from the secretome of miR-124 transfected cells (CT124). ET124 revealed better delivery effciency and higher potent effects in improving the stressed microglia status than CT124. Tricultures of human SH-SY5Y neuroblastoma cells (SH-*WT*) were established in the presence of the human microglia cell line (HMC3) and immortalized human astrocytes (IM-HA) in tricompartmentalized microfluidic devices. Replacement of SH-*WT* cells with those transfected with APP695 (SH-*SWE*) in the tricultures and addition of low doses of hydrogen peroxide were used to simulate late-onset AD. The system mimicked AD-associated neurodegeneration and neuroinflammation processes. Notably, ET124 exhibited neuroprotective properties across the three cell types in the

AD model by preventing neuronal apoptosis and neurite deficits, redirecting microglial profiles towards a steady state, and attenuating the inflammatory and miRNA fingerprints associated with astrocyte reactivity.

Conclusion: To the best of our knowledge, this is the first study supporting the neuro- and immunoprotective properties of miR-124-engineered exosomes in a microfluidic triculture platform, recapitulating age-related susceptibility to AD. Our system offers potential to develop personalized medicines in AD patient subtypes.

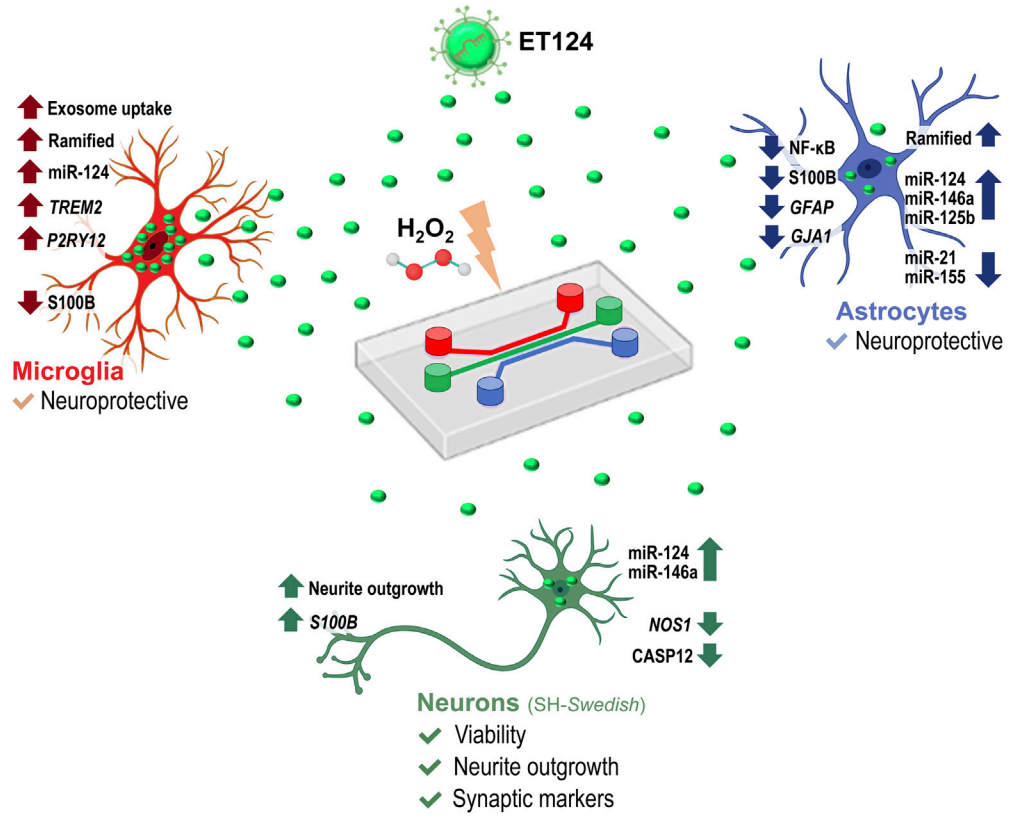
KEYWORDS

Alzheimer's disease modelling, human neural tricultures, microfluidic system, miRNA-engineered exosomes, miR-124-3p mimic, neuron-glia communication, SH-SY5Y cells transfected with APP695

1 Introduction

Alzheimer's disease (AD) is one of the biggest healthcare challenges of the 21st century, standing as the leading cause of dementia. The neuropathological progression typically begins in the temporal lobe and hippocampus, leading to cognitive decline and behavioural disabilities (Kumar et al., 2023). Amyloid plaques (aggregated amyloid beta-peptides, Aβ) and neurofibrillary tangles (NFTs) are the most common AD molecular hallmarks, but neuroinflammation, oxidative stress, and pre- and post-synaptic alterations, among other disturbed mechanisms, are equally associated risk factors (Tzioras et al., 2023). Limited therapeutic strategies, successive failed trials, and inaccurate translational AD models indicate that there is an unmet need for disruptive research and that stratification towards selection of patient subtypes is key to identifying and developing innovative and more effective treatments.

Small extracellular vesicles, also known as exosomes, are released from cells and are emerging as promising tools for both diagnostic and therapeutic purposes (Loch-Neckel et al., 2022). These lipid bilayer-bound exosomes, ranging from 30 to 150 nm, play a crucial role in synaptic plasticity and can permeate the blood–brain barrier (BBB), enabling bidirectional communication between the brain and the peripheral system (Yamashita et al., 2018). Exosomes, particularly those isolated from patients with neurodegenerative disorders, may also serve in early diagnosis once they revealed carrying specific biomarkers (Jia et al., 2021). Lately, the potential of exosomes as drug and miRNA mimic/inhibitor delivery systems



GRAPHICAL ABSTRACT

has been explored for treating neurodegenerative diseases (Cano et al., 2023; Rehman et al., 2023), capitalizing on their low immunogenicity and cytotoxicity, high selectivity, and protection of the encapsulated compound (Kimiz-Gebologlu and Oncel, 2022). Finally, exosomes can be delivered through several administration routes, such as intravenous, subcutaneous, intrathecal, intranasal, intraperitoneal, retro-orbital, intravitreal, and oral routes (Peng et al., 2020; Dong et al., 2021).

Among the several mediators involved in neuro-immune homoeostasis, microRNAs (miRNAs) are a class of non-coding RNAs that can induce post-transcriptional gene silencing (Ponomarev et al., 2013; Brites, 2020). They have been described as key players in dysregulated neuroinflammation associated with the development and progression of neurodegenerative diseases, such as AD (Parisi et al., 2013; Wang et al., 2019). One of the most predominant miRNAs in the CNS (mainly in neurons), with critical nervous and immune functions, is miRNA (miR)-124 (Soreq and Wolf, 2011; Wang et al., 2014). There are conflicting reports regarding miR-124 dysregulation in AD, with some studies on AD patients and models indicating increased levels (Wang et al., 2018; Brites, 2020; Garcia et al., 2021) and others showing decreased levels (Lukiw, 2007; An et al., 2017). We demonstrated that amongst hit inflammatory miRNAs, miR-124-3p is prominent as one of the most involved in the regulation of neuron–microglia paracrine signalling (Brites and Fernandes, 2015; Fernandes et al., 2018; Garcia et al., 2022). Using SH-SY5Y human neuroblastoma cells transfected with the amyloid precursor protein (APP)695 with the *Swedish* mutation (SH-*SWE*) and induced pluripotent stem cell (iPSC)-derived neurons obtained from presenilin1 (*PSEN1*) familial AD patients, similar to *in vitro* models, we showed that miR-124-3p mimic had preventive effects (e.g., inhibition of APP overexpression, of toxic amyloid accumulation, and of phosphorylated tau), while its inhibitor promoted harmful effects (e.g., reduction of dendritic spine density, enhanced APP processing, miR-146a upregulation, and tau phosphorylation) (Garcia et al., 2021). Data corroborate the association of miR-124 with neuroprotective mechanisms (Fang et al., 2012; An et al., 2017; Zhang F. et al., 2022). We also evidenced that neuronal-derived exosomes having miR-124 directly regulate microglia homoeostasis (Fernandes et al., 2018; Garcia et al., 2022), as previously stated for the effects of peripheral administration of miR-124 on the autoimmune encephalomyelitis activated microglia (Ponomarev et al., 2011). miR-124-loaded exosomes were tested in mouse models of several neuropathological disorders (Yang et al., 2017; Esteves et al., 2022; Mavroudis et al., 2023) but still not in AD.

Triculture systems using neurons, astrocytes, and microglia in microfluidic platforms, or in mixed cultures, have been used as models to assess neuron–glia signalling mechanisms as a basis for drug discovery in AD (Park et al., 2018; Guttikonda et al., 2021). However, the therapeutic application of exosomes loaded with miR-124 was never tested in such models.

In the present study, we developed an efficient miR-124-3p-engineered exosome delivery strategy and an improved human neuron–microglia–astrocyte model, allowing autocrine and paracrine signalling. For this, we used a microfabricated multi-compartment device with a fluid-independent circuit (De Vitis et al., 2021). Then, we established an *in vitro* age-AD model by using SH-*SWE* neuroblastoma cells in the presence of human microglia and astrocyte cell lines, under the stress of a low dose of hydrogen peroxide (H_2O_2). Finally, we tested exosomes loaded with miR-124 mimic for their ability in preserving AD-associated oxidative damage and ageing, as well as inflammation and neurodegeneration, by sustaining neuron–glial homoeostasis.

2 Materials and methods

2.1 Animals and ethics statement

For primary cortical microglia, we used mice with the strain B6SJLF1/J purchased from The Jackson Laboratory (Bar Harbor, ME, United States). Maintenance and handling were carried out at the Instituto de Medicina Molecular João Lobo Antunes (IMM) animal house facilities of the Faculty of Medicine, University of Lisbon, Portugal, where the colony was used for breeding. Animals were housed at 4–5 animals/cage, under 12 h light/12 h dark cycle, with room temperature (RT) at 22°C–24°C and 55% humidity, and received food and water *ad libitum*. Experiments were conducted in microglia isolated from the brain cortex of both male and female mouse pups.

All the procedures were carried out in compliance with Portuguese Legislation on Animal Care (Decreto-Lei 129/92, Portaria 1005/92, Portaria 466/95, Decreto-Lei 197/96, Portaria 1131/97) and in agreement with the European Community guidelines (Directives 86/609/EU and 2010/63/EU, Recommendation 2007/526/CE). The protocol was approved by the Institutional animal welfare body, ORBEA-iMM-FFUL, and the National competent autority, the DGAV (Direção Geral de Alimentação Veterinária). Every attempt was made to reduce the number of animals utilized and their suffering in accordance with the 3R principle.

2.2 Cortical microglia primary culture

Mixed glial cultures were obtained from the brain cortex of mouse pups, as previously described (Caldeira et al., 2014). In brief, animals were sacrificed at 7–8 days old; their brains were removed from the skull and placed in a Petri dish. The meninges, blood vessels, white matter, and cerebellum were removed under sterile conditions. After tissue homogenization, cells were sequentially passed through 230-μm and 104-μm filters, centrifuged, plated (4×10^5 cells/cm^2) on uncoated 12-well plates, and maintained with culture medium DMEM-Ham's F-12 medium (DMEM-F12) supplemented with 2 mM L-glutamine (1%), 1 mM sodium pyruvate (1%), 1× non-essential amino acids (NEAA) (1%), foetal bovine serum (FBS, 10%), and the Antibiotic-Antimycotic (AB/AM) solution (2%) at 37°C, 5% CO_2 in a Heracell 150 incubator (Thermo Fisher Scientific, Waltham, Massachusetts, United States). Every 7 days, the medium was changed. After 21 days *in vitro* (DIV), microglia were isolated from the astrocyte–microglia mixed culture by gently detaching the top layer of astrocytes with mild trypsinization. Microglia were then maintained until 2DIV, which correspond to a reactive/stressed microglia state, as we previously described (Caldeira et al., 2014). Next, we incubated

the microglia with the exosome formulations for 24 h and assessed the delivery efficiency of exosomal miR-124 into the cells, as well as microglia phenotypic markers by RT-qPCR (*Nos2, Arg1,* and Trem2) and immunocytochemistry (Iba1 and P2RY12) assays.

2.3 Culture of human cell lines

Wild-type human SH-SY5Y (SH-*WT*) cells and SH-SY5Y expressing the APP *Swedish* variant (SH-*SWE*) cells used in this study were a gift from Professor Anthony Turner (Belyaev et al., 2010). Cells were cultured in DMEM, supplemented with 10% FBS and 2% AB/AM in T75 flasks under a humidified atmosphere with 5% CO_2, at 37°C in a HERA cell 150 incubator (Thermo Fisher Scientific, Waltham, Massachusetts, United States), as performed in our laboratory (Garcia et al., 2021). For differentiation, cells were treated with 10 μM retinoic acid (RA) daily until 7DIV. The human microglial clone 3 cell line (HMC3) was kindly provided by Professor Marc Tardieu (Janabi et al., 1995). HMC3 microglial cells were cultured in DMEM, supplemented with 10% FBS, 2% AB/AM, and 1% L-glutamine in T75 flasks, under a humidified atmosphere with 5% CO_2 at 37°C, according to the established methods in our laboratory (Fernandes et al., 2018). Immortalized human astrocytes (IM-HA) were purchased from Innoprot (Ref: P10251-IM, Derio, Spain). Cells were cultured in DMEM, supplemented with 2% FBS, 2% AB/AM, and 1% N2 in T75 flasks under a humidified atmosphere with 5% CO_2 at 37°C. Media from every cell type were changed every other day until reaching 90% confluency. Then, cells were detached by trypsinization under a humidified atmosphere with 5% CO_2 and pelleted by centrifugation using a Hettich ROTOFIX 32 A centrifuge (Hettich, Tuttlingen, Germany). Pelleted cells were resuspended in the respective media described above and sub-cultured in new T75 culture flasks.

2.4 Tricultures in an organ-on-chip microfluidic system

Tricultures were established in tricompartment organ-on-chip (OoC) microfluidic devices, designed and described previously (De Vitis et al., 2021), with minor changes. In brief, the microfluidic device features three perfusable compartments, each measuring 500 μm in width, 250 μm in height, and 6 mm in length, with separate inlets and outlets (diameter of 6 mm). The compartments are connected by a series of tiny, parallel microgrooves, measuring 5 μm in width and 2.5 μm in height, which facilitate the separation of soma and neurites and simultaneously target neurite elongation while allowing direct and paracrine communication between compartments.

The microfluidic device was manufactured using conventional lithography techniques, specifically through a two-step photolithography process and subsequent soft lithography. Initially, silicon substrates measuring 2.5 × 2.5 cm were cleaned with acetone and isopropanol (Sigma-Aldrich, Milan, Italy) and utilized in the first lithography step to create the microgrooves. A uniform layer of photoresist (SU-8 2002, Kayaku Advanced Materials, Westborough, MA, United States) was spin-coated to obtain a resist thickness of 2.5 μm, soft-baked, and then exposed to UV radiation (λ = 365 nm) using a standard mask aligner (MA6, SUSS MicroTec, Garching, Germany). After post-baking, the photoresist was developed in a SU-8 developer solution (Kayaku Advanced Materials) and hard-baked. In the second lithography step, SU-8 2075 (Kayaku Advanced Materials) was spin-coated onto the substrate to achieve a resist thickness of 250 μm. After drying and soft-baking, the substrate was exposed to UV radiation, with a precise alignment of markers included in both the first-level pattern (on the substrate) and the second pattern (on the photomask) using the mask aligner. The substrate was then post-baked, developed, and finally hard-baked. Polydimethylsiloxane (PDMS) replicas were subsequently created by soft lithography using a prepolymer-to-curing agent ratio (Sylgard 184, Dow, Midland, MI, United States) of 10:1. Once polymerized, the cured PDMS layer was punctured with a 6-mm biopsy punch at the inlets and outlets. To assemble the final devices, the microstructured PDMS layer and a clean glass coverslip were treated in oxygen plasma apparatus (PICO low-pressure plasma system, Diener electronic, Ebhausen, Germany) at 100 W, 200 sccm, for 6 s, and heat-treated at 75°C for 4 h to irreversibly bond the two pieces.

SH-*WT* and/or SH-*SWE* neuroblastoma cells, HMC3 microglia, and IM-HA cells were individually seeded into their respective compartments of the microfluidic system, each pre-coated with poly-D-lysine (100 μg/mL) and laminin (4 μg/mL) to promote cell adhesion, after testing other coating formulations (Supplementary Figure S1). The SH-*WT*/SH-*SWE* neuroblastoma cells were plated in the central compartment at a final density of 1×10^6 cells/mL, making up 50% of the total cell population in the triculture setup. These cells were cultured in neural triculture media (NTM), composed of DMEM supplemented with 1% FBS, 2% AB/AM, and 1% N2 supplement. To induce neuronal differentiation, the NTM was further supplemented with 10 μM retinoic acid (RA), and the medium was refreshed daily until 3DIV. On the third day, HMC3 microglia and IM-HA cells were introduced into their respective lateral compartments of the microfluidic device. HMC3 cells were seeded at a final concentration of 4×10^5 cells/mL, constituting 20% of the triculture, while IM-HA astrocytes were seeded at 6×10^5 cells/mL, making up the remaining 30%. This cell ratio of 50% neurons, 30% astrocytes, and 20% microglia showed to be the best tested option (Supplementary Figure S2). After seeding microglia and astrocytes, RA was removed from the NTM media to ensure that all cell types were incubated under the same conditions for an additional 24 h, facilitating cell-to-cell interactions within the triculture system.

At 4DIV, triculture systems were simultaneously exposed to 10 μM H_2O_2, to induce oxidative stress and simulate neuronal cell ageing (Chadwick et al., 2010; Ismail et al., 2016). Such a minimal H_2O_2 concentration was previously described to not significantly affect the cell viability (Ustyantseva et al., 2022). Concurrently, exosomes transfected with miR-124-3p mimic (referred as ET124) were equally distributed in each cell compartment from the microfluidic system. At 5DIV, after 24 h of treatment, all cells were either fixed using 4% paraformaldehyde (PFA) for subsequent immunofluorescence analysis or separately harvested from each compartment for

further molecular analysis via RT-qPCR, providing an enriched sample of each cell type.

2.5 Exosome isolation, NTA, and labelling

For neuroblastoma-derived exosome collection, SH-*WT* cells were cultured in media with 1% of FBS (previously depleted in exosomes to prevent contamination). Exosomes were collected from the secretome of cultured SH-*WT* cells at confluency, via differential ultracentrifugation, as optimized in our laboratory (Pinto et al., 2017; Garcia et al., 2022). In brief, equal volumes of cell media were promptly centrifuged at 1000 g for 10 min to pellet cell debris. The supernatants were then centrifuged for 1 h at 16,000 g and filtered through a 0.22-µm pore size membrane, followed by centrifugation at 100,000 g for 2 h in an Ultra L-XP100 centrifuge (Beckman Coulter, Brea, CA, United States). The pellet was resuspended/washed in phosphate-buffered saline (PBS) and (re)centrifuged at 100,000 g for 2 h. The separated exosomes were quantified by nanoparticle tracking analysis (NTA) using the NanoSight instrument (model NS300, Malvern Instruments, Malvern, United Kingdom). Samples were injected into the system under controlled flow using a NanoSight syringe pump and an integrated scripting control system. At least three different videos up to 60-s long were produced, and particle movement was analysed by NTA-software (version 3.1). To track exosome cell internalization upon treatment, exosomes were stained with the PKH67 lipophilic dye. For this, exosomes were resuspended in Dulbecco's phosphate-buffered saline (DPBS) (1:1000) and mixed with an equal volume of PKH67 probe solution for 5 min at RT, using the PKH67 Green Fluorescent Membrane Labelling Kit (Sigma-Aldrich, St. Louis, MO, United States). Labelled exosomes were washed to remove the unbound dye before their addition to the cell cultures (Pinto et al., 2017).

2.6 Exosome transfection with Exo-Fect™ for miR-124-exosome loading

Before transfection, each exosome batch was individually characterized in terms of particle concentration and total exosomal protein content using NTA and Bradford assay, respectively. This characterization allowed for a precise quantification, estimating approximately $2.20 \pm 1.54 \times 10^7$ exosomes per µg of exosome protein to be used in each experimental setup. This was particularly relevant since the same number of exosomes not always corresponded to the same protein content. Therefore, we normalized for both the number and protein content.

To load neuroblastoma cell-derived exosomes with the miR-124-3p mimic (Ambion, Austin, TX, United States), we utilized the Exo-Fect™ Exosome Transfection Kit (Systems Bioscience, Palo Alto, CA, United States), according to manufacturer instructions, with minor changes. Transfection started by mixing 2 nmol of miR-124-3p mimic with 10 µL of the Exo-Fect reagent in a transfection tube, creating a total reaction volume of 30 µL. This mixture was gently vortexed and incubated at room temperature for 10 min to allow for optimal formation of the miRNA–reagent complex. Subsequently, 120 µL of freshly isolated exosomes from neuroblastoma cells, previously quantified and characterized, were added to the reaction mixture, increasing the total volume to 150 µL. The mixture was then incubated at 37°C for 10 min to facilitate the incorporation of miR-124-3p into the exosomes. During this incubation, the tube was manually agitated every 2 min to enhance the efficiency of the transfection process. To stop the transfection, 30 µL of the ExoQuick-TC reagent was added to the tube, which was then placed in ice for 30 min. To isolate exosomes, the tube sample was centrifuged at 14,000 rpm for 3 min. The supernatant was carefully removed, and the pellet containing the miR-124-3p-loaded exosomes (referred to as ET124) was then resuspended in 100 µL of sterile PBS. Successful loading of miR-124-3p into the exosomes was verified by RT-qPCR, utilizing specific predesigned primers for miR-124-3p (Supplementary Table S1). ET124 were immediately labelled with the PKH67 dye, as abovementioned (see the Exosome isolation, NTA and labelling section), and used as soon as possible to ensure highest fluorescence intensity for exosome tracking and their cell internalization in the different assays.

2.7 Evaluation of the neural cell viability by the nexin assay

To determine the viability of SH-*WT*/SH-*SWE* neuroblastoma cells, microglia, and IM-HA astrocytes in the triculture microfluidic system, in the absence or presence of H_2O_2, and before or after exosome treatment, the cells were detached by trypsinization and spun down at 500 g for 5 min. Pellets were resuspended in 1% bovine serum albumin (BSA) in PBS and stained with phycoerythrin-conjugated annexin V (V-PE) and 7-amino-actinomycin D (7-AAD), using the Guava Nexin Reagent® (Merck Millipore, Burlington, MA, United States). Stained cells were analysed using a flow cytometer (Guava easyCyte 5 HT, Merck-Millipore), operated by Guava Nexin software. Three cellular populations were distinguished in the nexin assay: viable cells (annexin V-PE and 7-AAD double-negative), early apoptotic cells (annexin V-PE positive and 7-AAD negative), and late apoptotic/necrotic cells (annexin V-PE and 7-AAD double-positive).

2.8 RT-qPCR assay

Primary cortical microglia were washed once with PBS and collected in TRIzol™ (Thermo Fisher Scientific, Waltham, Massachusetts, United States) for RNA extraction.

In the microfluidic triculture system, samples were collected by consecutively streaming TRIzol™ into each cell compartment, in a separate way for each cell type. This allowed us to collect neuronal, microglial, and astrocyte samples from the same microfluidic system, with a minimal cross-contamination of the cellular content.

Total RNA was extracted, according to the manufacturer's instructions, and quantified, as performed in our laboratory (Garcia et al., 2022). The NanoDrop ND100 Spectrophotometer (NanoDrop Technologies, Wilmington, United States) was used for RNA quantification.

For miRNA assessment, 5 ng/μL of total RNA was converted into cDNA using the miRCURY LNA™ RT Kit (QIAGEN) under controlled conditions: 60 min at 42°C, followed by heat inactivation of reverse transcriptase for 5 min at 95°C and subsequent cooling to 4°C for 24 h. RT-qPCR was performed on a QuantStudio 7 Flex Real-Time PCR System (Applied Biosystems, Life Technologies), using Power SYBR™ Green PCR Master Mix with the pre-designed primers listed in the Supplementary Table S1. RT-qPCR was done in 384-well plates with each sample measured in duplicate and non-template controls (NTCs) included for each amplification product. U6 and SNORD110, two reference genes, were used to normalize miRNA expression. The RT-qPCR conditions were as follows: polymerase activation/denaturation at 95°C for 10 min, followed by 50 amplification cycles at 95°C for 10 s and 60°C for 1 min (a ramp rate of 1.6°/s). Specificity of the amplified products was confirmed by melting curve analysis.

Regarding gene expression, 1000 ng/μL of total RNA was converted into cDNA using the Xpert cDNA Synthesis Supermix Kit (GRiSP, Porto, Portugal), according to the manufacturer's instructions at optimized conditions: 37°C for 15 min, 60°C for 10 min, and 95°C for 3 min. Subsequently, template cDNA was amplified by quantitative RT-qPCR using the Xpert Fast SYBR Mastermix BLUE Kit (GRiSP, Porto, Portugal), using the primer sequences indicated in Supplementary Table S2. RT-qPCR was performed in 384-well plates with each sample measured in duplicate and NTCs included for each amplification product. β-actin was used as an endogenous control to normalize gene expression levels. Running conditions for the RT-qPCR were as follows: 50°C for 2 min followed by 95°C for 2 min and 40 cycles at 95°C for 5 s and 62°C for 30 s. After amplification, the specificity of the amplified products was verified by melting curve analysis. Both miRNA and mRNA RT-qPCRs were run on the QuantStudio 7 Flex Real-Time PCR System (Thermo Fisher Scientific, Waltham, Massachusetts, United States).

Relative mRNA/miRNA expression levels were measured using the ΔΔCT method relative to the respective endogenous control, as previously published (Garcia et al., 2022). Normalized results were expressed as Log_2 ($2^{-\Delta\Delta CT}$) vs. the respective control sample.

2.9 Exosome protein quantification using the Micro BCA™ Protein Assay Kit

Total protein was extracted from concentrated exosome samples using a modified version of RIPA buffer [2% sodium deoxycholate; 20 mM HEPES buffer; 200 mM KCl; 1 mM EDTA pH 8.0; 0.2% sodium dodecyl sulphate (SDS); 20% glycerol and H_2O MilliQ]. Samples were diluted at least 20 times to prevent the buffer from interfering with the Micro-BCA™ Protein Assay Kit (Thermo Fisher Scientific, Waltham, Massachusetts, United States), following the manufacturer's recommendations. Protein concentration was measured using a Varioskan LUX multimode plate reader (Thermo Fisher Scientific™, Waltham, MA, United States). Absorbance was read at 562 nm.

2.10 Immunocytochemistry assay

For immunocytochemistry, primary microglia and neuroblastoma cells (referred to as neurons hereafter) were cultured in 12-well plates containing HCl-washed coverslips, while the microfluidic devices with neurons + microglia + astrocytes were directly used as the assay platform. In brief, primary cortical microglial cells and tricultures were fixed with 4% (w/v) paraformaldehyde in PBS for 20 min. Then, cells were permeabilized with 0.2% Triton X-100 in PBS for 10 min and further blocked with 3% BSA in PBS for 30 min. Afterwards, the cells were incubated with primary antibodies (Supplementary Table S3) at 4°C and overnight, as usual in our laboratory (Vaz et al., 2021). All antibodies were diluted in PBS (1% BSA). In the following day, cells were incubated with species-specific secondary antibodies (Supplementary Table S3) for 2 h. Coverslips were mounted into a glass in Fluoromount-G to be visualized by confocal microscopy. An extra washing step was performed by the addition of DPBS in the microfluidic device, followed by the application of a 40 μL drop of Fluoromount-G (Merck-Millipore) in each cell compartment.

2.11 Confocal microscopy analysis

Confocal fluorescence z-stack images of primary microglia and microfluidic cell triculture chips were acquired (under the navigator mode) using a Leica TCS SP8 inverted microscope (Leica Microsystems, Wetzlar, Germany), both with ×10 and ×40 (oil immersion) objectives, sequential laser excitation at 405/488/552/638 nm, and spectral detection adjusted for the emissions of AlexaFluor 405/488/594/647 dyes, respectively. The equipment was controlled by Leica LAS X software (Leica Microsystems).

2.12 Post-acquisition image treatment and analysis

Image treatment, including concatenation, and z-stack analysis (maximum fluorescence intensity) were performed using Fiji software (Schindelin et al., 2012). Pixel-integrated single-cell multiparametric analysis was done in AIVIA software v.12.0.0 (Leica Microsystems), using the following 2D recipes: neurite outgrowth; cell analysis, and particle count. Settings were adjusted for the identification of single cells, accordingly with each measurement requirements. In the images of the microfluidic cell triculture system, different regions of interest (ROIs) were created to perform a personalized analysis adjusted to the cell type of each compartment.

2.13 Statistical analysis

Statistical analyses were performed with GraphPad Prism 9 (GraphPad Software Inc., San Diego, CA, United States). All statistical comparisons were performed using one-way ANOVA when each dataset met the required assumptions for ANOVA, including homogeneity of variances and normality. Tukey's *post hoc* test was applied to determine statistical significance between experimental groups. Only $p < 0.05$ was considered statistically significant. Results from a minimum of three independent experiments ($n = 3$) are expressed as mean ± SEM. Individual replicates were visually represented in each graph, allowing for easy

verification of the sample sizes and distribution in each condition. In the triculture experiments, statistical analyses were carried out separately for neurons, microglia, and astrocytes. Whenever found, outliers were removed from the datasets to ensure the accuracy and robustness of the statistical analyses. For correlation analyses, RT-qPCR data were analysed using SRplot (Tang et al., 2023), including the basic correlation plot package (https://www.bioinformatics.com.cn/plot_basic_corrplot_corrlation_plot_082_en). Bivariate Pearson's correlation coefficients were calculated, and their significance was considered whenever $p < 0.05$. Raw data correlation matrix, Pearson correlation coefficients (R^2), and p-values are provided in Supplementary Datasheet S1.

3 Results

3.1 Exo-Fect™ exosomal transfection with miR-124-3p mimic reveals high efficiency and steers a neuroprotective phenotype on stressed microglia

Emerging studies have suggested that dysregulation of miR-124 is related to the pathogenesis of neurodegenerative diseases, such as AD (Han et al., 2019). Therefore, regulation of miR-124 expression may represent a promising therapeutic approach in patients where its downregulation is associated with the onset and progression of the disease. Indeed, we have previously showed that miR-124-3p regulation with its mimic counteracted AD neuronal impairments and restored microglial homoeostasis (Garcia et al., 2021; Garcia et al., 2022). Considering that exosomes are the main natural carriers of miRNAs (Loch-Neckel et al., 2022), we anticipated that delivery of exosomes loaded with miR-124 mimic could represent a promising strategy to recover homoeostatic neuron–glia balance in AD patients with defective neuronal values of miR-124.

Based on such background, we used two different loading strategies of miR-124 in neuronal exosomes, as schematized in Figure 1A, and as follows: one was the transfection of SH-*WT* cells with the miR-124-3p mimic and subsequent isolation of the released miR-124 enriched exosomes (CT124); and the other was the direct transfection of the miR-124-3p mimic in exosomes previously isolated from SH-*WT* cell secretome using the Exo-Fect™ kit (ET124). Then, CT124 and ET124 were first compared relatively to size distribution and particle count using the NTA assay, as described in the methods section (Figure 1B). No differences were found between CT124 and ET124 for the number and size, although ET124 revealed an enlarged variation in the exosome diameter size (from 100 to 200 nm). Next, we assessed CT124 and ET124 delivery efficiencies in the 2DIV cortical *WT* mouse microglia, by determining the microglial content in miR-124 vs. non-exosomal treated cells (untreated), mock-transfected (mock), and negative controls (NCs) (Figure 1C). Both approaches (CT124 and ET124) significantly upregulated microglial miR-124-3p vs. mock-transfected exosomes ($p < 0.001$) and vs. negative control-transfected exosomes ($p < 0.001$). Nevertheless, ET124 had a more efficient delivery (20-fold, $p < 0.001$), when compared to CT124.

Importantly, the neuroblastoma-derived exosomes used as mock and negative controls revealed to be natural miR-124-3p carriers, as we have previously demonstrated (Garcia et al., 2022). Based on the similar results of mock and negative controls, in the subsequent experiments, we used only the mock control.

To further evaluate how far CT124 and ET124 were able to regulate the originally stressed 2DIV microglia, we assessed core activity state biomarkers, namely, the genes encoding the nitric oxide synthase (*Nos2*), arginase 1 (*Arg1*), and the triggering receptor expressed on myeloid cells (*Trem2*). We also noted that exosomes, as we previously demonstrated (Pinto et al., 2017), can *per se* also promote microglial activation. This was the case for the increased *Nos2* ($p < 0.01$) and the decreased *Trem2* ($p < 0.05$) in mock samples relatively to non-exosomal treated cells (untreated), as shown in Figure 1D. Addition of CT124 was not able to significantly decrease *Nos2* or revert *Arg1* (despite the slight elevation) levels but significantly enhanced *Trem2* expression values, suggesting a "calming" effect and recovery of microglial metabolic fitness. More prominent effects were obtained for ET124 in mitigating *Nos2* overexpression relatively to both CT124 and mock samples (Figure 1D, $p < 0.05$, for both), as well as on upregulating *Arg1* and *Trem2*, as compared with both untreated and mock controls ($p < 0.001$, for both). Importantly, the ability to enhance the microglial phagocytosis rate was mainly sensed for ET124 and barely for CT124, when considering the *Trem2* overexpression ($p < 0.05$) and the trend towards *Arg1* upregulation ($p = 0.06$).

Given these promising results, we investigated whether such effects were caused by an increased exosome uptake of ET124 vs. CT124 by microglia. Correspondingly, we labelled exosomes (mock control, CT124, and ET124) with the PKH67 lipophilic dye to monitor and compare exosome internalization by the microglial cells. Although all exosomal formulations were successfully internalized by the 2DIV stressed cortical microglia, the uptake of ET124 was markedly higher ($p < 0.001$) than that of CT124 and mock control, as shown in Figures 1E, F.

Iba1 and the purinergic receptor P2Y12 (P2RY12) are considered specific and complementary microglia markers once they are not individually expressed by all microglia. Some subsets express Iba1, and some others lose P2RY12, as observed for the microglia around Aβ plaques (Kenkhuis et al., 2022). This means that they should be evaluated in combination, probably reflecting diverse functional phenotypes. Therefore, we assessed both markers in the microglia treated with CT124 and ET124 (Figures 1G, H) by immunocytochemistry. Our results suggest that the subtype induced by CT124 is considerably different from that triggered by ET124. Iba1 was sustained by CT124, with higher levels than mock ($p < 0.01$) or ET124 ($p < 0.001$), which showed lower levels than the untreated microglia ($p < 0.001$). On the contrary, untreated, mock, and ET124 experiments revealed between 60% and 70% of microglial positive cells for P2ry12 but only 40% in the case of the cells treated with CT124. The loss of Iba1 immunostaining seems to not be due to ET124, once it was also observed for the mock control. However, the loss of P2ry12 was determined only by CT124.

Together, such findings attest the higher efficiency of the exosomal direct transfection of miR-124-3p with Exo-Fect™ and suggest that ET124 redirects microglia into a more neuroprotective phenotype than CT124. Hereafter, the experiments were conducted only with ET124.

To later explore the potential neuroprotective properties of ET124 in a model recapitulating the homoeostatic imbalance

10.3389/fphar.2025.1474012

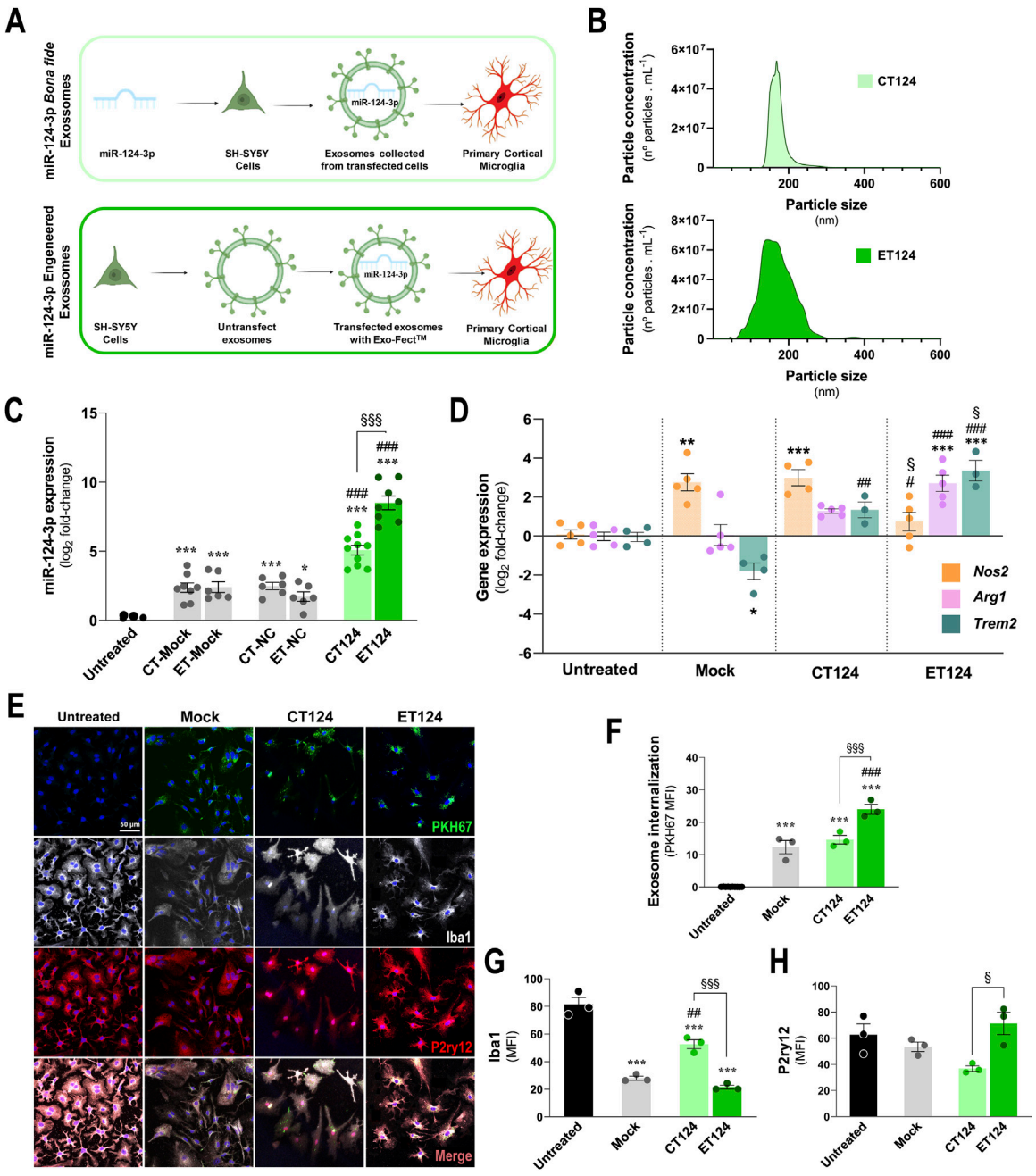


FIGURE 1
Comparative transfection processes, exosome delivery, and microglial targeting efficiencies of miR-124-engineered exosomes upon cell- and exosomal-enriched miR-124 strategies. CT124, obtained by transfecting SH-*WT* cells with the miR-124 mimic, followed by secretome collection and exosome isolation. ET124, obtained by separating exosomes from the secretome of SH-*WT* cells, followed by direct Exo-Fect transfection with the miR-124 mimic. **(A)** Schematic representation of the tested strategies for miR-124-3p exosome enrichment and delivery on cortical 2DIV stressed microglia. **(B)** Representative histograms of the size and concentration of CT124 and ET124 exosomes. **(C)** miR-124-3p expression levels in microglia treated with ET124 and CT124. **(D)** Expression levels of microglial *Nos2*, *Arg1*, and *Trem2* in each tested condition after exosome delivery. Both miRNA and gene expressions were determined by RT-qPCR. **(E)** Fluorescent images of microglia immunostained for Iba1 and P2RYy12, after incubation with PKH67-labelled CT124 and ET124. Internalization of PKH-67 labelled exosomes by microglia **(F)**, Iba1 **(G)** and P2ry12 **(H)** mean immunofluorescence intensities (MFI, arbitrary units), in each tested condition. Data are mean ± SEM, from at least n = 3 independent experiments. ***$p < 0.001$, **$p < 0.01$, and *$p < 0.05$ vs. untreated condition; $^{###}p < 0.001$, $^{##}p < 0.01$, and $^{#}p < 0.05$ vs. mock; $^{§§§}p < 0.001$, $^{§§}p < 0.01$, and $^{§}p < 0.05$ vs. CT124 cells; one-way ANOVA with Tukey's *post hoc* test. Microglia (human CHME3 cell line); Neuroblastoma SH-*WT*, SH-SY5Y *wild-type* cells; *Arg1*, arginase 1; Iba1, ionized calcium binding adaptor molecule 1; *Nos2*, inducible nitric oxide synthase-coding gene; P2ry12, purinergic receptor p2y12; *Trem2*, triggering receptor expressed on myeloid cell 2 coding gene.

associated with AD pathology, we developed a system with dynamic microglia–neuron–astrocyte tricultures in a microfluidic device, allowing paracrine signalling, and investigated the cell type-specific distribution of ET124 using the SH-*SWE* cells and H_2O_2 in the presence of human astrocytes and microglial cell lines. In this way, we envisioned to recreate the conditions of neurodegeneration, oxidative stress, neuroinflammation, and ageing usually linked to the onset and progression of AD.

3.2 Establishment of a microfluidic multicompartment system for sustained microglia–neuron–astrocyte crosstalk

Although microfluidic devices have been proposed for human triculture systems modelling neurodegeneration (Park et al., 2018; Amartumur et al., 2024; De Vitis et al., 2024), to the best of our knowledge, the present work is original in assessing ET124-based therapeutics to target neurodegeneration and neuroinflammation without cell-to-cell direct interactions. For this, we initially developed a triculture in a multicompartment microfluidic device, where three different human neural cell populations (neurons–astrocytes–microglia) were cultured in a fluidically dependent closed circuit of secretome (De Vitis et al., 2021) (Figure 2A). With this system, it is possible to follow the temporal-dependent paracrine signalling exerted all together by each cell type through their released soluble factors and extracellular vesicles. Considering the contradicting literature with different technical approaches for establishing triculture systems (Park et al., 2018; Guttikonda et al., 2021), we tested multiple procedures to optimize the cell triculture stability by defining the best setup to support each cell type (Supplementary Figure S1 for defining the cell coating; Supplementary Figure S2 for defining the best neuron–astrocyte–microglia cell ratio). We have decided to use a neuron–astrocyte–microglia ratio of 5:3:2, considering the better results achieved. It is noted that the interaction between the three cell types seems to improve the differentiation of SH-SY5Y cells, used as neuron-like cells.

We started by selecting the neural cell type to be plated in the system. For the neurons, we used neuron-like SH-*WT* differentiated cells because we are familiar with these cells, they are not expensive, and they are easy to use. They were plated in the middle compartment of the microfluidic device and differentiated for 2DIV (D1–D3, 48 h) with RA (Figure 2B). At 3DIV (D3), the human HMC3 cell line and the immortalized human astrocytes were plated on the top and bottom compartments, respectively, until 5DIV (D5). Cell images by phase contrast microscopy are shown in Figure 2C, upon the completion of the tricultures at D5. Here, we used devices with shorter microchannels (50 μm) across the cell compartments, to more easily follow the neurite extension between compartments using the fluorescence microscope and the immuno-specificity for βIII tubulin in neuronal cells (Figure 2D). Immunostaining of microglial P2RY12 (red), neuronal βIII-tubulin (green), and astrocytic S100 calcium-binding protein B (S100B, blue) expression predominance can be clearly identified in Figure 2E. Each cell type remained inside their specific compartment, except for neuronal neurites (visible in green) that transmigrated into the glial compartments through the narrow channels (white arrows), as shown in Figure 2E. Culture optimization was also validated in tricultures using SH-*SWE* cells, instead of SH-*WT* cells (data not shown).

Results confirm the success in establishing a viable neural cell triculture without cell-to-cell direct contact, reaching a state of equilibrium where the neurite outgrowth and the released secretome, enriched in cell-derived soluble factors and extracellular vesicles, contribute to a balanced signalling dynamics with paracrine and autocrine responses. The system will be fundamental to recreate a late-onset AD model (aged-related AD), a requisite to evaluate the ET124 cell-specific distribution and their subsequent neuroimmune modulatory effects in each neural cell type.

3.3 Microglia show the highest uptake of ET124 in the dynamic triculture microfluidic system recapitulating AD under stressful and ageing conditions

Tricultures were established as indicated in Section 2.2 but now using the SH-*SWE* cells instead of SH-*WT* cells to induce cell environmental pathology mediated by homoeostatic imbalance in the microglia–neuron–astrocyte cultures. We have previously demonstrated that SH-*SWE* cells release inflammatory mediators, mature and immature amyloid precursor protein (APP), and soluble APP alpha (sAPPα), as well as exosomes with an elevated cargo of inflammatory miRNAs that mimic their donor cells (Fernandes et al., 2018). In addition to the differentiation of the cells with RA, we used a low dose (10 μM) of H_2O_2 to trigger a viable neural phenotype in-part reminiscent of aged or damaged neuron derived from oxidative stress and neuroinflammation induction (Chadwick et al., 2010; Gunawardena et al., 2019), thus recreating our aged-related AD-like model before exposure to ET124 (Figure 3). Indeed, such conditions are known to be associated and further aggravate AD pathology (van Rensburg et al., 1997; Milton, 2004; Wang et al., 2023).

As shown in Supplementary Figure S3, the addition of H_2O_2 at 10 μM to SH-*SWE* cells in monoculture produced a dramatic reduction of total neurite length ($p < 0.001$), relatively to the SH-*WT* matched cells. Importantly, it caused a reduction of miR-124-3p expression levels, which was more prominent in SH-*SWE* cells when compared to SH-*WT* cells ($p < 0.01$ vs. untreated). These findings recapitulate a subtype of AD patients with defective miR-124 expression—which is our model of choice to test ET124 reparative benefits.

In previous studies from our group, exosomes isolated from SH-*WT* cells were characterized in terms of morphology by transmission electron microscopy (TEM), protein markers by Western blot, and number/size distribution by NTA (Fernandes et al., 2018; Garcia et al., 2021). Such exosomes typically showed a spherical morphology with the usual cup-shaped distortion by surface desiccation by TEM in high magnification, as well as the predictable presence of ALIX, CD63, and Flotillin-1 proteins. Therefore, in the present manuscript, we only characterized ET124 (obtained as previously described) in terms of concentration, size, and particle concentration per μg protein. Most of the samples of ET124 presented an average of 8×10^6 particles per mL (Figure 3A) and showed a mean particle size between 120 and 160 nm (Figure 3B). To obtain reproducibility among the experiments, we used both the number of exosomes and the exosomal protein concentration to estimate the amount of

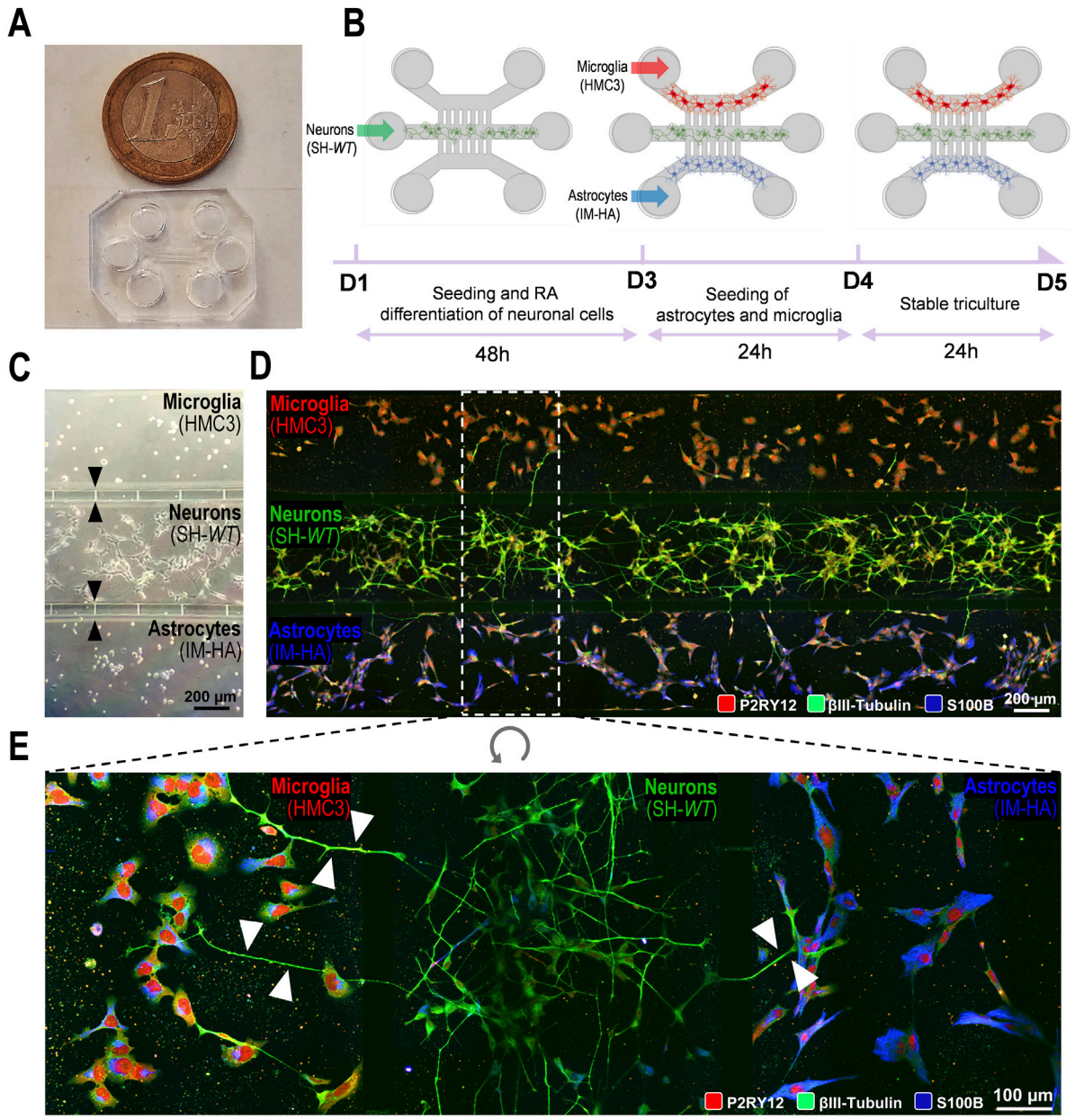


FIGURE 2
Generation and optimization of a 2D triple co-culture of neural cells (human neurons, microglia, and astrocytes) on a microfluid chip system to investigate paracrine signalling by neurites and cell-derived extracellular vesicles and soluble factors. **(A)** Photography of a microfluidic chip and size comparison to 1€ coin. **(B)** Schematic illustration of the experimental design implemented for microglia–neuron–astrocyte tricultures along the days in culture (day 1, D1 until the ending day 5, D5. **(C)** Phase contrast microscopic image of the three human cellular types (neuroblastoma SH-SY5Y cell line as neurons; CHME3 microglia cell line as microglia; and immortalized astrocyte cell line, IM-HA, as astrocytes) cultured in the microfluidic device, with intercellular communication via the microchannels with 5 µm in width and 50 µm in length (indicated by black arrows). **(D)** Fluorescent images of microglia (on the top compartment), neurons (on the middle compartment), and astrocytes (in the bottom compartment) cultured in the microfluidic device, evidencing immunostaining of microglial P2RY12 (red), of neuronal βIII-tubulin (green) and of astrocytic S100β (blue) expression predominance. **(E)** Inset image from panel D showing neurite transmigration from neuronal to both glial cell compartments through the 5-µm microchannels (indicated by white arrows). P2RY12, purinergic receptor P2Y12; S100B, S100 calcium-binding protein B.

ET124 to be added to each microfluidic triculture experiment. Indeed, the same number of exosomes may not represent the same concentration, which is why we used a ratio between the number of particles and the protein content (number of particles/µg of protein, Figure 3C). An average of $2.16 \pm 1.41 \times 10^7$ particles per µg of exosomal protein were administered to each triculture, divided in three doses equally distributed by individual cell compartment.

Before separately evaluating some of the resultant effects of the addition of ET124 in our AD-like triculture model, which will be addressed further, we tracked PKH67-labelled ET124 internalization by microglia (HMC3), neurons (SH-*SWE*), and astrocytes (IM-HA)

10.3389/fphar.2025.1474012

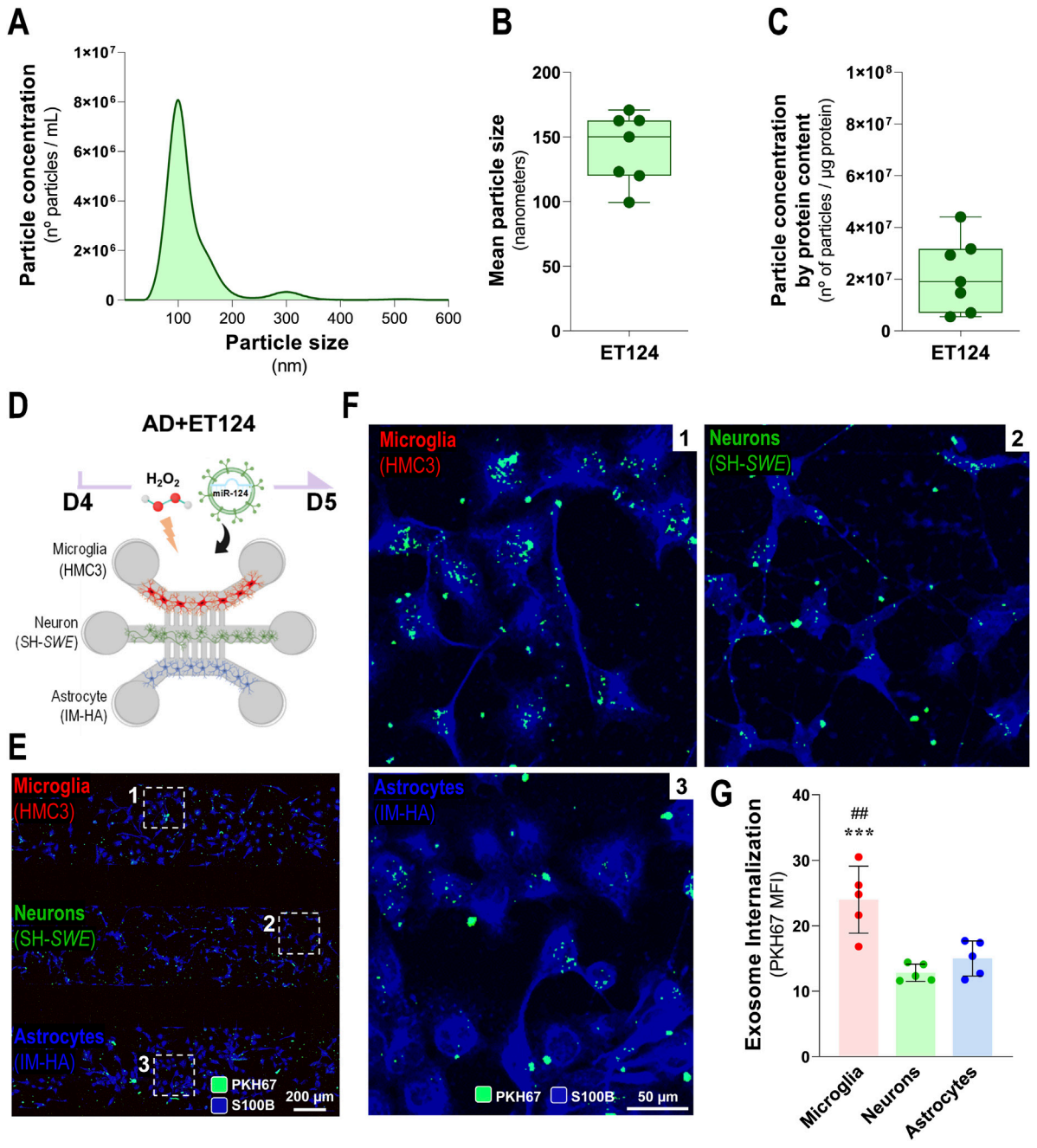


FIGURE 3
Characterization of ET124 for the size, number, and concentration and assessment of their delivery into microglia, neurons, and astrocytes in the AD-like microfluidic triculture model, after exosome labelling. **(A)** Representative histogram of ET124 for the particle size (nm) and number (particles/mL) by Nanosight tracking analysis (NTA). **(B)** Mean particle size of ET124 used in experiments. **(C)** Average ratio of particle number per microgram (µg) of exosomal protein used in experiments. **(D)** Schematic representation of the AD-like triculture model used in the experiments, with device microchannels of 5 µm diameter and 250 µm long. **(E)** Fluorescent images of the distribution of PKH67-labelled ET124 in the tricultures all positive for S100B with insets for zoomed-in images **(F)**, which reveal the internalization of PKH67-labelled ET124 by microglia (CHME3, **1**), neurons (SH-*Swe*, **2**), and astrocytes (IM-HA, **3**). **(G)** Pixel-integrated single-cell quantification of the mean fluorescent intensities (MFI, arbitrary units) for the number of PKH67-positive vesicles internalized by each cell type (from each cell compartment), as indicated in the Materials and methods section. Data are mean ±SEM, from at least three independent experiments. ***$p < 0.001$ vs. neurons and $^{\#\#}p < 0.01$ vs. astrocytes by one-way ANOVA with Tukey's *post hoc* test. AD, Alzheimer's disease. ET124, exosomes isolated from the SH-*WT* cell secretome after transfection with miR-124-3p mimic; SH-*WT*, *wild-type* human SH-SY5Y cells; neurons, SH-*SWE*, SH-SY5Y cells expressing the APP *Swedish* variant; Microglia (human CHME3 cell line); astrocytes; IM-HA, immortalized human astrocytes; S100B, S100 calcium-binding protein B; PKH67, green, fluorescent membrane linker.

under H_2O_2 treatment (Figures 3D, E). Here, we used the microfluidic devices with intercellular communication via the five longer inter-compartment microchannels (250 µm) to prevent the interference of neurites in the exosome cell distribution. Cells were stained for S100B to allow common but uncompartmentalized cell visualization. The pixel-integrated quantification of fluorescent

vesicles permitted their counting by AIVIA software. Images show that ET124 were internalized by all cell types (Figure 3F) with a significantly higher engulfment by microglia ($p < 0.001$ vs. neurons; $p < 0.01$ vs. astrocytes, Figure 3G). This is not without precedent if we consider microglia predominant phagocytic function and our previous data favouring microglial exosome uptake (Pinto et al., 2017; Garcia et al., 2022). As far as this ability to uptake ET124 will be reflected in more extended reparative effects on microglia than on astrocytes and neurons in the AD-like model, it will be a matter of evaluation at a later stage.

3.4 Delivery of ET124 into the microfluidic-based AD triculture model counteracts neuronal apoptosis and caspase-12 activation, as well as glial activation

As previously stated, our AD-like model is expected to be prone to neuroinflammation and neurodegeneration, leading to cell death. We already mentioned that the SH-*SWE* cells evidenced an increased loss of total neurite length upon the addition of H_2O_2, as compared to matched SH-*WT* cells (Supplementary Figure S3), suggesting increased neurotoxicity and ultimately cell demise. Here, we first evaluated how differently the neural cells behaved upon the addition of H_2O_2 (Control: SH-*WT* + HMC3 + IN-HA; AD: SH-*SWE* + HMC3 + IN-HA) and whether the addition of ET124 (AD+124) was effective in preventing the loss of cell viability, following the experiments schematized in Figure 4A. Results indicated a subtle but significant neuronal cell demise ($p < 0.05$, Figure 4B) in the AD-like model (SH-*SWE* cells + H_2O_2), without early apoptotic alterations (Figure 4C), but an increased percentage of late apoptotic/necrotic cells ($p < 0.05$, Figure 4D). Remarkably, this neurotoxicity was prevented in ET124-treated neurons. No changes were observed in the glial cells, although AD astrocytes (astrocytes in the presence of H_2O_2 and neuron-derived pathological signalling) revealed a slight lower viability (with a little more elevated number of apoptotic and necrotic cells).

Once caspase-12 was shown to mediate apoptosis and to be involved in endoplasmic reticulum-associated oxidative stress and Aβ-induced synaptic toxicity (Nakagawa et al., 2000; Quiroz-Baez et al., 2011), as well as in nuclear factor-kappa B (NF-κB) activation (Chow et al., 2021), we decided to evaluate these two parameters by immunocytochemistry (Figure 4E). Elevation of neuronal caspase-12 in the AD model ($p < 0.05$, Figure 4F) was prevented upon the addition of ET124 ($p < 0.01$). It should be noted that caspase-12 showed a trend to increase in astrocytes and microglia in AD and to be counteracted by ET124. NF-κB nuclear translocation was also enhanced in AD neurons and microglia relatively to control ($p < 0.01$, Figure 4G), but ET124 had no power to abrogate such effect, although the significance was reduced to $p < 0.05$ in AD + ET124 neurons. Specifically, ET124 prevented astrocytic NF-κB activation ($p < 0.05$ vs. AD astrocytes), sustaining control levels. Because NF-κB activation increases mitochondrial fragmentation (Albensi, 2019), we next evaluated *FIS1* and *MFN2* gene expression (encoding for dynamics-associated proteins involved in the mitochondrial fission and fusion mechanisms, respectively) (Kornfeld et al., 2018; Colpman et al., 2023). Our data clearly indicate a significant decrease in neuronal *MFN2* expression ($p < 0.01$) in the AD triculture not solved by the ET124 treatment (Figure 4H), suggesting mitochondria fragmentation. No other significant changes were observed in *FIS1* and *MFN2* gene expression levels across any cell type or condition. Since mitochondrial fusion and fission are involved in the regulation of cell proliferation (Dong et al., 2022), we next assessed the expression of the *MKI67* gene, which encodes the proliferation-associated protein Ki-67 (Figure 4I). However, no significant changes were detected, although neurons tended to exhibit lower levels of *MKI67* compared to microglia and astrocytes. These first data indicate that ET124 exert neuron–glia modulatory effects with promising applications in cell homoeostasis restoring.

3.5 Disease-associated alterations in microglia morphometric parameters and phenotypes are modulated by treating the AD-like tricultures with ET124

Data above indicated the presence of microglial activation in the age-AD neural triculture model, as suggested by the increased NF-κB nuclear translocation. In this section, we determined morphological, transcriptional, and immune-associated miRNA microglial changes, known as being associated with AD pathology (Brites, 2020; Franco-Bocanegra et al., 2021; Prater et al., 2023), to better explore the immune-regulatory effects of ET124.

Pixel-integrated image analysis in the age-associated AD model revealed morphological alterations in microglia, compatible with cell polarization (increased number of bipolar and round cells), when compared to control microglia, revealing ramifications (visualized by the white outline). It should be noted that the administration of ET124 to the AD compartment sustained the microglia ramifications and prevented the occurrence of the amoeboid shape (Figure 5A and insets). Although not statistically significant, we observed that microglia in the AD-associated ageing model showed both a reduced area (Figure 5B) and cell perimeter (Figure 5C, $p = 0.08$) that accounted to their significant increase in circularity/roundness shape ($p < 0.05$ vs. control, Figure 5D). Such morphology occurs when microglia switch to an activated phenotype with amoeboid and elongated rod bipolar morphotypes. Targeting of microglia with ET124 produced well-known beneficial effects in counteracting cell perimeter decrease ($p < 0.05$, vs. AD) and circularity increase ($p < 0.05$ vs. control and $p < 0.001$ vs. AD) in the AD condition, including a trend to also sustain cell area control values.

We next assessed S100B and P2RY12, which demonstrated to be upregulated and downregulated, respectively, in pro-inflammatory conditions (Gomez Morillas et al., 2021; Michetti et al., 2023). We observed a significant S100B increase, together with a P2RY12 decrease ($p < 0.01$ for both vs. control, Figures 5E, F), suggesting an activated dysfunctional microglia phenotype. This subtype was validated at the transcriptional level (Figure 5G) by S100B overexpression ($p < 0.01$ vs. control), although the elevation of P2RY12 did not reach significance. ET124 treatment avoided such altered immunoreactivity of S100B and P2RY12 ($p < 0.01$ for both vs. AD). However, no major significant effects were observed at

10.3389/fphar.2025.1474012

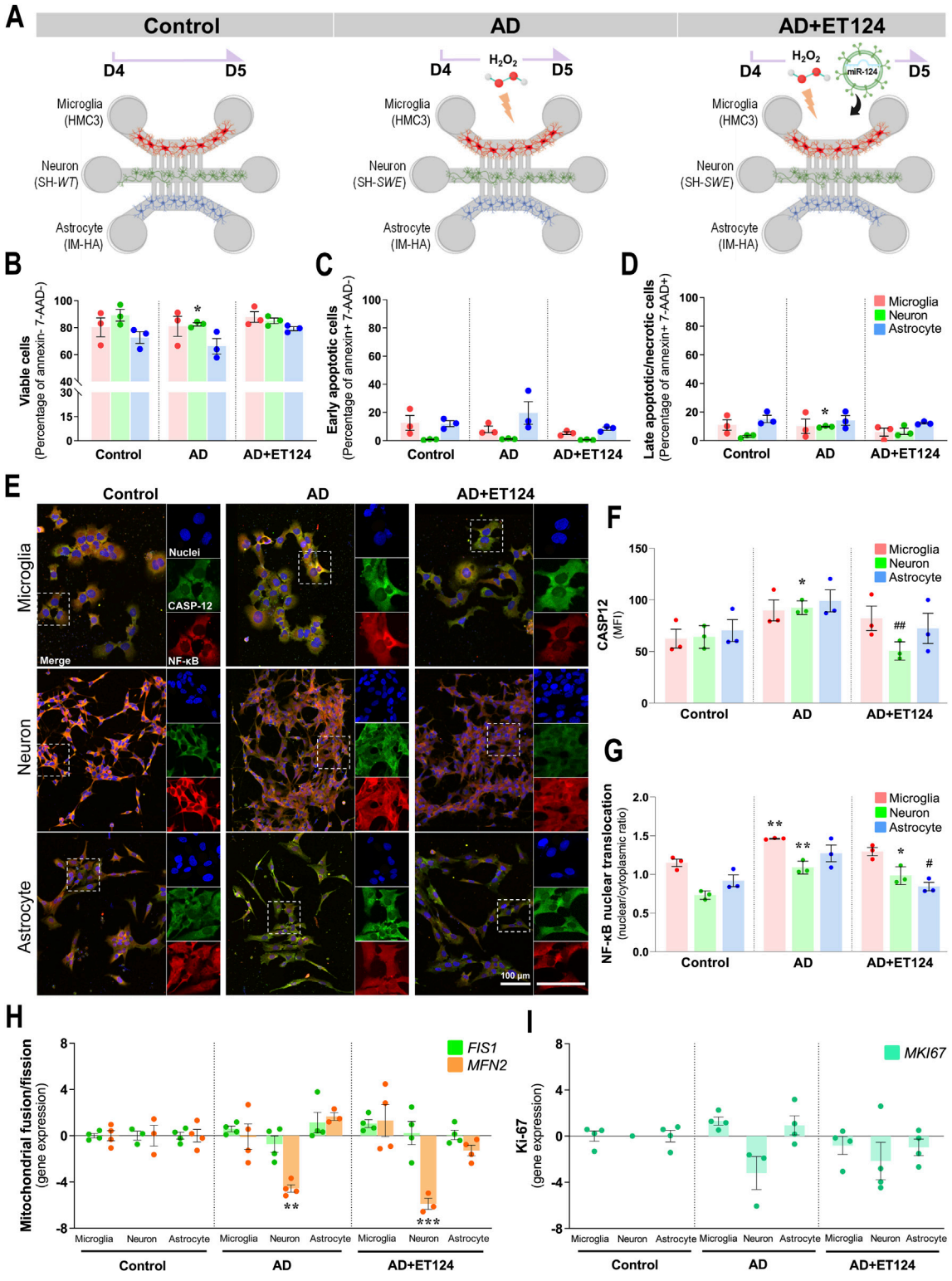


FIGURE 4
Delivery of ET124 into the AD-like microfluidic triculture model leads to preventive effects on neuronal demise and caspase-12 activation, as well as on neuron-glia NF-κB activation, without affecting mitochondria fragmentation or cell proliferation. **(A)** Schematic representation of ET targeting to control (untreated SH-*WT* cells), AD-like (SH-*SWE* + H_2O_2), and AD + ET124 (SH-*SWE* + H_2O_2 + ET124) tricultures (microglia–neurons–astrocytes). Evaluation of cell viability was as described in Materials and methods by flow cytometry. Three populations were distinguished: **(B)** Viable (annexin and 7-AAD double-negative); **(C)** early apoptotic (annexin-positive and 7-AAD-negative); and **(D)** late apoptotic (annexin and 7-AAD double-positive). **(E)** Representative immunofluorescence images of caspase-12 (green); NF-κB (red); cell nuclei stained with DAPI (blue) in neurons, microglia, and astrocytes in the microfluidic system tricultures. **(F)** Pixel-integrated measurement of caspase-12 mean fluorescence intensities (MFI, arbitrary unities) by each cell
(*Continued*)

FIGURE 4 (Continued)
type and condition. **(G)** NF-κB nuclear translocation ratio, obtained by dividing pixel-integrated nuclear/cytoplasmic NF-κB immunofluorescence intensities. Transcription analysis of FIS1 and MFN2 mitochondrial genes **(H)**, and of MKI67, coding for Ki-67 **(I)**, by RT-qPCR. All evaluations were performed in Control, AD, and AD treated with ET124 (AD + ET124). Data are mean ±SEM, from at least three independent experiments. ***$p < 0.001$ vs. Control and $^{\#\#}p < 0.01$ vs. matched cells in the AD-like model by one-way ANOVA with Tukey's *post hoc* test. SH-*WT, wild-type* human SH-SY5Y cells; SH-*SWE*, SH-SY5Y cells expressing the APP *Swedish* variant; ET124, exosomes isolated from the SH-*WT* cell secretome after transfection with miR-124-3p mimic; IM-HA, immortalized human astrocytes; microglia (human CHME3 cell line); 7-AAD, 7-aminoactinomycin D; CASP12, caspase-12; NF-κB, nuclear factor kappa of activated B cells; *FIS1*, fission 1 mitochondrial gene; *MFN2*, mitofusin2 mitochondrial gene; *MKI67*, Ki-67-coding gene.

transcriptional levels, despite the lower significance of S100B mRNA vs. control by the delivery of ET124 ($p < 0.05$ instead of the $p < 0.01$ in AD).

Among the microglia gene expression panel (Figure 5G), we detected upregulated *HLA-DRA* (that encodes the major histocompatibility complex class II, $p < 0.05$ vs. control), *ARG1* ($p < 0.05$ vs. control), and *S100B* ($p < 0.01$ vs. control), together with a nearly significant *TNF*α increase ($p = 0.07$ vs. control). We also found a microglial downregulation of *High Mobility Group Box protein 1* (*HMGB1*) and *TREM2* ($p < 0.05$ for both vs. control). All these changes in the AD model suggest the presence of heterogeneous microglial subtypes linked to cell adaptive immune-activation phenotypes. Beneficial outcomes from ET124 addition to the AD triculture were noticed on the sustained expression of *TREM2* near the control levels ($p < 0.05$ vs. AD) and on a slight effect on *HLA-DRA* and *HMGB1* mRNAs ($p = 0.07$ and $p = 0.1$ vs. control, respectively).

Regarding the miRNA profile, no significant miRNA alterations were detected in microglia from the AD system, despite the near-significant miR-146a decrease ($p = 0.05$ vs. control, Figure 5H), persisting after the addition of ET124 ($p = 0.09$). Interestingly, miR-146a levels were shown to inversely correlate with *HLA-DRA* ($p < 0.01$), as well as with *ARG1, S100B*, and *P2RY12* transcriptional levels ($p < 0.05$, Figure 5I), indicating that miR-146a may play a role in conditioning the microglial phenotype. Positive relationships were obtained between *TNF* and *ARG1/S100B/P2RY12* genes, as well as between *S100B* and *HLA-DRA* (at least $p < 0.05$), confirming their relevance in categorizing microglial subtypes. A more prominent effect was observed for the upregulation of miR-124-3p by ET124 ($p < 0.01$ vs. control and vs. AD) as we anticipated considering the higher ET124 delivery into microglia, which may account for the non-statistical decrease of miR-155-5p ($p = 0.10$ vs. AD). Such antagonism between microglial miR-124-3p and miR-155-5p was manifested by a significant negative correlation between both miRNAs ($p < 0.05$, Figure 5I). Together, these data suggest a more functional and homoeostatic microglia phenotype in the AD + ET124 model.

3.6 ET124 mitigates H_2O_2-induced neurite atrophy and prevents *NOS1, S100B*, and miR-146a AD-associated dysregulation

In this section, we focused on changes occurring preferentially in the neuronal compartment. As commented above, relatively to the increased loss of total neurite length upon the addition of H_2O_2, as compared to matched SH-*WT* cells in monocultures (Supplementary Figure S3), the same was observed in our AD tricultures, as revealed by projections identified with βIII-tubulin immunostaining ($p < 0.001$ vs. control, Figures 6A, B). Changes also included the reduction in total neurite length ($p < 0.001$ vs. control, Figure 6C) and neurite number per cell ($p < 0.01$ vs. control, Figure 6D). Marked preventive effects were observed upon ET124 treatment, for neurite length per cell and total neurite length ($p < 0.001$ vs. AD) with values like those of control, as well as for the neurite number per cell ($p < 0.05$ vs. AD).

Neuronal S100B is considered a reliable marker of active neural distress (Michetti et al., 2023). Although a slight elevation was identified in neuronal S100B immunofluorescence intensity in the AD system, no significant changes were observed for any tested condition (Figure 6E). Relatively to the number of transmigrating neurites (neurites that migrated through the microchannels towards microglial and astrocytic compartments) (Figure 6F), data suggest a reduced transmigration to the microglial and astrocyte compartments ($p = 0.09$ and $p = 0.05$, vs. control, respectively) in the age-AD model, as well as a protective effect by ET124 treatment, especially in the microglial compartment where values closer to control levels were observed.

By using specific discriminating primers, we confirmed that SH-*SWE* cells from the AD system express both *WT* and *SWE* transcript variants of the *APP* gene, unlike SH-*WT* used in the control system (Figure 6G). Nevertheless, a significant APP-WT downregulation ($p < 0.05$ vs. control) was detected in the AD system but not upon ET124 treatment ($p = 0.05$ vs. control). No changes were detected on APP-SWE expression, regardless of the ET124 treatment. Regarding other transcripts, the SH-*SWE* neurons from the AD triculture evidenced increased levels of *TNF* ($p < 0.001$ vs. control) and *NOS1* ($p = 0.07$ vs. control), together with decreased expression of *DLG4* (postsynaptic density protein 95 (PSD95)-coding gene) and *SYP* ($p < 0.05$ vs. control, for both), suggesting the presence of neuroinflammation and impaired synaptic dynamics (Figure 6H). Treatment with ET124 did not counteract *TNF* but led to a significant decrease in *NOS1* ($p < 0.05$ vs. AD) and to less defective *DLG4* and *SYP* mRNAs, together with a small significant increase in S100B ($p < 0.05$ vs. AD), suggested to be an Aβ42 suppressor (Cristóvão et al., 2018).

In what concerns the inflammation-associated miRNA profile (Figure 6I), no significant alterations were observed in the neurons from the AD triculture, as compared to the control condition. However, treatment with ET124 led to miR-146a upregulation ($p < 0.01$ vs. AD), as well as to moderate elevation of miR-124 ($p = 0.06$ vs. AD), not surprisingly if we consider that neurons are not the cells that most engulf ET124. When looking for correlations among microglial genes and miRNAs, we found a strong positive correlation of miR-124-3p with miR-146a-5p ($p < 0.001$) and a negative correlation between the expression of *TNF* and *DLG4* genes ($p < 0.01$), as shown in Figure 6J.

10.3389/fphar.2025.1474012

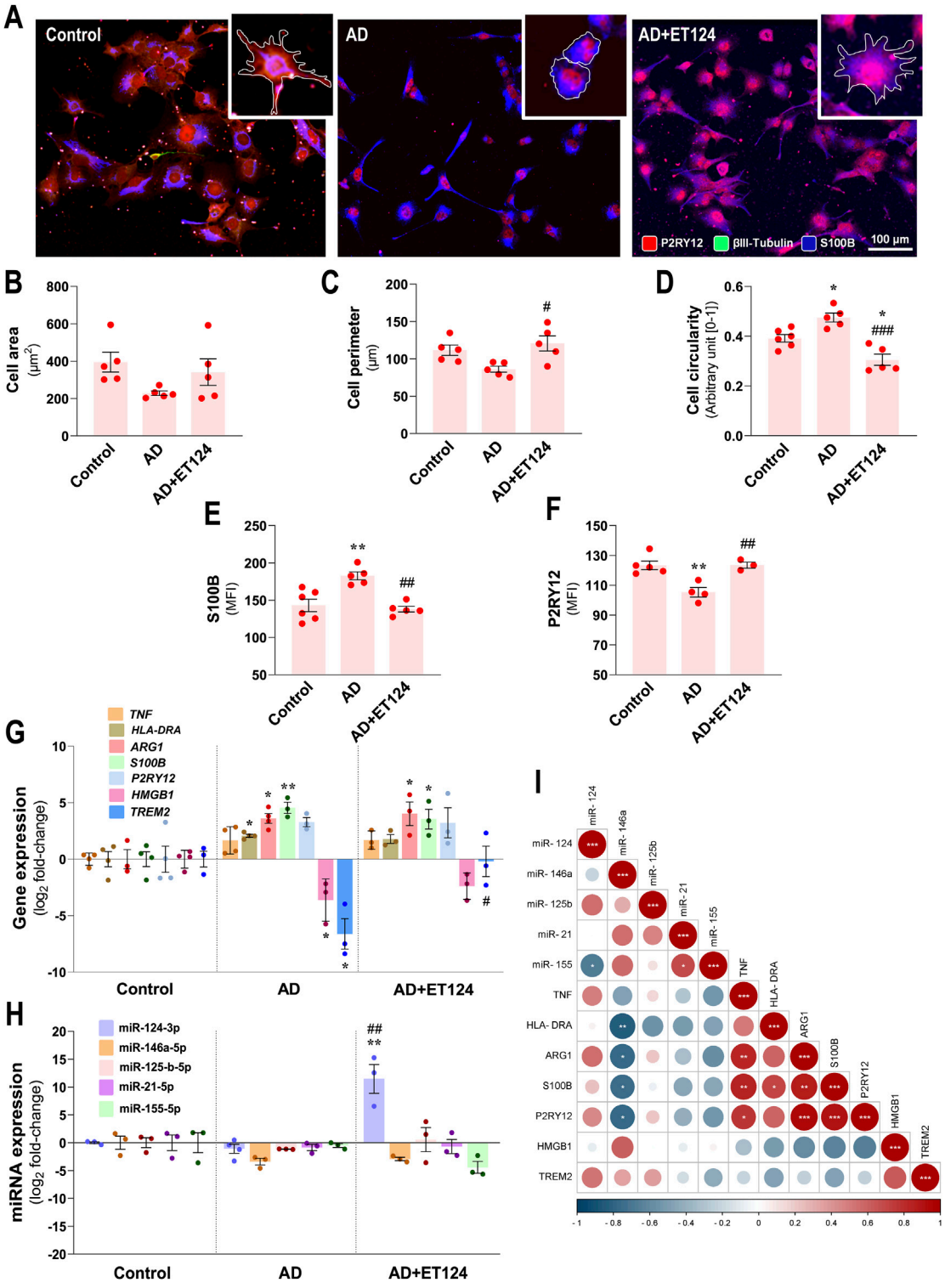


FIGURE 5
Phenotypic profile of microglia in the AD triculture (microglia–neurons–astrocytes) and consequences by ET124 treatment. **(A)** Representative fluorescence images of P2RY12, βIII tubulin, and S100B immunostaining in the microglial compartment showing P2RY12 specificity to HMC3 microglia with image top-right corner insets (with ×2.25 additional magnification), displaying the most representative cell morphological changes in each condition (white outline). Pixel-integrated fluorescence measurement of cell area **(B)**, cell perimeter **(C)**, and cell circularity **(D)** in each condition. Pixel-integrated mean fluorescence intensities (MFI, arbitrary units) for S100B **(E)** and P2RY12 **(F)**. **(G)** Transcriptional analysis of microglia-associated genes *TNF, HLA-DRA, ARG1, S100B, P2RY12, HMGB1*, and *TREM2*. **(H)** Evaluation of microglial expression of miR-124-3p, miR-146a-5p, miR-125b-5p, miR-21-5p, and miR-155-5p. Gene and miRNA expression levels were evaluated in control (untreated SH-WT cells, *wild-type* human SH-SY5Y cells), AD (SH-*SWE*, SH-SY5Y cells expressing the APP *Swedish* variant + H_2O_2), and AD + ET124 conditions by RT-qPCR. Actin (for genes) and U6 (for miRNAs) were used as internal references. **(I)** Correlation matrix based on Pearson's bivariate coefficients (R2) for pairwise comparisons of microglia-expressed miRNAs and genes. Negative correlations are shown in blue and positive correlations in red, both integrating a respective annotation whenever significant. Data are

(*Continued*)

FIGURE 5 (Continued)
mean ±SEM, from at least three independent experiments. ***$p < 0.001$ and **$p < 0.01$ vs. Control; ###$p < 0.001$, ##$p < 0.01$, and #$p < 0.05$ vs. AD, by one-way ANOVA with Tukey's *post hoc* test. ET124, exosomes isolated from the SH-*WT* cell secretome after transfection with miR-124-3p mimic; astrocytes, IM-HA or immortalized human astrocytes; microglia (human CHME3 cell line); *ARG1*, arginase-1 coding gene; *HLA-DRA*, major histocompatibility complex class II-coding gene; *HMGB1*, high mobility group box protein 1-coding gene; *P2RY12*, purinergic receptor P2Y12-coding gene; *S100B*, S100 calcium-binding protein B; *TNF*, tumour necrosis factor alpha-coding gene; and *TREM2*, triggering receptor expressed on myeloid cells 2 coding gene.

Altogether, these results support a neuroprotective effect of ET124 over the neuropathological features exhibited by the AD neuronal compartment in the microfluidic tricultures.

3.7 ET124 halts astrocyte morphological and immune dysregulation in the AD triculture model

Astrocytes, as the most abundant cell type in the CNS, show deleterious effects in AD, exacerbating Tau hyperphosphorylation and Aβ pathology (Cai et al., 2017), and acquiring several pathological phenotypes with altered morphologies and exacerbated reactivity (Kim et al., 2024). Here, morphological, transcriptional, and immune-associated miRNA astrocyte changes were investigated in the AD triculture model, similarly to that performed for microglia, together with the assessment on whether ET124 exerted a positive outcome on astrocyte-induced neuroinflammation.

As evidenced in Figure 7A, IM-HA cells with predominant S100B immunostaining showed bushy, spongy, and star-like morphologies in the control condition. Morphological deficits (decreased branching) were present predominantly in the AD-like system. Such a change is better visualized when comparing astrocyte morphologies in the insets (defined by the white outline). Astrocyte processes are visible in the control and ET124 experiments, indicating the efficacy of this treatment to sustain their native morphology. Morphometric studies revealed a non-significant reduction in the cell area (Figure 7B) and perimeter (Figure 7C) but an enhanced cell circularity in the age-AD model ($p < 0.01$ vs. control, Figure 7D), like those previously found for microglia in the same condition. ET124 treatment showed to prevent such morphological alterations by sustaining the cell area at control levels (p = 0.06 vs. AD) but mainly by preventing changes in the cell perimeter ($p < 0.01$ vs. AD) and circularity ($p < 0.001$ vs. AD). These regulatory effects of ET124 on astrocyte morphology and similarity to that observed for the microglial cells indicate that the targeting of ET124 equally prevents such a glial cell-altered shape in the AD compartment, despite the lower levels of PKH67 exosome internalization when compared to those in microglia (Figure 3G).

Like microglia, and in part neurons, astrocytes from the AD tricultures also exhibited increased S100B immunofluorescence ($p < 0.01$ vs. control, Figure 7E). Again, this reactivity-associated marker was prevented by the ET124 treatment ($p < 0.01$ vs. AD), further adding to its therapeutic potential in mitigating astrocyte-associated pathology in the triculture AD model.

Determination of astrocyte-associated inflammatory genes further validated reactive astrogliosis to the disturbed homoeostasis in the AD-like model (HMC3/IM-HA/SH-*SWE* and H_2O_2). Indeed, AD astrocytes showed a significant upregulation of the genes *S100B* ($p < 0.001$ vs. control), *AGER* (encoding the advanced glycosylation end-product-specific receptor, $p < 0.05$ vs. control), *GFAP* ($p < 0.05$ vs. control), and *GJA1* (encoding gap junction protein alpha 1, $p < 0.05$ vs. control). These findings were counteracted by ET124 (Figure 7F) that significantly diminished *S100B* upregulation ($p < 0.01$ vs. AD) and attenuated overexpression of *AGER*, *GFAP*, and *GJA1* genes (though not significantly vs. control or AD models). Data obtained so far validate the immunomodulatory potential of ET124 over the glial activation and neurodegeneration in our AD-like model.

Most important, we found a downregulation of several anti-inflammatory miRNAs in AD-related astrocytes, corroborating the homoeostatic imbalance and neuroimmune dysregulation in this system. We observed a defective expression of miR-124-3p ($p < 0.05$ vs. control), miR-146a-5p ($p < 0.01$ vs. control), and miR-125b-5p ($p < 0.05$ vs. control) (Figure 7G). A rebalancing action has been achieved by targeting the whole system with ET124, as evidenced by the upregulated anti-inflammatory miRNAs (miR-124-3p, $p < 0.001$; miR-146a-5p, $p < 0.001$; and miR-125b-5p, $p < 0.01$, all vs. AD). In addition, ET124 also inhibited the expression of miR-21-5p ($p < 0.05$ vs. control and AD), which regulates multiple AD pathologies, as well as miR-155-5p ($p < 0.05$ vs. AD), usually considered to be eliciting a pro-inflammatory response.

Such dynamic gene expression and miRNA profile led us to conduct Pearson's correlation analysis that highlighted interesting associations (Figure 7H). For instance, miR-124-3p showed to be positively correlated with miR-146a-5p and miR-125b-5p ($p < 0.001$, for both) and negatively correlated with *GFAP* ($p < 0.05$). Such findings support ET124 potential as a new and efficient therapeutic approach to halt astrocyte-induced AD pathogenesis. miR-146a-5p regulation by ET124 also have positive impact on miR-125b-5p ($p < 0.05$) and negative impact on *S100B* and *GFAP* ($p < 0.05$, for both). miR-21-5p directly correlated with miR-155 ($p < 0.01$) and inversely with *TNF* ($p < 0.05$), suggesting non-synergetic effects on inflammation. Other positive correlations included *HMGB1* with *AGER* ($p < 0.05$); *GJA1* with *GFAP* ($p < 0.001$); and *S100B* with *AGER*, *GFAP*, and *GJA1* ($p < 0.01$, $p < 0.05$, and $p < 0.05$, respectively). It should be additionally noted that intercellular direct correlations for the astrocytic miR-146a-5p and miR-125b-5p with matched miRNAs in neurons, and of miR-124-3p with the microglial one (Supplementary Figure S4), further pointed to miRNA paracrine signalling.

These last data confirm the ET124 potential to counteract astrocyte reactivity in a dynamics neuron–glial system that mimics the AD microenvironment, ultimately supporting their application to modulate inflammation and age-associated neurodegeneration.

10.3389/fphar.2025.1474012

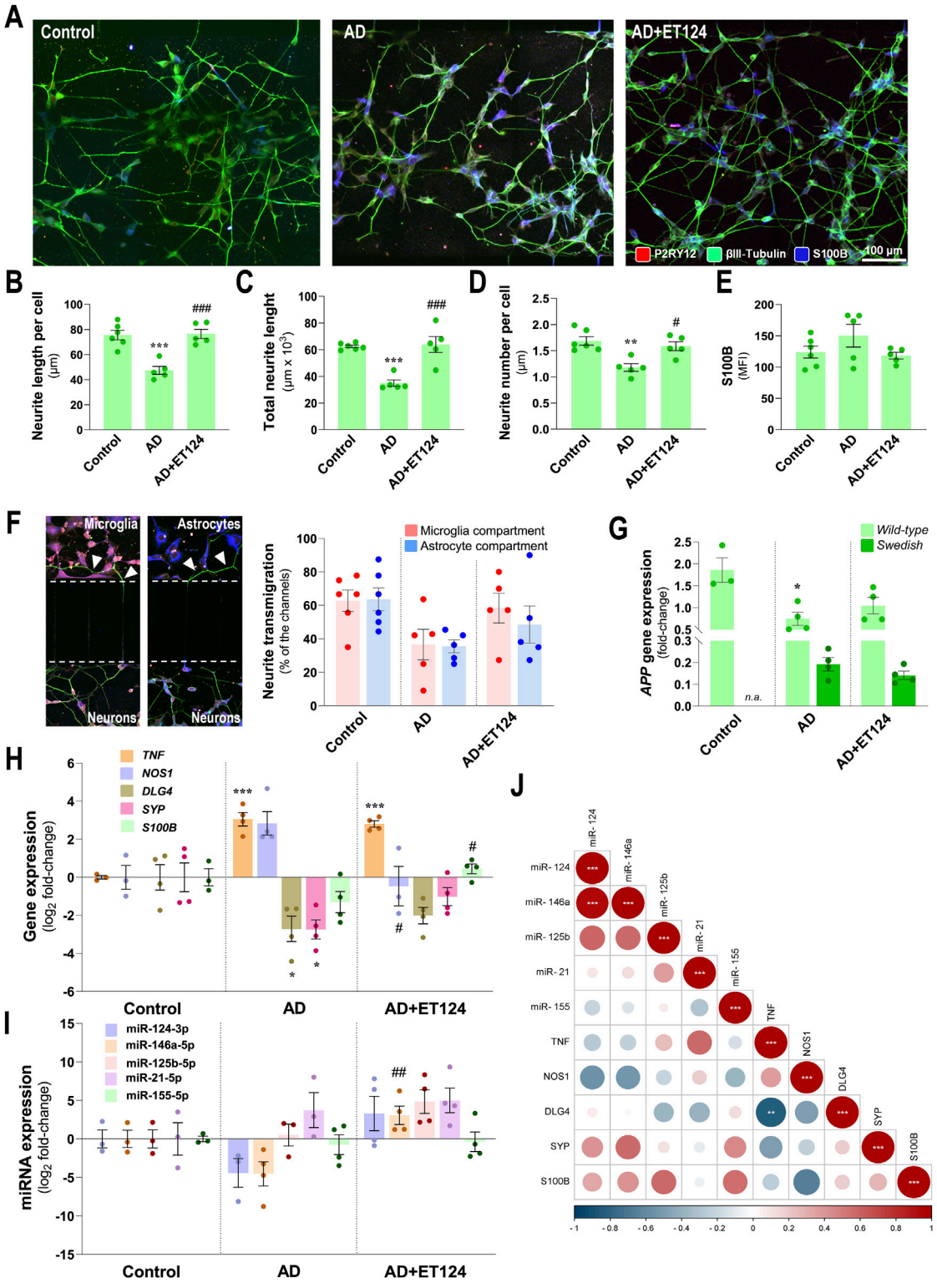


FIGURE 6
Characterization of the neuronal pathological features in the AD triculture (microglia–neurons–astrocytes) system and of the preventive effects by ET124 treatment. **(A)** Representative fluorescence images of P2RY12, βIII tubulin, and S100B immunostaining in the neuronal compartment, showing βIII tubulin specificity to neuronal cells/neurites in the three experimental conditions: SH-SY5Y neurons in non-treated tricultures (Control); SH-*SWE* in AD model tricultures treated with H_2O_2 (AD); and SH-*SWE* in AD model tricultures treated with ET124 (AD + ET124). Pixel-integrated fluorescence measurement of neurite length per cell **(B)**, total neurite length **(C)**, and neurite number per cell **(D)**. Pixel-integrated mean fluorescence intensities (MFI, arbitrary units) for S100B **(E)**. **(F)** Representative fluorescence image sections of the transmigrating neurites (neurites interacting with microglia and/or astrocyte compartments) through the silicon-separating block, accompanied by the percentage of transmigrating neurites counted in microglia and astrocyte compartments. **(G)** Transcriptional level of amyloid precursor protein (APP) using primers that discriminate *WT* and *SWE* forms by RT-qPCR. **(H)** Gene expression analysis of neuronal-associated TNF, NOS1, DLG4, SYP, and S100B. **(I)** Expression levels of the neuronal miR-124-3p, miR-146a-5p, (*Continued*)

FIGURE 6 (Continued)
miR-125b-5p, miR-21-5p, and miR-155-5p. Gene and miRNA expression levels were evaluated in Control (untreated SH-WT cells, *wild-type* human SH-SY5Y cells), AD (SH-*SWE*, SH-SY5Y cells expressing the APP *Swedish* variant + H_2O_2), and AD + ET124 conditions by RT-qPCR. **(J)** Correlation matrix based on Pearson's bivariate coefficients (R^2) for pairwise comparisons of neuron-expressed miRNAs and genes. Negative correlations are shown in blue, and positive correlations, in red, both integrating a respective annotation whenever significant. Data are mean ±SEM, from at least three independent experiments. ***$p < 0.001$, **$p < 0.01$, and *$p < 0.05$ vs. Control; ###$p < 0.001$, ##$p < 0.01$, and #$p < 0.05$ vs. AD, by one-way ANOVA with Tukey's *post hoc* test. ET124, exosomes isolated from the SH-*WT* cell secretome after transfection with miR-124-3p mimic. Astrocytes, IM-HA or immortalized human astrocytes; microglia (human CHME3 cell line); NOS1, neuronal nitric oxide synthase-coding gene; DLG4, postsynaptic density protein 95 (PSD95)-coding gene; S100B, S100 calcium-binding protein B-coding gene; SYP, synaptophysin-coding gene; TNF, tumour necrosis factor alpha-coding gene.

4 Discussion

AD persists as the most prominent form of dementia worldwide, being estimated to increase in the coming decades (Yiannopoulou and Papageorgiou, 2020). Treatments, such as memantine—an NMDA receptor antagonist that prevents nerve cell damage by excessive glutamate—and donepezil that slows the breakdown of acetylcholine improving mental and behavioural functions, do not inhibit the cognitive decline and death of brain cells (Korczyn and Grinberg, 2024). Lately, anti-Aβ therapy with monoclonal antibodies has shown some favourable effects, but only a small percentage of older adults with early cognitive impairment have been considered eligible (Pittock et al., 2023).

Therefore, better therapeutic approaches, effective biomarkers for identifying patients with preclinical AD, better translational models, and novel tools to more closely mimic AD pathology are required to connect basic and clinical research (Zhang Y. et al., 2023). Such experimental models recapitulating AD pathological hallmarks are crucial for gaining a better knowledge on the underlying mechanisms and for testing innovative therapeutic approaches. Translation of successful results in transgenic mice to clinics has shown a high-rate failure and limitations of the model (Drummond and Wisniewski, 2017). Using human cells as experimental models overcomes species differences.

Lately, miRNAs have been emerging as promising therapeutic molecules for brain diseases based on preclinical studies and clinical trials, although it is not clear their specific turnover mechanisms, feasibility, effectiveness, and safety (Ma and Zhao, 2023). Moreover, one of the key issues of miRNAs in therapeutics is their instability and rapid degradation that impair specificity and leads to off-target effects, as well as their difficulty in crossing biological barriers (Zhang et al., 2021). Exosomes have the advantage of crossing the BBB carrying signalling molecules, proteins, lipids, and non-coding RNAs (e.g., miRNAs) that control gene expression in the recipient cells (Cunha et al., 2016; Loch-Neckel et al., 2022). Several studies identified alterations in the miRNA expression profile in AD, and its modulation has successfully demonstrated neuroprotective effects in different models (Sun et al., 2018; Garcia et al., 2022). Mesenchymal and stem cell-derived exosomes have shown therapeutic potential in AD mouse models, as well as in rodent/human neuronal monoculture AD models (Xiong et al., 2021; Huber et al., 2022). Furthermore, exosomes have been loaded with different miRNAs for therapeutic purposes, such as with miR-146a mimic for immunomodulatory effects in rheumatoid arthritis and spinal cord injury (Tavasolian et al., 2020; Lai et al., 2022) or with the miR-155 inhibitor in oral cancer (Sayyed et al., 2021). Similarly, enriched miR-124-3p exosomes were used for diseases such as Huntington's [generated from transfected HEK 293 cells (Lee et al., 2017)] and Parkinson's [generated from human umbilical cord blood-derived mononuclear cells (Esteves et al., 2022)], or even for repetitive mild traumatic injury [generated from BV2 microglial cells (Ge et al., 2020)]. As far as we know, only engineered dendritic cell-derived miR-29b-2-exosomes were tested in diseased SH-SY5Y cells and 3xTg-AD mice, as in AD models (Lin et al., 2024).

Therefore, the present work was pioneer in developing miR-124-3p-loaded neuronal exosomes as a strategy to prevent AD progression and in using human neural tricultures in microfluidic devices, allowing cell-to-cell communication between neuron-like (SH-WT human neuroblastoma cells in control experiments or SH-SWE in the AD system), astrocytes and microglia cell lines (IM-HT and HMC3, respectively).

Like other authors, we used SH-*SWE* cells as an AD model (Joh and Choi, 2017; Fernandes et al., 2018; Garcia et al., 2021; Garcia et al., 2022). The use of the SH-SY5Y neuroblastoma cell line, a cloned subline of a neuroblastoma cell line from a bone marrow biopsy (Feles et al., 2022), has been commonly used, and most of the limitations of the model are associated with the fact that SH-SY5Y cells are undifferentiated (Lopez-Suarez et al., 2022), which was not the case in the present study, due to the differentiation protocol with RA that upregulates neuronal markers and the terminal phenotype (Xicoy et al., 2017). Because they are an immortalized cell line, SH-*SWE* cells may present carcinogenic factors (Maqsood et al., 2013) and genetic peculiarities that may lead to an unexpected response to a determined insult (Lopez-Suarez et al., 2022). Moreover, this and other cell lines do not mimic microenvironment perturbations. However, this aspect was surpassed using a triculture model that allows interactions between neurons and glial cells. Lately, induced pluripotent stem cells (iPSCs) generated from patient fibroblasts and differentiated into neurons were shown to better reproduce sporadic and familiar cases of AD (Poon et al., 2017), but limitations due to difficult recapitulation of cell ageing and phenotypic variation also need to be overcome (Volpato and Webber, 2020; Jothi and Kulka, 2024). Direct reprogramming minimizes safety concerns due to iPSCs, although poor proliferative ability and low efficiency limit its application (Zhang Y. X. et al., 2022). Therefore, we decided to use SH-*WT* and SH-*SWE* cells because they can be maintained in culture for long periods of time, are cost-effective, easy to work, more reproducible, provide more material, and bypass ethical concerns (Garcia et al., 2021). Furthermore, the culture of these cells in our multicompartment microfluidic system coated with poly-D-lysine and laminin allows their expansion, migration, and ramification under more physiologic conditions, if compared to a normal T-flask or Petri dish. Finally, SH-*SWE* cells were shown to release Aβ1-40, one of the hallmarks of AD (Fernandes et al., 2018).

In our previous studies, we identified that exosomes from SH-*SWE* cells have increased levels of miR-124, miR-21, and miR-125b,

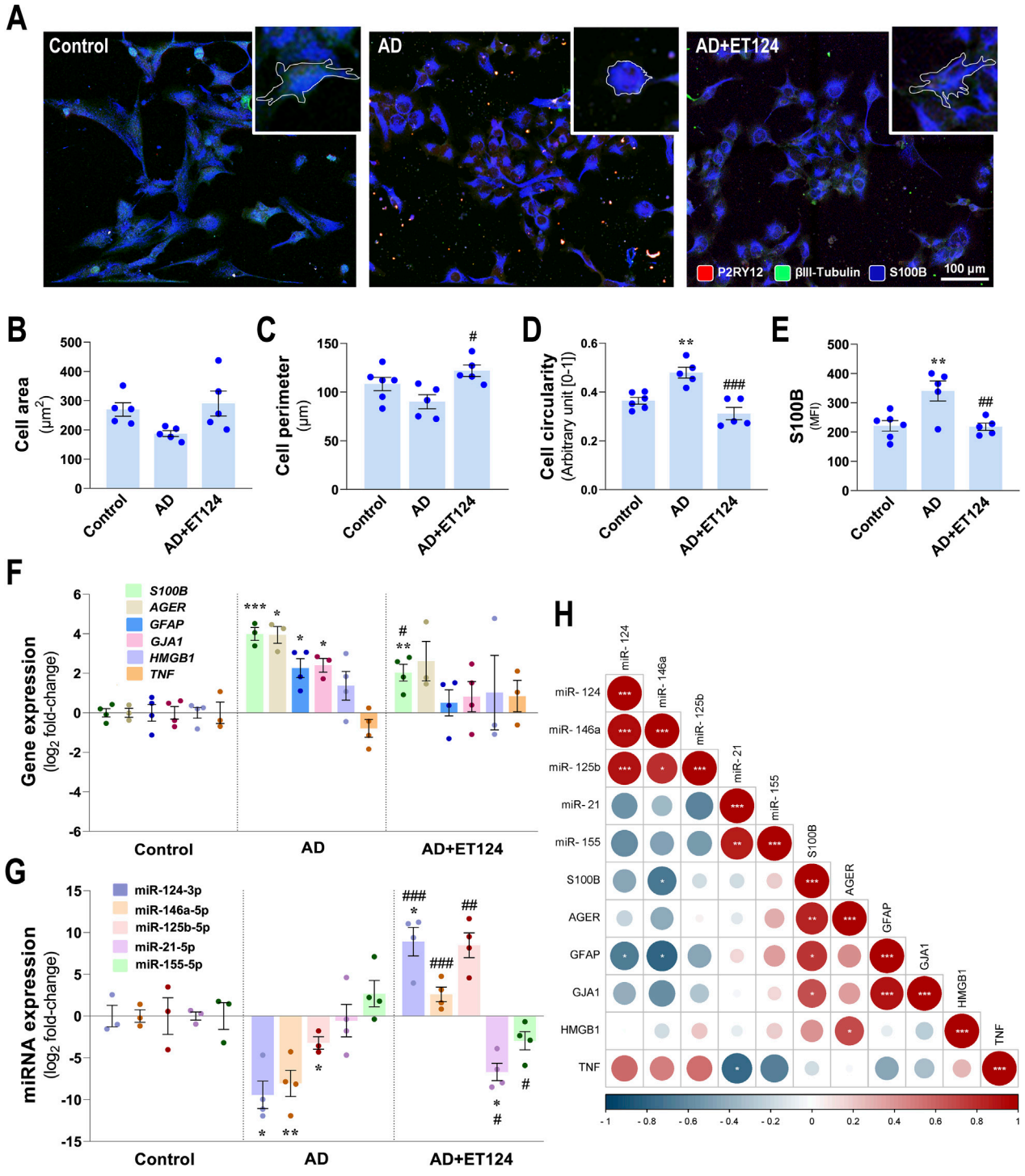


FIGURE 7
Phenotypic profile of astrocytes in the AD triculture (microglia–neurons–astrocytes) and benefits by ET124 treatment. **(A)** Representative fluorescence images of P2RY12, βIII tubulin, and preferential S100B immunostaining in the astrocyte compartment with image top-right corner insets (with ×2.25 additional magnification), displaying the most representative cell morphological changes in each condition (white outline). Pixel-integrated fluorescence measurement of the cell area **(B)**, cell perimeter **(C)**, and cell circularity **(D)** in each condition. Pixel-integrated mean fluorescence intensities (MFI, arbitrary units) for S100B **(E)**. **(F)** Transcriptional analysis of the astrocyte-associated genes *S100B*, *AGER*, *GFAP*, *GJA1*, *HMGB1*, and *TNF*. **(G)** Evaluation of astrocytic expression of miR-124-3p, miR-146a-5p, miR-125b-5p, miR-21-5p, and miR-155-5p. Gene and miRNA expression levels were evaluated in Control (untreated SH-WT cells, *wild-type* human SH-SY5Y cells), AD (SH-*SWE*, SH-SY5Y cells expressing the APP *Swedish* variant + H_2O_2), and AD + ET124 conditions, by RT-qPCR. Actin (for genes) and U6 (for miRNAs) were used as internal references. **(H)** Correlation matrix based on Pearson's bivariate coefficients (R^2) for pairwise comparisons of astrocyte-expressed miRNAs and genes. Negative correlations are shown in blue, and positive correlations, in red, both integrating a respective annotation whenever significant. Data are mean ±SEM, from at least three independent experiments. ***$p < 0.001$, **$p < 0.01$, *$p < 0.05$ vs. Control; $^{###}p < 0.001$, $^{##}p < 0.01$, and $^{#}p < 0.05$ vs. AD, by one-way ANOVA with Tukey's *post hoc* test.
(*Continued*)

FIGURE 7 (Continued)
ET124, exosomes isolated from the SH-*WT* cell secretome after transfection with miR-124-3p mimic. Astrocytes, IM-HA or immortalized human astrocytes; microglia (human CHME3 cell line); *AGER*, receptor for advanced glycation end product-coding gene; *GFAP*, glial fibrillary acidic protein coding gene; *GJA1*, gap junction protein alpha 1 gene (coding for connexin 43); *HMGB1*, high mobility group box protein 1-coding gene; *S100B*, S100 calcium-binding protein B-coding gene; *TNF*, tumour necrosis factor alpha-coding gene.

when compared to those from SH-*WT* cells, which revealed to be internalized by HMC3 microglia (the human microglial clone 3 cell line) after 24 h incubation and to co-localize with lysosomes (Fernandes et al., 2018). These lysosomes revealed to be degraded in the following 24 h. Microglia showed upregulated levels of miR-21, HMGB1, TNF-α, and S100B, thus supporting their activation by SH-*SWE*-derived exosomes. We also observed the existence of miR-124 in hippocampal microglia (*in situ* hybridization) from a Braak stage VI AD patient and homogenates (RT-qPCR) from postmortem biopsies of AD patients (Brites, 2020). In these last specimens from Braak stages II–V/VI AD patients, miR-124 upregulation was only observed in Braak stage III. Interestingly, we additionally identified increased miR-124 levels in the cortex, but not the hippocampus, of 3xTg-mice at 3 months, with downregulated levels at 9 months (Fernandes et al., 2022). It should be noted that miR-124 was shown to have neuroprotective properties in AD pathogenesis by targeting β-site APP cleaving enzyme 1 (BACE1) expression (Fang et al., 2012). Elevation of miR-155 in samples of the transgenic mice vs. WT at both 3- and 9-month-old in the cortex and hippocampus (except at the age of 3 months), together with *TNF-α*, *IL-1β*, *HMGB1*, and *iNOS* gene expression, mainly in the hippocampus, suggests the presence of neuroinflammation in this 3xTg-mouse model.

Although microglia and astrocytes have revealed regional diversity (Grabert et al., 2016; Batiuk et al., 2020), turning interesting to produce cortical and hippocampal regional tricultures, we faced the impossibility to obtain iPSC-derived regional microglial cultures and the limitation that only iPSC-derived cortical astrocytes are described in the literature (Hedegaard et al., 2020). Despite the possibility of modern genetic and cell lineage tracing tools, high-throughput sorting, and high-resolution sequencing technologies (Tan et al., 2020), such issues make it currently unfeasible to carry out regional human tricultures. With this in mind, we decided to proceed with human immortalized HCME3 microglia and human astrocyte (IM-HA) cell lines for tricultures with the SH-*SWE* and SH-*WT* human neuroblastoma cells.

Concerning the HMC3 cell line, established through SV40-dependent immortalization of human embryonic microglial cells, cells revealed surface markers, phagocytic properties, and inflammatory responses upon pro-inflammatory stimuli like primary microglia (https://bitesizebio.com/48560/microglial-cell-lines/). It should be noted, however, that the cells in homeostatic conditions were shown to produce significant amounts of reactive oxygen species (ROS) and IL-6 (Dello Russo et al., 2018). HMC3 cells present low-to-absent expression of CD14 and CD11b, like the human iPSC-derived microglia, and positivity for IBA1, Cx3CR1, TMEM119, P2RY12, and TREM2, which validates the model (Fazzina et al., 2024). To mention that when microglia are removed from the brain and placed into a plastic dish, in monoculture, they stop receiving brain-specific signals, such as the release of chemokines by neurons. However, in our triculture model, they were receiving signals from neurons and astrocytes about disturbances on their health, which turns the system a better recapitulation of the *in vivo* system. In addition, the use of H_2O_2 in low dose provided a better approximation to the physiologic oxidative exposure that these cells experiment *in vivo*, when ageing, and surpassed the lack of age-related features typical of immortalized cell lines.

Considering the IM-HA cells, they were established from primary cultures of human cortical astrocytes with a SV40 large T-antigen (https://cells-online.com/product/immortalized-human-astrocytes/). They are supplied as purified astrocytes, produce faster than primary cultures, and grow for extended periods of time. As limitations, they express reduced levels of GFAP but not of S100B and may behave phenotypically like reactive astrocytes (without oligodendrocyte-type 2 astrocyte progenitors' cells but with vimentin and nestin) (Morita et al., 2021). Similar to all immortalized cells, they differ from "normal" cells because they may express unique gene patterns. Furthermore, when the number of passages increases, immortalized cells may accumulate epigenetic changes (Voloshin et al., 2023). In our study, we only utilized astrocytes in early passages.

Tricultures were delivered into a tricompartmentalized microfluidic system, previously developed (De Vitis et al., 2021), which overcome the low yield of exosomes when generated from monocultures and have the advantage over the coculture mixed system (Park et al., 2018) to facilitate independent microglia–neuron–astrocyte signalling. This tool was the key to assess the effects of ET124 in each human cell type of the AD system. Neurons, microglia, and astrocytes were simultaneously stressed with H_2O_2 (in AD system) or co-treated with H_2O_2 + ET124 (in AD + ET124 system), while controls did not receive any treatment. The addition of H_2O_2 intended to stimulate ageing-associated disease features (Chadwick et al., 2010; Ismail et al., 2016). The model not only recapitulated AD pathological ageing features but also permitted to test ET124 in minimal amounts.

Our decision to upregulate miR-124 in the triculture microfluidic system derived from our previous experiments, where it showed neuroprotective properties (Garcia et al., 2021; Garcia et al., 2022) but also because miR-124 is the most predominant miRNA in the adult brain (Zhang W. H. et al., 2023). It is mostly expressed by neuronal cells and engaged in a variety of biological processes, including neuronal development and differentiation, synaptic plasticity, neurite outgrowth control, and even the acquisition and maintenance of neuronal identity (Yu et al., 2008; Sun et al., 2015). Using experimental *in vitro* models, we demonstrated that miR-124 inhibition in neurons affects the dendritic spine number and increases *APP* gene expression (Garcia et al., 2021). In contrast, in neurons differentiated from AD patient-derived iPSCs, miR-124 overexpression not only prevented *APP* overexpression and oligomerization of toxic

amyloid species but also reduced tau phosphorylation and preserved the dendritic spine number (Garcia et al., 2021). Therefore, our ET124 strategy may reveal particularly interesting in patients showing miR-124 downregulation, a condition previously found in hippocampal biopsy samples from AD individuals (Lukiw, 2007; Smith et al., 2011).

Additionally, miR-124-3p also acts through the inhibition of pro-apoptotic factors and by promotion of cellular survival pathways. For instance, miR-124 interacts with the STAT3 pathway, which is crucial for reducing oxidative stress and maintaining mitochondrial function (Geng et al., 2024). We previously demonstrated that neuronal overexpression of miR-124 also exerted a strong paracrine effect over cocultured IFNγ-stimulated microglia, by redirecting their proteomic profile towards a pro-regenerative and anti-inflammatory phenotype, in accordance with other studies (Ponomarev et al., 2011; Garcia et al., 2022). By proteomic analysis, we identified multiple Wilms tumor suppressor gene (WT1) regulators as differentially expressed according to miR-124-3p levels, including the PRKC apoptosis WT1 regulator (PAWR). Since 2011, several authors have demonstrated that miR-124 acts as a powerful immune modulator, suppressing pro-inflammatory microglial responses and inducing anti-inflammatory gene expression via targeting CCAAT/enhancer-binding protein-α (C/EBP-α) (Ponomarev et al., 2011; Yu et al., 2017; Veremeyko et al., 2019). Additionally, miR-124 has been shown to mitigate microglial activation triggered by surgical trauma (Chen et al., 2019) and to mediate morphine-induced inhibition of innate immunity in microglia (Qiu et al., 2015). Furthermore, miR-124 combined with bone marrow-derived exosomes has been shown to inhibit the p38 MAPK signalling pathway, leading to the upregulation of the glutamate transporter GLT-1, mitigating neural apoptosis (Zhuang et al., 2023). Although miR-124 has been poorly explored in AD, there are consistent lines of evidence, supporting its critical role in APP transcription and alternative splicing (Smith et al., 2011; Garcia et al., 2021), BACE1 expression (Fang et al., 2012; An et al., 2017), and tau hyperphosphorylation (Kang et al., 2017; Hou et al., 2020).

In summary, the regulation/modulation of miR-124 was envisaged, in this study, as a potential therapeutic strategy for AD, and the primary endpoint was to develop an exosome-based strategy for miR-124-3p delivery. For this, we first transfected miR-124 in SH-*WT* cells, followed by the isolation of miR-124-loaded exosomes (CT124), as other authors did with HEK 293 cells (Lee et al., 2017). Alternatively, we directly transfected SH-*SW*-exosomes with miR-124 (ET124), using Exo-Fect (de Abreu et al., 2021; Esteves et al., 2022). Although ET124 revealed to be the best approach in terms of transfection efficiency, both ET124 and CT124 were tested as cell targeting tools in 2DIV stressed cortical microglia. These microglia isolated from 2-day-old mice, cultured for 21 days in mixed culture with paired astrocytes, and then isolated and cultured for 2DIV revealed a pro-inflammatory phenotype when compared with the stabilized 10DIV microglia (Caldeira et al., 2014). In this condition, we could realize that both CT124 and ET124 modalities succeeded in raising microglial miR-124-3p expression levels, although ET124 was 20-fold more efficiently delivered than CT124. This finding is in line with studies from Abreu and colleagues, when several miR-155 loading processes were used and direct exosome transfection with Exo-Fect was shown as the best procedure (de Abreu et al., 2021). Our finding on increased ET124 internalization vs. CT124 may later deserve membrane lipidomic studies and elucidation of the engulfment process by electron microscopy.

Microglial phenotypes are governed by the surrounding environment and may show different coexistent phenotypes in neurodegenerative diseases, such as AD (Moore et al., 2015; Prater et al., 2023). Microglial upregulation of *Nos2* gene (encodes for iNOS) upon treatment with both the mock and CT124 exosomes but not with ET124 suggests a selective response to those exosome preparations, impacting on the generation of ROS and inflammation (Sierra et al., 2014). On the other hand, the higher *Arg1* upregulation by ET124 vs. CT124 indicates their increased anti-inflammatory potential, once Arg1 showed to antagonize iNOS in myeloid cells (Shosha et al., 2023). In the same way, *Trem2* upregulation by ET124 vs. CT124 is in line with an enhancement of microglial phagocytosis (Akhter et al., 2021). TREM2 was shown to be fundamental for promoting microglial activation in Aβ and tau pathologies and considered a target to restore homoeostatic microglia (Qin et al., 2021). These data favour ET124 over CT124 in supporting a neuroregenerative microglia subtype.

Co-expression patterns of microglia markers Iba1 and P2Ry12 were found in AD, and phenotypes Iba1^{high} and P2RY12^{low} were identified around Aβ plaques associated with cell activation and impaired phagocytosis. Microglia showing P2RY12^{high} are associated with the homeostatic state, having motility and migration potential abilities, while also occurring in early stages of activation and far from Aβ plaques (Gomez Morillas et al., 2021; Kenkhuis et al., 2022). Specifically, all incubations with exosomes attenuated *Iba1*, despite the strongest efficiency of ET124. The profile was the inverse for the *P2ry12* expression, where the decrease was only produced by CT124. By upregulating microglial *P2ry12* levels, ET124 further validated their promise as a therapeutic strategy.

Neurons are implicated in cognitive functions mediated by a complex and dynamic circuitry based on synaptic communication (Pan and Monje, 2020). Microglia and astrocytes coordinate each other and orchestrate most of the brain's inflammatory properties, with a direct participation on neuronal function (Garland et al., 2022). Therefore, to further explore the ET124 effects, we developed a novel advanced microfluidic system featuring human neuron–microglia–astrocyte tricultures, where SH-*SWE* cells and H_2O_2 (at low concentrations) were intended to recapitulate age-associated AD, as aforementioned. Several optimizations were necessary to establish functional tricultures in the tricompartmentalized microfluidic device. In addition to the definition of the most appropriate coating for the three cell types, we readjusted the media composition, as detailed in Material and methods. L-glutamine (a normal constituent in microglia media) was avoided due to potential side effects in the neuronal cells, including excitotoxicity and calcium dysregulation (Al-Nasser et al., 2022). Another optimization was the relative proportion of neurons/microglia/astrocytes in the tricultures. We employed 50% neurons, 30% astrocytes, and 20% microglia (5:3:2 ratio) that showed better stability during the 48 h of the triculture. The microfluidic device with microchannels of 5 μm in width, 2.5 μm in height, and 50/250 μm in length was fabricated (De Vitis et al.,

2021) to allow the passage of neurites (more easily with 50 μm length for some specific studies), cell-derived growth factors, and exosomes, as ET124. Such reduced dimensions provided the optimal tool in only requiring a small number of cells and exosomes, in contrast with other proposed systems (Bruce et al., 2015; Hajal et al., 2022).

Inflammation, ageing, and oxidative stress are mutually perpetuated in AD, contributing to the disease progression. These features were reproduced in our age-AD model with the SH-*SWE* cells and mild H_2O_2 concentration (van Rensburg et al., 1997; Milton, 2004; Wang et al., 2023). The addition of H_2O_2 was shown to induce cell stress and senescence (Chadwick et al., 2010). Downregulation of miR-124-3p in the monocultured SH-*SWE* cells (Supplementary Figure S3) was not observed in the triculture system, suggesting the presence of compensatory mechanisms by the glial cells, which are known to protect neurons against oxidative stress (Iwata-Ichikawa et al., 1999).

Following the administration of ET124 into the triculture system, its higher accumulation in the microglial compartment confirms the suggested tropism of neuron-derived exosomes for microglia (Bahrini et al., 2015; Peng et al., 2021). Furthermore, our study revealed that ET124 prevents neuronal death and inhibits late apoptosis in the AD triculture system, maintaining viability levels comparable to control. Such neuroprotective effects of ET124 were further evidenced by mitigating caspase-12, a protein known to respond to both amyloid toxicity and H_2O_2 oxidative stress in the AD context (Nakagawa et al., 2000; Quiroz-Baez et al., 2011). Hence, such mitigation of caspase-12 in neurons from the AD triculture model treated with ET124 is elucidative of the neuroprotective potential of miR-124 in mitigating ER stress and related apoptotic pathways previously mentioned.

The activation of NF-κB, described as implicated in Aβ deposition, neuroinflammation, and neurodegeneration (Sun et al., 2022), was inhibited by ET124 in astrocytes, despite the pronounced translocation exhibited by neurons and microglia in the AD triculture system. Intriguingly, ET124 had limited impact on the expression of mitochondrial fusion and fission genes, as well as in the proliferation marker Ki-67. These findings underscore the mitochondria neuroprotective effects under a slight rise of mitochondrial ROS associated with preconditioned tolerance (Correia et al., 2010).

Upon acute or chronic stimulation, microglia undergo context- and temporal-dependent changes that modify their morphology and inflammatory signature, becoming activated (Clarke and Patani, 2020). Sometimes, such an activation profile can be neurotoxic by excessive neuroinflammation that impairs neurons and astrocytes (Brites, 2020). Indeed, microglia in our AD microfluidic tricultures exhibited such morphological changes, manifested by a decreased cell area and perimeter but an increased cell circularity. In addition, *TREM2* downregulation, together with the low P2RY12 immunofluorescence in microglia at the AD microfluidic chips, indicate impaired phagocytic capacity, activation, and metabolism (Akhter et al., 2021). In AD, TREM2 promotes the clearance of neuronal toxic products (Li et al., 2022), being essential for the response to Aβ plaque-induced pathology (Ulland and Colonna, 2018). Furthermore, microglia from the AD microfluidic triculture exhibited upregulation of *HLA-DRA* (MHCII coding gene), *ARG1*, and *S100B*, consistent with activation and adaptive immune cell characteristics. ET124 treatment effectively increased microglial miR-124 levels and prevented alterations in their morphology, as well as in the expression of *P2RY12*, *TREM2*, *HLA-DRA*, and *HMGB1*. Such effects minimized the AD-related molecular signature and supported the preservation of neuroreparative and functional microglia. Future studies should additionally investigate the benefits of ET124 on the accumulation of microglia and neuronal lipid droplets, as well as in the dysfunctional inflammasome–autophagy interplay, as characteristic AD features (Claes et al., 2021; Lu et al., 2022; Li et al., 2024).

Neuronal expression of miR-124 is known to mediate neurite outgrowth by regulating genes involved in cytoskeleton organization (Yu et al., 2008). Indeed, such effects were observed in the AD triculture system, with the ET124 treatment sustaining neurite outgrowth in terms of number, length, and transmigration into other compartments. Furthermore, increased neuronal *NOS1* expression in the AD triculture system recapitulated data from postmortem AD patient samples, characterized by increased oxidative stress and activated glia (Luth et al., 2002). Remarkably, ET124 not only counteracted such *NOS1* overexpression but also further extended their benefits by partially recovering the expression of presynaptic (*SYN*) and post-synaptic (*DLG4)* genes, potentially improving synaptic function that is critically impaired in AD (Heffernan et al., 1998; Sultana et al., 2010). ET124 also switched miR-146a expression from negative towards positive levels, in accordance with the direct correction found in previous studies from our group (Vaz et al., 2021).

Astrocytes, in combination with microglia, contribute to homoeostasis, immune response, BBB regulation, and synaptic dynamics. Communication between microglia and astrocytes influences and coordinates each other and their effects on neural function and disease (Garland et al., 2022). In AD, astrocytes undergo morphological, molecular, and functional changes, designated as astrogliosis, becoming harmful to both neurons and microglia (Smit et al., 2021). Our data in the AD microfluidic system robustly support an increased astrocyte reactivity, based on the altered morphological changes and augmented *GFAP*, *GJA1*, *AGER*, and *S100B* gene expression levels together with their correspondent protein immunofluorescence detection, commonly identified in AD (Monterey et al., 2021). Importantly, AD astrocytes revealed a marked downregulation of miR-124-3p, miR-146a-5p, and miR-125-5p, implicated in AD-associated reactive astrocytosis and observed in AD patients (Iyer et al., 2012; Yashoa and Nabi, 2022; Papadimitriou et al., 2023). It should be noted that astrocytic miR-124-3p/miR-125b-5p/miR-146a-5p showed to be intercorrelated. Specifically, these astrocytic miRNAs not only correlated with neuronal miR-146a-5p and miR-125b-5p but also with microglial miR-124-3p, supporting intercellular crosstalk. Remarkably, treatment with ET124 prevented morphological changes in AD astrocytes, counteracted S100B increased expression levels, and upregulated miR-124-3p/miR-146-5p/miR-125b-5p. The regulatory effects of ET124 were also observed in the downregulation of astrocytic miR-155-5p, whose increased expression in astrocytes is associated with a pro-inflammatory medium (Korotkov et al., 2020) and of miR-21-5p that was shown to be associated with multiple AD-associated pathologies

10.3389/fphar.2025.1474012

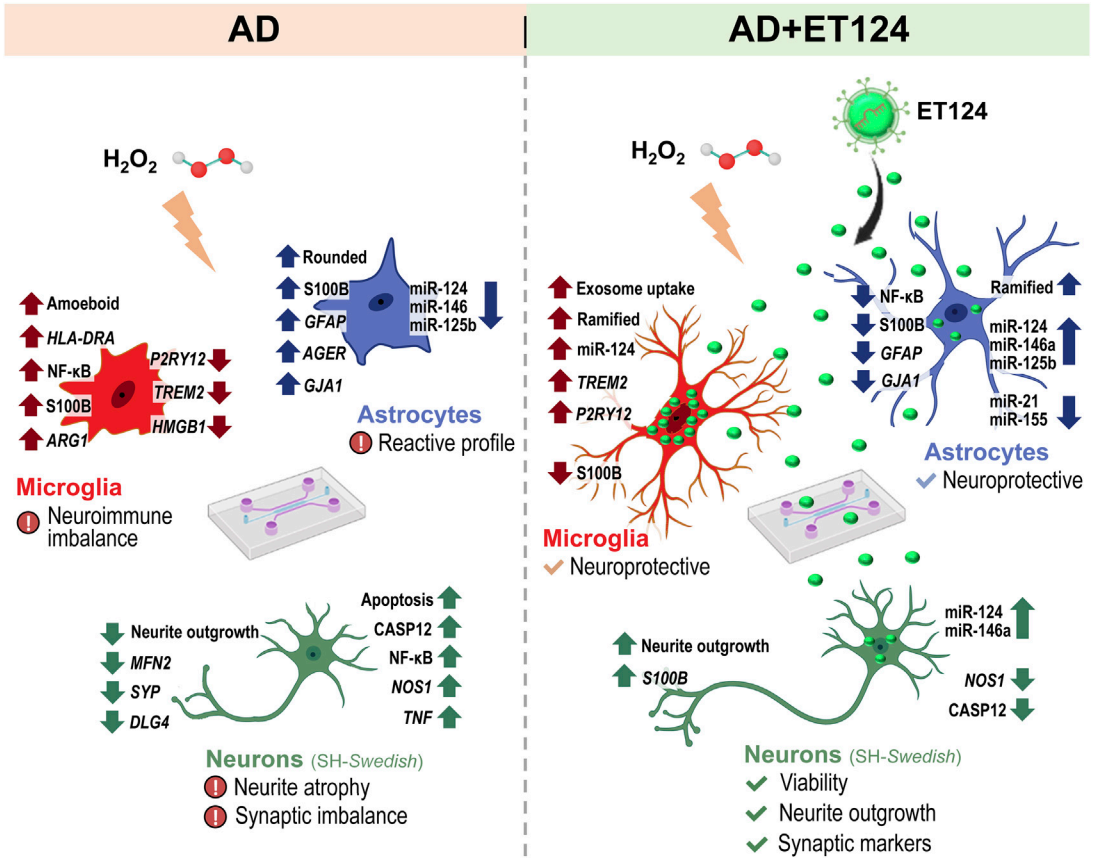


FIGURE 8
Schematic representation of the main alterations observed in the age-AD like model with microfluidic neural tricultures and the emerging role of miRNA-124-loaded exosomes (ET124) as novel therapeutics in Alzheimer's disease (AD). Data were obtained from neuron–glia human tricultures in tricompartmentalized microfluidic devices, allowing communication between neuron-like (SH-WT human neuroblastoma cells in control, or SH-SWE in AD system), astrocytes, and microglia human cell lines (IM-HT and HMC3, respectively). The three cell types were simultaneously stressed with H_2O_2 (in AD system), co-treated with H_2O_2 + ET124 (in AD + ET124 system), while control devices did not receive any treatment. The age-AD model (left panel, AD) depicts the most relevant alterations obtained in neuron-like cells, as well as in astrocytes and microglia, in the AD triculture model, which are predominantly associated with glial activation, oxidative stress, and neuroinflammation (including the presence of inflammatory-associated miRNAs). Treatment with ET124 (right panel, AD + ET124) that triggered the upregulation of miRNA-124 in all cell types; prevented alterations in neurite outgrowth, synaptic imbalance, and cell demise; as well as the appearance of inflammatory markers and miRNAs, thus sustaining neuroprotective glial phenotypes. Therefore, ET124 reveals to be a potential therapeutic tool capable of fostering neuroprotective effects through its unique capacity to modulate the neuron–glia immune response in the context of AD. AD, Alzheimer's disease; ET124, exosomes isolated from the SH-*WT* cell secretome after transfection with miR-124-3p mimic; SH-*WT*, *wild-type* human SH-SY5Y cells; neurons, SH-*SWE*, SH-SY5Y cells expressing the APP *Swedish* variant; Microglia (human CHME3 cell line); astrocytes; IM-HA, immortalized human astrocyte; NF-κB, nuclear factor kappa of activated B cells; S100B, S100 calcium-binding protein B; *HLA-DRA*, major histocompatibility complex class II (MHC-II)-coding gene; *ARG1*, arginase-1-coding gene; *P2RY12*, purinergic P2Y12 receptor-coding gene; *TREM2*, triggering receptor expressed on myeloid cells 2-coding gene; *HMGB1*, high mobility group box protein 1-coding gene; *GFAP*, glial fibrillary acidic protein-coding gene; *AGER*, advanced glycation end product receptor-coding gene; *GJA1*, gap junction protein alpha 1 gene (coding for connexin 43); *MFN2*, mitofusin2 mitochondrial gene; *SYP*, synaptophysin-coding gene; *DLG4*, postsynaptic density protein 95 (PSD95)-coding gene; CASP12, caspase-12; *NOS1*, neuronal nitric oxide synthase-coding gene; *TNF*, tumour necrosis factor alpha-coding gene (Created with BioRender.com).

(Kim et al., 2023). In summary, these data suggest ET124 immunoprotective effects on AD astrocytes.

Collectively, this study shows that the direct transfection of neuronal exosomes with miR-124 (ET124) is more efficient than the cell transfection to obtain miR-124-loaded exosomes (CT124). Likewise, it also supports the therapeutic benefits of delivering ET124 into an age-AD *in vitro* triculture model by preserving neurite outgrowth and viability, as well as neuron–glial cell morphology and overexpression of inflammatory markers, including miRNAs, as schematized in Figure 8. It was also clear that ET124 are increasingly phagocytosed by the microglia from mouse cortical primary cultures than CT124, suggesting that direct transfection with miR-124 may cause exosomal membrane modifications that facilitate recognition by microglial cells, an issue to be explored in the upcoming future.

To approach the clinic translation, we are now using intra-orbital injection of ET124 in 9-month-old 5xFAD mice, which exhibited the most harmful interrelationships between miRNAs and gene expression levels associated with neurodegeneration and neuroinflammation (Ianni et al., 2024). Preliminary results suggest a recovery in spatial learning and memory in the animals injected with ET124 when compared to treatments with PBS alone or empty exosomes (unpublished data). Hippocampal and brain cortex samples already collected will further

elucidate the regional aspect of the treatment and the eventual regeneration of the homoeostatic balance, following ET124 administration. Neuronal/glial/inflammatory markers selected from the Ianni et al., published study will be then investigated for preclinical validation of the miR-124-engineered neural exosomes. In addition to using the 5x FAD mice, we do not discard that additional models recapitulating AD pathogenesis may be required to enhance the robustness and reliability of this study conclusions. Moreover, numerous challenges should be addressed before bringing therapeutic miRNAs into clinical practice due to potential immunogenic reactions and off-target effects. Indeed, none of the miRNA-based therapeutics reached phase III clinical trials or was approved by the US Food and Drug Administration (FDA) so far (Seyhan, 2024). Finally, our innovative microfluidics-based triculture platform holds promise to assist as a detection tool in patient-centric stratification care, as recently proposed (Hauser et al., 2023), namely, in AD patients presenting innate immune activation or RNA dysregulation, recently categorized as pathophysiological subtypes 2 and 3, respectively (Tijms et al., 2020). Patients with defective miR-124 expression in neural cells (generated by transdifferentiation or iPSCs-derived), in monocultures, or in tricultures can then be treated with ET124. Ideally, in the future, ET124 can be even prepared from the patient cells to avoid treatment with immunosuppressors, although their applicability in clinical settings still requires further research. Microfluidic tricultures may additionally serve in the development of more precise immunotherapeutic agents, including exosome-based therapies, aligning with advancements in the precision medicine field and learning-assisted algorithmic analysis (Hua et al., 2024).

5 Conclusion

As far as we know, this research pioneers the impact of miR-124-engineered exosomes (ET124) in regulating the interactions between neurons, microglia, and astrocytes in an age-AD model supported by a microfluidic triculture system. The study offers novel proof, concerning the role of miR-124-loaded exosomes as an innovative tool in neurodegenerative diseases and highlights their therapeutic potential for AD by attenuating/suppressing neurodegeneration and neuroinflammation, as well as by potentially preventing disease dissemination through paracrine signalling regulation. In future studies, we will address the underlying mechanisms of ET124 treatment (and potentially other exosome-based formulations) in the 5xFAD mouse model and AD patient iPSC-derived brain cells. Lastly, the present study provides a prognostic assessment tool that can be used for patient-personalized medicine and as a foundation for future exosome-based therapeutical strategies and their clinical applications for counteracting AD progression.

Data availability statement

The original contributions presented in the study are included in the article/Supplementary Material; further inquiries can be directed to the corresponding author.

Ethics statement

Ethical approval was not required for the studies on humans in accordance with the local legislation and institutional requirements because only commercially available established cell lines were used. All the procedures carried out, complied with Portuguese Laws on Animal Care (Decreto-Lei 129/92, Portaria 1005/92, Portaria 466/95, Decreto-Lei 197/96, Portaria 1131/97), in agreement with the European Community guidelines (Directives 86/609/EU and 2010/63/EU, Recommendation 2007/526/CE). The protocol was approved by the Institutional animal welfare body, ORBEA-iMM-FFUL, and the National competent autority, DGAV (Direção Geral de Alimentação Veterinária). Every attempt was made to reduce the number of animals utilized and their suffering in accordance with the 3R principle. The study was conducted in accordance with the local legislation and institutional requirements.

Author contributions

AÉ: investigation, methodology, validation, visualization, writing–original draft, and software. GoG: formal analysis, investigation, methodology, visualization, writing–original draft, software, supervision, and validation. AR: investigation and writing–original draft. ED: methodology and writing–review and editing. AM: writing–review and editing and investigation. AV: methodology, writing–review and editing, and investigation. FG: writing–review and editing and methodology. GiG: writing–review and editing, supervision, and funding acquisition. AP: supervision, writing–review and editing, methodology, resources, and funding acquisition. DB: conceptualization, investigation, methodology, resources, supervision, validation, writing–review and editing, data curation, formal analysis, funding acquisition, project administration, and visualization.

Funding

The author(s) declare that financial support was received for the research, authorship, and/or publication of this article. This study was supported by grants from Fundação para a Ciência e Tecnologia (FCT) (PTDC/MED-NEU/2382/2021), La Caixa Foundation (HR21-00931), and Fundación Luzón (HR-00931) to DB, as well as by "Tecnopolo per la medicina di precisione" (TecnoMed Puglia)—Regione Puglia: DGR n.2117 del 21/11/2018, CUP: B84I18000540002 to GiG. Instituto de Investigação do Medicamento (iMed.ULisboa) acknowledges the support by FCT (UID 04138). AM and GoG acknowledge grants 2022.11128.BD and 5/2022/PTDC/MED-NEU/2382/2021, respectively, by FCT.

Acknowledgments

The authors thank Ema Podobnik (Erasmus student) for help with the preparation of some experiments, Rita Barbosa (Master Student) for help with mouse microglia cell isolation and culture, and Catarina Barros (PhD student) for help with the AIVIA software

analysis. Finally, they also thank Miriam Corraliza-Gomez (Margarita Salas granted junior postdoc) and Marta Ianni (Erasmus master training student) for help with a specific primer design.

Conflict of interest

The authors declare that the research was conducted in the absence of any commercial or financial relationships that could be construed as a potential conflict of interest.

The author(s) declared that they were an editorial board member of Frontiers, at the time of submission. This had no impact on the peer review process and the final decision.

Publisher's note

All claims expressed in this article are solely those of the authors and do not necessarily represent those of their affiliated organizations, or those of the publisher, the editors and the reviewers. Any product that may be evaluated in this article, or claim that may be made by its manufacturer, is not guaranteed or endorsed by the publisher.

Supplementary material

The Supplementary Material for this article can be found online at: https://www.frontiersin.org/articles/10.3389/fphar.2025.1474012/full#supplementary-material

References

Akhter, R., Shao, Y., Formica, S., Khrestian, M., and Bekris, L. M. (2021). TREM2 alters the phagocytic, apoptotic and inflammatory response to $A\beta_{42}$ in HMC3 cells. *Mol. Immunol.* 131, 171–179. doi:10.1016/j.molimm.2020.12.035

Albensi, B. C. (2019). What is nuclear factor kappa B (NF-kappaB) doing in and to the mitochondrion? *Front. Cell Dev. Biol.* 7, 154. doi:10.3389/fcell.2019.00154

Al-Nasser, M. N., Mellor, I. R., and Carter, W. G. (2022). Is L-glutamate toxic to neurons and thereby contributes to neuronal loss and neurodegeneration? A systematic review. *Brain Sci.* 12 (5), 577. doi:10.3390/brainsci12050577

Amartumur, S., Nguyen, H., Huynh, T., Kim, T. S., Woo, R. S., Oh, E., et al. (2024). Neuropathogenesis-on-chips for neurodegenerative diseases. *Nat. Commun.* 15 (1), 2219. doi:10.1038/s41467-024-46554-8

An, F., Gong, G., Wang, Y., Bian, M., Yu, L., and Wei, C. (2017). MiR-124 acts as a target for Alzheimer's disease by regulating BACE1. *Oncotarget* 8 (69), 114065–114071. doi:10.18632/oncotarget.23119

Bahrini, I., Song, J. H., Diez, D., and Hanayama, R. (2015). Neuronal exosomes facilitate synaptic pruning by up-regulating complement factors in microglia. *Sci. Rep.* 5, 7989. doi:10.1038/srep07989

Batiuk, M. Y., Martirosyan, A., Wahis, J., de Vin, F., Marneffe, C., Kusserow, C., et al. (2020). Identification of region-specific astrocyte subtypes at single cell resolution. *Nat. Commun.* 11 (1), 1220. doi:10.1038/s41467-019-14198-8

Belyaev, N. D., Kellett, K. A., Beckett, C., Makova, N. Z., Revett, T. J., Nalivaeva, N. N., et al. (2010). The transcriptionally active amyloid precursor protein (APP) intracellular domain is preferentially produced from the 695 isoform of APP in a {beta}-secretase-dependent pathway. *J. Biol. Chem.* 285 (53), 41443–41454. doi:10.1074/jbc.M110.141390

Brites, D. (2020). Regulatory function of microRNAs in microglia. *Glia* 68 (8), 1631–1642. doi:10.1002/glia.23846

Brites, D., and Fernandes, A. (2015). Neuroinflammation and depression: microglia activation, extracellular microvesicles and microRNA dysregulation. *Front. Cell Neurosci.* 9, 476. doi:10.3389/fncel.2015.00476

Bruce, A., Evans, R., Mezan, R., Shi, L., Moses, B. S., Martin, K. H., et al. (2015). Three-dimensional microfluidic tri-culture model of the bone marrow microenvironment for study of acute lymphoblastic leukemia. *PLoS One* 10 (10), e0140506. doi:10.1371/journal.pone.0140506

Cai, Z., Wan, C. Q., and Liu, Z. (2017). Astrocyte and Alzheimer's disease. *J. Neurol.* 264 (10), 2068–2074. doi:10.1007/s00415-017-8593-x

Caldeira, C., Oliveira, A. F., Cunha, C., Vaz, A. R., Falcao, A. S., Fernandes, A., et al. (2014). Microglia change from a reactive to an age-like phenotype with the time in culture. *Front. Cell Neurosci.* 8, 152. doi:10.3389/fncel.2014.00152

Cano, A., Munoz-Morales, A., Sanchez-Lopez, E., Ettcheto, M., Souto, E. B., Camins, A., et al. (2023). Exosomes-based nanomedicine for neurodegenerative diseases: current insights and future challenges. *Pharmaceutics* 15 (1), 298. doi:10.3390/pharmaceutics15010298

Chadwick, W., Zhou, Y., Park, S. S., Wang, L., Mitchell, N., Stone, M. D., et al. (2010). Minimal peroxide exposure of neuronal cells induces multifaceted adaptive responses. *PLoS One* 5 (12), e14352. doi:10.1371/journal.pone.0014352

Chen, Y., Sun, J. X., Chen, W. K., Wu, G. C., Wang, Y. Q., Zhu, K. Y., et al. (2019). miR-124/VAMP3 is a novel therapeutic target for mitigation of surgical trauma-induced microglial activation. *Signal Transduct. Target Ther.* 4, 27. doi:10.1038/s41392-019-0061-x

Chow, S. E., Chien, H. T., Chu, W. K., Lin, V., Shen, T. H., and Huang, S. F. (2021). Human caspase 12 enhances NF-κB activity through activation of IKK in nasopharyngeal carcinoma cells. *Int. J. Mol. Sci.* 22 (9), 4610. doi:10.3390/ijms22094610

Claes, C., Danhash, E. P., Hasselmann, J., Chadarevian, J. P., Shabestari, S. K., England, W. E., et al. (2021). Plaque-associated human microglia accumulate lipid droplets in a chimeric model of Alzheimer's disease. *Mol. Neurodegener.* 16 (1), 50. doi:10.1186/s13024-021-00473-0

Clarke, B. E., and Patani, R. (2020). The microglial component of amyotrophic lateral sclerosis. *Brain* 143 (12), 3526–3539. doi:10.1093/brain/awaa309

Colpman, P., Dasgupta, A., and Archer, S. L. (2023). The role of mitochondrial dynamics and mitotic fission in regulating the cell cycle in cancer and pulmonary arterial hypertension: implications for dynamin-related protein 1 and Mitofusin2 in hyperproliferative diseases. *Cells* 12 (14), 1897. doi:10.3390/cells12141897

Correia, S. C., Carvalho, C., Cardoso, S., Santos, R. X., Santos, M. S., Oliveira, C. R., et al. (2010). Mitochondrial preconditioning: a potential neuroprotective strategy. *Front. Aging Neurosci.* 2, 138. doi:10.3389/fnagi.2010.00138

Cristóvão, J. S., Morris, V. K., Cardoso, I., Leal, S. S., Martinez, J., Botelho, H. M., et al. (2018). The neuronal S100B protein is a calcium-tuned suppressor of amyloid-β aggregation. *Sci. Adv.* 4 (6), eaaq1702. doi:10.1126/sciadv.aaq1702

Cunha, C., Gomes, C., Vaz, A. R., and Brites, D. (2016). Exploring new inflammatory biomarkers and pathways during LPS-induced M1 polarization. *Mediat. Inflamm.* 2016, 6986175. doi:10.1155/2016/6986175

de Abreu, R. C., Ramos, C. V., Becher, C., Lino, M., Jesus, C., da Costa Martins, P. A., et al. (2021). Exogenous loading of miRNAs into small extracellular vesicles. *J. Extracell. Vesicles* 10 (10), e12111. doi:10.1002/jev2.12111

Dello Russo, C., Cappoli, N., Coletta, I., Mezzogori, D., Paciello, F., Pozzoli, G., et al. (2018). The human microglial HMC3 cell line: where do we stand? A systematic literature review. *J. Neuroinflammation* 15 (1), 259. doi:10.1186/s12974-018-1288-0

De Vitis, E., La Pesa, V., Gervaso, F., Romano, A., Quattrini, A., Gigli, G., et al. (2021). A microfabricated multi-compartment device for neuron and Schwann cell differentiation. *Sci. Rep.* 11 (1), 7019. doi:10.1038/s41598-021-86300-4

De Vitis, E., Stanzione, A., Romano, A., Quattrini, A., Gigli, G., Moroni, L., et al. (2024). The evolution of technology-driven *in vitro* models for neurodegenerative diseases. *Adv. Sci. (Weinh)* 11 (16), e2304989. doi:10.1002/advs.202304989

Dong, F., Zhu, M., Zheng, F., and Fu, C. (2022). Mitochondrial fusion and fission are required for proper mitochondrial function and cell proliferation in fission yeast. *FEBS J.* 289 (1), 262–278. doi:10.1111/febs.16138

Dong, X., Lei, Y., Yu, Z., Wang, T., Liu, Y., Han, G., et al. (2021). Exosome-mediated delivery of an anti-angiogenic peptide inhibits pathological retinal angiogenesis. *Theranostics* 11 (11), 5107–5126. doi:10.7150/thno.54755

Drummond, E., and Wisniewski, T. (2017). Alzheimer's disease: experimental models and reality. *Acta Neuropathol.* 133 (2), 155–175. doi:10.1007/s00401-016-1662-x

Esteves, M., Abreu, R., Fernandes, H., Serra-Almeida, C., Martins, P. A. T., Barao, M., et al. (2022). MicroRNA-124-3p-enriched small extracellular vesicles as a therapeutic approach for Parkinson's disease. *Mol. Ther.* 30 (10), 3176–3192. doi:10.1016/j.ymthe.2022.06.003

Fang, M., Wang, J., Zhang, X., Geng, Y., Hu, Z., Rudd, J. A., et al. (2012). The miR-124 regulates the expression of BACE1/β-secretase correlated with cell death in Alzheimer's disease. *Toxicol. Lett.* 209 (1), 94–105. doi:10.1016/j.toxlet.2011.11.032

Fazzina, M., Bergonzoni, M., Massenzio, F., Monti, B., Frabetti, F., and Casadei, R. (2024). Selection of suitable reference genes for gene expression studies in HMC3 cell line by quantitative real-time RT-PCR. *Sci. Rep.* 14 (1), 2431. doi:10.1038/s41598-024-52415-7

Feles, S., Overath, C., Reichardt, S., Diegeler, S., Schmitz, C., Kronenberg, J., et al. (2022). Streamlining culture conditions for the neuroblastoma cell line SH-SY5Y: a prerequisite for functional studies. *Methods Protoc.* 5 (4), 58. doi:10.3390/mps5040058

Fernandes, A., Caldeira, C., Cunha, C., Ferreiro, E., Vaz, A. R., and Brites, D. (2022). Differences in immune-related genes underlie temporal and regional pathological progression in 3xTg-AD mice. *Cells* 11 (1), 137. doi:10.3390/cells11010137

Fernandes, A., Ribeiro, A. R., Monteiro, M., Garcia, G., Vaz, A. R., and Brites, D. (2018). Secretome from SH-SY5Y APP(Swe) cells trigger time-dependent CHME3 microglia activation phenotypes, ultimately leading to miR-21 exosome shuttling. *Biochimie* 155, 67–82. doi:10.1016/j.biochi.2018.05.015

Franco-Bocanegra, D. K., Gourari, Y., McAuley, C., Chatelet, D. S., Johnston, D. A., Nicoll, J. A. R., et al. (2021). Microglial morphology in Alzheimer's disease and after Aβ immunotherapy. *Sci. Rep.* 11 (1), 15955. doi:10.1038/s41598-021-95535-0

Garcia, G., Fernandes, A., Stein, F., and Brites, D. (2022). Protective signature of ifnγ-stimulated microglia relies on miR-124-3p regulation from the secretome released by mutant APP Swedish neuronal cells. *Front. Pharmacol.* 13, 833066. doi:10.3389/fphar.2022.833066

Garcia, G., Pinto, S., Cunha, M., Fernandes, A., Koistinaho, J., and Brites, D. (2021). Neuronal dynamics and miRNA signaling differ between SH-SY5Y APPSwe and PSEN1 mutant iPSC-derived AD models upon modulation with miR-124 mimic and inhibitor. *Cells* 10 (9), 2424. doi:10.3390/cells10092424

Garland, E. F., Hartnell, I. J., and Boche, D. (2022). Microglia and astrocyte function and communication: what do we know in humans? *Front. Neurosci.* 16, 824888. doi:10.3389/fnins.2022.824888

Ge, X., Guo, M., Hu, T., Li, W., Huang, S., Yin, Z., et al. (2020). Increased microglial exosomal miR-124-3p alleviates neurodegeneration and improves cognitive outcome after rmTBI. *Mol. Ther.* 28 (2), 503–522. doi:10.1016/j.ymthe.2019.11.017

Geng, J., Feng, J., Ke, F., Fang, F., Jing, X., Tang, J., et al. (2024). MicroRNA-124 negatively regulates STAT3 to alleviate hypoxic-ischemic brain damage by inhibiting oxidative stress. *Aging (Albany NY)* 16 (3), 2828–2847. doi:10.18632/aging.205513

Gomez Morillas, A., Besson, V. C., and Lerouet, D. (2021). Microglia and neuroinflammation: what place for P2RY12? *Int. J. Mol. Sci.* 22 (4), 1636. doi:10.3390/ijms22041636

Grabert, K., Michoel, T., Karavolos, M. H., Clohisey, S., Baillie, J. K., Stevens, M. P., et al. (2016). Microglial brain region-dependent diversity and selective regional sensitivities to aging. *Nat. Neurosci.* 19 (3), 504–516. doi:10.1038/nn.4222

Gunawardena, D., Raju, R., and Munch, G. (2019). Hydrogen peroxide mediates pro-inflammatory cell-to-cell signaling: a new therapeutic target for inflammation? *Neural Regen. Res.* 14 (8), 1430–1437. doi:10.4103/1673-5374.253529

Guttikonda, S. R., Sikkema, L., Tchieu, J., Saurat, N., Walsh, R. M., Harschnitz, O., et al. (2021). Fully defined human pluripotent stem cell-derived microglia and tri-culture system model C3 production in Alzheimer's disease. *Nat. Neurosci.* 24 (3), 343–354. doi:10.1038/s41593-020-00796-z

Hajal, C., Offeddu, G. S., Shin, Y., Zhang, S., Morozova, O., Hickman, D., et al. (2022). Engineered human blood-brain barrier microfluidic model for vascular permeability analyses. *Nat. Protoc.* 17 (1), 95–128. doi:10.1038/s41596-021-00635-w

Han, D., Dong, X., Zheng, D., and Nao, J. (2019). MiR-124 and the underlying therapeutic promise of neurodegenerative disorders. *Front. Pharmacol.* 10, 1555. doi:10.3389/fphar.2019.01555

Hauser, J., Dale, M., Beck, O., Schwenk, J. M., Stemme, G., Fredolini, C., et al. (2023). Microfluidic device for patient-centric multiplexed assays with readout in centralized laboratories. *Anal. Chem.* 95 (2), 1350–1358. doi:10.1021/acs.analchem.2c04318

Hedegaard, A., Monzon-Sandoval, J., Newey, S. E., Whiteley, E. S., Webber, C., and Akerman, C. J. (2020). Pro-maturational effects of human iPSC-derived cortical astrocytes upon iPSC-derived cortical neurons. *Stem Cell Rep.* 15 (1), 38–51. doi:10.1016/j.stemcr.2020.05.003

Heffernan, J. M., Eastwood, S. L., Nagy, Z., Sanders, M. W., McDonald, B., and Harrison, P. J. (1998). Temporal cortex synaptophysin mRNA is reduced in Alzheimer's disease and is negatively correlated with the severity of dementia. *Exp. Neurol.* 150 (2), 235–239. doi:10.1006/exnr.1997.6772

Hou, T. Y., Zhou, Y., Zhu, L. S., Wang, X., Pang, P., Wang, D. Q., et al. (2020). Correcting abnormalities in miR-124/PTPN1 signaling rescues tau pathology in Alzheimer's disease. *J. Neurochem.* 154 (4), 441–457. doi:10.1111/jnc.14961

Hua, H., Zhou, Y., Li, W., Zhang, J., Deng, Y., and Khoo, B. L. (2024). Microfluidics-based patient-derived disease detection tool for deep learning-assisted precision medicine. *Biomicrofluidics* 18 (1), 014101. doi:10.1063/5.0172146

Huber, C. C., Callegari, E. A., Paez, M. D., Romanova, S., and Wang, H. (2022). Heat shock-induced extracellular vesicles derived from neural stem cells confer marked neuroprotection against oxidative stress and amyloid-β-caused neurotoxicity. *Mol. Neurobiol.* 59 (12), 7404–7412. doi:10.1007/s12035-022-03055-3

Ianni, M., Corraliza-Gomez, M., Costa-Coelho, T., Ferreira-Manso, M., Inteiro-Oliveira, S., Alemãn-Serrano, N., et al. (2024). Spatiotemporal dysregulation of neuron–glia related genes and pro-/anti-inflammatory miRNAs in the 5xFAD mouse model of Alzheimer's disease. *Int. J. Mol. Sci.* 25 (7), 9475. doi:10.3390/ijms25179475

Ismail, N., Ismail, M., Azmi, N. H., Abu Bakar, M. F., Basri, H., and Abdullah, M. A. (2016). Modulation of hydrogen peroxide-induced oxidative stress in human neuronal cells by thymoquinone-rich fraction and thymoquinone via transcriptomic regulation of antioxidant and apoptotic signaling genes. *Oxid. Med. Cell Longev.* 2016, 2528935. doi:10.1155/2016/2528935

Iwata-Ichikawa, E., Kondo, Y., Miyazaki, I., Asanuma, M., and Ogawa, N. (1999). Glial cells protect neurons against oxidative stress via transcriptional up-regulation of the glutathione synthesis. *J. Neurochem.* 72 (6), 2334–2344. doi:10.1046/j.1471-4159.1999.0722334.x

Iyer, A., Zurolo, E., Prabowo, A., Fluiter, K., Spliet, W. G., van Rijen, P. C., et al. (2012). MicroRNA-146a: a key regulator of astrocyte-mediated inflammatory response. *PLoS One* 7 (9), e44789. doi:10.1371/journal.pone.0044789

Janabi, N., Peudenier, S., Heron, B., Ng, K. H., and Tardieu, M. (1995). Establishment of human microglial cell lines after transfection of primary cultures of embryonic microglial cells with the SV40 large T antigen. *Neurosci. Lett.* 195 (2), 105–108. doi:10.1016/0304-3940(94)11792-h

Jia, L., Zhu, M., Kong, C., Pang, Y., Zhang, H., Qiu, Q., et al. (2021). Blood neuro-exosomal synaptic proteins predict Alzheimer's disease at the asymptomatic stage. *Alzheimers Dement.* 17 (1), 49–60. doi:10.1002/alz.12166

Joh, Y., and Choi, W. S. (2017). Mitochondrial complex I inhibition accelerates amyloid toxicity. *Dev. Reprod.* 21 (4), 417–424. doi:10.12717/DR.2017.21.4.417

Jothi, D., and Kulka, L. A. M. (2024). Strategies for modeling aging and age-related diseases. *NPJ Aging* 10 (1), 32. doi:10.1038/s41514-024-00161-5

Kang, Q., Xiang, Y., Li, D., Liang, J., Zhang, X., Zhou, F., et al. (2017). MiR-124-3p attenuates hyperphosphorylation of Tau protein-induced apoptosis via caveolin-1-PI3K/Akt/GSK3β pathway in N2a/APP695swe cells. *Oncotarget* 8 (15), 24314–24326. doi:10.18632/oncotarget.15149

Kenkhuis, B., Somarakis, A., Kleindouwel, L. R. T., van Roon-Mom, W. M. C., Hollt, T., and van der Weerd, L. (2022). Co-expression patterns of microglia markers Iba1, TMEM119 and P2RY12 in Alzheimer's disease. *Neurobiol. Dis.* 167, 105684. doi:10.1016/j.nbd.2022.105684

Kim, B., Tate, M., Wijeratne, H. R. S., Karahan, H., Philtjens, S., Sharify, A. D., et al. (2023). Deletion of microRNA-21 exacerbates multiple phenotypes associated with Alzheimer's disease through the RECK and ADAM10 pathway in a mouse model of Aβ amyloidosis. *Alzheimer's Dement.* 19 (Suppl. 13), e075961. doi:10.1002/alz.075961

Kim, J., Yoo, I. D., Lim, J., and Moon, J. S. (2024). Pathological phenotypes of astrocytes in Alzheimer's disease. *Exp. Mol. Med.* 56 (1), 95–99. doi:10.1038/s12276-023-01148-0

Kimiz-Gebologlu, I., and Oncel, S. S. (2022). Exosomes: large-scale production, isolation, drug loading efficiency, and biodistribution and uptake. *J. Control Release* 347, 533–543. doi:10.1016/j.jconrel.2022.05.027

Korczyn, A. D., and Grinberg, L. T. (2024). Is Alzheimer disease a disease? *Nat. Rev. Neurol.* 20 (4), 245–251. doi:10.1038/s41582-024-00940-4

Kornfeld, O. S., Qvit, N., Haileselassie, B., Shamloo, M., Bernardi, P., and Mochly-Rosen, D. (2018). Interaction of mitochondrial fission factor with dynamin related protein 1 governs physiological mitochondrial function *in vivo*. *Sci. Rep.* 8 (1), 14034. doi:10.1038/s41598-018-32228-1

Korotkov, A., Puhakka, N., Gupta, S. D., Vuokila, N., Broekaart, D. W. M., Anink, J. J., et al. (2020). Increased expression of miR142 and miR155 in glial and immune cells after traumatic brain injury may contribute to neuroinflammation via astrocyte activation. *Brain Pathol.* 30 (5), 897–912. doi:10.1111/bpa.12865

Kumar, A., Sidhu, J., Goyal, A., and Tsao, J. W. (2023). "Alzheimer disease," in StatPearls. *Treasure Island (FL) ineligible companies. Disclosure: jaskirat Sidhu declares no relevant financial relationships with ineligible companies. Disclosure: amandeep Goyal declares no relevant financial relationships with ineligible companies. Disclosure: jack Tsao declares no relevant financial relationships with ineligible companies*.

Lai, X., Wang, Y., Wang, X., Liu, B., and Rong, L. (2022). miR-146a-5p-modified hUCMSC-derived exosomes facilitate spinal cord function recovery by targeting neurotoxic astrocytes. *Stem Cell Res. Ther.* 13 (1), 487. doi:10.1186/s13287-022-03116-3

Lee, S. T., Im, W., Ban, J. J., Lee, M., Jung, K. H., Lee, S. K., et al. (2017). Exosome-based delivery of miR-124 in a huntington's disease model. *J. Mov. Disord.* 10 (1), 45–52. doi:10.14802/jmd.16054

Li, R. Y., Qin, Q., Yang, H. C., Wang, Y. Y., Mi, Y. X., Yin, Y. S., et al. (2022). TREM2 in the pathogenesis of AD: a lipid metabolism regulator and potential metabolic therapeutic target. *Mol. Neurodegener.* 17 (1), 40. doi:10.1186/s13024-022-00542-y

Li, Y., Munoz-Mayorga, D., Nie, Y., Kang, N., Tao, Y., Lagerwall, J., et al. (2024). Microglial lipid droplet accumulation in tauopathy brain is regulated by neuronal AMPK. *Cell Metab.* 36 (6), 1351–1370.e8. doi:10.1016/j.cmet.2024.03.014

Lin, E. Y., Hsu, S. X., Wu, B. H., Deng, Y. C., Wuli, W., Li, Y. S., et al. (2024). Engineered exosomes containing microRNA-29b-2 and targeting the somatostatin receptor reduce

presenilin 1 expression and decrease the β-amyloid accumulation in the brains of mice with Alzheimer's disease. *Int. J. Nanomedicine* 19, 4977–4994. doi:10.2147/IJN.S442876

Loch-Neckel, G., Matos, A. T., Vaz, A. R., and Brites, D. (2022). Challenges in the development of drug delivery systems based on small extracellular vesicles for therapy of brain diseases. *Front. Pharmacol.* 13, 839790. doi:10.3389/fphar.2022.839790

Lopez-Suarez, L., Awabdh, S. A., Coumoul, X., and Chauvet, C. (2022). The SH-SY5Y human neuroblastoma cell line, a relevant *in vitro* cell model for investigating neurotoxicology in human: focus on organic pollutants. *Neurotoxicology* 92, 131–155. doi:10.1016/j.neuro.2022.07.008

Lu, R., Zhang, L., and Yang, X. (2022). Interaction between autophagy and the NLRP3 inflammasome in Alzheimer's and Parkinson's disease. *Front. Aging Neurosci.* 14, 1018848. doi:10.3389/fnagi.2022.1018848

Lukiw, W. J. (2007). Micro-RNA speciation in fetal, adult and Alzheimer's disease hippocampus. *Neuroreport* 18 (3), 297–300. doi:10.1097/WNR.0b013e3280148e8b

Luth, H. J., Munch, G., and Arendt, T. (2002). Aberrant expression of NOS isoforms in Alzheimer's disease is structurally related to nitrotyrosine formation. *Brain Res.* 953 (1-2), 135–143. doi:10.1016/s0006-8993(02)03280-8

Ma, Y. M., and Zhao, L. (2023). Mechanism and therapeutic prospect of miRNAs in neurodegenerative diseases. *Behav. Neurol.* 2023, 8537296. doi:10.1155/2023/8537296

Maqsood, M. I., Matin, M. M., Bahrami, A. R., and Ghasroldasht, M. M. (2013). Immortality of cell lines: challenges and advantages of establishment. *Cell Biol. Int.* 37 (10), 1038–1045. doi:10.1002/cbin.10137

Mavroudis, I., Balmus, I. M., Ciobica, A., Nicoara, M. N., Luca, A. C., and Palade, D. O. (2023). The role of microglial exosomes and miR-124-3p in neuroinflammation and neuronal repair after traumatic brain injury. *Life (Basel)* 13 (9), 1924. doi:10.3390/life13091924

Michetti, F., Clementi, M. E., Di Liddo, R., Valeriani, F., Ria, F., Rende, M., et al. (2023). The S100B protein: a multifaceted pathogenic factor more than a biomarker. *Int. J. Mol. Sci.* 24 (11), 9605. doi:10.3390/ijms24119605

Milton, N. G. (2004). Role of hydrogen peroxide in the aetiology of Alzheimer's disease: implications for treatment. *Drugs Aging* 21 (2), 81–100. doi:10.2165/00002512-200421020-00002

Monterey, M. D., Wei, H., Wu, X., and Wu, J. Q. (2021). The many faces of astrocytes in Alzheimer's disease. *Front. Neurol.* 12, 619626. doi:10.3389/fneur.2021.619626

Moore, C. S., Ase, A. R., Kinsara, A., Rao, V. T., Michell-Robinson, M., Leong, S. Y., et al. (2015). P2Y12 expression and function in alternatively activated human microglia. *Neurol. Neuroimmunol. Neuroinflamm* 2 (2), e80. doi:10.1212/NXI.0000000000000080

Morita, M., Toida, A., Horiuchi, Y., Watanabe, S., Sasahara, M., Kawaguchi, K., et al. (2021). Generation of an immortalized astrocytic cell line from Abcd1-deficient H-2K(b)tsA58 mice to facilitate the study of the role of astrocytes in X-linked adrenoleukodystrophy. *Heliyon* 7 (2), e06228. doi:10.1016/j.heliyon.2021.e06228

Nakagawa, T., Zhu, H., Morishima, N., Li, E., Xu, J., Yankner, B. A., et al. (2000). Caspase-12 mediates endoplasmic-reticulum-specific apoptosis and cytotoxicity by amyloid-beta. *Nature* 403 (6765), 98–103. doi:10.1038/47513

Pan, Y., and Monje, M. (2020). Activity shapes neural circuit form and function: a historical perspective. *J. Neurosci.* 40 (5), 944–954. doi:10.1523/JNEUROSCI.0740-19.2019

Papadimitriou, E., Koutsoudaki, P. N., Thanou, I., Karagkouni, D., Karamitros, T., Chroni-Tzartou, D., et al. (2023). A miR-124-mediated post-transcriptional mechanism controlling the cell fate switch of astrocytes to induced neurons. *Stem Cell Rep.* 18 (4), 915–935. doi:10.1016/j.stemcr.2023.02.009

Parisi, C., Arisi, I., D'Ambrosi, N., Storti, A. E., Brandi, R., D'Onofrio, M., et al. (2013). Dysregulated microRNAs in amyotrophic lateral sclerosis microglia modulate genes linked to neuroinflammation. *Cell Death Dis.* 4 (12), e959. doi:10.1038/cddis.2013.491

Park, J., Wetzel, I., Marriott, I., Dreau, D., D'Avanzo, C., Kim, D. Y., et al. (2018). A 3D human triculture system modeling neurodegeneration and neuroinflammation in Alzheimer's disease. *Nat. Neurosci.* 21 (7), 941–951. doi:10.1038/s41593-018-0175-4

Peng, H., Harvey, B. T., Richards, C. I., and Nixon, K. (2021). Neuron-derived extracellular vesicles modulate microglia activation and function. *Biol. (Basel)* 10 (10), 948. doi:10.3390/biology10100948

Peng, H., Ji, W., Zhao, R., Yang, J., Lu, Z., Li, Y., et al. (2020). Exosome: a significant nano-scale drug delivery carrier. *J. Mater Chem. B* 8 (34), 7591–7608. doi:10.1039/d0tb01499k

Pinto, S., Cunha, C., Barbosa, M., Vaz, A. R., and Brites, D. (2017). Exosomes from NSC-34 cells transfected with hSOD1-g93a are enriched in miR-124 and drive alterations in microglia phenotype. *Front. Neurosci.* 11, 273. doi:10.3389/fnins.2017.00273

Pittock, R. R., Aakre, J. A., Castillo, A. M., Ramanan, V. K., Kremers, W. K., Jack, C. R., Jr., et al. (2023). Eligibility for anti-amyloid treatment in a population-based study of cognitive aging. *Neurology* 101 (19), e1837–e1849. doi:10.1212/WNL.0000000000207770

Ponomarev, E. D., Veremeyko, T., Barteneva, N., Krichevsky, A. M., and Weiner, H. L. (2011). MicroRNA-124 promotes microglia quiescence and suppresses EAE by deactivating macrophages via the C/EBP-α-PU.1 pathway. *Nat. Med.* 17 (1), 64–70. doi:10.1038/nm.2266

Ponomarev, E. D., Veremeyko, T., and Weiner, H. L. (2013). MicroRNAs are universal regulators of differentiation, activation, and polarization of microglia and macrophages in normal and diseased CNS. *Glia* 61 (1), 91–103. doi:10.1002/glia.22363

Poon, A., Zhang, Y., Chandrasekaran, A., Phanthong, P., Schmid, B., Nielsen, T. T., et al. (2017). Modeling neurodegenerative diseases with patient-derived induced pluripotent cells: possibilities and challenges. *N. Biotechnol.* 39 (Pt B), 190–198. doi:10.1016/j.nbt.2017.05.009

Prater, K. E., Green, K. J., Mamde, S., Sun, W., Cochoit, A., Smith, C. L., et al. (2023). Human microglia show unique transcriptional changes in Alzheimer's disease. *Nat. Aging* 3 (7), 894–907. doi:10.1038/s43587-023-00424-y

Qin, Q., Teng, Z., Liu, C., Li, Q., Yin, Y., and Tang, Y. (2021). TREM2, microglia, and Alzheimer's disease. *Mech. Ageing Dev.* 195, 111438. doi:10.1016/j.mad.2021.111438

Qiu, S., Feng, Y., LeSage, G., Zhang, Y., Stuart, C., He, L., et al. (2015). Chronic morphine-induced microRNA-124 promotes microglial immunosuppression by modulating P65 and TRAF6. *J. Immunol.* 194 (3), 1021–1030. doi:10.4049/jimmunol.1400106

Quiroz-Baez, R., Ferrera, P., Rosendo-Gutierrez, R., Moran, J., Bermudez-Rattoni, F., and Arias, C. (2011). Caspase-12 activation is involved in amyloid-β protein-induced synaptic toxicity. *J. Alzheimers Dis.* 26 (3), 467–476. doi:10.3233/JAD-2011-110326

Rehman, F. U., Liu, Y., Zheng, M., and Shi, B. (2023). Exosomes based strategies for brain drug delivery. *Biomaterials* 293, 121949. doi:10.1016/j.biomaterials.2022.121949

Sayyed, A. A., Gondaliya, P., Mali, M., Pawar, A., Bhat, P., Khairnar, A., et al. (2021). MiR-155 inhibitor-laden exosomes reverse resistance to cisplatin in a 3D tumor spheroid and xenograft model of oral cancer. *Mol. Pharm.* 18 (8), 3010–3025. doi:10.1021/acs.molpharmaceut.1c00213

Schindelin, J., Arganda-Carreras, I., Frise, E., Kaynig, V., Longair, M., Pietzsch, T., et al. (2012). Fiji: an open-source platform for biological-image analysis. *Nat. Methods* 9 (7), 676–682. doi:10.1038/nmeth.2019

Seyhan, A. A. (2024). Trials and tribulations of MicroRNA therapeutics. *Int. J. Mol. Sci.* 25 (3), 1469. doi:10.3390/ijms25031469

Shosha, E., Shahror, R. A., Morris, C. A., Xu, Z., Lucas, R., McGee-Lawrence, M. E., et al. (2023). The arginase 1/ornithine decarboxylase pathway suppresses HDAC3 to ameliorate the myeloid cell inflammatory response: implications for retinal ischemic injury. *Cell Death Dis.* 14 (9), 621. doi:10.1038/s41419-023-06147-7

Sierra, A., Navascues, J., Cuadros, M. A., Calvente, R., Martin-Oliva, D., Ferrer-Martin, R. M., et al. (2014). Expression of inducible nitric oxide synthase (iNOS) in microglia of the developing quail retina. *PLoS One* 9 (8), e106048. doi:10.1371/journal.pone.0106048

Smit, T., Deshayes, N. A. C., Borchelt, D. R., Kamphuis, W., Middeldorp, J., and Hol, E. M. (2021). Reactive astrocytes as treatment targets in Alzheimer's disease-Systematic review of studies using the APPswePS1dE9 mouse model. *Glia* 69 (8), 1852–1881. doi:10.1002/glia.23981

Smith, P., Al Hashimi, A., Girard, J., Delay, C., and Hebert, S. S. (2011). *In vivo* regulation of amyloid precursor protein neuronal splicing by microRNAs. *J. Neurochem.* 116 (2), 240–247. doi:10.1111/j.1471-4159.2010.07097.x

Soreq, H., and Wolf, Y. (2011). NeurimmiRs: microRNAs in the neuroimmune interface. *Trends Mol. Med.* 17 (10), 548–555. doi:10.1016/j.molmed.2011.06.009

Sultana, R., Banks, W. A., and Butterfield, D. A. (2010). Decreased levels of PSD95 and two associated proteins and increased levels of BCl2 and caspase 3 in hippocampus from subjects with amnestic mild cognitive impairment: insights into their potential roles for loss of synapses and memory, accumulation of Abeta, and neurodegeneration in a prodromal stage of Alzheimer's disease. *J. Neurosci. Res.* 88 (3), 469–477. doi:10.1002/jnr.22227

Sun, E., Motolani, A., Campos, L., and Lu, T. (2022). The pivotal role of NF-kB in the pathogenesis and therapeutics of Alzheimer's disease. *Int. J. Mol. Sci.* 23 (16), 8972. doi:10.3390/ijms23168972

Sun, P., Liu, D. Z., Jickling, G. C., Sharp, F. R., and Yin, K. J. (2018). MicroRNA-based therapeutics in central nervous system injuries. *J. Cereb. Blood Flow. Metab.* 38 (7), 1125–1148. doi:10.1177/0271678X18773871

Sun, Y., Luo, Z. M., Guo, X. M., Su, D. F., and Liu, X. (2015). An updated role of microRNA-124 in central nervous system disorders: a review. *Front. Cell Neurosci.* 9, 193. doi:10.3389/fncel.2015.00193

Tan, Y. L., Yuan, Y., and Tian, L. (2020). Microglial regional heterogeneity and its role in the brain. *Mol. Psychiatry* 25 (2), 351–367. doi:10.1038/s41380-019-0609-8

Tang, D., Chen, M., Huang, X., Zhang, G., Zeng, L., Zhang, G., et al. (2023). SRplot: a free online platform for data visualization and graphing. *PLoS One* 18 (11), e0294236. doi:10.1371/journal.pone.0294236

Tavasolian, F., Hosseini, A. Z., Soudi, S., and Naderi, M. (2020). miRNA-146a improves immunomodulatory effects of MSC-derived exosomes in rheumatoid arthritis. *Curr. Gene Ther.* 20 (4), 297–312. doi:10.2174/1566523220666200916120708

Tijms, B. M., Gobom, J., Reus, L., Jansen, I., Hong, S., Dobricic, V., et al. (2020). Pathophysiological subtypes of Alzheimer's disease based on cerebrospinal fluid proteomics. *Brain* 143 (12), 3776–3792. doi:10.1093/brain/awaa325

Tzioras, M., McGeachan, R. I., Durrant, C. S., and Spires-Jones, T. L. (2023). Synaptic degeneration in Alzheimer disease. *Nat. Rev. Neurol.* 19 (1), 19–38. doi:10.1038/s41582-022-00749-z

Ulland, T. K., and Colonna, M. (2018). TREM2 - a key player in microglial biology and Alzheimer disease. *Nat. Rev. Neurol.* 14 (11), 667–675. doi:10.1038/s41582-018-0072-1

Ustyantseva, E., Pavlova, S. V., Malakhova, A. A., Ustyantsev, K., Zakian, S. M., and Medvedev, S. P. (2022). Oxidative stress monitoring in iPSC-derived motor neurons using genetically encoded biosensors of H(2)O(2). *Sci. Rep.* 12 (1), 8928. doi:10.1038/s41598-022-12807-z

van Rensburg, S. J., Daniels, W. M., Potocnik, F. C., van Zyl, J. M., Taljaard, J. J., and Emsley, R. A. (1997). A new model for the pathophysiology of Alzheimer's disease. Aluminium toxicity is exacerbated by hydrogen peroxide and attenuated by an amyloid protein fragment and melatonin. *S Afr. Med. J.* 87 (9), 1111–1115.

Vaz, A. R., Vizinha, D., Morais, H., Colaco, A. R., Loch-Neckel, G., Barbosa, M., et al. (2021). Overexpression of miR-124 in motor neurons plays a key role in ALS pathological processes. *Int. J. Mol. Sci.* 22 (11), 6128. doi:10.3390/ijms22116128

Veremeyko, T., Kuznetsova, I. S., Dukhinova, M., A, W. Y. Y., Kopeikina, E., Barteneva, N. S., et al. (2019). Neuronal extracellular microRNAs miR-124 and miR-9 mediate cell-cell communication between neurons and microglia. *J. Neurosci. Res.* 97 (2), 162–184. doi:10.1002/jnr.24344

Voloshin, N., Tyurin-Kuzmin, P., Karagyaur, M., Akopyan, Z., and Kulebyakin, K. (2023). Practical use of immortalized cells in medicine: current advances and future perspectives. *Int. J. Mol. Sci.* 24 (16), 12716. doi:10.3390/ijms241612716

Volpato, V., and Webber, C. (2020). Addressing variability in iPSC-derived models of human disease: guidelines to promote reproducibility. *Dis. Model Mech.* 13 (1), dmm042317. doi:10.1242/dmm.042317

Wang, D., Zhang, H., Li, M., Frid, M. G., Flockton, A. R., McKeon, B. A., et al. (2014). MicroRNA-124 controls the proliferative, migratory, and inflammatory phenotype of pulmonary vascular fibroblasts. *Circ. Res.* 114 (1), 67–78. doi:10.1161/CIRCRESAHA.114.301633

Wang, M., Qin, L., and Tang, B. (2019). MicroRNAs in Alzheimer's disease. *Front. Genet.* 10, 153. doi:10.3389/fgene.2019.00153

Wang, X., Iyaswamy, A., Xu, D., Krishnamoorthi, S., Sreenivasmurthy, S. G., Yang, Y., et al. (2023). Real-time detection and visualization of amyloid-β aggregates induced by hydrogen peroxide in cell and mouse models of Alzheimer's disease. *ACS Appl. Mater Interfaces* 15 (1), 39–47. doi:10.1021/acsami.2c07859

Wang, X., Liu, D., Huang, H. Z., Wang, Z. H., Hou, T. Y., Yang, X., et al. (2018). A novel MicroRNA-124/PTPN1 signal pathway mediates synaptic and memory deficits in Alzheimer's disease. *Biol. Psychiatry* 83 (5), 395–405. doi:10.1016/j.biopsych.2017.07.023

Xicoy, H., Wieringa, B., and Martens, G. J. (2017). The SH-SY5Y cell line in Parkinson's disease research: a systematic review. *Mol. Neurodegener.* 12 (1), 10. doi:10.1186/s13024-017-0149-0

Xiong, W. P., Yao, W. Q., Wang, B., and Liu, K. (2021). BMSCs-exosomes containing GDF-15 alleviated SH-SY5Y cell injury model of Alzheimer's disease via AKT/GSK-3β/β-catenin. *Brain Res. Bull.* 177, 92–102. doi:10.1016/j.brainresbull.2021.09.008

Yamashita, T., Takahashi, Y., and Takakura, Y. (2018). Possibility of exosome-based therapeutics and challenges in production of exosomes eligible for therapeutic application. *Biol. Pharm. Bull.* 41 (6), 835–842. doi:10.1248/bpb.b18-00133

Yang, J., Zhang, X., Chen, X., Wang, L., and Yang, G. (2017). Exosome mediated delivery of miR-124 promotes neurogenesis after ischemia. *Mol. Ther. Nucleic Acids* 7, 278–287. doi:10.1016/j.omtn.2017.04.010

Yashoa, R. K., and Nabi, A. Q. (2022). The miR-146a-5p and miR-125b-5p levels as biomarkers for early prediction of Alzheimer's disease. *Hum. Gene* 34, 201129. doi:10.1016/j.humgen.2022.201129

Yiannopoulou, K. G., and Papageorgiou, S. G. (2020). Current and future treatments in alzheimer disease: an update. *J. Cent. Nerv. Syst. Dis.* 12, 1179573520907397. doi:10.1177/1179573520907397

Yu, A., Zhang, T., Duan, H., Pan, Y., Zhang, X., Yang, G., et al. (2017). MiR-124 contributes to M2 polarization of microglia and confers brain inflammatory protection via the C/EBP-α pathway in intracerebral hemorrhage. *Immunol. Lett.* 182, 1–11. doi:10.1016/j.imlet.2016.12.003

Yu, J. Y., Chung, K. H., Deo, M., Thompson, R. C., and Turner, D. L. (2008). MicroRNA miR-124 regulates neurite outgrowth during neuronal differentiation. *Exp. Cell Res.* 314 (14), 2618–2633. doi:10.1016/j.yexcr.2008.06.002

Zhang, F., Yao, Y., Miao, N., Wang, N., Xu, X., and Yang, C. (2022a). Neuroprotective effects of microRNA 124 in Parkinson's disease mice. *Arch. Gerontol. Geriatr.* 99, 104588. doi:10.1016/j.archger.2021.104588

Zhang, S., Cheng, Z., Wang, Y., and Han, T. (2021). The risks of miRNA therapeutics: in a drug target perspective. *Drug Des. Devel Ther.* 15, 721–733. doi:10.2147/DDDT.S288859

Zhang, W. H., Jiang, L., Li, M., and Liu, J. (2023a). MicroRNA-124: an emerging therapeutic target in central nervous system disorders. *Exp. Brain Res.* 241 (5), 1215–1226. doi:10.1007/s00221-022-06524-2

Zhang, Y., Chen, H., Li, R., Sterling, K., and Song, W. (2023b). Amyloid β-based therapy for Alzheimer's disease: challenges, successes and future. *Signal Transduct. Target Ther.* 8 (1), 248. doi:10.1038/s41392-023-01484-7

Zhang, Y. X., Chen, S. L., Li, Y. M., and Zheng, Y. W. (2022b). Limitations and challenges of direct cell reprogramming *in vitro* and *in vivo*. *Histol. Histopathol.* 37 (8), 723–737. doi:10.14670/HH-18-458

Zhuang, Z., Liu, M., Dai, Z., Luo, J., Zhang, B., Yu, H., et al. (2023). Bone marrow stromal cells-derived exosomes reduce neurological damage in traumatic brain injury through the miR-124-3p/p38 MAPK/GLT-1 axis. *Exp. Neurol.* 365, 114408. doi:10.1016/j.expneurol.2023.114408

frontiers | Frontiers in Oncology

TYPE Systematic Review
PUBLISHED 17 March 2025
DOI 10.3389/fonc.2025.1499163

Check for updates

OPEN ACCESS

EDITED BY
Alice Conigliaro,
University of Palermo, Italy

REVIEWED BY
Amudha Ganapathy,
University of Illinois Chicago, United States
Vivek Kumar,
University of South Florida, United States

*CORRESPONDENCE
Hong Zheng
zhenghonghq@hotmail.com
Jing Yang
844243123@qq.com

RECEIVED 25 September 2024
ACCEPTED 28 February 2025
PUBLISHED 17 March 2025

CITATION
Luo X, Li X, Chen C, Yang J and Zheng H (2025) The prognostic value of miR-34 family in ovarian cancer: a systematic review and meta-analysis.
Front. Oncol. 15:1499163.
doi: 10.3389/fonc.2025.1499163

COPYRIGHT
© 2025 Luo, Li, Chen, Yang and Zheng. This is an open-access article distributed under the terms of the Creative Commons Attribution License (CC BY). The use, distribution or reproduction in other forums is permitted, provided the original author(s) and the copyright owner(s) are credited and that the original publication in this journal is cited, in accordance with accepted academic practice. No use, distribution or reproduction is permitted which does not comply with these terms.

The prognostic value of miR-34 family in ovarian cancer: a systematic review and meta-analysis

Xiulan Luo, Xiaolu Li, Chaolin Chen, Jing Yang* and Hong Zheng*

Department of Pathology, Affiliated Hospital of Zunyi Medical University, Zunyi, Guizhou, China

Background: The aim of this study was to evaluate the association between miR-34 family expression and overall survival (OS) and progression-free survival (PFS) in women with ovarian cancer.

Methods: Literature searches were conducted using databases such as PubMed, Cochrane Library, EMBASE, Web of Science, Wanfang, and CNKI to identify studies reporting pooled hazard ratios (HRs) and 95% confidence intervals (CIs) examining the relationship between miR-34 family expression and overall survival (OS) or progression-free survival (PFS) in female patients with ovarian cancer. All potentially relevant studies were assessed and then pooled.

Results: There were a total of seven literatures included in this systematic review and meta-analysis, which included 672 women. There was a significant improvement in survival for women with ovarian cancer when miR-34s expression was higher (OS, HR = 0.70, 95% CI:0.57–0.86; PFS, HR = 0.48, 95% CI:0.31–0.75). A subgroup analysis of miR-34 family members showed that differences between groups greatly affected PFS (HR = 0.50, 95% CI: 0.40–0.63).

Conclusion: Based on the results of this review, it appears that ovarian cancer women with high expression of miR-34s may have a better chance of surviving.Systematic Review Registration: PROSPERO (CRD42024499203).

Systematic review registration: https://www.crd.york.ac.uk/PROSPERO/, identifier CRD42024499203.

KEYWORDS

meta-analysis, microRNA, miR-34s, ovarian cancer, prognosis

1 Introduction

Among female reproductive system tumors, ovarian cancer is the most common, and it is one of the most aggressive (1). Ovarian cancer is usually diagnosed at an advanced stage with a poor prognosis due to the absence of clinical symptoms in the early stages and the high failure rate of chemotherapy (2). It is estimated that in 2020, there will be around

3,13,959 new cases of ovarian cancer globally, with an incidence of 6.6 and a mortality rate of 4.4, according to the data survey (3). In spite of improvements in survival rates for women with ovarian cancer in the past few decades, the 5-year survival rate for women with stage I epithelial ovarian cancer remains below 30%. It is well known that the miR-34 family (miR-34s) is essential for the pathogenesis of epithelial ovarian cancer, and its inactivation might have significant implications for its progression (2). Therefore, in order to improve the prognosis of ovarian cancer patients, biomarkers relating to prognosis must be identified and new therapeutic targets explored.

There are approximately 22 nucleotides in the length of microRNA (miRNA; miR) that are endogenous non-coding RNA. The miRNA negatively regulates gene expression at the post-transcriptional and translational levels, and plays a significant role in cancer progression (4). miR-34s is a family of three miRNAs that is encoded by two different genes in the human body, miR-34a, miR-34b, and miR-34c. There is an individual transcript for miR-34a on chromosome 1p36.22; however, miR-34b and miR-34c share the same chromosome 11q23.1 for transcription and expression (5). Several processes in tumor development are regulated by the tumor suppressor miR-34s, which is low expressed in most tumors, including proliferation, migration, invasion, metabolism, apoptosis, and cancer stem-cell formation, cell cycle progression, epithelial mesenchymal transformation, and so on, the result is an inhibition of tumor growth and metastasis (2, 6). Direct transcriptional targets of p53 have been shown to be miR-34a and miR-34b/c (7). According to Hannah Welponer et al. (8)show that The levels of miR-34a/b/c in ovarian cancer were found to be significantly decreased compared to control tissues (p=0.002, p<0.001, p<0.001, respectively). Furthermore, the expression of each member of the miR-34 family was determined to have independent prognostic significance in relation to progression-free survival (PFS) (miR-34a: HR=0.6, p=0.033; miR-34b: HR=0.2, p=0.001; miR-34c: HR=0.3, p=0.002, respectively). It was determined that miR-34b (HR=0.4, p=0.016) and miR-34c (HR=0.6, p=0.049) have a prognostic value for overall survival (OS). Research conducted by Jia et al. (9) found no correlation between the presence of miR-34a and overall survival (HR=1.407, p=0.929) or progression-free survival (HR=0.855, p=0.727) in individuals with epithelial ovarian cancer. However, a study by Song et al. (10) found significant effects of tumor size, FIGO stage, histological type, and miR-34c expression on overall survival in ovarian cancer patients. An analysis of multivariate data found a significant association between miR-34c expression and shorter OS time (p=0.038). Consequently, it is necessary to evaluate miR-34s expression and ovarian cancer survival through meta-analysis in order to determine the diagnosis and prognosis assessment of the miR-34s.

In this study, in order to obtain more accurate information about the prognosis of ovarian cancer, miR-34s expression needs to be further studied. Reviewing relevant literature and using systematic reviews and meta-analyses to assess miR-34s prognostic value in ovarian cancer was the goal of this study.

2 Materials and methods

2.1 literature search strategy

We searched six electronic databases was conducted for studies published from 2007 until April 2023. and their creation (PubMed, Cochrane Library, EMBASE, Web of Science, Wanfang, and CNKI) for relevant literature. Based on the PICOS tool, a search strategy was formulated: (P) Population: Ovarian cancer patients; (I) Intervention: high expression of miR-34s; (C) Comparator: low expression of miR-34s; (O) Outcomes: OS or PFS; (S) Study Design: retrospective or prospective studies. An overview of the search strategy can be found in Table 1 and Supplementary Materials (The example used here is PubMed).

2.2 Inclusion criteria

The results of studies were included if they evaluated the following: (1) OS/PFS of ovarian cancer patients and miR-34s

TABLE 1 PubMed database strategy to conduct searches.

#1	(Ovarian Neoplasms [MeSH Terms]) OR (Carcinoma, Ovarian Epithelial [MeSH Terms])
#2	(Neoplasm, Ovarian[Title/Abstract])) OR (Ovarian Neoplasm[Title/Abstract])) OR (Neoplasm, Ovary[Title/Abstract])) OR (Neoplasms, Ovary [Title/Abstract])) OR (Ovary Neoplasm[Title/Abstract])) OR (Neoplasms, Ovarian[Title/Abstract])) OR (Ovary Cancer[Title/Abstract])) OR (Cancer, Ovary[Title/Abstract])) OR (Cancers, Ovary[Title/Abstract])) OR (Ovary Cancers[Title/Abstract])) OR (Ovarian Cancer[Title/Abstract])) OR (Cancer, Ovarian[Title/Abstract])) OR (Cancers, Ovarian[Title/Abstract])) OR (Ovarian Cancers[Title/Abstract])) OR (Cancer of Ovary[Title/Abstract])) OR (Cancer of the Ovary[Title/Abstract])) OR (Epithelial Carcinoma, Ovarian[Title/Abstract])) OR (Ovarian Epithelial Carcinomas [Title/Abstract])) OR (Epithelial Ovarian Cancer[Title/Abstract])) OR (Ovarian Epithelial Cancer[Title/Abstract])) OR (Cancer, Ovarian Epithelial[Title/Abstract])) OR (Epithelial Cancer, Ovarian[Title/Abstract])) OR (Ovarian Epithelial Cancers[Title/Abstract])) OR (Ovarian Cancer, Epithelial[Title/Abstract])) OR (Cancer, Epithelial Ovarian[Title/Abstract])) OR (Epithelial Ovarian Cancers[Title/Abstract])) OR (Ovarian Epithelial Carcinoma[Title/Abstract])) OR (Epithelial Ovarian Carcinoma[Title/Abstract])) OR (Carcinoma, Epithelial Ovarian[Title/Abstract])) OR (Epithelial Ovarian Carcinomas[Title/Abstract])) OR (Ovarian Carcinoma, Epithelial[Title/Abstract])) OR (Ovary Neoplasms[Title/Abstract])
#3	#1 OR #2
#4	MIRN34 microRNA, human [MeSH Terms]
#5	(hsa-mir-34 microRNA[Title/Abstract])) OR (miR-34, human[Title/Abstract])) OR (MIRN34B microRNA, human[Title/Abstract])) OR (hsa-mir-34b microRNA[Title/Abstract])) OR (microRNA-34b, human[Title/Abstract])) OR (MIRN34C microRNA, human[Title/Abstract])) OR (hsa-mir-34c microRNA[Title/Abstract])) OR (miR-34c, human[Title/Abstract])) OR (microRNA-34c, human[Title/Abstract])) OR (miR-34b-3, human[Title/Abstract])) OR (miR-34c-5p, human[Title/Abstract])) OR (Pri-miR-34b-c, human[Title/Abstract])) OR (MIRN34A microRNA, human[Title/Abstract])) OR (miR-34a, human[Title/Abstract])) OR (microRNA-34a, human[Title/Abstract])) OR (hsa-mir-34a microRNA [Title/Abstract])) OR (microRNA 34a, human[Title/Abstract])
#6	#4 OR #5
#7	#3 AND #6

expression; (2) A sufficient amount of information was provided to calculate hazard ratios (HRs) and 95% confidence intervals (CIs); and (3) Retrospective or prospective studies.

2.3 Exclusion criteria

(1) Data that is incomplete or unreported in studies; (2) Study results from non-observational studies[including reviews, cell experiments, animal experiments, correspondence, protocols, conference abstracts, or case reports.

2.4 Study selection

Utilizing the literature management software NoteExpress 3.8, we screened and excluded the literature. Research was conducted by two researchers to identify duplication, review papers, conference papers, protocols, and correspondence in the literature. It was then determined which literature should be included and which should be excluded by two researchers after reading the abstracts. Finally, literature not included in the study was read in full by both researchers and was identified for inclusion. This process involved both researchers screening the literature independently, then comparing the remaining literature. Those who remained the same were included, and those who differed were brought in to discuss and resolve the differences.

2.5 Data extraction

Data were extracted independently by two reviewers. Data were collected using nine standardized and preselected data extraction forms under the following headings for inclusion in the study: (1) author, (2) date of publication, (3) nation,(4) Study design,(5) miRNA, (6)miRNA cut-off value,(7) disease type, (8) mean age, (9) sample size, (10) assay, and (11) outcome. A 95% CI and *p* value are provided for the HRs of miR-34s expression for OS and PFS. In the absence of direct reporting of HR and 95% CI, we calculated them based on the number of reported patients and events observed in each group. The HRs were estimated from graphical survival plots if only Kaplan-Meier curves were available (11). In cases where univariate and multivariate analyses were reported simultaneously, only the multivariate analysis was analyzed. Due to the fact that multivariate analysis accounted for confounding factors, the results were more valuable. It was resolved through discussion among the first three authors that differences over data extraction could be resolved.

2.6 Individual studies may be biased

To evaluate included studies, independent researchers used the Newcastle Ottawa scale (NOS), a method for assessing the quality of observational studies and non-randomized trials. Study groups are compared based on three factors: participant selection, comparability of results, and outcome assessment. In total, nine stars were awarded, one for each item, with the exception of the item "Comparability of cohorts based on design or analysis," which was awarded two stars. Studies with quality scores less than 6 are considered low-quality studies. A study with a quality score of at least 6 is considered to be included in the meta-analysis. This meta-analysis follows the PRISMA guidelines. Under registration number CRD42024499203, it is registered with PROSPERO (International Register of Prospective Systems Evaluation).

2.7 Data analysis

A comprehensive statistical analysis was conducted using RevMan 5.4 software. OS and PFS were defined as the primary outcome indices. The hazard ratio (HR) and its corresponding 95% confidence interval (CI) were utilized as effect indices, calculated using the inverse variance (IV) method.

To assess the heterogeneity among included studies, we applied Cochran's Q test and calculated the I^2 statistic (12). If the I^2 value was less than or equal to 50% and the p-value was greater than or equal to 0.1, it indicated no significant heterogeneity among studies, and a fixed effects model was employed for the meta-analysis. Conversely, if the I^2 value exceeded 50% and the *p*-value was less than 0.1, indicating significant heterogeneity, we opted for a random effects model. In the event of high heterogeneity, we conducted subgroup analyses stratified by individual members of the miR-34 family (miR-34a, miR-34b, and miR-34c) to explore potential sources of variability. Additionally, we performed sensitivity analyses to further investigate the origin of the observed heterogeneity. To address the possibility of publication bias, we generated funnel plots for visual assessment.

3 Results

3.1 Study and identification and selection

An additional two literatures were manually searched in addition to 85 literatures retrieved from six electronic databases. Following the elimination of duplicates, to review the remaining 78 literatures, we read their titles and abstracts, and 34 papers were then excluded again. In total, 34 literatures were read in full, but 27 literatures were excluded (due to incomplete data, review, cell experiment, animal experiment, and interventions included in the review were not met). A total of 7 literatures remain for inclusion in this study. During the period 2009 to 2020, there were 7 literatures published including 672 ovarian cancer patients. Different ethnic groups were involved: 3 from China, 3 from Austria and 1 from Canada. miRs were mainly expressed in tissue samples. The detection method was qRT-PCR. In all 7 studies, 6 studies had survival indicators of OS and 5 studies had survival indicators of PFS. As shown in Figure 1, the included studies have a variety of characteristics.

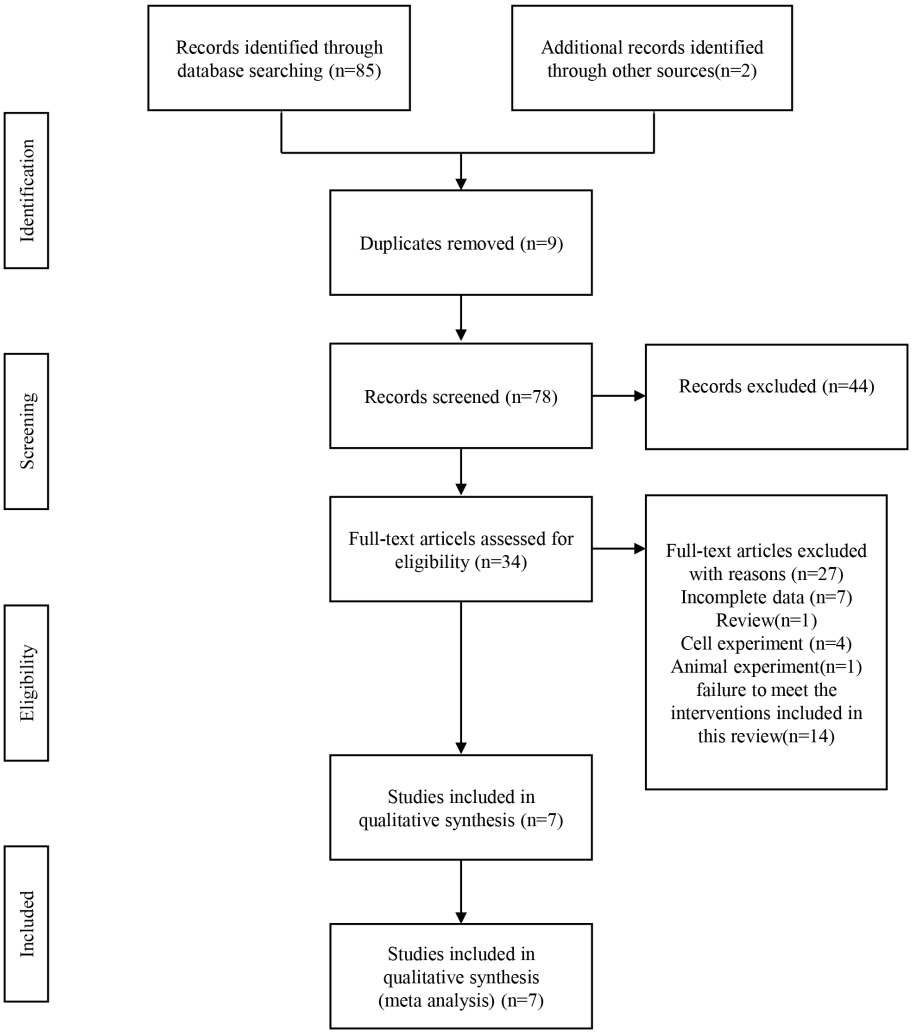


FIGURE 1
A flow chart for the systematic review process according to PRISMA.

3.2 An assessment of the quality of the included studies

7 literatures were eligible for inclusion, of which one was of low quality and eight were of medium quality, mainly because none of the papers described the non-response rate (Table 2).

3.3 Meta-analysis for miR-34s

3.1.1 OS

Since there was no heterogeneity in the included literatures (I^2 = 35%<50%, p>0.1), the analysis was conducted using a fixed-effects model. There was an association between higher miR-34s expression and improved OS (HR = 0.70,95% CI 0.57-0.86, Figure 2A) in women with ovarian cancer.

3.3.2 PFS

Due to heterogeneity among the included literatures (I^2 = 72% >50%, p <0.1), analyzing the data was done using a random effects model. According to the results, ovarian cancer patients with higher miR-34s expression had significantly better PFS (HR = 0.48,95% CI 0.31-0.75, Figure 2B).

3.4 Subgroup analysis

Since the outcome indicator PFS had significant heterogeneity, we conducted subgroup analysis to find the causes of heterogeneity. According to a stratified analysis by miR-34s member type, studies in the miR-34a and miR-34c groups showed no heterogeneity, while the heterogeneity between the three groups reached a high degree (I^2 = 67%, p<0.1, Figure 3), indicating that differences in the groups would greatly affect the results of meta-analysis.

10.3389/fonc.2025.1499163

TABLE 2 The meta-analysis included the following characteristics.

Author	Year	Nation	Study design	miRNA	miRNA cut-off value	Disease	Age(mean ± SD)	Sample size	Assay	Outcome	NOS score
Lee (13)	2009	Canada	Retro	miR-34c	Median	High grade serous carcinomas	NR	33	qRT-PCR	PFS	7
Reimer (14)	2011	Austria	Retro	miR-34a	Median	Epithelial ovarian cancer	NR	130	qRT-PCR	OS, PFS	8
Liu (9)	2015	China	Retro	miR-34a	Median	Epithelial ovarian cancer	57.48 ± 11.77	44	qRT-PCR	OS, PFS	8
Schmid (15)	2016	Austria	Retro	miR-34a	Median	Epithelial ovarian cancer	62.3	133	qRT-PCR	OS, PFS	8
Dong (16)	2016	China	Retro	miR-34a	Median	Serous ovarian cancer	NR	50	qRT-PCR	OS	6
Xiao (10)	2018	China	Pro	miR-34c	Median	Ovarian cancer	NR	54	qRT-PCR	OS	8
Welponer (8)	2020	Austria	Retro	miR-34a	Median	Epithelial ovarian cancer	61	228	qRT-PCR	OS, PFS	8
Welponer (8)	2020	Austria	Retro	miR-34b	Median	Epithelial ovarian cancer	61	228	qRT-PCR	OS, PFS	8
Welponer (8)	2020	Austria	Retro	miR-34c	Median	Epithelial ovarian cancer	61	228	qRT-PCR	OS, PFS	8

Pro prospective, *Retro* retrospective, *NR* not reported, *OS* overall survival, *PFS* progress-free survival, *NOS* Newcastle Ottawa scale.

3.5 Sensitivity analysis and publication bias

An analysis of OS and PFS sensitivity was conducted by eliminating individual studies, and it was found that no study had a significant impact on the overall results, and the results were relatively stable. According to both OS and PFS publication bias tests, it was found that the funnel plot was roughly symmetric and that there were no significant publication biases (Figure 4).

4 Discussion

Researchers have examined the relationship between miR-34s expression and survival in ovarian cancer patients. A total of 87 literatures were collected through six database and other ways, and 7 literatures were finally included. Firstly, a NOS quality assessment was conducted on the seven included studies, which were generally deemed to be of high quality. A pooled analysis of nine studies with 672 women, higher expression of miR-34s significantly increased OS and PFS for patients with ovarian cancer. Based on the significant heterogeneity of the outcome indicator PFS, stratified analysis by miR-34s member types identified miR-34a and miR-34c expression levels are higher as significantly associated with increased PFS. Lastly, sensitivity analysis found that no single study had a significant impact on overall results, and that the results were relatively stable and reliable. Using a publication bias test, the funnel plot was found to be roughly symmetrical, without evidence of publication bias.

The meta-analysis of research studies revealed that miR-34s expression was associated with a significant improvement in ovarian cancer patients' OS and PFS. These findings align with the results reported by Schmid et al. (15), indicating that ovarian cancer cases with reduced miR-34a expression exhibited a decrease in PFS ($p = 0.039$) and OS ($p = 0.016$). Researchers have found that miR-34s expression levels are lower in cancerous tissues than non-tumorous tissues in ovarian cancer tissues (8). Ovarian cancer exhibiting elevated miR-34a and miR-34c levels may demonstrate reduced malignant potential, decreased invasiveness, and limited dissemination (8). Kwan et al. (17) observed there is a notable decrease in miR-34s expression in a number of malignant tumors, including breast cancer and colon cancer. They further demonstrated that this downregulation facilitated tumor suppression by modulating key molecular pathways involved in tumorigenesis. Inhibition of lung squamous cell carcinoma proliferation, migration, and invasion was associated with high miR-34s expression, according to Sun et al. (18) By targeting miR-34c, Wang et al. (19) demonstrated *in vivo* and *in vitro* that miR-34c inhibited malignant behaviors such as invasion, migration, proliferation, and epithelial-mesenchymal transformation of nasopharyngeal carcinoma. According to Elena et al. (20), it is possible that miR-34a can serve as an important indicator of recurrence in patients with non-small cell lung cancer. The diminished expression of miR-34s in osteosarcoma and hepatoblastoma has been correlated with an unfavorable prognosis (21, 22). Hence, it is believed that reduced miR-34s

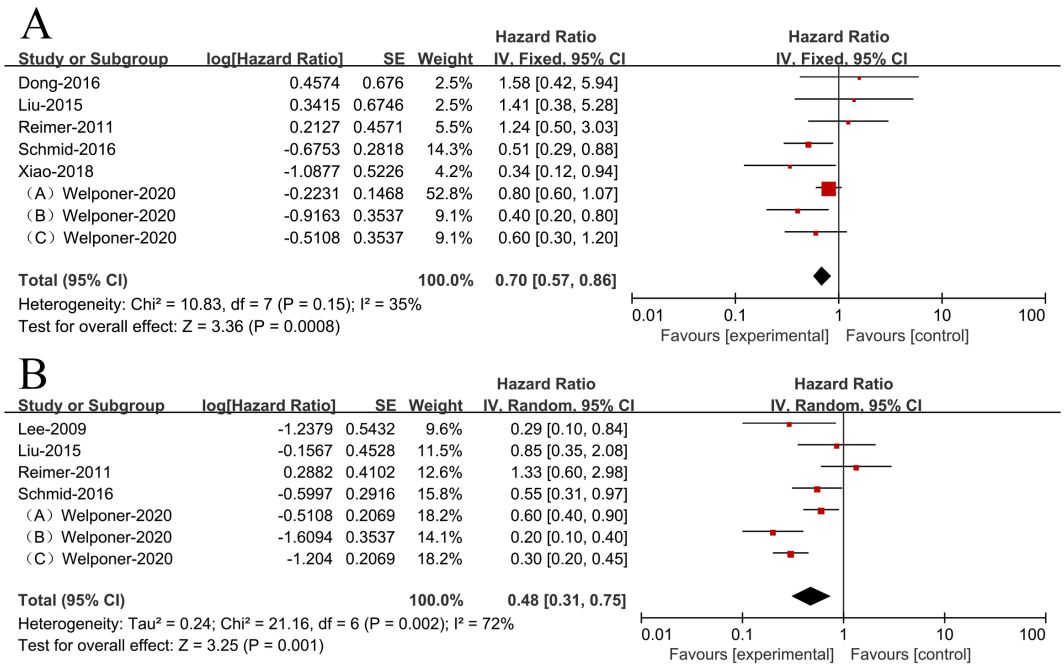


FIGURE 2
Patient survival plots for miR-34s expression in relation to overall survival **(A)** and progression-free survival **(B)**.

expression is a crucial factor in the initiation and progression of tumor growth.

We acknowledge that the heterogeneity for PFS in our study was high (I^2 = 72%), indicating significant differences among the included studies. To explore potential sources of this heterogeneity in more detail, we conducted a subgroup analysis to evaluate the impact of different RNA families on the results. Subsequently, we found that after performing the subgroup analysis, the I^2 value decreased to below 50%, suggesting that these subgroupings explain a substantial part of the heterogeneity. miR-34s represent the initial miRNA identified as being directly regulated by p53, with miR-34a demonstrating the most pronounced level of regulation by p53 (23). Furthermore, p53 and miR-34a expression is influenced by various indirect regulatory factors; for instance, miR-34a can enhance p53 activity by downregulating the expression of SIRT1, a NAD-dependent deacetylase involved in information regulation. Following the inhibition of p53 protein transcription, there is a subsequent down-regulation of p53 protein activity during the process of deacetylation (5, 24). In the context of epithelial-mesenchymal transition (EMT), miR-34 plays a crucial role by regulating the transcription factor Snail, which is pivotal in promoting EMT and invasion (16, 25). Additionally, miR-34a has

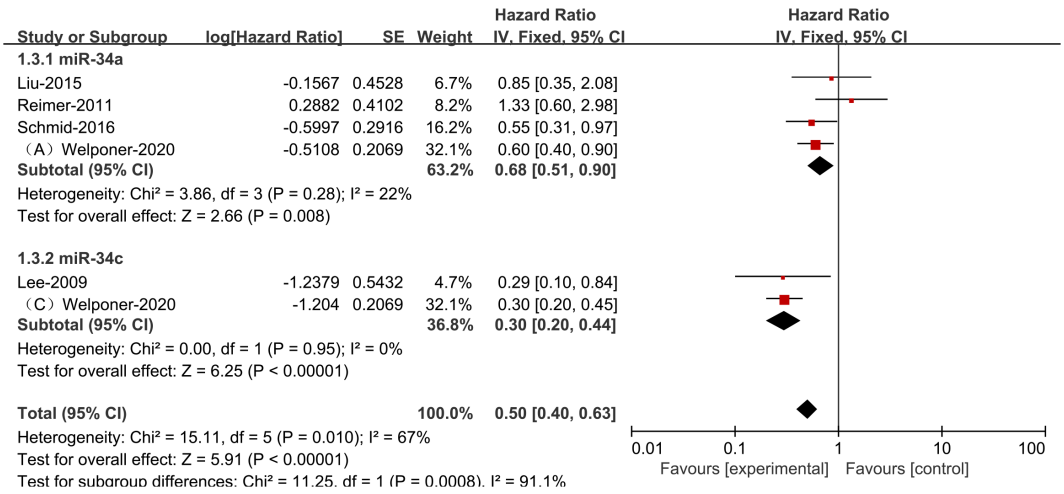


FIGURE 3
Plots showing specific miR-34s member expression and progression-free survival in ovarian cancer subgroups.

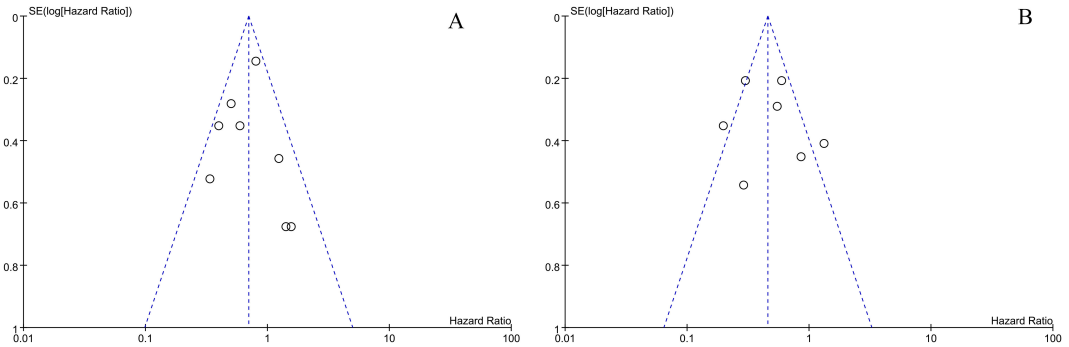


FIGURE 4
The overall survival and progression-free survival of miR-34s are depicted in a funnel plot **(A, B)**.

been shown to negatively regulate E2F3a, a key transcription factor that promotes cell proliferation and facilitates the G1/S transition. In ovarian cancer cells, knockdown of miR-34a resulted in a significant increase in E2F3 expression, highlighting its role in cell cycle regulation (14). Moreover, miR-34a's role extends to apoptosis, where its expression can influence apoptotic pathways, promoting cell death in cancer cells. This suggests that miR-34a not only acts as a tumor suppressor through cell cycle arrest and EMT regulation but also enhances apoptosis, thereby contributing to the suppression of malignant characteristics in ovarian cancer. For example, upregulation of miR-34a-5p has been shown to suppress the malignant characteristics of ovarian cancer cells by targeting TRIM44, impeding the advancement of the disease (26).Additionally, the miR-34 family members exhibit co-targeting of MET, a receptor protein tyrosine kinase, which influences the motility and invasion of epithelial ovarian cancer (27).Research has identified that MET is a target of miR-34c, enhancing the anti-tumor efficacy of cisplatin in ovarian cancer cells (28).In a study by Lu et al. (29), reverse transcriptional quantitative PCR demonstrated a significant reduction in exosome miR-34b expression in ovarian cancer cells, suggesting that exosome-derived miR-34b can diminish cell proliferation and hinder EMT in the SKOV3 ovarian cancer cell line. Based on these mechanistic studies, the findings collectively emphasize the importance of miR-34s in the cellular biology of ovarian cancer, particularly regarding their suppressive impact on proliferation, invasion, and promotion of apoptosis.

According to Kumar et al. (3), a MeDIP-NGS analysis revealed significant decreases in the relative expression levels of microRNA-34a in both tissue and serum samples of early epithelial ovarian cancer (p<0.0001). Furthermore, the functional analysis of microRNA-34a demonstrated that patients with stage III-IV and I-II epithelial ovarian cancer (EOC) had areas under curves of 92.0 (p<0.0001) and 82.7 (p<0.0001), respectively, suggesting that serum samples from these patients may be useful for monitoring cancer progression. In summary, miR-34s may serve as potential biomarkers in the diagnosis and prognosis of ovarian cancer. However, limitations such as varying sample sources, a paucity of literature, and inadequate sample sizes within studies may compromise the statistical robustness of miR-34s' prognostic value. By controlling for certain objective conditions, it is feasible to accurately forecast the prognosis of miR-34s expression in ovarian cancer.

4.1 The advantages

To our knowledge, this is the first systematic review and meta-analysis of miR-34s' prognostic value in ovarian cancer. From the methodological aspect, we conducted a two-person assessment, searched 6 databases, and further collected the literature comprehensively. We formulated inclusion and exclusion criteria according to PICOS principle, and the literature quality was relatively high.

4.2 The limitations

Due to the limited number of studies included in our analysis, consisting of three from China, three from Austria, and one from Canada, the data available for certain analyses and subgroup analyses was deemed insufficient. The findings of this study necessitate additional validation through large-scale, multicenter, multi-factorial, and high-quality clinical studies. Secondly, the potential for bias in the study may be influenced by variations in geographic regions and racial demographics. Thirdly, factors such as age, family history, and weight may also introduce bias.

5 Conclusions

Based on the results of this review, miR-34s could potentially serve as a prognostic indicator for an improved survival outcome for female ovarian cancer patients. However, due to the constraints of the present analysis, it is advisable to exercise caution when interpreting the conclusions. Additional clinical trials with rigorous

methodology, a substantial sample size, and an extended follow-up period are necessary to further elucidate the prognostic significance of miR-34s expression in ovarian cancer.

Data availability statement

The original contributions presented in the study are included in the article/Supplementary Material. Further inquiries can be directed to the corresponding authors.

Author contributions

XLu: Conceptualization, Data curation, Formal analysis, Methodology, Writing – original draft, Writing – review & editing. XLi: Conceptualization, Methodology, Writing – review & editing. CC: Data curation, Formal analysis, Writing – review & editing. JY: Writing – review & editing, Data curation, Methodology, Supervision, Funding acquisition, Resources. HZ: Conceptualization, Formal analysis, Writing – review & editing.

Funding

The author(s) declare that financial support was received for the research and/or publication of this article. This study was supported by the Guizhou Provincial Health Commission Science and Technology Fund (Project No. gzwkj2023-206).

Acknowledgments

We are grateful to all the authors for their individual contributions to the present study.

Conflict of interest

The authors declare that the research was conducted in the absence of any commercial or financial relationships that could be construed as a potential conflict of interest.

Publisher's note

All claims expressed in this article are solely those of the authors and do not necessarily represent those of their affiliated organizations, or those of the publisher, the editors and the reviewers. Any product that may be evaluated in this article, or claim that may be made by its manufacturer, is not guaranteed or endorsed by the publisher.

Supplementary material

The Supplementary Material for this article can be found online at: https://www.frontiersin.org/articles/10.3389/fonc.2025.1499163/full#supplementary-material

References

1. Shu C, Liu L, Chen X, Xue J, Fei J, Wang J, et al. ncRNA-mediated low expression of P2RY14 correlates with poor prognosis and tumor immune infiltration in ovarian carcinoma. *Ann Transl Med*. (2023) 11:10. doi: 10.21037/atm-22-6120

2. Tao F, Tian X, Lu M, Zhang Z. A novel lncrna, lnc-oc1, promotes ovarian cancer cell proliferation and migration by sponging mir-34a and mir-34c. *J Genet Genomics*. (2018) 45:137–45. doi: 10.1016/j.jgg.2018.03.001

3. Kumar V, Gupta S, Varma K, Chaurasia A, Sachan M. Diagnostic performance of microrna-34a, let-7f and microrna-31 in epithelial ovarian cancer prediction. *J Gynecol Oncol*. (2022) 33:e49. doi: 10.3802/jgo.2022.33.e49

4. Inoue J, Inazawa J. Cancer-associated mirnas and their therapeutic potential. *J Hum Genet*. (2021) 66:937–45. doi: 10.1038/s10038-021-00938-6

5. Pan W, Chai B, Li L, Lu Z, Ma Z. P53/microrna-34 axis in cancer and beyond. *Heliyon*. (2023) 9:e15155. doi: 10.1016/j.heliyon.2023.e15155

6. Rokavec M, Li H, Jiang L, Hermeking H. The P53/mir-34 axis in development and disease. *J Mol Cell Biol*. (2014) 6:214–30. doi: 10.1093/jmcb/mju003

7. He L, He X, Lim LP, de StanChina E, Xuan Z, Liang Y, et al. A microrna component of the P53 tumour suppressor network. *Nature*. (2007) 447:1130–4. doi: 10.1038/nature05939

8. Welponer H, Tsibulak I, Wieser V, Degasper C, Shivalingaiah G, Wenzel S, et al. The mir-34 family and its clinical significance in ovarian cancer. *J Cancer*. (2020) 11:1446–56. doi: 10.7150/jca.33831

9. Liu J ZY, Zhang L, Yan Y, Zheng H. Expression and clinical significance of four mirnas in epithelial ovarian cancer. *Tianjin Med J*. (2015) 43:996–1000. doi: 10.11958/i.issn.0253-9896.2015.09.0010

10. Xiao S, Li Y, Pan Q, Ye M, He S, Tian Q, et al. Mir-34c/sox9 axis regulates the chemoresistance of ovarian cancer cell to cisplatin-based chemotherapy. *J Cell Biochem*. (2019) 120:2940–53. doi: 10.1002/jcb.26865

11. Tierney JF, Stewart LA, Ghersi D, Burdett S, Sydes MR. Practical methods for incorporating summary time-to-event data into meta-analysis. *Trials*. (2007) 8:16. doi: 10.1186/1745-6215-8-16

12. Higgins JP, Thompson SG, Deeks JJ, Altman DG. Measuring inconsistency in meta-analyses. *Bmj*. (2003) 327:557–60. doi: 10.1136/bmj.327.7414.557

13. Lee CH, Subramanian S, Beck AH, Espinosa I, Senz J, Zhu SX, et al. Microrna profiling of brca1/2 mutation-carrying and non-mutation-carrying high-grade serous carcinomas of ovary. *PloS One*. (2009) 4:e7314. doi: 10.1371/journal.pone.0007314

14. Reimer D, Hubalek M, Kiefel H, Riedle S, Skvortsov S, Erdel M, et al. Regulation of transcription factor E2f3a and its clinical relevance in ovarian cancer. *Oncogene*. (2011) 30:4038–49. doi: 10.1038/onc.2011.119

15. Schmid G, Notaro S, Reimer D, Abdel-Azim S, Duggan-Peer M, Holly J, et al. Expression and promotor hypermethylation of mir-34a in the various histological subtypes of ovarian cancer. *BMC Cancer*. (2016) 16:102. doi: 10.1186/s12885-016-2135-2

16. Dong P, Xiong Y, Watari H, Hanley SJ, Konno Y, Ihira K, et al. Mir-137 and mir-34a directly target snail and inhibit emt, invasion and sphere-forming ability of ovarian cancer cells. *J Exp Clin Cancer Res*. (2016) 35:132. doi: 10.1186/s13046-016-0415-y

17. Wong KY, Yu L, Chim CS. DNA methylation of tumor suppressor mirna genes: A lesson from the mir-34 family. *Epigenomics*. (2011) 3:83–92. doi: 10.2217/epi.10.74

18. Sun D, Wu Y, Zhang S, Han Y, Shen J, Zheng W, et al. Distinct roles of miR-34 family members on suppression of lung squamous cell carcinoma. *BioMed Pharmacother*. (2021) 142:111967. doi: 10.1016/j.biopha.2021.111967

19. Wan FZ, Chen KH, Sun YC, Chen XC, Liang RB, Chen L, et al. Exosomes overexpressing mir-34c inhibit Malignant behavior and reverse the radioresistance of nasopharyngeal carcinoma. *J Transl Med*. (2020) 18:12. doi: 10.1186/s12967-019-02203-z

20. Gallardo E, Navarro A, Viñolas N, Marrades RM, Diaz T, Gel B, et al. Mir-34a as a prognostic marker of relapse in surgically resected non-small-cell lung cancer. *Carcinogenesis*. (2009) 30:1903–9. doi: 10.1093/carcin/bgp219

21. Wang Y, Jia LS, Yuan W, Wu Z, Wang HB, Xu T, et al. Low mir-34a and mir-192 are associated with unfavorable prognosis in patients suffering from osteosarcoma. *Am J Transl Res*. (2015) 7:111–9.

22. Jiao C, Zhu A, Jiao X, Ge J, Xu X. Combined low mir-34s are associated with unfavorable prognosis in children with hepatoblastoma: A chinese population-based study. *J Pediatr Surg*. (2016) 51:1355–61. doi: 10.1016/j.jpedsurg.2016.02.091

23. Hermeking H. Micrornas in the P53 network: micromanagement of tumour suppression. *Nat Rev Cancer*. (2012) 12:613–26. doi: 10.1038/nrc3318

24. Zhang DG, Zheng JN, Pei DS. P53/microrna-34-induced metabolic regulation: new opportunities in anticancer therapy. *Mol Cancer*. (2014) 13:115. doi: 10.1186/1476-4598-13-115

25. Jiang X, Ye Z, Jiang Y, Yu W, Fang Q. Lncrna oip5-as1 upregulates snail expression by sponging mir-34a to promote ovarian carcinoma cell invasion and migration. *Biol Res*. (2020) 53:49. doi: 10.1186/s40659-020-00315-1

26. Li HL, Duan YA, Zhao N. Mir-34a-5p directly targeting trim44 affects the biological behavior of ovarian cancer cells. *Eur Rev Med Pharmacol Sci*. (2021) 25:1250–60. doi: 10.26355/eurrev_202102_24829

27. Corney DC, Hwang CI, Matoso A, Vogt M, Flesken-Nikitin A, Godwin AK, et al. Frequent downregulation of mir-34 family in human ovarian cancers. *Clin Cancer Res*. (2010) 16:1119–28. doi: 10.1158/1078-0432.Ccr-09-2642

28. Yang S, Li Z, Luo R. miR-34c targets MET to improve the anti-tumor effect of cisplatin on ovarian cancer. *Onco Targets Ther*. (2020) 13:2887–97. doi: 10.2147/ott.S239425

29. Lu S, Liu W, Shi H, Zhou H. Exosomal miR-34b inhibits proliferation and the epithelial-mesenchymal transition by targeting Notch2 in ovarian cancer. *Oncol Lett*. (2020) 20:2721–8. doi: 10.3892/ol.2020.11837

frontiers | Frontiers in Immunology

TYPE Review
PUBLISHED 18 March 2025
DOI 10.3389/fimmu.2025.1525741

Check for updates

OPEN ACCESS

EDITED BY
Alice Conigliaro,
University of Palermo, Italy

REVIEWED BY
Nadeem Bhat,
University of Miami, United States
Mohd Shuaib,
Central University of Punjab, India

*CORRESPONDENCE
Weihua Yin
ywh1939@163.com

RECEIVED 10 November 2024
ACCEPTED 27 February 2025
PUBLISHED 18 March 2025

CITATION
Guo R, Shi L, Chen Y, Lin C and Yin W (2025) Exploring the roles of ncRNAs in prostate cancer via the PI3K/AKT/mTOR signaling pathway.
Front. Immunol. 16:1525741.
doi: 10.3389/fimmu.2025.1525741

COPYRIGHT
© 2025 Guo, Shi, Chen, Lin and Yin. This is an open-access article distributed under the terms of the Creative Commons Attribution License (CC BY). The use, distribution or reproduction in other forums is permitted, provided the original author(s) and the copyright owner(s) are credited and that the original publication in this journal is cited, in accordance with accepted academic practice. No use, distribution or reproduction is permitted which does not comply with these terms.

Exploring the roles of ncRNAs in prostate cancer via the PI3K/AKT/mTOR signaling pathway

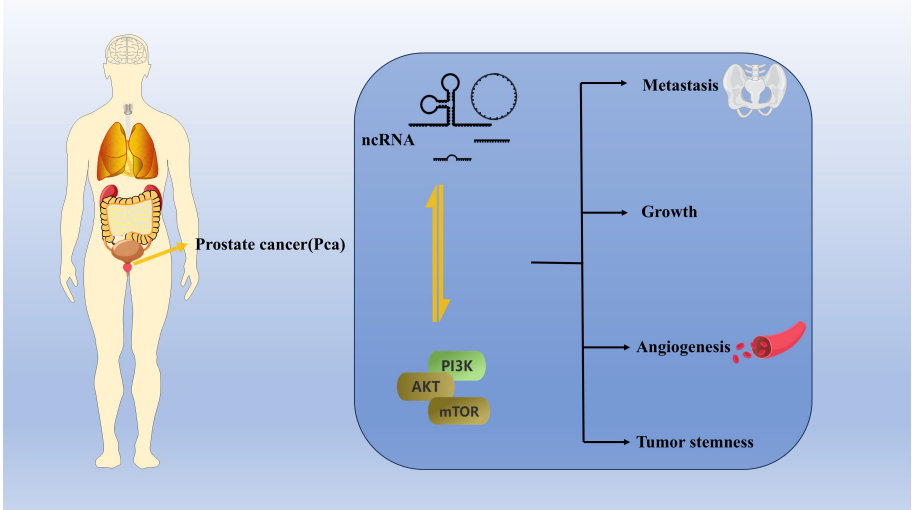
Rongwang Guo[1], Liji Shi[2], Yonghui Chen[2], Canling Lin[2] and Weihua Yin[3]*

[1]Nanchang University, 999 University Avenue, Honggutan District, Nanchang, China, [2]School of Chemical and Biological Engineering, Yichun College, Yichun, China, [3]Department of Oncology, Baoan Central Hospital of Shenzhen, Bao' an District, Shenzhen, China

Although various treatment options are available for prostate cancer (PCa), including androgen deprivation therapy (ADT) and chemotherapy, these approaches have not achieved the desired results clinically, especially in the treatment of advanced chemotherapy-resistant PCa. The PI3K/AKT/mTOR (PAM) signaling pathway is a classical pathway that is aberrantly activated in cancer cells and promotes the tumorigenesis, metastasis, resistance to castration therapy, chemoresistance, and recurrence of PCa. Noncoding RNAs (ncRNAs) are a class of RNAs that do not encode proteins. However, some ncRNAs have recently been shown to be differentially expressed in tumor tissues compared with noncancerous tissues and play important roles at the transcription and posttranscription levels. Among the types of ncRNAs, long noncoding RNAs (lncRNAs), microRNAs (miRNAs), circular RNAs (circRNAs), and Piwi-interacting RNAs (piRNAs) can participate in the PAM pathway to regulate PCa growth, metastasis, angiogenesis, and tumor stemness. Therefore, ncRNA therapy that targets the PAM signaling pathway is expected to be a novel and effective approach for treating PCa. In this paper, we summarize the types of ncRNAs that are associated with the PAM pathway in PCa cells as well as the functions and clinical roles of these ncRNAs in PCa. We hope to provide novel and effective strategies for the clinical diagnosis and treatment of PCa.

KEYWORDS

prostate cancer, ncRNA, PI3K/AKT/mTOR, metastasis, tumor growth



GRAPHICAL ABSTRACT

1 Introduction

According to Global Cancer Statistics 2022, prostate cancer (PCa) is the fourth most common malignant tumor worldwide (incidence of 7.3%), and it is the second most prevalent malignant tumor in men (prevalence of 14.2%) and the fifth leading cause of malignant tumor-related death in men (7.3% of tumor-related deaths) (1). Moreover, PCa has a heterogeneous regional distribution, and it is the most common cancer in 118 countries (e.g., around northern Europe, Australia-New Zealand, and the Caribbean) (1). Advanced PCa is the main cause of PCa-related death, and it is treated mainly with androgen deprivation therapy (ADT) and chemotherapy; however, advanced PCa is susceptible to drug resistance development after a period of treatment (2). Therefore, understanding the mechanisms underlying PCa development and progression is important for preventing and treating this condition.

The PI3K/AKT/mTOR (PAM) signaling pathway is highly conserved in eukaryotes, and it is the pathway that is most often abnormally activated in malignant tumors (3). Studies have shown that aberrant activation of the PAM pathway may be the result of gene mutation/amplification, epigenetic modification, and aberrant regulation of other signaling pathways; recently, the regulation of epigenetic modifications, which mainly include DNA methylation, histone posttranslational modification, and ncRNAs regulation, has become a popular research topic (3). The PAM signaling pathway regulates tumor cell proliferation, apoptosis, metastasis, and angiogenesis; thus, the PAM signaling pathway has become a target for the treatment of malignant tumors (4). For example, XL147 (an inhibitor of PI3K class 1 molecules) can inhibit the proliferation of breast cancer and PCa cells; inhibit the migration, invasion, and angiogenesis of melanoma cells *in vitro*; and increase the efficacy of chemotherapy in mice with breast cancer (5). Inhibition of the PAM signaling pathway enhances the immune checkpoint blockade response. Understanding the potential mechanisms underlying the aberrant activation of the PAM signaling pathway in PCa cells could provide valuable insights into overcoming PCa.

Noncoding RNAs (ncRNAs) are a class of RNAs that are not translated into proteins; these molecules are involved in gene modification, RNA transcription, protein translation, and functional travel (6). Current studies have briefly described the roles of several categories of ncRNAs, such as long noncoding RNAs (lncRNAs), microRNAs (miRNAs), circular RNAs (circRNAs), and piwi-interacting RNAs (piRNAs), in PCa. These ncRNAs show promise as diagnostic and prognostic markers of PCa (7). For example, the lncRNA *SChLAP1* is highly expressed specifically in PCa cells and is enriched mainly in high-risk patients and metastatic patients; thus, *SChLAP1* can be used to predict and diagnose the occurrence and metastasis of PCa (8). In addition, miR-145 overexpression can improve the radiosensitivity of PCa cells by impairing DNA gene repair (9), suggesting that the modulation of ncRNA expression is a promising strategy for treating PCa. In recent years, many studies have focused on the mechanism underlying ncRNA functions in PCa, and it has been shown that ncRNAs can regulate the growth, apoptosis, epithelial–mesenchymal transition (EMT), metastasis, immune microenvironment, and other behaviors of cancer cells by regulating the PAM signaling pathway (10); therefore, ncRNAs that are related to PAM signaling are likely to constitute a large class of targets for treating PCa.

In conclusion, in this review, we elucidate in detail the complex relationship between ncRNAs and the PAM signaling pathway in the development of PCa. Notably, to date, no relevant review has comprehensively reported the ncRNAs that are involved in the PAM signaling pathway in PCa cells.

2 Types of ncRNAs that are linked to the PAM signaling pathway

In prostate cancer, ncRNAs associated with the PAM signaling pathway can be divided into four categories by class: lncRNAs, miRNAs, circRNAs, and piRNAs (Table 1).

2.1 LncRNAs

LncRNAs are a class of RNAs that are more than 200 nucleotides in length and do not encode proteins; most of the lncRNAs that are involved in the PAM signaling pathway in PCa cells, such as *LINC01088* (11), *MALAT1* (26, 27), *RHPN1-AS1* (12), *DANCR* (13), *ZEB1-AS1* (15), and *LINC004600* (28), are oncogenes that can promote cancer cell viability, proliferation, metastasis, etc. In PCa cells, the lncRNAs that participate in the PAM signaling pathway as antioncogenes mainly include *MBNL1-AS1*, *HCG11*, and *GDPD4-2*, all of which are underexpressed in PCa cells compared with normal prostate cells (14, 16, 37). The lncRNAs that are the focus of this project regulate the PAM signaling pathway at multiple levels, and the direct targets that have been well studied include miRNAs, coding RNAs, and proteins. The current study indicates that most lncRNAs act as sponges for miRNAs, decreasing their expression. Nevertheless, some lncRNAs, such as the lncRNA *CHRF*, which positively regulates miR-10b expression, have also been shown to increase the transcription of miRNAs (22). Second, lncRNAs can also affect mRNAs; for example, *LINC00963* can transactivate Epidermal growth factor receptor (EGFR) (23). In addition, lncRNAs can interact with proteins that are involved in the PAM pathway; for example, the lncRNA *SNHG* interacts with EZH2 (19), the lncRNA *PCAT1* competes with PHLPP for binding to FKPB51 (31), and the lncRNA *NEAT1* binds to SRC3 at the promoter of IGF1R (25).

2.2 MiRNAs

MiRNAs can be fully or incompletely complementary to mRNAs, and their interaction with mRNA targets can lead to the failure or attenuation of mRNA translation. The target mRNAs of most of the miRNAs that regulate the PAM signaling pathway in PCa cells have been identified, and the most frequently targeted mRNA is Phosphatase and tensin homolog(PTEN) (14, 17, 49, 53–55). The miRNAs that regulate the PAM signaling pathway in PCa cells can be classified as oncogenes and antioncogenes according to their functions, and most of them are antioncogenes. Other genes, such as *miR-185-5p*, *miR-92a*, *miR-4534*, *miR-21*, *miR-22*, *miR-26a*, *miR-543*, *miR-10b*, and *miR-182*, are oncogenes, and the first six of these molecules can target PTEN (14, 16, 22, 49–51, 53–55). Five miRNAs were also found to be regulated by the PAM signaling pathway, which will be described in 2.3 later.

2.3 CircRNAs

The main function of circRNAs, which are ring-shaped ncRNAs, is to interact with ncRNAs or proteins to participate in regulating transcription and posttranscription processes, and a few circRNAs have recently been shown to serve as templates for translation (68). Current studies have shown that in PCa cells, circRNAs regulate the PAM signaling pathway mainly by acting as miRNA sponges; for example, *cir-ITCH* and *miR-17* inhibit each other to negatively regulate the PAM pathway (66). Moreover, *circMBOAT2* and *circSMARCC1* positively regulate the PAM signaling pathway via *miR-1271-5p* and *miR-1322*, respectively (64, 65). circRNAs are mainly stable in the cytoplasm in the form of covalent monocycles and are expressed in tissue- and cell-specific patterns; thus, they can be used as diagnostic markers (68). For example, *circMBOAT2* and *circSMARCC1* are highly expressed in PCa cells, and higher plasma levels of *CircSMARCC1* have been detected in PCa patients than in noncancer patients (64, 65). In addition, circRNAs are involved in the regulation of the immune microenvironment; *circSMARCC1* increases the number of M2 macrophages in PCa tissues by recruiting M2 macrophages via the CCL20–CCR6 axis and promoting M2 macrophage polarization (64). M1/M2 macrophages can be viewed as a scale in tumors, with M1 macrophages playing an antitumor role. M2 macrophages promote tumor development by regulating angiogenesis and lymphangiogenesis, immunosuppression, hypoxia induction, and cancer cell proliferation and metastasis (69). Therefore, circRNA imbalance is one of the etiological factors of PCa at the molecular level, and because of the specific expression and stable presence of circRNAs, it will be possible to identify circRNAs that can be used as high-quality diagnostic markers.

2.4 PiRNAs

piRNAs are a class of small noncoding RNAs that are 24–31 nucleotides in length. piRNAs form PIWI complexes with piwi proteins that are involved in transcriptional and posttranscriptional regulation (70). PCDH9 can competitively inhibit the formation of PI3K by binding to P85α, which is a regulatory subunit of PI3K, thereby affecting the phosphorylation of PIPs (67). In PCa cells, *piR-001773* and *piR-017184* can bind to PIWIL4 to form a PIWI/piRNA complex and silence the expression of PCDH9, thereby activating the PAM signaling pathway to promote PCa development (67). In addition, *piR-001773* and *piR-017184* were found to be correlated with the T stage and Gleason score of PCa patients, and high expression of *piR-001773* and *piR-017184* suggest a poor prognosis (67).

3 Functions of ncRNAs in the PAM signaling pathway in PCa cells

3.1 Metastasis

Metastatic PCa strongly affects the prognosis of PCa patients and is the leading cause of death in advanced PCa patients.

10.3389/fimmu.2025.1525741

TABLE 1 Type and role of ncRNAs associated with the PAM signaling pathway in PCa progression.

	ncRNA	Effect on the PAM pathway	Function	Signaling network	Ref.
LncRNA	LINC01088	Activate	Promote cell viability, migration, and invasion	miR-22/CDC6	(11)
	RHPN1-AS1	Activate	Promote cell proliferation and invasion Inhibit apoptosis and autophagy	miR-7-5p/EGFR	(12)
	DANCR	Activate	Promote cell proliferation, G1-S transformation, EMT, migration, and invasion	miR-185-5p/LASP1	(13)
	MBNL1-AS1	Inhibit	Inhibit cell proliferation, migration, and invasion	miR-181a-5p/PTEN	(14)
	ZEB1-AS1	Activate	Promote cell viability, migration, and invasion	miR-342-3p/CUL4B	(15)
	HCG11	Inhibit	Inhibit cell viability, migration, invasion, EMT, and tumor growth in nude mice Promote apoptosis	miR-543	(16)
	GAS5	—	Inhibit cell viability and proliferation Promote cell autophagy	miR-21/PDCD4, PTEN miR-1284/AKT	(17)
	SNHG3	Activate	Promote cell proliferation, migration, invasion, EMT, and tumor growth in nude mice	miR-1827	(18)
	SNHG1	Activate	Promote cell viability, proliferation, migration, invasion, and tumor growth in nude mice Inhibit apoptosis and autophagy	miR-377-3p/AKT2, EZH2	(19, 20)
	CASC11	Activate	Promote cell proliferation, migration, and invasion	miR-145/IGF1R	(21)
	CHRF	Activate	Promote cell proliferation and EMT Inhibit apoptosis	miR-10b	(22)
	LINC00963	Activate	Promote cell viability, migration, and invasion Inhibit apoptosis	EGFR	(23)
	PCAT1	Activate	Promote cell viability, proliferation, and tumor growth in nude mice Inhibit apoptosis	FKPB51–IKKα–PHLPP	(24)
	NEAT1	Activate	Promote cell viability	SRC3/IGF1R	(25)
	MALAT1	Activate	Promote cell viability, proliferation, migration, invasion, EMT, and tumor growth in nude mice Inhibit apoptosis	—	(26, 27)
	LINC00460	Activate	Promote cell proliferation, and cell cycle progression Inhibit apoptosis	—	(28)
	SNHG25	Activate	Promote cell proliferation, migration, invasion, and tumor growth in nude mice Inhibit apoptosis	—	(29)
	lncRNA-ATB	Activate	Promote cell proliferation and EMT	—	(30)
	PlncRNA-1	Activate	Promote cell proliferation, migration, invasion, and cell cycle Inhibit apoptosis	PTEN	(31)
	LINC01296	Activate	Promote cell proliferation, migration, invasion, and EMT	—	(32)
	AC245100.4	Activate	Promote cell proliferation	PAR2	(33)
	MIR4435-2HG	Activate	Promote cell proliferation, migration, invasion, and tumor growth in nude mice	ST8SIA1/FAK	(34)
	UCA1	Activate	Promote cell proliferation and cell cycle	—	(35)
	SPRY4-IT1	Activate	Promotes cell proliferation and cell cycle Increase cellular resistance to hypoxia	—	(36)
	GDPD4-2	Inhibit	Inhibit tumor growth in nude mice	—	(37)

(Continued)

TABLE 1 Continued

	ncRNA	Effect on the PAM pathway	Function	Signaling network	Ref.
miRNA	miR-139-5p	Inhibit	Inhibit cell viability and EMT	ZNF217	(38)
	miR-151	Inhibit	Inhibit cell viability, migration, and invasion Promote apoptosis	—	(39)
	miR-101-3p	Inhibit	Inhibit cell viability, migration, and invasion Promote apoptosis	CUL4B	(40)
	miR-129	Inhibit	Inhibit cell viability, proliferation, EMT, migration, invasion, and tumor growth in nude mice Promote apoptosis	ETS1	(41)
	miR-101	Inhibit	Inhibit cell viability Promote apoptosis	RLIP76	(42)
	miR-4638-5p	Inhibit	Inhibit cell proliferation, tumor angiogenesis, and tumor growth in nude mice Promote apoptosis	Kidins220	(43)
	miR-133a-3p	Inhibit	Inhibit tumor stemness Attenuate resistance to anoikis	EGFR, FGFR1, IGF1R, MET	(44)
	miR -7	Inhibit	Inhibit tumor stemness, cell proliferation, tumor growth in nude mice, and cell cycle progression	KLF4	(45)
	miR-218	Inhibit	Inhibit tumor angiogenesis, tumor growth in nude mice, cell viability, proliferation, migration, invasion, EMT, and cell cycle progression	RICTOR, GAB2, LGR4	(46–48)
	miR-4534	Activate	Promote cell proliferation, migration, invasion, cell cycle, and tumor growth in nude mice Inhibit apoptosis	PTEN	(49)
	miR-21	Activate	Inhibit apoptosis in chemoresistant cells	PTEN	(50)
	miR-182	Activate	Promote cell proliferation, tumor growth in nude mice	ST6GALNAC5	(51)
	miR -149	Inhibit	Inhibit cell proliferation, migration, invasion, EMT, and cell cycle Promote apoptosis	AKT1	(52)
	miR-125b	Inhibit	Inhibit cell migration and invasion	ErbB2/3	(53)
	miR-22	Activate	Promote cell proliferation, migration, and invasion	PTEN	(53)
	miR-19b	—	Promotes cell proliferation and cell cycle	PTEN	(54)
	miR-23b	—	Promotes cell proliferation and cell cycle	PTEN	(54)
	miR-26a	—	Promotes cell proliferation and cell cycle	PTEN	(54)
	miR-92a	—	Promote cell proliferation, migration, invasion, and cell cycle Inhibit apoptosis	PTEN	(54, 55)
	miR-151a-3p	Inhibit	Inhibit cell proliferation and migration	NEK2	(56)
	miR-188-5p	Inhibit	Inhibit cell proliferation, migration, invasion, tumor growth and metastasis in nude mice	LAPTM4B	(57)
	miR-605	Inhibit	Inhibit cell proliferation and cell cycle	EN2/PTEN	(58)
	miR-137	—	Inhibit H3K4 methylation	KDM5B	(59)
	miR-106a-5p	—	Promote cell migration and invasion	TIMP2	(60)
	miR-106b	—	Promote cell growth (in the presence of prolactin)	P21	(61)
	miR-27a	—	Inhibit cell proliferation, cell cycle, and migration Promote apoptosis	MAP2K4	(62)
	miR-135a	—	Inhibit cell proliferation, cell cycle, and migration Promote apoptosis	RBAK, MMP11	(63)

(Continued)

TABLE 1 Continued

	ncRNA	Effect on the PAM pathway	Function	Signaling network	Ref.
circRNA	CircSMARCC1	Activate	Promote cell proliferation, migration, invasion, tumor growth and metastasis in nude mice	miR-1322/CCL20	(64)
	circMBOAT2	Activate	Promote cell proliferation, migration, invasion, tumor growth and metastasis in nude mice	miR- 1271-5p/mTOR	(65)
	circ-ITCH	Inhibit	Inhibit cell proliferation, migration, and invasion	miR-17	(66)
piRNA	piR-001773	Activate	Promote cell proliferation, migration, invasion, and tumor growth in nude mice	PCDH9	(67)
	piR-017184	Activate	Promotes cell proliferation, migration, invasion, and tumor growth in nude mice	PCDH9	(67)

Cancer cell metastasis occurs through a certain process; this process starts with cancer cell acquisition of a migratory and invasive phenotype through EMT, after which the cancer cell passes through the extracellular matrix (ECM) and stromal cells to dislodge them from their primary foci (71). Upon loss of epithelial cell contact with the ECM, cancer cells undergo a form of cysteine-dependent apoptosis that is induced by death receptors and mitochondria that is known as anoikis (72). However, the resistance of cancer cells to anoikis leads to the progression of tumor metastasis (73). Therefore, EMT, anoikis, and migration and invasion assays are commonly used in experiments to assess the metastatic ability of tumors.

3.1.1 Inhibition of metastasis

ncRNAs associated with the PAM signaling pathway inhibit PCa metastasis (Figure 1). The skeletal system is the most common site of the distant metastasis of PCa. *miR-133a-3p* was shown to be expressed at lower levels in PCa bone metastatic tissues than in nonmetastatic cancer tissues, and its expression is negatively correlated with bone metastasis-free survival in PCa patients (44). Further studies revealed that overexpression of *miR-133a-3p* attenuates anoikis resistance and thus inhibits PCa bone metastasis, which may be mediated by *miR-133a-3p* targeting EGFR, FGFR1, IGF1R and MET to regulate the PAM signaling pathway (44). These findings suggest that *miR-133a-3p* may be a potential target for the treatment of PCa bone metastases. PTEN, which is a classic inhibitor of the PAM signaling pathway, is lacking in up to 60% of PCa tumors (74). The *MBNL1-AS1* inhibits the invasion and migration of PCa cells through the *miR-181a-5p*/PTEN axis [18]. Cullin 4B (CUL4B) is a scaffold for the Cullin4B-Ring E3 ligase complex (CRL4B), which is involved in protein hydrolysis (75). CUL4B is highly expressed in PCa patients, and

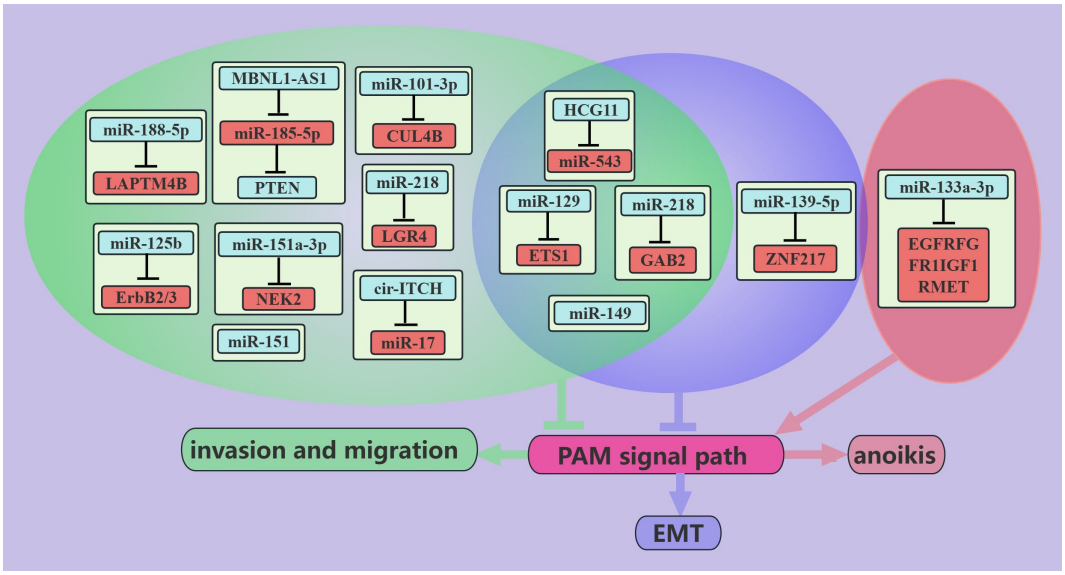


FIGURE 1
ncRNAs inhibit PCa metastasis through the PAM signaling pathway. This figure illustrates that ncRNAs associated with the PAM signaling pathway inhibit PCa metastasis by regulating invasion, migration, anoikis, and EMT. Blue represents the role of suppressing the PAM signaling pathway. Red represents roles that facilitate the PAM signaling pathway. Cyan color represents an association with invasion and migration, purple color represents an association with EMT, and light red color represents an association with anoikis.

miR-101-3p can target CUL4B to inhibit its expression and thus inhibit PCa migration and invasion; this is mediated by inhibiting the PAM signaling pathway (40). Yongguang Jiang reported that *miRNA-149* directly inhibits AKT1 mRNA expression in CRPC, thus inhibiting tumor EMT, migration, and metastasis; however, this process does not involve PI3K (52).

The expression level of *miR-218* in metastatic PCa tissues is much lower than that in primary PCa tissues (46), and *miR-218* can inhibit the EMT, migration, and metastasis of cancer cells via GAB2/PI3K/AKT/GSK-3β (47). Recent studies have shown that PCa is associated with chronic inflammation (76), and leucine-rich repeat-containing G protein-coupled receptor (LGR) 4 is a key molecule in the progression of PCa whose expression is induced by the proinflammatory factor IL-6 [69]. *miR-218* inhibits the migration and metastasis of IL-6-treated PCa cells by directly targeting LGR4 to inhibit the PAM pathway (48). ETS1, which is an independent prognostic molecule in breast cancer (77), is a proto-oncogene that is expressed mainly in triple-negative breast cancers (78). Higher expression of ETS1 was observed in PC cells than in noncancerous cells, especially in desmoplasia-resistant prostate cancer cells (41). miR-129 can directly target ETS1 and thus negatively regulate the PAM signaling pathway, thereby inhibiting the EMT, migration, and invasion of PCa cells (41).

In addition, other ncRNAs that are associated with the PAM signaling pathway, such as *HCG11/miR-543* (16), *miR-125b* (53), *miR-151a-3p* (56), *miR-188-5p* (57), *miR-151* (39), and *miR-139-5p* (38), inhibit the migration and metastasis of PCa cells through different pathways. *cir-ITCH* was found to negatively regulate the PAM signaling pathway and thus inhibit the EMT, migration, and invasion of PCa cells, possibly through *miR-17* (66). In addition, some miRNAs are negatively regulated by the PAM signaling pathway, such as *miR-27a* and *miR-135a*, which inhibit migration and invasion of PCa cells through MAP2K4 and MMP11, respectively (62, 63).

3.1.2 Promotion of metastasis

It is also very common for ncRNAs to positively regulate the PAM signaling pathway and thus promote PCa metastasis(Figure 2). For example, the *DANCR* can activate the PAM signaling pathway through the *miR-185-5p*/LASP1 axis to promote the EMT, migration, and invasion of PCa cells (13). The expression of the *DANCR* and LASP1 was also found to be positively correlated with PCa metastasis, whereas the expression of *miR-185-5p* was negatively correlated with PCa metastasis (13). These findings suggest that the lncRNA *DANCR/miR-185-5p*/LASP1 axis plays an important role in the process of PCa metastasis. Dysregulation of EGFR promotes the progression of PCa to bone metastasis (79), and both *LINC00963* and the lncRNA *RHPN1-AS* can contribute to the overexpression of the EGFR gene and increase the migration and invasion of PCa cells; these effects may be mediated via the PAM pathway (12, 23). These findings suggest that drugs that target EGFR potentially inhibit PCa metastasis. PTEN is a tumor suppressor molecule that acts on PIPs. *miR-22, miR-4534, miR-92a*, and *PlncRNA-1* can reduce PTEN expression, thereby promoting the migration and invasion of PCa cells (31, 49, 53, 55). CircRNAs are stably expressed because they exist in a cyclic form. *CircSMARCC1*- and *CircMBOAT2*-overexpressing PC3 cells were injected into the tail vein of nude mice, and more pulmonary and/or abdominal metastases were detected in the nude

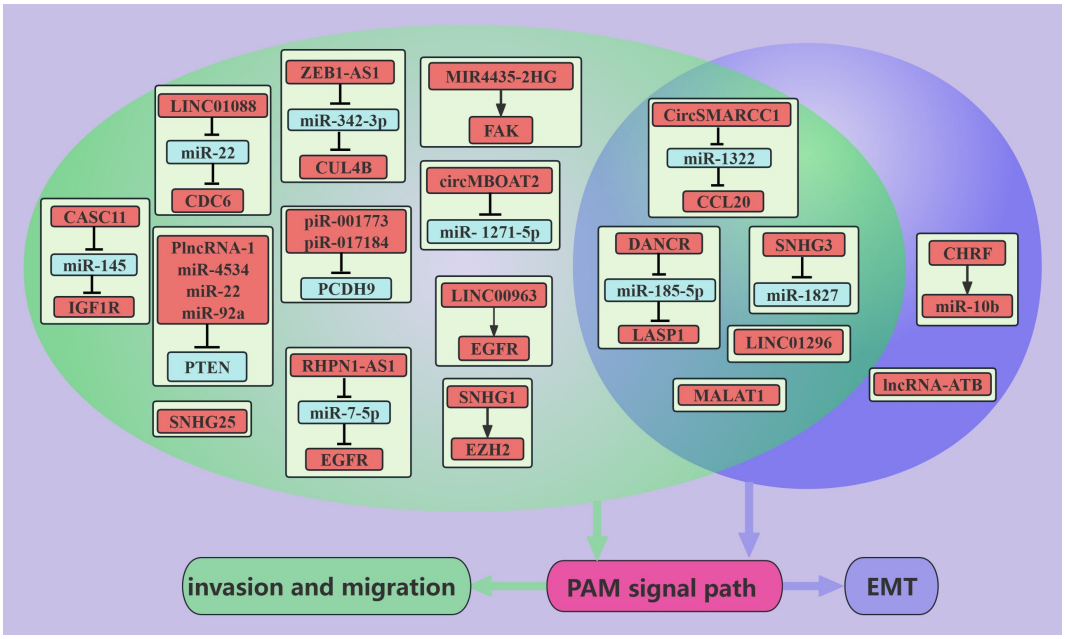


FIGURE 2
ncRNAs promote PCa metastasis through the PAM signaling pathway. This figure illustrates that ncRNAs associated with the PAM signaling pathway promote PCa metastasis through regulating invasion, migration, and EMT. Blue represents the role of suppressing the PAM signaling pathway. Red represents roles that facilitate the PAM signaling pathway. Cyan color represents association with invasion and migration and purple color represents association with EMT.

mice than in the control group (64, 65). Second, *in vitro* experiments have demonstrated that *circSMARCC1* promotes the EMT, migration, and invasion of PCa cells through *miR-22*/CCL20 and that *circMBOAT2* promotes the migration and invasion of PCa cells through *miR-1271-5p*/mTOR (64, 65). These effects may be mediated via the PAM signaling pathway (64, 65). pCDH9, which is a member of the calcineurin superfamily, inhibits the metastasis of hepatocellular carcinoma, gastric carcinoma, and malignant melanoma (80–82). In PCa cells, *piR-001773* and *piR-01718* inhibit PCDH9 and abolish the inhibitory effect of PCDH9 on the PAM signaling pathway, thus promoting the migration and metastasis of PCa cells (67).

Obesity is strongly associated with PCa, with an 8–11% increase in specific mortality in advanced PCa patients who are obese compared with nonobese advanced PCa patients, and the presence of obesity also decreases the efficacy of surgical treatments, radiotherapy and ADT in the treatment of PCa (83). Mediators between obesity and PCa may include insulin and the IGF-axis, sex hormone concentrations, and adipokine signaling (83). PC3 cells with low expression of Apelin, which is an adipokine, were implanted into the prostates of nude mice, and Apelin promoted the liver metastasis and bone metastasis of PC3 cells by increasing the level of TIMP2 (60). Further studies revealed that Apelin increases the level of *miR-106a-5p* through the C-Src/PI3K/AKT axis and that *miR-106a-5p* sponges TIMP2, thereby promoting the migration and invasion of PCa cells (60). IGF1R is a membrane receptor of IGF, and more than 90% of the regions in PCa tissue sections are positive for IGF1R (84). The lncRNA *CASC11* can upregulate the PAM signaling pathway through IGF1R, thereby promoting the migration and invasion of PCa cells (21). These findings suggest that drugs that target IGF1R potentially inhibit PCa metastasis. Therefore, with further in-depth studies of obesity and PCa, obesity has been shown to promote PCa metastasis, and weight loss is likely beneficial for the treatment of PCa.

MALAT1 mediates the development and metastasis of digestive system and sex hormone-related tumors, and *MALAT1* levels in plasma and urine could be a marker for the diagnosis and prediction of PCa metastasis and recurrence (85). *MALAT1* can promote the EMT, migration, and metastasis of PCa cells by activating the PAM signaling pathway (26, 27), and METTL3 acts as a methyltransferase to methylate *MALAT1* adenosine and thus stabilize its expression (26).

In addition to these novel ncRNAs, *LINC01088*/miR-22 (11), *ZEB1-AS1*/*miR-342-3p* (15), *SNHG3*/*miR-1827* (18), *SNHG1* (19), *SNHG25* (29), *LINC01296* (32), and *MIR4435-2HG* (34) can promote the migration, invasion or/and EMT of PCa cells via the PAM signaling pathway. Also worth mentioning is *miR-106a-5p*, which is positively regulated by the PAM signaling pathway and promotes PCa migration and invasion (60).

3.2 Tumor growth

Tumor growth represents a dysregulation of the balance between cancer cell generation and cell loss; cancer cell generation occurs mainly through cell division, and cancer cell loss occurs mainly through apoptosis and autophagy. In PCa cells, ncRNAs can regulate tumor growth through the PAM signaling pathway, and the elucidation of these mechanisms can provide guidance for the clinical treatment of PCa.

3.2.1 Promotion of tumor growth

NcRNAs associated with the PAM signaling pathway promote PCa growth (Figure 3). These ncRNAs can promote cancer cell growth via the PTEN-dependent induction of cell cycle progression through cell cycle checkpoints (86). For example, in PCa cells, *miR-4534* promotes the passage of cancer cells through the G0/G1 phase (49); *PlncRNA-1* promotes the passage of cancer cells through the G2/M phase (31); and *miR-19b, miR-23b, miR-26a*, and *miR-92a* promote the passage of cancer cells through the G1/S phase via the cell cycle protein D1 (54). In addition, ncRNAs, such as *miR-4534, PlncRNA-1, miR-92a*, and *miR-21*, can inhibit apoptosis to promote PCa growth via PTEN (31, 49, 50, 55). Interestingly, *miR-21* inhibits apoptosis in chemotherapy-resistant PCa cells, which may be mediated by *miR-21* inhibition of cancer cell exocytosis of toxic drugs taken up via PTEN (50). The hypoxic environment of PCa can induce tumor progression and metastasis (87). PCa cells express high levels of *SPRY4-IT1* in hypoxic environments, and *SPRY4-IT1* may promote the growth of cancer cells by regulating the PAM pathway and cell cycle progression (36). High expression of *UCA1* was observed in radiotherapy-resistant PCa, in contrast to the radiotherapy-sensitive PCa (35). *UCA1* may promote the passage of cancer cells through the G0/G1 phase via the PAM pathway [90]. Moreover, EGFR expression is higher in CRPC than in ADPC (23). Linc00963 was found to transactivate EGFR and mediate the apoptosis of CRPC cells (23). In addition, in PCa, *RHPN1-AS1*/*miR-7-5P*/EGFR could promote cancer cell growth through the PAM signaling pathway (12). This may be mediated by the PAM axis, which promotes apoptosis and autophagy and induces cancer cells to pass the G2/M checkpoint (12).

3.2.2 Inhibition of tumor growth

ncRNAs inhibit PCa growth through the PAM signaling pathway (Figure 4). PCa is an androgen-dependent tumor, and *miR-149* can inhibit AR signaling (52). In addition, *miR-149* can target AKT1 to inhibit the proliferation of CRPC cells, which may be mediated by promoting apoptosis and inducing G1/S phase arrest in cancer cells (52). *miR-7* can inhibit the proliferation of PCa cells, possibly because *miR-7* can increase the nuclear localization of P21 through the KLF4/PI3K/AKT axis, which in turn prolongs the cell cycle [91]. Interestingly, *miR-7* increases P-P21 expression but does not seem to interfere with apoptosis (45).

IL-6 stimulation increases PCa viability and invasiveness, suggesting that PCa is closely associated with inflammation (88). *miR-218* inhibits cell cycle progression through LRG4, and this inhibition is suppressed in the presence of IL-6 (48). Therefore, anti-inflammatory therapy can be used as an adjuvant treatment for PCa. RLIP76 depletion therapy can cause the nearly complete regression of PCa cell xenografts and can improve sensitivity to radiotherapy (89). *miR-101* can

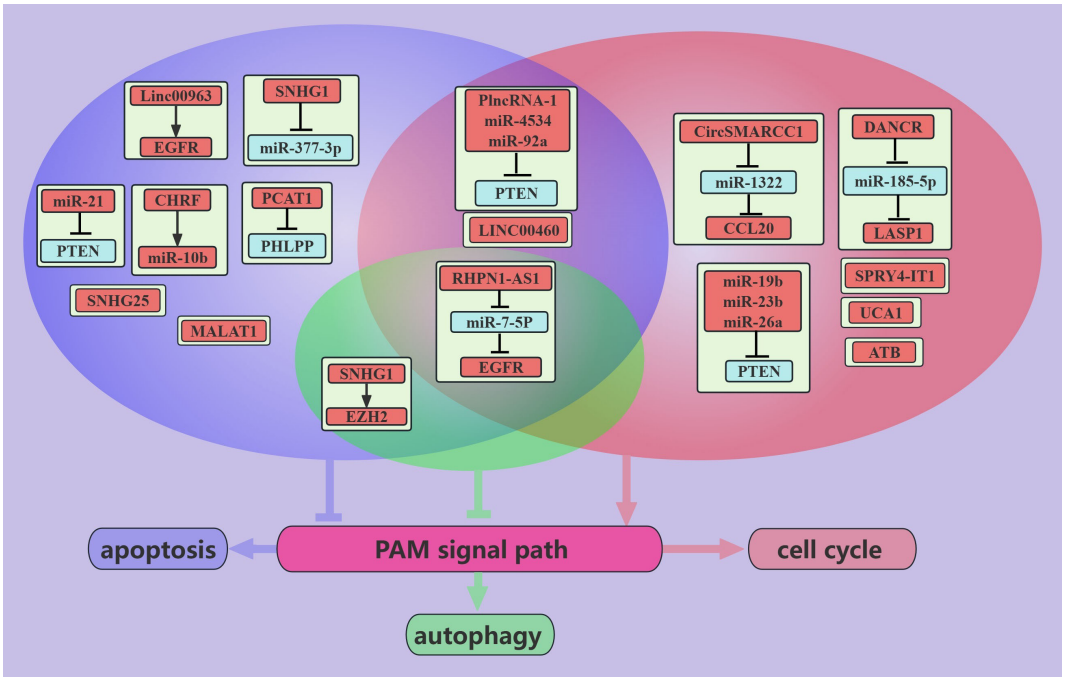


FIGURE 3
ncRNAs promote PCa growth through the PAM signaling pathway. This figure illustrates that ncRNAs associated with the PAM signaling pathway promote PCa growth through regulating apoptosis, autophagy, and cell cycle. Blue represents the role of suppressing the PAM signaling pathway. Red represents roles that facilitate the PAM signaling pathway. Cyan color represents an association with autophagy, purple color represents an association with apoptosis, and light red color represents an association with the cell cycle.

target and inhibit RLIP76, thereby promoting the apoptosis of PCa cells. *miR-101*-based depletion therapy targeting RLIP76 is promising for the treatment of PCa (42). *miRNA-605* was found to differentiate between inert and aggressive PCa, and further studies found that *miRNA-605* can arrest the cell cycle in the G0/G1 phase by the EN2/PTEN axis (58). In addition, some miRNAs, such as *miR-27a* and *miR-135a*, are negatively regulated by the PAM signaling pathway. These miRNAs arrest PCa cells in the G1/S phase and promote apoptosis through MAP2K4 and RBAK, respectively (62, 63).

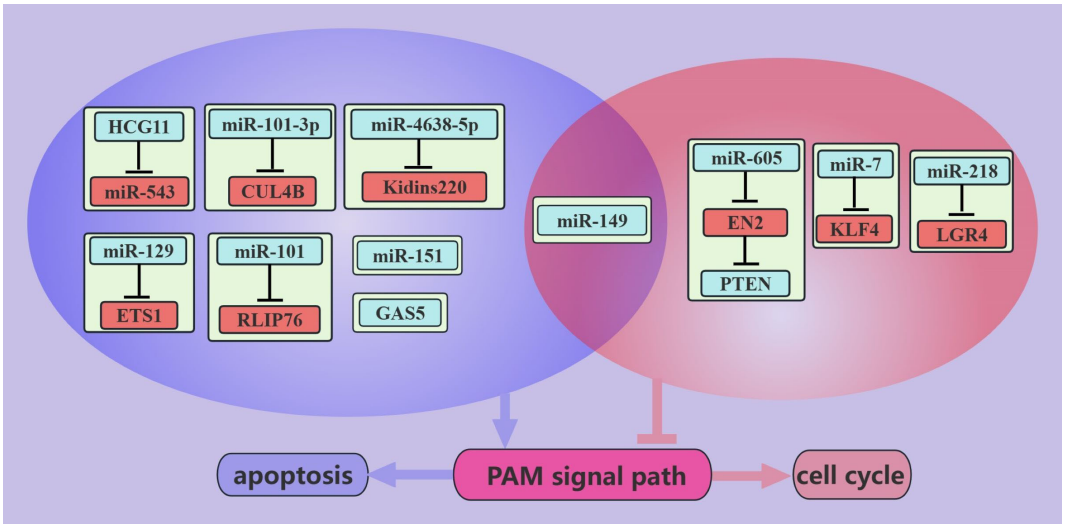


FIGURE 4
ncRNAs inhibit PCa growth through the PAM signaling pathway. This figure illustrates that ncRNAs associated with the PAM signaling pathway inhibit PCa growth by regulating apoptosis and cell cycle. Blue represents the role of suppressing the PAM signaling pathway. Red represents roles that facilitate the PAM signaling pathway. purple color represents an association with apoptosis and light red color represents an association with the cell cycle.

3.3 Angiogenesis

Rapid tumor proliferation is inevitably accompanied by neoangiogenesis because without blood vessels to provide nutrients for tumor cells, the tumor size cannot exceed 1–2 mm (90). NcRNAs regulate PCa angiogenesis through the PAM signaling pathway (Figure 5). The interaction of VEGF with VEGFR on the surface of vascular endothelial cells (ECs) is crucial for the proliferation, migration, and tube formation of ECs (91). *miR-4638-5p* can inhibit the secretion of VEGF by PCa cells, thereby inhibiting neovascularization (43). *miR-4638-5p* may inhibit the PAM signaling pathway by targeting the inhibition of Kidins220, thereby reducing the production of VEGF (43). In addition, *miR-218* can inhibit VEGFA secretion by PCa cells, thereby inhibiting neovascularization (46). The effect of *miR-218* on VEGFA is mediated by the RICTOR/AKT/HIF1&2α axis (46). To date, we have elucidated the mechanism by which miRNAs regulate angiogenesis in PCa cells through the PAM signaling pathway.

3.4 Tumor stemness

The presence of cancer stem cells (CSCs) in tumors is an important cause of tumor treatment failure and tumor recurrence, and tumors are considered to be cured only when CSCs are completely eliminated (92). miRNAs mediate the biological regulation of CSCs through the PAM signaling pathway (Figure 6) (92). *miR-133a-3p* can inhibit PCa stemness through the PAM signaling pathway. This may be mediated by *miR-133a-3p*, which targets and inhibits EGFR, FGFR1, IGF1R, and MET (44). *miR-133a-3p* was also shown to inhibit the expression of some stemness-related factors, such as NANOG, BMI-1, OCT4, and SOX2 (44). In addition, *microRNA-7* can inhibit PCa stemness by targeting and inhibiting the stemness factor KLF4, possibly because the stemness factor KLF4 activates the transcription of P110δ (the catalytic subunit of PI3K) (45). *MicroRNA-7* inhibits PCa stemness through KLF4 in several generations of cells and prevents the transition from nonstem cells to stem cells (45). Thus, *miR-133a-3p* and *microRNA-7* are promising targets for PCa treatments that target tumor stemness.

4 Clinical roles of ncRNAs in the PAM pathway

The ncRNAs associated with the PAM signaling pathway in PCa are of clinical significance (Table 2).

4.1 Diagnosis

The diagnosis of PCa is the basis of treatment, and ncRNAs that are involved in the PAM pathway were found to help confirm the diagnosis of PCa by ROC curve analysis. For example, an analysis of 52 paired samples revealed an AUC of 0.915 for *SNHG25* (29), an

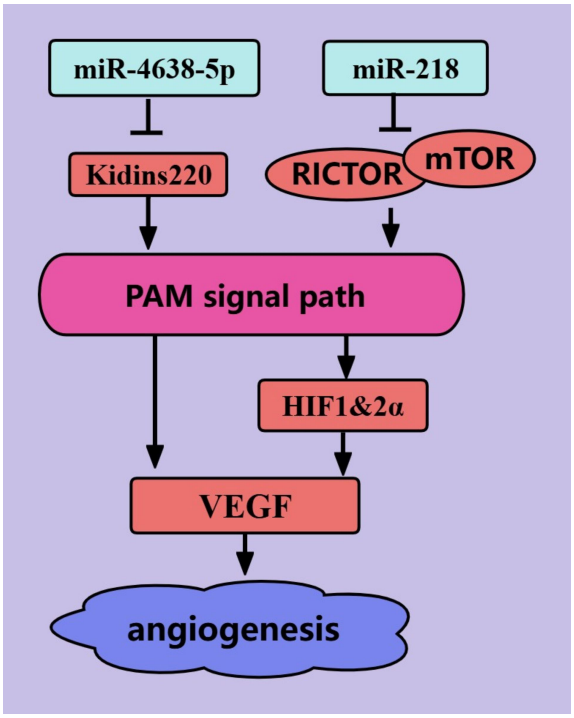


FIGURE 5
ncRNAs regulate PCa angiogenesis through the PAM signaling pathway. The blue color represents the inhibition of angiogenesis in PCa. The red color represents the promotion of angiogenesis in PCa.

10.3389/fimmu.2025.1525741

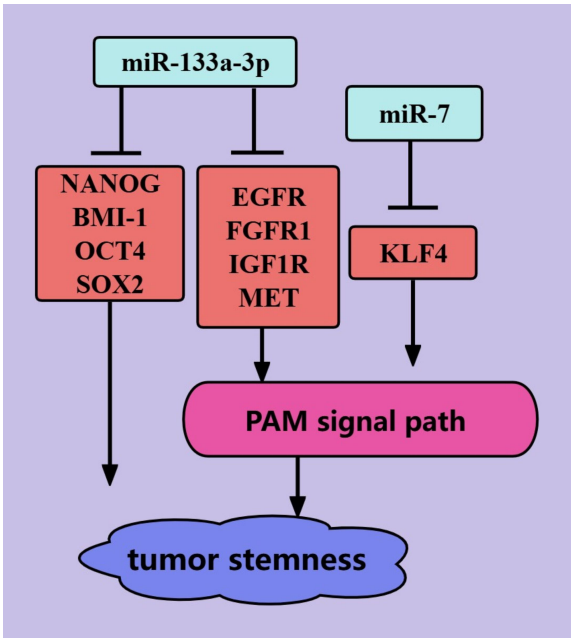


FIGURE 6
ncRNAs regulate PCa tumor stemness through the PAM signaling pathway. The blue color represents the inhibition of PCa tumor stemness. The red color represents the promotion of PCa tumor stemness.

TABLE 2 Clinical applications of ncRNAs associated with the PAM signaling pathway in PCa.

	ncRNA	Expression in PCa	Diagnosis	Prognosis	Clinical significance	Ref.
LncRNA	LINC01088	↑	Profitable	Disease-free survival	—	(67)
	RHPN1-AS1	↑	Profitable	—	—	(78)
	DANCR	↑	Profitable	Overall 5-year survival	Pathological grade and tumor metastasis	(34)
	MBNL1-AS1	↓	Profitable	—	—	(31)
	ZEB1-AS1	↑	Profitable	—	—	(77)
	HCG11	↓	Profitable	—	Tumor metastasis	(90)
	GAS5	Associated with SNPs	—	Overall survival	Gleason score and tumor stage	(93)
	SNHG3	↑	Profitable	Overall survival	—	(65)
	SNHG1	↑	Profitable	Overall survival	T stage	(12, 24)
	CASC11	↑	Profitable	—	Gleason score	(26)
	CHRF	—	—	—	—	(52)
	LINC00963	CRPC↑vs. ADPC	Profitable	—	—	(58)
	PCAT1	CRPC↑vs. ADPC	Profitable	Overall survival and recurrence-free survival	—	(84)
	NEAT1	↑	Profitable	—	Tumor metastasis and PSA recurrence	(94)
	MALAT1	↑	Profitable	Tumor recurrence rate	Gleason score, lymphatic node transfer and Quercetin therapy	(41, 76)
	LINC00460	↑	Profitable	—	T stage and Gleason score	(17)

(Continued)

TABLE 2 Continued

	ncRNA	Expression in PCa	Diagnosis	Prognosis	Clinical significance	Ref.
	SNHG25	↑	Profitable (AUC=0.915)	Disease-free survival	—	(47)
	lncRNA-ATB	↑	Profitable (AUC=0.931)	Biochemical recurrence-free survival	Histologic grade, preoperative PSA level, pathologic stage, Gleason score, lymph node metastasis, vascular lymphatic infiltration, and biochemical recurrence	(95)
	PlncRNA-1	↑	Profitable	—	T stage	(96)
	LINC01296	↑	Profitable	Biochemical recurrence-free survival	Preoperative PSA level, lymph node metastasis, Gleason score, and tumor stage	(97)
	AC245100.4	↑	Profitable	—	—	(98)
	MIR4435-2HG	↑	Profitable	—	—	(99)
	UCA1	Radiotherapy-resistant cells ↑ vs. radiotherapy-sensitive cells	Profitable	—	Radiotherapy sensitivity	(54)
	SPRY4-IT1	↑	Profitable	—	Gleason score	(83)
	GDPD4-2	↓	Profitable	—	Astragaloside IV-PESV therapy	(100)
miRNA	miR-139-5p	—	—	—	—	(4)
	miR-151	↓	Profitable	—	Chemosensitivity	(28)
	miR-101-3p	↓	Profitable	—	TNM stage, tumor size, Gleason score, and preoperative PSA level	(51)
	miR-129	↓	Profitable	—	—	(101)
	miR-101	—	—	—	—	(102)
	miR-4638-5p	CRPC↓vs. ADPC	Profitable	—	—	(91)
	miR-133a-3p	↓	Profitable	Bone metastasis-free survival	Gleason score, T stage, N stage, M stage, and bone metastases	(87)
	MicroRNA-7	↓	Profitable	—	—	(27)
	miR-218	↓	Profitable	—	Tumor metastasis	(35, 68, 70)
	miR-4534	↑	Profitable (AUC=0.9)	Overall survival, recurrence-free survival	Gleason score, T stage, PSA recurrence, and genistein treatment	(63)
	miR-21	Chemoresistant cells ↑ vs. chemosensitive cells	Profitable	—	chemotherapy resistance	(103)
	miR-182	↑	Profitable	—	Distant metastasis, lymph node metastasis, and tumor size	(6)
	MicroRNA-149	—	—	—	—	(104)
	miR-125b	↓	Profitable	—	—	(11)
	miR-22	↑	Profitable	—	—	(11)
	miR-19b	—	—	—	—	(45)
	miR-23b	—	—	—	—	(45)
	miR-26a	—	—	—	—	(45)
	miR-92a	—	—	—	—	(45, 105)
	miR-151a-3p	↓	Profitable	—	—	(101)

(Continued)

TABLE 2 Continued

	ncRNA	Expression in PCa	Diagnosis	Prognosis	Clinical significance	Ref.
	miR-188-5p	—	—	Biochemical recurrence-free survival and overall survival	Lymph node metastasis, T stage, preoperative PSA level, vascular lymphatic infiltration, biochemical recurrence, and chemosensitivity	(106)
	miR-605	↓	Profitable	—	—	(107)
	miR-137	—	—	—	—	(64)
	miR-106a-5p	↑	Profitable	—	—	(74)
	miR-106b	—	—	—	Prolactin therapy	(13)
	miR-27a	↓	Profitable	—	—	(89)
	miR-135a	↓	Profitable	Biochemical recurrence-free survival	Gleason score, T stage, biochemical recurrence	(42)
circRNA	CircSMARCC1	↑	Profitable (AUC=0.713)	—	Gleason score, and T stage	(108)
	circMBOAT2	↑	Profitable	Disease-free survival	Gleason score and T stage	(21)
	cir-ITCH	↓	Profitable	—	—	(71)
piRNA	piR-001773	↑	Profitable	—	Gleason score and T stage	(109)
	piR-017184	↑	Profitable	—	Gleason score	(109)

↑ represents elevated levels of ncRNA in cancerous tissues compared to non-cancerous tissues. ↓ represents that ncRNA is reduced in cancerous tissues compared to non-cancerous tissues. ↓vs. represents a lower content of the former than of the latter. ↑vs. represents a higher content of the former than the latter.

analysis of 57 paired patients revealed an AUC of 0.931 for *LncRNA-ATB* (30), and a study of 28 unpaired patients reported an AUC of 0.9 for *miR-4534* (49). We aimed to detect and diagnose prostate cancer by noninvasive methods, and we detected elevated *circSMARCC1* levels in the plasma of PCa patients compared with those in the plasma of noncancerous patients (64). ROC curve analysis revealed that the AUC of *CircSMARCC1* was 0.713, which was not as good as that of PSA in identifying PCa (64). However, the specificity of *circSMARCC1* was high enough to discriminate between patients with PCa and those with BPH, and *CircSMARCC1* levels were also found to be elevated only in colorectal cancer tissues (97). ncRNAs that are associated with the PAM signaling pathway can also predict various stages of PCa. For example, lower expression of *miR-185-5p*, *miR-218*, and *miR-133-3p* and higher expression of *DANCR* were observed in metastatic patients than in nonmetastatic PCa patients (13, 44, 46). Interestingly, *miR-185-5p* expression was more significantly decreased in patients with bone metastatic PCa than in patients without bone metastatic PCa (44). High expression of *PCAT1* and *NEAT1* suggests CRPC (24, 25), high expression of *miR-21* suggests chemoresistance (50), and high expression of *UCA1* suggests radioresistance (35). Thus, ncRNAs are expected to be novel markers for the diagnosis of PCa.

4.2 Prognosis

Prognostic information on PCa helps in the selection of optimal treatment strategies (108), and the levels of ncRNAs that are related to the PAM signaling pathway can indicate the prognosis of PCa patients. These ncRNAs are closely associated with overall survival, progression-free survival, biochemical recurrence-free survival, bone metastasis-free survival, and recurrence-free survival in PCa patients. For example, the levels of *lncRNA-ATB*, *LINC01296*, and *miR-188-5p* can be used as independent prognostic factors for the biochemical recurrence-free survival of PCa patients (30, 32, 57). The *miR-133a-3p* level can be used as an independent prognostic factor for the bone metastasis-free survival of PCa patients (44). Second, these ncRNAs are closely associated with pathological features that affect prognosis; for example, plasma *CircSMARCC1* levels are positively correlated with the Gleason score and T stage in patients with PCa (64). In addition, single nucleotide polymorphisms (SNPs) of ncRNAs have the potential to predict the prognosis of PCa (17). For example, two SNPs on chromosome *GAS5* are correlated with overall survival, Gleason score, and TNM stage in patients with PCa (17).

4.3 Treatment

The targeted regulation of ncRNAs can inhibit PCa growth, metastasis, angiogenesis, and drug resistance via the PAM signaling pathway; this provides a basis for developing PCa therapies that target ncRNAs. For example, agomir-133a-3p inhibits bone metastasis of PCa in mice (44), knockdown of *UCA1* reduces radiotherapy resistance in PCa cells (35), and inhibition of *miR-21* increases the chemosensitivity of PCa cells (50). ncRNAs are natural molecules in the body, and they can interfere in a given pathway with broad specificity via multiple targets or target

different pathways to inhibit tumors (99), leading to increased benefits in ncRNA therapy. For example, *miR-218* can target LGR4 to reduce AKT levels in PCa cells, target RICTOR to inhibit the phosphorylation of AKT at Ser473, and target GAB2 to disrupt the coexistence environment of PI3K and PIPs to inhibit the PAM signaling pathway (46–48). In addition, *miR-218* not only inhibits the PAM pathway but also interferes with the Wnt/β-catenin pathway in PCa cells (48). Drugs that specifically target ncRNA therapeutics include antisense oligonucleotides(ASOs), siRNAs, shRNAs, RNA sponges, antmiRs, therapeutic circRNAs, miRNA mimics (Figure 7A), and the drugs that are currently being developed are mainly miRNA-based siRNAs and antisense oligonucleotides (99). However, therapies that target ncRNAs have limitations associated with specificity, delivery, and tolerance when translated into the clinic, resulting in the failure of the development of these drugs (99). The use of novel drug delivery strategies, such as the possible use of nanomaterials, liposomes, cationic polymers, etc., for drug delivery, has shown promising advantages in overcoming these difficulties (94). Nanocarrier-based drug therapies for ASOs are currently the most hotly researched option (Figure 7), and better structures have been achieved in other diseases.

To date, there are only two ncRNA drugs in human trials regarding PCa. Apatorsen (OGX-427) is a 2′-methoxyethyl-modified ASO that inhibits Hsp27 expression. A Phase I clinical trial including 42 (22 CRPC patients) showed that OGX-427 was tolerated at the highest dose (101). Then a phase II trial showed that OGX-427+prednisone did not improve the 12-week progression-free period in CRPC patients compared to prednisone alone, but only significantly reduced PSA in patients, so further clinical trials of OGX-427 are in limbo (95) There is another drug Custirsen (OGX-011) that is an ASO targeting clusterin inhibition. A meta-analysis including 3 RCTs pointed out that OGX-011 did not significantly improve OS in mCRPC patients, so it has been terminated from development in the clinic (102).

A cohort study including 1132 patients revealed that the use of traditional Chinese medicine reduced PCa-related mortality (32.8% vs. 21.9%) compared with the nonuse of traditional Chinese medicine (105). Traditional Chinese medicine (TCM) has multitarget properties, and TCM is involved in the entire process of PCa treatment (100). Recently, traditional Chinese medicine has been shown to modulate ncRNAs and thus treat PCa; for example, quercetin can downregulate *MALAT1* in a time- and dose-dependent manner to inhibit the growth, migration, invasion, and EMT of PCa cells. This may be mediated by targeting the PAM signaling pathway via *MALAT1* (27). Astragaloside IV-PESV can upregulate *GDPD4-2* to inhibit the PAM pathway and PCa growth (37). However, silencing *GDPD4-2* does not completely block the antitumor effect of astragaloside IV-PESV, suggesting that astragaloside IV-PESV may also act on other targets to inhibit PCa growth (37). In addition, traditional Chinese medicine can be used together with other antitumor drugs not only to exert antitumor effects alone but also to produce synergistic effects and improve the sensitivity of tumor cells to antitumor drugs (100, 106). For example, the use of quercetin together with docetaxel can significantly improve the antitumor effect of docetaxel on chemotherapy-resistant PCa (106). Moreover, traditional Chinese medicine makes it easier to achieve clinical translation than specific drugs do; thus, traditional Chinese medicine has broad prospects in the treatment of tumors.

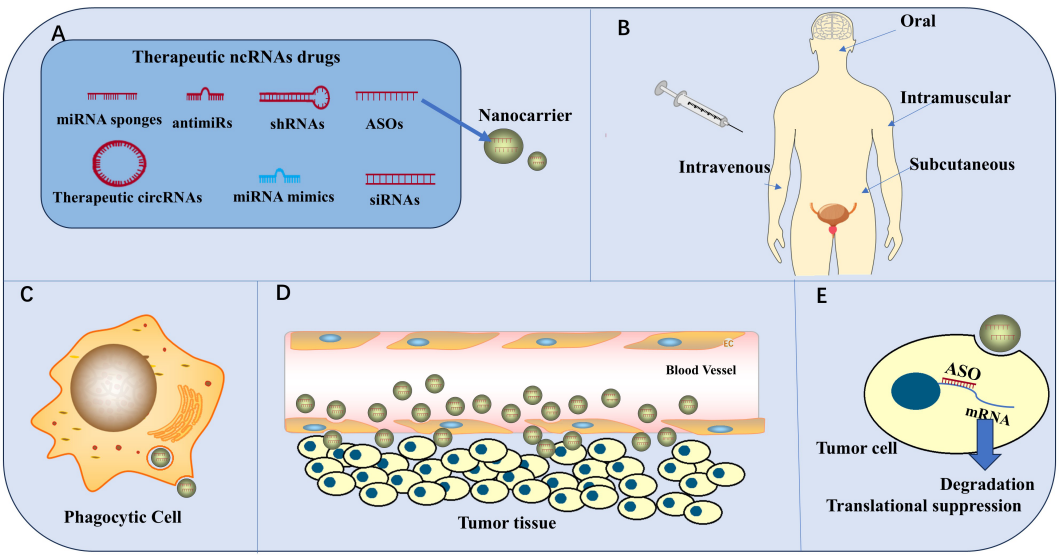


FIGURE 7
ncRNAs for clinical therapy. **(A)** Therapeutic ncRNA drugs include ASOs, siRNAs, shRNAs, RNA sponges, antmiRs, therapeutic circRNAs, and miRNA mimics. ASOs were the first ncRNA drugs to be developed. Nanomaterials are the most common carriers for ncRNA drugs. **(B)** The administration routes of ncRNA drugs include oral, intramuscular, subcutaneous, and intravenous administration **(C)** Phagocytic cells destroy the efficacy of the drug. **(D)** Drugs cross blood vessel walls through intercellular spaces or channels and endocytosis. **(E)** ASOs enter tumor cells to cause mRNA degradation and translation suppression, thus achieving anti-tumor effects.

5 Discussion

This paper summarizes the types, functions and specific mechanisms of action of ncRNAs that are associated with the PAM signaling pathway in PCa cells. Most of these ncRNAs act at the transcription level. lncRNAs and circRNAs mostly function as miRNA sponges, and miRNAs and piRNAs mostly function by suppressing mRNA transcription. In addition, some ncRNAs, mainly lncRNAs, act posttranscriptionally to regulate the PAM pathway. The PAM signaling pathway is abnormally activated in PCa cells and interacts with the RAS/MAPK, AR, and WNT pathways (110). This paper explore the roles of ncRNAs in the apoptosis, cellular autophagy, cell cycle progression, EMT, invasion, migration, angiogenesis, and tumor stemness of PCa cells via the PAM pathway. We analyzed the effects of these ncRNAs on PCa cell apoptosis, autophagy and cell cycle regulation in PCa growth and their effects on EMT, invasion and migration in PCa metastasis, and we presented these functions in the form of Venn diagrams, which can allow a more comprehensive understanding of the regulatory effects of these ncRNAs on PCa growth and metastasis. We found that some ncRNAs affect PCa growth and metastasis through dual or triple mechanisms, which more clearly highlights the importance of certain ncRNAs and may provide guidance for subsequent studies. For example, *miR-149* can inhibit the growth of PCa cells by affecting apoptosis and cell cycle progression, and it can inhibit PCa metastasis through EMT, migration, and invasion (52). If the role of *miR-149* is further explored, it can be found that *miR-149* can inhibit AR signaling via the PAM pathway (52). In fact, cell growth, metastasis, angiogenesis and tumor stemness are intertwined with each other, and the roles of these ncRNAs in the interactions of these processes can be further explored. In addition, we explored how these ncRNAs affect PCa growth, metastasis, angiogenesis and tumor stemness via the PAM pathway. We found that the regulatory effect of these ncRNAs on PCa angiogenesis depended on VEGF; that EGFR mediated the effects of *miR-7-5p*, *miR-133a-3p*, and *LINC0096* on PCa growth, metastasis, and tumor stemness; and that PTEN mediated the effects of *miR-181a-5p, miR-4534, miR-22, miR-21, miR-26a, miR-23b, miR-92a*, and *miR-19* on PCa growth and metastasis.

We also discussed the prospects for the clinical application of these ncRNAs in diagnosis, prognosis, and treatment. In terms of diagnosis and prognosis, most of the ncRNA content in cancer tissues can be detected, and some of the ncRNA content shows high sensitivity for diagnosing PCa and determining patient prognosis. However, these ncRNAs are not easy to sample and analyze, they cannot be included in a dynamic detection index, and most ncRNAs do not have high specificity for the diagnosis of PCa. It is hoped that more *circSMARCC1*-like ncRNAs will be discovered and that diagnostic and prognostic markers with high specificity will be available in the bloodstream. Therapeutically, drugs that target these ncRNAs are based mainly on ASO, siRNAs, shRNAs, RNA sponges, antmiRs, therapeutic circRNAs, and miRNA mimics, and these drugs have shown excellent therapeutic effects in animal and cellular experiments. However, when these drugs are used in humans, their efficacy is greatly reduced. For example, Custirsen is an antisense nucleotide drug that targets human CLU mRNA and was developed to treat chemotherapy-resistant mCRPC patients (98). However, in a phase III clinical trial that included 635 patients, it was shown that there was no statistically significant difference in overall survival in the Custirsen + chemotherapy group compared to the chemotherapy control group (14.2 moon vs. 13.4 moon, $p = 0.529$) (98).

This loss of efficacy is mainly because the drug will face delivery challenges. ncRNA drugs cannot be delivered efficiently to the cells of interest due to their own instability and lack of cell specificity. Secondly, crossing cell membranes is also a great challenge. Scientists have proposed to solve the delivery problem by altering the internal chemical modifications, such as 2′-deoxy-2′-fluoro-RNA, 2′-O-methyl-RNA, the phosphorothioates, and bicyclic nucleic acids, of ncRNA drugs to improve resistance to nucleases and enhance interaction with proteins to improve stability and uptake (109). Custirsen was dual-modified with alternating 2′-O-methyl and the phosphorothioates, but phase III clinical trials showed that the effect was not significant and was halted (98, 111). Apatorsen (OGX-427) is also an ASO doped with phosphorothioates and 2′-methoxyethyl modification to prolong half-life and improve specificity aimed at treating mCRPC patients (101). However, phase II trials have shown that Apatorsen (OGX-427) does not alter mCRPC disease progression, but only reduces PSA concentrations in patients (95). These failures suggest the need to improve the efficacy of the drug in other ways, so recently scientists have thought of solving this problem through novel delivery systems. For example, nanoparticles, which can be synthesized from liposomes, polymers, micelles, proteins, antibodies, gold nanoparticles, USPIO nanoparticles, and nanotubes, in addition to enhancing the stability of RNA drugs, due to their small size can also enhance the permeability and retention (EPR effect) of tumor tissue to increase the concentration of the drug inside the tumor tissue (112). The miR-145 therapy based on gold nanoparticle-based nanocarrier and miR-34a therapy based on micelle-based nanocarrier have achieved good therapeutic efficacy in cellular and animal tests (103, 107). Based on nanoparticles, some scientists combine Ultrasound-induced microbubble cavitation technology to increase the permeability of cell membranes and the capillary gap, which further facilitates the entry of drugs into cancer cells (93). However, these have yet to be proven in human trials and the safety of nanoparticles needs to be explored further. The side effects of nanoparticles are also due to the EPR effect, which leads to the aggregation of nanoparticles in vascular leakage tissues. The side effects are caused by reactive oxygen species (ROS), DNA damage, modification of protein structures and functions, and disruption of membrane integrity mechanisms leading to damage in these tissues (113). Viral-constituted delivery carriers have also been believed to enhance the efficacy of RNA drugs by loading the target RNA into the viral genome. Viral-constituted delivery carriers deliver RNA drugs into tumor tissues through viral oncolytic properties and stability. For example, the current delivery of miRNAs for PCa therapy using herpes simplex virus-1 and recombinant adeno-

associated virus has shown good results in animal studies (96, 114). However, the exact efficacy has to be observed in humans and the safety is worth considering. In addition to viral delivery and nano-delivery systems, membrane vesicles, bacteria, and ligand-receptor delivery systems are also explored in ncRNA therapy for PCa (99).

In the future, the internal modification of ncRNA itself to make ncRNA more stable, the carrier delivery system to further stabilize the ncRNA and increase the drug concentration in the tumor region, and the ligand-receptor refinement to navigate the drug into the target tumor cells will make ncRNAs as clinical drugs a reality. While these enhance the efficacy of ncRNA drugs, the carrier system itself can cause some toxic effects, which need to be addressed. In addition, the human immune system recognizes single- or double-stranded RNA inside and outside the cell through the PAMP receptor, which reduces the drug's efficacy and causes an immune-inflammatory response (99). As PCa is a "cold tumor" in immunotherapy, could the immune-inflammatory response by such ncRNAs potentiate the immunotherapy of PCa? Nanocarriers have been shown to enhance the antitumor efficacy and specificity of immunopharmaceuticals through enhanced immunostimulatory activity and favorable modulatory pharmacological properties (104). Therefore, whether treatment with ncRNAs in combination with vectors could make PCa a "hot tumor" in terms of immunotherapy. Currently, the translation from cell and animal trials to clinical trials is the biggest obstacle to ncRNA drug therapy, which may be solved in the future by the combined delivery of ncRNA drugs through multiple mechanisms.

Previously OGX-427 and OGX-011 were considered to be promising for clinical use, but the therapeutic effect was not shown to be significant in clinical trials. Therefore, attempts can be made to develop other ncRNAs for the treatment of PCa. miR-218 gene is located on chromosome 4p15.31, which is transcribed as an intron into an ncRNA and is expressed in various malignant tumors at lower levels than in the surrounding normal tissues (115). It can be used as a tumor suppressor gene. Earlier Katia R M Leite and other scholars have found that miR-218 is highly expressed in metastatic PCa compared to high-grade PCa patients (116). In recent years, many studies have shown that miR-218 may regulate the PAM signaling pathway in PCa, and basically, it works by binding to the 3'-UTR of the downstream genes' mRNA and blocking the mRNAs' translation process. miR-218 can target LGR4 to reduce the content of AKT, target RICTOR to inhibit the phosphorylation of AKT ser-473 and target GAB2 to destroy the coexistence environment of PI3K and PIPs to inhibit the PAM signaling pathway (46–48). miR-218 can effectively inhibit the viability, migration, and invasion of PCa cells and inhibit tumor angiogenesis through multi-targeting inhibiting PAM signaling. miR-218's multi-targeting properties may improve its efficacy in the clinical translational process, and have the opportunity to be applied in the clinic. In addition, miR-133a-3p may play an important role in the treatment of PCa bone metastasis (44). It was shown that upregulation of miR-133a-3p inhibited PCa bone metastasis and stem cell characteristics and that miR-133a-3p levels were strongly associated with bone metastasis-free survival in PCa patients (44). Moreover, miR-133a-3p can target multiple receptors, such as EGFR, FGFR1, IGF1R, and MET receptors, to inhibit tumor cells (44). Therefore, the development of miR-133a-3p as a novel drug for PCa patients with bone metastasis is promising, but the specific effects are still waiting to be observed in clinical trials.

There is a lack of effective treatment for mCRPC. From the current clinical data, the PAM signaling pathway inhibitor (Ipatasertib) brings the best efficacy, which can prolong the survival of patients by 2 months. However, there is still much room for improvement (117). Based on the above, this review summarizes the ncRNAs in the PAM signaling pathway of PCa and tries to find AKT inhibitor breakthroughs from the function and clinical use of these ncRNAs for better treatment of PCa. We also discussed the prospect of clinical translation of ncRNAs in PCa, but we found that only a few clinical studies show that ncRNA drugs' efficacy in PCa is still poor and that ncRNAs are unstable. There is still a long way to go before they can be applied to the clinic; In addition to the ncRNA strategy, there may be other pathways implicit in the PAM signaling pathway to treat PCa, which is the shortcoming of this review. Therefore, we wrote this review for the next study on the use of ncRNA in PCa.

We can refer to ncRNA drug development strategies that have been successfully used in the clinic in other diseases, and more data are needed in the future to explore the next step of ncRNA therapies for PCa. This review investigates ncRNAs under the PAM pathway in PCa to provide a reference for the next step in the study of ncRNAs for new drugs or new strategies.

Author contributions

RG: Writing – original draft. LS: Writing – review & editing. YC: Writing – review & editing. CL: Writing – review & editing. WY: Writing – review & editing.

Funding

The author(s) declare that financial support was received for the research and/or publication of this article. This work was supported by the Jiangxi Provincial Natural Science Foundation (20202BABL206079).

Conflict of interest

The authors declare that the research was conducted in the absence of any commercial or financial relationships that could be construed as a potential conflict of interest.

Generative AI statement

The author(s) declare that no Generative AI was used in the creation of this manuscript.

Publisher's note

All claims expressed in this article are solely those of the authors and do not necessarily represent those of their affiliated organizations, or those of the publisher, the editors and the reviewers. Any product that may be evaluated in this article, or claim that may be made by its manufacturer, is not guaranteed or endorsed by the publisher.

References

1. Bray F, Laversanne M, Sung H, Ferlay J, Siegel RL, Soerjomataram I, et al. Global cancer statistics 2022: GLOBOCAN estimates of incidence and mortality worldwide for 36 cancers in 185 countries. *CA Cancer J Clin*. (2024) 74:229–63. doi: 10.3322/caac.21834

2. Teo MY, Rathkopf DE, Kantoff P. Treatment of advanced prostate cancer. *Annu Rev Med*. (2019) 70:70479–499. doi: 10.1146/annurev-med-051517-011947

3. Glaviano A, Foo ASC, Lam HY, Yap KCH, Jacot W, Jones RH, et al. PI3K/AKT/mTOR signaling transduction pathway and targeted therapies in cancer. *Mol Cancer*. (2023) 22:22138. doi: 10.1186/s12943-023-01827-6

4. He Y, Sun MM, Zhang GG, Yang J, Chen KS, Xu WW, et al. Targeting PI3K/akt signal transduction for cancer therapy. *Signal Transduction Targeting Ther*. (2021) 6:425. doi: 10.1038/s41392-021-00828-5

5. Foster P, Yamaguchi K, Hsu PP, Qian F, Du X, Wu J, et al. The selective PI3K inhibitor XL147 (SAR245408) inhibits tumor growth and survival and potentiates the activity of chemotherapeutic agents in preclinical tumor models. *Mol Cancer Ther*. (2015) 14:931–40. doi: 10.1158/1535-7163.MCT-14-0833

6. Slack FJ, Chinnaiyan AM. The role of non-coding RNAs in oncology. *Cell*. (2019) 179:1033–55. doi: 10.1016/j.cell.2019.10.017

7. Mitobe Y, Takayama K, Horie-Inoue K, Inoue S. Prostate cancer-associated lncRNAs. *Cancer Lett*. (2018) 418:418159–166. doi: 10.1016/j.canlet.2018.01.012

8. Prensner JR, Zhao S, Erho N, Schipper M, Iyer MK, Dhanasekaran SM, et al. Nomination and validation of the long noncoding RNA SChLAP1 as a risk factor for metastatic prostate cancer progression: A multi-institutional high-throughput analysis. *Lancet Oncol*. (2014) 15:1469–80. doi: 10.1016/S1470-2045(14)71113-1

9. Gong P, Zhang T, He D, Hsieh J-T. MicroRNA-145 modulates tumor sensitivity to radiation in prostate cancer. *Radiat Res*. (2015) 184:630–8. doi: 10.1667/RR14185.1

10. Mirzaei S, Paskeh MDA, Okina E, Gholami MH, Hushmandi K, Hashemi M, et al. Molecular landscape of lncRNAs in prostate cancer: A focus on pathways and therapeutic targets for intervention. *J Exp Clin Cancer Res CR*. (2022) 41:41214. doi: 10.1186/s13046-022-02406-1

11. Li J, Huang X, Chen H, Gu C, Ni B, Zhou J. LINC01088/miR-22/CDC6 axis regulates prostate cancer progression by activating the PI3K/AKT pathway. *Mediators Inflammation*. (2023) 2023:20239207148. doi: 10.1155/2023/9207148

12. Ma X, Ren H, Zhang Y, Wang B, Ma H. LncRNA RHPN1-AS1 Inhibition Induces Autophagy and Apoptosis in Prostate Cancer Cells via the miR-7-5p/EGFR/PI3K/AKT/mTOR Signaling Pathway. *Environ Toxicol*. (2022) 37:3013–27. doi: 10.1002/tox.23656

13. Sun W, Zu S, Shao G, Wang W, Gong F. Long Non-Coding DANCR Targets miR-185-5p to Upregulate LIM and SH3 Protein 1 Promoting Prostate Cancer via the FAK/PI3K/AKT/GSK3β/Snail Pathway. *J Gene Med*. (2021) 23:e3344. doi: 10.1002/jgm.3344

14. Ding X, Xu X, He X-F, Yuan Y, Chen C, Shen X-Y, et al. Muscleblind-like 1 antisense RNA 1 inhibits cell proliferation, invasion, and migration of prostate cancer by sponging miR-181a-5p and regulating PTEN/PI3K/AKT/mTOR signaling. *Bioengineered*. (2021) 12:803–14. doi: 10.1080/21655979.2021.1890383

15. Ma T, Chen H, Wang P, Yang N, Bao J. Downregulation of lncRNA ZEB1-AS1 Represses Cell Proliferation, Migration, and Invasion Through Mediating PI3K/AKT/mTOR Signaling by miR-342-3p/CUL4B Axis in Prostate Cancer. *Cancer Biother Radiopharm*. (2020) 35:661–72. doi: 10.1089/cbr.2019.3123

16. Wang Y-C, He W-Y, Dong C-H, Pei L, Ma Y-L. lncRNA HCG11 regulates cell progression by targeting miR-543 and regulating AKT/mTOR pathway in prostate cancer. *Cell Biol Int*. (2019) 43:1453–62. doi: 10.1002/cbin.11194

17. Zhu L, Zhu Q, Wen H, Huang X, Zheng G. Mutations in GAS5 affect the transformation from benign prostate proliferation to aggressive prostate cancer by affecting the transcription efficiency of GAS5. *J Cell Physiol*. (2019) 234:8928–40. doi: 10.1002/jcp.27561

18. Hu M, Ren M, Zhao Z, Cui X, Shi M, Yang Y, et al. Long non-coding RNA SNHG3 promotes prostate cancer progression by sponging microRNA-1827. *Oncol Lett*. (2022) 24:281. doi: 10.3892/ol.2022.13401

19. Chen J, Wang F, Xu H, Xu L, Chen D, Wang J, et al. Long non-coding RNA SNHG1 regulates the wnt/β-catenin and PI3K/AKT/mTOR signaling pathways via EZH2 to affect the proliferation, apoptosis, and autophagy of prostate cancer cell. *Front Oncol*. (2020) 10:10552907. doi: 10.3389/fonc.2020.552907

20. Xie M, Zhang Z, Cui Y. Long noncoding RNA SNHG1 contributes to the promotion of prostate cancer cells through regulating miR-377-3p/AKT2 axis. *Cancer Biother Radiopharm*. (2020) 35:109–19. doi: 10.1089/cbr.2019.3177

21. Capik O, Sanli F, Kurt A, Ceylan O, Suer I, Kaya M, et al. CASC11 Promotes Aggressiveness of Prostate Cancer Cells through miR-145/IGF1R Axis. *Prostate Cancer Prostatic Dis*. (2021) 24:891–902. doi: 10.1038/s41391-021-00353-0

22. Liu S, Wang L, Li Y, Cui Y, Wang Y, Liu C. Long Non-Coding RNA CHRF Promotes Proliferation and Mesenchymal Transition (EMT) in Prostate Cancer Cell Line PC3 Requiring up-Regulating microRNA-10b. *Biol Chem*. (2019) 400:1035–45. doi: 10.1515/hsz-2018-0380

23. Wang L, Han S, Jin G, Zhou X, Li M, Ying X, et al. Linc00963: A novel, long non-coding RNA involved in the transition of prostate cancer from androgen-dependence to androgen-independence. *Int J Oncol*. (2014) 44:2041–9. doi: 10.3892/ijo.2014.2363

24. Shang Z, Yu J, Sun L, Tian J, Zhu S, Zhang B, et al. LncRNA PCAT1 activates AKT and NF-κB signaling in castration-resistant prostate cancer by regulating the PHLPP/FKBP51/IKKα Complex. *Nucleic Acids Res*. (2019) 47:4211–25. doi: 10.1093/nar/gkz108

25. Xiong W, Huang C, Deng H, Jian C, Zen C, Ye K, et al. Oncogenic Non-Coding RNA *NEAT1* promotes the prostate cancer cell growth through the SRC3/IGF1R/AKT pathway. *Int J Biochem Cell Biol*. (2018) 94:94125–132. doi: 10.1016/j.biocel.2017.12.005

26. Mao Y, Li W, Weng Y, Hua B, Gu X, Lu C, et al. METTL3-Mediated m6A Modification of lncRNA MALAT1 Facilitates Prostate Cancer Growth by Activation of PI3K/AKT Signaling. *Cell Transplant*. (2022) 31:319636897221122997. doi: 10.1177/09636897221122997

27. Lu X, Chen D, Yang F, Xing N. Quercetin Inhibits Epithelial-to-Mesenchymal Transition (EMT) Process and Promotes Apoptosis in Prostate Cancer via Downregulating lncRNA MALAT1. *Cancer Manage Res*. (2020) 12:121741–1750. doi: 10.2147/CMAR.S241093

28. Dong Y, Quan H-Y. Downregulated LINC00460 inhibits cell proliferation and promotes cell apoptosis in prostate cancer. *Eur Rev Med Pharmacol Sci*. (2019) 23:6070–8. doi: 10.26355/eurrev_201907_18420

29. Liu Z, Ke S, Wang Q, Gu X, Zhai G, Shao H, et al. Analyzing roles of small nucleolar RNA host gene 25 from clinical, molecular target and tumor formation in prostate cancer. *Exp Cell Res*. (2023) 429:113686. doi: 10.1016/j.yexcr.2023.113686

30. Xu S, Yi X-M, Tang C-P, Ge J-P, Zhang Z-Y, Zhou W-Q. Long non-coding RNA ATB promotes growth and epithelial-mesenchymal transition and predicts poor prognosis in human prostate carcinoma. *Oncol Rep*. (2016) 36:10–22. doi: 10.3892/or.2016.4791

31. LncRNA PlncRNA-1 accelerates the progression of prostate cancer by regulating PTEN/Akt axis . Available online at (Accessed May 27, 2024).

32. Wu J, Cheng G, Zhang C, Zheng Y, Xu H, Yang H, et al. Long noncoding RNA LINC01296 is associated with poor prognosis in prostate cancer and promotes cancer-cell proliferation and metastasis. *OncoTargets Ther*. (2017) 10:101843–1852. doi: 10.2147/OTT.S129928

33. Zhang K, Liu C, Hu C, Lin P, Qi Q, Jia H, et al. Long non-coding RNA AC245100.4 activates the PI3K/AKT pathway to promote PCa cell proliferation by elevating PAR2. *Heliyon*. (2023) 9:e16870. doi: 10.1016/j.heliyon.2023.e16870

34. Xing P, Wang Y, Zhang L, Ma C, Lu J. Knockdown of lncRNA MIR4435–2HG and ST8SIA1 expression inhibits the proliferation, invasion and migration of prostate cancer cells *in vitro* and *in vivo* by blocking the activation of the FAK/AKT/B–catenin signaling pathway. *Int J Mol Med*. (2021) 47:93. doi: 10.3892/ijmm.2021.4926

35. Fotouhi Ghiam A, Taeb S, Huang X, Huang V, Ray J, Scarcello S, et al. Long non-coding RNA urothelial carcinoma associated 1 (UCA1) mediates radiation response in prostate cancer. *Oncotarget*. (2017) 8:4668–89. doi: 10.18632/oncotarget.13576

36. Sang W, Zhu R, Liu D, Gong M. LncRNA SPRY4–IT1 is upregulated and promotes the proliferation of prostate cancer cells under hypoxia *in vitro*. *Oncol Lett*. (2023) 25:138. doi: 10.3892/ol.2023.13724

37. You X, Wu Y, Li Q, Sheng W, Zhou Q, Fu W. Astragalus-scorpion drug pair inhibits the development of prostate cancer by regulating GDPD4-2/PI3K/AKT/mTOR pathway and autophagy. *Front Pharmacol*. (2022) 13:13895696. doi: 10.3389/fphar.2022.895696

38. Azhati B, Reheman A, Dilixiati D, Rexiati M. FTO-stabilized miR-139-5p targets ZNF217 to suppress prostate cancer cell Malignancies by inactivating the PI3K/akt/mTOR signal pathway. *Arch Biochem Biophys*. (2023) 741:741109604. doi: 10.1016/j.abb.2023.109604

39. Chen S, Ke S, Cheng S, Wu T, Yang Y, Liao B. MicroRNA-151 regulates the growth, chemosensitivity and metastasis of human prostate cancer cells by targeting PI3K/AKT. *J BUON Off J Balk Union Oncol*. (2020) 25:2045–50.

40. Gu Z, You Z, Yang Y, Ding R, Wang M, Pu J, et al. Inhibition of microRNA miR-101-3p on prostate cancer progression by regulating cullin 4B (CUL4B) and PI3K/AKT/mTOR signaling pathways. *Bioengineered*. (2021) 12:4719–35. doi: 10.1080/21655979.2021.1949513

41. Xu S, Ge J, Zhang Z, Zhou W. MiR-129 inhibits cell proliferation and metastasis by targeting ETS1 via PI3K/AKT/mTOR pathway in prostate cancer. *Biomed Pharmacother Biomedecine Pharmacother*. (2017) 96:96634–641. doi: 10.1016/j.biopha.2017.10.037

42. Yang J, Song Q, Cai Y, Wang P, Wang M, Zhang D. RLIP76-dependent suppression of PI3K/AKT/bcl-2 pathway by miR-101 induces apoptosis in prostate cancer. *Biochem Biophys Res Commun*. (2015) 463:900–6. doi: 10.1016/j.bbrc.2015.06.032

43. Wang Y, Shao N, Mao X, Zhu M, Fan W, Shen Z, et al. MiR-4638-5p inhibits castration resistance of prostate cancer through repressing kidins220 expression and PI3K/AKT pathway activity. *Oncotarget*. (2016) 7:47444–64. doi: 10.18632/oncotarget.10165

44. Tang Y, Pan J, Huang S, Peng X, Zou X, Luo Y, et al. Downregulation of miR-133a-3p Promotes Prostate Cancer Bone Metastasis via Activating PI3K/AKT Signaling. *J Exp Clin Cancer Res CR*. (2018) 37:37160. doi: 10.1186/s13046-018-0813-4

45. Chang Y-L, Zhou P-J, Wei L, Li W, Ji Z, Fang Y-X, et al. MicroRNA-7 inhibits the stemness of prostate cancer stem-like cells and tumorigenesis by repressing KLF4/PI3K/akt/P21 pathway. *Oncotarget*. (2015) 6:24017–31. doi: 10.18632/oncotarget.4447

46. Guan B, Wu K, Zeng J, Xu S, Mu L, Gao Y, et al. Tumor-Suppressive microRNA-218 Inhibits Tumor Angiogenesis via Targeting the mTOR Component RICTOR in Prostate Cancer. *Oncotarget*. (2016) 8:8162–72. doi: 10.18632/oncotarget.14131

47. Tian J, Zhang H, Mu L, Wang M, Li X, Zhang X, et al. The miR-218/GAB2 Axis Regulates Proliferation, Invasion and EMT via the PI3K/AKT/GSK-3β Pathway in Prostate Cancer. *Exp Cell Res*. (2020) 394:112128. doi: 10.1016/j.yexcr.2020.112128

48. Li F, Gu C, Tian F, Jia Z, Meng Z, Ding Y, et al. miR-218 impedes IL-6-induced prostate cancer cell proliferation and invasion via suppression of LGR4 expression. *Oncol Rep*. (2016) 35:2859–65. doi: 10.3892/or.2016.4663

49. Nip H, Dar AA, Saini S, Colden M, Varahram S, Chowdhary H, et al. Oncogenic microRNA-4534 regulates PTEN pathway in prostate cancer. *Oncotarget*. (2016) 7:68371–84. doi: 10.18632/oncotarget.12031

50. Zhao W, Ning L, Wang L, Ouyang T, Qi L, Yang R, et al. miR-21 inhibition reverses doxorubicin-resistance and inhibits PC3 human prostate cancer cells proliferation. *Andrologia*. (2021) 53:e14016. doi: 10.1111/and.14016

51. Bai L, Luo L, Gao W, Bu C, Huang J. miR-182 modulates cell proliferation and invasion in prostate cancer via targeting ST6GALNAC5. *Braz J Med Biol Res Rev Bras Pesqui Medicas E Biol*. (2021) 54:e9695. doi: 10.1590/1414-431X2020e9695

52. MicroRNA–149 inhibits cancer cell Malignant phenotype by regulating Akt1 in C4–2 CRPC cell line . Available online at (Accessed May 27, 2024).

53. Budd WT, Seashols-Williams SJ, Clark GC, Weaver D, Calvert V, Petricoin E, et al. Dual action of miR-125b as a tumor suppressor and oncomiR-22 promotes prostate cancer tumorigenesis. *PloS One*. (2015) 10:e0142373. doi: 10.1371/journal.pone.0142373

54. Tian L, Fang Y, Xue J, Chen J. Four microRNAs promote prostate cell proliferation with regulation of PTEN and its downstream signals *in vitro*. *PloS One*. (2013) 8:e75885. doi: 10.1371/journal.pone.0075885

55. Yanshen Z, Lifen Y, Xilian W, Zhong D, Huihong M. miR-92a promotes proliferation and inhibits apoptosis of prostate cancer cells through the PTEN/akt signaling pathway. *Libyan J Med*. (2021) 16:1971837. doi: 10.1080/19932820.2021.1971837

56. Zhang Y, Hao T, Zhang H, Wei P, Li X. Over-expression of miR-151a-3p inhibits proliferation and migration of PC-3 prostate cancer cells. *Xi Bao Yu Fen Zi Mian Yi Xue Za Zhi Chin J Cell Mol Immunol*. (2018) 34:247–52.

57. Zhang H, Qi S, Zhang T, Wang A, Liu R, Guo J, et al. miR-188-5p inhibits tumour growth and metastasis in prostate cancer by repressing LAPTM4B expression. *Oncotarget*. (2015) 6:6092–104. doi: 10.18632/oncotarget.3341

58. Zhou Y-J, Yang H-Q, Xia W, Cui L, Xu R-F, Lu H, et al. Down-Regulation of miR-605 Promotes the Proliferation and Invasion of Prostate Cancer Cells by up-Regulating EN2. *Life Sci*. (2017) 190:1907–14. doi: 10.1016/j.lfs.2017.09.028

59. Khan MI, Hamid A, Rath S, Ateeq B, Khan Q, Siddiqui IA, et al. AKT inhibition modulates H3K4 demethylase levels in PTEN-null prostate cancer. *Mol Cancer Ther*. (2019) 18:356–63. doi: 10.1158/1535-7163.MCT-18-0141

60. Lin T-H, Chang SL-Y, Khanh PM, Trang NTN, Liu S-C, Tsai H-C, et al. Apelin Promotes Prostate Cancer Metastasis by Downregulating TIMP2 via Increases in miR-106a-5p Expression. *Cells*. (2022) 11:3285. doi: 10.3390/cells11203285

61. Chen K-HE, Bustamante K, Nguyen V, Walker AM. Involvement of miR-106b in tumorigenic actions of both prolactin and estradiol. *Oncotarget*. (2017) 8:36368–82. doi: 10.18632/oncotarget.16755

62. Wan X, Huang W, Yang S, Zhang Y, Zhang P, Kong Z, et al. Androgen-induced miR-27A acted as a tumor suppressor by targeting MAP2K4 and mediated prostate cancer progression. *Int J Biochem Cell Biol*. (2016) 79:79249–260. doi: 10.1016/j.biocel.2016.08.043

63. Wan X, Pu H, Huang W, Yang S, Zhang Y, Kong Z, et al. Androgen-Induced miR-135a Acts as a Tumor Suppressor through Downregulating RBAK and MMP11, and Mediates Resistance to Androgen Deprivation Therapy. *Oncotarget*. (2016) 7:51284–300. doi: 10.18632/oncotarget.9992

64. Xie T, Fu D, Li Z, Lv D, Song X-L, Yu Y, et al. CircSMARCC1 Facilitates Tumor Progression by Disrupting the Crosstalk between Prostate Cancer Cells and Tumor-Associated Macrophages via miR-1322/CCL20/CCR6 Signaling. *Mol Cancer*. (2022) 21:21173. doi: 10.1186/s12943-022-01630-9

65. Shi J, Liu C, Chen C, Guo K, Tang Z, Luo Y, et al. Circular RNA circMBOAT2 Promotes Prostate Cancer Progression via a miR-1271-5p/mTOR Axis. *Aging*. (2020) 12:13255–80. doi: 10.18632/aging.103432

66. Li S, Yu C, Zhang Y, Liu J, Jia Y, Sun F, et al. Circular RNA cir-ITCH is a potential therapeutic target for the treatment of castration-resistant prostate cancer. *BioMed Res Int*. (2020) 2020:20207586521. doi: 10.1155/2020/7586521

67. Zhang L, Meng X, Li D, Han X. piR-001773 and piR-017184 promote prostate cancer progression by interacting with PCDH9. *Cell Signal*. (2020) 96:76109780. doi: 10.1016/j.cellsig.2020.109780

68. Zhang Z, Wang Y, Zhang Y, Zheng S-F, Feng T, Tian X, et al. The function and mechanisms of action of circular RNAs in urologic cancer. *Mol Cancer*. (2023) 22:2261. doi: 10.1186/s12943-023-01766-2

69. Boutilier AJ, Elsawa SF. Macrophage polarization states in the tumor microenvironment. *Int J Mol Sci*. (2021) 22:6995. doi: 10.3390/ijms22136995

70. Liu Y, Dou M, Song X, Dong Y, Liu S, Liu H, et al. The emerging role of the piRNA/piwi complex in cancer. *Mol Cancer*. (2019) 18:18123. doi: 10.1186/s12943-019-1052-9

71. Paolillo M, Schinelli S. Extracellular matrix alterations in metastatic processes. *Int J Mol Sci*. (2019) 20:4947. doi: 10.3390/ijms20194947

72. Simpson CD, Anyiwe K, Schimmer AD. Anoikis resistance and tumor metastasis. *Cancer Lett*. (2008) 272:177–85. doi: 10.1016/j.canlet.2008.05.029

73. Sakamoto S, Kyprianou N. Targeting anoikis resistance in prostate cancer metastasis. *Mol Aspects Med*. (2010) 31:205–14. doi: 10.1016/j.mam.2010.02.001

74. Zhang S, Yu D. PI(3) king apart PTEN's role in cancer. *Clin Cancer Res*. (2010) 16:4325–30. doi: 10.1158/1078-0432.CCR-09-2990

75. Li Y, Wang X. The role of cullin4B in human cancers. *Exp Hematol Oncol*. (2017) 6:617. doi: 10.1186/s40164-017-0077-2

76. De Nunzio C, Kramer G, Marberger M, Montironi R, Nelson W, Schröder F, et al. The controversial relationship between benign prostatic hyperplasia and prostate cancer: the role of inflammation. *Eur Urol*. (2011) 60:106–17. doi: 10.1016/j.eururo.2011.03.055

77. Dittmer J. The biology of the ets1 proto-oncogene. *Mol Cancer*. (2003) 2:229. doi: 10.1186/1476-4598-2-29

78. Dittmer J. The role of the transcription factor ets1 in carcinoma. *Semin Cancer Biol*. (2015) 35:520–38. doi: 10.1016/j.semcancer.2015.09.010

79. Day KC, Hiles GL, Kozminsky M, Dawsey SJ, Paul A, Broses LJ, et al. HER2 and EGFR overexpression support metastatic progression of prostate cancer to bone. *Cancer Res*. (2017) 77:74–85. doi: 10.1158/0008-5472.CAN-16-1656

80. Zhu P, Lv J, Yang Z, Guo L, Zhang L, Li M, et al. Protocadherin 9 inhibits epithelial-mesenchymal transition and cell migration through activating GSK-3β in hepatocellular carcinoma. *Biochem Biophys Res Commun*. (2014) 452:567–74. doi: 10.1016/j.bbrc.2014.08.101

81. Chen Y, Xiang H, Zhang Y, Wang J, Yu G. Loss of PCDH9 is associated with the differentiation of tumor cells and metastasis and predicts poor survival in gastric cancer. *Clin Exp Metastasis*. (2015) 32:417–28. doi: 10.1007/s10585-015-9712-7

82. Zhang J, Yang H-Z, Liu S, Islam MO, Zhu Y, Wang Z, et al. PCDH9 suppresses melanoma proliferation and cell migration. *Front Oncol*. (2022) 12:12903554. doi: 10.3389/fonc.2022.903554

83. Wilson RL, Taaffe DR, Newton RU, Hart NH, Lyons-Wall P, Galvão DA. Obesity and prostate cancer: A narrative review. *Crit Rev Oncol Hematol*. (2022) 169:169103543. doi: 10.1016/j.critrevonc.2021.103543

84. Liao Y, Abel U, Grobholz R, Hermani A, Trojan L, Angel P, et al. Up-regulation of insulin-like growth factor axis components in human primary prostate cancer correlates with tumor grade. *Hum Pathol*. (2005) 36:1186–96. doi: 10.1016/j.humpath.2005.07.023

85. Zhao M, Wang S, Li Q, Ji Q, Guo P, Liu X. MALAT1: A long non-coding RNA highly associated with human cancers. *Oncol Lett*. (2018) 16:19–26. doi: 10.3892/ol.2018.8613

86. Brandmaier A, Hou S-Q, Shen WH. Cell cycle control by PTEN. *J Mol Biol*. (2017) 429:2265–77. doi: 10.1016/j.jmb.2017.06.004

87. Mohamed OAA, Tesen HS, Hany M, Sherif A, Abdelwahab MM, Elnaggar MH. The role of hypoxia on prostate cancer progression and metastasis. *Mol Biol Rep*. (2023) 50:3873–84. doi: 10.1007/s11033-023-08251-5

88. Cheng K, Batbatan C, Jia Q. IL-6 enhances the viability and invasion ability of prostate cancer cells. *Stud Health Technol Inform*. (2023) 308:308521–526. doi: 10.3233/SHTI230879

89. Singhal SS, Roth C, Leake K, Singhal J, Yadav S, Awasthi S. Regression of prostate cancer xenografts by RLIP76 depletion. *Biochem Pharmacol*. (2009) 77:1074–83. doi: 10.1016/j.bcp.2008.11.013

90. Liu L-Z, Li C, Chen Q, Jing Y, Carpenter R, Jiang Y, et al. MiR-21 induced angiogenesis through AKT and ERK activation and HIF-1α Expression. *PloS One*. (2011) 6:e19139. doi: 10.1371/journal.pone.0019139

91. Ahmad A, Nawaz MI. Molecular mechanism of VEGF and its role in pathological angiogenesis. *J Cell Biochem*. (2022) 123:1938–65. doi: 10.1002/jcb.30344

92. Najafi M, Farhood B, Mortezaee K. Cancer stem cells (CSCs) in cancer progression and therapy. *J Cell Physiol*. (2019) 234:8381–95. doi: 10.1002/jcp.27740

93. Wang Z, Chen C, Tao Y, Zou P, Gao F, Jia C, et al. Ultrasound-induced microbubble cavitation combined with miR-34a-loaded nanoparticles for the treatment of castration-resistant prostate cancer. *J Biomed Nanotechnol*. (2021) 17:78–89. doi: 10.1166/jbn.2021.3020

94. Toden S, Zumwalt TJ, Goel A. Non-coding RNAs and potential therapeutic targeting in cancer. *Biochim Biophys Acta Rev Cancer*. (2021) 1875:188491. doi: 10.1016/j.bbcan.2020.188491

95. Yu EY, Ellard SL, Hotte SJ, Gingerich JR, Joshua AM, Gleave ME, et al. A randomized phase 2 study of a HSP27 targeting antisense, apatorsen with prednisone versus prednisone alone, in patients with metastatic castration resistant prostate cancer. *Invest New Drugs*. (2018) 36:278–87. doi: 10.1007/s10637-017-0553-x

96. Ai J, Li J, Su Q, Ma H, He R, Wei Q, et al. rAAV-based and intraprostatically delivered miR-34a therapeutics for efficient inhibition of prostate cancer progression. *Gene Ther*. (2022) 29:418–24. doi: 10.1038/s41434-021-00275-5

97. Chen M, Lin C, Huang L, Qiu X. CircRNA SMARCC1 sponges miR-140-3p to regulate cell progression in colorectal cancer. *Cancer Manage Res*. (2020) 12:124899–4910. doi: 10.2147/CMAR.S254185

98. Fizazi K, Hotte SJ, Saad F, Alekseev B, Matveev VB, Flechon A, et al. Genitourinary tumours, prostate final overall survival (OS) from the AFFINITY phase 3 trial of custirsen and cabazitaxel/prednisone in men with previously treated metastatic castration-resistant prostate cancer (mCRPC). *Ann Oncol*. (2016) 27:27vi564. doi: 10.1093/annonc/mdw435.20

99. Winkle M, El-Daly SM, Fabbri M, Calin GA. Noncoding RNA therapeutics — Challenges and potential solutions. *Nat Rev Drug Discovery*. (2021) 20:629–51. doi: 10.1038/s41573-021-00219-z

100. Kong F, Wang C, Zhang J, Wang X, Sun B, Xiao X, et al. Chinese herbal medicines for prostate cancer therapy: from experimental research to clinical practice. *Chin Herb Med*. (2023) 15:485–95. doi: 10.1016/j.chmed.2023.05.003

101. Chi KN, Yu EY, Jacobs C, Bazov J, Kollmannsberger C, Higano CS, et al. A phase I dose-escalation study of apatorsen (OGX-427), an antisense inhibitor targeting heat shock protein 27 (Hsp27) , in patients with castration-resistant prostate cancer and other advanced cancers. *Ann Oncol*. (2016) 27:1116–22. doi: 10.1093/annonc/mdw068

102. Zhang X, Liu C, Li K, Wang K, Zhang Q, Cui Y. Meta-analysis of efficacy and safety of custirsen in patients with metastatic castration-resistant prostate cancer. *Med (Baltimore)*. (2019) 98:e14254. doi: 10.1097/MD.0000000000014254

103. Ekin A, Karatas OF, Culha M, Ozen M. Designing a Gold Nanoparticle-Based Nanocarrier for microRNA Transfection into the Prostate and Breast Cancer Cells. *J Gene Med*. (2014) 16:331–5. doi: 10.1002/jgm.2810

104. Rana I, Oh J, Baig J, Moon JH, Son S, Nam J. Nanocarriers for cancer nano-immunotherapy. *Drug Deliv Transl Res*. (2023) 13:1936–54. doi: 10.1007/s13346-022-01241-3

105. Liu J-M, Lin P-H, Hsu R-J, Chang Y-H, Cheng K-C, Pang S-T, et al. Complementary traditional chinese medicine therapy improves survival in patients with metastatic prostate cancer. *Med (Baltimore)*. (2016) 95:e4475. doi: 10.1097/MD.0000000000004475

106. Lu X, Yang F, Chen D, Zhao Q, Chen D, Ping H, et al. Quercetin reverses docetaxel resistance in prostate cancer via androgen receptor and PI3K/akt signaling pathways. *Int J Biol Sci*. (2020) 16:1121–34. doi: 10.7150/ijbs.41686

107. Wen D, Peng Y, Lin F, Singh RK, Mahato RI. Micellar delivery of miR-34a modulator rubone and paclitaxel in resistant prostate cancer. *Cancer Res*. (2017) 77:3244–54. doi: 10.1158/0008-5472.CAN-16-2355

108. Adamaki M, Zoumpourlis V. Prostate cancer biomarkers: from diagnosis to prognosis and precision-guided therapeutics. *Pharmacol Ther*. (2021) 228:228107932. doi: 10.1016/j.pharmthera.2021.107932

109. Egli M, Manoharan M. Re-engineering RNA molecules into therapeutic agents. *Acc Chem Res*. (2019) 52:1036–47. doi: 10.1021/acs.accounts.8b00650

110. Shorning BY, Dass MS, Smalley MJ, Pearson HB. The PI3K-AKT-mTOR pathway and prostate cancer: at the crossroads of AR, MAPK, and WNT signaling. *Int J Mol Sci*. (2020) 21:4507. doi: 10.3390/ijms21124507

111. Al-Asaaed S, Winquist E. Custirsen (OGX-011): clusterin inhibitor in metastatic prostate cancer. *Curr Oncol Rep*. (2013) 15:113–8. doi: 10.1007/s11912-012-0285-1

112. Mitchell MJ, Billingsley MM, Haley RM, Wechsler ME, Peppas NA, Langer R. Engineering precision nanoparticles for drug delivery. *Nat Rev Drug Discovery*. (2021) 20:101–24. doi: 10.1038/s41573-020-0090-8

113. Najahi-Missaoui W, Arnold RD, Cummings BS. Safe nanoparticles: are we there yet? *Int. J Mol Sci*. (2020) 22:385. doi: 10.3390/ijms22010385

114. Lee CYF, Rennie PS, Jia WWG. MicroRNA regulation of oncolytic herpes simplex virus-1 for selective killing of prostate cancer cells. *Clin Cancer Res*. (2009) 15:5126–35. doi: 10.1158/1078-0432.CCR-09-0051

115. Tatarano S, Chiyomaru T, Kawakami K, Enokida H, Yoshino H, Hidaka H, et al. miR-218 on the genomic loss region of chromosome 4p15.31 functions as a tumor suppressor in bladder cancer. *Int J Oncol*. (2011) 39:13–21. doi: 10.3892/ijo.2011.1012

116. Leite KRM, Sousa-Canavez JM, Reis ST, Tomiyama AH, Camara-Lopes LH, Sañudo A, et al. Change in Expression of miR-Let7c, miR-100, and miR-218 from High Grade Localized Prostate Cancer to Metastasis. *Urol Oncol Semin Orig Investig*. (2011) 29:265–9. doi: 10.1016/j.urolonc.2009.02.002

117. Sweeney C, Bracarda S, Sternberg CN, Chi KN, Olmos D, Sandhu S, et al. Ipatasertib plus abiraterone and prednisolone in metastatic castration-resistant prostate cancer (IPATential150): A multicentre, randomised, double-blind, phase 3 trial. *Lancet Lond Engl*. (2021) 398:131–42. doi: 10.1016/S0140-6736(21)00580-8

frontiers | Frontiers in Pharmacology

TYPE Systematic Review
PUBLISHED 19 March 2025
DOI 10.3389/fphar.2025.1502107

Check for updates

OPEN ACCESS

EDITED BY
Heike Wulff,
University of California, Davis, United States

REVIEWED BY
Gonçalo Garcia,
Research Institute for Medicines (iMed.ULisboa), Portugal
Sankar Jagadeeshan,
Ben-Gurion University of the Negev, Israel

*CORRESPONDENCE
Babban Jee,
babban.jee@manipal.edu

‡PRESENT ADDRESS
Sayan Kumar Das,
Department of Pharmacology, Apollo Institute of Medical Sciences and Research Chittoor, Andhra Pradesh, India
Sameer Khasbage,
Department of Pharmacology, All India Institute of Medical Sciences, Raipur, India
Ashim Mishra,
Department of Forensic Medicine, Rohilkhand Medical College, Bareilly, Uttar Pradesh, India

RECEIVED 26 September 2024
ACCEPTED 18 February 2025
PUBLISHED 19 March 2025

CITATION
Das SK, Khasbage S, Mishra A and Jee B (2025) Prognostic and clinicopathological roles of circular RNA expression in chemoresistance in head and neck squamous cell carcinoma: a systematic review.
Front. Pharmacol. 16:1502107.
doi: 10.3389/fphar.2025.1502107

COPYRIGHT
© 2025 Das, Khasbage, Mishra and Jee. This is an open-access article distributed under the terms of the Creative Commons Attribution License (CC BY). The use, distribution or reproduction in other forums is permitted, provided the original author(s) and the copyright owner(s) are credited and that the original publication in this journal is cited, in accordance with accepted academic practice. No use, distribution or reproduction is permitted which does not comply with these terms.

Prognostic and clinicopathological roles of circular RNA expression in chemoresistance in head and neck squamous cell carcinoma: a systematic review

Sayan Kumar Das[1‡], Sameer Khasbage[2‡], Ashim Mishra[3‡] and Babban Jee[4*]

[1]Department of Pharmacology, Manipal Tata Medical College, Manipal Academy of Higher Education, Manipal, India, [2]Department of Pharmacology, People's College of Medical Sciences and Research, Bhopal, India, [3]Department of Forensic Medicine, Manipal Tata Medical College, Manipal Academy of Higher Education, Manipal, India, [4]Department of Research, Manipal Tata Medical College, Manipal Academy of Higher Education, Manipal, India

Background: Characterized by a poor prognosis and survivability, head and neck squamous cell carcinoma (HNSCC) is an aggressive neoplastic condition with a propensity for recurrence where the development of chemoresistance adversely affects the prognostic outcome. Recently, it was shown that circular RNAs (circRNAs) augment the cellular survivability and chemoresistance of malignant cells. Hence, biomarkers for early detection of chemoresistance in these patients can significantly aid in preventing a poor prognostic outcome.

Objective: The present study aimed to systematically identify circRNAs that play a vital role in the development of chemoresistance in HNSCC and understand their mechanisms of action in HNSCC chemoresistance.

Methods: The protocol was prospectively registered on PROSPERO with protocol no. CRD42024532291. A six-stage methodological and PRISMA recommendations were followed for the review.

Results and Discussion: 13 studies were identified which yielded 13 circRNAs which have been investigated for their role in the chemoresistance in HNSCC. Of these, 11 circRNAs were reported to be upregulated while only 2 circRNAs were found to be downregulated. Moreover, we found that circRNAs can modulate autophagy (circPARD3, circPKD2, circAP1M2 and circPGAM1), apoptosis (circ-ILF2, circANKS1B, circTPST2, circPUM1 and circ_0001971), drug efflux (circ-ILF2, has_circ_0005033 and circTPST2), EMT (circANKS1B, circCRIM1, circ_0001971), tumor microenvironment (circ-ILF2. circ-ILF2, circCRIM1 and circTPST2), DNA damage (circTPST2) and malignant potential (hsa_circ_0000190 and hg19_circ_0005033).

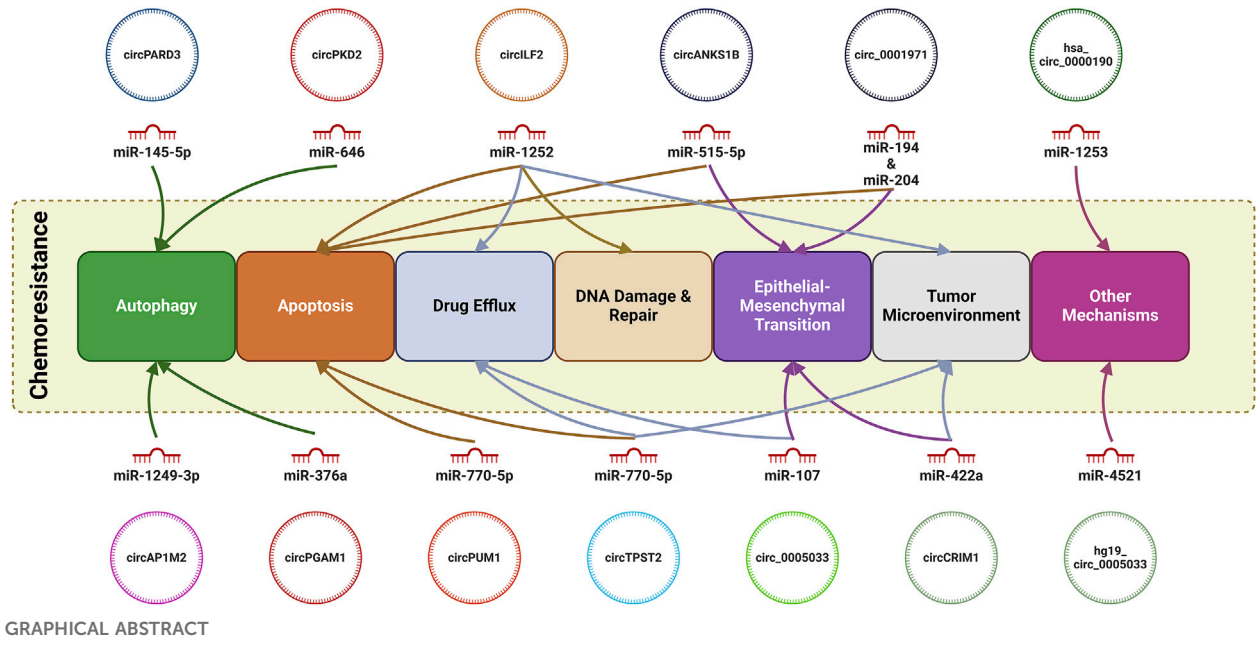
Conclusion: The present study identified 13 circRNAs which may serve as biomarkers for prognosis as well as response to chemotherapy in HNSCC.

10.3389/fphar.2025.1502107

Systematic Review Registration: PROSPERO, identifier CRD42024532291.

KEYWORDS

circular RNA, microRNA, biomarker, chemoresistance, head and neck squamous cell carcinoma, systematic review



GRAPHICAL ABSTRACT

1 Introduction

Malignancies arising from the squamous cell lining of the tissues of the oral cavity, nasal cavity, pharynx, larynx, lip, paranasal sinuses and salivary glands, collectively are termed as head and neck squamous cell carcinoma (HNSCC). With a prevalence of an estimated 890,000 new cases and 450,000 deaths per year, HNSCC poses a serious health problem in especially in South and Southeast Asian countries and accounts for 4.5% of cancer diagnosis globally. With an annual incidence of about 380,000 cases, oral squamous cell carcinomas (OSCCs) are the most common form of HNSCC, followed by laryngeal squamous cell carcinoma (LSCC), nasopharyngeal carcinoma, and cancers of the hypopharynx and salivary glands (Barsouk et al., 2023).

Risk factors for the development of HNSCC can be both non-infectious such as consumption of tobacco with or without areca nut and alcohol, exposure to carcinogenic environmental pollutants including organic, inorganic chemicals, particulate matter (PM), poor oral hygiene, malnutrition/diet lacking fruit and green vegetables, ageing or infectious such as human papillomavirus (HPV) for oropharyngeal carcinoma and Epstein-Barr virus (EBV) for nasopharyngeal carcinoma (Johnson et al., 2020).

Depending on the primary tumor location and TNM staging, the treatment options entail surgery, radiation and chemotherapy in various combinations. In 40% of the patients, presenting at an early stage (Stage I and II) of the disease, surgery is the primary modality of treatment whereas for patients with advanced disease (Stage II and IV), irrespective of the resectability of the tumor, the palliative treatment involves platinum-based chemotherapy and radiation, with or without induction chemotherapy (Marur and Forastiere, 2016). The addition of targeted therapy along with cytotoxic chemotherapy although has resulted in the prolongation of the median survival time to 10 months, this is indicative of the lack of chemotherapeutic efficacy for these patients (Sacco and Cohen, 2015). The development of chemoresistance in patients of HNSCC remains a major cause of concern as it worsens the prognostic outcome. A plethora of mechanisms for development of chemoresistance in HNSCC have been postulated which includes aberrant modulation of pathways regulating apoptosis, DNA damage and repair, epithelial mesenchymal transition (EMT),

Abbreviations: circRNA, Circular RNA; ceRNA, Competitive endogenous RNA; EBV, Epstein-Barr virus; EGFR, Epidermal growth factor; EMT, Epithelial mesenchymal transition; FOXQ1, Forkhead box Q1; HDGF, Hepatoma-derived growth factor; HNSCC, Head and neck squamous cell carcinoma; HPV, Human papillomavirus; IGF1R, Insulin-like growth factor 1 receptor; KFL8, Krüppel-like factor 8; LC3B-II, Light chain 3B-II; LSCC, Laryngeal squamous cell carcinoma; MMP-2, Matrix metalloproteinase-2; NAP1L1, Nucleosome assembly protein 1-like 1 protein; ncRNA, Non-coding RNA; NPC, nasopharyngeal carcinoma; NSCLC, Non-small cell lung cancer; OSCC, Oral squamous cell carcinoma; p-FAK, Phospho-focal adhesion kinase; PIK3CA/AKT-mTOR, Phosphatidylinositol 3-kinase alpha/AKT-mammalian target of rapamycin; PM, Particulate matter; TGF- α, Transforming growth factor-α; VEGF, Vascular endothelial growth factor.

modulation of cell cycle phases, cancer stem cells, epigenetic modulation, non-coding RNA (ncRNA) processing, regulation of autophagy and immune cell interactions (Khera et al., 2023). Stemming from a poor understanding of the molecular mechanism(s) of malignancy, patients of HNSCC are subjected to the same standardized regimen irrespective of their genetic variability. Hence, investigation for the elicitation of molecular biomarkers of HNSCC will not only aid in the stratification of the patients by personalizing the therapeutic approaches but also aid in minimizing toxicity and predicting the prognostic and therapeutic outcome (Khera et al., 2023).

Circular RNAs (circRNAs) are covalently closed circular molecules of endogenous RNA which are refractory to the actions of RNA exonuclease due to the absence of 5′ or 3′ termini, thus, making them more stable than linear RNA molecules such as microRNAs (miRNAs) or long non-coding RNAs (lncRNAs) and this feature makes them ideal candidates for use as biomarkers (Liu and Chen, 2022). CircRNAs have been implicated as key regulators of various physiological and pathological conditions, including malignancies and their expression is tissue and cell specific (Hwang and Kim, 2024). Acting primarily as competing endogenous RNAs (ceRNAs), circRNAs, by sponging of miRNAs, regulate the expression of downstream miRNA target genes by alleviating the inhibitory effects of the miRNA. Additionally, some circRNA, by binding to RNA-binding proteins or translating into proteins can modulate biological functions (Bach et al., 2019). In cancers, circRNAs have been observed to induce the development of chemoresistance by augmenting the efflux of drugs, regulation of apoptosis, modulation of the tumor microenvironment, autophagy and dysregulation of DNA repair (Liu et al., 2022).

In this review, we aim to systematically identify circRNAs played regulatory role in chemoresistance and explore their underlying mechanism(s) in HNSCC for application as predictive biomarkers for prognosis and response to chemotherapy.

2 Methods

2.1 Protocol and registration

The present systematic review was done as per the "PRISMA (Preferred Reporting Items for Systematic Reviews and Meta-Analyses)" statement (PRISMA statement, 2024). The protocol was prospectively registered with PROSPERO (International Prospective Register of Systematic Reviews) (Protocol No. CRD42024532291).

2.2 Criteria for study selection

Randomized and non-randomized controlled trials, observational studies, animal studies, *in vitro* studies were considered for the inclusion whereas systematic reviews (with or without meta-analysis), narrative reviews, editorials, letters to the editor, conference proceedings and abstracts and *in silico* studies were excluded. Studies which were published in English language or could be translated to English language were considered for the review.

2.3 Search strategy and study selection

The search strategy was created after reviewing published literature and discussion among the coauthors. An electronic literature search was performed in PubMed, Embase, Web of Science and Cochrane Library using predetermined keywords and MeSH terms. A bibliographic search of the articles included in the review was also performed. The detailed search strategy was mentioned in the Supplementary Material (Supplementary Table S1).

2.4 Data extraction

The search of four databases yielded a total of 161 articles on 27 March 2024. Of 161 articles, 46 articles were retrieved from PubMed, 97 articles from Embase, 18 articles from Web of Science and zero articles from Cochrane Library (Figure 1). All articles were exported to Microsoft Excel. Duplicates were removed using the Title-Author-Date of Publication criteria. In the first phase, title/abstract screening was performed by two individual reviewers (AM and SK) to remove 19 duplicates. The remaining 142 articles were screened for each step of the screening process in the second phase (SKD and SK) and full text screening for the assessment of eligibility for inclusion was performed by two independent authors (SKD and BJ). The bibliography of the articles included for review was also screened for identification of eligible articles for inclusion by two authors (AM and BJ). Two authors (SKD and SK) independently extracted the data using a pre-structured form where the details were recorded as: author, year, country, type of HNSCC, circRNA, circRNA regulation, target miRNA and other downstream effectors. Any discrepancy, arising at any stage of the of the review was addressed by discussion among the authors till a consensus was reached.

2.5 Study outcome

This study aimed primarily to evaluate the role of circRNAs in chemoresistance in HNSCC as well as to assess their prognostic potential in HNSCC cases.

2.6 Quality assessment of studies

Two authors (SKD and SK) assessed the risk of bias and applicability concerns independently using QUADAS-2 tool (A tool for the quality assessment for diagnostic accuracy studies) (QUADAS-2, 2024). The studies were assessed for Risk of Bias and Applicability Concerns. The risk of bias dimension had four domains whereas the dimension of applicability concerns had three domains. For risk of bias assessment, each domain was graded as "yes," "no" and "unclear" whereas each domain for applicability concern was graded as "high" "low" or "unclear."

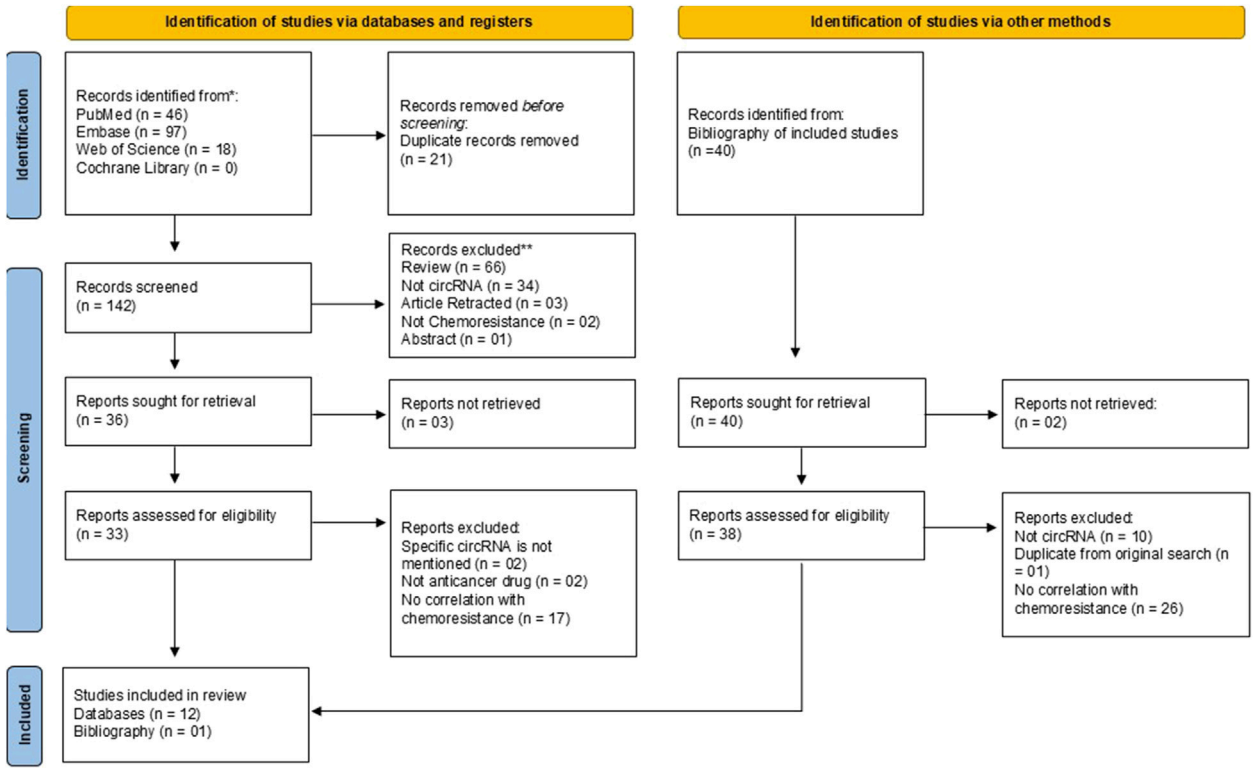


FIGURE 1
PRISMA flow diagram.

2.7 Data synthesis and summary measures

The data extracted were categorized, interpreted, and grouped according to the similarity of the data for the narrative synthesis.

3 Results

3.1 Study selection

Following the search, a total of 161 records from four databases were obtained. After the removal of duplicates, there were 142 records screened for eligibility, out of which 36 records were sought for retrieval. A total of 12 studies from three databases were included for the review. From the bibliography of the included 12 studies, 40 studies were identified and sought for retrieval, out of which 38 were assessed for inclusion into the review. Of 38, only 1 study was found eligible. The PRISMA flow diagram (Figure 1) outlines the process of selections for the included studies.

3.2 Risk of bias and applicability concerns within studies

A summary of the quality assessment of the included studies using QUADAS-2 has been given in Figure 2. Only one study fulfilled all the domains as mentioned under risk of bias in the QUADAS-2 quality assessment tool whereas most studies satisfied only 2 domains. Only four studies satisfied 2 domains pertaining to applicability concerns and none satisfied all three domains.

3.3 Study characteristics

The characteristics of studies included in the review have been summarized in Table 1.

3.4 Differentially expressed circRNAs

3.4.1 circPARD3

Gao et al., in their study, identified a novel autophagy-suppressive cytoplasmic circRNA, i.e., circPARD3, which was significantly upregulated in LSCC samples. miR-145-5p was identified as a downstream target for circPARD3, where the sponging of miR-145-5p by circPARD3 alleviated its inhibitory effects resulting in the overexpression of oncogene PRKCI. circPARD3 was found to inhibit autophagy via the modulation of the miR-145-5p-PRKCI-Akt-mTOR pathway, resulting in augmentation of the neoplastic potential of LSCC and precipitation of chemoresistance. The level of expression of circPARD3 is LSCC was seen to be directly corelated with the malignant progression and worsening of the prognostic outcome (Gao et al., 2020).

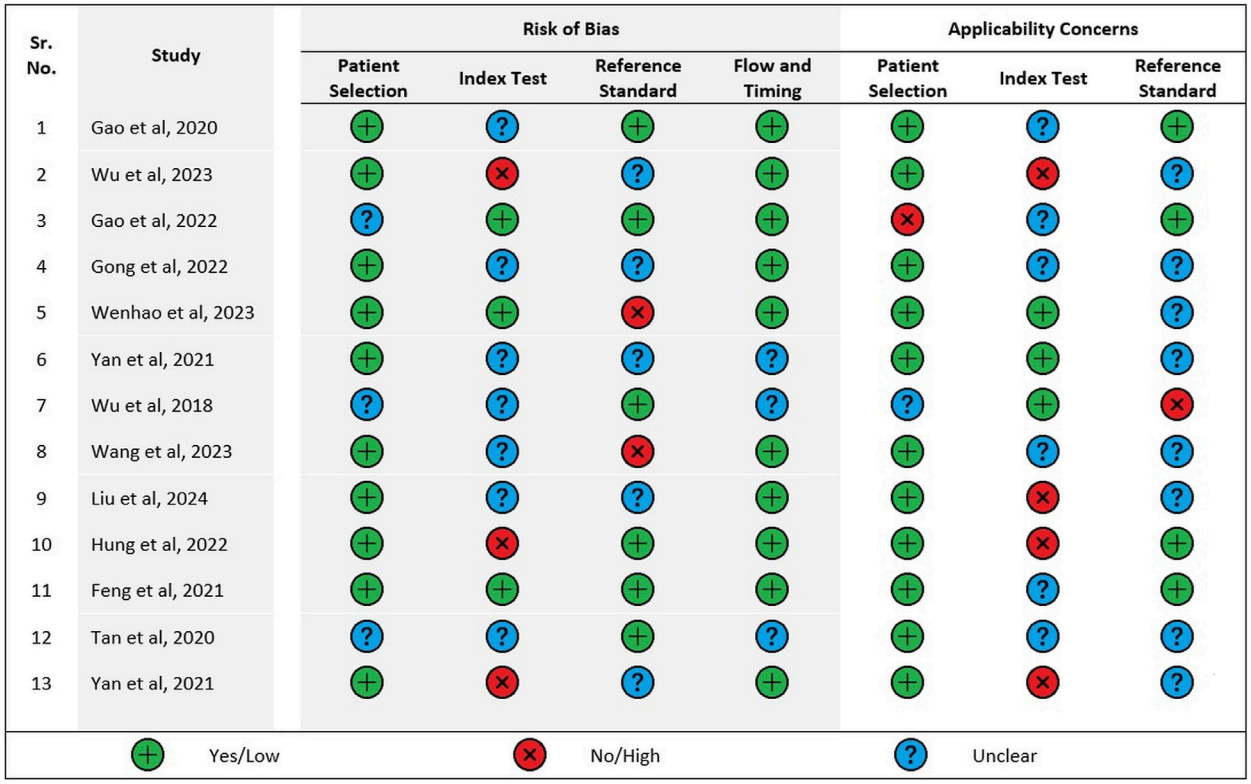


FIGURE 2
Quality assessment of included studies using QUADAS-2.

3.4.2 circPKD2

Gao and his colleagues observed that circPKD2 was significantly downregulated in OSCC cells. Further, they found that circPKD2 promotes autophagy by sponging of miR-646 which in turn negated its suppressive effects on Atg13. The decreased expression of circ-PKD3 in OSCC cells was associated with tumor proliferation, invasion and chemoresistance (Gao et al., 2022).

3.4.3 circAP1M2 (hsa_circ_0049282)

In the study conducted by Wenhao and his group, an increased expression of circAP1M2 in OSCC tissue was observed. In comparison to parental cells, circAP1M2 was noted to be significantly overexpressed in cisplatin-resistant OSCC cells. circAP1M2 was found to regulate autophagy by sponging of miR-1249-3p which in turn modulates the expression of ATG9A (Wenhao et al., 2023).

3.4.4 circPGAM1

Feng et al. observed the upregulation of circPGAM1 in laryngocarcinoma tumors where the level of expression of circPGAM1 showed a positive correlation with the higher stages (Stages III and IV) of malignancy in comparison to the lower stages (Stages I and II). circPGAM1 was seen to promote chemoresistance as its downregulation was associated with a decrease in cell viability in the presence of cisplatin. MiR-376a was identified as the downstream target of circPGAM. MiR-376a inhibited the circPGAM1 induced increase in cell viability under cisplatin. ATG2A was identified as a downstream factor for miR-376a where the miR-mediated inhibition of ATG2A promoted cisplatin sensitivity (Feng et al., 2021).

3.4.5 circ-ILF2 (hsa_circ_00428)

Wu et al. identified upregulated circ-ILF2 (hsa_circ_00428) in CDDP-resistant OSCC cells. miR-1252 was identified as a target for circ-ILF2, where sponging of miR-1252 inhibited the latter's effects on KLF8 expression, resulting in the development of cisplatin resistance in OSCC cells because of impairment of cisplatin-induced apoptotic machinery. circ-ILF2 was also found to promote the M2 polarization of macrophages (Wu et al., 2023).

3.4.6 circ_0005033 (hsa_circ-0005033)

In a study, Gong and co-workers observed that circ_0005033 was upregulated in LSCC specimens. miR-107 was identified as the target for circ_0005033 and the relationship was seen to be an inverse linear correlation. The upregulation of circ_0005033 and inhibition of miR107 were associated with augmentation of LSCC cell viability, proliferation, metastasis and chemoresistance to cisplatin. The downstream effector for miR107 was identified to be IGF1R (Gong et al., 2022).

3.4.7 circANKS1B (hsa_circ_0007294)

In a study, we demonstrated the elevated levels of circANKS1B and TGF-β1 in OSCC tissues in comparison to the para-tumor samples and suggested a positive correlation where circANKS1B was found to regulate the expression of TGF-β1 in OSCC. circANKS1B

TABLE 1 Characteristics of included studies.

No	Author (Year)	Country	Type of HNSCC	circRNA	circRNA regulation	Chemotherapeutic agent	Target miRNA	Other downstream targets
1	Gao et al. (2020)	China	Laryngeal squamous cell carcinoma (LSCC)	circPARD3	Upregulated	Cisplatin	miR-145-5p	PRKCI
2	Wu et al. (2023)	China	Oral squamous cell carcinoma (OSCC)	circ-ILF2 (hsa_circ_001428)	Upregulated	Cisplatin	miR-1252	KLF8
3	Gao et al. (2022)	China	Oral squamous cell carcinoma (OSCC)	circ-PKD2	Downregulated	Cisplatin	miR-646	Atg13
4	Gao et al. (2022)	China	Laryngeal squamous cell carcinoma (LSCC)	hsa_circ_0005033	Upregulated	Cisplatin	miR-107	IGF1R
5	Wenhao et al. (2023)	China	Oral squamous cell carcinoma (OSCC)	circAP1M2	Upregulated	Cisplatin	miR-1249-3p	ATG9A
6	Yan and Xu (2021)	China	Oral squamous cell carcinoma (OSCC	circANKS1B	Upregulated	Cisplatin	miR-515-5p	TGF- β1
7	Wu et al. (2018a)	China	Laryngeal squamous cell carcinoma (LSCC)	hg19_circ_0005033	Upregulated	Cisplatin	miR-4521	-
8	Wang et al. (2023)	China	HNSCC subtype not specified	circTPST2	Upregulated	Cisplatin	miR-770-5p	Nucleolin
9	Liu et al. (2024)	China	Oral squamous cell carcinoma (OSCC)	circPUM1	Upregulated	Cisplatin	miR-770-5p	NK cells & NAP1L1
10	Hung et al. (2022)	Taiwan	Oral squamous cell carcinoma (OSCC)	hsa_circ_0000190	Downregulated	Cisplatin	-	-
11	Feng et al. (2021)	China	Laryngeal squamous cell carcinoma (LSCC)	circPGAM1	Upregulated	Cisplatin	miR-376a	ATG2A
12	Tan et al. (2020)	China	Oral squamous cell carcinoma (OSCC)	circ_0001971	Upregulated	Cisplatin	miR-194 & miR-204	-
13	Hong et al. (2020)	China	Nasopharyngeal carcinoma	circCRIM1	Upregulated	Docetaxel	miR-422a	FOXQ1

upregulation was associated with an elevation of the metastatic potential of the OSCC cells. Downregulation of circANKS1B resulted in decreased cell viability when exposed to cisplatin and an increase in the activity of caspase-3. The expression of miR-515-5p was seen to be noticeably downregulated in OSCC and a direct interaction with circANKS1B was noted suggesting of miRNA sponging. miR-515-5p was observed to reduce the mRNA levels of TGF- β1 suggestive of a circANKS1B/miR-515-5p/TGF- β1 axis (Yan and Xu, 2021).

3.4.8 hg19_circ_0005033

Wu et al., in their study, observed high level expression of hg19_circ_0005033 in TDP cells of LSCC. siRNA transfection induced downregulation of hg19_circ_0005033 which inhibited proliferation, migration and invasion of TDP cells and an enhancement of chemosensitivity. An inverse relationship between hg19_circ_0005033 and miR-4521 was observed which suggests that hg19_circ_0005033 exerts its action via the sponging of miR-4521. STAT5A was identified as the target for miR4521 and downregulation of miR-4521, due to the sponging by hg19_circ_0005033, upregulated the expression of hg19_circ_0005033 via the hg19_circ_0005033/miR-4521/STAT5A axis (Wu Q. et al., 2018).

3.4.9 circTPST2

Wang et al. identified circTPST2 to be relatively highly expressed in HNSCC in comparison to the adjacent tissue. miR-770-5p was identified as the downstream target for circTPSP2. Further, physical interaction between circPTST2 and nucleolin and regulation of nucleolin by miR-770-5p were established. We found that circTPSP2 regulates cisplatin chemosensitivity by sponging miR-770-5p which in turn modulated the Nucleolin dual pathway (Wang et al., 2023).

3.4.10 circPUM1

Liu et al. observed the overexpression of circPUM1 in OSCC and this overexpression was regulated by the upstream factor, SP2. An inverse relationship was observed between circPUM1 and susceptibility of NK cells where high expression of circPUM1 decreased the susceptibility of OSCC cells to NK cells. The downstream target for circPUM1 was identified to be miR-770-5p playing a role in cisplatin chemoresistance and susceptibility to NK cells of OSCC cells. Overexpression of miR-770-5p was associated with a decrease in cellular viability whereas downregulation was associated with an increase in cellular viability. Nucleosome assembly protein 1-like 1 protein (NAP1L1) was identified as a downstream target for miR-770-5p which shows an inversely correlated relationship whereas an elevated expression of miR-770-5p inhibits NAP1L1 expression. Similarly, an elevated expression of circPUM1 was found to downregulate the expression of NAP1L1 which is suggestive of an axis comprising of circPUM1/miR-770-5p/NAP1L1 (Liu et al., 2024).

3.4.11 circ_0001971

Tan et al. observed significant upregulation of circ_0001971 in OSCC tumor tissues in comparison to normal tissue and the elevated expression was seen to be associated with increase in cellular proliferation, migration, invasion and EMT. The expression of circ_0001971 was significantly elevated in higher stages (Stage III and IV) of the malignancy in comparison to the lower stages (Stages I and II) and was suggestive of a relationship where the level of expression has direct correlation with the five-year survival rate. Suppression of circ_0001971 expression inhibited tumorigenesis and progression while augmenting the induction of apoptosis and chemosensitivity to cisplatin. miR-194 and miR-204 were identified as downstream targets for circ_0001971 where overexpression of the two miRNAs inhibited the expression and function of circ_0001971 suggesting that circ_0001971 functions as a ceRNA for the two miRNAs (Tan et al., 2020).

3.4.12 circCRIM1 (has_circ_0002346)

Hong et al. observed overexpression of circCRIM1 in highly metastatic nasopharyngeal carcinoma (NPC) cells. circCRIM1 was found to induce migration, invasion and EMT in NPC cells. miR-422a was identified as a downstream target for circCRIM1 and was found to be downregulated. Transcription factor forkhead box Q1 (FOXQ1), an oncogene, was identified as a target for miR-422a. circCRIM1 was noted to upregulate FOXQ1 by the attenuation of the posttranscriptional suppression activity of miR-422a. circCRIM1 downregulation enhanced docetaxel sensitivity of NPC cells. Hence, circCRIM1, functioning as a ceRNA, sponges miR-422a to alleviate its inhibitory effects on FOXQ1 in nasopharyngeal carcinoma, promoting metastasis and chemoresistance (Hong et al., 2020).

3.4.13 hsa_circ_0000190

Hung et al. investigated the expression of hsa_circ_0000190 and hsa_circ_0001649, which have previously been reported as potential cancer biomarkers, in plasma of OSCC patients with an aim of improving risk stratification of recurrence, metastasis and chemoresistance. Both hsa_circ_0000190 and hsa_circ_0001649 were found to be downregulated in OSCC in comparison to normal healthy individuals with the downregulation of hsa_circ_0000190 being highly statistically significant ($p < 0.0001$) in the late stage. hsa_circ_0000190 could effectively differentiate OSCC from normal healthy individuals. Decreased expression of hsa_circ_0001649 in OSCC patients was correlated with an increased risk of early recurrence and poor overall survival. When the pre- and post-induction of chemotherapy expression levels of both circRNAs were evaluated, a trend of increase in expression of hsa_circ_0000190 was observed which is suggestive of a correlation to induction chemotherapy in OSCC whereas no such correlation was observed with hsa_circ_0001649 (Hung et al., 2022).

4 Discussion

A comprehensive literature search was performed using four databases followed by a bibliographic search of included articles was performed from which a total of 13 studies investigating the role of circRNAs in the development of chemoresistance in HNSCC were included for the present review. We identified 13 cirRNAs which have a pivotal role in chemotherapy resistance in HNSCC cases. Of these 13 circRNAs, 12 circRNAs (circPARD3, circ-ILF2, cricPKD2, hsa_circ_0005033, circAP1M2, circANKS1B, hg19_circ_0005033, circTPST2, circPUM1, has_circ_0000190, circPGAM1, and circ_0001971) were investigated for drug-resistance with cisplatin whereas only 1 circRNA (circCRIM1) was investigated for Docetaxel. While most circRNAs were upregulated, only circRNA has_circ_0000190 was found to be downregulated.

Autophagy, mediated by autophagosomes, is a physiological intracellular pathway responsible for the degradation and elimination of misfolded proteins and damaged cell organelles during stressful cellular environments for maintaining cellular metabolism, energy homeostasis and promoting cellular survival (Yun and Lee, 2018). Autophagy can play a dual role in tumorigenesis as it modulates both, as a mechanism of tumor suppression or as a mechanism of cyto-protection, promoting cellular adaptation to hypoxic microenvironment which in turn facilitates chemoresistance (Yang et al., 2011). Chemotherapeutic agents like cisplatin exert their anti-neoplastic activity by the induction of autophagy, whereas modulation of autophagy can be an important aspect of enhancing chemotherapeutic sensitivity while decreasing chemoresistance specially pertaining to drug like cisplatin (Xu and Gewirtz, 2022). Hence, modulation of autophagy may aid in reducing chemoresistance and augment the sensitivity of the neoplastic cells to these chemotherapeutic agents (Pu et al., 2022). Studies demonstrated that circPARD3 inhibits autophagy by the modulation of circPARD3/miR-145-5p/PRKCI axis which in turn inhibits the PIK3CA/AKT-mTOR signaling pathway. mTOR activation via the PIK3CA/AKT-mTOR signaling pathway regulates multiple cellular processes, such as growth, proliferation, metabolism and survival which, due to constitutive activation in malignancies, drives uncontrolled cellular growth and proliferation while inhibiting apoptosis (Zheng et al., 2024). MiR-145-5p is a suppressor of tumorigenesis and an enhancer of autophagy (Gao et al., 2020). CircPARD3, by sponging miR-145-5p, downregulates its expression. The downregulation of miR-145-5p in turn

suppresses the expression of PRKCI (Kim et al., 2020). First classified as a human oncogene in lung and ovarian carcinomas, PRKCI, via the inhibition of PIK3CA/AKT-mTOR signaling pathway, inhibits autophagy as reflected by a decrease in the light chain 3B-II (LC3B-II) protein, increase in p62 and weakened degradation of both endogenous and exogenous autophagic substrates (Qu et al., 2016; Inman et al., 2022). Due to the downregulation of the inhibitory effect of miR-145-5p by circPARD3, the resultant overexpression of PRKCI potentiated the migration and invasion of the LSCC cells while making them refractory to the therapeutic effects of cisplatin. Although no established PRKCI inhibitors are available for clinical use (Jiao et al., 2023), PI3K enzyme inhibitors such as buparlisib and alpelisib have the potential to improve the therapeutic outcome in patients with HNSCC (Jung et al., 2018; Razak et al., 2023). Similarly, mTOR inhibitors like everolimus have been investigated for used as an adjuvant therapy in advanced HNSCC with promising therapeutic outcomes (Nathan et al., 2022; Massarelli et al., 2015).

Cytoprotective autophagy, by the degradation of damaged organelles and preventing DNA damage, enhances cellular survival in turn promoting tumorigenesis and predisposes the development of resistance to chemotherapeutic agents (Zhang et al., 2022). Autophagosomes are double layered vesicles which form an integral component of the intracellular degradation pathway in autophagy where they deliver degraded cytoplasmic components to the lysosome for recycling (Yun and Lee, 2018). Although primarily aimed at maintaining homeostasis by facilitating the recycling of damaged cell organelles and in turn preventing tumorigenesis, autophagy under conditions of cellular stress, such as hypoxia, nutrient deprivation and chemotherapy-induced therapeutic pressure and under the influence of factors secreted by immune and stromal cells of the tumor microenvironment, aids in the recycling of cellular components which facilitates equitable distribution of nutrients and energy among the cancer cells (Chavez-Dominguez et al., 2020). The activation of autophagy-related genes, such as ATG5 and ATG7, facilitates the shift from tumor suppression to cytoprotective autophagy and hence, alteration in expression of these gene may improve the effectiveness of chemotherapeutic agents (Chavez-Dominguez et al., 2020).

CircPKD2 was observed to augment cytoprotective autophagy via the modulation of the circPKD2/miR-646/Atg13 pathway (Gao et al., 2022). Atg13 is an essential component in the early stages of autophagosome formation which, depending on its state of phosphorylation, can promote or inhibit autophagy (Bhattacharya et al., 2024). Moreover, circPKD2 was found to promote apoptosis via autophagy and in turn promoting cisplatin sensitivity by up-regulating Atg13. circPKD2 augments caspase-8 and caspase-3 cleavage (Xu and Gewirtz, 2022). Caspase-8 acts as the initiator caspase for extrinsic apoptosis (Fritsch et al., 2019) whereas caspase-3 is a part of the intrinsic apoptotic pathway and plays a role in DNA and cytoskeletal protein degradation (Brentnall et al., 2013). It was previously observed that caspase-8 activation can induce caspase-9 (Li et al., 1998), but in some studies, it was demonstrated that cisplatin-induced apoptosis was associated with the upregulation of caspase-9 activity whereas caspase-8 activity was seen to be unchanged (Park et al., 2002; Garcia-Berrocal et al., 2007). Hence, further work is warranted for examining the role of circPKD2 induced caspase-8 activity in relation to chemoresistance to cisplatin.

circAP1M2 via the regulation of miR-1249-3p modulated the expression of ATG9A (Wenhao et al., 2023). ATG9A is a multi-spanning membrane protein and plays a role in the early stages of autophagy by contributing to the expansion of the phagophore and lipid mobilization from the lipid droplets to the autophagosomes and mitochondria (Mailler et al., 2021). MiR-1249-3p has previously been implicated in augmenting the malignant potential of multiple cancers (Chen et al., 2019). The expression of miR-1249-3p was seen to be downregulated in the OSCC cells and this was primarily due to the overexpression of circAP1M2 suggesting a relationship which was negatively correlated. Sponging of the miR-1249-3p alleviated its inhibitory effects on ATG9A. This phenomenon suggested that the underlying mechanism of cisplatin resistance in OSCC may be induction of cytoprotective autophagy. Earlier it was observed that cisplatin induces both, non-protective as well as cytotoxic autophagy, which can be modulated via an "autophagic switch" stemming from the alteration of expression of specific genes (Xu and Gewirtz, 2022). Although no therapeutic modality is available for the negation of ATG, concomitant administration of mTOR inhibitors, chloroquine and hydroxychloroquine, which have been seen to play a role in the regulation of autophagy, may aid in the alleviation of chemoresistance by the modulation of this "autophagic switch" (Wang G. J. et al., 2020).

Similarly, circPGAM1, by sponging miR-376a, upregulated the expression of ATG2A (Feng et al., 2021). MiR-376a is a known tumor suppressor as well as a promoter of apoptosis in multiple cancers such as renal cell carcinoma (Fan et al., 2019) and osteosarcoma (Fellenberg et al., 2019), among others. In HNSCC, miR-376a has been observed to play a similar role by inhibiting ATG2A (Feng et al., 2021). ATG2A is a lipid transfer protein which plays a role in autophagosome assembly and transfer of lipids from membrane vesicles to other vesicles (Maeda et al., 2019). As a part of the ATG9/ATG12-WIPI complex, it plays a role in the recruitment of ATG9 for the expansion of autophagosomes (Li et al., 2020). The downregulation of ATG2A has been observed to induce an accumulation of immature autophagosome membranes which in turn promote the activation of non-canonical caspase-8 via an intracellular death-inducing signaling complex (DISC) (Tang et al., 2017). Hence, circPAGM1 mediated upregulation of ATG2A resulted in the induction of cytoprotective autophagy which precipitates cisplatin chemoresistance. Figure 3 delineates the roles of the identified circRNA in the autophagy pathway in cancer chemoresistance.

An important mechanism of development of chemoresistance is an increase in the efflux of cytotoxic drugs (Kannampuzha and Gopalakrishnan, 2023). The upregulation of circILF2 (hsa_circ_00428) in OSCC, by sponging miR-1252, alleviated its inhibitory effects on KFL8 which in turn preventing cisplatin-induced apoptosis (Wu et al., 2023). As a regulator of gene transcription, Krüppel-like factor 8 (KFL8), plays a vital role in multiple cellular process such as differentiation, apoptosis, drug resistance and inflammation, and has been implicated in the progression of various neoplastic conditions including triple negative breast cancer (TNBC), lung adenocarcinoma, hepatocellular carcinoma, gastric carcinoma and osteosarcoma among others (Liu et al., 2017; Le Minh et al., 2023; Kumar et al., 2021). KLF8 has been observed to promote chemoresistance via PARP-1 dependent DNA damage response in HCC cells. In solid tumors, KLF8, on binding to the

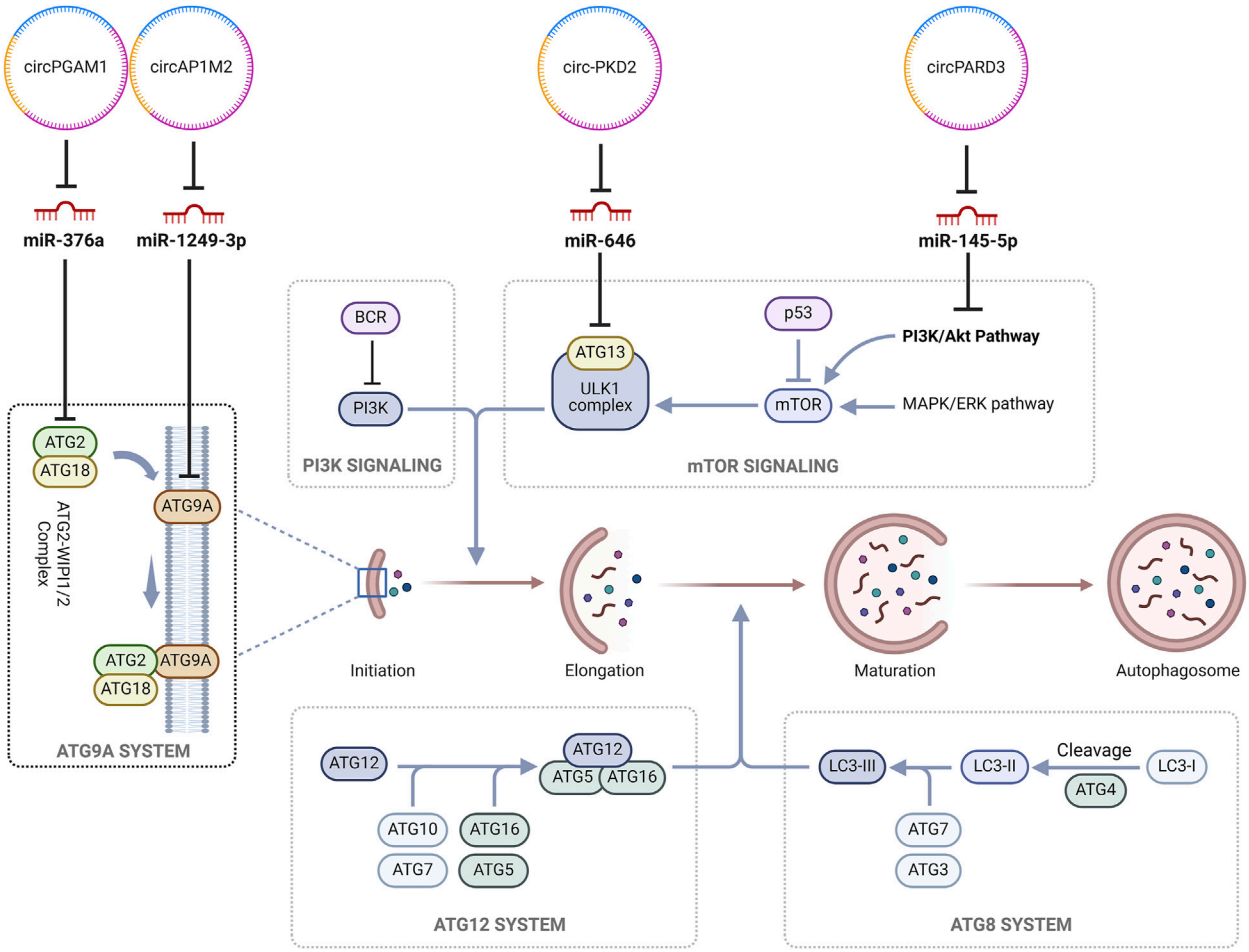


FIGURE 3
CircRNAs regulating autophagy in cancer chemoresistance. (circ, circRNAs; ATG2, Autophagy-related protein 2; ATG18, Autophagy-related protein 18; miR, MicroRNAs; BCR, breakpoint cluster region protein; PI3K, Phosphatidylinositol-3-kinase; ULK1, Unc-51-like autophagy-activating kinases 1; p53, tumor protein p53; MAPK/ERK, Mitogen-activated protein kinase/extracellular signal-regulated kinase; LC3-II, Microtubule-associated protein 1A/1B-light chain 3; mTOR, Mammalian target of rapamycin).

upstream region of the MDR1, promotes translational activity in the tumour microenvironment under hypoxic conditions and thus, inhibiting apoptosis and augmenting the rate of efflux of the chemotherapeutic agent (Xu et al., 2010). M2 macrophages have been noted to induce chemoresistance and radioprotection by the secretion of growth factors and inhibition of apoptotic pathways in neoplastic cells (Jayasingam et al., 2020). Hence, circILF2 plays a role in the development of chemoresistance via two mechanisms, augmenting KLF8 expression and M2 polarization of macrophages.

circ_0005033 was upregulated in LSCC and by sponging miR-107 increased the expression of IGF1R (Gong et al., 2022). IGF1R signaling is a tightly regulated network essential for cellular proliferation and survival. Commonly overexpressed in neoplasms, this growth factor and receptor is responsible for sustained proliferative signals, inhibition of apoptosis, metastasis and chemoresistance. IGF1R induced chemoresistance includes promotion of proliferation, inhibition of apoptosis, increased expression of ABC transporter proteins and changes in the extracellular matrix (Yuan et al., 2018). Although miR-107 was found to be downregulated in LSCC, but in the hypoxic microenvironment of breast and colon cancers, it was overexpressed where it inhibits VEGF-mediated angiogenesis via the downregulation of HIF-1β-mediated signaling pathway (Bao et al., 2012). Upregulation of circ_0005033 alleviated the inhibitory effects of miR-107 on IGF1R precipitating the development of chemoresistance to cisplatin.

circANKS1B, by sponging miR-515-5p, elevated the expression of TGF-β in OSCC (Yan and Xu, 2021). Although TGF-β1 initially acts as a tumor suppressor, but later its role as a promoter of tumor growth was demonstrated. The role of TGF-β1 in the stromal-epithelial interactions and stromal fibroblast cell autonomous effects have implicated this cytokine in the regulation of tumor progression in malignancies (Bierie and Moses, 2006). The activation of alternate pathways of cellular survival or prevention of apoptosis by TGF-β1 has primarily been hypothesized for the development of chemoresistance but, it has been observed that downregulation of TGF-β1 expression too can play a role in EMT and chemoresistance. Downregulation of SMAD3 or absence of SMAD4 suppresses the expression of TGF-β1 which in turn induced the expression of anti-apoptotic proteins such as Bcl-2 and Bcl-w enhancing cell

survivability to response to platinum coordinated compounds in NSCLC and 5-FU in CRC (Zhang et al., 2021). In cisplatin-resistant OSCC, TGF-β1 modulates the cancer cell stemness where it inhibited the tumor suppressor gene FOXO3a via AKT pathway, a non-canonical, SMAD-independent pathway, resulting in the increased expression of SOX2 and ABCG2, which are markers of stemness (Zhang et al., 2021).

hg19_circ_0005033 was found to be upregulated in TDP cells of LSCC and by sponging miR-4521 elevated the expression of STAT5A (Wu Q. et al., 2018). STAT5A has been implicated in various neoplastic conditions, for example, it is overexpressed in hematological malignancies and glioblastoma and suppressed in malignancies of the breast and ovaries suggesting a dual role of STAT5A as a tumor promoter or as a tumor suppressor depending on the underlying pathophysiology (Maninang et al., 2023). Further investigation is warranted to delineate the exact role of STAT5a in the augmentation of neoplastic potential of LSCC (Han et al., 2022). In mice models, the overexpression of STAT5A has been associated with the initiation of breast cancer, a contradictory observation to the tumor suppressive effects of STAT5, where the STAT5 signaling augments the expression TGF- α and in turn enhances the expression of EGFR predisposing the development of malignant changes (Halim et al., 2020). In colorectal cancer, STAT5 overexpression has been associated with a poor prognostic outcome where IL-23 signaling inhibits the expression of SOCS3, an inhibitor of STATs expression and activation. Activation of STATs downregulates p16, p21 and p27 while upregulating the expression of cyclin D1m Bcl-2 and survivin leading to the augmentation of cellular proliferation and inhibition of apoptosis. The STAT mediated overexpression of p-FAK, VEGF and MMP-2 levels and downregulation of E-cadherin expression raises the invasiveness and metastatic potential (Halim et al., 2020). Hence, therapeutic inhibition of STAT5 can aid in the restoration of chemosensitivity in these conditions. STAT5, by augmenting cellular proliferation, cancer stem cell population and EMT can predispose increased invasion and metastasis in hepatocellular carcinoma whereas in prostate cancer, it induces stem-like cell properties and EMT (Wu Y. et al., 2018; Halim et al., 2020).

As multifunctional protein playing a role in rDNA transcription, RNA metabolism and ribosome assembly, the expression of nucleolin in cancers have been hypothesized to be aberrant. Overexpression of nucleolin has been associated with the worsening of the prognostic outcome whereas the presence of cell surface nucleolin has been implicated in augmentation of the malignant potential and metastasis (Chen and Xu, 2016). circTPST2 was observed to be upregulated in HNSCC and by modulation of miR-770-5p regulated the expression of nucleolin. A physical interaction between circPTST2 and nucleolin was observed. Taken together, it is suggestive of a dual nucleolin pathway (Wang et al., 2023). MiR-770-5p has been implicated in the modulation of chemoresistance in multiple cancers like ovarian and colorectal adenocarcinomas. The upregulation of miR-770-5p, by its action as an anti-oncogene, promotes cisplatin sensitivity in ovarian cancers through downregulating the expression of NEAT1 (Zhu M. et al., 2020). In colon adenocarcinoma, miR-770-5p downregulates HIPK1 to modulate methotrexate resistance (Zhang et al., 2020). In HNSCC, circTPST2, by sponging miR-770-5p, modulates chemoresistance via upregulating nucleolin. circTPST2 was found to physically interact and induce the expression of nucleolin where the expression of nucleolin was found to be inversely corelated with the prognostic outcome of chemotherapy in HNSCC. The inhibition of nucelolin increased the number of late apoptotic cells (Wang et al., 2023). In cervical cancers, nucleolin modulates the expression of MDR1 in a YB1-dependent manner precipitating chemoresistance by augmenting drug efflux and reducing intra-cellular accumulation of the drug (Ke et al., 2021).

The expression of circPUM1 was found to be elevated in OSCC. Overexpression of circPUM1 was associated with a decrease in the susceptibility of NK cells and modulation of miR-770-5p which in turn downregulated the expression of NAP1L1 (Liu et al., 2024). The upregulation of miR-770-5p has been observed to promote EMT, invasion and metastasis in OSCC leading to an overall poor prognostic outcome (Khalilian et al., 2023). In a study carried out by Jia and colleagues, it was observed that miR-770-5p downregulates the expression of Sirt7 via the Sirt7/Smad4 signaling pathway to promote cellular migration (Jia et al., 2021). NAP1L1 overexpression has been associated with a poor prognostic outcome and has previously been found to promote cellular proliferation in various neoplastic conditions including colorectal cancer, HCC, lung adenocarcinoma, and neuroendocrine cancers (Zhu et al., 2022). Le et al. observed that NAP1L1 overexpression in HCC was associated with an augmentation of the neoplastic potential and chemoresistance to doxorubicin (Le et al., 2019). In glioma and ovarian cancers, NAP1L1, via its interaction with HDGF, activated c-Jun, an oncogenic transcription factor, to induce CCND1/CDK4/CDK6 expression resulting in cellular proliferation and chemoresistance to cisplatin (Zhu et al., 2022; Chen et al., 2021).

circRNAs function via the modulation of downstream RNA transcripts by competing with shared miRNAs (Salmena et al., 2011). circ_0001971 was highly expressed in OSCC cases and miR-194 as well as miR-204 were its downstream targets (Tan et al., 2020). miR-194 was found to inhibit cellular proliferation in OSCC by suppressing acylglycerol kinase (AGK) expression via the PI3K/AKT/FoxO3a signaling pathway acting as a tumor suppressor (Chi, 2015). AGK is an oncogene which has been observed to be overexpressed in a myriad of malignancies and plays a crucial role as a regulator of cellular growth and proliferation, invasion and metastasis and resistance to chemotherapy (Chu et al., 2021). AGK was also considered to be a promoter of resistance to paclitaxel in nasopharyngeal carcinomas and this chemoresistance properties which eventually mediate tumor growth and metastasis is facilitated by overexpressed FOXM1 via JAK2/STAT3 signaling pathway (Zhao et al., 2021; Zhu Q. et al., 2020). Depending on the underlying neoplastic condition, miR-204 has been observed to either play the role of a tumor suppressor or an oncomiR. Wu et al., in their study, observed the low expression level of miR-204 in HNSCC with JAK2 being its direct target. Attenuation of JAK2 by miR-204 in HNSCC inhibited the JAK2/JAK3 pathway preventing tumor angiogenesis and increased sensitivity to cetuximab suggesting a tumor suppressive activity (Wu Y. et al., 2018). The tumor suppressive actions and chemotherapy sensitivity enhancement activity of miR-204, via the inhibition of RAB22A, an oncogene, has been investigated for

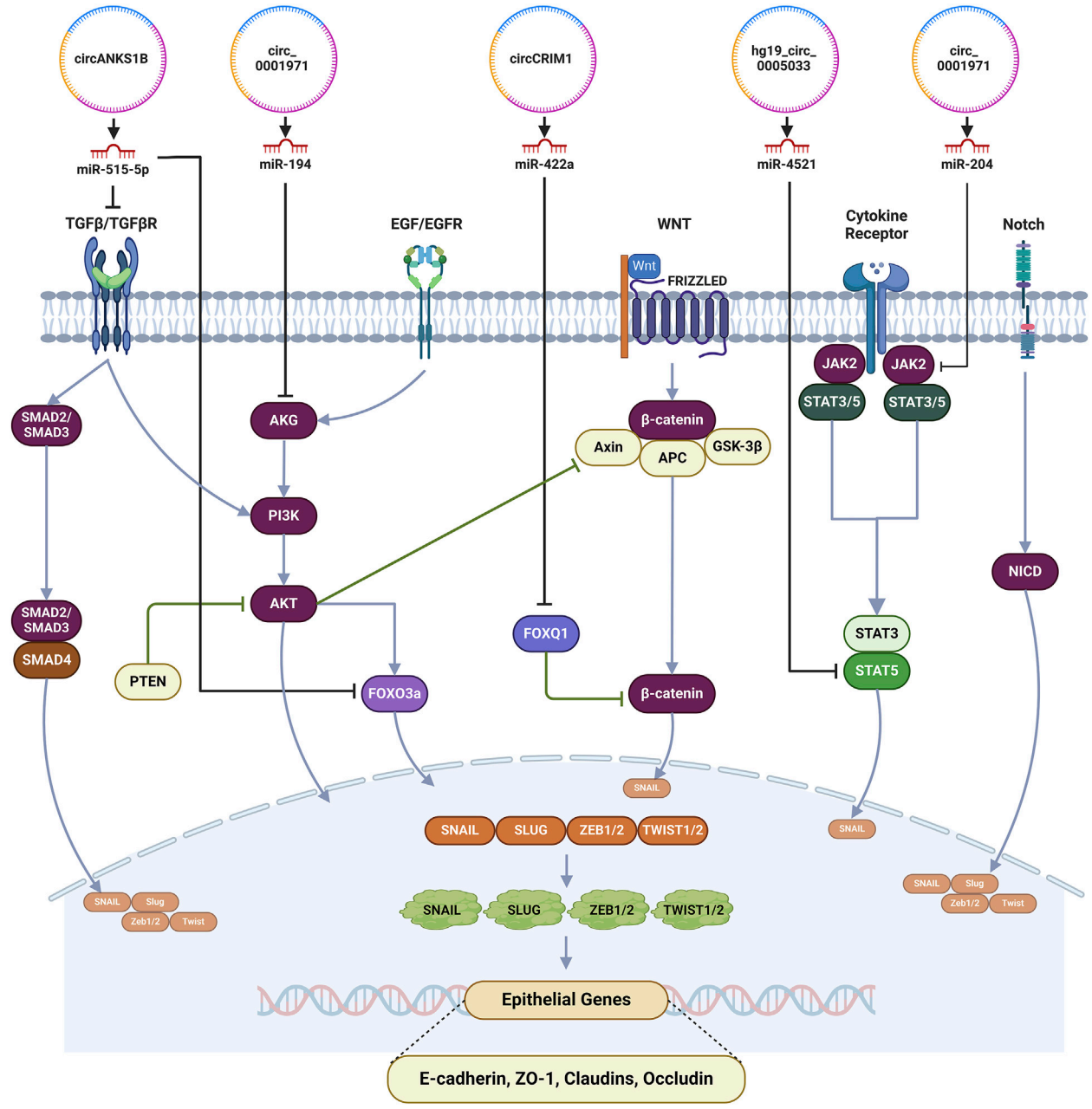


FIGURE 4
Regulation of EMT by circRNAs in HNSCC. (circ, circRNAs; ATG2, Autophagy-related protein 2; ATG18, Autophagy-related protein 18; miR, MicroRNAs; BCR, breakpoint cluster region protein; PI3K, Phosphatidylinositol-3-kinase; ULK1, Unc-51-like autophagy-activating kinases 1; p53, tumor protein p53; MAPK/ERK, Mitogen-activated protein kinase/extracellular signal-regulated kinase; LC3-II, Microtubule-associated protein 1A/1B-light chain 3; mTOR, Mammalian target of rapamycin).

multiple cancers including nasopharyngeal carcinoma (Rajan et al., 2021; Yin et al., 2014). Further studies are warranted for identification of downstream targets for miR-194 and miR-204 in OSCC and establishment of the regulatory axis.

circCRIM1 was observed to be upregulated in NPC cells and by sponging miR-422a alleviated the inhibitory effect on FOXQ1 in nasopharyngeal carcinoma (Hong et al., 2020). miR-422a which primarily functions as a tumor suppressor was downregulated in nasopharyngeal carcinoma (Hong et al., 2020) as well as in other neoplastic conditions like gastric carcinoma (He et al., 2018), colorectal cancer (Li et al., 2018) and osteosarcoma (Zhang et al., 2018). Moreover, miR-422a exerts its tumor suppressive effects by inhibiting the expression of FOXQ1. FOXQ1 has been implicated in the regulation of various physiological processes such as glucose metabolism, synthesis of lactic acid, cardiac fibrosis and cellular senescence. In neoplastic conditions, FOXQ1 plays a role of promoter of tumor progression and has been involved in the regulation of invasion, EMT and apoptosis (Dong et al., 2022).

Zhang et al., demonstrated that FOXQ1 expression was elevated in laryngeal carcinoma and inhibition of FOXQ1 under experimental conditions impairs the cellular proliferation and invasion by arresting the cell cycle progression in G0/G1 phase (Zhang et al., 2015). Although further research is warranted to delineate the underlying mechanism(s) of FOXQ1-mediated chemoresistance in HNSCC, Meng et al. identified Twist1, Zeb2, PDGFRA and PDGFRB as potential downstream targets in breast carcinoma which are downregulated by FOXQ1 (Baumeister et al., 2021). Hence, therapeutic modalities targeting these transcription factors may play a role in the inhibition of growth, invasion and metastasis while promoting apoptosis in HNSCC. The regulation of EMT pathway by circRNA in HNSCC has been delineated in Figure 4.

Hung and colleagues investigated the clinical implications of hsa_circ_0000190 and hsa_circ_0001649 as potential biomarkers for prognosis and response to chemotherapy in OSCC. Although both circRNAs were found to be downregulated, the decreased expression of hsa_circ_0000190 in the late stage of the disease was statistically significant and it could effectively differentiate OSCC cases from normal healthy individuals. A correlation was observed between the expression of hsa_circ_0000190 and response to chemotherapy. Although the decreased expression of hsa_circ_0001649 correlated with an increased risk of early recurrence and decreased survivability, no correlation was observed between its expression and response to chemotherapy (Hung et al., 2022). Hsa_circ_0000190 has been investigated in multiple cancers where the expression varies depending on the underlying neoplastic conditions. hsa_circ_0000190 was highly expressed in non-small cell lung cancer (NSCLC) (Luo et al., 2021) while, in OSCC (Hung et al., 2022) and gastric cancer (Chen et al., 2017), it was downregulated. Although there is a paucity of data pertaining to the downstream targets and delineation of the exact role of hsa_circ_0000190 in HNSCC, a series of studies have investigated its role in the tumor progression and chemoresistance to cisplatin in NSCLC (Luo et al., 2021; Chen et al., 2017). Further, we found that hsa_circ_0000190 by sponging miR-1253 upregulated IL-6 in NSCLC to induce chemoresistance (He and Li, 2024). IL-6 has been implicated as mediator of tumor progression and chemoresistance in multiple cancers such as NSCLC and colorectal cancer wherein IL-6 has been observed to modulate autophagy by inducing phosphorylation of BECN1 via the IL-6/JAK2/BECN1 signaling pathway (He and Li, 2024; Hu et al., 2021). The phosphorylation of BECN1 at the tyrosine residue Y333 by JAK2 augments its interaction with VPS34, a component of the PI3KC3 complex, which is essential for the formation of autophagosomes in turn aiding the malignant cells to survive the stress induced by chemotherapeutic agents (Hu et al., 2021). Like in OSCC, hsa_circ_0000190 has been found to be downregulated in gastric carcinoma. miR-1252 was identified as a direct target for hsa_circ_0000190 and it directly targeted PAK3. The hsa_circ_0000190/miR-1252/PAK3 was found to modulate the malignant potential of the cells by regulating the expression of p27 and cyclin D inducing cell cycle arrest at G1 phase due to inhibition of DNA synthesis, apoptosis, cellular proliferation and migration (Wang Y. et al., 2020). As the expression of hsa_circ_0000190 varies depending on the underlying neoplastic conditions, it is a view that circRNAs exert their influence on different biological processes depending on the underlying pathology.

Similarly, hsa_circ_0001649 which is thought to be an anti-oncogenic circRNA was downregulated in multiple malignancies such as osteosarcoma (Sun and Zhu, 2020), gastric carcinoma (Li et al., 2017) and retinoblastoma (Xing et al., 2018) and is associated with a poor prognostic outcome. In osteosarcoma, it has been observed that hsa_circ_0001649, by sponging miR-338-5p, miR-647 and miR-942, inhibits the STAT signaling pathway to decrease cellular proliferation and promote apoptosis (Sun and Zhu, 2020) whereas, in retinoblastoma, hsa_circ_0001649 was observed to exert its actions via the modulation of the AKT/mTOR signaling pathway (Xing et al., 2018) and this suggests that even though dysregulated circRNA may play a role in the pathogenesis of cancer, they may not be useful as biomarkers of prognosis and response to chemotherapy.

In brief, the mechanism of development of chemoresistance in HNSCC is quite complex and involves multiple pathways regulated by a wide range of circRNAs. In present study, we found that circular RNAs circPARD3, circPKD2, circAP1M2 and circPGAM1 can modulate autophagy; circ-ILF2, circANKS1B, circTPST2, circPUM1 and circ_0001971 can regulate apoptosis and circ-ILF2, has_circ_0005033 and circTPST2 augment the efflux of the chemotherapeutic agent; EMT is enhanced by circANKS1B, circCRIM1, circ_0001971 and has_circ_0005033) whereas DNA damage and repair capacity of the cells is modulated by circ-ILF2. circ-ILF2, circCRIM1 and circTPST2 may also play a role in modulation of the tumor microenvironment. Moreover, malignant potential of cancerous cells is regulated by has_circ_0000190 and hg19_circ_0005033. Interestingly, circTPST2 circRNA is involved in regulation of apoptosis, augmentation of drug efflux, and modulation of the tumor microenvironment. Similarly, circ-ILF2 augments the drug efflux, modulates the tumor microenvironment and DNA damage.

As discussed elsewhere, the present review identifies 13 circRNAs which have been investigated for their role in chemoresistance in HNSCC. We have provided insight into their possible mechanism of action, their target miRNAs, and regulatory pathways involved in the development of chemoresistance while highlighting the potential roles of predictors of chemotherapy response in HNSCC. However, the present study has some limitations. Although we strived to conduct a comprehensive literature search involving four databases, it is possible that we may have missed literature from the grey areas. As most of the studies reported in our review have been conducted in People's Republic of China, hence, a population bias may exist. A variation in study design including sample size, control groups and experimental designs was noted which may have contributed to some inconsistences in the results which have been reported. Majority of the studies investigated chemoresistance to cisplatin whereas only one study investigated the therapeutic response to docetaxel which may restrict the applicability to other chemotherapeutic drugs and chemotherapy regimens.

5 Conclusion

In this review, we have systematically identified 13 circRNAs that played a vital role in the development of chemoresistance in HNSCC. These identified circRNAs may be considered as predictive biomarkers not only for prognosis but also for response to

chemotherapy. Further, these circRNAs may aid in the personalization of therapeutic modalities in HNSCC cases. The development of chemoresistance is not unidimensional but involves the modulation of multiple pathways which in turn control various cellular processes by multiple circRNAs, their target miRNAs and downstream effectors. Hence, integration of circRNAs with other biomarkers such as proteins and other ncRNAs can provide a comprehensive and more accurate understanding of the underlying pathophysiological process, treatment response and even serve as potential therapeutic targets in cancer and for deterring chemoresistance. Although all identified circRNAs should be investigated for their potential role as biomarkers, of the identified circRNAs, the authors would like to propose the four most promising candidates for further evaluation, namely, circPARD3 which modulates autophagy via the PRKCI-Akt-mTOR pathway, circTPST2 which modulates apoptosis, drug efflux and tumor microenvironment and shows a strong correlation with chemotherapy response, circANKS1B which modulation of EMT and TGF-β1 pathway (responsible for cell survival, growth and immune response) and circ_0000190 which modulates autophagy via the IL-6/JAK2/BECN1 signaling pathway and the expression of which has been reported to correlate with response to chemotherapy. Although dysregulation of expression of a circRNAs can predict the malignant potential of the cells, further exploration is required to ascertain their role in chemoresistance. Validation of the identified circRNAs and their incorporation into clinical practice warrants the conduction of longitudinal studies for observing the change in response to chemotherapy whereas *in vivo* experiments may shed light on extrapolating the role of these circRNAs in cancer at a cellular level. As discussed earlier, circRNAs are inherently more resistant to degradation than other ncRNAs owing to their closed circular structures, they hold immense potential as biomarkers, a correlation between tissue and plasma samples will aid in easier applicability. The existence of validated biomarkers with good specificity and sensitivity can aid in the early detection of chemoresistance minimizing therapy failure resulting in a better therapeutic outcome. Hence, further well-planned studies are warranted from clinical perspectives to establish the role and utility of circRNAs in chemoresistance to some other anti-cancer drugs and explore their potential as novel biomarkers for predicting prognosis and chemotherapy response.

Data availability statement

The original contributions presented in the study are included in the article/Supplementary Material, further inquiries can be directed to the corresponding author.

Author contributions

SKD: Conceptualization, Data curation, Methodology, Writing–original draft. SK: Data curation, Methodology, Writing–original draft. AM: Data curation, Methodology, Writing–original draft. BJ: Data curation, Methodology, Writing–original draft, Writing–review and editing.

Funding

The author(s) declare that no financial support was received for the research, authorship, and/or publication of this article.

Acknowledgments

Figure 3: Adapted from "Autophagy in Cancer Pathways", by BioRender.com (2024). Retrieved from https://app.biorender.com/biorender-templates. Figure 4: Created with BioRender.com.

Conflict of interest

The authors declare that the research was conducted in the absence of any commercial or financial relationships that could be construed as a potential conflict of interest.

Generative AI statement

The author(s) declare that no Generative AI was used in the creation of this manuscript.

Publisher's note

All claims expressed in this article are solely those of the authors and do not necessarily represent those of their affiliated organizations, or those of the publisher, the editors and the reviewers. Any product that may be evaluated in this article, or claim that may be made by its manufacturer, is not guaranteed or endorsed by the publisher.

Supplementary material

The Supplementary Material for this article can be found online at: https://www.frontiersin.org/articles/10.3389/fphar.2025.1502107/full#supplementary-material

References

Bach, D. H., Lee, S. K., and Sood, A. K. (2019). Circular RNAs in cancer. *Mol. Ther. Nucleic Acids* 16, 118–129. doi:10.1016/j.omtn.2019.02.005

Bao, B., Azmi, A. S., Ali, S., Ahmad, A., Li, Y., Banerjee, S., et al. (2012). The biological kinship of hypoxia with CSC and EMT and their relationship with deregulated expression of miRNAs and tumor aggressiveness. *Biochim. Biophys. Acta Rev. Cancer* 1826, 272–296. doi:10.1016/j.bbcan.2012.04.008

Barsouk, A., Aluru, J. S., Rawla, P., Saginala, K., and Barsouk, A. (2023). Epidemiology, risk factors, and prevention of head and neck squamous cell carcinoma. *Med. Sci.* 11, 42. doi:10.3390/medsci11020042

Baumeister, P., Zhou, J., Canis, M., and Gires, O. (2021). Epithelial-to-mesenchymal transition-derived heterogeneity in head and neck squamous cell carcinomas. *Cancers* 13, 5355. doi:10.3390/cancers13215355

Bhattacharya, A., Torggler, R., Reiter, W., Romanov, N., Licheva, M., Ciftci, A., et al. (2024). Decoding the function of Atg13 phosphorylation reveals a role of Atg11 in bulk autophagy initiation. *EMBO Rep.* 25, 813–831. doi:10.1038/s44319-023-00055-9

Bierie, B., and Moses, H. L. (2006). TGF-beta and cancer. *Cytokine Growth Factor Rev.* 17, 29–40. doi:10.1016/j.cytogfr.2005.09.006

Brentnall, M., Rodriguez-Menocal, L., De Guevara, R. L., Cepero, E., and Boise, L. H. (2013). Caspase-9, caspase-3 and caspase-7 have distinct roles during intrinsic apoptosis. *BMC Cell Biol.* 14, 32. doi:10.1186/1471-2121-14-32

Chavez-Dominguez, R., Perez-Medina, M., Lopez-Gonzalez, J. S., Galicia-Velasco, M., and Aguilar-Cazares, D. (2020). The double-edge sword of autophagy in cancer: from tumor suppression to pro-tumor activity. *Front. Oncol.* 10, 578418. doi:10.3389/fonc.2020.578418

Chen, S., Li, T., Zhao, Q., Xiao, B., and Guo, J. (2017). Using circular RNA hsa_circ_0000190 as a new biomarker in the diagnosis of gastric cancer. *Clin. Chim. Acta* 466, 167–171. doi:10.1016/j.cca.2017.01.025

Chen, X., Zeng, K., Xu, M., Liu, X., Hu, X., Xu, T., et al. (2019). P53-induced miR-1249 inhibits tumor growth, metastasis, and angiogenesis by targeting VEGFA and HMGA2. *Cell Death Dis.* 10, 131. doi:10.1038/s41419-018-1188-3

Chen, Z., Xie, Y., Luo, H., Song, Y., Que, T., Hu, R., et al. (2021). NAP1L1 promotes proliferation and chemoresistance in glioma by inducing CCND1/CDK4/CDK6 expression through its interaction with HDGF and activation of c-Jun. *Aging (Albany NY)* 13, 26180–26200. doi:10.18632/aging.203805

Chen, Z., and Xu, X. (2016). Roles of nucleolin: focus on cancer and anti-cancer therapy. *Saudi Med. J.* 37, 1312–1318. doi:10.15537/smj.2016.12.15972

Chi, H. (2015). miR-194 regulated AGK and inhibited cell proliferation of oral squamous cell carcinoma by reducing PI3K-Akt-FoxO3a signaling. *Biomed. Pharmacother.* 71, 53–57. doi:10.1016/j.biopha.2015.02.011

Chu, B., Hong, Z., and Zheng, X. (2021). Acylglycerol kinase-targeted therapies in oncology. *Front. Cell Dev. Biol.* 9, 659158. doi:10.3389/fcell.2021.659158

Dong, Q., Yan, L., Xu, Q., Hu, X., Yang, Y., Zhu, R., et al. (2022). Pan-cancer analysis of forkhead box Q1 as a potential prognostic and immunological biomarker. *Front. Genet.* 13, 944970. doi:10.3389/fgene.2022.944970

Fan, X. R., Zhang, Z. Y., Wang, R. H., Li, Y., and Mao, Q. Z. (2019). MiR-376a functions as tumor suppressor by targeting SGK3 in renal cell carcinoma. *Eur. Rev. Med. Pharmacol. Sci.* 23, 3726–3732. doi:10.26355/eurrev_201905_17798

Fellenberg, J., Lehner, B., Saehr, H., Schenker, A., and Kunz, P. (2019). Tumor suppressor function of miR-127-3p and miR-376a-3p in osteosarcoma cells. *Cancers* 11, 2019. doi:10.3390/cancers11122019

Feng, B., Chen, K., Zhang, W., Zheng, Q., and He, Y. (2021). circPGAM1 enhances autophagy signaling during laryngocarcinoma drug resistance by regulating miR-376a. *Biochem. Biophys. Res. Commun.* 534, 966–972. doi:10.1016/j.bbrc.2020.10.063

Fritsch, M., Günther, S. D., Schwarzer, R., Albert, M. C., Schorn, F., Werthenbach, J. P., et al. (2019). Caspase-8 is the molecular switch for apoptosis, necroptosis and pyroptosis. *Nature* 575, 683–687. doi:10.1038/s41586-019-1770-6

Gao, L., Zhang, Q., Li, S., Zheng, J., Ren, W., and Zhi, K. (2022). Circ-PKD2 promotes Atg13-mediated autophagy by inhibiting miR-646 to increase the sensitivity of cisplatin in oral squamous cell carcinomas. *Cell Death Dis.* 13, 192. doi:10.1038/s41419-021-04497-8

Gao, W., Guo, H., Niu, M., Zheng, X., Zhang, Y., Xue, X., et al. (2020). circPARD3 drives malignant progression and chemoresistance of laryngeal squamous cell carcinoma by inhibiting autophagy through the PRKCI-Akt-mTOR pathway. *Mol. Cancer* 19, 166–222. doi:10.1186/s12943-020-01279-2

Garcia-Berrocal, J. R., Nevado, J., Ramirez-Camacho, R., Sanz, R., González-García, J. A., Sánchez-Rodríguez, C., et al. (2007). The anticancer drug cisplatin induces an intrinsic apoptotic pathway inside the inner ear. *Br. J. Pharmacol.* 152, 1012–1020. doi:10.1038/sj.bjp.0707405

Gong, L., Chen, J., and Jiang, X. (2022). Circ_0005033 is an oncogene in laryngeal squamous cell carcinoma and regulates cell progression and Cisplatin sensitivity via miR-107/IGF1R axis. *Anti-Cancer Drugs* 33, 245–256. doi:10.1097/CAD.0000000000001260

Halim, C. E., Deng, S., Ong, M. S., and Yap, C. T. (2020). Involvement of STAT5 in oncogenesis. *Biomedicines* 8, 316. doi:10.3390/biomedicines8090316

Han, X., Tian, R., Wang, C., Li, Y., and Song, X. (2022). CircRNAs: roles in regulating head and neck squamous cell carcinoma. *Front. Oncol.* 12, 1026073. doi:10.3389/fonc.2022.1026073

He, H., and Li, T. (2024). Hsa_circ_0000190 promotes NSCLC cell resistance to cisplatin via the modulation of the miR-1253/IL-6 Axis. *Anal. Cell. Pathol.* 2024, 6647810. doi:10.1155/2024/6647810

He, Z., Li, Z., Zhang, X., Yin, K., Wang, W., Xu, Z., et al. (2018). MiR-422a regulates cellular metabolism and malignancy by targeting pyruvate dehydrogenase kinase 2 in gastric cancer. *Cell Death Dis.* 9, 505. doi:10.1038/s41419-018-0564-3

Hong, X., Liu, N., Liang, Y., He, Q., Yang, X., Lei, Y., et al. (2020). Circular RNA CRIM1 functions as a ceRNA to promote nasopharyngeal carcinoma metastasis and docetaxel chemoresistance through upregulating FOXQ1. *Mol. Cancer* 19, 33–36. doi:10.1186/s12943-020-01149-x

Hu, F., Song, D., Yan, Y., Huang, C., Shen, C., Lan, J., et al. (2021). IL-6 regulates autophagy and chemotherapy resistance by promoting BECN1 phosphorylation. *Nat. Commun.* 12, 3651. doi:10.1038/s41467-021-23923-1

Hung, K. F., Chen, B. H., Wang, T. Y., Yang, Y. P., Chien, Y., Lo, J. F., et al. (2022). Identification of plasma hsa_circ_0000190 and 0001649 as biomarkers for predicting the recurrence and treatment response of patients with oral squamous cell carcinoma. *J. Chin. Med. Assoc.* 85, 431–437. doi:10.1097/JCMA.0000000000000700

Hwang, H. J., and Kim, Y. K. (2024). Molecular mechanisms of circular RNA translation. *Exp. Mol. Med.* 56, 1272–1280. doi:10.1038/s12276-024-01220-3

Inman, K. S., Liu, Y., Scotti Buzhardt, M. L., Leitges, M., Krishna, M., Crawford, H. C., et al. (2022). Prkci regulates autophagy and pancreatic tumorigenesis in mice. *Cancers* 14, 796. doi:10.3390/cancers14030796

Jayasingam, S. D., Citartan, M., Thang, T. H., Mat Zin, A. A., Ang, K. C., and Ch'ng, E. S. (2020). Evaluating the polarization of tumor-associated macrophages into M1 and M2 phenotypes in human cancer tissue: technicalities and challenges in routine clinical practice. *Front. Oncol.* 9, 1512. doi:10.3389/fonc.2019.01512

Jia, B., Zhang, S., Wu, S., Zhu, Q., and Li, W. (2021). MiR-770 promotes oral squamous cell carcinoma migration and invasion by regulating the Sirt7/Smad4 pathway. *IUBMB Life* 73, 264–272. doi:10.1002/iub.2426

Jiao, J., Ruan, L., Cheng, C. S., Wang, F., Yang, P., and Chen, Z. (2023). Paired protein kinases PRKCI-RIPK2 promote pancreatic cancer growth and metastasis via enhancing NF-κB/JNK/ERK phosphorylation. *Mol. Med.* 29, 47. doi:10.1186/s10020-023-00648-z

Johnson, D. E., Burtness, B., Leemans, C. R., Lui, V. W., Bauman, J. E., and Grandis, J. R. (2020). Head and neck squamous cell carcinoma. *Nat. Rev. Dis. Prim.* 6, 92. doi:10.1038/s41572-020-00224-3

Jung, K., Kang, H., and Mehra, R. (2018). Targeting phosphoinositide 3-kinase (PI3K) in head and neck squamous cell carcinoma (HNSCC). *Cancers Head. Neck* 3, 3. doi:10.1186/s41199-018-0030-z

Kannampuzha, S., and Gopalakrishnan, A. V. (2023). Cancer chemoresistance and its mechanisms: associated molecular factors and its regulatory role. *Med. Oncol.* 40, 264. doi:10.1007/s12032-023-02138-y

Ke, J., Gu, C., Zhang, H., Liu, Y., Zhang, W., Rao, H., et al. (2021). Nucleolin promotes cisplatin resistance in cervical cancer by the YB1-MDR1 pathway. *J. Oncol.* 2021, 9992218. doi:10.1155/2021/9992218

Khalilian, S., Imani, S. Z., Hosseini, S. A., and Ghafouri-Fard, S. (2023). The important role of miR-770 as a novel potential diagnostic and therapeutic target for human cancer and other diseases. *Pathol. Res. Pract.* 248, 154586. doi:10.1016/j.prp.2023.154586

Khera, N., Rajkumar, A. S., Abdulkader, M. A., Liu, Z., Ma, H., Waseem, A., et al. (2023). Identification of multidrug chemoresistant genes in head and neck squamous cell carcinoma cells. *Mol. Cancer* 22, 146. doi:10.1186/s12943-023-01846-3

Kim, K. W., Qiao, J., Kim, J. Y., Park, K., and Chung, D. H. (2020). Overexpression of microRNA-145 inhibits tumorigenesis through autophagy in chemotherapy and radiation resistant neuroblastoma cells. *Oncoscience* 7, 1–9. doi:10.18632/oncoscience.496

Kumar, S., Behera, A., Saha, P., and Srivastava, A. K. (2021). The role of Krüppel-like factor 8 in cancer biology: current research and its clinical relevance. *Biochem. Pharmacol.* 183, 114351. doi:10.1016/j.bcp.2020.114351

Le, Y., Kan, A., Li, Q. J., He, M. K., Chen, H. L., and Shi, M. (2019). NAP1L1 is a prognostic biomarker and contribute to doxorubicin chemotherapy resistance in human hepatocellular carcinoma. *Cancer Cell Int.* 19, 228. doi:10.1186/s12935-019-0949-0

Le Minh, G., Esquea, E. M., Dhameliya, T. T., Merzy, J., Lee, M. H., Ball, L. E., et al. (2023). Kruppel-like factor 8 regulates triple negative breast cancer stem cell-like activity. *Front. Oncol.* 13, 1141834. doi:10.3389/fonc.2023.1141834

Li, H., Zhu, H., Xu, C. J., and Yuan, J. (1998). Cleavage of BID by caspase 8 mediates the mitochondrial damage in the Fas pathway of apoptosis. *Cell* 94, 491–501. doi:10.1016/s0092-8674(00)81590-1

Li, P., Li, Q., Zhang, Y., Sun, S., Liu, S., and Lu, Z. (2018). MiR-422a targets MAPKK6 and regulates cell growth and apoptosis in colorectal cancer cells. *Biomed. Pharmacother.* 104, 832–840. doi:10.1016/j.biopha.2018.03.013

Li, W. H., Song, Y. C., Zhang, H., Zhou, Z. J., Xie, X., Zeng, Q. N., et al. (2017). Decreased expression of Hsa_circ_00001649 in gastric cancer and its clinical significance. *Dis. Markers* 2017, 4587698. doi:10.1155/2017/4587698

Li, X., He, S., and Ma, B. (2020). Autophagy and autophagy-related proteins in cancer. *Mol. Cancer* 19, 12. doi:10.1186/s12943-020-1138-4

Liu, C. X., and Chen, L. L. (2022). Circular RNAs: characterization, cellular roles, and applications. *Cell* 185, 2390–2034. doi:10.1016/j.cell.2022.06.001

Liu, L., Zou, C., Lv, X., Wei, H., Wu, S., Song, J., et al. (2024). SP2-induced circPUM1 modulates chemoresistance and nature killer cell toxicity in oral squamous cell carcinoma. *J. Cell. Mol. Med.* 28, e17888. doi:10.1111/jcmm.17888

Liu, X. Y., Zhang, Q., Guo, J., Zhang, P., Liu, H., Tian, Z. B., et al. (2022). The role of circular RNAs in the drug resistance of cancers. *Front. Oncol.* 11, 790589. doi:10.3389/fonc.2021.790589

Liu, Y., Yao, X., Zhang, Q., Qian, L., Feng, J., Bian, T., et al. (2017). Expression of Kruppel like factor 8 and Ki67 in lung adenocarcinoma and prognosis. *Exp. Ther. Med.* 14, 1351–1356. doi:10.3892/etm.2017.4632

Luo, Y. H., Yang, Y. P., Chien, C. S., Yarmishyn, A. A., Adekunle Ishola, A., Chien, Y., et al. (2021). Circular RNA hsa_circ_0000190 facilitates the tumorigenesis and immune evasion by upregulating the expression of soluble PD-L1 in non-small-cell lung cancer. *Int. J. Mol. Sci.* 23, 64. doi:10.3390/ijms23010064

Maeda, S., Otomo, C., and Otomo, T. (2019). The autophagic membrane tether ATG2A transfers lipids between membranes. *Elife* 8, e45777. doi:10.7554/eLife.45777

Mailler, E., Guardia, C. M., Bai, X., Jarnik, M., Williamson, C. D., Li, Y., et al. (2021). The autophagy protein ATG9A enables lipid mobilization from lipid droplets. *Nat. Commun.* 12, 6750. doi:10.1038/s41467-021-26999-x

Maninang, C., Li, J., and Li, W. X. (2023). Expression and prognostic role of STAT5a across cancer types. *Biosci. Rep.* 43, BSR20230612. doi:10.1042/BSR20230612

Marur, S., and Forastiere, A. A. (2016). Head and neck squamous cell carcinoma: update on epidemiology, diagnosis, and treatment. *Mayo Clin. Proc.* 91, 386–396. doi:10.1016/j.mayocp.2015.12.017

Massarelli, E., Lin, H., Ginsberg, L. E., Tran, H. T., Lee, J. J., Canales, J. R., et al. (2015). Phase II trial of everolimus and erlotinib in patients with platinum-resistant recurrent and/or metastatic head and neck squamous cell carcinoma. *Ann. Oncol.* 26, 1476–1480. doi:10.1093/annonc/mdv194

Nathan, C. A., Hayes, D. N., Karrison, T., Harismendy, O., Flores, J. M., Moore-Medlin, T., et al. (2022). A randomized multi-institutional phase II trial of everolimus as adjuvant therapy in patients with locally advanced squamous cell cancer of the head and neck. *Clin. Cancer Res.* 28, 5040–5048. doi:10.1158/1078-0432.CCR-21-4290

Park, M. S., De Leon, M., and Devarajan, P. (2002). Cisplatin induces apoptosis in LLC-PK1 cells via activation of mitochondrial pathways. *J. Am. Soc. Nephrol.* 13, 858–865. doi:10.1681/ASN.V134858

PRISMA statement (2024). Available at: https://www.prisma-statement.org/(Accessed August 28, 2024).

Pu, Y., Wang, J., and Wang, S. (2022). Role of autophagy in drug resistance and regulation of osteosarcoma. *Mol. Clin. Oncol.* 16, 1–6. doi:10.3892/mco.2022.2505

Qu, L., Li, G., Xia, D., Hongdu, B., Xu, C., Lin, X., et al. (2016). PRKCI negatively regulates autophagy via PIK3CA/AKT–MTOR signaling. *Biochem. Biophys. Res. Commun.* 470, 306–312. doi:10.1016/j.bbrc.2016.01.059

QUADAS-2 (2024). *Bristol medical school: population health sciences*. University of Bristol. Available at: https://www.bristol.ac.uk/population-health-sciences/projects/quadas/quadas-2/(Accessed August 28, 2024).

Rajan, C., Roshan, V. D., Khan, I., Manasa, V. G., Himal, I., Kattoor, J., et al. (2021). MiRNA expression profiling and emergence of new prognostic signature for oral squamous cell carcinoma. *Sci. Rep.* 11, 7298. doi:10.1038/s41598-021-86316-w

Razak, A. R., Wang, H. M., Chang, J. Y., Ahn, M. J., Munster, P., Blumenschein, G., Jr., et al. (2023). A phase 1b/2 study of alpelisib in combination with cetuximab in patients with recurrent or metastatic head and neck squamous cell carcinoma. *Target. Oncol.* 18, 853–868. doi:10.1007/s11523-023-00997-z

Sacco, A. G., and Cohen, E. E. (2015). Current treatment options for recurrent or metastatic head and neck squamous cell carcinoma. *J. Clin. Oncol.* 33, 3305–3313. doi:10.1200/JCO.2015.62.0963

Salmena, L., Poliseno, L., Tay, Y., Kats, L., and Pandolfi, P. P. (2011). A ceRNA hypothesis: the Rosetta Stone of a hidden RNA language? *Cell* 146, 353–358. doi:10.1016/j.cell.2011.07.014

Sun, D., and Zhu, D. (2020). Circular RNA hsa_circ_0001649 suppresses the growth of osteosarcoma cells via sponging multiple miRNAs. *Cell Cycle* 19, 2631–2643. doi:10.1080/15384101.2020.1814026

Tan, X., Zhou, C., Liang, Y., and Lai, Y. F. (2020). Circ_0001971 regulates oral squamous cell carcinoma progression and chemosensitivity by targeting miR-194/miR-204 *in vitro* and *in vivo*. *Eur. Rev. Med. Pharmacol. Sci.* 24, 2470–2481. doi:10.26355/eurrev_202003_20515

Tang, Z., Takahashi, Y., Chen, C., Liu, Y., He, H., Tsotakos, N., et al. (2017). Atg2A/B deficiency switches cytoprotective autophagy to non-canonical caspase-8 activation and apoptosis. *Cell Death Differ.* 24, 2127–2138. doi:10.1038/cdd.2017.133

Wang, G. J., Yu, T. Y., Li, Y. R., Liu, Y. J., and Deng, B. B. (2020a). Circ_0000190 suppresses gastric cancer progression potentially via inhibiting miR-1252/PAK3 pathway. *Cancer Cell Int.* 20, 351–353. doi:10.1186/s12935-020-01422-5

Wang, T., Xin, C., Zhang, S., Tian, X., Hu, Y., Wang, Y., et al. (2023). Circular RNA from tyrosylprotein sulfotransferase 2 gene inhibits cisplatin sensitivity in head and neck squamous cell carcinoma by sponging miR-770-5p and interacting with nucleolin. *Cancers* 15, 5351. doi:10.3390/cancers15225351

Wang, Y., Liu, Z., Shu, S., Cai, J., Tang, C., and Dong, Z. (2020b). AMPK/mTOR signaling in autophagy regulation during cisplatin-induced acute kidney injury. *Front. Physiol.* 11, 619730. doi:10.3389/fphys.2020.619730

Wenhao, R., Yali, C., Shaoming, L., Jingjing, Z., Ling, G., and Keqian, Z. (2023). circAP1M2 activates ATG9A-associated autophagy by inhibiting miR-1249-3p to promote cisplatin resistance in oral squamous cell carcinoma. *J. Cell. Physiol.* 238, 2612–2624. doi:10.1002/jcp.31116

Wu, Q., Zhao, Y., and Wang, P. (2018a). miR-204 inhibits angiogenesis and promotes sensitivity to cetuximab in head and neck squamous cell carcinoma cells by blocking JAK2-STAT3 signaling. *Biomed. Pharmacother.* 99, 278–285. doi:10.1016/j.biopha.2018.01.055

Wu, S., Lv, X., Wei, H., Chen, W., Zheng, J., Li, X., et al. (2023). Circ-ILF2 in oral squamous cell carcinoma promotes cisplatin resistance and induces M2 polarization of macrophages. *J. Cell. Mol. Med.* 27, 4133–4144. doi:10.1111/jcmm.17998

Wu, Y., Zhang, Y., Niu, M., Shi, Y., Liu, H., Yang, D., et al. (2018b). Whole-transcriptome analysis of CD133+ CD144+ cancer stem cells derived from human laryngeal squamous cell carcinoma cells. *Cell. Physiol. biochem.* 47, 1696–1710. doi:10.1159/000490992

Xing, L., Zhang, L., Feng, Y., Cui, Z., and Ding, L. (2018). Downregulation of circular RNA hsa_circ_0001649 indicates poor prognosis for retinoblastoma and regulates cell proliferation and apoptosis via AKT/mTOR signaling pathway. *Biomed. Pharmacother.* 105, 326–333. doi:10.1016/j.biopha.2018.05.141

Xu, J., and Gewirtz, D. A. (2022). Is autophagy always a barrier to cisplatin therapy? *Biomolecules* 12, 463. doi:10.3390/biom12030463

Xu, X. L., Xing, B. C., Han, H. B., Zhao, W., Hu, M. H., Xu, Z. L., et al. (2010). The properties of tumor-initiating cells from a hepatocellular carcinoma patient's primary and recurrent tumor. *Carcinogenesis* 31, 167–174. doi:10.1093/carcin/bgp232

Yan, J., and Xu, H. (2021). Regulation of transforming growth factor-beta1 by circANKS1B/miR-515-5p affects the metastatic potential and cisplatin resistance in oral squamous cell carcinoma. *Bioengineered* 12, 12420–12430. doi:10.1080/21655979.2021.2005221

Yang, Z. J., Chee, C. E., Huang, S., and Sinicrope, F. A. (2011). The role of autophagy in cancer: therapeutic implications. *Mol. Cancer Ther.* 10, 1533–1541. doi:10.1158/1535-7163.MCT-11-0047

Yin, Y., Zhang, B., Wang, W., Fei, B., Quan, C., Zhang, J., et al. (2014). miR-204-5p inhibits proliferation and invasion and enhances chemotherapeutic sensitivity of colorectal cancer cells by downregulating RAB22A. *Clin. Cancer Res.* 20, 6187–6199. doi:10.1158/1078-0432.CCR-14-1030

Yuan, J., Yin, Z., Tao, K., Wang, G., and Gao, J. (2018). Function of insulin like growth factor 1 receptor in cancer resistance to chemotherapy. *Oncol. Lett.* 15, 41–47. doi:10.3892/ol.2017.7276

Yun, C. W., and Lee, S. H. (2018). The roles of autophagy in cancer. *Int. J. Mol. Sci.* 19, 3466. doi:10.3390/ijms19113466

Zhang, D., Li, Y., and Sun, P. (2020). miR 770 5p modulates resistance to methotrexate in human colorectal adenocarcinoma cells by downregulating HIPK1. *Exp. Ther. Med.* 19, 339–346. doi:10.3892/etm.2019.8221

Zhang, H., He, Q. Y., Wang, G. C., Tong, D. K., Wang, R. K., Ding, W. B., et al. (2018). miR-422a inhibits osteosarcoma proliferation by targeting BCL2L2 and KRAS. *Biosci. Rep.* 38, BSR20170339. doi:10.1042/BSR20170339

Zhang, J., Li, W., Dai, S., Tai, X., Jia, J., and Guo, X. (2015). FOXQ1 is overexpressed in laryngeal carcinoma and affects cell growth, cell cycle progression and cell invasion. *Oncol. Lett.* 10, 2499–2504. doi:10.3892/ol.2015.3530

Zhang, L., Zhu, Y., Zhang, J., Zhang, L., and Chen, L. (2022). Inhibiting cytoprotective autophagy in cancer therapy: an update on pharmacological small-molecule compounds. *Front. Pharmacol.* 13, 966012. doi:10.3389/fphar.2022.966012

Zhang, M., Zhang, Y. Y., Chen, Y., Wang, J., Wang, Q., and Lu, H. (2021). TGF-β signaling and resistance to cancer therapy. *Front. Cell Dev. Biol.* 9, 786728. doi:10.3389/fcell.2021.786728

Zhao, C., Chen, H. Y., Zhao, F., Feng, H. J., and Su, J. P. (2021). Acylglycerol kinase promotes paclitaxel resistance in nasopharyngeal carcinoma cells by regulating FOXM1 via the JAK2/STAT3 pathway. *Cytokine* 148, 155595. doi:10.1016/j.cyto.2021.155595

Zheng, S., He, S., Liang, Y., Tan, Y., Liu, Q., Liu, T., et al. (2024). Understanding PI3K/Akt/mTOR signaling in squamous cell carcinoma: mutated PIK3CA as an example. *Mol. Biomed.* 5, 13. doi:10.1186/s43556-024-00176-0

Zhu, M., Yang, L., and Wang, X. (2020a). NEAT1 knockdown suppresses the cisplatin resistance in ovarian cancer by regulating miR-770-5p/PARP1 axis. *Cancer Manag. Res.* 12, 7277–7289. doi:10.2147/CMAR.S257311

Zhu, Q., Zhong, A. L., Hu, H., Zhao, J. J., Weng, D. S., Tang, Y., et al. (2020b). Acylglycerol kinase promotes tumour growth and metastasis via activating the PI3K/AKT/GSK3β signalling pathway in renal cell carcinoma. *J. Hematol. Oncol.* 13, 2–6. doi:10.1186/s13045-019-0840-4

Zhu, X., Xie, Y., Huang, W., Chen, Z., and Guo, S. (2022). NAP1L1 promotes tumor proliferation through HDGF/C-JUN signaling in ovarian cancer. *BMC Cancer* 22, 339. doi:10.1186/s12885-022-09356-z

frontiers | Frontiers in Immunology

TYPE Review
PUBLISHED 04 April 2025
DOI 10.3389/fimmu.2025.1480447

Check for updates

OPEN ACCESS

EDITED BY
Margarida Gama-Carvalho,
University of Lisbon, Portugal

REVIEWED BY
Matias I. Hepp,
Universidad Católica de la Santísima Concepción, Chile
Valentina Gonzalez-Pecchi,
Universidad Católica de la Santísima Concepción, Chile

*CORRESPONDENCE
Fangteng Liu
15807031758@163.com
Ting Lou
jiwenhan1216@163.com

RECEIVED 14 August 2024
ACCEPTED 17 March 2025
PUBLISHED 04 April 2025

CITATION
Liu Q, Huang H, Zhang S, Liu F and Lou T (2025) A novel cancer-associated lncRNA, LINC01123, participates in tumor progression, metabolism, immune escape, and resistance. *Front. Immunol.* 16:1480447. doi: 10.3389/fimmu.2025.1480447

COPYRIGHT
© 2025 Liu, Huang, Zhang, Liu and Lou. This is an open-access article distributed under the terms of the Creative Commons Attribution License (CC BY). The use, distribution or reproduction in other forums is permitted, provided the original author(s) and the copyright owner(s) are credited and that the original publication in this journal is cited, in accordance with accepted academic practice. No use, distribution or reproduction is permitted which does not comply with these terms.

A novel cancer-associated lncRNA, LINC01123, participates in tumor progression, metabolism, immune escape, and resistance

Qiang Liu[1], He Huang[2], Shuwen Zhang[3], Fangteng Liu[2*] and Ting Lou[4*]

[1]Department of General Surgery, Jiujiang Hospital of Traditional Chinese Medicine, Jiujiang, Jiangxi, China, [2]Department of Gastrointestinal Surgery, The Second Affiliated Hospital, Jiangxi Medical College, Nanchang University, Nanchang, Jiangxi, China, [3]Queen Mary College, Nanchang University, Nanchang, Jiangxi, China, [4]Department of Hospital Admission and Medical Record Management, The Second Medical Center & National Clinical Research Center for Geriatric Diseases, Chinese People's Liberation Army (PLA) General Hospital, Beijing, China

Long Intergenic Non-Protein Coding RNA 1123 (LINC01123), located on human chromosome 2q13, is a pivotal factor in tumorigenesis, exerting multifaceted oncogenic effects. Its expression strongly correlates with clinicopathological features, patient survival, and disease progression. *In vivo* and *in vitro* experiments further demonstrate that LINC01123 influences diverse cellular processes, including proliferation, apoptosis, viability, migration, invasion, stemness, and tumor growth. Notably, it also regulates metabolic reprogramming, immune escape, and tumor cell resistance to treatment. LINC01123 is regulated by multiple transcription factors and participates in gene regulation through protein interactions and competitive endogenous RNA (ceRNA) networks, thereby modulating cancer-promoting effects. This work systematically elucidates its primary functions and molecular mechanisms driving cancer initiation and progression, suggesting that LINC01123 might serve as a novel potential oncogenic driver and biomarker in various cancers.

KEYWORDS

LINC01123, human tumors, biological functions, regulatory mechanism, cancer biomarker

1 Introduction

Long non-coding RNAs (lncRNAs) are RNA molecules longer than 200 nucleotides that do not encode proteins (1–4). Initially considered "junk" RNA, they are now recognized as crucial players in human diseases (5–7), particularly cancer (8–10). LncRNAs are classified based on their proximity to protein-coding genes, including

sense, antisense, intronic, bidirectional, or intergenic types (11–13). Mechanistically, one of the main functions of lncRNAs involves the ceRNA network (14–16). Acting as "sponges" for microRNAs (miRNAs), lncRNAs bind to miRNAs and modulate their availability for target mRNAs, thereby indirectly regulating gene expression. Disruptions in the ceRNA network involving lncRNAs are evident in various cancers (17–19). Accumulating evidence underscores the pivotal role of lncRNAs in cancer development and progression, highlighting their potential as targets for innovative therapeutic strategies (20–22).

Homo sapiens (human) Long Intergenic Non-Protein Coding RNA 1123 (LINC01123) is classified as a lncRNA gene located on chromosome 2q13. Spanning a length of 8302 nucleotides (nt), this gene comprises four exons (https://www.ncbi.nlm.nih.gov/gene/440894). The LINC01123 gene produces two splice variants: ENST00000419296.1, which is 2436 base pairs (bp) long, and ENST00000336905.3, which spans 2271 bp (Source: https://www.ensembl.org/Homo_sapiens/Gene/Summary?g=ENSG00000204588;r=2:109987063-109996140). LINC01123 has recently emerged as a key player in the pathogenesis of various diseases, including deep vein thrombosis (23), atherosclerosis (AS) (24), and acute cerebral infarction (25). Notably, its role in cancer progression has sparked considerable interest (26–28). LINC01123 is upregulated in a wide array of human tumors, and elevated expression levels of LINC01123 in cancerous samples correlate with adverse clinicopathological features and poor prognosis, including lymph node metastasis, tumor size, clinical stage, overall survival (OS), disease-free survival (DFS), and biochemical recurrence (BCR)-free survival. Furthermore, LINC01123 plays a critical role in crucial biological processes such as epithelial-mesenchymal transition (EMT), tumor cell growth, and invasion. Given its pivotal role in tumor progression, LINC01123 is expected to serve as a valuable tumor biomarker and contribute to the development of effective therapeutic strategies across various malignancies.

In this work, we provide a comprehensive summary of the latest research on the roles of LINC01123 in tumor development. We focus on LINC01123 expression patterns, associated clinical characteristics, its potential as a cancer biomarker, and its biological functions in tumor progression. Additionally, we examine the underlying mechanisms driving LINC01123's effects in various malignancies. This review highlights the promising prospects of LINC01123 as a target for therapeutic interventions in different cancer types.

2 Expression and clinical significance of LINC01123 in human tumors

Recently identified as an oncogenic lncRNA, LINC01123 demonstrates significant upregulation across multiple cancer types originating from various organ systems (26–37). These include cancers of the nervous system (glioma) (29), respiratory system (lung cancer, LC) (28, 30), head and neck region (oral squamous cell carcinoma, OSCC; head and neck squamous cell carcinoma, HNSCC) (26, 27), digestive system (hepatocellular carcinoma, HCC; colorectal cancer, CRC; intrahepatic cholangiocarcinoma) (31–35), and reproductive system (ovarian cancer, OC; cervical cancer, CC) (36, 37), as summarized in Table 1.

Research has investigated the relationship between LINC01123 expression and clinicopathological features across various cancer types (see Table 1). In OSCC, elevated expression of LINC01123 is associated with lymph node metastasis and advanced TNM stage (26). In non-small cell lung cancer (NSCLC), LINC01123

TABLE 1 Relationship between LINC01123 expression in tumor samples and clinicopathological features and prognosis in cancer patients.

Cancer type	Expression	Significant clinical variables	End-points	Unfavorable	Ref.
Colorectal cancer	Up-regulated	TNM stage, lymph-node metastasis	OS, DFS	High expression	(32)
Non-small cell lung cancer	Up-regulated	TNM stages, T stage, lymph node metastasis, mortality	OS	High expression	(28)
Hepatocellular carcinoma	Up-regulated	Tumor size, venous infiltration, TNM stage	OS	High expression	(31)
Oral squamous cell carcinoma	Up-regulated	Lymph node metastasis, TNM stage	OS	High expression	(26)
Colorectal cancer	Up-regulated	–	OS	High expression	(33)
Head and neck squamous cell carcinoma	Up-regulated	–	OS	High expression	(27)
Prostate cancer	–	–	BCR-free survival	High expression	(38)
Cervical cancer	Up-regulated	Lymph node metastasis, FIGO stage	–	–	(37)
Colon cancer	Up-regulated	–	–	–	(34)
Intrahepatic cholangiocarcinoma	Up-regulated	–	–	–	(35)
Ovarian cancer	Up-regulated	–	–	–	(36)
Glioma	Up-regulated	–	–	–	(29)
Lung adenocarcinoma	Up-regulated	–	–	–	(30)

TNM, Tumor; Node, Metastasis; FIGO, International Federation of Gynecology and Obstetrics; OS, Overall Survival; DFS, Disease-Free Survival; BCR, Biochemical Recurrence.

expression is significantly related to TNM stages, T stage, and lymph node metastasis (28). In HCC, increased levels of LINC01123 indicate larger tumor size, venous infiltration, and advanced TNM stage (31). In CRC, higher LINC01123 expression is observed in patients with advanced TNM stage and lymph node metastasis (32). Similarly, in CC, LINC01123 shows a significant positive correlation with lymph node metastasis and higher International Federation of Gynecology and Obstetrics (FIGO) stage (37). Additionally, high LINC01123 expression correlates highly with shorter OS in patients with OSCC (26), HNSCC (27), NSCLC (28), and HCC (31). And high LINC01123 expression levels are associated with worse OS and DFS in CRC patients (32), and LINC01123 is negatively associated with BCR-free survival in prostate cancer (38).

3 Upstream regulation of LINC01123 by trans-acting factors

Research has shown that the expression of LINC01123 is regulated by multiple key transcription factors across various tumors (Figure 1) (28, 39, 40). In triple-negative breast cancer (TNBC), LINC01123 is transcriptionally amplified by FOXC1, which directly binds to the LINC01123 promoter and promotes malignant cellular processes in tumor cells (39). This regulatory mechanism suggests that targeting FOXC1 or its interaction with LINC01123 could potentially disrupt tumor progression in TNBC. In lung cancer, studies demonstrate that ZEB1 binds to the LINC01123 promoter regions, initiating transcription and upregulating LINC01123 (40). This upregulation enhances malignant functions in lung adenocarcinoma (LUAD) cells through the miR-449b-5p/NOTCH1 axis, highlighting the potential of targeting this pathway to suppress LUAD progression. Additionally, the transcription factor c-Myc also induces LINC01123 expression, functioning as an oncogene by promoting proliferation and aerobic glycolysis in NSCLC through the miR-199a-5p/c-Myc feedback loop (28). These findings collectively underscore the critical role of transcription factors in regulating LINC01123 and suggest that disrupting these regulatory networks could offer novel therapeutic strategies for multiple cancer types.

4 Oncogenic roles of LINC01123 in tumorigenesis and development

Recent studies have extensively examined the role of LINC01123 across eleven different types of tumors, including glioma (29), OSCC (27), HNSCC (27), TNBC (39), NSCLC (28), LUAD (30, 40, 41), HCC (31), CRC (32–34, 42), OC (36), CC (37) and osteosarcoma (43). These investigations highlight the multifaceted role of LINC01123, as evidenced by various *in vivo* and *in vitro* experiments summarized in Table 2.

A consistent finding across these studies is the elevated expression of LINC01123 in numerous tumor cell lines. This observation suggests that LINC01123 could serve as a potential biomarker for tumor aggressiveness, providing an avenue for further research into its prognostic value. At the subcellular level, LINC01123 predominantly localizes to the cytoplasm in six types of cancer cells: colon cancer (32, 34), breast cancer (39), HNSCC (27), LUAD (30, 40), NSCLC (28), glioma (29). This cytoplasmic localization is crucial, as it implicates LINC01123 in the regulation of cytoplasmic processes, including interaction with microRNAs and other cellular components.

The oncogenic role of LINC01123 in tumorigenesis and development is multifaceted, influencing a variety of biological processes (see Figure 2). Notably, LINC01123 has been implicated in promoting EMT, which facilitates the metastatic capacity of tumors. By enhancing cell proliferation and inhibiting apoptosis, LINC01123 effectively increases cell viability, thereby supporting tumor growth. Moreover, LINC01123 facilitates not only cell migration and invasion but also induces a stem-like phenotype

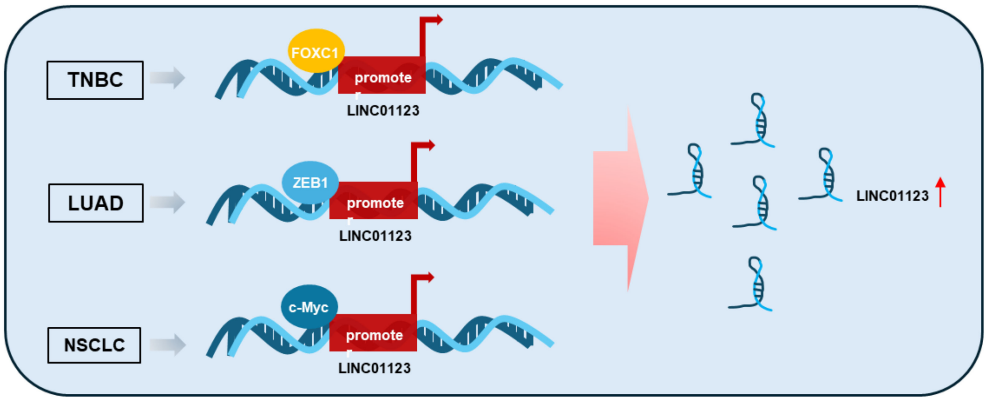


FIGURE 1
Mechanism by which the expression of LINC01123 is increased in tumors. Specific transcription factors such as FOXC1, ZEB1, and c-Myc bind to the promoter region of LINC01123, thereby initiating its transcription. TNBC, Triple-Negative Breast Cancer; LUAD, Lung Adenocarcinoma; NSCLC, Non-Small Cell Lung Cancer.

TABLE 2 The functions and regulatory mechanisms of LINC01123 in human cancers.

Cancer type	Experiments	Cellular functions	Related molecule/pathway	Role	Ref.
Glioma	*In vitro* and *in vivo*	Cell proliferation, apoptosis, radioresistance, tumor growth	LINC01123/miR-151a/CENPB	Cancer-promoting	(29)
Oral squamous cell carcinoma	*In vitro*	Cell proliferation, migration, invasion	LINC01123/miR-34a-5p	Cancer-promoting	(26)
Head and neck squamous cell carcinoma	*In vitro* and *in vivo*	Cell proliferation, migration, and invasion, immune escape, tumor growth	LINC01123/miR-214-3p/B7–H3	Cancer-promoting	(27)
Triple negative breast cancer	*In vitro*	Cell proliferation, cell apoptosis, cell viability	LINC01123/miR-663a/CMIP	Cancer-promoting	(39)
Lung adenocarcinoma	–	Cisplatin resistance	LINC01123/hsa–miR–152–3p/MED12, LINC01123/hsa–miR–152–3P/NCAM1, LINC01123/hsa–miR–152–3P/ARF4, LINC01123/hsa–miR–762/NCAM1, LINC01123/hsa–miR–762/RHBG	Cancer-promoting	(41)
Lung adenocarcinoma	*In vitro* and *in vivo*	Cell proliferation, migration, tumor growth	LINC01123/miR-4766-5p/PYCR1	Cancer-promoting	(30)
Non-small cell lung cancer	*In vitro* and *in vivo*	Cell proliferation, metabolic reprogramming (glycolysis), tumor growth	LINC01123/miR-199a-5p/c-Myc	Cancer-promoting	(28)
Lung adenocarcinoma	*In vitro*	Cell proliferation, apoptosis, migration, EMT, stemness	LINC01123/miR-449b-5p/NOTCH1, NOTCH signaling pathway	Cancer-promoting	(40)
Hepatocellular carcinoma	*In vitro* and *in vivo*	Cell proliferation, migration, invasion, tumor growth	LINC01123/miR-34a-5p/TUFT1	Cancer-promoting	(31)
Colorectal cancer	*In vitro*	Cell proliferation, invasion	LINC01123/miR-625-5p/LASP1	Cancer-promoting	(32)
Colorectal cancer	*In vitro* and *in vivo*	Cell proliferation, migration, invasion, tumor growth	LINC01123/SRSF7	Cancer-promoting	(33)
Colon cancer	*In vitro*	Cell proliferation, apoptosis, invasion, angiogenesis, chemosensitivity	LINC01123/miR-34c-5p/VEGFA	Cancer-promoting	(34)
Colorectal cancer	*In vitro* and *in vivo*	Cell viability, proliferation, apoptosis, migration, invasion, EMT, tumor growth	LINC01123/miR-625-5p/LASP1	Cancer-promoting	(42)
Ovarian cancer	*In vitro*	Cell proliferation, apoptosis, migration, invasion, EMT	LINC01123/miR-516b-5p/VEGFA	Cancer-promoting	(36)
Cervical cancer	*In vitro* and *in vivo*	Cell viability, migration, invasion, tumor growth	LINC01123/miR-361-3p/TSPAN1	Cancer-promoting	(37)
Osteosarcoma	*In vitro* and *in vivo*	Cell proliferation, apoptosis, migration, invasion, stemness, tumor growth	LINC01123/miR-516b-5p/Gli1, Hedgehog pathway	Cancer-promoting	(43)

associated with tumor-initiating properties. This shift towards stemness suggests that LINC01123 may contribute to tumor recurrence and treatment resistance, as cancer stem cells are often implicated in these phenomena. Furthermore, LINC01123 promotes metabolic reprogramming and immune escape, thereby enabling tumors to thrive in hostile environments. This capability underscores the potential for targeted therapies that could disrupt LINC01123 interactions, rendering tumors more susceptible to immune responses and conventional treatments. Lastly, LINC01123's involvement in angiogenesis and therapy resistance further highlights its critical role in sustaining tumor growth and resilience against treatment. Given these implications, LINC01123 emerges as a promising target for future therapeutic strategies aimed at combating a variety of cancers.

4.1 LINC01123 promotes tumor cell malignancy

LINC01123 has emerged as a pivotal regulator in various types of cancer, exerting significant influence on tumor cell malignancy through intricate molecular mechanisms.For example, in OSCC (26) and HCC (31), LINC01123 acts as a ceRNA by sequestering miR-34a-5p, which in turn upregulates TUFT1 expression. This regulatory interaction enhances cancer cell proliferation and invasion, highlighting LINC01123 as a potential therapeutic target to inhibit oncogenic processes. In TNBC (39), LINC01123 protects CMIP from miR-663a-mediated suppression. By acting as a miRNA sponge, LINC01123 promotes TNBC progression, implicating its role in modulating cellular processes crucial for tumor growth and metastasis. Studies in LUAD and CRC reveal that LINC01123 interacts with miR-4766-5p and miR-625-5p, respectively. In LUAD (30), LINC01123 regulates PYCR1 expression, influencing cancer cell proliferation and metastasis. Similarly, in CRC (42), LINC01123 competitively interacts with miR-625-5p to enhance LASP1 expression, thereby promoting tumor cell invasion and migration. In OC (36), LINC01123 regulates VEGFA through hsa-miR-516b-5p, impacting angiogenesis and tumor progression. Meanwhile, in CC (37), LINC01123 modulates the miR-361-3p/TSPAN1 axis to affect cell viability, migration, and invasion, underscoring its diverse roles in cancer cell behaviors. In osteosarcoma (43), LINC01123 promotes proliferation and metastasis via the miR-516b-5p/Gli1 axis, highlighting its oncogenic potential in bone cancer progression. Experimental evidence consistently shows that LINC01123 depletion inhibits tumor growth in preclinical models across these cancer types (30, 31, 33, 37, 42, 43). This underscores LINC01123 as a promising therapeutic target to disrupt oncogenic processes and improve patient outcomes. LINC01123 emerges as a critical regulator of tumor cell malignancy, exerting its effects through intricate ceRNA networks and signaling pathways. Understanding its multifaceted roles in promoting cancer progression provides a compelling rationale for further investigating targeted therapies aimed at suppressing LINC01123 activity in cancer cells.

4.2 LINC01123 regulates tumor metabolism and immunity

LINC01123 plays a critical role in shaping the tumor microenvironment through its dual regulation of metabolism and immunity in cancer (27, 28). Notably, in NSCLC, LINC01123 acts as a ceRNA, sequestering miR-199a-5p to enhance c-Myc expression (28). This interaction promotes metabolic adaptations, particularly increased glycolysis, which serves as a key energy source that fuels tumor growth and aggressiveness. The implication here is that by enhancing these metabolic pathways, LINC01123 not only supports tumor viability but also positions tumors to thrive under metabolic stress, further exacerbating their malignancy.

Moreover, LINC01123 establishes a positive feedback loop with c-Myc, which further amplifies these metabolic changes and facilitates tumor progression and metabolic reprogramming (28). This relationship highlights the potential for targeting this loop therapeutically; disrupting the feedback mechanism could impair tumor growth and shift metabolic reliance, rendering cancers more vulnerable to treatment.

Beyond its metabolic implications, LINC01123 significantly influences tumor immunity (27). In HNSCC, LINC01123 interacts with B7-H3 (27), a protein intricately linked to both immune escape and non-immune pathways of tumor invasion (44–46). The consequences of this interaction are profound; LINC01123 overexpression or the downregulation of miR-214-3p in HNSCC cells leads to dysfunctional CD8+ T cells (27). This dysfunction is characterized by decreased expression levels of key immune markers such as TNF-α, IFN-γ, perforin, and granzyme B (27). These markers are crucial for effective CD8+ T cell-mediated immune responses against tumors (47–49). The reversibility of LINC01123's detrimental effects through miR-214-3p silencing suggests promising therapeutic strategies aimed at restoring immune function and enhancing anti-tumor responses in HNSCC (27). By re-establishing the balance in this regulatory axis, it may be feasible to reinvigorate the immune response, offering a potential avenue for improving treatment outcomes.

Overall, understanding the intricate roles of LINC01123 in both metabolic reprogramming and immune evasion underscores its

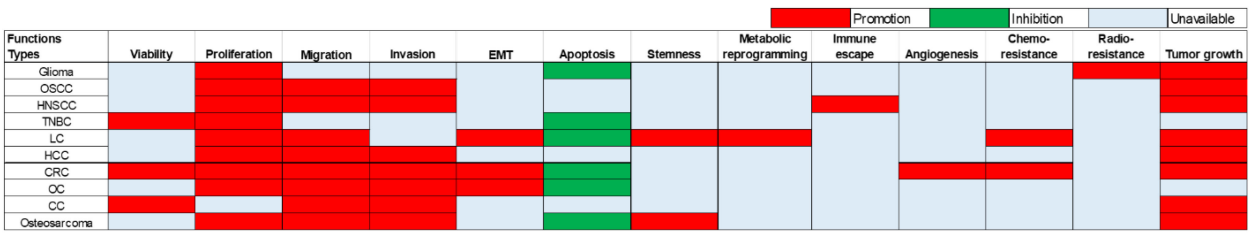


FIGURE 2
Diverse roles of oncogenic LINC01123 across ten different types of tumors. This underscores its wide-ranging impact in various cancers. These functions encompass the regulation of critical cellular processes such as proliferation, invasion, tumor growth, and more. OSCC, Oral Squamous Cell Carcinoma; HNSCC, Head and Neck Squamous Cell Carcinoma; TNBC, Triple-Negative Breast Cancer; LC, Lung Cancer; HCC, Hepatocellular Carcinoma; CRC, Colorectal Cancer; OC, Ovarian Cancer; CC, Cervical Cancer.

significance as a target in the development of novel therapies. By addressing both the metabolic and immune facets of tumor biology, strategies targeting LINC01123 could yield substantial improvements in combating tumor progression and enhancing the efficacy of existing treatments in cancer.

4.3 LINC01123 enhances treatment resistance

LINC01123 exhibits a crucial role in promoting resistance to treatment across different types of cancer. In glioma, LINC01123 is significantly upregulated in radioresistant cells (U251R), where it acts as a ceRNA by binding to miR-151a (29). This interaction decreases miR-151a levels, resulting in increased expression of CENPB. Elevated CENPB expression contributes to radioresistance by facilitating DNA repair mechanisms, as validated through *in vitro* and *in vivo* experiments involving xenograft tumors exposed to irradiation (29). In LUAD, LINC01123 is implicated in mediating cisplatin resistance through ceRNA pathways involving other lncRNAs such as HOXD-AS2 and FIRRE (41). This suggests a broader role for LINC01123 in modulating chemotherapy resistance mechanisms. In colon cancer, LINC01123 localizes predominantly in the cytoplasm, where it competes with VEGFA for binding to miR-34c-5p (34). By sequestering miR-34c-5p, LINC01123 upregulates VEGFA expression at both mRNA and protein levels, promoting angiogenesis and potentially contributing to chemoresistance (34). LINC01123 plays a pivotal role in enhancing resistance to treatment in various cancers by regulating ceRNA networks and influencing key downstream effectors. Targeting LINC01123 and its ceRNA networks could potentially reverse treatment resistance.

5 Mechanisms of LINC01123 in regulating biological functions

5.1 Regulation through ceRNA networks

The role of LINC01123 as a ceRNA has been comprehensively studied across a variety of tumors (26–32, 34, 36, 37, 39–43), revealing diverse mechanisms through which it influences tumor biology. For instance, in glioma, LINC01123 has been shown to regulate the miR-151a/CENPB pathway, thereby enhancing radioresistance (29). This suggests that targeting LINC01123 could potentially improve therapeutic outcomes in glioma treatment by overcoming resistance. Similarly, in OSCC, LINC01123 promotes tumor progression by sponging miR-34a-5p (26). The implication here is significant; by inhibiting a key microRNA associated with tumor suppression, LINC01123 may facilitate a more aggressive tumor phenotype, highlighting the need for strategies that disrupt this interaction. In HNSCC, LINC01123 regulates the expression of B7-H3 through sponging miR-214-3p. This interaction leads to B7-H3 upregulation, which inhibits CD8+ T cell activation and contributes to immune evasion (27). Consequently, targeting this pathway may enhance immunotherapeutic efficacy against HNSCC by reinstating T cell activation. In TNBC, LINC01123 exerts influence over tumor growth via the LINC01123/miR-663a/CMIP axis (39). This suggests a potential therapeutic avenue; by disrupting this axis, it may be possible to mitigate tumor growth and progression in TNBC. In LUAD, Li et al. (41) demonstrated that LINC01123 could contribute to cisplatin resistance. This is achieved through ceRNA networks involving hsa-miR-152-3p/MED12-NCAM1-ARF4 and hsa-miR-762/NCAM1-RHBG axes. These findings stress the importance of LINC01123 in chemoresistance, suggesting that targeting it could enhance the effectiveness of cisplatin in LUAD therapy. Additionally, both *in vitro* and *in vivo* studies have shown that LINC01123 accelerates malignancy in NSCLC by acting as a ceRNA, thereby influencing multiple axes including miR-4766-5p/PYCR1 (30), miR-199a-5p/c-Myc (28), and miR-449b-5p/NOTCH1 (40). These findings highlight the multifaceted role of LINC01123 in promoting NSCLC, reinforcing the notion of its potential as a target for therapeutic intervention. In HCC, it promotes tumor cell proliferation and invasion by modulating the miR-34a-5p/TUFT1 axis (31). This suggests that LINC01123 could be a valuable marker for HCC aggressiveness. In CRC, LINC01123 drives tumor progression by regulating miR-34c-5p/VEGFA (34) and miR-625-5p/LASP1 axes (32, 42). These interactions underline the potential of LINC01123 as a therapeutic target to impede CRC advancement. Furthermore, in ovarian cancer, LINC01123 enhances malignancy by competitively binding to hsa-miR-516b-5p, leading to VEGFA upregulation (36). This pathway suggests a critical role for LINC01123 in fostering an angiogenic tumor environment. In cervical cancer, LINC01123 stimulates proliferation, migration, and invasion by inhibiting miR-361-3p and upregulating TSPAN1 (37). This interplay underscores the necessity of investigating LINC01123's mechanisms in cervical cancer to potentially hinder its metastatic capabilities. Lastly, LINC01123 enhances osteosarcoma proliferation and metastasis via the miR-516b-5p/Gli1 axis (43). This highlights the potential for LINC01123 to serve as a therapeutic target across various cancer types. All LINC01123-associated ceRNA networks are illustrated in Figure 3.

5.2 Formation of RNA-protein complexes

The primary function of lncRNAs involves their interaction with cellular macromolecules, which is crucial for various regulatory processes within the cell (50–52). Specifically, LINC01123 is capable of forming RNA-protein complexes, utilizing specific proteins as structural components. This interaction not only facilitates the modulation of LINC01123 but also significantly affects the expression and functionality of subsequent molecular targets.

In CRC, Liu et al. (33) provided compelling evidence that LINC01123 specifically interacts with SRSF7, a notable member of the splicing factor family involved in critical cellular processes such as splicing, transport, and polypeptide synthesis (53–55). The expression levels of LINC01123 positively correlate with those of

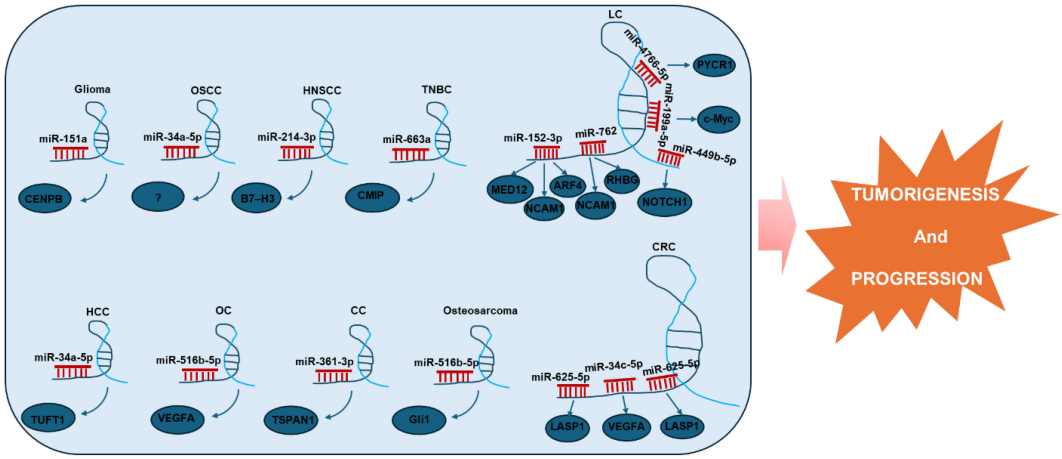


FIGURE 3
LINC01123 participates in a complex ceRNA network, competitively binding with miRNAs in various cancers. This interaction regulates the downregulation of oncogenic targets, thereby promoting tumorigenesis and disease progression. OSCC, Oral Squamous Cell Carcinoma; HNSCC, Head and Neck Squamous Cell Carcinoma; TNBC, Triple-Negative Breast Cancer; LC, Lung Cancer; HCC, Hepatocellular Carcinoma; CRC, Colorectal Cancer; OC, Ovarian Cancer; CC, Cervical Cancer.

SRSF7, indicating that higher levels of LINC01123 may enhance the activity of SRSF7. SRSF7 has been found to be overexpressed in various cancers and plays a significant role in regulating the alternative splicing of key oncogenes (56–59). This raises important implications: by forming RNA-protein complexes with SRSF7, LINC01123 may alter alternative splicing processes, potentially leading to the upregulation of downstream oncogenes that drive tumorigenesis.

The functional consequences of this interaction are substantial; experimental studies have demonstrated that through these RNA-protein complexes, LINC01123 not only influences splicing but also promotes tumor growth and migration (33). Such effects have been validated in both *in vitro* and *in vivo* experiments (33), indicating a potential pathway through which LINC01123 contributes to CRC progression and underscores its role as a critical factor in cancer biology.

6 Future perspectives

A huge amount of evidence recent suggested that lncRNAs play a vital role in the development of human diseases (60–62). Further investigation into different lncRNAs in human cancers, particularly their involvement in both the onset and advancement of tumors, is valuable and warrants exploration and consolidation. Here, we comprehensively examine current research the clinical values and roles of LINC01123 in human tumors and provides insights into its molecular regulatory mechanisms.

LINC01123, a newly identified lncRNA, consistently exhibits upregulation in various cancerous tissues and cell lines (26–38), suggesting its potential as an oncogene in tumorigenesis. Similarly, overexpression of LINC01089 is associated with advanced clinicopathological features across different cancer types (26, 28, 31, 32, 37), including larger tumor size, lymph node metastasis, and higher TNM stage. Elevated levels of LINC01089 also correlate with poorer prognosis (26–28, 31–33, 38), leading to shorter overall survival and accelerated cancer progression. Thus, LINC01123 serve as a promising prognostic biomarker in multiple tumors.

Recent experimental investigations have characterized the functional roles of LINC01123 across eleven distinct cancer types (Table 2), including glioma (29), OSCC (27), HNSCC (27), TNBC (39), LUAD (30, 40, 41), NSCLC (28), HCC (31), CRC (32–34, 42), OC (36), CC (37) and osteosarcoma (43). These studies have elucidated its regulatory interactions with critical molecular targets, key signaling pathways, and essential biological processes that drive tumorigenesis and cancer progression, as illustrated in Figure 4. LINC01123 functions as a pivotal oncogenic factor by regulating tumor cell proliferation, apoptosis, viability, invasion, migration, and EMT. Notably, LINC01123 is also implicated in stemness, glycolysis, angiogenesis, and resistance to various tumor therapies. These effects are mediated through diverse mechanisms, including the lncRNA-miRNA-mRNA ceRNA network, NOTCH and Hedgehog pathways, and interactions with SRSF7. Consequently, LINC01123 plays critical roles in tumor progression, glycolysis, tumor immunity, and therapy resistance. Targeting LINC01123 has thus emerged as a promising therapeutic strategy for cancer treatment.

Research on LINC01123 indicates its expression has been studied in nine types of solid tumors (Table 1), including glioma (29), lung cancer (LUAD, NSCLC) (28, 30), OSCC (26), HNSCC (27), HCC (31), CRC (32–34), intrahepatic cholangiocarcinoma (35), OC (36) and CC (37), yet its presence in hematologic malignancies and other solid cancers remains unexplored. To establish its broader relevance, future studies should investigate

10.3389/fimmu.2025.1480447

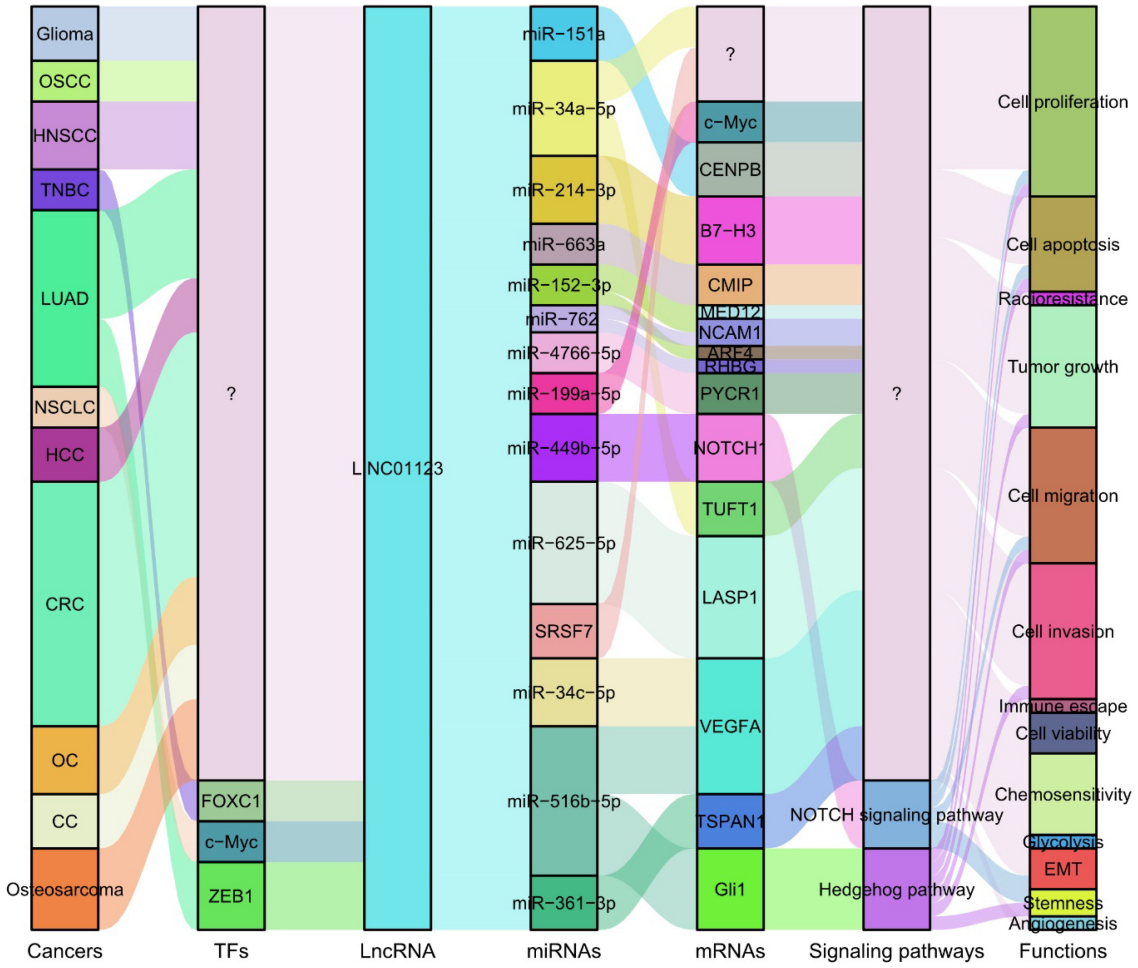


FIGURE 4
Summary of the mechanisms by which LINC01123 participates in various biological processes associated with tumor pathogenesis and progression. LINC01123 is regulated by key transcription factors, including FOXC1, c-Myc, and ZEB1. LINC01123 participates in multiple lncRNA-miRNA-mRNA ceRNA networks and regulates critical signaling pathways such as NOTCH and Hedgehog. Through these mechanisms, LINC01123 functions as a pivotal oncogenic factor, modulating various tumor processes. OSCC, Oral Squamous Cell Carcinoma; HNSCC, Head and Neck Squamous Cell Carcinoma; TNBC, Triple-Negative Breast Cancer; LUAD, Lung Adenocarcinoma; NSCLC, Non-Small Cell Lung Cancer; HCC, Hepatocellular Carcinoma; CRC, Colorectal Cancer; OC, Ovarian Cancer; CC, Cervical Cancer; TFs, Transcription Factors; EMT, Epithelial-Mesenchymal Transition.

its expression across hematologic malignancies and additional solid cancer types. Moreover, while LINC01123 has shown prognostic implications in seven tumor types (26–28, 31–33, 38), its clinical significance across diverse cancer stages and types requires validation through larger patient cohorts. On the other hand, LINC01123 has been implicated in various tumors, indicating a need for further *in vivo* and *in vitro* studies to delineate its specific roles and mechanisms in different cancer contexts. Its complex functions underscore the importance of gaining comprehensive insights into its involvement in distinct pathways and ceRNA networks, as well as lncRNA-protein interactions across different cancers. Additionally, studies have explored its potential associations with tumor metabolism in NSCLC (28) and immunity in HNSCC (27), while research into drug resistance is currently limited to radioresistance in glioma (29), chemotherapy resistance in LUAD (41), and colon cancer (34). Further studies are needed to explore these associations in more depth, mechanistically and across more cancer types.

7 Conclusion

In conclusion, LINC01123 has emerged as a newly identified and dysregulated cancer-associated lncRNA, highlighting its potential as both a promising biomarker and a key player in multiple critical aspects of tumor progression, metabolism, immune evasion, and therapeutic resistance. Targeting LINC01123 may offer new therapeutic avenues and enhance the efficacy of existing treatment options. However, further mechanistic investigations and large-scale comprehensive clinical studies are essential to elucidate its precise role in human cancer pathogenesis and to assess its clinical applicability.

Author contributions

QL: Data curation, Formal analysis, Investigation, Methodology, Validation, Visualization, Writing – original draft. HH: Formal analysis, Methodology, Resources, Validation, Visualization, Writing – original draft. SZ: Methodology, Resources, Validation, Writing – original draft. FL: Investigation, Project administration, Supervision, Writing – review & editing, Writing – original draft, Conceptualization, Formal analysis, Methodology, Validation, Visualization. TL: Investigation, Project administration, Supervision, Validation, Writing – original draft, Writing – review & editing.

Funding

The author(s) declare that no financial support was received for the research and/or publication of this article.

Conflict of interest

The authors declare that the research was conducted in the absence of any commercial or financial relationships that could be construed as a potential conflict of interest.

Publisher's note

All claims expressed in this article are solely those of the authors and do not necessarily represent those of their affiliated organizations, or those of the publisher, the editors and the reviewers. Any product that may be evaluated in this article, or claim that may be made by its manufacturer, is not guaranteed or endorsed by the publisher.

References

1. Statello L, Guo CJ, Chen LL, Huarte M. Gene regulation by long non-coding RNAs and its biological functions. *Nat Rev Mol Cell Biol*. (2021) 22:96–118. doi: 10.1038/s41580-020-00315-9

2. Quinn JJ, Chang HY. Unique features of long non-coding RNA biogenesis and function. *Nat Rev Genet*. (2016) 17:47–62. doi: 10.1038/nrg.2015.10

3. Rinn JL, Chang HY. Genome regulation by long noncoding RNAs. *Annu Rev Biochem*. (2012) 81:145–66. doi: 10.1146/annurev-biochem-051410-092902

4. Mercer TR, Dinger ME, Mattick JS. Long non-coding RNAs: insights into functions. *Nat Rev Genet*. (2009) 10:155–9. doi: 10.1038/nrg2521

5. Wapinski O, Chang HY. Long noncoding RNAs and human disease. *Trends Cell Biol*. (2011) 21:354–61. doi: 10.1016/j.tcb.2011.04.001

6. Chen Y, Li Z, Chen X, Zhang S. Long non-coding RNAs: From disease code to drug role. *Acta Pharm Sin B*. (2021) 11:340–54. doi: 10.1016/j.apsb.2020.10.001

7. Long F, Zhou X, Zhang J, Di C, Li X, Ye H, et al. The role of lncRNA HCG18 in human diseases. *Cell Biochem Funct*. (2024) 42:e3961. doi: 10.1002/cbf.v42.2

8. Wang J, Luo H, Yang L, Yuan H. ARAP1-AS1: a novel long non-coding RNA with a vital regulatory role in human cancer development. *Cancer Cell Int*. (2024) 24:270. doi: 10.1186/s12935-024-03435-w

9. Liao B, Wang J, Xie Y, Luo H, Min J. LINK-A: unveiling its functional role and clinical significance in human tumors. *Front Cell Dev Biol*. (2024) 12:1354726. doi: 10.3389/fcell.2024.1354726

10. Hu Y, Hu Y, Lu X, Luo H, Chen Z. LINC00839 in Human Disorders: Insights into its Regulatory Roles and Clinical Impact, with a Special Focus on Cancer. *J Cancer*. (2024) 15:2179–92. doi: 10.7150/jca.93820

11. Liu Y, Ding W, Yu W, Zhang Y, Ao X, Wang J. Long non-coding RNAs: Biogenesis, functions, and clinical significance in gastric cancer. *Mol Ther oncolytics*. (2021) 23:458–76. doi: 10.1016/j.omto.2021.11.005

12. Ransohoff JD, Wei Y, Khavari PA. The functions and unique features of long intergenic non-coding RNA. *Nat Rev Mol Cell Biol*. (2018) 19:143–57. doi: 10.1038/nrm.2017.104

13. Mattick JS, Amaral PP, Carninci P, Carpenter S, Chang HY, Chen L-L, et al. Long non-coding RNAs: definitions, functions, challenges and recommendations. *Nat Rev Mol Cell Biol*. (2023) 24:430–47. doi: 10.1038/s41580-022-00566-8

14. Xu J, Xu J, Liu X, Jiang J. The role of lncRNA-mediated ceRNA regulatory networks in pancreatic cancer. *Cell Death discovery*. (2022) 8:287. doi: 10.1038/s41420-022-01061-x

15. Kartha RV, Subramanian S. Competing endogenous RNAs (ceRNAs): new entrants to the intricacies of gene regulation. *Front Genet*. (2014) 5:8. doi: 10.3389/fgene.2014.00008

16. Thomson DW, Dinger ME. Endogenous microRNA sponges: evidence and controversy. *Nat Rev Genet*. (2016) 17:272–83. doi: 10.1038/nrg.2016.20

17. Nejadi Orang F, Abdoli Shadbad M. CircRNA and lncRNA-associated competing endogenous RNA networks in medulloblastoma: a scoping review. *Cancer Cell Int*. (2024) 24:248. doi: 10.1186/s12935-024-03427-w

18. Ma H, Weng F, Tong X, Li H, Yao Y, Yuan J. LncRNA TRPM2-AS promotes endometrial carcinoma progression and angiogenesis via targeting miR-497-5p/SPP1 axis. *Cell Mol Biol letters*. (2024) 29:93. doi: 10.1186/s11658-024-00612-7

19. Wang M, Niu X, Wang M, Zheng P, Liu X, Cao Z, et al. Long non-coding RNA RP11-197K6.1 as ceRNA promotes colorectal cancer progression via miR-135a-5p/DLX5 axis. *J Trans Med*. (2024) 22:469. doi: 10.1186/s12967-024-05286-5

20. Coan M, Haefliger S, Ounzain S, Johnson R. Targeting and engineering long non-coding RNAs for cancer therapy. *Nat Rev Genet*. (2024) 25:578–95. doi: 10.1038/s41576-024-00693-2

21. Kadian LK, Verma D, Lohani N, Yadav R, Ranga S, Gulshan G, et al. Long non-coding RNAs in cancer: multifaceted roles and potential targets for immunotherapy. *Mol Cell Biochem*. (2024) 479:3229–3254. doi: 10.1007/s11010-024-04933-1

22. Peng WX, Koirala P, Mo YY. LncRNA-mediated regulation of cell signaling in cancer. *Oncogene*. (2017) 36:5661–7. doi: 10.1038/onc.2017.184

23. Yang B, Zhang Z. Suppression of long intergenic non-protein coding RNA 1123 constrains lower extremity deep vein thrombosis via microRNA-125a-3p to target interleukin 1 receptor type 1. *Bioengineered*. (2022) 13:13452–61. doi: 10.1080/21655979.2022.2076496

24. Weng G, Gu M, Zhang Y, Zhao G, Gu Y. LINC01123 promotes cell proliferation and migration via regulating miR-1277-5p/KLF5 axis in ox-LDL-induced vascular smooth muscle cells. *J Mol histology*. (2021) 52:943–53. doi: 10.1007/s10735-021-10010-4

25. Ding SW, Wang JJ. Diagnostic value and clinical significance of lncRNA LINC01123 combined with fibrinogen in acute cerebral infarction. *Clin Neurol Neurosurg*. (2024) 241:108309. doi: 10.1016/j.clineuro.2024.108309

26. Qin H, Wang C, Hua Y. LINC01123 is associated with prognosis of oral squamous cell carcinoma and involved in tumor progression by sponging miR-34a-5p. *Oral Surg Oral Med Oral Pathol Oral Radiol*. (2022) 133:50–9. doi: 10.1016/j.oooo.2021.07.013

27. Li H, Yang Z, Yang X, Zhang F, Wang J, Wu Z, et al. LINC01123 promotes immune escape by sponging miR-214-3p to regulate B7-H3 in head and neck squamous-cell carcinoma. *Cell Death disease*. (2022) 13:109. doi: 10.1038/s41419-022-04542-0

28. Hua Q, Jin M, Mi B, Xu F, Li T, Zhao L, et al. LINC01123, a c-Myc-activated long non-coding RNA, promotes proliferation and aerobic glycolysis of non-small cell lung cancer through miR-199a-5p/c-Myc axis. *J Hematol Oncol*. (2019) 12:91. doi: 10.1186/s13045-019-0773-y

29. Tian W, Zhang Y, Liu H, Jin H, Sun T. LINC01123 potentially correlates with radioresistance in glioma through the miR-151a/CENPB axis. *Neuropathology*. (2022) 42:3–15. doi: 10.1111/neup.12764

30. Wang H, He D. LINC01123 acts as an oncogenic driver in lung adenocarcinoma by regulating the miR-4766-5p/PYCR1 axis. *Histol Histopathol*. (2023) 38:1475–86. doi: 10.14670/HH-18-610

31. Xiao Z, Liu Y, Zhao J, Li L, Hu L, Lu Q, et al. Long noncoding RNA LINC01123 promotes the proliferation and invasion of hepatocellular carcinoma cells by modulating the miR-34a-5p/TUFT1 axis. *Int J Biol Sci*. (2020) 16:2296–305. doi: 10.7150/ijbs.45457

32. Shang T, Zhou X, Chen W. LINC01123 Promotes the Progression of Colorectal Cancer via miR-625-5p/LASP1 Axis. *Cancer biotherapy radiopharmaceuticals*. (2021) 36:765–73. doi: 10.1089/cbr.2020.3740

33. Liu Z, Ma L, Gu Y, Huang Y, Liang X, Kong L, et al. Long non-coding RNA LINC01123 promotes cell proliferation, migration and invasion via interacting with SRSF7 in colorectal cancer. *Pathology Res practice*. (2022) 232:153843. doi: 10.1016/j.prp.2022.153843

34. Ye S, Sun B, Wu W, Yu C, Tian T, Lian Z, et al. LINC01123 facilitates proliferation, invasion and chemoresistance of colon cancer cells. *Bioscience Rep*. (2020) 40:BSR20194062. doi: 10.1042/BSR20194062

35. Yang W, Li Y, Song X, Xu J, Xie J. Genome-wide analysis of long noncoding RNA and mRNA co-expression profile in intrahepatic cholangiocarcinoma tissue by RNA sequencing. *Oncotarget*. (2017) 8:26591–9. doi: 10.18632/oncotarget.15721

36. Dong B, Li C, Xu X, Wang Y, Li Y, Li X. LncRNA LINC01123 promotes Malignancy of ovarian cancer by targeting hsa-miR-516b-5p/VEGFA. *Genes Genomics*. (2024) 46:231–9. doi: 10.1007/s13258-023-01440-3

37. Li C, Li Y, Zhang Y, Yan H, Huang C. Knockdown of LINC01123 inhibits cell viability, migration and invasion via miR-361-3p/TSPAN1 targeting in cervical cancer. *Exp Ther Med*. (2021) 22:1184. doi: 10.3892/etm.2021.10618

38. Huang TB, Dong CP, Zhou GC, Lu SM, Luan Y, Gu X, et al. A potential panel of four-long noncoding RNA signature in prostate cancer predicts biochemical recurrence-free survival and disease-free survival. *Int Urol Nephrol*. (2017) 49:825–35. doi: 10.1007/s11255-017-1536-8

39. Zhang P, Long Q, Zeng S, Wen M, Lu Q. FOXC1-induced LINC01123 acts as a mediator in triple negative breast cancer. *Cancer Cell Int*. (2020) 20:199. doi: 10.1186/s12935-020-01258-z

40. Zhang M, Han Y, Zheng Y, Zhang Y, Zhao X, Gao Z, et al. ZEB1-activated LINC01123 accelerates the Malignancy in lung adenocarcinoma through NOTCH signaling pathway. *Cell Death disease*. (2020) 11:981. doi: 10.1038/s41419-020-03166-6

41. Li Y, Huang S, Wei Z, Yang B. A putative competing endogenous RNA network in cisplatin-resistant lung adenocarcinoma cells identifying potentially rewarding research targets. *Oncol letters*. (2020) 19:4040–52. doi: 10.3892/ol.2020.11483

42. Shang T, Pang S, Dong Y. Knockdown of long non-coding RNA LINC01123 plays a molecular sponge on miR-625-5p to inhibit the process of colorectal cancer cells via LASP1. *J Mol histology*. (2023) 54:521–37. doi: 10.1007/s10735-023-10141-w

43. Pan X, Tan J, Tao T, Zhang X, Weng Y, Weng X, et al. LINC01123 enhances osteosarcoma cell growth by activating the Hedgehog pathway via the miR-516b-5p/Gli1 axis. *Cancer science*. (2021) 112:2260–71. doi: 10.1111/cas.v112.6

44. Chapoval AI, Ni J, Lau JS, Wilcox RA, Flies DB, Liu D, et al. B7-H3: a costimulatory molecule for T cell activation and IFN-gamma production. *Nat Immunol*. (2001) 2:269–74. doi: 10.1038/85339

45. Zang X, Thompson RH, Al-Ahmadie HA, Serio AM, Reuter VE, Eastham JA, et al. B7-H3 and B7x are highly expressed in human prostate cancer and associated with disease spread and poor outcome. *Proc Natl Acad Sci United States America*. (2007) 104:19458–63. doi: 10.1073/pnas.0709802104

46. Sun Y, Wang Y, Zhao J, Gu M, Giscombe R, Lefvert AK, et al. B7-H3 and B7-H4 expression in non-small-cell lung cancer. *Lung Cancer*. (2006) 53:143–51. doi: 10.1016/j.lungcan.2006.05.012

47. Koh C-H, Lee S, Kwak M, Kim B-S, Chung Y. CD8 T-cell subsets: heterogeneity, functions, and therapeutic potential. *Exp Mol Med*. (2023) 55:2287–99. doi: 10.1038/s12276-023-01105-x

48. St Paul M, Ohashi PS. The roles of CD8(+) T cell subsets in antitumor immunity. *Trends Cell Biol*. (2020) 30:695–704. doi: 10.1016/j.tcb.2020.06.003

49. Wang J, Wu H, Chen Y, Zhu J, Sun L, Li J, et al. B7-H5 blockade enhances CD8(+) T-cell-mediated antitumor immunity in colorectal cancer. *Cell Death discovery*. (2021) 7:248. doi: 10.1038/s41420-021-00628-4

50. Zhu J, Fu H, Wu Y, Zheng X. Function of lncRNAs and approaches to lncRNA-protein interactions. *Sci China Life Sci*. (2013) 56:876–85. doi: 10.1007/s11427-013-4553-6

51. Yao R-W, Wang Y, Chen L-L. Cellular functions of long noncoding RNAs. *Nat Cell Biol*. (2019) 21:542–51. doi: 10.1038/s41556-019-0311-8

52. Li Y. Non-coding RNA performs its biological function by interacting with macromolecules. *Int J Mol Sci*. (2023) 24:16246. doi: 10.3390/ijms242216246

53. Könige V, de Oliveira Freitas MaChado C, Arnold B, Blümel N, Solovyeva A, Löbbert S, et al. SRSF7 maintains its homeostasis through the expression of Split-ORFs and nuclear body assembly. *Nat Struct Mol Biol*. (2020) 27:260–73. doi: 10.1038/s41594-020-0385-9

54. Zheng X, Peng Q, Wang L, Zhang X, Huang L, Wang J, et al. Serine/arginine-rich splicing factors: the bridge linking alternative splicing and cancer. *Int J Biol Sci*. (2020) 16:2442–53. doi: 10.7150/ijbs.46751

55. Wagner RE, Frye M. Noncanonical functions of the serine-arginine-rich splicing factor (SR) family of proteins in development and disease. *Bioessays*. (2021) 43:e2000242. doi: 10.1002/bies.202000242

56. Bei M, Xu J. SR proteins in cancer: function, regulation, and small inhibitor. *Cell Mol Biol letters*. (2024) 29:78. doi: 10.1186/s11658-024-00594-6

57. Shen W, Yuan L, Cheng F, Wu Z, Li X. SRSF7 is a promising prognostic biomarker in hepatocellular carcinoma and is associated with immune infiltration. *Genes Genomics*. (2024) 46:49–64. doi: 10.1007/s13258-023-01463-w

58. Fu Y, Wang Y. SRSF7 knockdown promotes apoptosis of colon and lung cancer cells. *Oncol letters*. (2018) 15:5545–52. doi: 10.3892/ol.2018.8072

59. Boguslawska J, Sokol E, Rybicka B, Czubaty A, Rodzik K, Piekielko-Witkowska A. microRNAs target SRSF7 splicing factor to modulate the expression of osteopontin splice variants in renal cancer cells. *Gene*. (2016) 595:142–9. doi: 10.1016/j.gene.2016.09.031

60. López-Jiménez E, Andrés-León E. The implications of ncRNAs in the development of human diseases. *Non-coding RNA*. (2021) 7:17. doi: 10.3390/ncrna7010017

61. Zhang X, Hong R, Chen W, Xu M, Wang L. The role of long noncoding RNA in major human disease. *Bioorganic Chem*. (2019) 92:103214. doi: 10.1016/j.bioorg.2019.103214

62. Srinivas T, Mathias C, Oliveira-Mateos C, Guil S. Roles of lncRNAs in brain development and pathogenesis: Emerging therapeutic opportunities. *Mol Ther*. (2023) 31:1550–61. doi: 10.1016/j.ymthe.2023.02.008

frontiers | Frontiers in Immunology

TYPE Review
PUBLISHED 25 April 2025
DOI 10.3389/fimmu.2025.1523190

Check for updates

OPEN ACCESS

EDITED BY
Alice Conigliaro,
University of Palermo, Italy

REVIEWED BY
Jin-Fen Xiao,
University of Texas MD Anderson Cancer Center, United States
Mengsha Shi,
Nanjing Medical University, China
Baojie Mao,
Zhejiang University, China

*CORRESPONDENCE
Minjie Chen
chenminjiedoctor@163.com
Xiaoguang Wang
xiaoguangwangs@163.com
Zhengwei Song
doctorsongzw@zjxu.edu.cn

†These authors share first authorship

RECEIVED 05 November 2024
ACCEPTED 02 April 2025
PUBLISHED 25 April 2025

CITATION
Zhao S, Chen F, Hu L, Li X, Gao Z, Chen M, Wang X and Song Z (2025) Long non-coding rnas as key modulators of the immune microenvironment in hepatocellular carcinoma: implications for Immunotherapy. *Front. Immunol.* 16:1523190. doi: 10.3389/fimmu.2025.1523190

COPYRIGHT
© 2025 Zhao, Chen, Hu, Li, Gao, Chen, Wang and Song. This is an open-access article distributed under the terms of the Creative Commons Attribution License (CC BY). The use, distribution or reproduction in other forums is permitted, provided the original author(s) and the copyright owner(s) are credited and that the original publication in this journal is cited, in accordance with accepted academic practice. No use, distribution or reproduction is permitted which does not comply with these terms.

Long non-coding rnas as key modulators of the immune microenvironment in hepatocellular carcinoma: implications for Immunotherapy

Siqi Zhao†, Fei Chen†, Lingyu Hu†, Xiaoping Li, Zhaofeng Gao, Minjie Chen*, Xiaoguang Wang* and Zhengwei Song*

Department of Surgery, the Second Affiliated Hospital of Jiaxing University, Jiaxing, Zhejiang, China

Hepatocellular carcinoma (HCC) represents a major global health challenge, characterized by its complex immune microenvironment that plays a pivotal role in tumor progression and therapeutic response. Long non-coding RNAs (lncRNAs) have emerged as critical regulators of various biological processes, including gene expression and immune cell function. This review explores the multifaceted roles of lncRNAs in modulating the immune microenvironment of HCC. We discuss how lncRNAs influence the infiltration and activation of immune cells, shape cytokine profiles, and regulate immune checkpoint molecules, thereby affecting the tumor's immunogenicity and response to immunotherapy. Furthermore, we highlight specific lncRNAs implicated in immune evasion mechanisms and their potential as biomarkers and therapeutic targets. By elucidating the intricate interplay between lncRNAs and the immune landscape in HCC, this review aims to provide insights into novel strategies for enhancing immunotherapeutic efficacy and improving patient outcomes.

KEYWORDS

lncRNAs, HCC, immune microenvironment, immunotherapy, immune evasion

1 Introduction

HCC is the most common type of primary liver cancer and ranks as one of the leading causes of cancer-related mortality worldwide (1, 2). Its development is often associated with underlying liver diseases, including chronic hepatitis B and C infections, cirrhosis, and metabolic disorders (3–5). Despite advances in surgical and systemic therapies, the prognosis for patients with HCC remains poor, largely due to the tumor's aggressive nature and its ability to evade the host immune response (6).

The tumor microenvironment (TME) plays a crucial role in HCC progression and therapeutic resistance (7). It is composed of various cell types, including tumor cells, immune cells, fibroblasts, and endothelial cells, all of which interact dynamically to

influence tumor behavior (7–9). These immune cells can either promote anti-tumor immunity or facilitate tumor growth through immunosuppressive mechanisms, contributing to the challenges faced in effective treatment (8, 10).

At present, cancer immunotherapies such as immune checkpoint inhibitors (ICIs) (such as anti-PD-1/PD-L1 monoclonal antibody) and CAR-T cell therapy have made breakthroughs in a variety of tumors, but their efficacy in HCC is still limited to a certain extent (11–13). Although checkpoint inhibitors partially improve the survival of patients with advanced HCC, their overall response rate is less than 20% and they are prone to secondary drug resistance (14). CAR-T therapy is effective in hematologic tumors, but progress is slow due to the high heterogeneity of HCC, immunosuppressive microenvironment and physical barrier of solid tumors (15). In addition, HCC is often accompanied by chronic inflammation and cirrhosis, leading to depletion of immune cell function and increased infiltration of immunosuppressive cells (such as Treg and MDSC), further weakening treatment response (8). These limitations highlight the urgent need for in-depth analysis of HCC-specific immune regulatory mechanisms, such as lncrNA-mediated immune escape, to develop combination strategies.

Recent studies have identified lncRNAs as critical regulators of gene expression and cellular processes in cancer (16, 17). These RNA molecules, which are over 200 nucleotides in length and do not code for proteins, have been shown to play diverse roles in modulating cellular behavior, including apoptosis, proliferation, and immune responses (18, 19). Emerging evidence suggests that lncRNAs are involved in shaping the immune microenvironment of various tumors, including HCC, by regulating the functions of immune cells and influencing the expression of immune-related genes (20).

In this review, we will explore the intricate relationships between lncRNAs and the immune microenvironment in HCC. We will discuss how lncRNAs contribute to immune cell infiltration, modulation of cytokine secretion, and regulation of immune checkpoints, thereby impacting the tumor's immunogenicity and response to therapies. By understanding these mechanisms, we aim to highlight the potential of lncRNAs as biomarkers and therapeutic targets in HCC, paving the way for novel strategies to enhance immunotherapy outcomes.

2 HCC and immune microenvironment

The immune microenvironment in HCC is a complex network that significantly influences tumor progression and therapeutic outcomes (3, 21). Comprised of various immune and stromal cell types, the immune landscape of HCC is characterized by both pro-tumor and anti-tumor activities. A critical feature of this microenvironment is its ability to foster immune evasion, which allows tumors to grow and metastasize (7, 22).

In HCC, diverse immune cell populations, including T cells, natural killer (NK) cells, dendritic cells, and myeloid-derived suppressor cells (MDSCs), contribute to the tumor immune landscape. The balance between these cell types can determine the effectiveness of the immune response against tumors. A high infiltration of MDSCs and regulatory T cells (Tregs) is often associated with poor prognosis, as these cells can suppress the activity of effector T cells and promote an immunosuppressive microenvironment (23, 24). Conversely, a robust presence of activated cytotoxic T lymphocytes (CTLs) and NK cells is linked to better patient outcomes, as these cells can effectively target and destroy tumor cells (25–27).

The immune microenvironment in HCC is heavily influenced by the local cytokine milieu, which can dictate the behavior of immune and tumor cells (28, 29). Pro-inflammatory cytokines such as IL-6 and TNF-α often dominate the microenvironment, promoting tumor proliferation and facilitating immune evasion (30, 31). These cytokines can enhance the recruitment of immunosuppressive cells while inhibiting the function of effector immune cells. Moreover, a dysregulated cytokine profile can lead to chronic inflammation, which is a hallmark of HCC development. This chronic inflammatory state not only supports tumor growth but also contributes to the creation of an immune environment that is unfavorable for effective anti-tumor responses (32, 33).

Immune checkpoint molecules, including PD1, PD-L1, and CTLA-4, play a crucial role in regulating immune responses in HCC (34, 35). The expression of these checkpoints can be upregulated in response to theTME, leading to diminished T cell activation and function (36).

The upregulation of PD-L1 on tumor cells, in particular, has been associated with poor clinical outcomes in HCC, as it enables cancer cells to evade immune detection (37, 38). ICIs targeting PD1 and CTLA-4 have shown promise in clinical settings, offering new avenues for immunotherapy in HCC (39, 40). However, the effectiveness of these therapies can be hindered by the complexity of the immune microenvironment and the various mechanisms of immune evasion employed by HCC.

lncRNAs have emerged as important regulators of the immune microenvironment in HCC, influencing various aspects of immune cell behavior and interactions (41). The formation process of lncRNAs involves several steps. First, lncRNAs are transcribed from genomic DNA by RNA polymerase II, typically existing adjacent to or independently from protein-coding genes. After transcription, lncRNAs undergo processing, including 5' capping, 3' polyadenylation, and splicing, to become mature. Mature lncRNAs can function in the nucleus or cytoplasm, regulating gene expression and cellular functions through interactions with DNA, RNA, or proteins. They can act as "sponges" to absorb specific miRNAs or participate in transcriptional regulation and chromatin remodeling, thus playing various important biological roles (Figure 1) (42, 43).

Abbreviations: HCC, Hepatocellular carcinoma; lncRNAs, Long non-coding RNAs; TME, Tumor microenvironment; NK, Natural killer; MDSCs, Myeloid-derived suppressor cells; Tregs, Regulatory T cells; CTLs, Cytotoxic T lymphocytes; EVs, Extracellular vesicles; TAMs, Tumor-associated macrophages; ceRNA, Competitive endogenous RNA; EMT, Epithelial-mesenchymal transition; ICIs, Immune checkpoint inhibitor; VEGF, Vascular endothelial growth factor; ASOs, Antisense oligonucleotides.

These lncRNAs can modulate the infiltration and activity of immune cells, alter cytokine production, and regulate immune checkpoint expression (44). For instance, certain lncRNAs have been shown to enhance the recruitment of immunosuppressive cells, such as MDSCs and Tregs, thereby promoting an immunosuppressive environment conducive to tumor growth. Conversely, other lncRNAs may activate effector immune responses by enhancing the function of cytotoxic T cells and NK cells (45–47). By shaping the immune landscape, lncRNAs play a critical role in determining the efficacy of immunotherapies in HCC. Targeting specific lncRNAs could offer a novel approach to reprogram the immune microenvironment, restore anti-tumor immunity, and improve patient responses to existing therapies (48). Thus, further investigation into the functional roles of lncRNAs in HCC's immune landscape is essential for developing innovative therapeutic strategies.

3 LncRNA regulation of the immune Microenvironment in HCC

3.1 Regulation of immune cells by lncRNAs in HCC

As mentioned above, in the complex immune microenvironment of HCC, lncRNAs play a crucial regulatory role. Recent studies have demonstrated that lncRNAs not only participate in the biological processes of tumor cells but also significantly influence the immune evasion mechanisms of HCC by modulating the functions and interactions of immune cells (Figure 2A). These lncRNAs can shape the TME through various mechanisms, including affecting the differentiation, activation, and functional status of immune cells, as well as regulating intercellular signaling. In this chapter, we will delve into the regulatory mechanisms of lncRNAs on specific immune cells, such as T cells, B cells, macrophages, and dendritic cells, analyze their potential roles in HCC, and discuss the prospects of targeting them for therapeutic interventions.

3.1.1 T cell

T cells play a crucial role in the immune response of HCC, and lncRNAs regulate T cell function and activity through various mechanisms. They influence T cell development, differentiation, and effector functions, thereby altering the immune balance within the TME. Previous studies have demonstrated the overexpression of several oncogenic lncRNAs in HCC, including TUG1, LINC01116, CRNDE, MIAT, E2F1, LINC01132, and Lnc-Tim3. These lncRNAs can influence T cell activity and function through various pathways or cascading effects, thereby promoting tumor progression. lncRNAs often modulate T cell co-stimulation by regulating downstream miRNAs. Research has shown that NEAT1 and Tim-3 are significantly upregulated in the PBMCs of HCC patients. Downregulation of NEAT1 can inhibit the apoptosis of CD8+ T cells and enhance their cytolytic activity against HCC cells, while interference with miR-155 shows the opposite effect, promoting the upregulation of Tim-3. This study confirms the binding and interaction of NEAT1 with miR-155 in CD8+ T cells. By regulating the miR-155/Tim-3 pathway, downregulation of NEAT1 can inhibit CD8+ T cell apoptosis and enhance their cytolytic activity against HCC, indicating that NEAT1 is an effective target for improving immunotherapy outcomes (49). Lnc-Tim3 can specifically bind to Tim-3, preventing its interaction with Bat3, thereby inhibiting downstream signaling in the Lck/NFAT1/AP-1 pathway, leading to the nuclear localization of Bat3. This enhances the transcriptional activation of pro-

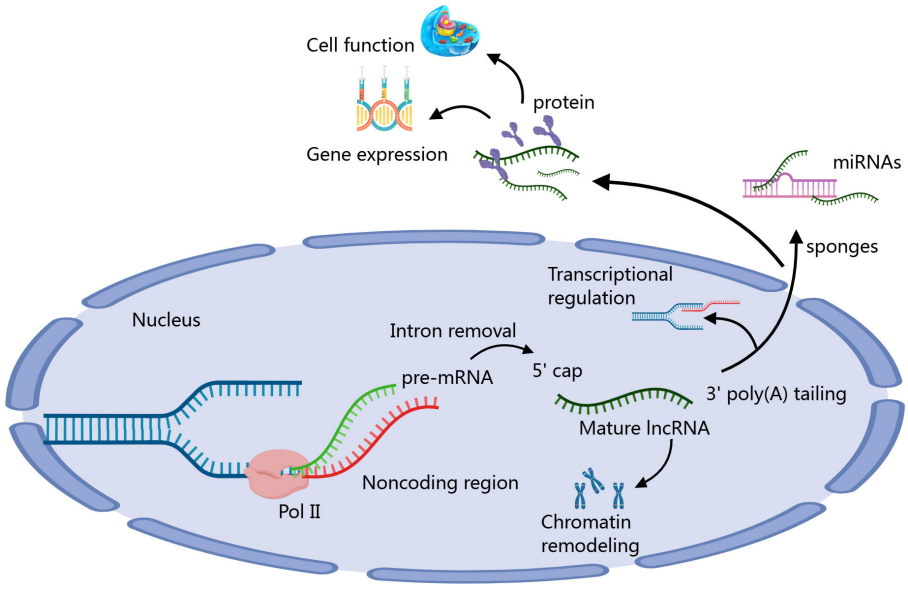


FIGURE 1
The formation process and function diagram of lncRNAs (37, 38).

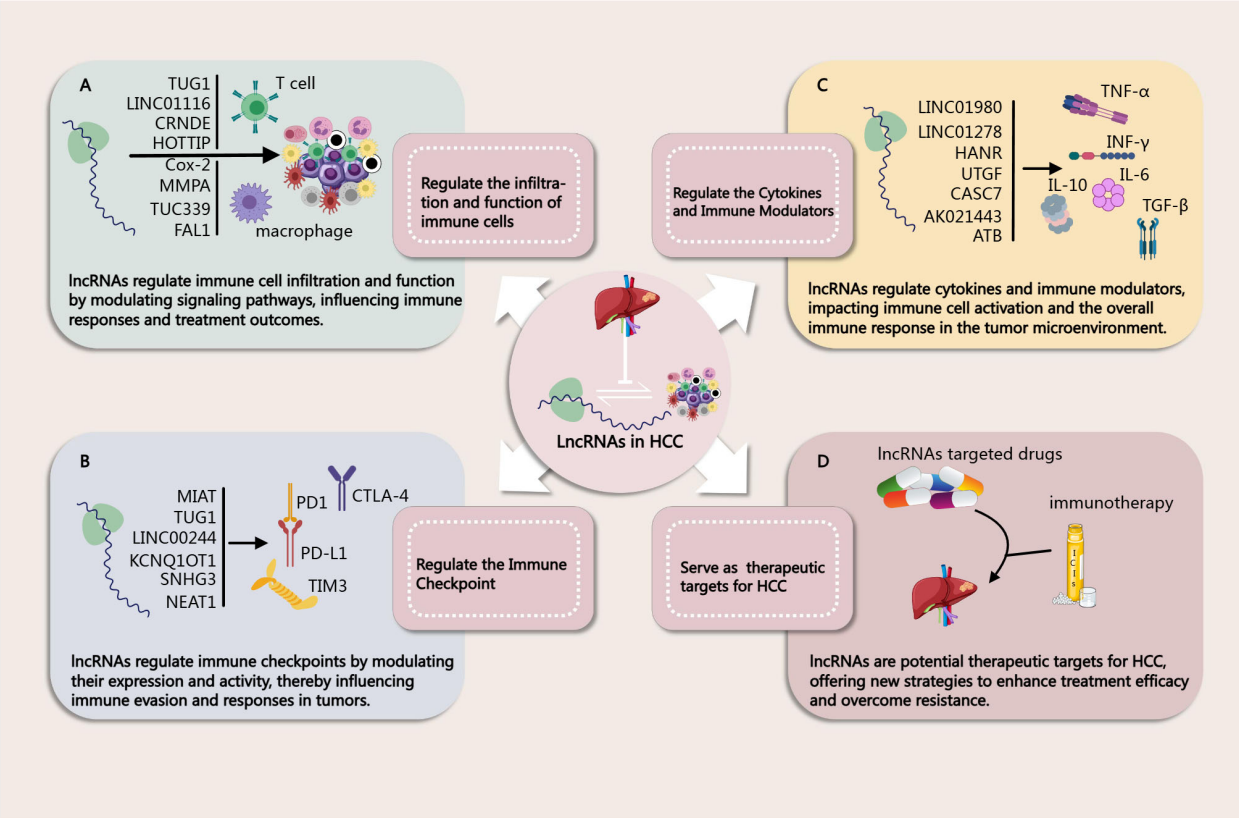


FIGURE 2
(A) Regulation of immune Cells by lncRNAs in HCC (46, 49, 50, 52, 65–67, 72). **(B)** Regulation of Immune Checkpoint by lncRNAs in HCC (44, 46, 47, 63, 91, 92). **(C)** Regulation of Cytokines and Immune Modulators by lncRNAs in HCC (94–96, 98–100, 106). **(D)** lncRNAs as Biomarkers in HCC Immunotherapy (46, 47, 65, 96).

apoptotic genes (such as MDM2 and Bcl-2) by p300-dependent p53 and RelA, promoting T cell exhaustion. This suggests that Lnc-Tim3 and its associated signaling pathways may impact the effectiveness of cancer therapies targeting the adaptive immune system (50).

Some lncRNAs can affect T cell function by regulating the expression of immune checkpoints. For instance, TUG1 is upregulated in HCC due to METTL3-mediated m6A modification. Knockdown of TUG1 can inhibit tumor growth and metastasis while increasing the infiltration of CD8+ T cells and M1 macrophages in tumors. TUG1 activates CD8+ T cells through PD-L1 and enhances macrophage phagocytosis via CD47. Mechanistically, TUG1 acts as a "sponge" for miR-141 and miR-340 to regulate the expression of PD-L1 and CD47 while interacting with YBX1 to promote their transcription. Clinical data also indicate a positive correlation between TUG1 and PD-L1 and CD47 in HCC tissues. Co-treatment with Tug1-siRNA and Pdl1 antibodies effectively inhibits tumor growth (51). Additionally, MIAT promotes STAT3 expression by negatively regulating miR-411-5p, thereby increasing the transcription level of PD-L1. Knockdown of MIAT enhances T cell cytotoxicity against HCC cells, and inhibiting miR-411-5p can reverse the decrease in STAT3 and PD-L1 expression caused by MIAT knockdown (52). The lncRNA CTD-2510F5.4 is significantly upregulated under hypoxic conditions and is expressed in Huh7 and HepG2 cells. Overexpression of CTD-2510F5.4 promotes the proliferation, invasion, and metastasis of HCC cells. Patients with high expression of CTD-2510F5.4 have poor prognoses and higher TP53 mutation rates, increased infiltration of immunosuppressive Tregs, and elevated expression of immune checkpoint molecules, leading to impaired immune function. Notably, patients with low expression of CTD-2510F5.4 show higher sensitivity to immunotherapy and anti-angiogenic therapy, while those with high expression respond better to chemotherapy (53).

Some lncRNAs can also influence the immune microenvironment by regulating tumor metabolism. For example, LINC01116 inhibits RAD18-mediated ubiquitination, stabilizing the EWSR1 protein and upregulating the expression of PPARA and long-chain fatty acid transporter FABP1, leading cancer cells to preferentially uptake linoleic acid and other long-chain fatty acids, resulting in T cell dysfunction and malignant progression of HCC. In mouse models, blocking LINC01116 enhances the efficacy of anti-PD1 therapy, increasing the infiltration of cytotoxic T cells and reducing the proportion of exhausted T cells (54).

Additionally, some lncRNAs can influence T cell infiltration and function through various cascading pathways, thereby affecting tumor progression. CRNDE is primarily found in malignant tumor cells and promotes tumor cell growth, recruits a large number of granulocyte-

MDSCs (G-MDSCs), and restricts T cell infiltration, thereby facilitating HCC progression. Mechanistically, CRNDE binds to TLR3, activating the NF-κB signaling pathway and increasing the secretion of CXCL3. Knockdown of CRNDE significantly reduces G-MDSC accumulation and enhances T cell infiltration in the TME (55). LINC01132 has been identified as a novel oncogenic lncRNA, with its expression significantly higher in HCC tumor tissues compared to normal tissues, correlating with poor survival rates in patients, primarily driven by copy number amplification. Functional studies indicate that overexpression of LINC01132 promotes cell growth, proliferation, invasion, and metastasis. Mechanistically, LINC01132 enhances DPP4 expression through physical interaction with NRF1, acting as an oncogenic driver. Furthermore, silencing LINC01132 can induce CD8+ T cell infiltration, and when combined with anti-PD-L1 treatment, can improve anti-tumor immunity, suggesting that LINC01132 may serve as a novel immunotherapeutic target in HCC. Therefore, LINC01132 promotes HCC development through the NRF1/DPP4 axis, and targeting LINC01132 may enhance the efficacy of anti-PD-L1 immunotherapy (56).

These findings highlight the complex roles of lncRNAs in the immune microenvironment, suggesting that developing therapeutic strategies targeting specific lncRNAs may provide new avenues to enhance the efficacy of immunotherapy in HCC. Further related studies are summarized in Table 1.

3.1.2 Macrophage

Macrophages play a dual role in the immune microenvironment of HCC, capable of both promoting tumor progression and inhibiting tumor growth. LncRNAs regulate macrophage function through various mechanisms, influencing their polarization states, secretory characteristics, and interactions with tumor cells.

Extracellular vesicles (EVs) in the TME play a crucial role in regulating the tumor immune microenvironment. Studies have shown that tumor-associated macrophages (TAMs) secrete exosomes containing the lncRNA MMPA, enhancing aerobic glycolysis and proliferation in HCC cells. Mechanistically, lncMMPA not only promotes M2 macrophage polarization but also acts as a sponge for miR-548, increasing ALDH1A3 mRNA expression and thereby facilitating glucose metabolism and cell proliferation. Clinical data indicate that lncMMPA expression correlates with TAM glycolysis and decreased survival rates in HCC patients (70). Additionally, HCC cell-derived exosomes are found to contain high levels of TUC339, which can be absorbed by macrophages (THP-1 cells). Inhibition of TUC339 enhances the production of pro-inflammatory factors, expression of co-stimulatory molecules, and phagocytic capacity in macrophages, while overexpression of TUC339 suppresses these functions. TUC339 is highly expressed in M2 macrophages and exhibits distinct regulatory patterns during the polarization switch between M1 and M2 macrophages, indicating its key role in M1/M2 polarization. TUC339 is also associated with cytokine receptor interactions, chemokine receptor binding, Toll-like receptor signaling, FcγR-mediated phagocytosis, cytoskeletal regulation, and cell proliferation (71).

Furthermore, the lncRNA FAL1 is highly enriched in exosomes from the serum of HCC patients and promotes tumor progression. Exosomes enriched with FAL1 can induce M2 polarization in macrophages, enhancing the proliferation, invasion, and clonogenicity of HCC cells while inhibiting apoptosis and sensitivity to sorafenib. Interfering with FAL1 can reverse these effects. FAL1 promotes malignant progression in HCC by activating the Wnt/β-catenin signaling pathway (72). Another study reveals the role of the EZH2-related lncRNA HEIH, which is abnormally upregulated in HCC and correlates with poor prognosis in tumor tissues and cell lines. HEIH is enriched in exosomes found in plasma and cell supernatants and is transported to macrophages by HCC-derived exosomes, inducing M2 polarization and promoting HCC cell proliferation, migration, and invasion. Mechanistically, HEIH acts as a miRNA sponge, binding to miR-98-5p, leading to STAT3 upregulation. This provides evidence for the novel regulatory role of tumor-derived exosomal lncRNA HEIH targeting the miR-98-5p/STAT3 axis in macrophages, aiding the understanding of the complex interactions between the TME and immune cells in HCC treatment (73).

HMMR-AS1, an lncRNA associated with poor prognosis, promotes M2 polarization in macrophages by competitively binding to miR-147a, preventing the degradation of ARID3A, and accelerates HCC progression. Additionally, in hypoxic conditions, HIF-1α enhances HMMR-AS1 transcription by binding to its promoter, increasing exosome secretion (74).

Apart from exosomes, lncRNAs can also influence macrophage polarization and function through EVs. The lncRNA PART1 can be transported to macrophages via tumor-derived EVs, regulating macrophage polarization in HCC. PART1 binds to miR-372-3p, inhibiting its expression, while miR-372-3p negatively regulates TLR4 expression in macrophages. EVs containing PART1, TLR4 overexpression, or miR-372-3p inhibition all induce macrophage polarization toward M2. Thus, EVs from HCC cells may promote M2 polarization by transporting PART1 to inhibit miR-372-3p, leading to upregulation of TLR4 (75).

Metabolic reprogramming is also an important pathway through which lncRNAs influence macrophage status. Research has identified that the lncRNA miR4458HG promotes carcinogenesis in HCC, particularly in glucose metabolism. High expression of miR4458HG enhances HCC cell proliferation, activates glycolytic pathways, and induces polarization of TAMs. Mechanistically, miR4458HG stabilizes its target mRNAs (e.g., HK2 and SLC2A1) by binding to IGF2BP2, a key RNA m6A recognition protein, thereby enhancing glycolysis and altering the physiology of tumor cells. Moreover, miR4458HG secreted by HCC can increase ARG1 expression via exosomes, further promoting M2 polarization in macrophages (76).

The aforementioned studies reveal the complex mechanisms by which lncRNAs regulate macrophage polarization and function within the TME, underscoring their significance in the progression of HCC. Notably, lncRNAs such as lncMMPA, TUC339, and FAL1 influence glucose metabolism, inflammatory responses, and cellular signaling pathways, promoting M2 macrophage polarization and thereby creating a favorable environment for the survival and proliferation of HCC cells. These findings not only deepen our understanding of the roles of lncRNAs in the tumor immune microenvironment but also suggest

TABLE 1 Regulation of T Cells by lncRNAs in HCC.

LncRNAs	Mechanism and Effect	Clinical significance	Ref
TUG1	TUG1, upregulated by METTL3-mediated m6A, regulates PD-L1 and CD47 by sponging miR-141/miR-340 and interacting with YBX1; its knockdown inhibits tumor growth, enhances CD8+T/M1 macrophage infiltration, activates CD8+T via PD-L1, and boosts macrophage phagocytosis through CD47.	TUG1-siRNA combined with PD-L1 antibody can effectively inhibit tumor growth, providing a new target and strategy for HCC immunotherapy.	(51)
LINC01116	LINC01116 inhibits RAD18-mediated ubiquitination, stabilizes EWSR1, upregulates PPARA and FABP1, promotes long-chain fatty acid uptake (e.g., linoleic acid), induces T cell dysfunction, and drives HCC progression.	The LINC01116-EWSR1-PPARA-FABP1 axis may be a new target for cancer immunotherapy.	(54)
CRNDE	CRNDE drives HCC progression by enhancing tumor growth, recruiting G-MDSCs, and inhibiting T cell invasion via TLR3 binding, NF-κB activation, and CXCL3 upregulation.	The CRNDE - NF-κB - CXCL3 axis plays an important role in promoting the immunosuppressive environment and tumor progression in HCC.	(55)
HOTTIP	HOTTIP promotes HCC cell viability by suppressing miR-205; HOTTIP knockdown or miR-205 upregulation inhibits HCC proliferation, while miR-205 downregulation reverses HOTTIP knockdown effects.	LncRNA HOTTIP regulates the carcinogenic mechanism of miR-205 in HCC and provides a potential target for the treatment of HCC.	(57)
MIAT	MIAT and PD-L1 are upregulated in HCC; MIAT promotes STAT3 by inhibiting miR-411-5p, increasing PD-L1 transcription. MIAT knockdown enhances T cell cytotoxicity, while miR-411-5p inhibition reverses STAT3 and PD-L1 reduction.	This study suggests a new lncRNA-mediated immune escape mechanism of HCC cells, and the MIAT/miR-411-5p/STAT3/PD-L1 pathway may be a new therapeutic target for HCC.	(52)
AC099850.3	AC099850.3 promotes tumorigenesis via the PRR11/PI3K/AKT axis, correlates positively with T helper cells and M0 macrophages but negatively with M2 macrophages, monocytes, NK cells, and CD8+ T cells, and is strongly linked to immune checkpoint molecules like PD-1 and PD-L1.	AC099850.3 promotes HCC malignancy and serves as a potential biomarker and therapeutic target for immunotherapy.	(58)
GAS5	lncRNA-GAS5 levels are reduced in PBMC-CD4+ T cells and tumor tissues compared to healthy controls and adjacent non-tumor tissues. Del/Del genotype increases lncRNA-GAS5 expression, lowers postoperative pain, and improves survival. lncRNA-GAS5 negatively correlates with IL-6, IL-17, and Th17 polarization index (RORγT/CD3).	LncRNA-GAS5 expression and its promoter rs145204276 polymorphism are prognostic biomarkers for predicting postoperative pain in patients with hepatectomy.	(59)
XIST	XIST is associated with high tumor and peritumoral CD4 inflammation, higher CD25+ cell counts (p=0.01), and elevated intratumoral CD25 expression.	LncRNA XIST is expressed in CHB-HCC and strongly correlates with inflammatory TME, particularly CD25+ Treg presence and quantity.	(60)
NEAT1	NEAT1 and Tim-3 are upregulated in HCC patients' PBMCs. NEAT1 downregulation inhibits CD8+T cell apoptosis and enhances cytotoxicity, while miR-155 interference promotes Tim-3 upregulation.	NEAT1 downregulation, via the miR-155/Tim-3 pathway, inhibits CD8+T cell apoptosis and enhances cytotoxicity against HCC, highlighting its potential as an immunotherapy target.	(49)
E2F1	E2F1 positively correlates with memory CD4+T cells, memory B cells, eosinophils, and T helper cells but negatively with monocytes, initial B cells, and resting memory CD4+T cells. It is also positively linked to immune checkpoints (PDCD1, CTLA4, LAG3) and potentially sensitive to 39 drugs.	This study provides an important direction for the study of E2F1, which may contribute to the identification of HCC related molecular biotherapy and immunotherapy targets.	(61)
AIFM2-1	Lnc-AIFM2-1 reduces HBV clearance by CD8+T cells via miR-330-3p inhibition and CD244 accumulation; Lnc-AIFM2-1-siRNA, miR-330-3p mimic, or CD244-siRNA restore CD8+T cell function.	Lnc-AIFM2-1 acts as a ceRNA for miR-330-3p, upregulating CD244 to promote HBV immune escape, revealing lncRNA-miRNA-mRNA interactions in immune evasion. It highlights Lnc-AIFM2-1 and CD244 as potential targets for CHB diagnosis and treatment.	(62)
MIAT	MIAT in HCC negatively correlates with tumor purity but positively with immune cells (B cells, T lymphocytes, macrophages) and checkpoint molecules (PD-1, PD-L1, CTLA4). MIAT-TF interactions regulate genes (JAK2, SLC6A6, KCND1, MEIS3, RIN1) to influence the immune microenvironment and are linked to sensitivity to anticancer drugs, particularly Sorafenib.	This study provides a meaningful attempt to reveal the immune escape mechanism of HCC and find the effectiveness of targeted drugs.	(63)
LINC01132	LINC01132 overexpression drives cell growth, proliferation, invasion, and metastasis by interacting with NRF1 to upregulate DPP4. Silencing LINC01132 induces CD8+ T cell infiltration, enhancing anti-tumor immunity when combined with anti-PD-L1 therapy.	LINC01132 promotes the development of HCC through the NRF1/DPP4 axis, and targeted silencing of LINC01132 is expected to enhance the effect of anti-PD-L1 immunotherapy.	(56)
Lnc-Tim3	Lnc-Tim3 is upregulated in tumor-infiltrating CD8 T cells, inversely correlating with IFN-γ and IL-2 production. It drives CD8 T cell exhaustion and survival by binding to Tim-3, blocking BAT3 interaction, inhibiting Lck/NFAT1/AP-1 signaling, and promoting nuclear Bat3-mediated activation of p300-dependent anti-apoptotic genes (MDM2, Bcl-2).	Lnc-Tim3 drives T cell exhaustion, weakening anti-tumor immunity, and may impact the efficacy of therapies targeting acquired immune system regulation.	(50)

(Continued)

TABLE 1 Continued

LncRNAs	Mechanism and Effect	Clinical significance	Ref
PCED1B-AS1	PCED1B-AS1 inhibits PD-Ls expression by sponging hsa-miR-194-5p, inducing PD-Ls-mediated T cell immunosuppression. HCC exosomes containing PCED1B-AS1 enhance PD-Ls in recipient cells while suppressing T cells and macrophages. Blood exosome PCED1B-AS1 correlates with PD-Ls expression in HCC.	PCED1B-AS1 enhances the expression and function of PD-Ls through spongification of hsa-miR-194-5p and induces immunosuppression of HCC.	(64)
XIST	Somatic CD4+T cell infiltration, especially resting memory CD4+T cell infiltration, was positively correlated with lncRNA and its related mirnas, while Th1 CD4+T cell infiltration was negatively correlated.	These findings provide new insights into the mechanism of immune dysregulation of CD4+T cells in HCC.	(65)
GIHCG	GIHCG is overexpressed in HCC, correlating with poor clinicopathological features, shorter survival, and reduced infiltration of memory CD4+/CD8+ T cells, NK cells, macrophages, dendritic cells, neutrophils, and monocytes.	GIHCG can be used as a biomarker to predict prognosis in HCC patients and is associated with immune cell infiltration in HCC.	(66)
LINC00261	LINC00261, MiR105-5p, and selectin L(SELL) may be potential new biomarkers for patient prognosis and immunotherapy.	The findings provide important insights into the selection of the LINC00261/MiR105-5p/SELL signaling pathway as a novel marker associated with overall survival of HCC and may impact the effectiveness of HCC immunotherapy.	(67)
SNHG3	SNHG3 promotes PD1 expression by regulating ASF1B. Ultimately, elevated ASF1B predicted poor outcomes for HCC patients in subgroups with B cells, CD8+ T cells, or neutropenia, and in subgroups with CD4+ T cell enrichment.	It was found that the novel lncRNA SNHG3/miR-214-3p/ASF1B axis may promote HCC recurrence by regulating immune infiltration.	(68)
FENDRR	FENDRR regulates GADD45B by competitively binding miR-423-5p, which targets GADD45B. FENDRR and GADD45B are downregulated in HCC, while miR-423-5p is upregulated. FENDRR overexpression and miR-423-5p downregulation inhibit HCC proliferation, promote apoptosis, and regulate Treg-mediated immune escape.	miR-423-5p up-regulates GADD45B, thereby inhibiting Treg-mediated immune escape of HCC cells.	(69)
CTD-2510F5.4	CTD-2510F5.4 overexpression promotes HCC proliferation, invasion, and metastasis, correlating with poor prognosis, higher TP53 mutation, increased Treg infiltration, elevated immune checkpoint expression, and impaired immunity. Low CTD-2510F5.4 enhances sensitivity to immunotherapy and anti-angiogenic therapy, while high expression favors chemotherapy response.	CTD-2510F5.4 is crucial in HCC progression and immune regulation, warranting further study as a prognostic biomarker and treatment response predictor to develop personalized HCC therapies.	(53)

that future therapeutic strategies should consider targeting these specific lncRNAs to reverse macrophage polarization and enhance the efficacy of immunotherapy for HCC. Further research should focus on the interactions between lncRNAs and other components of the TME to comprehensively elucidate their potential mechanisms in tumor progression. Additional relevant studies are summarized in Table 2.

3.1.3 Others

In addition to T cells and macrophages, other cell types in the tumor immune microenvironment are also regulated by lncrnas. Previous studies have shown that a variety of lncRNAs are associated with tumor invasion of B cells. For example, lncRNA AC099850.3 and E2F1 are positively correlated with the level of memory B cells (58, 61), while RNASEH1-AS1 is negatively correlated with the invasion of B cells (88). NK, as an immune cell responsible for recognizing and killing tumor cells, can also be regulated by LncRNAs through a variety of mechanisms.For example, LINC00707 can interact with YTHDF2, promoting ubiquitination dependent degradation of YTHDF2 protein. It can also influence the cytotoxicity of NK-92MI cells to HCC cells through its interaction with YTHDF2 (89). Treg is an immunosuppressive cell. Previous studies have shown that lncRNA FENDRR up-regulates GADD45B by adsorbing miR-423-5p, and inhibits Treg-mediated immune escape of HCC cells (69).

The previous sections primarily focused on immune-suppressive lncRNAs; however, in addition to those lncRNAs that promote tumor growth and immune suppression, several lncRNAs have been identified as tumor suppressors, playing critical roles in enhancing immune responses and improving survival outcomes in HCC. For example, MEG3 expression increases during LPS/IFNγ-induced M1 polarization, while it decreases during IL4/IL13-induced M2 polarization. Overexpression of MEG3 suppresses M2 polarization markers in mice. Mechanistically, MEG3 regulates DAB2 expression by binding to miR-145-5p. Overexpressing MEG3 inhibits HCC cell metastasis and angiogenesis induced by M2 polarization, and it suppresses tumor growth *in vivo* (82). Knockdown of MALAT1 inhibited VEGF-A production, impaired the angiogenesis of HUVECs, and promoted the polarization of macrophages to the M1 subgroup. Mechanistic studies confirmed the interaction between MALAT1 and miR-140 and between miR-140 and VEGF-A, revealing a negative correlation between MALAT1 and miR-140 in HCC tissues. In addition, inhibition of miR-140 significantly increased VEGF-A expression, promoted angiogenesis in HUVECs, and polarized macrophages toward the M2 subpopulation (87). LINC00261 has been shown to act as a tumor suppressor in various cancers. Studies indicate that in HCC, LINC00261 expression is downregulated in tumor tissues and is associated with better prognosis. Furthermore,

TABLE 2 Regulation of Macrophage by lncRNAs in HCC.

LncRNAs	Mechanism and Effect	Clinical significance	Ref
Cox-2	lncRNA Cox-2 is highly expressed in M1 macrophages; its knockdown reduces pro-inflammatory factors (IL-12, iNOS, TNF-α) in M1 and increases anti-inflammatory factors (IL-10, Arg-1, Fizz-1) in M2. It also weakens M1's ability to inhibit HCC proliferation, invasion, and migration while enhancing M2's pro-tumor effects.	LncRNA Cox-2 inhibits immune escape and tumor growth of HCC by inhibiting the polarization of M2-type macrophages.	(77)
MMPA	TAMs promote HCC aerobic glycolysis and proliferation via exosomal lncMMPA, which polarizes M2 macrophages and upregulates ALDH1A3 mRNA by sponging miR-548, enhancing glucose metabolism and cell growth.	LncMMPA plays an important role in malignant transformation and metabolic reprogramming of HCC by regulating miR-548/ALDH1A3 pathway.	(70)
TUC339	HCC exosomes containing TUC339 are absorbed by macrophages; TUC339 inhibition enhances proinflammatory cytokine production, co-stimulatory molecule expression, and phagocytosis, while its overexpression suppresses these functions. TUC339 is highly expressed in M2 macrophages and regulates M1/M2 polarization, impacting cytokine receptor interactions, chemokine binding, toll-like receptor signaling, phagocytosis, cytoskeletal regulation, and cell proliferation.	Tumor-derived exosomal lncRNA TUC339 regulates macrophage behavior, revealing a key mechanism of tumor-immune cell communication via exosomal lncRNAs.	(71)
ELMO1-AS1	High levels of ELMO1-AS1 are associated with better treatment outcomes and may be an independent prognostic marker for HCC. Overexpression of ELMO1-AS1 can inhibit the proliferation, migration and invasion of HCC cells, and its target may be ELMO1.	ELMO1-AS1 may be an important regulator of liver cancer progression and has potential as a prognostic marker and therapeutic target.	(78)
HMMR-AS1	HMMR-AS1 is upregulated in HCC, correlating with poor prognosis; its inhibition suppresses tumor growth. It promotes M2 macrophage polarization and HCC progression by competitively binding miR-147a to stabilize ARID3A. HIF-1α enhances HMMR-AS1 transcription and exosome secretion under hypoxia.	These findings provide new ideas for the study of HCC pathogenesis and the development of targeted therapies.	(74)
FAL1	FAL1-enriched exosomes induce M2 macrophage polarization, enhancing HCC proliferation, invasion, and clonal formation while reducing apoptosis and sorafenib sensitivity. FAL1 interference reverses these effects by inhibiting the Wnt/β-catenin pathway. FAL1-enriched exosomal macrophages also promote tumor growth in mouse models.	FAL1 in exosomes promotes HCC progression by inducing M2-type polarization in macrophages and activating the Wnt/beta-catenin signaling pathway.	(72)
MEG3	MEG3 overexpression promotes M1 macrophage polarization, increases Th1 cytokines, and reduces CSF-1 and PD-1/PD-Ls, inhibiting HCC growth, invasion, and migration. MEG3 knockdown (KD) induces M2 polarization, elevates Th2 cytokines, CSF-1, and PD-1/PD-Ls, and promotes tumor growth. *In vivo*, MEG3 OE inhibits tumor growth and PD-1/PD-Ls while enhancing Th1 immunity, whereas MEG3 KD has the opposite effect.	MEG3 regulates the TME of HCC by influencing macrophage polarization and T cell immune balance, and becomes a potential therapeutic target.	(79)
miR4458HG	miR4458HG promotes HCC proliferation, activates glycolysis, and induces TAM polarization by stabilizing target mRNAs (e.g., HK2, SLC2A1) via IGF2BP2 binding. HCC-secreted miR4458HG exosomes increase ARG1 expression, further driving M2 macrophage polarization.	MiR4458HG is considered to be a pro-cancer factor in HCC, and targeting this pathway may provide new strategies for HCC patients with high glucose metabolism.	(76)
HEIH	HCC exosomes deliver HEIH to macrophages, inducing M2 polarization and promoting HCC proliferation, migration, and invasion. HEIH acts as a miR-98-5p sponge, upregulating STAT3, as confirmed in tumor xenograft models.	This study reveals the novel role of tumor-derived exosomal lncRNA HEIH in regulating macrophages via the miR-98-5p/STAT3 axis, advancing understanding of TME-immune cell interactions in HCC therapy.	(73)
MEG3	MEG3 promotes M1 polarization and inhibits M2 polarization of BMDM by binding HuR, which suppresses CCL5 transcription. MEG3 overexpression inhibits HCC metastasis, invasion, and angiogenesis by blocking M2 polarization. MEG3 suppresses tumorigenesis by enhancing M1 and inhibiting M2 polarization, while CCL5 absence in M2 macrophages reverses MEG3's inhibitory effects on migration, invasion, and lumen formation.	MEG3 inhibits HCC progression by binding to HuR and upregulating CCL5.	(80)
MAAS	HBeAg secreted by HBV+HCC cells up-regulates MAAS expression in M2 macrophages by influencing m6A modification of MAAS, and then transfers to HBV+HCC cells via exosomes to promote their proliferation and target c-Myc	/	(81)
MEG3	MEG3 expression rises during LPS/IFN-γ-induced M1 polarization but declines during IL4/IL13-induced M2 polarization. MEG3 overexpression suppresses M2 markers *in vitro* and *in vivo* by binding miR-145-5p to upregulate DAB2, inhibiting M2-induced HCC metastasis, angiogenesis, and tumor growth.	LncRNA MEG3 inhibits the polarization of M2 macrophages through the miR-145-5p/DAB2 axis, thereby inhibiting the development of HCC.	(82)
CRNDE	Conditioned medium (CM) of M2 cells and CRNDE overexpressed M0 macrophages promoted HCC cell survival, migration, and invasion, while CRNDE knockdown of M0 cell	CRNDE regulates metabolic reprogramming of M2 macrophages through the ERK pathway, thereby	(83)

(Continued)

TABLE 2 Continued

LncRNAs	Mechanism and Effect	Clinical significance	Ref
	CM reversed this effect. CRNDE overexpressed M0 cells promoted tumor growth and the expression of Ki67 and CD206.	promoting the proliferation, migration and invasion of HCC.	
TP73-AS1	TP73-AS1 negatively regulates miR-539, and its knockdown inhibits MMP-8 expression and M2 macrophage polarization. miR-539 overexpression also suppresses M2 polarization by downregulating MMP-8. MMP-8 knockdown limits M2 polarization by inhibiting TGF-β1 signaling. TP73-AS1 knockdown or miR-539 overexpression inhibits HCC tumor growth and M2 macrophage infiltration.	LncRNA TP73-AS1 promotes the expression of MMP-8 by negatively regulating miR-539, and then activates TGF-β1 signaling pathway to induce polarization of M2 macrophages in HCC.	(84)
MA301	Lnc-MA301 is upregulated during M2-to-M1 polarization of U937 macrophages. In HCC, its expression is lower than in adjacent tissues and correlates with poor prognosis. Lnc-MA301 activation inhibits HCC proliferation, migration, EMT, and lung metastasis in mice by interacting with caprin-1 via the Akt/Erk1 pathway.	Lnc-MA301 may play a regulatory role in the development and metastasis of HCC.	(85)
PART1	PART1 and TLR4 are upregulated, while miR-372-3p is downregulated in HCC. PART1 promotes HCC proliferation, migration, invasion, and EMT by binding miR-372-3p, which negatively regulates TLR4. PART1-containing EVs or miR-372-3p inhibition induces M2 macrophage polarization. PART1 EVs drive HCC progression and M2 polarization via the miR-372-3p/TLR4 axis.	HCC cell-derived EVs may inhibit miR-372-3p through PART1 transport, thereby up-regulating TLR4 and promoting M2 polarization of macrophages in HCC.	(75)
LINC00662	LINC00662 activates Wnt/β-catenin signaling in macrophages via WNT3A secretion, driving M2 polarization. This promotes HCC tumor growth and metastasis by enhancing Wnt/β-catenin signaling and M2 macrophage polarization.	Targeting LINC00662 may provide a new therapeutic strategy for HCC.	(86)
MALAT1	MALAT1 knockdown reduces VEGF-A production, impairs HUVEC angiogenesis, and promotes M1 macrophage polarization. MALAT1 interacts with miR-140, which targets VEGF-A, and their levels are negatively correlated in HCC. miR-140 inhibition increases VEGF-A, enhances HUVEC angiogenesis, and drives M2 polarization.	This study reveals the mechanism by which MALAT1 acts as a promoter of HCC, possibly by inhibiting miR-140. Therefore, targeting MALAT1 or miR-140 may help slow the progression of HCC.	(87)

the LINC00261/MiR105-5p/SELL axis is involved in B-cell dysfunction. These findings provide significant insights into selecting the LINC00261/MiR105-5p/SELL signaling pathway as a new biomarker related to overall survival in HCC and may influence the effectiveness of HCC immunotherapy (67). Previous research has shown that JPX-induced XIST inhibits liver cancer progression by sequestering miR-155-5p (90). XIST is more highly expressed in patients with high tumor and peritumoral CD4 inflammation. The number of CD25-positive cells is significantly higher in tumors with XIST expression, suggesting its potential regulatory role in the immune microenvironment (60). It is worth noting that the clinical application of these lncRNAs still faces significant challenges and requires further clinical validation. These relevant lncRNAs are summarized in the corresponding table according to the above classification.

3.2 LncRNAs in immune checkpoint regulation

In the TME, lncRNAs play a crucial role in immune regulation by modulating the expression of PD1 and its ligand PD-L1 (Figure 2B). These lncRNAs are involved in the mechanisms of immune evasion and influence the signaling between tumor cells and immune cells through interactions with miRNAs or transcription factors. Research indicates that the upregulation of certain lncRNAs is closely associated with the expression of PD1/PD-L1, thereby promoting the survival and proliferation of tumor cells.

Previous studies have indicated that various lncRNAs are positively correlated with the expression of PD1/PD-L1 or can promote their expression. For example, AC099850.3 is significantly positively correlated with key immune checkpoint molecules (PD1, PD-L1, PD-L2, and CTLA4) (58). MIAT promotes the expression of PD-L1 at the transcriptional level by downregulating miR-411-5p, which in turn enhances STAT3 expression (52). SNHG3 can also promote PD1 expression by regulating ASF1B (68). Hypoxia induces the interaction between MIR155HG and ILF3, stabilizing HIF-1α mRNA and increasing PD-L1 expression, thereby facilitating immune evasion in HCC (91). Additionally, MIR155HG functions as a competitive endogenous RNA (ceRNA) that regulates PD-L1 expression through the miR-223/STAT1 axis (92). HOXA-AS3 is highly expressed in HCC cells and enhances PD-L1 expression by adsorbing miR-455-5p, thereby increasing the proliferation, migration, and invasion abilities of HCC cells, regulating the cell cycle, and inhibiting apoptosis (93).

Multiple mechanisms are involved in the regulation of PD1/PD-L1 by lncRNAs. PCED1B-AS1 enhances the expression of PD-L1 and PD-L2 by adsorbing hsa-miR-194-5p, thereby increasing the immune suppressive ability of HCC cells. Furthermore, HCC cells release exosomes containing PCED1B-AS1, transmitting this immune suppressive mechanism to other HCC cells, T cells, and macrophages. High expression of PCED1B-AS1 is closely related to the overexpression of PD-Ls in HCC and promotes tumor cell

proliferation and tumor formation while inhibiting apoptosis (64). METTL3-mediated m6A modification upregulates TUG1, promoting tumor immune evasion. Silencing TUG1 inhibits tumor growth and metastasis, enhances the infiltration of CD8+ T cells and M1 macrophages, and activates CD8+ T cells through PD-L1 while promoting macrophage phagocytosis via CD47. TUG1 regulates the expression of PD-L1 and CD47 by adsorbing miR-141 and miR-340, respectively, and interacts with YBX1 to promote their transcriptional upregulation, ultimately facilitating tumor immune evasion (51).

In addition to PD1/PD-L1, lncRNAs are also associated with other checkpoints such as CTLA-4 and TIM-3, and they can even regulate their levels and functions. For example, Lnc-Tim3 specifically binds to Tim-3, obstructing its interaction with Bat3, which inhibits the downstream Lck/NFAT1/AP-1 signaling pathway, leading to the nuclear localization of Bat3 and enhancing the transcriptional activity of p300-dependent p53 and RelA. This promotes the transcriptional activation of anti-apoptotic genes (such as MDM2 and Bcl-2), contributing to T cell exhaustion, which is linked to diminished anti-tumor immunity (50). Furthermore, a study established a prognostic model for HCC composed of 12 ferroptosis-related lncRNAs, dividing HCC patients into high-risk and low-risk groups. In the high-risk group, the expression of various immune checkpoint molecules, including PD1, CTLA-4, and CD86, was significantly elevated (94). Another study constructed a new feature comprising three ferroptosis-related lncRNAs, which was associated with immune cell infiltration (such as macrophages, myeloid dendritic cells, and neutrophils) and immune checkpoint blockade targets (including PD1, CTLA-4, and TIM-3) (95).

The above studies clearly demonstrate the significant role of lncRNAs in regulating immune checkpoints in HCC. We have summarized the related research in Table 3 for a more intuitive presentation.

3.3 Regulatory roles of LncRNA in cytokines and immune modulators

Gaining a deeper understanding of the role of lncRNAs in cytokines and immune regulatory molecules is also a crucial aspect of providing new strategies and targets for tumor immunotherapy.

TGF-β plays a dual role in HCC. In the early stages, it inhibits cell proliferation and induces apoptosis, serving an anti-tumor role. However, in later stages of HCC, TGF-β promotes tumor cell migration, invasion, and fibrosis in the TME, thereby facilitating tumor progression. Therefore, TGF-β is an important target in HCC treatment. Previous studies have shown that lncRNAs can interact with TGF-β. Research indicates that some lncRNAs can be activated by TGF-β-related pathways in HCC, thereby exerting downstream effects. For instance, lnc-UTGF is transcriptionally induced by TGF-β. Under TGF-β stimulation, SMAD2/3 bind to the lnc-UTGF promoter and activate its expression. Overexpression of lnc-UTGF enhances TGF-β/SMAD signaling, while its knockdown suppresses this signaling. lnc-UTGF interacts with the mRNAs of SMAD2 and SMAD4 through complementary base pairing, thereby increasing the stability of SMAD2/4 mRNA. This indicates the existence of a novel TGF-β/SMAD/lnc-UTGF positive feedback loop (99). Additionally, LINC01980 promotes HCC metastasis via the miR-376b-5p/E2F5 axis under classical TGF-β/SMAD pathway activation (100). TGF-β-activated lncRNA-ATB is upregulated in HCC metastasis and is associated with poor prognosis. lncRNA-ATB induces epithelial-mesenchymal transition (EMT) and cell invasion by competitively binding to the miR-200 family, leading to the upregulation of ZEB1 and ZEB2. Furthermore, lncRNA-ATB promotes the autocrine induction of IL-11 by binding to IL-11 mRNA, activating the STAT3 signaling pathway, and further facilitating the organ colonization of disseminated tumor cells (101). Other studies have shown that some lncRNAs can exert effects by regulating TGF-β secretion. For example, PRR34-AS1 stabilizes the mRNA level of the exosomal protein Rab27a by recruiting DDX3X, thereby promoting the exosomal secretion of VEGF and TGF-β in HCC cells (102). CASC7 can also promote HCC progression by binding to miR-30a-5p, regulating KLF10 and its downstream TGF-β/SMAD3 pathway (103). The downregulation of LINC01278 can reduce HCC cell migration and invasion induced by β-catenin and TGF-β1 (104). HANR and miR-214 jointly regulate EZH2, affecting the level of TGFBR2 (105). Additionally, some lncRNAs participate in TGF-β-induced biological processes. For instance, lncRNA SLC7A11-AS1 and hsa_circ_0006123 are involved in the TGF-β-induced EMT process and may promote HCC metastasis (106).

In addition to TGF-β, lncRNAs also interact with various cytokines and immune regulatory factors such as IL-6, IL-10, INF-γ, and TNF-α (Figure 2C). For instance, lnc-DILC exerts its effects by inhibiting the autocrine IL-6/STAT3 signaling pathway, and there are binding sites between lnc-DILC and the IL-6 promoter. Furthermore, lnc-DILC mediates the interaction between TNF-α/NF-κB signaling and IL-6/STAT3 signaling (107). Both TNF-α and IL-6 can also regulate the expression of lncRNA 00607 (108). The downregulation of lncRNA cox-2 using siRNA significantly decreased the expression of IL-12, iNOS, and TNF-α in M1 macrophages, while increasing the expression of IL-10, Arg-1, and Fizz-1 in M2 macrophages (77). Relevant studies are summarized in Table 4 for a more intuitive presentation.

4 Potential of lncRNAs in HCC immunotherapy

4.1 lncRNAs as biomarkers in HCC immunotherapy

LncRNAs have emerged as promising biomarkers for predicting responses to immunotherapy in HCC. Their unique expression profiles in tumor tissues and circulation provide valuable insights into the TME and immune landscape.

TABLE 3 Regulation of Immune Checkpoint by lncRNAs in HCC.

LncRNAs	Mechanism and Effect	Clinical significance	Ref
MIAT	MIAT and PD-L1 are upregulated in HCC. MIAT promotes STAT3 by downregulating miR-411-5p, increasing PD-L1 transcription. MIAT knockdown enhances T cell cytotoxicity, and miR-411-5p inhibition reverses STAT3 and PD-L1 suppression.	This study reveals the MIAT-mediated mechanism of immune evasion in HCC, suggesting that the MIAT/miR-411-5p/STAT3/PD-L1 axis could serve as a novel therapeutic target for HCC treatment.	(52)
MIR155HG	HIF-1α binds to the MIR155HG promoter, enhancing its transcription. Hypoxia promotes ILF3 nuclear export, increasing ILF3-MIR155HG interaction, stabilizing HIF-1α mRNA, and elevating PD-L1 expression.	This study reveals that hypoxia promotes HCC immune evasion by inducing the interaction between MIR155HG and ILF3, which stabilizes HIF-1α mRNA and enhances PD-L1 expression.	(91)
PCED1B-AS1	PCED1B-AS1 enhances HCC immunosuppression by sponging hsa-miR-194-5p, increasing PD-L1 and PD-L2 expression. It blocks hsa-miR-194-5p's inhibition of PD-Ls, leading to their overexpression. HCC exosomes containing PCED1B-AS1 spread this mechanism to other HCC cells, T cells, and macrophages.	PCED1B-AS1 induces immune evasion in HCC by regulating the expression of PD-Ls, suggesting it may serve as a novel therapeutic target for HCC treatment.	(64)
HOXA-AS3	HOXA-AS3 is highly expressed in HCC cells and promotes PD-L1 expression by sequestering miR-455-5p, thereby enhancing HCC cell proliferation, migration, and invasion, regulating the cell cycle, and inhibiting apoptosis.	HOXA-AS3 exerts its effects in HCC by regulating the miR-455-5p/PD-L1 axis, suggesting it may serve as a new therapeutic target for HCC treatment.	(93)
TUG1	TUG1, upregulated by METTL3-mediated m6A modification, promotes immune evasion. TUG1 knockdown inhibits tumor growth and metastasis, enhances CD8+ T cell and M1 macrophage infiltration, activates CD8+ T cells via PD-L1, and promotes macrophage phagocytosis via CD47. TUG1 sequesters miR-141 and miR-340 to regulate PD-L1 and CD47, respectively, and interacts with YBX1 to upregulate their transcription, facilitating immune escape.	This mechanism provides new insights for enhancing immune therapy in HCC.	(51)
MIR155HG	LPS induces PD-1 and PD-L1 expression, significantly upregulating PD-L1 in HCC. LPS enhances METTL14, promoting m6A methylation of MIR155HG, which is stabilized by ELAVL1. MIR155HG acts as a ceRNA, regulating PD-L1 via the miR-223/STAT1 axis.	This mechanism provides new therapeutic targets for the immunotherapy of HCC, particularly in cases associated with liver cirrhosis.	(92)
AC099850.3	AC099850.3 is significantly positively correlated with immune checkpoint molecules (PD-1, PD-L1, PD-L2, and CTLA4).	This indicates its potential as a therapeutic target for immunotherapy in HCC.	(58)
LINC00244	Long non-coding RNA LINC00244 can downregulate the expression of PD-L1, thereby inhibiting the proliferation, invasion, and metastasis of HCC.	High expression of LINC00244 is associated with better clinical prognosis, suggesting that it may be a potential therapeutic target for HCC.	(96)
KCNQ1OT1	KCNQ1OT1, as a ceRNA for miR-506, elevates PD-L1 expression in sorafenib-resistant HCC cells.	KCNQ1OT1 promotes PD-L1-mediated immune evasion and resistance in sorafenib-resistant HCC cells by inhibiting miR-506.	(97)
FOXD1-AS1	FOXD1-AS1, upregulated in malignancies, correlates with poor prognosis and enhances HCC immune evasion by increasing PD-L1 as a ceRNA for miR-615-3p. It also regulates CTC EMT via PI3K/AKT signaling.	This study provides strong evidence supporting the role of FOXD1-AS1 as a miRNA sponge, sequestering miR-615-3p and protecting PD-L1 from inhibition.	(98)
SNHG3	SNHG3 promotes the expression of PD1 by regulating ASF1B.	The study identified a novel lncRNA SNHG3/miR-214-3p/ASF1B axis that promotes the recurrence of HCC by modulating immune infiltration.	(68)
Lnc-Tim3	Lnc-Tim3 binds Tim-3, blocking its interaction with Bat3 and suppressing the Lnc/NFAT1/AP-1 pathway. This drives Bat3 nuclear localization, enhancing p300-dependent p53 and RelA transcriptional activity, activating anti-apoptotic genes (e.g., MDM2, Bcl-2), and promoting T cell exhaustion.	This suggests that Lnc-Tim3 and its associated signaling pathways may influence the efficacy of cancer therapies aimed at modulating the adaptive immune system.	(50)
NEAT1	In the PBMCs of HCC patients, the expression levels of NEAT1 and Tim-3 are significantly elevated. Downregulation of NEAT1 inhibits CD8+ T cell apoptosis and enhances their cytolytic activity, while interference with miR-155 shows the opposite effect by upregulating Tim-3.	NEAT1 may serve as an effective target for enhancing the efficacy of immunotherapy.	(49)

TABLE 4 Regulation of Cytokines and Immune Modulators by lncRNAs in HCC.

LncRNAs	Mechanism and Effect	Clinical significance	Ref
LINC01980	Under the activation of the classical TGF-β/SMAD pathway, LINC01980 promotes HCC metastasis through the miR-376b-5p/E2F5 axis.	LINC01980 may serve as a potential prognostic biomarker and therapeutic target for HCC.	(100)
ATB	TGF-β-activated lncRNA-ATB is upregulated in HCC metastasis and linked to poor prognosis. It induces EMT and invasion by sponging miR-200 family, upregulating ZEB1 and ZEB2. lncRNA-ATB also binds IL-11 mRNA, promoting autocrine IL-11 induction and STAT3 activation, enhancing tumor cell colonization.	lncRNA-ATB, a TGF-β signaling mediator, increases HCC metastasis risk and represents a potential anti-metastatic therapy target.	(101)
LINC01278	The downregulation of LINC01278 reduces the migration and invasion of HCC cells induced by β-catenin and TGF-β1.	The study uncovers the β-catenin/TCF-4-LINC01278-miR-1258-Smad2/3 feedback loop in HCC metastasis, highlighting LINC01278 as a potential therapeutic target.	(104)
MIR4435-2HG	HSC-released CXCL1 exacerbates the malignant behavior of HCC cells through the MIR4435-2HG/miR-506-3p/TGFB1 axis.	CXCL1 and the MIR4435-2HG/miR-506-3p/TGFB1 axis may also represent potential therapeutic targets for HCC treatment.	(109)
SLC7A11-AS	LncRNA SLC7A11-AS1 and hsa_circ_0006123 are involved in the TGF-β-induced EMT process and may promote the metastasis of HCC.	These findings advance clinical diagnostic and therapeutic approaches, offering new avenues for research into TGF-β-induced EMT molecular mechanisms.	(106)
HANR	Both HANR and miR-214 jointly regulate EZH2, thereby affecting the levels of TGFBR2.	The study reveals the HANR/miR-214/EZH2/TGF-β axis as a novel regulatory mechanism in HCC tumorigenesis and progression, providing insights for therapeutic strategies and diagnostic biomarkers targeting HANR.	(105)
UTGF	Lnc-UTGF is induced by TGF-β via SMAD2/3 binding to its promoter. Its overexpression enhances TGF-β/SMAD signaling, while knockdown inhibits it. Lnc-UTGF stabilizes SMAD2/4 mRNAs through base pairing, forming a TGF-β/SMAD/lnc-UTGF positive feedback loop.	The lnc-UTGF-mediated positive feedback loop in TGF-β signaling, coupled with its role in liver cancer metastasis, highlights its potential as a therapeutic target for HCC metastasis.	(99)
CASC7	CASC7 regulates KLF10 and its downstream TGF-β/SMAD3 pathway by binding to miR-30a-5p, thereby promoting the progression of HCC cells.	CASC7 is involved in the tumorigenesis and progression of HCC by regulating miR-30a-5p and its target KLF10.	(103)
NNT-AS1	Inhibition of NNT-AS1 significantly reduces the levels of TGF-β, TGFBR1, and SMAD5 in HCC cells.	NNT-AS1 activates the TGF-β signaling pathway, inhibiting CD4+ T cell infiltration and offering new insights into HCC immune evasion.	(110)
AK021443	Overexpression of AK021443 significantly increases the release of inflammatory factors such as TGF-β, interleukin-1β, platelet-derived growth factor, epidermal growth factor, and ROS.	Overexpression of AK021443 enhances the proliferation, activation, and pro-inflammatory response of HSCs, suggesting its potential significant role in exacerbating liver fibrosis.	(111)
PRR34-AS1	PRR34-AS1 stabilizes the mRNA levels of the exosomal protein Rab27a by recruiting DDX3X, thereby promoting the secretion of VEGF and TGF-β in HCC cells.	This study uncovers PRR34-AS1's role in enhancing exosomal secretion in HCC cells, offering new insights into lncRNA-mediated regulation of tumor cell biology.	(102)
LINC00974	LINC00974 acts as a ceRNA for miR-642, upregulating KRT19. Its elevation results from promoter hypomethylation, activating Notch and TGF-β signaling pathways.	The LINC00974-KRT19 interaction may serve as a novel diagnostic marker for HCC growth and metastasis, while LINC00974 itself could be a therapeutic target to prevent HCC progression.	(112)
DANCR	DANCR activates the IL-6/STAT3 signaling pathway through PSMD10. The study also found that the activation of the IL-6/STAT3 signaling pathway enhances the transcription of DANCR, creating a positive feedback loop.	This study reveals DANCR's role in sorafenib resistance via the PSMD10-IL-6/STAT3 axis, offering new therapeutic targets for HCC.	(113)
DLGAP1-AS1	DLGAP1-AS1 sponges miR-26a/b-5p, elevating IL-6 and activating JAK2/STAT3 signaling, which enhances DLGAP1-AS1 transcription, forming a positive feedback loop.	The study reveals DLGAP1-AS1's role in HCC progression and EMT, highlighting its potential as a therapeutic target.	(114)
MALAT1	MALAT1 promotes the binding of NF-κB to the promoter regions of IL-6 and CXCL8 by recruiting the catalytic subunit BRG1 of the chromatin remodeling complex SWI/SNF, thereby inducing the expression of these inflammatory factors.	Inhibiting MALAT1 may represent a novel strategy for the treatment of HCC.	(115)

(Continued)

TABLE 4 Continued

LncRNAs	Mechanism and Effect	Clinical significance	Ref
TPTEP1	TPTEP1 interacts with STAT3 to inhibit its phosphorylation, homodimerization, nuclear transport, and the transcription of downstream genes.	TPTEP1 suppresses the progression of HCC cells by affecting the IL-6/STAT3 signaling pathway, revealing its tumor-suppressive role in HCC chemotherapy.	(116)
DILC	Lnc-DILC inhibits IL-6/STAT3 signaling by binding to the IL-6 promoter and mediates crosstalk between TNF-α/NF-κB and IL-6/STAT3 pathways.	Lnc-DILC may not only serve as a prognostic biomarker for HCC but also as a potential therapeutic target against liver cancer stem cells.	(107)
Cox-2	The downregulation of lncRNA cox-2 using siRNA significantly reduced the expression of IL-12, iNOS, and TNF-α in M1 macrophages, while increasing the expression of IL-10, Arg-1, and Fizz-1 in M2 macrophages.	lncRNA cox-2 inhibits the polarization of M2 macrophages, thereby suppressing immune evasion and tumor growth in HCC.	(77)
Lnc-00607	TNF-α and IL-6 can regulate the expression of lncRNA 00607. lncRNA 00607 inhibits the transcription of NF-κB p65 by binding to its promoter region, thereby promoting the elevation of p53 levels in HCC.	The TNF-α/IL-6-lncRNA 00607-NF-κB p65/p53 signaling pathway may offer a novel therapeutic strategy for cancer chemotherapy.	(108)
PRRT3-AS1	PRRT3-AS1 knockdown increases IL-10 and TGF-β1 (anti-inflammatory) and decreases IL-1β, TNF-α, and IL-6 (pro-inflammatory) in the cell supernatant.	This has significant clinical implications for predicting patient prognosis and guiding personalized treatment for HCC patients, although further prospective validation is needed.	(117)
TUC339	Inhibiting TUC339 in macrophages reduces the expression of M (IL-4) markers after IL-4 treatment, while overexpressing TUC339 following IFN-γ + LPS treatment enhances the expression of M(IL-4) markers.	The study highlights tumor-derived exosomal lncRNA TUC339's role in regulating environmental macrophages, uncovering complex tumor-immune cell interactions mediated by exosomal lncRNAs.	(71)
Lnc-Tim3	Lnc-Tim3 is upregulated in tumor-infiltrating CD8 T cells of HCC patients and is negatively correlated with the production of IFN-γ and IL-2.	Lnc-Tim3 and its associated signaling pathways may influence the efficacy of cancer treatments targeting the regulatory adaptive immune system.	(50)

In the previous sections, we discussed specific lncRNAs that are associated with immune cell infiltration, cytokine profiles, and overall immune responses, making them potential prognostic indicators for HCC patients undergoing immunotherapy. For example, lnc-TUG1, lnc-MMPA, lnc-MIAT, and lnc-ATB are lncRNAs whose expression levels are correlated with the state of the tumor immune microenvironment in HCC, suggesting their roles in regulating immune responses (51, 52, 70, 101).

Furthermore, the expression levels of lncRNAs can serve as predictive markers for patient outcomes. By assessing lncRNA profiles, clinicians may better stratify patients, identifying those who are more likely to benefit from immunotherapeutic approaches. This stratification could lead to more personalized treatment strategies, maximizing efficacy while minimizing unnecessary exposure to ineffective therapies. Previous studies have constructed various risk prediction models composed of lncRNAs. For example, one study developed a nine-lncRNA ferroptosis-related signature (CTD-2033A16.3, CTD-2116N20.1, CTD-2510F5.4, DDX11-AS1, LINC00942, LINC01224, LINC01231, LINC01508, and ZFPM2-AS1) to predict the prognosis and immune response in liver cancer. This lncRNA signature may regulate the immune microenvironment of HCC by interfering with TNF-α/NF-κB, IL-2/STAT5 and cytokine/receptor signaling pathways (118). Other studies have also constructed prognostic models using nine copper nephropathy-related lncRNAs. The low-risk group had significantly higher infiltration of immune cells, which primarily have anti-tumor immune functions, and showed a higher sensitivity to ICIs therapy, possibly acting through the AL365361.1/hsa-miR-17-5p/NLRP3 axis. In addition, NLRP3 mutation-sensitive drugs such as VNLG/124, Sunitinib, and rifampicin may achieve better clinical outcomes in high-risk patients (119). More relevant models are summarized in Table 5.

4.2 Combination therapy

In Chapter Three, we discuss how lncRNAs can regulate the TME, influencing the infiltration and function of immune cells, thereby enhancing the efficacy of immunotherapy. Certain lncRNAs can alter the immune status of the TME by inhibiting the expression of immunosuppressive factors or promoting the release of immune-activating factors. This underscores the promising therapeutic prospects of combining lncRNA-targeted therapy with immunotherapy. For example, TUG1 can regulate the expression of PD-L1 and CD47 by acting as a "sponge" for miR-141 and miR-340. Knockdown of TUG1 can inhibit tumor growth and metastasis, increase the infiltration of CD8+ T cells and M1 macrophages in the tumor, and activate CD8+ T cells through PD-L1 while enhancing macrophage phagocytosis through CD47. Therefore, TUG1-siRNA combined with PD-L1 antibodies can effectively suppress tumor growth, providing new targets and strategies for HCCimmunotherapy (51). Additionally, various lncRNAs discussed earlier, such as MIAT (52), LINC01132 (56), MIR155HG (91), PCED1B-AS1 (64), NEAT1 (49), can serve as potential combined treatment targets to enhance the effects of HCC immunotherapy (Figure 2D). However, it is worth noting that, despite the promising therapeutic prospects of combination

TABLE 5 Various risk prediction models composed of lncRNAs in HCC.

LncRNAs	Mechanism and Effect	Clinical significance	Ref
CTD-2033A16.3, CTD-2116N20.1, CTD-2510F5.4, DDX11-AS1, LINC00942, LINC01224, LINC01231, LINC01508, and ZFPM2-AS1	This lncRNA signature may modulate the HCC immune microenvironment by affecting TNF-α/NF-κB, IL-2/STAT5, and cytokine/receptor signaling pathways.	It provides a personalized prediction tool for prognosis and immune response of HCC patients.	(118)
AC073611.1, AL050341.2, LINC02321, LUCAT1, LINC02362, LINC01871, ZNF582-AS	High ATLS scores correlate with poor prognosis, increased tumor mutations, immune activation, elevated T cell proliferation regulators, anti-PD-L1 response, and abnormal sensitivity to oxaliplatin/fluorouracil/Lenvatinib.	ATLS can be used as a powerful biomarker to improve the clinical prognosis and precision treatment of HCC.	(120)
LUCAT1, AC010761.1, AC006504.7 and MIR210HG	MIR210HG silencing inhibits HCC growth and migration by up-regulating PFKFB4 and SPAG4.	This angiogenesis-associated risk model serves as a reliable and promising tool for predicting HCC prognosis.	(121)
MIR4435-2HG/hsa-miR-1-3p/MMP9/hsa-miR-29-3p/DUXAP8	The MIR4435-2HG/hsa-miR-1-3p/MMP9/hsa-miR-29-3p/DUXAP8 ceRNA network correlates with tumor stage and invasion depth. MMP9 positively associates with resting M0 macrophages and NK cells but negatively with activated/resting mast cells, monocytes, and activated NK cells. DUXAP8 positively links to M2 macrophages but negatively to MIR4435-2HG, which itself negatively associates with activated mast cells, CD8+ T cells, and follicular helper T cells.	These findings enhance understanding of immune-related gene interactions with non-coding RNAs in HCC development and progression. Relevant RNAs may serve as diagnostic/prognostic biomarkers and molecular targets for HCC patients.	(122)
GSEC/miR-101-3p/SNX16/PAPOLG	The GSEC/miR-101-3p/SNX16/PAPOLG axis is linked to HCC prognosis. GSEC, SNX16, and PAPOLG are highly expressed in HCC with poor prognosis, while miR-101-3p is low with good prognosis. This axis may influence macrophage polarization.	The GSEC/miR-101-3p/SNX16/PAPOLG axis may be an important factor related to HCC prognosis and immune infiltration.	(123)
LINC01134, C2orf27A, LINC00501, AC104066.3, AC034229.4, CASC8, FAM225B, AL451069.3, AL161669.3, AC116025.2 and LINC00632.	Among the 11-LNCPS lncRNAs, LINC01134 and AC116025.2 are particularly critical. Their upregulation impacts immune cell infiltration, correlates with TCE, poorer OS, and reduced immune response in liver cancer.	LncRNAs in 11-LNCPS influence cancer-related biological processes and signaling pathways, particularly in immune function and metabolism. 11-LNCPS can predict HCC prognosis and immune response.	(124)
AC012073.1, AL031985.3, AL355574.1, LINC01224, SNHG4	The low-risk group showed better OS, an independent HCC prognostic indicator. A nomogram combining features and TNM stages was constructed. TP53 mutations were more frequent in high-risk individuals. CD4+ T cells, NK cells, and macrophages differed significantly between groups. High-risk individuals had increased immune checkpoint molecule expression. The low-risk group responded better to sorafenib and cisplatin.	This study provides promising insights into DDR-associated lncrnas in HCC and provides a personalized predictive tool for prognosis and treatment response.	(125)
AC022007.1, AC023090.1, AC099850.4, ACSL6-AS1, CYTOR, LHFPL3-AS2, AL365361.1, LINC02362, and MSC-AS1	The proportion of Tregs and M0 and M2 macrophages in high-risk group was higher.	These lncRNAs may influence mitochondrial function, ferroptosis, and immune cell infiltration in HCC via specific pathways, offering valuable insights into HCC progression and treatment.	(126)
m6A-lncRNA	Many lncrnas are predictive risk factors for HCC prognosis, and the expression of M6A-lncrnas is significantly upregulated in tumor tissues, which can predict HCC prognosis independently of other clinical features.	m6A-lncRNA is closely linked to HCC occurrence and progression. Its prognostic model aids in predicting HCC outcomes, while m6A-lncRNA and immune cell infiltration in the TME offer new therapeutic targets, warranting further research.	(127)
Cuproptosis-related lncRNA	High CLS is associated with more aggressive tumor characteristics and treatment resistance. TP53, CSMD1, and RB1 mutations are more frequent in high CLS samples, which also show more amplifications and deletions. High CLS patients are more sensitive to 5-fluorouracil, gemcitabine, and doxorubicin, while low CLS patients respond better to immunotherapy.	In this study, we used machine learning to create CLs-based prognostic profiles and conducted comprehensive analyses in the areas of function, immunity, mutation, and clinical application.	(128)

(Continued)

TABLE 5 Continued

LncRNAs	Mechanism and Effect	Clinical significance	Ref
Cuproptosis-related lncRNAs	The high-risk group had a higher TMB and a poorer prognosis, while the low-risk group had a higher activity of NK cells and less infiltration of Tregs, indicating a better prognosis.	CupRLSig serves as a prognostic tool for HCC, predicting immune invasion levels and potential tumor immunotherapy efficacy.	(129)
Cuproptosis-Related LncRNAs	The low-risk group exhibited higher infiltration of anti-tumor immune cells and greater sensitivity to ICIs, potentially mediated by the AL365361.1/hsa-miR-17-5p/NLRP3 axis. NLRP3 mutation-sensitive drugs like VNLG/124, Sunitinib, and rifampicin may benefit high-risk patients.	The crLncRNAs model has good specificity and sensitivity, and can be used to classify and treat sensitive populations and predict the prognosis of HCC patients.	(119)
Ferroptosis-related lncRNAs	A 12 ferroptosis-related lncRNA prognostic model for HCC stratifies patients into high-risk and low-risk groups, with the high-risk group showing elevated immune checkpoint molecule expressions (PD-1, CTLA-4, CD86).	This model may serve as a new indicator for the response and adverse reactions of HCC to immunotherapy.	(94)
Ferroptosis-related lncRNAs	A ferroptosis-associated lncRNA feature has been established, linked to immune checkpoint blockade targets like PD-1, CTLA-4, and TIM-3.	The three lncRNAs may act as potential therapeutic targets for HCC patients, and their profiles could aid in prognostic prediction for HCC.	(95)

therapies, large-scale clinical trials of lncRNA-targeted drugs alone or in combination with immunotherapy for treating HCC have not yet been widely conducted.

In addition to the combination with immunotherapy, significant progress has been made in the study of lncRNA targeting drugs in combination with chemotherapy, anti-angiogenic drugs or targeted kinase inhibitors in tumors. The mechanism mainly focuses on the synergistic regulation of tumor drug resistance, angiogenesis and signaling pathways. Studies have shown that lncrnas can affect the expression of apoptosis-related genes by regulating DNA damage repair or adsorbing mirnas as ceRNA, thus reversing chemotherapy resistance (130). In addition, lncrnas can also regulate vascular endothelial growth factor (VEGF) related pathways, such as linc00173.v1, which promotes angiogenesis through the miR-511-5p/VEGFA axis (131). Other studies have shown that lncrnas recruit kinase complexes through scaffold action (e.g., WDR5/KAT2A complex regulates SOD2 gene (132)) or regulate kinase-related signaling pathways (e.g., STAT3/VEGFA axis (133)). However, current research still faces challenges, such as *in vivo* safety verification of lncRNA targeted delivery systems (such as lipid nanoparticles and viral vectors), as well as dose optimization of combination regimenes and analysis of drug resistance mechanisms. Overall, this combination strategy provides a new direction to overcome the limitations of traditional therapies by regulating the TME and molecular networks in multiple dimensions.

5 Future perspectives and challenges

Recent advancements in the understanding of lncRNAs have provided valuable insights into their roles within the immune microenvironment of HCC. Research has revealed that lncRNAs are not merely passive players but active regulators of immune cell behavior, influencing tumor progression and response to therapy (134). For instance, studies have highlighted specific lncRNAs that modulate T cell activity, macrophage polarization, and the overall cytokine profile within the TME (135). These findings suggest that lncRNAs can serve as critical mediators of immune evasion and resilience in HCC.

Moreover, the identification of lncRNAs as potential biomarkers for prognosis and treatment response has opened new avenues for personalized immunotherapy approaches in HCC (136). By integrating lncRNA profiling into clinical practice, oncologists may better predict patient responses to immunotherapeutic strategies and tailor treatments accordingly (94, 137). This perspective shift emphasizes the potential for lncRNAs to enhance the efficacy of existing therapies and improve patient outcomes.

Despite the promising insights gained from current research, several challenges remain in translating lncRNA findings into clinical practice. One of the primary obstacles is the complex regulatory mechanisms underlying lncRNA functions. The interactions between lncRNAs and their target genes, as well as the pathways they influence, can be intricate and context-dependent, complicating efforts to target them effectively (138, 139).

Additionally, the identification of specific lncRNA targets poses another challenge. Given the pleiotropic effects of many lncRNAs, achieving specificity in targeting their functions can be difficult (140). This challenge underscores the need for advanced methodologies to elucidate lncRNA interactions and their precise roles within the HCC immune microenvironment.

Drug delivery systems also represent a significant hurdle in lncRNA-based therapies. Ensuring efficient and targeted delivery of lncRNA modulators to tumor tissues while minimizing off-target effects is critical for maximizing therapeutic efficacy (141). Advances in nanotechnology and RNA delivery systems may provide solutions to these challenges, enabling more effective clinical applications of lncRNA therapeutics (142–144).

Although most current studies focus on lncRNAs as biomarkers, some lncRNAs play regulatory roles in the tumor immune microenvironment that render them potential direct therapeutic targets. For example, lncRNA NEAT1 promotes

immune evasion by modulating PD-L1 expression, thereby affecting the sensitivity of tumor cells to immunotherapy; inhibition of NEAT1 may enhance immunotherapeutic efficacy (145–147). Similarly, lncRNA MALAT1 influences T cell infiltration and augments tumor immune suppression by modulating the STAT3 signaling pathway (148, 149). In addition, antisense oligonucleotides (ASOs) targeting MALAT1 have demonstrated promising therapeutic potential (150, 151). Moreover, lncRNA UCA1 regulates PD-L1 expression via miR-148a, and its inhibition could improve the efficacy of ICIs (152). Therefore, the design of lncRNA-targeted intervention strategies—such as RNAi, ASOs, or CRISPR-Cas13-mediated lncRNA degradation—could represent a novel immunotherapeutic approach (153–155).

Despite the potential of lncRNAs as therapeutic targets, several challenges remain. Many lncRNAs exhibit tissue- or cell type-specific expression, and strategies to precisely target specific cells without affecting normal tissues need further exploration. Furthermore, the complex structure of lncRNAs, with some harboring highly stable secondary structures, makes them difficult to degrade or inhibit effectively. Although *in vitro* studies often demonstrate promising intervention outcomes, *in vivo* delivery of RNA-based therapeutics faces challenges including degradation, immunogenicity, and hepatic clearance.

Various RNA delivery strategies have been developed; however, systems optimized specifically for lncRNAs still require refinement. LNPs, which have been approved by the FDA for mRNA vaccine delivery, can be used for lncRNA modulators but still need improvements in tissue specificity (156, 157). Viral vectors, such as AAVs, can facilitate the stable expression of shRNAs to knock down pathogenic lncRNAs, although they may trigger immune responses (158). Chemical modifications like 2'-O-methylation and locked nucleic acid modifications can enhance the stability of lncRNA interference molecules (159, 160).

Meanwhile, the off-target effects of lncRNA modulators should not be overlooked. Many lncRNAs possess highly homologous sequences, so interference with a specific lncRNA may inadvertently affect other non-target RNAs, leading to unexpected biological effects (161, 162). Additionally, lncRNAs may interact with miRNAs through ceRNA mechanisms, whereby targeting a particular lncRNA could trigger cascade effects in miRNA-associated pathways (160). To evaluate such off-target phenomena, techniques such as single-cell sequencing, RNA pull-down assays, and RBP interaction studies can be employed to assess the specificity of lncRNA modulators (163, 164).

Previous studies, as summarized in this review, have shown that the potential of lncRNAs in HCC immunotherapy has been validated in several preclinical studies, demonstrating their significant potential in regulating the immune microenvironment, promoting immune evasion, and serving as therapeutic targets. However, these findings are still far from mature and lack sufficient clinical validation. Currently, most related studies remain in the basic and preclinical research stages, with a lack of clinical trials targeting lncRNA-based therapies for HCC. For example, ASOs targeting MALAT1 have shown preliminary therapeutic effects in mouse models, but their clinical efficacy still needs further confirmation (151, 165). Similarly, although interventions targeting PVT1 and HOTAIR have shown promising results in preclinical studies, there is still a lack of relevant clinical data to assess their therapeutic potential (166). Furthermore, it is important to acknowledge the many challenges in implementing lncRNA-targeted therapeutic strategies, such as those mentioned earlier regarding the specificity of drug delivery to lncRNAs and the avoidance of systemic toxicity, as well as off-target effects that may cause adverse reactions. Therefore, before advancing lncRNA-targeted therapies into clinical practice, these technical barriers must be addressed, and their safety and efficacy should be validated through more extensive clinical trials. As a result, research on lncRNAs as immune therapy targets remains in its early stages. Despite their potential demonstrated in preclinical experiments, there are still many technical and clinical challenges to overcome before applying them in clinical settings. Future research should place greater emphasis on critically evaluating the feasibility and limitations of these therapeutic strategies and strengthening clinical validation efforts.

Looking ahead, future research directions may focus on the development of lncRNA-based therapies that can be integrated into existing treatment regimens. Exploring combination therapies that leverage the immune-modulating effects of lncRNAs alongside ICIs or targeted therapies could yield synergistic benefits. Furthermore, the continued investigation of lncRNA dynamics in response to various treatment modalities will be crucial for optimizing therapeutic strategies.

In summary, while the field of lncRNAs in HCC presents exciting opportunities for enhancing our understanding of tumor-immune interactions, significant challenges remain. Continued research efforts will be essential to unravel the complexities of lncRNA functions and translate these findings into effective clinical interventions.

Author contributions

SZ: Conceptualization, Writing – original draft, Writing – review & editing. FC: Visualization, Writing – original draft, Writing – review & editing. LH: Visualization, Writing – original draft. XL: Visualization, Writing – original draft. ZG: Visualization, Writing – original draft. MC: Writing – original draft, Writing – review & editing. XW: Conceptualization, Writing – original draft, Writing – review & editing. ZS: Conceptualization, Funding acquisition, Visualization, Writing – original draft, Writing – review & editing.

Funding

The author(s) declare that financial support was received for the research and/or publication of this article. This research was supported by the Medical Health Science and Technology Project of Zhejiang Provincial Health Commission (2022KY1246), and the Science and Technology Bureau of Jiaxing City (2023AZ31002 and 2022AZ10009).

Conflict of interest

The authors declare that the research was conducted in the absence of any commercial or financial relationships that could be construed as a potential conflict of interest.

Generative AI statement

The author(s) declare that no Generative AI was used in the creation of this manuscript.

Publisher's note

All claims expressed in this article are solely those of the authors and do not necessarily represent those of their affiliated organizations, or those of the publisher, the editors and the reviewers. Any product that may be evaluated in this article, or claim that may be made by its manufacturer, is not guaranteed or endorsed by the publisher.Abbreviation

References

1. Sung H, Ferlay J, Siegel RL, Laversanne M, Soerjomataram I, Jemal A, et al. Global cancer statistics 2020: GLOBOCAN estimates of incidence and mortality worldwide for 36 cancers in 185 countries. *CA Cancer J Clin*. (2021) 71:209–49. doi: 10.3322/caac.21660

2. Rajendran L, Ivanics T, Claasen MP, Muaddi H, Sapisochin G. The management of post-transplantation recurrence of hepatocellular carcinoma. *Clin Mol Hepatol*. (2022) 28:1–16. doi: 10.3350/cmh.2021.0217

3. Llovet JM, Willoughby CE, Singal AG, Greten TF, Heikenwalder M, El-Serag HB, et al. Nonalcoholic steatohepatitis-related hepatocellular carcinoma: pathogenesis and treatment. *Nat Rev Gastroenterol Hepatol*. (2023) 20:487–503. doi: 10.1038/s41575-023-00754-7

4. Leone V, Ali A, Weber A, Tschaharganeh DF, Heikenwalder M. Liver inflammation and hepatobiliary cancers. *Trends Cancer*. (2021) 7:606–23. doi: 10.1016/j.trecan.2021.01.012

5. Huang DQ, El-Serag HB, Loomba R. Global epidemiology of NAFLD-related HCC: trends, predictions, risk factors and prevention. *Nat Rev Gastroenterol Hepatol*. (2021) 18:223–38. doi: 10.1038/s41575-020-00381-6

6. Reig M, Forner A, Rimola J, Ferrer-Fabrega J, Burrel M, Garcia-Criado A, et al. BCLC strategy for prognosis prediction and treatment recommendation: The 2022 update. *J Hepatol*. (2022) 76:681–93. doi: 10.1016/j.jhep.2021.11.018

7. Shen KY, Zhu Y, Xie SZ, Qin LX. Immunosuppressive tumor microenvironment and immunotherapy of hepatocellular carcinoma: current status and prospectives. *J Hematol Oncol*. (2024) 17:25. doi: 10.1186/s13045-024-01549-2

8. Llovet JM, Castet F, Heikenwalder M, Maini MK, Mazzaferro V, Pinato DJ, et al. Immunotherapies for hepatocellular carcinoma. *Nat Rev Clin Oncol*. (2022) 19:151–72. doi: 10.1038/s41571-021-00573-2

9. Donne R, Lujambio A. The liver cancer immune microenvironment: Therapeutic implications for hepatocellular carcinoma. *Hepatology*. (2023) 77:1773–96. doi: 10.1002/hep.32740

10. Sun G, Liu H, Zhao J, Zhang J, Huang T, Sun G, et al. Macrophage GSK3beta-deficiency inhibits the progression of hepatocellular carcinoma and enhances the sensitivity of anti-PD1 immunotherapy. *J Immunother Cancer*. (2022) 10. doi: 10.1136/jitc-2022-005655

11. Lin X, Kang K, Chen P, Zeng Z, Li G, Xiong W, et al. Regulatory mechanisms of PD-1/PD-L1 in cancers. *Mol Cancer*. (2024) 23:108. doi: 10.1186/s12943-024-02023-w

12. Baker DJ, Arany Z, Baur JA, Epstein JA, June CH. CAR T therapy beyond cancer: the evolution of a living drug. *Nature*. (2023) 619:707–15. doi: 10.1038/s41586-023-06243-w

13. Macek Jilkova Z, Aspord C, Decaens T. Predictive factors for response to PD-1/PD-L1 checkpoint inhibition in the field of hepatocellular carcinoma: current status and challenges. *Cancers (Basel)*. (2019) 11. doi: 10.3390/cancers11101554

14. Rimassa L, Finn RS, Sangro B. Combination immunotherapy for hepatocellular carcinoma. *J Hepatol*. (2023) 79:506–15. doi: 10.1016/j.jhep.2023.03.003

15. Zhou Y, Wei S, Xu M, Wu X, Dou W, Li H, et al. CAR-T cell therapy for hepatocellular carcinoma: current trends and challenges. *Front Immunol*. (2024) 15:1489649. doi: 10.3389/fimmu.2024.1489649

16. Chen B, Dragomir MP, Yang C, Li Q, Horst D, Calin GA. Targeting non-coding RNAs to overcome cancer therapy resistance. *Signal Transduct Target Ther*. (2022) 7:121. doi: 10.1038/s41392-022-00975-3

17. Nemeth K, Bayraktar R, Ferracin M, Calin GA. Non-coding RNAs in disease: from mechanisms to therapeutics. *Nat Rev Genet*. (2024) 25:211–32. doi: 10.1038/s41576-023-00662-1

18. Huang W, Li H, Yu Q, Xiao W, Wang DO. LncRNA-mediated DNA methylation: an emerging mechanism in cancer and beyond. *J Exp Clin Cancer Res*. (2022) 41:100. doi: 10.1186/s13046-022-02319-z

19. Imamura K, Akimitsu N. Long non-coding RNAs involved in immune responses. *Front Immunol*. (2014) 5:573. doi: 10.3389/fimmu.2014.00573

20. Mai H, Zhou B, Liu L, Yang F, Conran C, Ji Y, et al. Molecular pattern of lncRNAs in hepatocellular carcinoma. *J Exp Clin Cancer Res*. (2019) 38:198. doi: 10.1186/s13046-019-1213-0

21. Llovet JM, Pinyol R, Yarchoan M, Singal AG, Marron TU, Schwartz M, et al. Adjuvant and neoadjuvant immunotherapies in hepatocellular carcinoma. *Nat Rev Clin Oncol*. (2024) 21:294–311. doi: 10.1038/s41571-024-00868-0

22. Giraud J, Chalopin D, Blanc JF, Saleh M. Hepatocellular carcinoma immune landscape and the potential of immunotherapies. *Front Immunol*. (2021) 12:655697. doi: 10.3389/fimmu.2021.655697

23. Yin S, Jin W, Qiu Y, Fu L, Wang T, Yu H. Solamargine induces hepatocellular carcinoma cell apoptosis and autophagy via inhibiting LIF/miR-192-5p/CYR61/Akt signaling pathways and eliciting immunostimulatory tumor microenvironment. *J Hematol Oncol*. (2022) 15:32. doi: 10.1186/s13045-022-01248-w

24. Wang H, Zhang H, Wang Y, Brown ZJ, Xia Y, Huang Z, et al. Regulatory T-cell and neutrophil extracellular trap interaction contributes to carcinogenesis in non-alcoholic steatohepatitis. *J Hepatol*. (2021) 75:1271–83. doi: 10.1016/j.jhep.2021.07.032

25. Liu N, Wang X, Steer CJ, Song G. MicroRNA-206 promotes the recruitment of CD8(+) T cells by driving M1 polarisation of Kupffer cells. *Gut*. (2022) 71:1642–55. doi: 10.1136/gutjnl-2021-324170

26. Zhang PF, Gao C, Huang XY, Lu JC, Guo XJ, Shi GM, et al. Cancer cell-derived exosomal circUHRF1 induces NK cell exhaustion and may cause resistance to anti-PD1 therapy in hepatocellular carcinoma. *Mol Cancer*. (2020) 19:110. doi: 10.1186/s12943-020-01222-5

27. Wang S, Wu Q, Chen T, Su R, Pan C, Qian J, et al. Blocking CD47 promotes antitumour immunity through CD103(+) dendritic cell-NK cell axis in murine hepatocellular carcinoma model. *J Hepatol*. (2022) 77:467–78. doi: 10.1016/j.jhep.2022.03.011

28. Finkin S, Yuan D, Stein I, Taniguchi K, Weber A, Unger K, et al. Ectopic lymphoid structures function as microniches for tumor progenitor cells in hepatocellular carcinoma. *Nat Immunol*. (2015) 16:1235–44. doi: 10.1038/ni.3290

29. Heinrich B, Gertz EM, Schaffer AA, Craig A, Ruf B, Subramanyam V, et al. The tumour microenvironment shapes innate lymphoid cells in patients with hepatocellular carcinoma. *Gut*. (2022) 71:1161–75. doi: 10.1136/gutjnl-2021-325288

30. Chan LC, Li CW, Xia W, Hsu JM, Lee HH, Cha JH, et al. IL-6/JAK1 pathway drives PD-L1 Y112 phosphorylation to promote cancer immune evasion. *J Clin Invest*. (2019) 129:3324–38. doi: 10.1172/JCI126022

31. Qi D, Lu M, Xu P, Yao X, Chen Y, Gan L, et al. Transcription factor ETV4 promotes the development of hepatocellular carcinoma by driving hepatic TNF-alpha signaling. *Cancer Commun (Lond)*. (2023) 43:1354–72. doi: 10.1002/cac2.v43.12

32. Kuraji R, Sekino S, Kapila Y, Numabe Y. Periodontal disease-related nonalcoholic fatty liver disease and nonalcoholic steatohepatitis: An emerging concept of oral-liver axis. *Periodontol 2000*. (2021) 87:204–40. doi: 10.1111/prd.12387

33. Arvanitakis K, Mitroulis I, Germanidis G. Tumor-associated neutrophils in hepatocellular carcinoma pathogenesis, prognosis, and therapy. *Cancers (Basel)*. (2021) 13. doi: 10.3390/cancers13122899

34. Pinter M, Scheiner B, Pinato DJ. Immune checkpoint inhibitors in hepatocellular carcinoma: emerging challenges in clinical practice. *Lancet Gastroenterol Hepatol*. (2023) 8:760–70. doi: 10.1016/S2468-1253(23)00147-4

35. Sangro B, Chan SL, Meyer T, Reig M, El-Khoueiry A, Galle PR. Diagnosis and management of toxicities of immune checkpoint inhibitors in hepatocellular carcinoma. *J Hepatol*. (2020) 72:320–41. doi: 10.1016/j.jhep.2019.10.021

36. Wang Z, Wang Y, Gao P, Ding J. Immune checkpoint inhibitor resistance in hepatocellular carcinoma. *Cancer Lett*. (2023) 555:216038. doi: 10.1016/j.canlet.2022.216038

37. Zhu AX, Abbas AR, de Galarreta MR, Guan Y, Lu S, Koeppen H, et al. Molecular correlates of clinical response and resistance to atezolizumab in combination with bevacizumab in advanced hepatocellular carcinoma. *Nat Med*. (2022) 28:1599–611. doi: 10.1038/s41591-022-01868-2

38. Lu LG, Zhou ZL, Wang XY, Liu BY, Lu JY, Liu S, et al. PD-L1 blockade liberates intrinsic antitumourigenic properties of glycolytic macrophages in hepatocellular carcinoma. *Gut*. (2022) 71:2551–60. doi: 10.1136/gutjnl-2021-326350

39. Wei CY, Zhu MX, Zhang PF, Huang XY, Wan JK, Yao XZ, et al. PKCalpha/ZFP64/CSF1 axis resets the tumor microenvironment and fuels anti-PD1 resistance in hepatocellular carcinoma. *J Hepatol*. (2022) 77:163–76. doi: 10.1016/j.jhep.2022.02.019

40. Gao X, Xu N, Li Z, Shen L, Ji K, Zheng Z, et al. Safety and antitumour activity of cadonilimab, an anti-PD-1/CTLA-4 bispecific antibody, for patients with advanced solid tumours (COMPASSION-03): a multicentre, open-label, phase 1b/2 trial. *Lancet Oncol*. (2023) 24:1134–46. doi: 10.1016/S1470-2045(23)00411-4

41. Ye W, Li H, Zhao J, Lu D, Tao T, Zhu X. Graphene therapy-related lncRNAs as prognostic and immune microenvironmental biomarkers in hepatocellular carcinoma. *Transl Oncol*. (2024) 43:101915. doi: 10.1016/j.tranon.2024.101915

42. Tzur YB. lncRNAs in fertility: redefining the gene expression paradigm? *Trends Genet*. (2022) 38:1170–9. doi: 10.1016/j.tig.2022.05.013

43. Herman AB, Tsitsipatis D, Gorospe M. Integrated lncRNA function upon genomic and epigenomic regulation. *Mol Cell*. (2022) 82:2252–66. doi: 10.1016/j.molcel.2022.05.027

44. Zhang N, Zhang H, Wu W, Zhou R, Li S, Wang Z, et al. Machine learning-based identification of tumor-infiltrating immune cell-associated lncRNAs for improving outcomes and immunotherapy responses in patients with low-grade glioma. *Theranostics*. (2022) 12:5931–48. doi: 10.7150/thno.74281

45. Safarzadeh E, Asadzadeh Z, Safaei S, Hatefi A, Derakhshani A, Giovannelli F, et al. MicroRNAs and lncRNAs-A new layer of myeloid-derived suppressor cells regulation. *Front Immunol*. (2020) 11:572323. doi: 10.3389/fimmu.2020.572323

46. Zhang J, Luo Q, Li X, Guo J, Zhu Q, Lu X, et al. Novel role of immune-related non-coding RNAs as potential biomarkers regulating tumour immunoresponse via MICA/NKG2D pathway. *Biomark Res*. (2023) 11:86. doi: 10.1186/s40364-023-00530-4

47. Gao F, He S, Jin A. MiRNAs and lncRNAs in NK cell biology and NK/T-cell lymphoma. *Genes Dis*. (2021) 8:590–602. doi: 10.1016/j.gendis.2020.08.006

48. Saadi W, Fatmi A, Pallardo FV, Garcia-Gimenez JL, Mena-Molla S. Long non-coding RNAs as epigenetic regulators of immune checkpoints in cancer immunity. *Cancers (Basel)*. (2022) 15. doi: 10.3390/cancers15010184

49. Yan K, Fu Y, Zhu N, Wang Z, Hong JL, Li Y, et al. Repression of lncRNA NEAT1 enhances the antitumor activity of CD8(+)T cells against hepatocellular carcinoma via regulating miR-155/Tim-3. *Int J Biochem Cell Biol*. (2019) 110:1–8. doi: 10.1016/j.biocel.2019.01.019

50. Ji J, Yin Y, Ju H, Xu X, Liu W, Fu Q, et al. Long non-coding RNA Lnc-Tim3 exacerbates CD8 T cell exhaustion via binding to Tim-3 and inducing nuclear translocation of Bat3 in HCC. *Cell Death Dis*. (2018) 9:478. doi: 10.1038/s41419-018-0528-7

51. Xi Q, Yang G, He X, Zhuang H, Li L, Lin B, et al. M(6)A-mediated upregulation of lncRNA TUG1 in liver cancer cells regulates the antitumor response of CD8(+) T cells and phagocytosis of macrophages. *Adv Sci (Weinh)*. (2024) 11:e2400695. doi: 10.1002/advs.202400695

52. Zhang X, Pan B, Qiu J, Ke X, Shen S, Wang X, et al. lncRNA MIAT targets miR-411-5p/STAT3/PD-L1 axis mediating hepatocellular carcinoma immune response. *Int J Exp Pathol*. (2022) 103:102–11. doi: 10.1111/iep.12440

53. AbuliHaiti Z, Li W, Yang L, Zhang H, Du A, Tang N, et al. Hypoxia-driven lncRNA CTD-2510F5.4: a potential player in hepatocellular carcinoma's prognostic stratification, cellular behavior, tumor microenvironment, and therapeutic response. *Mol Biol Rep*. (2024) 51:905. doi: 10.1007/s11033-024-09826-6

54. Ma K, Chu J, Liu Y, Sun L, Zhou S, Li X, et al. Hepatocellular carcinoma LINC01116 outcompetes T cells for linoleic acid and accelerates tumor progression. *Adv Sci (Weinh)*. (2024) 11:e2400676. doi: 10.1002/advs.202400676

55. Li X, Liang S, Fei M, Ma K, Sun L, Liu Y, et al. LncRNA CRNDE drives the progression of hepatocellular carcinoma by inducing the immunosuppressive niche. *Int J Biol Sci*. (2024) 20:718–32. doi: 10.7150/ijbs.85471

56. Zhang J, Pan T, Zhou W, Zhang Y, Xu G, Xu Q, et al. Long noncoding RNA LINC01132 enhances immunosuppression and therapy resistance via NRF1/DPP4 axis in hepatocellular carcinoma. *J Exp Clin Cancer Res*. (2022) 41:270. doi: 10.1186/s13046-022-02478-z

57. Chen W, Chen F, Gong M, Jin Z, Shu L, Wang ZW, et al. Comprehensive analysis of lncRNA-mediated ceRNA networkfor hepatocellular carcinoma. *Front Oncol*. (2022) 12:1042928. doi: 10.3389/fonc.2022.1042928

58. Zhong F, Liu S, Hu D, Chen L. LncRNA AC099850.3 promotes hepatocellular carcinoma proliferation and invasion through PRR11/PI3K/AKT axis and is associated with patients prognosis. *J Cancer*. (2022) 13:1048–60. doi: 10.7150/jca.66092

59. Sha Z, Zhang P. LncRNA-GAS5 and its promoter region polymorphism associate with helper th17 polarization and predict postoperative pain and the prognosis of the patients with hepatocellular carcinoma undergoing hepatectomy. *Iran J Immunol*. (2022) 19:349–57. doi: 10.22034/IJI.2022.92678.2168

60. Pehlivanoglu B, Aysal A, Agalar C, Egeli T, Ozbilgin M, Unek T, et al. lncRNA XIST interacts with regulatory T cells within the tumor microenvironment in chronic hepatitis B-associated hepatocellular carcinoma. *Turk Patoloji Derg*. (2024) 40:101–8. doi: 10.5146/tjpath.2023.13161

61. Dong W, Zhan C. Bioinformatic-based mechanism identification of E2F1-related ceRNA and E2F1 immunoassays in hepatocellular carcinoma. *J Gastrointest Oncol*. (2022) 13:1915–26. doi: 10.21037/jgo-22-674

62. Xie C, Wang S, Zhang H, Zhu Y, Jiang P, Shi S, et al. Lnc-AIFM2-1 promotes HBV immune escape by acting as a ceRNA for miR-330-3p to regulate CD244 expression. *Front Immunol*. (2023) 14:1121795. doi: 10.3389/fimmu.2023.1121795

63. Peng L, Chen Y, Ou Q, Wang X, Tang N. LncRNA MIAT correlates with immune infiltrates and drug reactions in hepatocellular carcinoma. *Int Immunopharmacol*. (2020) 89:107071. doi: 10.1016/j.intimp.2020.107071

64. Fan F, Chen K, Lu X, Li A, Liu C, Wu B. Dual targeting of PD-L1 and PD-L2 by PCED1B-AS1 via sponging hsa-miR-194-5p induces immunosuppression in hepatocellular carcinoma. *Hepatol Int*. (2021) 15:444–58. doi: 10.1007/s12072-020-10101-6

65. Huang LH, Rau CS, Liu YW, Wu CJ, Chien PC, Lin HP, et al. Exploring the regulatory role of XIST-microRNAs/mRNA network in circulating CD4(+) T cells of hepatocellular carcinoma patients. *Biomedicines*. (2023) 11. doi: 10.3390/biomedicines11071848

66. Xiao S, Huang S, Yang J. Overexpression of GIHCG is associated with a poor prognosis and immune infiltration in hepatocellular carcinoma. *Onco Targets Ther*. (2020) 13:11607–19. doi: 10.2147/OTT.S271966

67. Song H, Huang XF, Hu SY, Lu LL, Yang XY. The LINC00261/MiR105-5p/SELL axis is involved in dysfunction of B cell and is associated with overall survival in hepatocellular carcinoma. *PeerJ*. (2022) 10:e12588. doi: 10.7717/peerj.12588

68. Zhan T, Gao X, Wang G, Li F, Shen J, Lu C, et al. Construction of novel lncRNA-miRNA-mRNA network associated with recurrence and identification of immune-related potential regulatory axis in hepatocellular carcinoma. *Front Oncol*. (2021) 11:626663. doi: 10.3389/fonc.2021.626663

69. Yu Z, Zhao H, Feng X, Li H, Qiu C, Yi X, et al. Long non-coding RNA FENDRR acts as a miR-423-5p sponge to suppress the treg-mediated immune escape of hepatocellular carcinoma cells. *Mol Ther Nucleic Acids*. (2019) 17:516–29. doi: 10.1016/j.omtn.2019.05.027

70. Xu M, Zhou C, Weng J, Chen Z, Zhou Q, Gao J, et al. Tumor associated macrophages-derived exosomes facilitate hepatocellular carcinoma Malignance by transferring lncMMPA to tumor cells and activating glycolysis pathway. *J Exp Clin Cancer Res*. (2022) 41:253. doi: 10.1186/s13046-022-02458-3

71. Li X, Lei Y, Wu M, Li N. Regulation of macrophage activation and polarization by HCC-derived exosomal lncRNA TUC339. *Int J Mol Sci*. (2018) 19. doi: 10.3390/ijms19102958

72. Lv S, Wang J, Li L. Extracellular vesicular lncRNA FAL1 promotes hepatocellular carcinoma cell proliferation and invasion by inducing macrophage M2 polarization. *J Physiol Biochem*. (2023) 79:669–82. doi: 10.1007/s13105-022-00922-4

73. Ai JH, Wen YZ, Dai SJ, Zhang LD, Huang ZJ, Shi J. Exosomal lncRNA HEIH, an essential communicator for hepatocellular carcinoma cells and macrophage M2 polarization through the miR-98-5p/STAT3 axis. *J Biochem Mol Toxicol*. (2024) 38:e23686. doi: 10.1002/jbt.23686

74. Wang X, Zhou Y, Dong K, Zhang H, Gong J, Wang S. Exosomal lncRNA HMMR-AS1 mediates macrophage polarization through miR-147a/ARID3A axis under hypoxia and affects the progression of hepatocellular carcinoma. *Environ Toxicol*. (2022) 37:1357–72. doi: 10.1002/tox.23489

75. Zhou J, Che J, Xu L, Yang W, Zhou W, Zhou C. Tumor-derived extracellular vesicles containing long noncoding RNA PART1 exert oncogenic effect in hepatocellular carcinoma by polarizing macrophages into M2. *Dig Liver Dis*. (2022) 54:543–53. doi: 10.1016/j.dld.2021.07.005

76. Ye Y, Wang M, Wang G, Mai Z, Zhou B, Han Y, et al. lncRNA miR4458HG modulates hepatocellular carcinoma progression by activating m6A-dependent glycolysis and promoting the polarization of tumor-associated macrophages. *Cell Mol Life Sci*. (2023) 80:99. doi: 10.1007/s00018-023-04741-8

77. Ye Y, Xu Y, Lai Y, He W, Li Y, Wang R, et al. Long non-coding RNA cox-2 prevents immune evasion and metastasis of hepatocellular carcinoma by altering M1/M2 macrophage polarization. *J Cell Biochem*. (2018) 119:2951–63. doi: 10.1002/jcb.v119.3

78. Luo T, Chen M, Zhao Y, Wang D, Liu J, Chen J, et al. Macrophage-associated lncRNA ELMO1-AS1: a novel therapeutic target and prognostic biomarker for hepatocellular carcinoma. *Onco Targets Ther*. (2019) 12:6203–16. doi: 10.2147/OTT.S213833

79. Lin J, Huang J, Tan C, Wu S, Lu X, Pu J. LncRNA MEG3 suppresses hepatocellular carcinoma by stimulating macrophage M1 polarization and modulating immune system via inhibiting CSF-1 *in vivo*/vitro studies. *Int J Biol Macromol*. (2024) 281:136459. doi: 10.1016/j.ijbiomac.2024.136459

80. Wei H, Wu X, Huang L, Long C, Lu Q, Huang Z, et al. LncRNA MEG3 reduces the ratio of M2/M1 macrophages through the huR/CCL5 axis in hepatocellular carcinoma. *J Hepatocell Carcinoma*. (2024) 11:543–62. doi: 10.2147/JHC.S449090

81. Tao L, Li D, Mu S, Tian G, Yan G. LncRNA MAPKAPK5_AS1 facilitates cell proliferation in hepatitis B virus -related hepatocellular carcinoma. *Lab Invest*. (2022) 102:494–504. doi: 10.1038/s41374-022-00731-9

82. Wei Q, Liu G, Huang Z, Huang Y, Huang L, Huang Z, et al. LncRNA MEG3 Inhibits Tumor Progression by Modulating Macrophage Phenotypic Polarization via miR-145-5p/DAB2 Axis in Hepatocellular Carcinoma. *J Hepatocell Carcinoma*. (2023) 10:1019–35. doi: 10.2147/JHC.S408800

83. Lin C, Jiang T EC, Wang L, Chen T, Wang X, Xiang Y. LncRNA CRNDE promotes hepatoma cell proliferation by regulating the metabolic reprogramming of M2 macrophages via ERK pathway. *Cancer Cell Int*. (2024) 24:193. doi: 10.1186/s12935-024-03380-8

84. Chen J, Huang ZB, Liao CJ, Hu XW, Li SL, Qi M, et al. LncRNA TP73-AS1/miR-539/MMP-8 axis modulates M2 macrophage polarization in hepatocellular carcinoma via TGF-beta1 signaling. *Cell Signal*. (2020) 75:109738. doi: 10.1016/j.cellsig.2020.109738

85. Luo HL, Luo T, Liu JJ, Wu FX, Bai T, Ou C, et al. Macrophage polarization-associated lnc-Ma301 interacts with caprin-1 to inhibit hepatocellular carcinoma metastasis through the Akt/Erk1 pathway. *Cancer Cell Int*. (2021) 21:422. doi: 10.1186/s12935-021-02133-1

86. Tian X, Wu Y, Yang Y, Wang J, Niu M, Gao S, et al. Long noncoding RNA LINC00662 promotes M2 macrophage polarization and hepatocellular carcinoma progression via activating Wnt/beta-catenin signaling. *Mol Oncol*. (2020) 14:462–83. doi: 10.1002/1878-0261.12606

87. Hou ZH, Xu XW, Fu XY, Zhou LD, Liu SP, Tan DM. Long non-coding RNA MALAT1 promotes angiogenesis and immunosuppressive properties of HCC cells by sponging miR-140. *Am J Physiol Cell Physiol*. (2020) 318:C649–63. doi: 10.1152/ajpcell.00510.2018

88. Sun J, Li Y, Tian H, Chen H, Li J, Li Z. Comprehensive analysis identifies long non-coding RNA RNASEH1-AS1 as a potential prognostic biomarker and oncogenic target in hepatocellular carcinoma. *Am J Cancer Res*. (2024) 14:996–1014. doi: 10.62347/JPHF4071

89. Wei M, Lu L, Ma J, Luo Z, Tan X, Wang J. LINC00707 impairs the Natural Killer cell antitumour activity in hepatocellular carcinoma through decreasing YTHDF2 stability. *J Cell Mol Med*. (2024) 28:e18106. doi: 10.1111/jcmm.18106

90. Lin XQ, Huang ZM, Chen X, Wu F, Wu W. XIST induced by JPX suppresses hepatocellular carcinoma by sponging miR-155-5p. *Yonsei Med J*. (2018) 59:816–26. doi: 10.3349/ymj.2018.59.7.816

91. Qiu J, Zhong F, Zhang Z, Pan B, Ye D, Zhang X, et al. Hypoxia-responsive lncRNA MIR155HG promotes PD-L1 expression in hepatocellular carcinoma cells by enhancing HIF-1alpha mRNA stability. *Int Immunopharmacol*. (2024) 136:112415. doi: 10.1016/j.intimp.2024.112415

92. Peng L, Pan B, Zhang X, Wang Z, Qiu J, Wang X, et al. Lipopolysaccharide facilitates immune escape of hepatocellular carcinoma cells via m6A modification of lncRNA MIR155HG to upregulate PD-L1 expression. *Cell Biol Toxicol*. (2022) 38:1159–73. doi: 10.1007/s10565-022-09718-0

93. Zeng C, Ye S, Chen Y, Zhang Q, Luo Y, Gai L, et al. HOXA-AS3 Promotes Proliferation and Migration of Hepatocellular Carcinoma Cells via the miR-455-5p/PD-L1 Axis. *J Immunol Res*. (2021) 2021:9289719. doi: 10.1155/2021/9289719

94. Dong L, Zhou S, Bai X, He X. Construction of a prognostic model for HCC based on ferroptosis-related lncRNAs expression and its potential to predict the response and irAEs of immunotherapy. *Front Pharmacol*. (2023) 14:1090895. doi: 10.3389/fphar.2023.1090895

95. Liang J, Zhi Y, Deng W, Zhou W, Li X, Cai Z, et al. Dong Y, et al. Development and validation of ferroptosis-related lncRNAs signature for hepatocellular carcinoma. *PeerJ*. (2021) 9:e11627. doi: 10.7717/peerj.11627

96. Sun Z, Xue C, Li J, Zhao H, Du Y, Du N. LINC00244 suppresses cell growth and metastasis in hepatocellular carcinoma by downregulating programmed cell death ligand 1. *Bioengineered*. (2022) 13:7635–47. doi: 10.1080/21655979.2022.2050073

97. Zhang J, Zhao X, Ma X, Yuan Z, Hu M. KCNQ1OT1 contributes to sorafenib resistance and programmed death–ligand–1–mediated immune escape via sponging miR–506 in hepatocellular carcinoma cells. *Int J Mol Med*. (2020) 46:1794–804. doi: 10.3892/ijmm.2020.4710

98. Guo BL, Zheng QX, Jiang YS, Zhan Y, Huang WJ, Chen ZY. Long non-coding RNAFOXD1-AS1 modulated CTCs epithelial-mesenchymal transition and immune escape in hepatocellular carcinoma *in vitro* by sponging miR-615-3p. *Cancer Rep (Hoboken)*. (2024) 7:e2050. doi: 10.1002/cnr2.2050

99. Wu MZ, Yuan YC, Huang BY, Chen JX, Li BK, Fang JH, et al. Identification of a TGF-beta/SMAD/lnc-UTGF positive feedback loop and its role in hepatoma metastasis. *Signal Transduct Target Ther*. (2021) 6:395. doi: 10.1038/s41392-021-00781-3

100. Sheng J, Luo Y, Lv E, Liang H, Tao H, Yu C, et al. LINC01980 induced by TGF-beta promotes hepatocellular carcinoma metastasis via miR-376b-5p/E2F5 axis. *Cell Signal*. (2023) 112:110923. doi: 10.1016/j.cellsig.2023.110923

101. Yuan JH, Yang F, Wang F, Ma JZ, Guo YJ, Tao QF, et al. A long noncoding RNA activated by TGF-beta promotes the invasion-metastasis cascade in hepatocellular carcinoma. *Cancer Cell*. (2014) 25:666–81. doi: 10.1016/j.ccr.2014.03.010

102. Zhang Z, Zhou Y, Jia Y, Wang C, Zhang M, Xu Z. PRR34-AS1 promotes exosome secretion of VEGF and TGF-beta via recruiting DDX3X to stabilize Rab27a mRNA in hepatocellular carcinoma. *J Transl Med*. (2022) 20:491. doi: 10.1186/s12967-022-03628-9

103. Li D, Lu L, Liu M, Sun J. Inhibition of long noncoding RNA cancer susceptibility candidate 7 attenuates hepatocellular carcinoma development by targeting microRNA-30a-5p. *Bioengineered*. (2022) 13:11296–308. doi: 10.1080/21655979.2022.2068289

104. Huang WJ, Tian XP, Bi SX, Zhang SR, He TS, Song LY, et al. The beta-catenin/TCF-4-LINC01278-miR-1258-Smad2/3 axis promotes hepatocellular carcinoma metastasis. *Oncogene*. (2020) 39:4538–50. doi: 10.1038/s41388-020-1307-3

105. Shi Y, Yang X, Xue X, Sun D, Cai P, Song Q, et al. HANR promotes hepatocellular carcinoma progression via miR-214/EZH2/TGF-beta axis. *Biochem Biophys Res Commun*. (2018) 506:189–93. doi: 10.1016/j.bbrc.2018.10.038

106. Liang J, Liao J, Liu T, Wang Y, Wen J, Cai N, et al. Comprehensive analysis of TGF-beta-induced mRNAs and ncRNAs in hepatocellular carcinoma. *Aging (Albany NY)*. (2020) 12:19399–420. doi: 10.18632/aging.v12i19

107. Wang X, Sun W, Shen W, Xia M, Chen C, Xiang D, et al. Long non-coding RNA DILC regulates liver cancer stem cells via IL-6/STAT3 axis. *J Hepatol*. (2016) 64:1283–94. doi: 10.1016/j.jhep.2016.01.019

108. Sun QM, Hu B, Fu PY, Tang WG, Zhang X, Zhan H, et al. Long non-coding RNA 00607 as a tumor suppressor by modulating NF-kappaB p65/p53 signaling axis in hepatocellular carcinoma. *Carcinogenesis*. (2018) 39:1438–46. doi: 10.1093/carcin/bgy113

109. Li S, Hu X, Yu S, Yi P, Chen R, Huang Z, et al. Hepatic stellate cell-released CXCL1 aggravates HCC Malignant behaviors through the MIR4435-2HG/miR-506-3p/TGFB1 axis. *Cancer Sci*. (2023) 114:504–20. doi: 10.1111/cas.v114.2

110. Wang Y, Yang L, Dong X, Yang X, Zhang X, Liu Z, et al. Overexpression of NNT-AS1 activates TGF-beta signaling to decrease tumor CD4 lymphocyte infiltration in hepatocellular carcinoma. *BioMed Res Int*. (2020) 2020:8216541. doi: 10.1155/2020/8216541

111. Yang Y, Min Z. Effect of long non−coding RNA AK021443 on promoting hepatic fibrosis *in vitro*. *Mol Med Rep*. (2021) 23. doi: 10.3892/mmr.2021.12518

112. Tang J, Zhuo H, Zhang X, Jiang R, Ji J, Deng L, et al. A novel biomarker Linc00974 interacting with KRT19 promotes proliferation and metastasis in hepatocellular carcinoma. *Cell Death Dis*. (2014) 5:e1549. doi: 10.1038/cddis.2014.518

113. Liu Y, Chen L, Yuan H, Guo S, Wu G. LncRNA DANCR promotes sorafenib resistance via activation of IL-6/STAT3 signaling in hepatocellular carcinoma cells. *Onco Targets Ther*. (2020) 13:1145–57. doi: 10.2147/OTT.S229957

114. Lin Y, Jian Z, Jin H, Wei X, Zou X, Guan R, et al. Long non-coding RNA DLGAP1-AS1 facilitates tumorigenesis and epithelial-mesenchymal transition in hepatocellular carcinoma via the feedback loop of miR-26a/b-5p/IL-6/JAK2/STAT3 and Wnt/beta-catenin pathway. *Cell Death Dis*. (2020) 11:34. doi: 10.1038/s41419-019-2188-7

115. Huang M, Wang H, Hu X, Cao X. lncRNA MALAT1 binds chromatin remodeling subunit BRG1 to epigenetically promote inflammation-related hepatocellular carcinoma progression. *Oncoimmunology*. (2019) 8:e1518628. doi: 10.1080/2162402X.2018.1518628

116. Ding H, Liu J, Zou R, Cheng P, Su Y. Retraction Note: Long non-coding RNA TPTEP1 inhibits hepatocellular carcinoma progression by suppressing STAT3 phosphorylation. *J Exp Clin Cancer Res*. (2023) 42:123. doi: 10.1186/s13046-023-02700-6

117. Ma A, Sun Y, Ogbodu RO, Xiao L, Deng H, Zhou H. Identification of biomarkers of hepatocellular carcinoma gene prognosis based on the immune-related lncRNA signature of transcriptome data. *Funct Integr Genomics*. (2023) 23:104. doi: 10.1007/s10142-023-01019-x

118. Xu Z, Peng B, Liang Q, Chen X, Cai Y, Zeng S, et al. Construction of a ferroptosis-Related nine-lncRNA signature for predicting prognosis and immune response in hepatocellular carcinoma. *Front Immunol*. (2021) 12:719175. doi: 10.3389/fimmu.2021.719175

119. Mao Z, Nie Y, Jia W, Wang Y, Li J, Zhang T, et al. Revealing prognostic and immunotherapy-sensitive characteristics of a novel cuproptosis-related lncRNA model in hepatocellular carcinoma patients by genomic analysis. *Cancers (Basel)*. (2023) 15. doi: 10.3390/cancers15020544

120. Wang X, Chen J, Lin L, Li Y, Tao Q, Lang Z, et al. Machine learning integrations develop an antigen-presenting-cells and T-Cells-Infiltration derived LncRNA signature for improving clinical outcomes in hepatocellular carcinoma. *BMC Cancer*. (2023) 23:284. doi: 10.1186/s12885-023-10766-w

121. Xie S, Zhong J, Zhang Z, Huang W, Lin X, Pan Y, et al. Novel risk model based on angiogenesis-related lncRNAs for prognosis prediction of hepatocellular carcinoma. *Cancer Cell Int*. (2023) 23:159. doi: 10.1186/s12935-023-02975-x

122. Zhang L, Hu S, Chen J, Ma S, Liu F, Liu C, et al. Comprehensive analysis of the MIR4435-2HG/miR-1-3p/MMP9/miR-29-3p/DUXAP8 ceRNA network axis in hepatocellular carcinoma. *Discov Oncol*. (2021) 12:38. doi: 10.1007/s12672-021-00436-3

123. Hu S, Zhang J, Guo G, Zhang L, Dai J, Gao Y. Comprehensive analysis of GSEC/miR-101-3p/SNX16/PAPOLG axis in hepatocellular carcinoma. *PloS One*. (2022) 17:e0267117. doi: 10.1371/journal.pone.0267117

124. Li X, Zhang Z, Liu M, Fu X, A J, Chen G, et al. Establishment of a lncRNA-based prognostic gene signature associated with altered immune responses in HCC. *Front Immunol*. (2022) 13:880288. doi: 10.3389/fimmu.2022.880288

125. Huang F, Zhang C, Yang W, Zhou Y, Yang Y, Yang X, et al. Identification of a DNA damage repair-related LncRNA signature for predicting the prognosis and immunotherapy response of hepatocellular carcinoma. *BMC Genomics*. (2024) 25:155. doi: 10.1186/s12864-024-10055-1

126. Xia W, Zeng C, Zheng Z, Huang C, Zhou Y, Bai L. Development and validation of a novel mitochondrion and ferroptosis-related long non-coding RNA prognostic signature in hepatocellular carcinoma. *Front Cell Dev Biol*. (2022) 10:844759. doi: 10.3389/fcell.2022.844759

127. Yu ZL, Zhu ZM. Comprehensive analysis of N6-methyladenosine -related long non-coding RNAs and immune cell infiltration in hepatocellular carcinoma. *Bioengineered*. (2021) 12:1708–24. doi: 10.1080/21655979.2021.1923381

128. Lu D, Liao J, Cheng H, Ma Q, Wu F, Xie F, et al. Construction and systematic evaluation of a machine learning-based cuproptosis-related lncRNA score signature to predict the response to immunotherapy in hepatocellular carcinoma. *Front Immunol*. (2023) 14:1097075. doi: 10.3389/fimmu.2023.1097075

129. Huang EM, Ma N, Ma T, Zhou JY, Yang WS, Liu CX, et al. Cuproptosis-related long non-coding RNAs model that effectively predicts prognosis in hepatocellular carcinoma. *World J Gastrointest Oncol*. (2022) 14:1981–2003. doi: 10.4251/wjgo.v14.i10.1981

130. Wilusz JE, Sunwoo H, Spector DL. Long noncoding RNAs: functional surprises from the RNA world. *Genes Dev*. (2009) 23:1494–504. doi: 10.1101/gad.1800909

131. Chen J, Liu A, Wang Z, Wang B, Chai X, Lu W, et al. LINC00173.v1 promotes angiogenesis and progression of lung squamous cell carcinoma by sponging miR-511-5p to regulate VEGFA expression. *Mol Cancer*. (2020) 19:98. doi: 10.1186/s12943-020-01217-2

132. Sun TT, He J, Liang Q, Ren LL, Yan TT, Yu TC, et al. LncRNA GClnc1 promotes gastric carcinogenesis and may act as a modular scaffold of WDR5 and KAT2A complexes to specify the histone modification pattern. *Cancer Discov*. (2016) 6:784–801. doi: 10.1158/2159-8290.CD-15-0921

133. Zhao J, Du P, Cui P, Qin Y, Hu C, Wu J, et al. LncRNA PVT1 promotes angiogenesis via activating the STAT3/VEGFA axis in gastric cancer. *Oncogene*. (2018) 37:4094–109. doi: 10.1038/s41388-018-0250-z

134. Li Y, Jiang T, Zhou W, Li J, Li X, Wang Q, et al. Pan-cancer characterization of immune-related lncRNAs identifies potential oncogenic biomarkers. *Nat Commun*. (2020) 11:1000. doi: 10.1038/s41467-020-14802-2

135. Xu Z, Chen Y, Ma L, Chen Y, Liu J, Guo Y, et al. Role of exosomal non-coding RNAs from tumor cells and tumor-associated macrophages in the tumor microenvironment. *Mol Ther*. (2022) 30:3133–54. doi: 10.1016/j.ymthe.2022.01.046

136. Nakagawa C, Kadlera Nagaraj M, Hernandez JC, Uthay Kumar DB, Shukla V, Machida R, et al. beta-CATENIN stabilizes HIF2 through lncRNA and inhibits intravenous immunoglobulin immunotherapy. *Front Immunol*. (2023) 14:1204907. doi: 10.3389/fimmu.2023.1204907

137. Jia X, Wang Y, Yang Y, Fu Y, Liu Y. Constructed risk prognosis model associated with disulfidptosis lncRNAs in HCC. *Int J Mol Sci*. (2023) 24. doi: 10.3390/ijms242417626

138. Yamamura S, Imai-Sumida M, Tanaka Y, Dahiya R. Interaction and cross-talk between non-coding RNAs. *Cell Mol Life Sci*. (2018) 75:467–84. doi: 10.1007/s00018-017-2626-6

139. Zhang L, Zou J, Wang Z, Li L. A subpathway and target gene cluster-based approach uncovers lncRNAs associated with human primordial follicle activation. *Int J Mol Sci*. (2023) 24. doi: 10.3390/ijms241310525

140. Lim LJ, Wong SYS, Huang F, Lim S, Chong SS, Ooi LL, et al. Roles and regulation of long noncoding RNAs in hepatocellular carcinoma. *Cancer Res*. (2019) 79:5131–9. doi: 10.1158/0008-5472.CAN-19-0255

141. Zuo X, Chen Z, Gao W, Zhang Y, Wang J, Wang J, et al. M6A-mediated upregulation of LINC00958 increases lipogenesis and acts as a nanotherapeutic target in hepatocellular carcinoma. *J Hematol Oncol*. (2020) 13:5. doi: 10.1186/s13045-019-0839-x

142. Vilaca A, de Windt LJ, Fernandes H, Ferreira L. Strategies and challenges for non-viral delivery of non-coding RNAs to the heart. *Trends Mol Med*. (2023) 29:70–91. doi: 10.1016/j.molmed.2022.10.002

143. Machyna M, Kiefer L, Simon MD. Enhanced nucleotide chemistry and toehold nanotechnology reveals lncRNA spreading on chromatin. *Nat Struct Mol Biol*. (2020) 27:297–304. doi: 10.1038/s41594-020-0390-z

144. Horns F, Martinez JA, Fan C, Haque M, Linton JM, Tobin V, et al. Engineering RNA export for measurement and manipulation of living cells. *Cell*. (2023) 186:3642–3658 e3632. doi: 10.1016/j.cell.2023.06.013

145. Yuan J, Yang J, Wang R, Hao H, Li J. LncRNA NEAT1 regulate diffuse large B-cell lymphoma by targeting miR-495-3p/PD-L1 axis. *Immunopharmacol Immunotoxicol*. (2022) 44:429–36. doi: 10.1080/08923973.2022.2052896

146. Yin L, Wang Y. Extracellular vesicles derived from M2-polarized tumor-associated macrophages promote immune escape in ovarian cancer through NEAT1/miR-101-3p/ZEB1/PD-L1 axis. *Cancer Immunol Immunother*. (2023) 72:743–58. doi: 10.1007/s00262-022-03305-2

147. Toker J, Iorgulescu JB, Ling AL, Villa GR, Gadet J, Parida L, et al. Clinical importance of the lncRNA NEAT1 in cancer patients treated with immune checkpoint inhibitors. *Clin Cancer Res*. (2023) 29:2226–38. doi: 10.1158/1078-0432.CCR-22-3714

148. Yang Q, Chen W, Xu Y, Lv X, Zhang M, Jiang H. Polyphyllin I modulates MALAT1/STAT3 signaling to induce apoptosis in gefitinib-resistant non-small cell lung cancer. *Toxicol Appl Pharmacol*. (2018) 356:1–7. doi: 10.1016/j.taap.2018.07.031

149. Jing Z, Liu Q, Xie W, Wei Y, Liu J, Zhang Y, et al. NCAPD3 promotes prostate cancer progression by up-regulating EZH2 and MALAT1 through STAT3 and E2F1. *Cell Signal*. (2022) 92:110265. doi: 10.1016/j.cellsig.2022.110265

150. Goyal B, Yadav SRM, Awasthee N, Gupta S, Kunnumakkara AB, Gupta SC. Diagnostic, prognostic, and therapeutic significance of long non-coding RNA MALAT1 in cancer. *Biochim Biophys Acta Rev Cancer*. (2021) 1875:188502. doi: 10.1016/j.bbcan.2021.188502

151. Barker SJ, Thayer MB, Kim C, Tatarakis D, Simon MJ, Dial R, et al. Targeting the transferrin receptor to transport antisense oligonucleotides across the mammalian blood-brain barrier. *Sci Transl Med*. (2024) 16:eadi2245. doi: 10.1126/scitranslmed.adi2245

152. Wang X, Zhang Y, Zheng J, Yao C, Lu X. LncRNA UCA1 attenuated the killing effect of cytotoxic CD8 + T cells on anaplastic thyroid carcinoma via miR-148a/PD-L1 pathway. *Cancer Immunol Immunother*. (2021) 70:2235–45. doi: 10.1007/s00262-020-02753-y

153. Yang LZ, Wang Y, Li SQ, Yao RW, Luan PF, Wu H, et al. Dynamic imaging of RNA in living cells by CRISPR-cas13 systems. *Mol Cell*. (2019) 76:981–997 e987. doi: 10.1016/j.molcel.2019.10.024

154. Chen Y, Li Z, Chen X, Zhang S. Long non-coding RNAs: From disease code to drug role. *Acta Pharm Sin B*. (2021) 11:340–54. doi: 10.1016/j.apsb.2020.10.001

155. Zhang L, Xu W, Gao X, Li W, Qi S, Guo D, et al. lncRNA sensing of a viral suppressor of RNAi activates non-canonical innate immune signaling in drosophila. *Cell Host Microbe*. (2020) 27:115–128 e118. doi: 10.1016/j.chom.2019.12.006

156. Han S, Chen X, Huang L. The tumor therapeutic potential of long non-coding RNA delivery and targeting. *Acta Pharm Sin B*. (2023) 13:1371–82. doi: 10.1016/j.apsb.2022.12.005

157. Niu X, Zhang J, Zhang J, Bai L, Hu S, Zhang Z, et al. Lipid nanoparticle-mediated oip5-as1 delivery preserves mitochondrial function in myocardial ischemia/reperfusion injury by inhibiting the p53 pathway. *ACS Appl Mater Interfaces*. (2024) 16:61565–82. doi: 10.1021/acsami.4c10032

158. Sarangi P, Senthilkumar MB, Amit S, Kumar N, Jayandharan GR. AAV mediated repression of Neat1 lncRNA combined with F8 gene augmentation mitigates pathological mediators of joint disease in haemophilia. *J Cell Mol Med*. (2024) 28:e18460. doi: 10.1111/jcmm.v28.11

159. Wu H, Qin W, Lu S, Wang X, Zhang J, Sun T, et al. Long noncoding RNA ZFAS1 promoting small nucleolar RNA-mediated 2'-O-methylation via NOP58 recruitment in colorectal cancer. *Mol Cancer*. (2020) 19:95. doi: 10.1186/s12943-020-01201-w

160. Amodio N, Stamato MA, Juli G, Morelli E, Fulciniti M, Manzoni M, et al. Drugging the lncRNA MALAT1 via LNA gapmeR ASO inhibits gene expression of proteasome subunits and triggers anti-multiple myeloma activity. *Leukemia*. (2018) 32:1948–57. doi: 10.1038/s41375-018-0067-3

161. Gao P, Lyu Q, Ghanam AR, Lazzarotto CR, Newby GA, Zhang W, et al. Prime editing in mice reveals the essentiality of a single base in driving tissue-specific gene expression. *Genome Biol*. (2021) 22:83. doi: 10.1186/s13059-021-02304-3

162. Sehgal A, Vaishnaw A, Fitzgerald K. Liver as a target for oligonucleotide therapeutics. *J Hepatol*. (2013) 59:1354–9. doi: 10.1016/j.jhep.2013.05.045

163. Li G, Zhu X, Wang Y, Ma H, Wang Y, Wu H, et al. Transcription-wide impact by RESCUE-induced off-target single-nucleotide variants in mammalian cells. *J Mol Cell Biol*. (2023) 15. doi: 10.1093/jmcb/mjad011

164. Zhang L, Liang D, Chen C, Wang Y, Amu G, Yang J, et al. Circular siRNAs for reducing off-target effects and enhancing long-term gene silencing in cells and mice. *Mol Ther Nucleic Acids*. (2018) 10:237–44. doi: 10.1016/j.omtn.2017.12.007

165. Mortberg MA, Gentile JE, Nadaf NM, Vanderburg C, Simmons S, Dubinsky D, et al. A single-cell map of antisense oligonucleotide activity in the brain. *Nucleic Acids Res*. (2023) 51:7109–24. doi: 10.1093/nar/gkad371

166. Mo H, Wang X, Ji G, Liang X, Yang Y, Sun W, et al. The effect of SNPs in lncRNA as ceRNA on the risk and prognosis of hepatocellular carcinoma. *BMC Genomics*. (2022) 23:769. doi: 10.1186/s12864-022-09010-9

frontiers | Frontiers in Pharmacology

TYPE Review
PUBLISHED 16 May 2025
DOI 10.3389/fphar.2025.1577496

Check for updates

OPEN ACCESS

EDITED BY
Chiara De Santi,
Royal College of Surgeons in Ireland, Ireland

REVIEWED BY
Antonio Leo,
University Magna Graecia of Catanzaro, Italy
Imran Shair Mohammad,
City of Hope National Medical Center, United States

*CORRESPONDENCE
Marta Biagioli,
marta.biagioli@unitn.it
Jasmin Morandell,
jasmin.morandell@unitn.it

RECEIVED 15 February 2025
ACCEPTED 02 May 2025
PUBLISHED 16 May 2025

CITATION
Galli V, Vinciguerra S, Biagioli M and Morandell J (2025) Circular RNAs as disease modifiers of complex neurologic disorders.
Front. Pharmacol. 16:1577496.
doi: 10.3389/fphar.2025.1577496

COPYRIGHT
© 2025 Galli, Vinciguerra, Biagioli and Morandell. This is an open-access article distributed under the terms of the Creative Commons Attribution License (CC BY). The use, distribution or reproduction in other forums is permitted, provided the original author(s) and the copyright owner(s) are credited and that the original publication in this journal is cited, in accordance with accepted academic practice. No use, distribution or reproduction is permitted which does not comply with these terms.

Circular RNAs as disease modifiers of complex neurologic disorders

Veronica Galli, Sara Vinciguerra, Marta Biagioli* and Jasmin Morandell*

NeuroEpigenetics Laboratory, Department of Cellular, Computational and Integrative Biology - CIBIO, University of Trento, Trento, Italy

Circular RNAs are a large class of non-coding RNA molecules, conserved across species and produced by back-splicing. While their molecular functions are still elusive, the ones primarily retained in the nucleus are usually associated to regulation of transcription and mRNA processing patterns. Instead, the majority, are transported to the cytoplasm where they elicit micro-RNA (miRNA) or RNA binding protein (RBP)-sponging functions, or could be translated. CircRNAs are abundantly expressed in brain tissue, where they do not only act as regulators of brain development and physiology, but can also contribute to complex neurological conditions. In fact, deregulated circRNA expression levels were described in neurodevelopmental and neurodegenerative disorders, like Alzheimer's disease, Parkinson's disease and Huntington's disease. Because of their described roles in pathology, these molecules may not only represent possible disease bio-markers, but they could even function as disease modifiers. As such, they could be targeted or protected in search of novel routes of therapeutic intervention. In this review, we highlight recent developments in the field, first discussing circRNAs involved in physiologic brain development and function, then reviewing studies that implicate circRNAs in neurodevelopmental and neurodegenerative disorders, with major attention to experimental studies exploring circRNA function and their role in neuropathologic processes. Such experimental strategies are mainly based on depletion or over-expression approaches and provide important insights into the modulatory potential of these molecules. They are relevant for clinical translation of basic research findings to drug development, possibly generating a positive impact for patients' quality of life.

KEYWORDS

circRNA, non-coding RNA, alternative splicing, neurodevelopment, neurodegeneration

Introduction

Circular RNAs are a recently re-discovered, evolutionary conserved, large class of RNA molecules (Wang et al., 2014). Eukaryotic circRNAs are produced by a process called back-splicing, leading to the formation of a covalent bond between a pre-mRNA 3′-splice donor (down-stream) and a 5′-splice acceptor (up-stream) site, resulting in the generation of a unique junction, the back-splice sequence (BSJ) (Jeck et al., 2013; Memczak et al., 2013) (Figure 1A). Still, it is the canonical splicing machinery that generates these continuous loops of RNA while processing exons, introns, or both exon-introns of, primarily, protein coding genes. The precise details of circRNA biogenesis are not yet fully elucidated, but

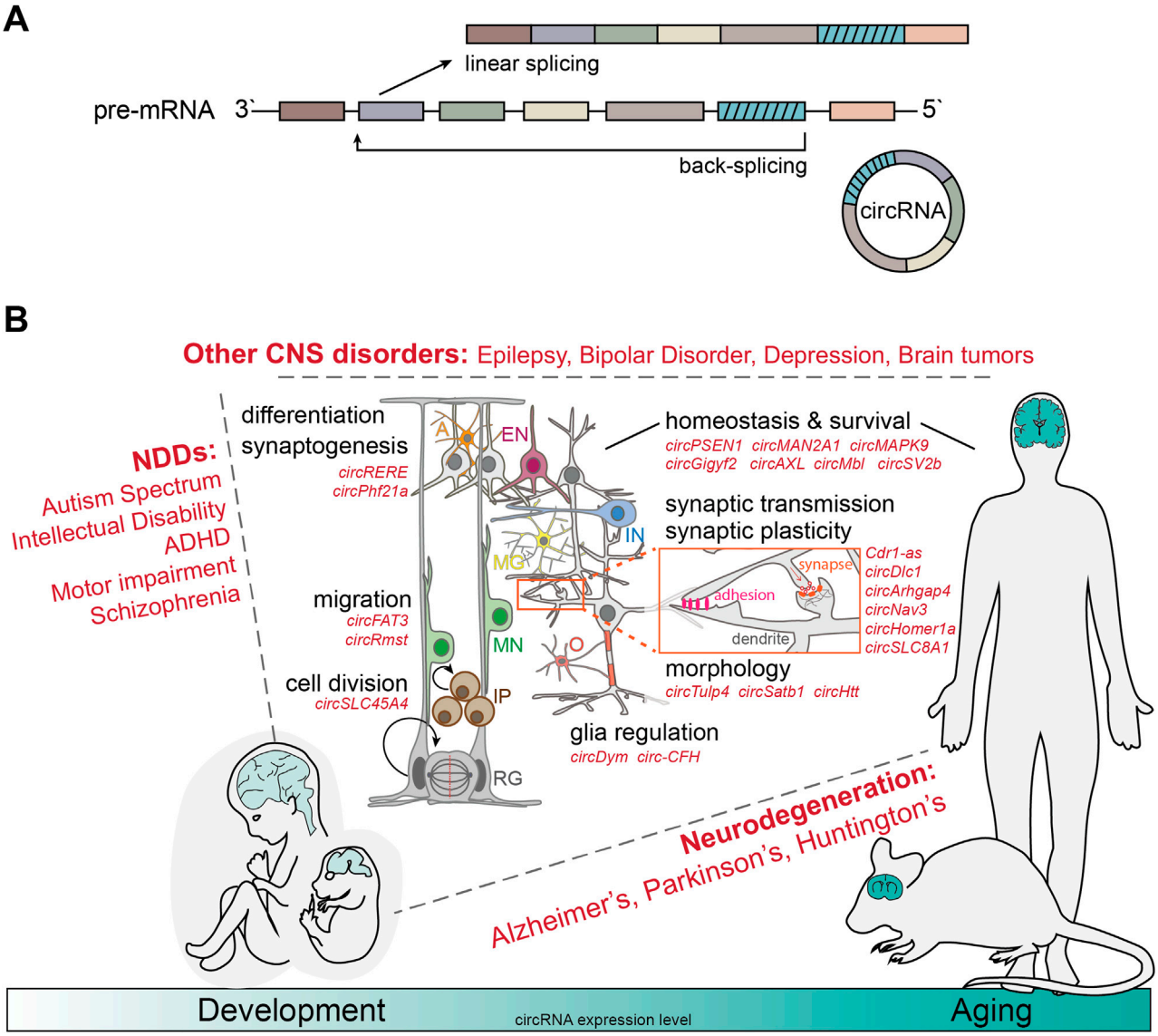


FIGURE 1
CircRNAs as modifiers of complex brain disorders. **(A)** Schematic of linear splicing (top) vs back-splicing (bottom). Back-splicing leads to the formation of a covalent bond between the 3′-splice donor and a 5′-splice acceptor site of unprocessed pre-mRNAs, generating the unique back-splicing sequence and rendering the resulting circRNAs extremely resistant against degradation through exoribonucleases. **(B)** CircRNAs are evolutionarily conserved and especially abundant in the nervous system of a large number of different species and especially mammals. Globally, circRNA expression increases during brain development, maturation and aging (bottom). In the last decade, numerous studies have linked deregulation of a variety of circRNAs with both, neurodevelopmental disorders (NDDs) such as Autism Spectrum Disorders and Schizophrenia (left); neurodegenerative (NDG) processes such as Alzheimer's, Parkinson's and Huntington's Disease, as well as Frontotemporal dementia and Amyotropic lateral sclerosis (right); and other complex brain disorders such as Epilepsy, Depression and brain tumor development (top). Relevant circRNAs (in red) have been shown to regulate the cell cycle of neural stem cells (radial glia -RG, intermediate progenitors–IP), the migration of newborn neurons (MN), the differentiation into inhibitory (IN) and excitatory (EN) post-mitotic neurons, astrocytes (A), microglia (MG), and oligodendrocytes (O), synaptogenesis, and mechanisms involved in mature brain function, homeostasis and survival- synaptic transmission and plasticity, neuronal and dendritic morphology, as well as brain immune activation.

evidence underscores the importance of base-pairing of the two introns adjacent to the circularizing exons, with typically long length (>10 kilobases), enriched in inverted ALU repeats (Jeck et al., 2013). In other cases, specific binding of RBPs (such as FUS and QKI) to the intronic sequences adjacent to circularizing exons drives circularization (Ashwal-Fluss et al., 2014; Starke et al., 2015).

The circular conformation of these RNA molecules confers a unique resistance against degradation, since 3′–5′ exonucleases preferentially digest linear RNAs while leaving most circRNAs intact (Suzuki et al., 2006). Thus, circRNAs are much more stable than linear RNA transcripts (Hwang and Kim, 2024), with a median half-life that is at least 2.5 times longer (Enuka et al., 2016; Jeck et al., 2013). Nonetheless, most circRNAs are expressed at low levels when compared to their cognate linear counterparts (Santer et al., 2019), but in a highly tissue-, cell type-, and time point-dependent context. To date, based on large scale, bulk RNA

sequencing (RNAseq) studies, multiple databases have been constructed to help annotate circRNA expression patterns of millions of circRNAs across different cell lines, tissues and organisms (Chen et al., 2016; Dong et al., 2018; Glažar et al., 2014; Meng et al., 2019; Wu et al., 2020). Furthermore, with the advent of single cell RNA sequencing, efforts have been made to resolve the complexity of circRNA expression landscapes also at the single cell level (Fan et al., 2015; W. Wu et al., 2022; Zhong et al., 2017).

While a molecular and functional characterization remains neglected for the majority of circRNAs, some circular RNA molecules that are primarily retained in the nucleus, have been described to act on the transcription and splicing regulation of their host and/or nearby located genes (Mai et al., 2022). Others are primarily exported into the cytoplasm, where they can act as miRNA "sponges" (Hansen et al., 2013; Peng et al., 2017), or interact with RBPs (Holdt et al., 2016; Ikeda et al., 2023), thus competing with linear mRNAs. Furthermore, some circRNAs appear to be translated in a cap-independent fashion, via internal ribosomal entry sites (IRES) (Chen et al., 2021), although the peptide coding potential of circRNAs, at endogenous levels and in physiological context, remains under discussion. CircRNAs expression is especially abundant in the brain and increases during aging, independently from the host gene mRNA expression (Hanan et al., 2017; Knupp and Miura, 2018; Rybak-Wolf et al., 2015). Over the last decade, abnormal levels of circRNAs have been associated with a large number of complex human neurologic disorders, ranging from ischemic stroke, over neurodevelopmental disorders (such as epilepsy, schizophrenia and autism spectrum disorders), Alzheimer's Disease and Parkinson's Disease, as well as Huntington's Disease (Mai et al., 2022; Morandell et al., 2024; Titze-de-Almeida & Titze-de-Almeida, 2023; Wang et al., 2023).

Recent work has further identified the dedicated mechanism by which circRNAs are exported to the cytoplasm, dependent upon Ran-GTP/Exportin-2, underscoring the potential relevance of circRNA localization for cell function (Ngo et al., 2024).

While for a vast majority of the identified deregulated circRNAs associated with human neurologic disorders their biologic function and relevance for the disease pathogenesis/progression remains elusive, in the past decade a number of studies have discovered important regulatory roles for some circRNAs in neuronal development, function and homeostasis with the detailed analysis of their molecular mechanisms of action. This review will put these most recent functional studies into the spotlight and consequently discuss how deregulation of circRNAs can modify complex neurologic disorders, from neurodevelopment to neurodegeneration.

CircRNAs in physiologic brain development and function

CircRNAs are most abundantly expressed in brain tissues (Hanan et al., 2017). The majority of neuronal circRNAs were shown to be localized both at the cell body and dendrites of neurons. Additionally, their expression pattern changes according to the developmental stage of the cell, suggesting a functional role of circRNAs during development and the mature brain (Hollensen et al., 2020; Venø et al., 2015). In line with these observations, circRNAs found in dopaminergic and pyramidal neurons are predominantly expressed from gene loci relevant for synaptic activity, underscoring their potential functional role in determining activity of these neuronal subtypes, but also the whole neuronal network (Dong et al., 2023; You et al., 2015). Single cell RNAseq efforts have furthermore shown that circRNAs display specific expression patterns in different neuronal cell types, presumably contributing to cell diversity and identity (Dong et al., 2023).

Arguably the most thoroughly studied neuronal circRNA is complementary determining region 1 antisense (*Cdr1-as*). *Cdr1-as* contains >70 binding sites for the neuronal microRNA (miRNA) *miR-7* and acts as *miR-7* sponge (Hansen et al., 2013), as part of a complex non-coding regulatory network (Kleaveland et al., 2018; Piwecka et al., 2017). Interestingly, binding of *miR-7* seems to actively mediate the circularization of *Cdr1-as* (Belter et al., 2022), while loss of *Cdr1-as* leads to miR-7 destabilization and alters excitatory synaptic transmission, driving schizophrenia-associated behaviours (Piwecka et al., 2017). Moreover, synaptic localization of *Cdr1-as* is required for fear-memory extinction (Zajaczkowski et al., 2023), while, in cortical neurons, *Cdr1-as* buffers *miR-7* activity to control glutamatergic excitatory transmission and neuronal connectivity. As such, these observations highlight the possible relevance of circRNAs for memory formation and long-lasting synaptic adaptations (Cerda-Jara et al., 2024).

Human *circSLC45A4*, one of the highest expressed circRNAs in the developing human frontal cortex, was reported to be necessary in maintaining the pool of neural progenitors *in vivo*, and its knock-down promoted Cajal-Retius cell differentiation in the cortical plate during early embryonic development (Suenkel et al., 2020). Similarly important for neural progenitor differentiation and cell positioning in the developing cortex is *circFAT3*. As shown by Seeler et al., it is especially relevant for differentiation of human embryonic stem cells into rostral and caudal neural progenitors. While *circFAT3* knock-down caused minimal changes in bulk RNA expression, it had significant effects at the single-cell level in human cerebral organoids, disrupting expression patterns linked to neural differentiation and migration of telencephalic radial glial cells and mature cortical neurons (Seeler et al., 2023).

Morphology and migration of midbrain dopamine neurons (mDA), crucial for motor and cognitive behaviours and linked to various brain disorders, are critically regulated by *circRmst* (Rybiczka-Tešulov et al., 2024). While single-molecule fluorescence *in situ* hybridization (smFISH) did not reveal any specific compartmentalization of highly expressed circRNAs in the cell, *in vitro* knock-down of the candidate *circRmst* had wide-spread effects in *in vitro* primary cultures, such as increased soma size, soma-to-nucleus ratio, reduced numbers of tyrosine hydroxylase positive neurons and, *in vivo*, accelerated neuronal migration and lateral mislocalization of the mDA neuron pool (Rybiczka-Tešulov et al., 2024). On the other hand, *circTulp4* depletion, also highly expressed in developing mDA neurons, only led to milder effects, causing a small decrease in neurite length and increase in secondary branch formation (Rybiczka-Tešulov et al., 2024). Its primary function, in fact, is thought to lie in the regulation of general brain physiology and synaptic activity,

due to its compartmentalized enrichment at the synapse. Concordantly, depletion of *circTulp4* - by the alteration of the splice acceptor site responsible for its biogenesis - modulated the strength of excitatory neurotransmission in primary cultures and sensitivity to aversive stimuli in behavioral assays (Giusti et al., 2024). While *circTulp4* molecular mechanism is unlikely to be driven by miRNA-sponging or translation from the circular molecule, its mode of action remains to be identified (Giusti et al., 2024).

Synaptogenesis and dendritic spine formation was further shown to be strictly regulated by *circRERE and circPhf21a* expression in rat hippocampal neurons. *CircRERE* depletion led to the formation of electrophysiologically silent synapses, and Kelly et al. could demonstrate *circRERE*-mediated stabilization of *miR-128-3p* as a novel molecular mechanism to modulate the formation of silent excitatory synaptic co-clusters (Kelly et al., 2024, 2025).

The miRNA-sponging ability of circRNAs, implies also the capability of these molecules to regulate gene expression through circRNA/miRNA/mRNA interaction networks. In line with this molecular mechanism, *circDlc1* was shown to bind to *miR-130b-5p*, controlling its synaptic localization and regulating the expression of different mRNAs in the glutamatergic circuit. Thereby it plays an important role in synaptic transmission, regulating glutamatergic signaling and plasticity in cortico-striatal pathways. In line with these findings, loss of *circDlc1* lead to hyperactivity behaviour in a knock-out mouse model (Silenzi et al., 2024).

Taken together, these studies highlight important regulatory functions of circRNAs for physiologic brain development, modulating all steps of the process, from neural progenitor positioning and neurogenesis, over migration and differentiation of newborn neurons, to dendritic spine formation, synaptogenesis, synaptic function and plasticity (Figure 1B).

CircRNAs in neurodevelopmental disorders

Because of their enrichment in the central nervous system (CNS) and their crucial roles in neurogenesis, synaptic plasticity and neuronal identity not surprisingly, circRNAs have been associated with neurodevelopmental (NDDs) and neuropsychiatric disorders, were they are increasingly recognized as key regulators of pathological processes (Nemeth et al., 2024). According to the DSM-5, NDDs include autism spectrum disorders (ASD), intellectual disability (ID), attention deficit hyperactivity disorder (ADHD), communication and motor disorders. These diagnostic categories, defined by specific sets of symptoms, show considerable comorbidity and phenotypic overlap, complicating diagnosis and management of the disorders. In fact, genetic research supports the hypothesis that ID, ASD, ADHD and schizophrenia lie on a neurodevelopmental continuum, rather than representing independent conditions (Morris-Rosendahl and Crocq, 2020).

The phenotypic heterogeneity of ASD and the co-morbid other neurodevelopmental syndromes is mirrored by the large complexity in underlying genetic architecture and altered biologic pathways, which have been studied in detail over the last 4 decades (reviewed here (Choi and An, 2021) and here (Parenti et al., 2020)). Instead, the exploration of long non-coding (lnc) RNAs, of which circRNAs are an important subgroup, and their contribution to the etiology of NDDs is yet in its infancy, and has been, so far, primarily focused on ASD and schizophrenia, but can possibly be extrapolated to other NDDs (Ghafouri-Fard et al., 2022; Jiang et al., 2023; Stott et al., 2023). A comprehensive study utilizing previously published RNAseq data sets from total RNA (ribosomal RNA-depleted RNAs without poly(A)-selection) derived from a large collection of *post mortem* brain tissue of control and ASD cases (Parikshak et al., 2016; Wu et al., 2016), represents the first systematic investigation of circRNA dysregulation in ASD. In the study, the authors identified 60 circRNAs and three co-regulated modules that were perturbed in ASD. By integrating circRNA, microRNA, and mRNA dysregulation data derived from the same cortical samples, 8170 ASD-associated circRNA/miRNA/mRNA networks were identified. The 2302 putative target genes of these axes were enriched for ASD risk genes and genes encoding inhibitory postsynaptic density (PSD) proteins, but not for genes implicated in monogenic forms of other brain disorders or genes encoding excitatory PSD proteins. Functionally, only *circARID1A* was tested: upregulated in ASD brain samples and working as *miR-204-3p* sponge, the corresponding circRNA/miRNA/mRNA regulatory network was further characterized *in vitro* employing knock-down and over-expression experiments, supporting the notion that circRNAs may serve as efficient miRNA sponges, influencing the expression dynamics of ASD-associated risk genes and leading to synaptic dysfunction and abnormal neural development (Huang et al., 2023). Furthermore, the genomic study by Te-Lun Mai et al. focused on quantitative trait loci (QTL) associated with the expression of nearby circRNAs (circQTL). They integrated RNAseq and genotyping data from *post mortem* brain tissues of individuals with ASD, to identify circQTLs that *cis*-regulate nearby circRNAs expression and, in turn, *trans*-regulate distant gene expression (*trans*-eGenes). The researchers identified 3,619 circQTLs, constructing 19,804 circQTL-circRNA-trans-eGene regulatory axes. 291 of these circQTLs overlapped with ASD-related genetic variants identified in genome-wide association studies (GWAS), suggesting a potential link between these circQTLs, SFARI risk factor genes, and ASD pathogenesis (Mai et al., 2022). Such findings highlight the complexity of gene regulation in ASD and suggest that circRNAs may serve as key intermediaries in the genetic architecture of the disorder.

On the other hand, additional insights on the importance of circRNAs in NDDs can be derived from studies using animal models. Wang et al. identified a vast array of differentially expressed circRNAs following valproate treatment in the mouse brain. By exploring a circRNA-based competing endogenous RNA (ceRNA) network, the study revealed possible interactions between circRNAs, miRNAs, and mRNAs, highlighting the complex regulatory networks that might potentially contribute to neurodevelopmental pathology (Wang et al., 2021). Similarly, Gasparini et al. explored the differential expression of hippocampal circRNAs, such as *circCdh9*, in the BTBR mouse model of ASD (Meyza and Blanchard, 2017). Their findings suggest that these circRNAs may contribute to synaptic dysfunctions observed in ASD (Gasparini et al., 2020).

In the context of SCZ, *circHOMER1* expression levels were significantly reduced in *post mortem* orbitofrontal cortex samples of patients, and *circHOMER1* levels positively correlated with the

age of SCZ onset. *CircHomer1a* regulated the expression of specific isoforms of synaptic plasticity-related genes with relevance for psychiatric disorders. Knock-down of *circHomer1a* in the orbitofrontal cortex was sufficient to disrupt cognitive flexibility *in vivo* (Zimmerman et al., 2020). In SCZ, circRNAs have also been intensely studied as potential class of novel diagnostic and therapeutic biomarkers (Huang et al., 2023; Tan et al., 2021; Yao et al., 2019). For instance, circRNA expression was profiled in plasma samples of very early-onset schizophrenia (VEOS) patients and 235 circRNAs (1 upregulated, 234 downregulated) were shown to be differentially expressed. A circRNA/miRNA/mRNA network was then constructed and identified target genes that were involved in signal transduction, the cytoskeleton and transport pathways. Thus, plasma circRNAs in this network may be potential diagnostic biomarkers for VEOS and could play an important role in the onset and development of VEOS symptoms (Huang et al., 2023).

Taken together, although with much room for further exploration, circRNA dysregulation might lead to aberrant gene expression, contributing to the development and progression of neurodevelopmental and neuropsychiatric disorders. As modulators of altered neurodevelopment, they may also represent promising therapeutic targets, offering new avenues for treating neuropsychiatric conditions or be used as diagnostic or therapeutic biomarkers in easily accessible biofluids.

CircRNAs in the aging brain and neurodegenerative diseases

Neurodegenerative disorders, including Alzheimer's disease (AD), Parkinson's disease (PD), amyotrophic lateral sclerosis (ALS), and Huntington's disease (HD), are marked by the progressive degeneration and loss of neurons in distinct regions of the brain and spinal cord. These conditions are currently irreversible, with no effective treatments available, eventually leading to decline and death of the affected patient. Although, in certain cases, clear genetic causes can be identified, aging still represents an important risk factor for most neurodegenerative diseases (Hou et al., 2019). Thus, in line with the ever increasing life expectancy and increasing numbers of individuals with advanced age, especially in industrialized countries, neurodegenerative disorders are considered a leading cause of death by the World Health Organization (WHO).

Alzheimer's disease

Global changes in circRNA expression levels in AD have first been explored in detail by Dube et al., demonstrating that collectively, the expression changes of ten circRNAs, in the human *post mortem* parietal cortex, had a higher predictive value for cognitive impairment and dementia, than, e.g., the number of *APOE4* alleles (Dube et al., 2019). Additionally, an association of circRNA expression levels with AD has also been found in other brain regions (Cochran et al., 2021; Lo et al., 2020), such as the frontal lobe, temporal cortex and hippocampus. Importantly, circRNAs from two AD-associated genes, *presenilin 1* (*PSEN1*) and *tau* have further been studied more in detail. *CircPSEN1* levels increase during autosomal-dominant Alzheimer's disease progression which may be related to neuro-inflammatory events and amyloid beta accumulation (Chen et al., 2022). Instead, after undergoing RNA editing, circular RNAs from the *tau* pre-mRNA encompassing the microtubule binding sites were shown to be translated into proteins that promote tau aggregation *in vitro,* and are therefore hypothesized to contribute to tauopathies more in general (Welden et al., 2022).

Maquera et al. provided initial evidence for a role of translated circRNAs in the development of AD. Through RNAseq based analysis of the mRNA and circRNA composition in *post mortem* human cortical tissues during AD progression, as characterized by the spread of neurofibrillary tangles from the entorhinal cortex (early stages) to the whole brain, they identified *circMAN2A1* expression to be correlated with AD progression. Transfection experiments indicated that RNA editing promoted its translation using start codons out of frame with linear mRNAs, which generates novel proteins (Arizaca Maquera et al., 2023).

In a study by Puri et al., RNAseq analysis of neuropathologically confirmed AD brains and controls (n = 2027) identified 4,092 deregulated circRNAs in the hippocampus and 4,912 in the cortex. The study aimed to assess the relationship between circRNA expression patterns and AD clinical and pathological outcomes (Puri et al., 2023). CircRNA expression was correlated with the Clinical Dementia Rating (CDR) and AD-related neuropathological traits, including CERAD neuritic plaque score and Braak stage. Among 48 differentially expressed circRNAs, 69% were significantly associated with all three parameters. Key circRNAs such as *circSLC8A1* (linked also with Parkinson's disease) and *circHOMER1*, associated with synaptic function and calcium signaling, were significantly downregulated in AD patients, correlating with synaptic loss and cognitive decline. The downregulation of the validated circRNAs following treatment with oligomeric Tau (oTau) highlighted the responsiveness of AD-associated circRNAs in neuro progenitor cells (NPC). *CircMAPK9* exhibited downregulation by oTau exposure, independent of its linear transcript counterpart. These observations raised the possibility that some of the changes in circRNA expression in the AD brain might reflect the response to oTau toxicity, consistent with Cervera-Carles et al., who noted similar responses of circRNAs between FTD-tau (but not FTD-TDP-43) and AD (Cervera-Carles et al., 2020).

Using the 5xFAD genetic mouse model, which exhibits early Aβ plaque deposition and progressive cognitive decline (Forner et al., 2021), Wang et al., investigated circRNA alterations at critical disease stages (5 and 7 months). A-tailing RNAseq combined with the CARP algorithm revealed 342 and 467 differentially expressed (DE) circRNAs in the cortex at these time points, with additional 264 DE circRNAs in the hippocampus (Wang et al., 2024). To determine human relevance, they compared these findings with RNAseq data from the Mount Sinai Brain Bank (MSBB), confirming that many DE circRNAs were also dysregulated in AD patient brains. One of the most significantly altered circRNAs, *circGigyf2*, was highly expressed in healthy brains but showed marked downregulation at 7 months in 5xFAD mice and in human AD cortical regions. Notably, *circGigyf2* interacts with CPSF6, a critical RNA-processing factor involved in 3′-end

cleavage and polyadenylation. Its loss correlated with increased CPSF6 availability, leading to altered poly-(A)-site (PAS) selection and disrupted gene expression in thousands of transcripts, suggesting a role in AD pathogenesis. They also observed alternative splicing events within circRNAs, affecting their interactions with miRNAs and RBPs. For example, *circCcdc50* exhibited exon 4 skipping in the 7-month 5xFAD cortex, impacting *miR-335-5p*, a miRNA linked to AD-related gene expression changes. More broadly, miRNA sequestration appeared to be dynamically regulated by circRNA clusters, where multiple low-abundance circRNAs collectively influenced miRNA activity. Although individual circRNAs within a cluster may not achieve statistical significance in DE analysis, they can collectively function as a regulatory unit.

Additionally, Li et al. found that *circAXL* plays a key role in regulating BACE1, a protein associated with amyloid-beta production (Li et al., 2022). Over-expression of *circAXL*, which, in turn, negatively regulated *miR-328*, led to increased neuronal apoptosis, reduced neurite outgrowth, and heightened inflammation in AD models. In contrast, *miR-328* over-expression had protective effects, suggesting that *circAXL* and its modulation of BACE1 through *miR-328* may serve as potential therapeutic targets for AD.

These findings demonstrate that circRNAs are not passive byproducts of splicing but active regulators of gene expression in AD, as they affect both miRNA function and RNA-processing pathways. Their brain region-specific disruptions observed in both mice and AD patients highlight their potential as biomarkers and therapeutic targets in neurodegeneration.

Parkinson's disease

Secondly to AD, PD is one of the most common neurodegenerative disorders with loss of dopamine production from substantia nigra dopaminergic neurons, leading to overt motor impairment and psychological decline. RNAseq studies on PD mouse models highlighted several dysregulated circRNAs, among which *circSV2b* which was further studied. Evidence shows that its over-expression, in PD induced mice, results in the restoration of dopamine synthesis and a normal nigro-striatal function. *CircSV2b* regulates the activity of *mirR-5107-5p* which modulates the transcription of *Foxk1* mRNA and acts on the *Akt1* signaling pathway, participating in PD–related oxidation. These data suggest that *circSV2b* may not only be investigated to understand the pathogenesis of PD, but could also be a promising candidate for PD treatment or even exploited as a molecular biomarker (Cheng et al., 2022). Furthermore, studies on PD patients revealed an over-expression of *circSLC8A1,* predicted to bind *mir-128,* in patients. Over-expression of this circRNA is strongly linked to the oxidative stress, a crucial characteristic of PD and most neurodegenerative disorders (Hanan et al., 2020).

Frontotemporal dementia

The human microtubule-associated protein tau (MAPT) stabilizes microtubules in neurons through up to four microtubule binding repeats, mainly formed by exons 7–12. Exon 10 - encoding the second microtubule-binding repeat - is alternatively spliced in the adult human brain leading to a mixture of tau proteins with 3 or 4 microtubule binding repeats. This ratio can be altered in disease, especially in several forms of frontotemporal dementia with parkinsonism linked to chromosome 17 (*FTDP-17*) (Corsi et al., 2022). Margvelani et al. investigated the impact of *FTDP-17* mutations on the formation and translation of circular RNAs derived from the *MAPT* gene (Margvelani et al., 2023). Interestingly, five *FTDP-17* mutations increased the formation of circRNA involving back-splicing from exon 12 to exon 7 (*circTau (7,8,9,10,11,12)*), while 3 other different mutations elevated the levels of circRNA from exon 12 to exon 10 (*circTau(10,11,12)*). These circRNAs undergo RNA editing through the interferon-induced ADAR1-p150 isoform which promotes the translation of *circTau* RNAs.

Atrian et al. further support the role of circRNAs and N6-methyladenosine (m6A) modification, a key epitranscriptome mark affecting RNA stability and processing, in tau-induced neurotoxicity, by using both *Drosophila* models and human induced pluripotent stem cell (iPSC)-derived neurons. RNAseq analysis found, among others, *circMbl* to be significantly upregulated in tauopathy models. Depletion of *circMbl* reduced tau-induced cell death in *Drosophila* neurons, suggesting that increased *circMbl* contributes to neurotoxicity. Further experiments revealed an overall increase in m6A levels, which led to enhanced back-splicing and circRNA biogenesis in *tau* transgenic *Drosophila*. By m6A-RIP sequencing, tau-induced *circMbl* upregulation was confirmed to be m6A-dependent with suppression of RNA methylation factors mitigating tau-induced neurotoxicity. Taken together, these findings underscore a complex interplay between RNA editing and *FTDP-17* mutations in regulating circRNA dynamics and their potential contribution to disease pathology. On the other hand, they also highlight a novel molecular mechanism where tau-driven m6A modifications might promote circRNA formation and contribute to neurotoxicity, thus opening a possible therapeutic strategy for tauopathies (Atrian et al., 2024).

Amyotrophic lateral sclerosis

Amyotrophic lateral sclerosis (ALS) is a progressive neurodegenerative disease affecting both upper and lower motor neurons, leading to muscle atrophy, speech difficulties, and respiratory failure (Brown and Al-Chalabi, 2017). With an average life expectancy of just 30 months from symptom onset, early and accurate diagnosis is critical (Hardiman et al., 2017). Given the variability in clinical presentation, especially in patients without genetic mutations or familial history, reliable biomarkers are essential for timely detection and intervention. There are very few studies available exploring the role of circRNAs in ALS, with most focusing on their dysregulation rather than their functional significance. For instance, Dolinar et al. identified 274 upregulated and 151 downregulated circRNAs in ALS patients compared to healthy controls using microarray assays. Based on these findings and the functional relevance of their host genes in ALS, 10 circRNAs were selected for further PCR validation in a larger sample set. Of the

ones experimentally validated, two are of particular interest based on their host gene identity, namely *hsa_circ_0000567*, which is derived from *SETD3*, linked to muscle differentiation, and *hsa_circ_0023919*, derived from *PICALM*, which plays a role in clathrin-mediated endocytosis at neuromuscular junctions and has been associated with AD. Notably, all selected circRNAs contain predicted binding sites for one or more RBPs. Further analysis revealed that *hsa_circ_0000567*, *hsa_circ_0023919*, and *hsa_circ_0088036* were negatively correlated with patient age at blood collection, while *hsa_circ_0000567* and *hsa_circ_0088036* were also negatively associated with the age of disease onset (Dolinar et al., 2019).

Aquilina-Reid et al. assessed circRNA expression levels in spinal cord tissues and explored the functional interactions between circRNAs, miRNAs and mRNAs in ALS, identifying 92 differentially expressed circRNAs (Aquilina-Reid et al., 2022). TargetScanHuman database based prediction of targeted mRNAs by selected miRNAs, then, revealed 55 genes whose targets were both significantly upregulated and differentially expressed in ALS (Friedman et al., 2009; Garcia et al., 2011; Grimson et al., 2007; Lewis et al., 2005). These genes were enriched for Gene Ontology terms such as "cell-cell signaling by Wnt" and "positive regulation of proteasomal ubiquitin-dependent protein catabolic process," both linked to ALS pathology (Chen et al., 2012).

Taken together these findings first demonstrate the potential significance of circRNA in ALS progression and for biomarker development, although follow up experiments are needed to validate these initial observations.

Huntington's disease

Huntington's disease (HD) is a hereditary, fatal neurodegenerative disorder caused by a CAG trinucleotide expansion within exon 1 of the *HTT* gene. A polymorphic CAG tract up to 35 repeats is found in unaffected individuals, whereas alleles bearing 39 or more repeats lead to HD symptoms. Among the various dysfunctional mechanisms linked to the disease, RNA processing and alternative splicing (AS) alterations are emerging as crucial regulators of HD (Nguyen et al., 2025). Coherently, as the splicing machinery is also instrumental to circRNA biogenesis, different evidence is suggesting a functional role of circRNAs in HD. An initial study, using a circRNA microarray, compared expression patterns of rat cell lines expressing mutant or wild-type huntingtin (Marfil-Marin et al., 2021). A total of 23 circRNAs were differentially expressed, most of which downregulated. CircRNA/miRNA/mRNAs interactions were predicted, suggesting that changes in these regulatory networks might impact neuronal function and survival in HD. Capitalizing on accurate genetic mouse models of the disease, Ayyildiz et al. examined AS and circRNA biogenesis in HD by RNAseq approach (Ayyildiz et al., 2023). While circRNA expression was generally higher in NPCs compared to embryonic stem cells (ESC), cells expressing mutant huntingtin exhibit a mis-shaped repertoire of linear and back-spliced circular RNA isoforms. A negative correlation between CAG length and circRNA expression was noted in NPCs, suggesting a mutation-dependent disruption of circularization. A significant proportion (32.7%) of differentially expressed circRNAs were found to be modified by m6A. This indicates that mutant huntingtin may impact circRNA biogenesis through m6A-mediated regulation. Interestingly, these splicing defects were most prominent in neural progenitors, with minimal changes observed in ESCs, highlighting the early vulnerability of neural cells to RNA dysregulation in HD. Interestingly, a highly conserved circRNA is also stemming from the HD gene locus itself, *circHTT(2,3,4,5,6)*. *CircHTT(2,3,4,5,6)* expression significantly correlates with the length of the CAG-repeat tract in exon-1 of *HTT* in human and mouse HD model systems. Mouse *circHtt(2,3,4,5,6)*, is expressed during embryogenesis and increases during nervous system development. *CircHtt(2,3,4,5,6)* over-expression experiments in the HD-relevant ST*Hdh* striatal cells further revealed its ability to modulate CAG expansion-driven cellular defects in cell-to-substrate adhesion, acting as novel modifier of HD pathology and potential drug target (Morandell et al., 2024). These three studies underscore the potential for targeting splicing, back-splicing and RNA modifications as therapeutic strategies in HD.

CircRNAs in other disorders of the CNS

Deregulation of circRNAs has also been described in the context of other disorders of the central nervous system, that are not strictly of neurodevelopmental or neurodegenerative nature. These disorders range from epilepsy, depression and bipolar disorder, the inflammatory disease multiple sclerosis, to brain tumors. All these conditions are similarly complex and heterogeneous in their etiology, phenotypic composition and therapeutic management, as the typical neurodevelopmental and neurodegenerative disorders.

Temporal lobe epilepsy

CircRNAs can regulate synaptogenesis and synaptic transmission, thus they are directly linked with neural network activity and the excitation-inhibition interplay in the brain. In line with this notion, numerous circRNAs have been investigated to provide a better understanding of the pathogenesis of mesial temporal lobe epilepsy (mTLE), the most common form of refractory focal epilepsy. Through high-throughput sequencing of mTLE patients-derived samples, thousands of circRNAs were identified; *circSATB1*, *circSATB2* and *cirLRP6* showed an interesting downregulation in the hippocampus of patients when compared to controls. Functionally, *circSatb1* regulates dendritic spine morphology and function (Venø et al., 2015). The deregulated expression of circRNAs in mTLE was also confirmed by Gomes-Duarte et al., highlighting aberrant increase in *circArhgap4* and *circNav3* expression from early to late stage of experimental epilepsy, likely as consequence of recurrent spontaneous seizures. Abnormal electrical brain activity, in turn, could be potentially correlated to the bioavailability of miRNA pathophysiologic drivers, binding targets of the dysregulated circRNAs with predicted miRNA-sponging activity (Gomes-Duarte et al., 2021). The hypothesis that circRNAs may interfere with the abundance and availability of miRNAs in the context of TLE is particularly relevant since different studies previously reported dysregulated miRNA levels in TLE patients' circulation, miRNAs as disease modifiers as well as

their importance for drug resistance in TLE [reviewed here (Guarnieri et al., 2024)].

Depression

Major depressive disorder (MDD) is a very common disorder, severely limiting psychosocial functioning and diminishing quality of life of affected individuals. The WHO ranked MDD as the third cause of burden of disease worldwide and projected that it will rank first by 2030 (Malhi and Mann, 2018). The etiology of MDD is believed to be multifactorial, with biological, genetic, environmental, and psychosocial contributing factors (Cui et al., 2024). Pathophysiologic mechanisms include neuroinflammation and alterations in neuroplasticity and epigenetics. Several long noncoding RNAs, including miRNAs and circRNAs, have been found to be deregulated in MDD, and could represent potential biomarkers for clinical diagnosis and monitoring of the therapeutic outcomes (Shi et al., 2021b). A small pilot study on 129 participants showed that individuals affected by MDD have increased plasma levels of *circHIPK2* (Yu et al., 2024), which is consistent with previous findings in a mouse model system of depression (Zhang et al., 2019). In this study, the authors also speculated about a possible involvement of *circHIPK2* in the gut-brain axis: Previously implicated in astrocyte activation in brain physiology (Huang et al., 2017), alterations of *circHIPK2*-regulated astrocyte activity in response to changes in the microbiome could modify the MDD behavioral characteristics (Hao et al., 2022; Zhang et al., 2019).

Furthermore, data from samples of MDD patients and two mouse models of depression (chronic unpredictable stress (CUS) and lipopolysaccharide (LPS) models), revealed increased *circMBML1* levels and reduced expression of *circFKBP8* (Shi et al., 2021a), *hsa_circRNA_103636* (Cui et al., 2016) and *circDYM(4,5,6)* (Zhang et al., 2020) in peripheral blood samples. Interestingly, overexpression of *circDym(4,5,6)* in the mouse hippocampus, regulated immune activation by sponging miR-9, which, in turn, led to a consequent decrease of microglial activation upon CUS and LPS treatment, a hallmark of MDD, with depression-like behaviors ameliorated in these mice (Zhang et al., 2020). These findings suggest that, i) peripheral blood *circDYM(4,5,6)* levels may represent a promising biomarker, and ii) *circDYM(4,5,6)* over-expression may represent a novel treatment strategy for MDD. While these represent exciting initial observations, follow up studies in independent patient cohorts, alternative mouse models of depression and human *in vitro* model systems are imperative to assess the true value of these findings for clinical translation.

Bipolar disorder

Bipolar disorder (BD) is a psychiatric disorder characterized by the alternation of depressive and maniacal phases during the lifetime of the affected individuals (Tondo et al., 2017). In recent years, studies explored the role of gene regulation and non-coding RNAs in the pathophysiology of BD. Analyzing the expression of circRNAs in peripheral blood mononuclear cells (PBMCs) from patients with BD, in comparison to samples from a non-psychiatric group, found around 33 circRNAs to be significantly dysregulated (Mahmoudi et al., 2021). Additionally, RNAseq analysis on samples from anterior cingulate cortex of individuals with BD compared to neurotypical controls, identified several dysregulated circRNAs among which, *circCCNT2* showed a significant upregulation in the BD cohort (Lin et al., 2021). Many studies focused on the function of *circHomer1* as a psychiatric disease-related circular RNA: its expression is reduced in BD as well as other diseases such as SCZ. Using knock-down mouse models, low levels of *circHomer1* were shown to be associated with changes in animal cognitive ability and behaviour, possibly explained by *circHomer1* ability to modulate the expression of genes involved in synaptic plasticity, thus affecting neuronal function (Zimmerman et al., 2020, 2024).

The differential expression of *circNEBL* and *circEPHA3* - altered in RNAseq data from *post-mortem* brains of BD patients versus healthy controls - could further provide new insights into the role of circRNAs in BD (Luykx et al., 2019). Specifically, the upregulation of *circEPHA3* may be of particular relevance since EPHA3's role in mediating axon growth (Javier-Torrent et al., 2019) could be linked to the neurodevelopmental aspects of BD.

Multiple sclerosis

Multiple sclerosis (MS) is a complex autoimmune disease of the CNS characterized by demyelination, chronic inflammation, neuronal loss, and axonal damage (Thompson et al., 2018). The most common form, affecting 80% of patients, is relapsing-remitting MS, characterized by attacks followed by complete or partial remissions (Lublin et al., 2014). Although the pathogenic factors underlying MS remain largely unknown, several recent studies pointed to alterations in AS and RNA processing as new molecular mechanisms potentially involved in the pathogenesis. Coherently, some AS events as well as ncRNAs have been proposed as novel biomarkers for MS (D'Ambrosio et al., 2015; Hecker et al., 2019; Paraboschi et al., 2015; Spurlock et al., 2015). While functional investigation of circRNAs has been largely neglected, circRNAs were first implicated in MS by Cardamone et al., identifying the *GSMDB* derived *hsa_circ_0106803* circRNA as upregulated in PBMCs of 30 RR-MS patients compared to 30 healthy controls (Cardamone et al., 2017). Subsequently, Iparraguirre and colleagues detected 406 differentially expressed circRNAs through a microarray analysis on peripheral blood leucocytes of four RR-MS patients and four healthy controls; two downregulated circRNAs, both deriving from the *ANXA2* host gene, were validated in an independent cohort of 20 RR-MS patients and 18 healthy controls (Iparraguirre et al., 2017). In addition, through an RNAseq based analysis of blood samples, a global, specific and sex-dependent deregulation of circRNA expression in MS was observed in a cohort of 30 patients and 20 controls, with candidate circRNAs further examined in a second, independent cohort of 70 M cases, revealing 6 upregulated circRNAs (e.g., *circPADI4*) as potential biomarkers (Iparraguirre et al., 2020). CircRNAs were furthermore shown to be enriched at MS *loci*, emerging from genome wide studies, with further characterization of *hsa_circ_0043813* derived from the MS-associated *STAT3* gene (Paraboschi et al., 2018). Similarly, expression analysis in another patient cohort, revealed

166 differentially expressed circRNAs in MS patients, 125 of which were downregulated. One of the top dysregulated circRNAs, *hsa_circ_0007990*, derives from the *PGAP3* gene, relevant for the control of autoimmune responses. Later analysis of two independent replication cohorts confirmed the downregulation of *circPGAP3* suggesting its implementation as a possible RNA-based biomarker (Cardamone et al., 2023).

Brain tumor development

CircRNAs play a complex role in cancer development, influencing tumor progression through exosomal transfer and facilitating communication between cancer cells and the surrounding microenvironment. Certain circRNAs can contribute to metastasis by promoting pre-metastatic niches (Dai et al., 2018; Wang et al., 2019). Additionally, the failure of transcription termination and uncontrolled gene transcription into the downstream gene followed by back-splicing can give rise to read-through circRNAs, which incorporate exons from adjacent genes (Liang et al., 2017; Vo et al., 2019). These aberrant circRNAs are associated with oncogenic processes, potentially driving tumor growth and malignant transformation.

Invasion and metastasis of tumor cells are the primary causes of mortality in patients with malignant tumors (Asif et al., 2021). Despite the growing interest in circRNAs in cancer, few studies specifically address their role in brain tumor development (Ahmed et al., 2022; Katsushima et al., 2023; Zhang et al., 2024). Among the multiple pathways implicated in circRNA-mediated tumorigenesis, such as p53, JAK/STAT, and ERK signaling, the PI3K/AKT/mTOR axis is particularly significant.

mTOR is a key downstream signaling molecule in the AMPK, MAPK, and PI3K/AKT pathways, playing a central role in cancer progression (Tee et al., 2003). PI3K activation promotes the transition from PIP2 to PIP3, a process reversed by PTEN, and subsequently leads to mTORC1 and mTORC2 activation, either directly or through Rheb regulation via TSC1/2 inhibition (Ma et al., 2005).

Xin et al. (2019) identified *hsa_circ_0067934* as a critical modulator of glioblastoma progression through its regulation of the epithelial-mesenchymal transition (EMT) process and the PI3K/AKT/mTOR signaling pathway. In their study, they analyzed 157 human brain samples from glioblastoma patients and healthy controls. qRT-PCR revealed that *hsa_circ_0067934* was significantly overexpressed in glioblastoma tissues compared to adjacent noncancerous tissues. To investigate the functional role of *hsa_circ_0067934*, siRNA-mediated knock-down experiments were conducted *in vitro*. The results demonstrated a significant reduction in cell proliferation of glioblastoma cell lines post-transfection, while apoptosis levels increased notably upon *hsa_circ_0067934* silencing. *Hsa_circ_0067934* knock-down, furthermore, significantly impaired the migratory ability of glioblastoma cells in wound healing assays. At molecular level, *hsa_circ_0067934* silencing resulted in a marked decrease of phosphorylated PI3K and phosphorylated AKT, while total PI3K and AKT levels remained unchanged. This suggests that *hsa_circ_0067934* promotes glioblastoma progression by activating the PI3K-AKT signaling pathway (Xin et al., 2019).

Moreover, Bian et al., 2018 identified *circ-CFH* as a novel oncogenic circRNA, upregulated in glioma tissues. *Hsa_circ_0015758* (*circ-CFH*) is a single exon-derived circRNA transcribed from the GRCh37/hg19 fragment of chromosome 1, sharing homology with the protein-coding gene complement factor H (*CFH*) and functioning as a *miR-149* sponge, thereby upregulating *AKT1* expression. To investigate the biological role of *circ-CFH* in glioma cells, siRNA-mediated knock-down was performed. Silencing *circ-CFH* significantly decreased cell proliferation and cells' ability to form colonies *in vitro*, while subcutaneous injection of *circ-CFH* -suppressing cells into nude mice significantly decreased tumor volume and weight. Finally, the RNA sponging activity of *circ-CFH* was explored, confirming miR-149 as a direct target through luciferase reporter assays, regulating miR-149-target mRNAs, such as *AKT1* mRNA (Bian et al., 2018). Taken together, these studies highlight the possibility for circRNAs targeting in order to modulate the activity of the PI3K/AKTAkt/mTOR signaling pathway in the context of brain tumor development.

CircRNAs as biomarkers for brain disorders

Circularity renders RNA largely resistant to exonuclease cleavage and, therefore, circRNAs are extremely stable, as demonstrated by their long half lives in cells (Memczak et al., 2015). Furthermore, they show remarkable tissue specificity in their expression patterns, can be secreted into the extracellular space via extracellular vesicles, - both exosomes (30–100 nm) and microvesicles (100–1,000 nm) (Hon et al., 2019; Lasda and Parker, 2016; Zhao et al., 2024), and have previously been detected in easily accessible biofluids such as saliva, blood and urine (Hutchins et al., 2021; Memczak et al., 2015; Zhao et al., 2018). All these characteristics render circRNAs ideal candidates for being reliable biomarkers. Biomarkers can support diagnosis, provide information about disease prognosis, and progression, and can be used to monitor the efficacy and safety of drug therapy. In fact, when it comes to complex brain disorders, reliable peripheral biomarkers would be extremely useful. Disease relevant circRNAs could enter the blood via blood brain barrier leakage and be measured in biofluids. They could aid 1) diagnosis, which, for instance, is still very difficult in ASD and ALS (Hus and Segal, 2021), 2) disease progression and staging, which is critical for clinical trial design and endpoint assessment, 3) patient care, as sampling is much less invasive when compared with the collection of cerebrospinal fluid, as commonly done in HD (Pellegrini et al., 2022). In line with these requirements, recently, a study utilizing two large publicly available datasets with longitudinal clinical and blood transcriptomic data of PD patients, identified 71 circRNAs that were sufficient to differentiate between genetic PD, at risk-individuals and controls, highlighting the potential of these circRNAs to aid PD diagnosis. Importantly, five circRNAs significantly correlated with PD severity, yet the identified circRNAs had no better predictive value than linear RNA, limiting their utility (Beric et al., 2024). This example, amongst many others discussed above, highlights important considerations in using circRNAs as biomarkers for complex brain disorders. First,

10.3389/fphar.2025.1577496

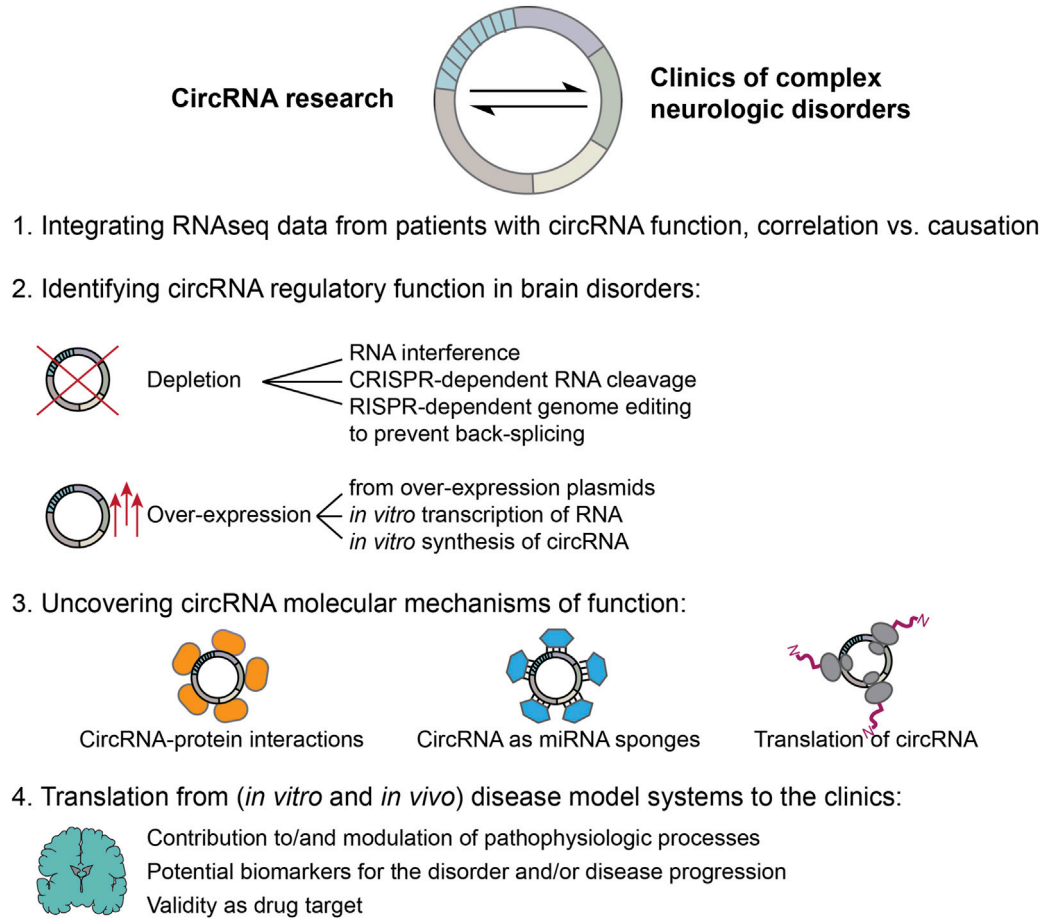


FIGURE 2
Moving forward: steps towards integrating results from circRNA basic research with the clinics of complex neurologic disorders. 1. Numerous RNA sequencing studies have found deregulated circRNA expression levels in samples derived from human patients. However, much fewer studies were able to experimentally validate a functional role and its molecular mechanism for the identified circRNAs in the pathophysiologic processes of the respective disorder. Future studies need to address this current gap in knowledge to avoid fallacy of causation. 2. This requires high quality follow up-experiments to identify circRNA regulatory functions. Experimental approaches can be based on circRNA depletion as well as over-expression. Both strategies face methodological difficulties unique to the circRNA field. CircRNA depletion approaches need to be highly specific to exclusively target the circRNA without simultaneously changing the linear RNA counterparts, or other unintended off-targets. Targeting circRNAs is especially difficult as sequence specificity is restricted to the back-splice junction, while genomic removal of sites required for back-splicing may unintentionally also alter linear splicing dynamics. Over-expression approaches, instead, can lead to difficult interpretation, since linear cognate RNAs can be produced (from plasmids), or co-transfected with *in vitro* transcribed or synthetized circRNAs; unintended immune activation may be induced, while over-expressed circRNA levels may reach extremely high levels leading to cellular effects that could be irrelevant in the physiologic context. 3. If depletion or over-expression of a circRNA of interest produces an effect, the underlying molecular mechanism should be investigated. A number of different molecular mechanisms have been proposed for circRNAs, including sequestration of RNA-binding proteins or activity as protein scaffolds, sponging of miRNAs as well as the production of circRNA related peptides through translation. When molecular mechanisms of function are investigated, it is of utmost importance to first determine endogenous expression levels of the involved components in the disorder of interest, to be able to draw physiologically relevant conclusions. 4. Finally, findings obtained from studying *in vivo* and *in vitro* model systems need to be translated back to the clinics in order to be useful for patients suffering from complex neurologic disorders. To that end, evaluation of a true contribution of the circRNA molecular function to the pathophysiologic processes, either on initiation or progression of the disease or modulation thereof, and/or its potential as biomarker as well as novel drug target need to be carefully assessed and tested.

most studies that are available to date and propose individual circRNAs as biomarkers are based on small sample sizes, i.e., few patients, and limited datasets, and only few have validated their primary findings in additional, independent patient cohorts. Secondly, gender-differences have not been taken into consideration in the majority of cases, which could hamper their potential for clinical translation. And third, the tissue-origin of the deregulated circRNAs proposed as biomarkers remains unexplored, thus it is unclear whether they truly represent a "window into the diseased brain" or whether their deregulation is a secondary, unspecific result. Therefore, more standardised and carefully designed studies, will clarify their true potential as biomarkers in the future and for other neurologic disorders.

Moving forward: challenges and outstanding questions

The last decade has seen the circRNA research field explode, and experimental evidence highlighting the important regulatory

functions of these peculiar molecules for brain physiology and complex neurologic disorders has continuously piled up over the years. Nonetheless, despite the rightful excitement about the discovery of a new regulatory layer that could modulate still untreatable, severe and -in some cases- lethal disorders, measures need to be taken to validate findings derived from RNAseq studies of *post mortem* human, or model organism brain samples, demonstrating a clear functional role of the deregulated circRNAs in the pathogenesis, and/or disease progression by experimental scrutiny to avoid misinterpreting correlation with causation. The circRNA field thereby faces unique challenges, caused by the -mostly- low expression levels, extremely high sequence similarity with the linear RNA counterparts, as well as high stability of these molecules, in addition to issues related to a lack of standardized protocols and detection tools that limit the precision and specificity of experimental approaches. In Figure 2 we suggest a roadmap in moving the circRNA field from performing RNAseq studies, to being able to eventually translate discoveries back to the clinics in order to benefit patients' outcomes. Until very recently, the absence of a standardized circRNA nomenclature severely complicated the communication of results and replication of circRNA related data. This issue, however, was recently addressed by Chen et al. proposing guidelines for a unified circRNA nomenclature. Now the scientific community should push for the implementation of these guidelines, to benefit the circRNA research field as a whole (Chen et al., 2023). Additionally, best practice standards have been recently put forward by leading experts in the field, highlighting important pitfalls and considerations when designing experiments to ensure reproducibility of findings (Nielsen et al., 2022). Experimental strategies to identify regulatory functions are, currently, primarily based on circRNA depletion or over-expression approaches (Figure 2, step 2), which can give valuable first insights into the modulatory potential of the deregulated circRNAs. Since specific targeting is challenging when it comes to circRNAs, as their sequence is unique exclusively at the BSJ, extra care needs to be taken to avoid simultaneously altering the levels of linear RNA transcripts and splicing. When it comes to over-expression strategies, circRNAs can be either synthetically produced, or transcribed RNA or over-expression plasmids can be transfected into *in vitro* model systems. Next to issues relating to immune activation by the synthetic molecules, these strategies often also lead to delivery/production of linear cognate RNAs and extremely high expression levels of the circRNA of interest, far away from any physiological relevant levels. Thus, the results obtained by such over-expression approaches need to be critically evaluated and, ideally, confirmed with a second strategy.

In general, only few circRNA studies have been able to conclusively demonstrate the molecular action of function of the identified DE circRNA, but merely provide a description of the cellular effects of the modulation of their expression. In order to move the field forward, it will be necessary to thoroughly investigate the molecular mechanisms of action of the candidate circRNAs across different disorders (Figure 2, step 3) to objectively assess their true potential as druggable target, therapeutic agent or biomarker. Once these goals have been reached for a specific candidate circRNA, additional challenges need to be overcome. In case the expression of a candidate circRNA is beneficial and counteracts pathophysiological processes, then the circRNA would need to be overexpressed. Should, instead, a reduction of a candidate circRNA demonstrate desirable effects, knock-down or knock-out approaches would be needed. In either case, all the considerations for overexpression and knock-down strategies discussed above, need to be addressed for a successful translation into the clinics. Independently of a desired up-or downregulation, still, the best approach for reaching the brain needs to be identified. This requires a successful crossing of the blood-brain barrier of a therapeutic agent or small molecule, intracranial injections or intrathecal administration, the targeting of a specific brain region or cell type exclusively, while leaving surrounding areas/cells unaffected. Further limitations are arising from the potential toxicity of all viral and non viral approaches, which may either integrate into the host genome and cause insertional mutagenesis or cause inflammation in the brain. Only when all these hurdles are overcome, then, eventually, circRNAs may benefit patients affected by these complex brain disorders for real (Figure 2, step 4), a milestone that has yet to be achieved by this young research field.

Author contributions

VG: Writing – original draft. SV: Writing – original draft. MB: Funding acquisition, Resources, Supervision, Writing – original draft. JM: Conceptualization, Funding acquisition, Project administration, Supervision, Writing – original draft.

Funding

The author(s) declare that financial support was received for the research and/or publication of this article. This work was supported by the University of Trento, the Huntington Society of Canada's NEW PATHWAYS award, the European Huntington's Disease Network (EHDN) seed fund project #1041 and the Hereditary Disease Foundation research grant #990845, the HD Human Biology Project 2018 by the Huntington's Disease Society of America (HDSA) and the MUR PNRR National Center RNA and gene Therapy Spoke 3, Bando a Cascata "RAPID" to MB. MB. was also a recipient of a Marie Skłodowska Curie reintegration fellowship (The European Union's Horizon 2020 Research and Innovation Program, GA n°706567). JM was/is supported by a EMBO postdoctoral fellowship (ALTF 897-2021) and by the European Union (under GA n°101062297- BrainCircHD).

Conflict of interest

The authors declare that the research was conducted in the absence of any commercial or financial relationships that could be construed as a potential conflict of interest.

Generative AI statement

The author(s) declare that no Generative AI was used in the creation of this manuscript.

Publisher's note

All claims expressed in this article are solely those of the authors and do not necessarily represent those of their affiliated organizations, or those of the publisher, the editors and the reviewers. Any product that may be evaluated in this article, or claim that may be made by its manufacturer, is not guaranteed or endorsed by the publisher.

References

Ahmed, S. P., Castresana, J. S., and Shahi, M. H. (2022). Role of circular RNA in brain tumor development. *Cells* 11 (14), 2130. doi:10.3390/cells11142130

Aquilina-Reid, C., Brennan, S., Curry-Hyde, A., Teunisse, G. M., and Janitz, M. (2022). Circular RNA expression and interaction patterns are perturbed in amyotrophic lateral sclerosis. *Int. J. Mol. Sci.* 23 (23), 14665. doi:10.3390/ijms232314665

Arizaca Maquera, K. A., Welden, J. R., Margvelani, G., Miranda Sardón, S. C., Hart, S., Robil, N., et al. (2023). Alzheimer's disease pathogenetic progression is associated with changes in regulated retained introns and editing of circular RNAs. *Front. Mol. Neurosci.* 16, 1141079. doi:10.3389/fnmol.2023.1141079

Ashwal-Fluss, R., Meyer, M., Pamudurti, N. R., Ivanov, A., Bartok, O., Hanan, M., et al. (2014). circRNA biogenesis competes with pre-mRNA splicing. *Mol. Cell* 56 (1), 55–66. doi:10.1016/j.molcel.2014.08.019

Asif, P. J., Longobardi, C., Hahne, M., and Medema, J. P. (2021). The role of cancer-associated fibroblasts in cancer invasion and metastasis. *Cancers* 13 (18), 4720. doi:10.3390/cancers13184720

Atrian, F., Ramirez, P., Mange, J. D., Marquez, M., Gonzalez, E. M., Minaya, M., et al. (2024). m6A-dependent circular RNA formation mediates tau-induced neurotoxicity. *bioRxiv*. doi:10.1101/2024.01.25.577211

Ayyildiz, D., Bergonzoni, G., Monziani, A., Tripathi, T., Döring, J., Kerschbamer, E., et al. (2023). CAG repeat expansion in the Huntington's disease gene shapes linear and circular RNAs biogenesis. *PLOS Genet.* 19 (10), e1010988. doi:10.1371/journal.pgen.1010988

Belter, A., Popenda, M., Sajek, M., Woźniak, T., Naskręt-Barciszewska, M. Z., Szachniuk, M., et al. (2022). A new molecular mechanism of RNA circularization and the microRNA sponge formation. *J. Biomol. Struct. and Dyn.* 40 (7), 3038–3045. doi:10.1080/07391102.2020.1844802

Beric, A., Sun, Y., Sanchez, S., Martin, C., Powell, T., Kumar, R., et al. (2024). Circulating blood circular RNA in Parkinson's Disease; from involvement in pathology to diagnostic tools in at-risk individuals. *NPJ Parkinson's Dis.* 10 (1), 222. doi:10.1038/s41531-024-00839-3

Bian, A., Wang, Y., Liu, J., Wang, X., Liu, D., Jiang, J., et al. (2018). Circular RNA complement factor H (CFH) promotes glioma progression by sponging miR-149 and regulating AKT1. *Med. Sci. Monit. Int. Med. J. Exp. Clin. Res.* 24, 5704–5712. doi:10.12659/MSM.910180

Brown, R. H., and Al-Chalabi, A. (2017). Amyotrophic lateral sclerosis. *N. Engl. J. Med.* 377 (2), 162–172. doi:10.1056/NEJMra1603471

Cardamone, G., Paraboschi, E. M., Rimoldi, V., Duga, S., Soldà, G., and Asselta, R. (2017). The characterization of GSDMB splicing and backsplicing profiles identifies novel isoforms and a circular RNA that are dysregulated in multiple sclerosis. *Int. J. Mol. Sci.* 18 (3), 576. doi:10.3390/ijms18030576

Cardamone, G., Paraboschi, E. M., Soldà, G., Liberatore, G., Rimoldi, V., Cibella, J., et al. (2023). The circular RNA landscape in multiple sclerosis: disease-specific associated variants and exon methylation shape circular RNA expression profile. *Multiple Scler. Relat. Disord.* 69, 104426. doi:10.1016/j.msard.2022.104426

Cerda-Jara, C. A., Kim, S. J., Thomas, G., Farsi, Z., Zolotarov, G., Dube, G., et al. (2024). miR-7 controls glutamatergic transmission and neuronal connectivity in a Cdr1as-dependent manner. *EMBO Rep.* 25 (7), 3008–3039. doi:10.1038/s44319-024-00168-9

Cervera-Carles, L., Dols-Icardo, O., Molina-Porcel, L., Alcolea, D., Cervantes-Gonzalez, A., Muñoz-Llahuna, L., et al. (2020). Assessing circular RNAs in Alzheimer's disease and frontotemporal lobar degeneration. *Neurobiol. Aging* 92, 7–11. doi:10.1016/j.neurobiolaging.2020.03.017

Chen, C.-K., Cheng, R., Demeter, J., Chen, J., Weingarten-Gabbay, S., Jiang, L., et al. (2021). Structured elements drive extensive circular RNA translation. *Mol. Cell* 81 (20), 4300–4318.e13. doi:10.1016/j.molcel.2021.07.042

Chen, H.-H., Eteleeb, A., Wang, C., Fernandez, M. V., Budde, J. P., Bergmann, K., et al. (2022). Circular RNA detection identifies circPSEN1 alterations in brain specific to autosomal dominant Alzheimer's disease. *Acta Neuropathol. Commun.* 10 (1), 29. doi:10.1186/s40478-022-01328-5

Chen, L.-L., Bindereif, A., Bozzoni, I., Chang, H. Y., Matera, A. G., Gorospe, M., et al. (2023). A guide to naming eukaryotic circular RNAs. *Nat. Cell Biol.* 25 (1), 1–5. doi:10.1038/s41556-022-01066-9

Chen, X., Han, P., Zhou, T., Guo, X., Song, X., and Li, Y. (2016). circRNADb: a comprehensive database for human circular RNAs with protein-coding annotations. *Sci. Rep.* 6 (1), 34985. doi:10.1038/srep34985

Chen, Y., Guan, Y., Zhang, Z., Liu, H., Wang, S., Yu, L., et al. (2012). Wnt signaling pathway is involved in the pathogenesis of amyotrophic lateral sclerosis in adult transgenic mice. *Neurological Res.* 34 (4), 390–399. doi:10.1179/1743132812Y.0000000027

Cheng, Q., Wang, J., Li, M., Fang, J., Ding, H., Meng, J., et al. (2022). CircSV2b participates in oxidative stress regulation through miR-5107-5p-Foxk1-Akt1 axis in Parkinson's disease. *Redox Biol.* 56, 102430. doi:10.1016/j.redox.2022.102430

Choi, L., and An, J.-Y. (2021). Genetic architecture of autism spectrum disorder: lessons from large-scale genomic studies. *Neurosci. Biobehav. Rev.* 128, 244–257. doi:10.1016/j.neubiorev.2021.06.028

Cochran, K. R., Veeraraghavan, K., Kundu, G., Mazan-Mamczarz, K., Coletta, C., Thambisetty, M., et al. (2021). Systematic identification of circRNAs in Alzheimer's disease. *Genes* 12 (8), 1258. doi:10.3390/genes12081258

Corsi, A., Bombieri, C., Valenti, M. T., and Romanelli, M. G. (2022). Tau isoforms: gaining insight into MAPT alternative splicing. *Int. J. Mol. Sci.* 23 (23), 15383. doi:10.3390/ijms232315383

Cui, L., Li, S., Wang, S., Wu, X., Liu, Y., Yu, W., et al. (2024). Major depressive disorder: hypothesis, mechanism, prevention and treatment. *Signal Transduct. Target. Ther.* 9 (1), 30–32. doi:10.1038/s41392-024-01738-y

Cui, X., Niu, W., Kong, L., He, M., Jiang, K., Chen, S., et al. (2016). hsa_circRNA_103636: potential novel diagnostic and therapeutic biomarker in Major depressive disorder. *Biomarkers Med.* 10 (9), 943–952. doi:10.2217/bmm-2016-0130

Dai, X., Chen, C., Yang, Q., Xue, J., Chen, X., Sun, B., et al. (2018). Exosomal circRNA_100284 from arsenite-transformed cells, via microRNA-217 regulation of EZH2, is involved in the malignant transformation of human hepatic cells by accelerating the cell cycle and promoting cell proliferation. *Cell Death and Dis.* 9 (5), 454. doi:10.1038/s41419-018-0485-1

D'Ambrosio, A., Pontecorvo, S., Colasanti, T., Zamboni, S., Francia, A., and Margutti, P. (2015). Peripheral blood biomarkers in multiple sclerosis. *Autoimmun. Rev.* 14 (12), 1097–1110. doi:10.1016/j.autrev.2015.07.014

Dolinar, A., Koritnik, B., Glavač, D., and Ravnik-Glavač, M. (2019). Circular RNAs as potential blood biomarkers in amyotrophic lateral sclerosis. *Mol. Neurobiol.* 56 (12), 8052–8062. doi:10.1007/s12035-019-1627-x

Dong, R., Ma, X.-K., Li, G.-W., and Yang, L. (2018). CIRCpedia v2: an updated database for comprehensive circular RNA annotation and expression comparison. *Genomics, Proteomics and Bioinforma.* 16 (4), 226–233. doi:10.1016/j.gpb.2018.08.001

Dong, X., Bai, Y., Liao, Z., Gritsch, D., Liu, X., Wang, T., et al. (2023). Circular RNAs in the human brain are tailored to neuron identity and neuropsychiatric disease. *Nat. Commun.* 14 (1), 5327. doi:10.1038/s41467-023-40348-0

Dube, U., Del-Aguila, J. L., Li, Z., Budde, J. P., Jiang, S., Hsu, S., et al. (2019). An atlas of cortical circular RNA expression in Alzheimer disease brains demonstrates clinical and pathological associations. *Nat. Neurosci.* 22 (11), 1903–1912. doi:10.1038/s41593-019-0501-5

Enuka, Y., Lauriola, M., Feldman, M. E., Sas-Chen, A., Ulitsky, I., and Yarden, Y. (2016). Circular RNAs are long-lived and display only minimal early alterations in response to a growth factor. *Nucleic Acids Res.* 44 (3), 1370–1383. doi:10.1093/nar/gkv1367

Fan, X., Zhang, X., Wu, X., Guo, H., Hu, Y., Tang, F., et al. (2015). Single-cell RNA-seq transcriptome analysis of linear and circular RNAs in mouse preimplantation embryos. *Genome Biol.* 16 (1), 148. doi:10.1186/s13059-015-0706-1

Forner, S., Kawauchi, S., Balderrama-Gutierrez, G., Kramár, E. A., Matheos, D. P., Phan, J., et al. (2021). Systematic phenotyping and characterization of the 5xFAD mouse model of Alzheimer's disease. *Sci. Data* 8 (1), 270. doi:10.1038/s41597-021-01054-y

Friedman, R. C., Farh, K. K.-H., Burge, C. B., and Bartel, D. P. (2009). Most mammalian mRNAs are conserved targets of microRNAs. *Genome Res.* 19 (1), 92–105. doi:10.1101/gr.082701.108

Garcia, D. M., Baek, D., Shin, C., Bell, G. W., Grimson, A., and Bartel, D. P. (2011). Weak seed-pairing stability and high target-site abundance decrease the proficiency of lsy-6 and other microRNAs. *Nat. Struct. and Mol. Biol.* 18 (10), 1139–1146. doi:10.1038/nsmb.2115

Gasparini, S., Del Vecchio, G., Gioiosa, S., Flati, T., Castrignano, T., Legnini, I., et al. (2020). Differential expression of hippocampal circular RNAs in the BTBR mouse model for autism spectrum disorder. *Mol. Neurobiol.* 57 (5), 2301–2313. doi:10.1007/s12035-020-01878-6

Ghafouri-Fard, S., Noroozi, R., Brand, S., Hussen, B. M., Eghtedarian, R., Taheri, M., et al. (2022). Emerging role of non-coding RNAs in autism spectrum disorder. *J. Mol. Neurosci.* 72 (2), 201–216. doi:10.1007/s12031-021-01934-3

Giusti, S. A., Pino, N. S., Pannunzio, C., Ogando, M. B., Armando, N. G., Garrett, L., et al. (2024). A brain-enriched circular RNA controls excitatory neurotransmission and restricts sensitivity to aversive stimuli. *Sci. Adv.* 10 (21), eadj8769. doi:10.1126/sciadv.adj8769

Glažar, P., Papavasileiou, P., and Rajewsky, N. (2014). circBase: a database for circular RNAs. *RNA (New York, N.Y.)* 20 (11), 1666–1670. doi:10.1261/rna.043687.113

Gomes-Duarte, A., Bauer, S., Venø, M. T., Norwood, B. A., Henshall, D. C., Kjems, J., et al. (2021). Enrichment of circular RNA expression deregulation at the transition to recurrent spontaneous seizures in experimental temporal lobe epilepsy. *Front. Genet.* 12, 627907. doi:10.3389/fgene.2021.627907

Grimson, A., Farh, K. K.-H., Johnston, W. K., Garrett-Engele, P., Lim, L. P., and Bartel, D. P. (2007). MicroRNA targeting specificity in mammals: determinants beyond seed pairing. *Mol. Cell* 27 (1), 91–105. doi:10.1016/j.molcel.2007.06.017

Guarnieri, L., Amodio, N., Bosco, F., Carpi, S., Tallarico, M., Gallelli, L., et al. (2024). Circulating miRNAs as novel clinical biomarkers in temporal lobe epilepsy. *Non-Coding RNA* 10 (2), 18. doi:10.3390/ncrna10020018

Hanan, M., Simchovitz, A., Yayon, N., Vaknine, S., Cohen-Fultheim, R., Karmon, M., et al. (2020). A Parkinson's disease CircRNAs Resource reveals a link between circSLC8A1 and oxidative stress. *EMBO Mol. Med.* 12 (9), e11942. doi:10.15252/emmm.201911942

Hanan, M., Soreq, H., and Kadener, S. (2017). CircRNAs in the brain. *RNA Biol.* 14 (8), 1028–1034. doi:10.1080/15476286.2016.1255398

Hansen, T. B., Jensen, T. I., Clausen, B. H., Bramsen, J. B., Finsen, B., Damgaard, C. K., et al. (2013). Natural RNA circles function as efficient microRNA sponges. *Nature* 495 (7441), 384–388. doi:10.1038/nature11993

Hao, W.-Z., Chen, Q., Wang, L., Tao, G., Gan, H., Deng, L.-J., et al. (2022). Emerging roles of long non-coding RNA in depression. *Prog. Neuro-Psychopharmacology Biol. Psychiatry* 115, 110515. doi:10.1016/j.pnpbp.2022.110515

Hardiman, O., Al-Chalabi, A., Brayne, C., Beghi, E., van den Berg, L. H., Chio, A., et al. (2017). The changing picture of amyotrophic lateral sclerosis: lessons from European registers. *J. Neurology, Neurosurg. Psychiatry* 88 (7), 557–563. doi:10.1136/jnnp-2016-314495

Hecker, M., Rüge, A., Putscher, E., Boxberger, N., Rommer, P. S., Fitzner, B., et al. (2019). Aberrant expression of alternative splicing variants in multiple sclerosis—a systematic review. *Autoimmun. Rev.* 18 (7), 721–732. doi:10.1016/j.autrev.2019.05.010

Holdt, L. M., Stahringer, A., Sass, K., Pichler, G., Kulak, N. A., Wilfert, W., et al. (2016). Circular non-coding RNA ANRIL modulates ribosomal RNA maturation and atherosclerosis in humans. *Nat. Commun.* 7 (1), 12429. doi:10.1038/ncomms12429

Hollensen, A. K., Thomsen, H. S., Lloret-Llinares, M., Kamstrup, A. B., Jensen, J. M., Luckmann, M., et al. (2020). circZNF827 nucleates a transcription inhibitory complex to balance neuronal differentiation. *eLife* 9, e58478. doi:10.7554/eLife.58478

Hon, K. W., Ab-Mutalib, N. S., Abdullah, N. M. A., Jamal, R., and Abu, N. (2019). Extracellular Vesicle-derived circular RNAs confers chemoresistance in Colorectal cancer. *Sci. Rep.* 9 (1), 16497. doi:10.1038/s41598-019-53063-y

Hou, Y., Dan, X., Babbar, M., Wei, Y., Hasselbalch, S. G., Croteau, D. L., et al. (2019). Ageing as a risk factor for neurodegenerative disease. *Nat. Rev. Neurol.* 15 (10), 565–581. doi:10.1038/s41582-019-0244-7

Huang, H., Luo, J., Qi, Y., Wu, Y., Qi, J., Yan, X., et al. (2023). Comprehensive analysis of circRNA expression profile and circRNA-miRNA-mRNA network susceptibility to very early-onset schizophrenia. *Schizophrenia* 9 (1), 70. doi:10.1038/s41537-023-00399-0

Huang, R., Zhang, Y., Han, B., Bai, Y., Zhou, R., Gan, G., et al. (2017). Circular RNA HIPK2 regulates astrocyte activation via cooperation of autophagy and ER stress by targeting MIR124–2HG. *Autophagy* 13 (10), 1722–1741. doi:10.1080/15548627.2017.1356975

Hus, Y., and Segal, O. (2021). Challenges surrounding the diagnosis of autism in children. *Neuropsychiatric Dis. Treat.* 17, 3509–3529. doi:10.2147/NDT.S282569

Hutchins, E., Reiman, R., Winarta, J., Beecroft, T., Richholt, R., De Both, M., et al. (2021). Extracellular circular RNA profiles in plasma and urine of healthy, male college athletes. *Sci. Data* 8 (1), 276. doi:10.1038/s41597-021-01056-w

Hwang, H. J., and Kim, Y. K. (2024). Molecular mechanisms of circular RNA translation. *Exp. and Mol. Med.* 56 (6), 1272–1280. doi:10.1038/s12276-024-01220-3

Ikeda, Y., Morikawa, S., Nakashima, M., Yoshikawa, S., Taniguchi, K., Sawamura, H., et al. (2023). CircRNAs and RNA-binding proteins involved in the pathogenesis of cancers or central nervous system disorders. *Non-Coding RNA* 9 (2), 23. doi:10.3390/ncrna9020023

Iparraguirre, L., Alberro, A., Sepúlveda, L., Osorio-Querejeta, I., Moles, L., Castillo-Triviño, T., et al. (2020). RNA-Seq profiling of leukocytes reveals a sex-dependent global circular RNA upregulation in multiple sclerosis and 6 candidate biomarkers. *Hum. Mol. Genet.* 29 (20), 3361–3372. doi:10.1093/hmg/ddaa219

Iparraguirre, L., Muñoz-Culla, M., Prada-Luengo, I., Castillo-Triviño, T., Olascoaga, J., and Otaegui, D. (2017). Circular RNA profiling reveals that circular RNAs from ANXA2 can be used as new biomarkers for multiple sclerosis. *Hum. Mol. Genet.* 26 (18), 3564–3572. doi:10.1093/hmg/ddx243

Javier-Torrent, M., Marco, S., Rocandio, D., Pons-Vizcarra, M., Janes, P. W., Lackmann, M., et al. (2019). Presenilin/γ-secretase-dependent EphA3 processing mediates axon elongation through non-muscle myosin IIA. *eLife* 8, e43646. doi:10.7554/eLife.43646

Jeck, W. R., Sorrentino, J. A., Wang, K., Slevin, M. K., Burd, C. E., Liu, J., et al. (2013). Circular RNAs are abundant, conserved, and associated with ALU repeats. *RNA (New York, N.Y.)* 19 (2), 141–157. doi:10.1261/rna.035667.112

Jiang, M., Wang, Z., Lu, T., Li, X., Yang, K., Zhao, L., et al. (2023). Integrative analysis of long noncoding RNAs dysregulation and synapse-associated ceRNA regulatory axes in autism. *Transl. Psychiatry* 13 (1), 375. doi:10.1038/s41398-023-02662-5

Katsushima, K., Joshi, K., and Perera, R. J. (2023). Diagnostic and therapeutic potential of circular RNA in brain tumors. *Neuro-Oncology Adv.* 5 (1), vdad063. doi:10.1093/noajnl/vdad063

Kelly, D., Bicker, S., Winterer, J., Nanda, P., Germain, P.-L., Dieterich, C., et al. (2024). A functional screen uncovers circular RNAs regulating excitatory synaptogenesis in hippocampal neurons. *bioRxiv*. doi:10.1101/2024.04.09.588686

Kelly, D., Bicker, S., Winterer, J., Nanda, P., Germain, P.-L., Dieterich, C., et al. (2025). A functional screen uncovers circular RNAs regulating excitatory synaptogenesis in hippocampal neurons. *Nat. Commun.* 16 (1), 3040. doi:10.1038/s41467-025-58070-4

Kleaveland, B., Shi, C. Y., Stefano, J., and Bartel, D. P. (2018). A network of noncoding regulatory RNAs acts in the mammalian brain. *Cell* 174 (2), 350–362.e17. doi:10.1016/j.cell.2018.05.022

Knupp, D., and Miura, P. (2018). CircRNA accumulation: a new hallmark of aging? *Mech. Ageing Dev.* 173, 71–79. doi:10.1016/j.mad.2018.05.001

Lasda, E., and Parker, R. (2016). Circular RNAs Co-precipitate with extracellular vesicles: a possible mechanism for circRNA clearance. *PLOS ONE* 11 (2), e0148407. doi:10.1371/journal.pone.0148407

Lewis, B. P., Burge, C. B., and Bartel, D. P. (2005). Conserved seed pairing, often flanked by adenosines, indicates that thousands of human genes are microRNA targets. *Cell* 120 (1), 15–20. doi:10.1016/j.cell.2004.12.035

Li, Y., Han, X., Fan, H., Sun, J., Ni, M., Zhang, L., et al. (2022). Circular RNA AXL increases neuron injury and inflammation through targeting microRNA-328 mediated BACE1 in Alzheimer's disease. *Neurosci. Lett.* 776, 136531. doi:10.1016/j.neulet.2022.136531

Liang, D., Tatomer, D. C., Luo, Z., Wu, H., Yang, L., Chen, L.-L., et al. (2017). The output of protein-coding genes shifts to circular RNAs when the pre-mRNA processing machinery is limiting. *Mol. Cell* 68 (5), 940–954.e3. doi:10.1016/j.molcel.2017.10.034

Lin, R., Lopez, J. P., Cruceanu, C., Pierotti, C., Fiori, L. M., Squassina, A., et al. (2021). Circular RNA circCCNT2 is upregulated in the anterior cingulate cortex of individuals with bipolar disorder. *Transl. Psychiatry* 11 (1), 629–638. doi:10.1038/s41398-021-01746-4

Lo, Ij., Hill, J., Vilhjálmsson, B. J., and Kjems, J. (2020). Linking the association between circRNAs and Alzheimer's disease progression by multi-tissue circular RNA characterization. *RNA Biol.* 17 (12), 1789–1797. doi:10.1080/15476286.2020.1783487

Lublin, F. D., Reingold, S. C., Cohen, J. A., Cutter, G. R., Sørensen, P. S., Thompson, A. J., et al. (2014). Defining the clinical course of multiple sclerosis: the 2013 revisions. *Neurology* 83 (3), 278–286. doi:10.1212/WNL.0000000000000560

Luykx, J. J., Giuliani, F., Giuliani, G., and Veldink, J. (2019). Coding and non-coding RNA abnormalities in bipolar disorder. *Genes* 10 (11), 946. doi:10.3390/genes10110946

Ma, L., Chen, Z., Erdjument-Bromage, H., Tempst, P., and Pandolfi, P. P. (2005). Phosphorylation and functional inactivation of TSC2 by Erk implications for tuberous sclerosis and cancer pathogenesis. *Cell* 121 (2), 179–193. doi:10.1016/j.cell.2005.02.031

Mahmoudi, E., Green, M. J., and Cairns, M. J. (2021). Dysregulation of circRNA expression in the peripheral blood of individuals with schizophrenia and bipolar disorder. *J. Mol. Med.* 99 (7), 981–991. doi:10.1007/s00109-021-02070-6

Mai, T.-L., Chen, C.-Y., Chen, Y.-C., Chiang, T.-W., and Chuang, T.-J. (2022). Trans-genetic effects of circular RNA expression quantitative trait loci and potential causal mechanisms in autism. *Mol. Psychiatry* 27 (11), 4695–4706. doi:10.1038/s41380-022-01714-4

Malhi, G. S., and Mann, J. J. (2018). Depression. *Lancet London, Engl.* 392 (10161), 2299–2312. doi:10.1016/S0140-6736(18)31948-2

Marfil-Marin, E., Santamaría-Olmedo, M., PerezGrovas-Saltijeral, A., Valdes-Flores, M., Ochoa-Morales, A., Jara-Prado, A., et al. (2021). circRNA regulates dopaminergic synapse, MAPK, and long-term depression pathways in Huntington disease. *Mol. Neurobiol.* 58 (12), 6222–6231. doi:10.1007/s12035-021-02536-1

Margvelani, G., Welden, J. R., Maquera, A. A., Eyk, J. E. V., Murray, C., Sardon, S. C. M., et al. (2023). Influence of FTDP-17 mutants on circular Tau RNAs. *bioRxiv*. doi:10.1101/2023.09.08.556913

Memczak, S., Jens, M., Elefsinioti, A., Torti, F., Krueger, J., Rybak, A., et al. (2013). Circular RNAs are a large class of animal RNAs with regulatory potency. *Nature* 495 (7441), 333–338. doi:10.1038/nature11928

Memczak, S., Papavasileiou, P., Peters, O., and Rajewsky, N. (2015). Identification and characterization of circular RNAs as a new class of putative biomarkers in human blood. *PloS One* 10 (10), e0141214. doi:10.1371/journal.pone.0141214

Meng, X., Hu, D., Zhang, P., Chen, Q., and Chen, M. (2019). CircFunBase: a database for functional circular RNAs. *Database* 2019, baz003. doi:10.1093/database/baz003

Meyza, K. Z., and Blanchard, D. C. (2017). The BTBR mouse model of idiopathic autism—current view on mechanisms. *Neurosci. Biobehav. Rev.* 76 (Pt A), 99–110. doi:10.1016/j.neubiorev.2016.12.037

Morandell, J., Monziani, A., Lazioli, M., Donzel, D., Döring, J., Oss Pegorar, C., et al. (2024). *CircHTT(2,3,4,5,6)*- co-evolving with the *HTT* CAG-repeat tract - modulates Huntington's disease phenotypes. *Nucleic acids.* 35 (3), 102234. doi:10.1016/j.omtn.2024.102234

Morris-Rosendahl, D. J., and Crocq, M.-A. (2020). Neurodevelopmental disorders-the history and future of a diagnostic concept. *Dialogues Clin. Neurosci.* 22 (1), 65–72. doi:10.31887/DCNS.2020.22.1/macrocq

Nemeth, K., Bayraktar, R., Ferracin, M., and Calin, G. A. (2024). Non-coding RNAs in disease: from mechanisms to therapeutics. *Nat. Rev. Genet.* 25 (3), 211–232. doi:10.1038/s41576-023-00662-1

Ngo, L. H., Bert, A. G., Dredge, B. K., Williams, T., Murphy, V., Li, W., et al. (2024). Nuclear export of circular RNA. *Nature* 627 (8002), 212–220. doi:10.1038/s41586-024-07060-5

Nguyen, T. B., Miramontes, R., Chillon-Marinas, C., Maimon, R., Vazquez-Sanchez, S., Lau, A. L., et al. (2025). Aberrant splicing in Huntington's disease accompanies disrupted TDP-43 activity and altered m6A RNA modification. *Nat. Neurosci.* 28 (2), 280–292. doi:10.1038/s41593-024-01850-w

Nielsen, A. F., Bindereif, A., Bozzoni, I., Hanan, M., Hansen, T. B., Irimia, M., et al. (2022). Best practice standards for circular RNA research. *Nat. Methods* 19 (10), 1208–1220. doi:10.1038/s41592-022-01487-2

Paraboschi, E. M., Cardamone, G., Rimoldi, V., Gemmati, D., Spreafico, M., Duga, S., et al. (2015). Meta-analysis of multiple sclerosis microarray data reveals dysregulation in RNA splicing regulatory genes. *Int. J. Mol. Sci.* 16 (10), 23463–23481. doi:10.3390/ijms161023463

Paraboschi, E. M., Cardamone, G., Soldà, G., Duga, S., and Asselta, R. (2018). Interpreting non-coding genetic variation in multiple sclerosis genome-wide associated regions. *Front. Genet.* 9, 647. doi:10.3389/fgene.2018.00647

Parenti, I., Rabaneda, L. G., Schoen, H., and Novarino, G. (2020). Neurodevelopmental disorders: from genetics to functional pathways. *Trends Neurosci.* 43 (8), 608–621. doi:10.1016/j.tins.2020.05.004

Parikshak, N. N., Swarup, V., Belgard, T. G., Irimia, M., Ramaswami, G., Gandal, M. J., et al. (2016). Genome-wide changes in lncRNA, splicing, and regional gene expression patterns in autism. *Nature* 540 (7633), 423–427. doi:10.1038/nature20612

Pellegrini, M., Bergonzoni, G., Perrone, F., Squitieri, F., and Biagioli, M. (2022). Current diagnostic methods and non-coding RNAs as possible biomarkers in Huntington's disease. *Genes* 13 (11), 2017. doi:10.3390/genes13112017

Peng, L., Chen, G., Zhu, Z., Shen, Z., Du, C., Zang, R., et al. (2017). Circular RNA ZNF609 functions as a competitive endogenous RNA to regulate AKT3 expression by sponging miR-150-5p in Hirschsprung's disease. *Oncotarget* 8 (1), 808–818. doi:10.18632/oncotarget.13656

Piwecka, M., Glažar, P., Hernandez-Miranda, L. R., Memczak, S., Wolf, S. A., Rybak-Wolf, A., et al. (2017). Loss of a mammalian circular RNA locus causes miRNA deregulation and affects brain function. *Sci. (New York, N.Y.)* 357 (6357), eaam8526. doi:10.1126/science.aam8526

Puri, S., Hu, J., Sun, Z., Lin, M., Stein, T. D., Farrer, L. A., et al. (2023). Identification of circRNAs linked to Alzheimer's disease and related dementias. *Alzheimer's and Dementia J. Alzheimer's Assoc.* 19 (8), 3389–3405. doi:10.1002/alz.12960

Rybak-Wolf, A., Stottmeister, C., Glažar, P., Jens, M., Pino, N., Giusti, S., et al. (2015). Circular RNAs in the mammalian brain are highly abundant, conserved, and dynamically expressed. *Mol. Cell* 58 (5), 870–885. doi:10.1016/j.molcel.2015.03.027

Rybiczka-Tešulov, M., Garritsen, O., Venø, M. T., Wieg, L., Dijk, R., Rahimi, K., et al. (2024). Circular RNAs regulate neuron size and migration of midbrain dopamine neurons during development. *Nat. Commun.* 15 (1), 6773. doi:10.1038/s41467-024-51041-1

Santer, L., Bär, C., and Thum, T. (2019). Circular RNAs: a novel class of functional RNA molecules with a therapeutic perspective. *Mol. Ther. J. Am. Soc. Gene Ther.* 27 (8), 1350–1363. doi:10.1016/j.ymthe.2019.07.001

Seeler, S., Andersen, M. S., Sztanka-Toth, T., Rybiczka-Tešulov, M., Van Den Munkhof, M. H., Chang, C.-C., et al. (2023). A circular RNA expressed from the FAT3 locus regulates neural development. *Mol. Neurobiol.* 60 (6), 3239–3260. doi:10.1007/s12035-023-03253-7

Shi, Y., Song, R., Wang, Z., Zhang, H., Zhu, J., Yue, Y., et al. (2021a). Potential clinical value of circular RNAs as peripheral biomarkers for the diagnosis and treatment of major depressive disorder. *eBioMedicine* 66, 103337. doi:10.1016/j.ebiom.2021.103337

Shi, Y., Wang, Q., Song, R., Kong, Y., and Zhang, Z. (2021b). Non-coding RNAs in depression: promising diagnostic and therapeutic biomarkers. *EBioMedicine* 71, 103569. doi:10.1016/j.ebiom.2021.103569

Silenzi, V., D'Ambra, E., Santini, T., D'Uva, S., Setti, A., Salvi, N., et al. (2024). A tripartite circRNA/mRNA/miRNA interaction regulates glutamatergic signaling in the mouse brain. *Cell Rep.* 43 (10), 114766. doi:10.1016/j.celrep.2024.114766

Spurlock, C. F., Tossberg, J. T., Guo, Y., Sriram, S., Crooke, P. S., and Aune, T. M. (2015). Defective structural RNA processing in relapsing-remitting multiple sclerosis. *Genome Biol.* 16 (1), 58. doi:10.1186/s13059-015-0629-x

Starke, S., Jost, I., Rossbach, O., Schneider, T., Schreiner, S., Hung, L.-H., et al. (2015). Exon circularization requires canonical splice signals. *Cell Rep.* 10 (1), 103–111. doi:10.1016/j.celrep.2014.12.002

Stott, J., Wright, T., Holmes, J., Wilson, J., Griffiths-Jones, S., Foster, D., et al. (2023). A systematic review of non-coding RNA genes with differential expression profiles associated with autism spectrum disorders. *PloS One* 18 (6), e0287131. doi:10.1371/journal.pone.0287131

Suenkel, C., Cavalli, D., Massalini, S., Calegari, F., and Rajewsky, N. (2020). A highly conserved circular RNA is required to keep neural cells in a progenitor state in the mammalian brain. *Cell Rep.* 30 (7), 2170–2179.e5. doi:10.1016/j.celrep.2020.01.083

Suzuki, H., Zuo, Y., Wang, J., Zhang, M. Q., Malhotra, A., and Mayeda, A. (2006). Characterization of RNase R-digested cellular RNA source that consists of lariat and circular RNAs from pre-mRNA splicing. *Nucleic Acids Res.* 34 (8), e63. doi:10.1093/nar/gkl151

Tan, G., Wang, L., Liu, Y., Zhang, H., Feng, W., and Liu, Z. (2021). The alterations of circular RNA expression in plasma exosomes from patients with schizophrenia. *J. Cell. Physiology* 236 (1), 458–467. doi:10.1002/jcp.29873

Tee, A. R., Manning, B. D., Roux, P. P., Cantley, L. C., and Blenis, J. (2003). Tuberous sclerosis complex gene products, Tuberin and Hamartin, control mTOR signaling by acting as a GTPase-activating protein complex toward Rheb. *Curr. Biol. CB* 13 (15), 1259–1268. doi:10.1016/s0960-9822(03)00506-2

Thompson, A. J., Baranzini, S. E., Geurts, J., Hemmer, B., and Ciccarelli, O. (2018). Multiple sclerosis. *Lancet London, Engl.* 391 (10130), 1622–1636. doi:10.1016/S0140-6736(18)30481-1

Titze-de-Almeida, S. S., and Titze-de-Almeida, R. (2023). Progress in circRNA-targeted Therapy in experimental Parkinson's disease. *Pharmaceutics* 15 (8), 2035. doi:10.3390/pharmaceutics15082035

Tondo, L., Vázquez, G. H., and Baldessarini, R. J. (2017). Depression and mania in bipolar disorder. *Curr. Neuropharmacol.* 15 (3), 353–358. doi:10.2174/1570159X14666160606210811

Venø, M. T., Hansen, T. B., Venø, S. T., Clausen, B. H., Grebing, M., Finsen, B., et al. (2015). Spatio-temporal regulation of circular RNA expression during porcine embryonic brain development. *Genome Biol.* 16, 245. doi:10.1186/s13059-015-0801-3

Vo, J. N., Cieslik, M., Zhang, Y., Shukla, S., Xiao, L., Zhang, Y., et al. (2019). The landscape of circular RNA in cancer. *Cell* 176 (4), 869–881.e13. doi:10.1016/j.cell.2018.12.021

Wang, F., Li, Y., Shen, H., Martinez-Feduchi, P., Ji, X., Teng, P., et al. (2024). Identification of pathological pathways centered on circRNA dysregulation in association with irreversible progression of Alzheimer's disease. *Genome Med.* 16 (1), 129. doi:10.1186/s13073-024-01404-6

Wang, J., Yang, Z., Chen, C., Xu, Y., Wang, H., Liu, B., et al. (2021). Comprehensive circRNA expression profile and construction of circRNAs-related ceRNA network in a mouse model of autism. *Front. Genet.* 11, 623584. doi:10.3389/fgene.2020.623584

Wang, P. L., Bao, Y., Yee, M.-C., Barrett, S. P., Hogan, G. J., Olsen, M. N., et al. (2014). Circular RNA is expressed across the eukaryotic tree of life. *PLOS ONE* 9 (3), e90859. doi:10.1371/journal.pone.0090859

Wang, X., Xie, J., Tan, L., Lu, Y., Shen, N., Li, J., et al. (2023). N6-methyladenosine-modified circRIMS2 mediates synaptic and memory impairments by activating GluN2B ubiquitination in Alzheimer's disease. *Transl. Neurodegener.* 12 (1), 53. doi:10.1186/s40035-023-00386-6

Wang, Y., Liu, J., Ma, J., Sun, T., Zhou, Q., Wang, W., et al. (2019). Exosomal circRNAs: biogenesis, effect and application in human diseases. *Mol. Cancer* 18 (1), 116. doi:10.1186/s12943-019-1041-z

Welden, J. R., Margvelani, G., Arizaca Maquera, K. A., Gudlavalleti, B., Miranda Sardón, S. C., Campos, A. R., et al. (2022). RNA editing of microtubule-associated protein tau circular RNAs promotes their translation and tau tangle formation. *Nucleic Acids Res.* 50 (22), 12979–12996. doi:10.1093/nar/gkac1129

Wu, W., Ji, P., and Zhao, F. (2020). CircAtlas: an integrated resource of one million highly accurate circular RNAs from 1070 vertebrate transcriptomes. *Genome Biol.* 21 (1), 101. doi:10.1186/s13059-020-02018-y

Wu, W., Zhang, J., Cao, X., Cai, Z., and Zhao, F. (2022). Exploring the cellular landscape of circular RNAs using full-length single-cell RNA sequencing. *Nat. Commun.* 13 (1), 3242. doi:10.1038/s41467-022-30963-8

Wu, Y. E., Parikshak, N. N., Belgard, T. G., and Geschwind, D. H. (2016). Genome-wide, integrative analysis implicates microRNA dysregulation in autism spectrum disorder. *Nat. Neurosci.* 19 (11), 1463–1476. doi:10.1038/nn.4373

Xin, J., Zhang, X.-Y., Sun, D.-K., Tian, L.-Q., and Xu, P. (2019). Up-regulated circular RNA hsa_circ_0067934 contributes to glioblastoma progression through activating

PI3K-AKT pathway. *Eur. Rev. Med. Pharmacol. Sci.* 23 (8), 3447–3454. doi:10.26355/eurrev_201904_17709

Yao, G., Niu, W., Zhu, X., He, M., Kong, L., Chen, S., et al. (2019). hsa_circRNA_104597: a novel potential diagnostic and therapeutic biomarker for schizophrenia. *Biomarkers Med.* 13 (5), 331–340. doi:10.2217/bmm-2018-0447

You, X., Vlatkovic, I., Babic, A., Will, T., Epstein, I., Tushev, G., et al. (2015). Neural circular RNAs are derived from synaptic genes and regulated by development and plasticity. *Nat. Neurosci.* 18 (4), 603–610. doi:10.1038/nn.3975

Yu, X., Fan, Z., Yang, T., Li, H., Shi, Y., Ye, L., et al. (2024). Plasma circRNA HIPK2 as a putative biomarker for the diagnosis and prediction of therapeutic effects in major depressive disorder. *Clin. Chim. Acta* 552, 117694. doi:10.1016/j.cca.2023.117694

Zajaczkowski, E. L., Zhao, Q., Liau, W.-S., Gong, H., Madugalle, S. U., Periyakaruppiah, A., et al. (2023). Localised Cdr1as activity is required for fear extinction memory. *Neurobiol. Learn. Mem.* 203, 107777. doi:10.1016/j.nlm.2023.107777

Zhang, B., Zhang, H., Wang, Z., Cao, H., Zhang, N., Dai, Z., et al. (2024). The regulatory role and clinical application prospects of circRNA in the occurrence and development of CNS tumors. *CNS Neurosci. and Ther.* 30 (4), e14500. doi:10.1111/cns.14500

Zhang, Y., Du, L., Bai, Y., Han, B., He, C., Gong, L., et al. (2020). CircDYM ameliorates depressive-like behavior by targeting miR-9 to regulate microglial activation via HSP90 ubiquitination. *Mol. Psychiatry* 25 (6), 1175–1190. doi:10.1038/s41380-018-0285-0

Zhang, Y., Huang, R., Cheng, M., Wang, L., Chao, J., Li, J., et al. (2019). Gut microbiota from NLRP3-deficient mice ameliorates depressive-like behaviors by regulating astrocyte dysfunction via circHIPK2. *Microbiome* 7 (1), 116. doi:10.1186/s40168-019-0733-3

Zhao, J., Li, Q., Hu, J., Yu, H., Shen, Y., Lai, H., et al. (2024). Circular RNA landscape in extracellular vesicles from human biofluids. *Genome Med.* 16 (1), 126. doi:10.1186/s13073-024-01400-w

Zhao, S.-Y., Wang, J., Ouyang, S.-B., Huang, Z.-K., and Liao, L. (2018). Salivary circular RNAs Hsa_Circ_0001874 and Hsa_Circ_0001971 as novel biomarkers for the diagnosis of oral squamous cell carcinoma. *Cell. Physiology Biochem. Int. J. Exp. Cell. Physiology, Biochem. Pharmacol.* 47 (6), 2511–2521. doi:10.1159/000491624

Zhong, C., Yu, S., Han, M., Chen, J., and Ning, K. (2017). Heterogeneous circRNA expression profiles and regulatory functions among HEK293T single cells. *Sci. Rep.* 7 (1), 14393. doi:10.1038/s41598-017-14807-w

Zimmerman, A. J., Hafez, A. K., Amoah, S. K., Rodriguez, B. A., Dell'Orco, M., Lozano, E., et al. (2020). A psychiatric disease-related circular RNA controls synaptic gene expression and cognition. *Mol. Psychiatry* 25 (11), 2712–2727. doi:10.1038/s41380-020-0653-4

Zimmerman, A. J., Weick, J. P., Papageorgiou, G., Mellios, N., and Brigman, J. L. (2024). Aberrant encoding of event saliency in the orbitofrontal cortex following loss of the psychiatric-associated circular RNA, circHomer1. *Transl. Psychiatry* 14 (1), 480–514. doi:10.1038/s41398-024-03188-0

frontiers | Frontiers in Oncology

TYPE Review
PUBLISHED 04 July 2025
DOI 10.3389/fonc.2025.1549046

Check for updates

OPEN ACCESS

EDITED BY
Chiara De Santi,
Royal College of Surgeons in Ireland, Ireland

REVIEWED BY
Anna Lucia Tornesello,
G. Pascale National Cancer Institute Foundation (IRCCS), Italy
Xiaolin Wang,
University of Science and Technology of China, China

*CORRESPONDENCE
Surajit Pathak
drsurajitpathak@care.edu.in;
drsurajitpathak@gmail.com
Asim K. Duttaroy
a.k.duttaroy@medisin.uio.no

RECEIVED 20 December 2024
ACCEPTED 18 June 2025
PUBLISHED 04 July 2025

CITATION
Nambidi S, Shruthi KB, Kanimozhe SP, Banerjee A, Kondaveeti SB, Duttaroy AK and Pathak S (2025) A review of circular RNAs in colorectal cancer: insights into biomarker discovery and therapeutic targeting. *Front. Oncol.* 15:1549046. doi: 10.3389/fonc.2025.1549046

COPYRIGHT
© 2025 Nambidi, Shruthi, Kanimozhe, Banerjee, Kondaveeti, Duttaroy and Pathak. This is an open-access article distributed under the terms of the Creative Commons Attribution License (CC BY). The use, distribution or reproduction in other forums is permitted, provided the original author(s) and the copyright owner(s) are credited and that the original publication in this journal is cited, in accordance with accepted academic practice. No use, distribution or reproduction is permitted which does not comply with these terms.

A review of circular RNAs in colorectal cancer: insights into biomarker discovery and therapeutic targeting

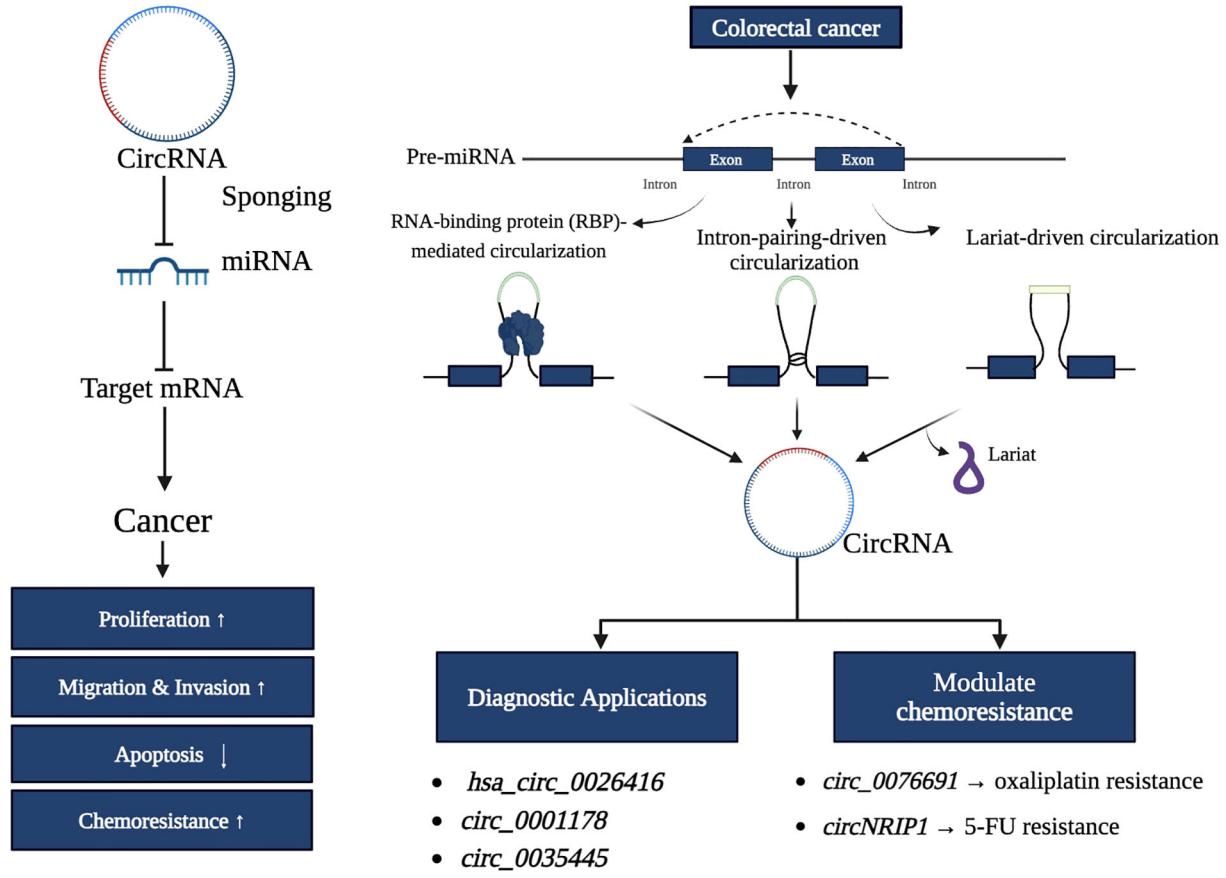
Sibin Nambidi[1], Karunakaran Bhuvaneswari Shruthi[1], Sujatha Padmanaban Kanimozhe[1], Antara Banerjee[1], Suresh Babu Kondaveeti[2], Asim K. Duttaroy[3*] and Surajit Pathak[1*]

[1]Medical Biotechnology Lab, Faculty of Allied Health Sciences, Chettinad Academy of Research and Education (CARE), Chettinad Hospital and Research Institute (CHRI), Chennai, India, [2]Department of Biochemistry, Symbiosis Medical College For Women, Symbiosis International (Deemed University), Pune, India, [3]Department of Nutrition, Institute of Basic Medical Sciences, Faculty of Medicine, University of Oslo, Oslo, Norway

Colorectal cancer (CRC) is one of the most common cancers, with an incidence that has increased significantly over the last 20 years. The World Health Organization (WHO), under its cancer program, identifies CRC as the third most prevalent cancer worldwide with a high mortality rate, especially in patients under the age of 50. Despite advances in surgery, chemotherapy, radiotherapy, and molecular targeted therapy, CRC shares a low survival rate and poor prognosis due to late diagnosis. To address these challenges, research into alternative diagnostic and therapeutic strategies has increasingly focused on molecular mechanisms, including noncoding RNAs (ncRNAs). Circular RNAs (circRNAs), a subclass of endogenous ncRNAs characterized by their covalently enclosed loop structure, demonstrate greater stability than linear RNAs, making them potential candidates for clinical applications. The circRNAs possess differential expressions in cancers and function as tumor suppressive or oncogenic activities. This review discusses the recent findings on circRNAs and their potential for biomarkers and therapeutic targets in CRC. As circRNAs can serve as miRNA sponges, increase or decrease mRNA expression, and function to regulate an oncogenic or tumor suppressor pathway, there may be the possibility for an early diagnosis, prognosis, or therapeutic role of circRNAs in CRC. Highlighting the clinical implications of circRNAs, this review discusses their potential to transform current CRC management strategies and address critical gaps in timely diagnosis and effective treatment. It also emphasized the need for further clinical research to validate their utility and translate these findings into practice.

KEYWORDS

colorectal cancer, circular RNA, noncoding RNA, diagnosis, biomarker, prognosis, miRNA sponges



GRAPHICAL ABSTRACT

1 Overview of the CRC

Colorectal cancer (CRC) is the third most commonly diagnosed cancer and continues to be a leading cause of cancer-related deaths (1). In 2020, there were approximately 1.93 million new cases of CRC reported globally, resulting in nearly 0.94 million deaths. The projected number of new CRC cases worldwide will be 3.2 million by 2040 (2). The development of CRC is influenced by various interactions between genetic and environmental factors, including nutrition, diet, physical inactivity, insulin-like growth factors, and supplements (3). About 20% of colon or rectal tumors are believed to emerge from an inherited mutation in genetic code, including familial adenomatous polyposis (FAP), hereditary non-polyposis 5colorectal cancer (HNPCC), and tumors with a significant family history (4, 5). Obesity has also been shown to be a considerable risk factor in CRC development, and studies repeatedly show that physically inactive individuals are possibly prone to CRC (6). A diet high in protein, red meat, and alcohol and low in fruits, vegetables, and dairy foods further enhances CRC risk. Johnson C.M., et al. (2013) performed a meta-analysis. He summarized a number of modifiable risk factors for CRC incidence, which included higher BMI, cigarette smoking, red meat intake, low fruit and vegetable intake, post-menopausal hormone therapy, and inflammatory bowel disease (IBD) (7).

Early diagnosis is crucial for improving patient outcomes and overall survival rates in CRC (8). As such, discovering new biomarkers and developing better treatment strategies are essential because they will allow for early detection, personalized treatment, and ultimately better management of CRC for better prognoses and quality of life (8). The Centers for Disease Control and Prevention estimates that in 2024, there will be about 97,220 new colon cancer cases and about 43,030 new rectal cancer cases diagnosed in the United States (9). However, the incidence of CRC has been declining for the last few decades. The incidence rate in the United States went from 60.5 cases per 100,000 in 1976 to 46.4 in 2005, and 40.7 between 2009 and 2013 (9). Although this overall trend does not hold for younger populations, between 2003 and 2012, the incidence of CRC declined by approximately 3% annually, and the overall mortality decreased by 51% from its peak in 1976 until 2014. Overall, this progress can mainly be attributed to increased detection via screening and improved therapeutic interventions (9).

It is predicted that in the United States, the incidence rates for colon and rectal cancer for people ages 20–34 years could increase by 90% and 124%, respectively, by the year 2030. For people ages 35–49 years, incidence rates could increase by 27.7% and 46%, respectively (10, 11). CRC is most prevalent in industrialized countries, but incidence rates are rising in low and middle-

income countries due to the growing propensity to adopt Western dietary and lifestyle measures (12). The highest incidence rates by country are Australia and New Zealand, followed by European countries and North America (12). Central Eastern Europe demonstrates some of the highest mortality rates for any cancer. Conversely, South Asia and Africa display the lowest incidence and mortality rates but face higher mortality-to-incidence ratios due to a lack of access to screenings and treatments (12). In Italy, CRC incidence increased among men from 30 to 70 per 100,000 between 1970 and 2010, while among women, incidence rates stabilized at approximately 38 per 100,000 in the late 1990s (13). Colon cancer (CC) is more common than rectal cancer (RC) in developed countries, though markedly more common among women (14). Thus, CC is more prevalent than RC (ratios as high as 2 or 3:1). In Europe, there are more than 250,000 new cases of CC each year, corresponding to around 9% of cases diagnosed yearly. Urbanization and industrialization have been key contributors to the increasingly high incidence of CRC cases in developed countries (14, 15). Globally, CRC incidence remains low in Africa and Asia. North America, Europe, and Australia are considered high-risk regions, while Central and South America, Asia, and Africa are classified as low-risk areas (16, 17). CRC prevalence significantly increases with age, rising from approximately 20 cases per 100,000 per year in individuals aged 45–54 years to 55 per 100,000 in those aged 55–64 years, 150 per 100,000 in the 65–74 age group, and 250 per 100,000 among individuals over 75 years (18). CRC survival rates have improved over time, especially in Europe, but with important regional discrepancies; for example, by the late 1990s, the five-year survival rate rose to 54%, although the rate was notably lower in Europe than the higher reported rates in the US (19, 20). The incidence of CRC in Italy in the North was double compared with the South in men and women (21, 22).

Adenocarcinoma is the predominant histological type of colon cancer and makes up 92–95% of tumors in the bowel. Mucinous or colloid adenocarcinomas make up about 17% of tumors in the bowel (23). The rare epithelial cancers (adeno-squamous carcinomas and squamous cell carcinomas (adenoacanthoma) are rarely seen. CRC lesions are assessed for differentiation (well, moderate, poorly), and differentiation is assessed via standard glandular morphology and cytology (23). Poorly differentiated cancers tend to carry a worse prognosis, often secondary to genetic defects, but it is unclear what mutations correlate with this differentiation. Recognizable differentiation was absent in 20–25% of colon malignancies. Polyps, commonly designated precursor lesions for CRC, are mainly recognized in the lower GI tract, the rectum or appendix, but can happen anywhere in the colon (24). Recent developments in the molecular pathophysiology of CRC have led to the opportunity to identify several aspects that can be considered as potential biomarkers, genetic as well as epigenetic and protein-based markers from fecal, serum, and tissue samples. Some examples of key research areas include DNA methylation, microRNAs, circular RNAs, long non-coding RNAs, and exosomes (25).

Although various imaging techniques are available, CT imaging remains the most widely accessible, reliable, and versatile tool for cancer staging and assessing local tumor characteristics (26). While PET/CT colonography, a combination of PET and CT imaging, has also shown great potential for cancer detection and staging. Its proficiency in identifying metastatic lymph nodes is of particular importance in rectal cancer management, in which it is more common for patients to undergo preoperative treatment with node-positive disease (27). Sigmoidoscopy and colonoscopy are utilized extensively for both screening and diagnostic purposes (28). The current most utilized diagnostic biomarker for CRC is the fecal immunochemical test (FIT), the foundation of population-based CRC screening programs intended to reduce CRC mortality (29). Fecal immunochemical tests are also used to diagnose in symptomatic patients and to perform surveillance following adenoma removal (30). FIT's ability to detect human hemoglobin in stool using antibodies and without necessitating dietary restrictions results in greater participation in screening programs (31). The guaiac fecal occult blood test (g-FOBT) is another commonly utilized method for detecting blood in stool and is a chemical test that relies on peroxidase activity. g-FOBT tests are inexpensive, relatively easy to perform, and readily available (32). Many randomized controlled studies have shown that g-FOBT tests can decrease CRC mortality rates due to tumors being identified earlier. However, there is concern that g-FOBT tests with limited sensitivity for detecting colorectal adenomas may fail to prevent the onset of CRC (33).

Choosing an appropriate therapeutic strategy and determining the dosing regimen continue to be a large challenge in cancer therapy. For CRC, there are different modes of treatment, including surgical intervention, cryosurgery, chemotherapy, radiation therapy, and targeted therapies (34). Physicians use chemotherapy most frequently, which is the administration of different drugs that block cancer cell growth. Still, often, these agents have adverse effects like chemotherapy-induced leukopenia, fatigue, palmar-plantar erythrodysesthesia, chemotherapy-induced gastrointestinal toxicity, chemotherapy-induced oral mucositis, nausea, vomiting, aches, anemia, hematologic complications, and liver impairment (35). Side effects diminish the quality of life, lessen the efficacy of treatment, and cause drug resistance over time. Surgical intervention remains the most essential treatment for CRC, addressing approximately 50% of cases successfully, where recurrence of the cancer after surgery remains one major limitation, leading to poor outcomes and often causing death (34, 35). Even with early detection and treatment advances, patient clinical outcomes remain unfavorable. While radiation and chemotherapy are standard approaches, these methods of treatment have limitations, reinforcing the need for more efficient alternative therapies. As a result, there are more efforts to establish molecular biomarkers for diagnostic and therapeutic purposes (35). There is an urgent need to develop better diagnostic and therapeutic approaches while understanding the molecular mechanisms of CRC progression (36).

2 Role of CircRNAs

The first single-stranded, covalently closed circRNAs were identified in human HeLa cells using electron microscopy in 1979

(37). Subsequent research revealed that numerous species, including viruses, prokaryotic cells, single-celled eukaryotes, and mammals, have evolved to produce circular forms of RNA. High-throughput RNA sequencing and bioinformatics analyses have established circRNAs as a ubiquitous component of the human transcriptome, present across many metazoans (38). CircRNAs exhibit greater stability than linear RNAs due to their resistance to RNases (39). This inherent stability and distinct expression patterns have established circRNAs as biomarkers and potential therapeutic targets, particularly in cancer (39). CircRNAs perform diverse cellular functions, including serving as protein scaffolds, miRNA sponges, and templates for polypeptide translation (40). Despite their biological significance, the precise mechanisms underlying their aberrant expression in diseases such as cancer remain incompletely understood. CircRNAs regulate physiological and pathological processes through interactions with cellular components, often indirectly modulating gene expression. For instance, circRNAs can act as competitive endogenous RNAs (ceRNAs) by sequestering miRNAs, freeing mRNA targets, and influencing critical signaling pathways (40).

Detection and quantification of circRNAs involve northern blotting, RT-qPCR with divergent primers, RNA sequencing (RNA-seq), circRNA profiling, and *in situ* hybridization targeting the back-splice junction (41). While advances in RNA sequencing technologies have enhanced circRNA identification, challenges remain, such as distinguishing circular from linear transcripts and elucidating their biological roles (42). CDR1as, the antisense transcript of CDR1, a circRNA, was among the first circRNAs investigated for its functional significance. Recent findings indicate that CDR1 interacts with p53 to inhibit pro-metastatic activities by preventing its binding to MDM2 (42). This interaction highlights the ability of circRNAs to influence key regulatory proteins, underscoring their profound potential in tumor biology. The diverse function of CircRNA is represented in Figure 1.

2.1 Classification and types of circRNAs

Depending on their genomic origin, circRNAs are organized into various categories: exonic circ RNAs (ecircRNAs), intronic circRNAs (ciRNAs), exon-intron circRNAs (EI ciRNAs), intergenic circRNAs, and tRNA-derived circRNAs (triRNAs) (43). Exonic circRNAs are derived from the exonic sequences of protein-coding genes. They are primarily cytoplasmic, often acting as miRNA sponges to impact gene expression in the post-transcriptional phase (44). Intronic circRNAs are formed at in the intronic region and are located in the nucleus, with ciRNAs being reported to regulate transcription. Exon-intron circRNAs are formed from the components of both exons and introns and can exist in both nuclear and cytoplasmic compartments. The functionality of exon-intron circRNAs is variable in their precise composition and cellular location (43, 44). Intergenic circRNAs originate from non-coding genome regions between annotated genes and can act as a further regulatory layer. Furthermore, a subset of circRNAs is thought to come from tRNA sequences called triRNAs (44). These circRNA subtypes involve different cellular biology processes, including gene regulation and protein interactions. They are potentially relevant to the pathology of many human diseases, indicating their biological and clinical significance (44, 45).

The ecircRNAs, intronic circRNAs, and EIciRNAs are diverse in their cellular localization and functions (45). EcircRNAs are often cytoplasmic and serve primarily as miRNA sponges, sequestering these regulatory miRNAs from influencing their mRNA targets (45). On the other hand, ciRNAs and EIciRNAs are predominatly located within the nucleus and regulate their parental genes transcriptionally. CirRNAs can interact with RNA polymerase II and transcription factors to regulate expression and EIciRNAs not only regulate transcription of their source genes but also interact with RNA polymerase II and the U1 snRNP complex, indicating a role in transcriptional activation (46, 47).

2.2 Biogenesis of circRNAs

Since circRNAs are formed from pre-mRNAs, the standard spliceosome machinery may also regulate their synthesis. The biogenesis of circRNAs and their mechanisms of action remain incompletely understood. While exon skipping is considered a key regulator of circRNA production through alternative splicing, the exact primary process driving circRNA generation has yet to be determined (48). Three distinct theories have been proposed to explain the synthesis of exonic circRNAs, which are the dominant type in eukaryotes: Lariat-driven circularization (exon skipping), Intron-pairing-driven circularization (back splicing), and RNA-binding protein (RBP)-mediated circularization (24).

In exon skipping, non-canonical 'back splicing' processes are thought to occur during RNA synthesis. For instance, an early study on the human cytochrome P450 2C18 gene reported a connection between exon skipping and circular RNA isoforms, identifying four alternative circularization patterns and their associated exon-skipped transcripts (49). Back splicing involves a bridging mechanism that reduces the distance between the splice sites of neighboring introns, facilitating the formation of circRNAs. Additionally, the splicing process utilizes specific elements, such as an 11-nucleotide GU-rich sequence at the 5′ splice site and a 7-nucleotide C-rich element at the 3′ branch point of introns, which promote circRNA synthesis (34, 49). A study by Li et al. (2024) identified ZC3H14, a conserved RNA-binding protein, as a new regulator of circRNA biogenesis. ZC3H14 promotes back-splicing binding at exon-intron boundaries (EIBs) and 3' untranslated regions (UTRs) to encourage recruitment of the spliceosome by dimerization (50). Furthermore, ZC3H14 does not directly impact BSS–3'UTR distance, suggesting that ZC3H14 may play a prominent post-transcriptional silencing role in regulating circRNA biogenesis. The strong binding of ZC3H14 at 3'UTRs stabilizes the interaction with EIBs, bringing splice sites closer and increasing the likelihood of circularization (50). Therefore, these findings expand the current knowledge about the regulation of circRNA biogenesis beyond the previously defined intronic repeat

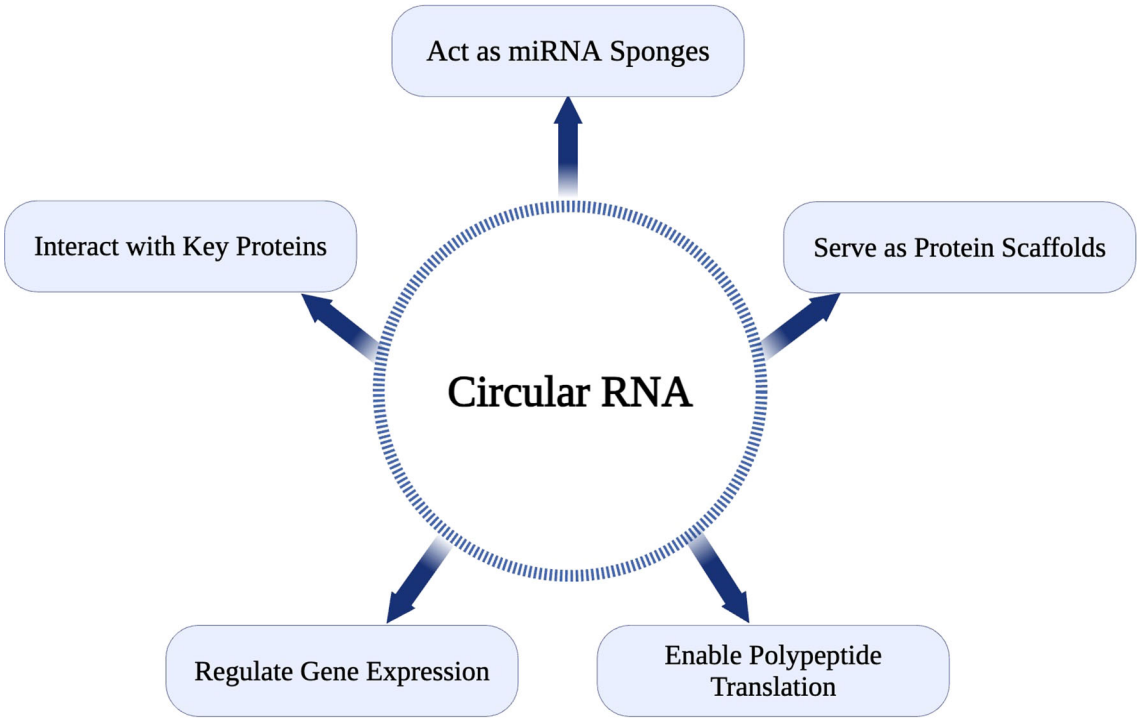


FIGURE 1
Functional roles of circRNAs in cellular processes.

element (50). Figure 2 illustrates the process of pre-mRNA to circRNA, incorporating the spliceosome machinery and three primary circularization mechanisms: RNA-binding protein-mediated circularization, intron-pairing circularization, and lariat circularization. In the lariat circularization mechanism, exon-skipping gives rise to a lariat that is further processed into circRNA. These mechanisms facilitate back-splicing, resulting in covalently stabilized or closed circRNAs forming.

It was recently discovered that circRNAs are formed through a back-splicing event during pre-mRNA processing. CircRNAs are considered a specialized product of RNA processing, where spliceosome activity preferentially removes introns from the ring region (51). Unlike canonical splicing, which joins exons linearly, back-splicing covalently links a downstream 5′ splice site to an upstream 3′ splice site, forming a stable circular structure (52). CircRNAs play critical roles in CRC, influencing cell growth, invasion, movement, and apoptosis. Depending on the context, they can function as tumor suppressors or oncogenes (53). This dual functionality is shaped by their interactions with miRNAs, RNA-binding proteins, and chromatin regulators. For example, circRNAs bind and sponge oncogenic or tumor-suppressive miRNAs, thereby modulating the expression of downstream target genes involved in key oncogenic pathways. This miRNA sponge activity regulates gene expression and contributes to chemoresistance and metastasis in CRC (54, 55). Figure 3 illustrates the processing pathways for generating linear mRNA and circRNA from a single pre-mRNA molecule. Canonical splicing produces linear mRNA by joining exons in a sequential order.

3 Role of circRNA in CRC diagnosis

CircRNAs are a significant diagnostic biomarker due to their conservative nature, abundance, and tissue-specificity (56). Two RNA types are contained in the circRNA-microRNA code, and they work together to control the expression of genes. As a result, cancer can be predicted early (57). circRNAs have potential use in monitoring therapy effectiveness and determining cancer prognosis (58). Understanding circRNAs and their expression patterns could eventually result in the development of biomarkers for cancer diagnosis, including colon, breast, gastric, lung, and hepatocellular carcinoma (58). Figure 4 shows the systematic workflow for discovering biomarkers using circRNAs and developing diagnostic tools. The first phase consists of subject sample collection, RNA extraction including circRNAs, and then circRNA profiling using RNA sequencing (RNA-Seq) or circRNA microarrays. Candidate circRNA biomarkers are identified based on their differential expression profiles and clinical relevance for potential use as a diagnostic or prognostic tool. The clinical samples from which circRNA biomarkers were selected will be used to undergo clinical evaluation for their diagnostic or prognostic potential.

CircRNAs play a significant role in the initiation and progression of cancer. The formation of circRNAs is believed to result from the binding of RNA-binding proteins and specific repeating sequences in the introns adjacent to the circularizing exons (59). CircRNAs are thought to influence cancer development through multiple mechanisms, including interacting with proteins, sponging miRNAs, altering gene transcription or splicing, and even translating into

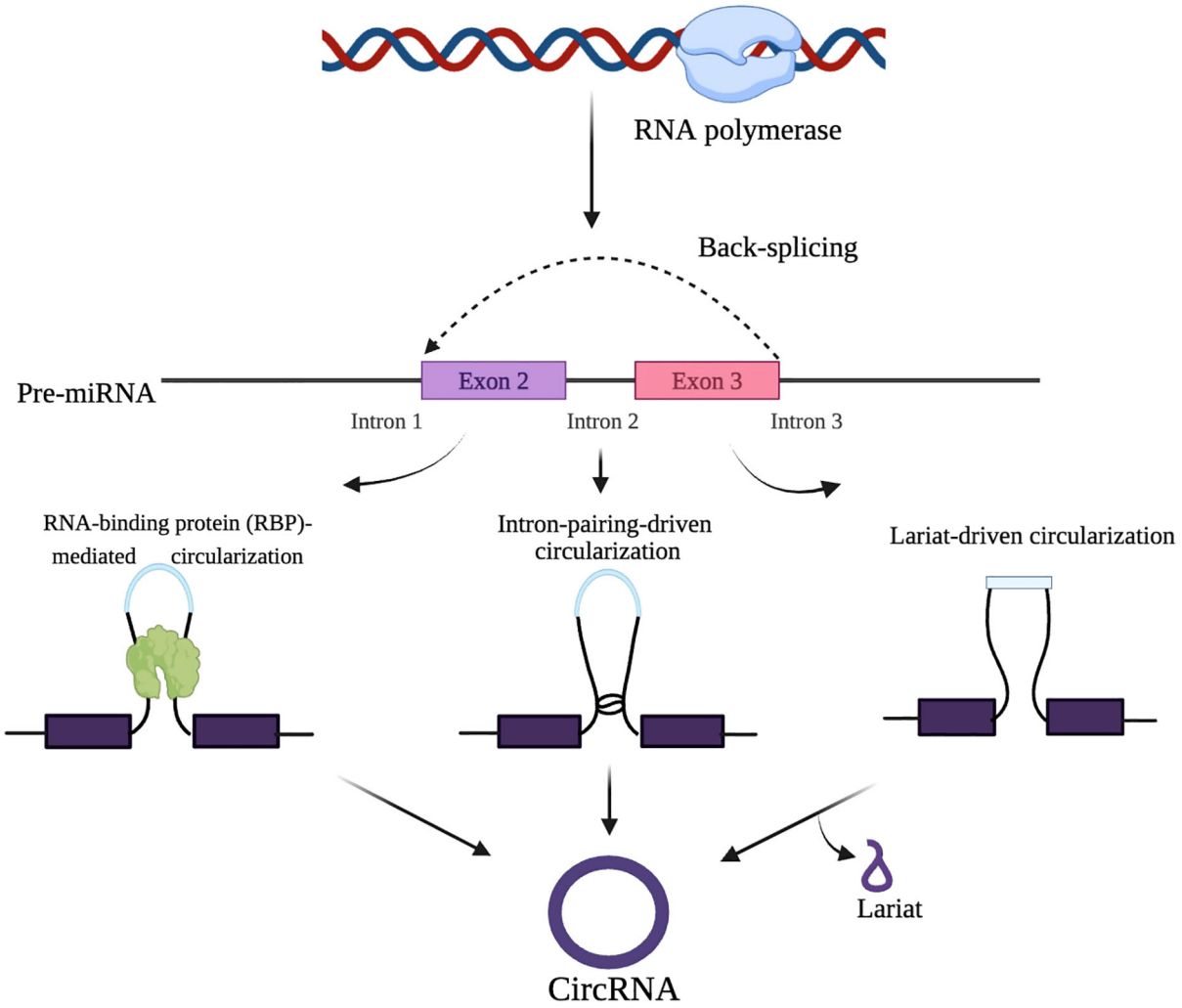


FIGURE 2
Mechanisms of circRNA biogenesis. CircRNAs are formed through the back-splicing of precursor mRNA via RNA-binding proteins, intron pairing, or lariat-driven circularization.

proteins or short peptides (60). Abnormal expression patterns of circRNAs have been linked to the development of various human malignancies, including colon cancer. Several circRNAs have been identified as abnormally expressed in CRC tissues, regulating carcinogenesis (61). The circRNA circPPP1R12A is highly expressed in CRC patient tissues, and its overexpression correlates with a lower life expectancy (62). Similarly, CRC tissues show overexpression of circPIP5K1A, which promotes cell proliferation and invasion while reducing the expression of the corresponding protein, thereby impairing cell viability. Consequently, circPIP5K1A enhances colon oncogenesis by blocking miR-1273a. Furthermore, higher circCTIC1 expression in CRC tissues has been associated with poor tumor prognosis. CircRNAs can regulate gene expression at multiple levels, as seen in their potential to be translated into peptides or proteins (63).

circRNAs play a pivotal role in CRC progression by interacting with various proteins and miRNAs, thereby influencing key tumorigenic processes such as proliferation, migration, invasion, and epithelial-mesenchymal transition (63). These molecules serve as critical regulators of gene expression, acting as sponges for specific miRNAs, and participate in modulating signaling pathways associated with cancer progression (64). For instance, circ-0053277, significantly upregulated in CRC tissues, functions as a sponge for miR-2467-3p. By sequestering miR-2467-3p, circ-0053277 enhances cell migration, proliferation, and EMT, contributing to increased metastatic potential and poorer clinical outcomes in CRC patients (65). These findings highlight circ-0053277's role as an oncogenic factor, underscoring its potential as a therapeutic target. Thus, inhibiting circ-0053277 could offer novel strategies to reduce metastatic spread and improve patient prognosis, especially in advanced CRC (64, 65).

Similarly, hsa_circ_0026416 is another circRNA overexpressed in CRC tissues and plasma, acting as a sponge for miR-346 (66). Functional studies have demonstrated its role in promoting CRC growth in both *in vivo* and *in vitro* models, emphasizing its contribution to tumorigenesis. Importantly, detecting hsa_circ_0026416 in plasma positions it as a promising non-invasive

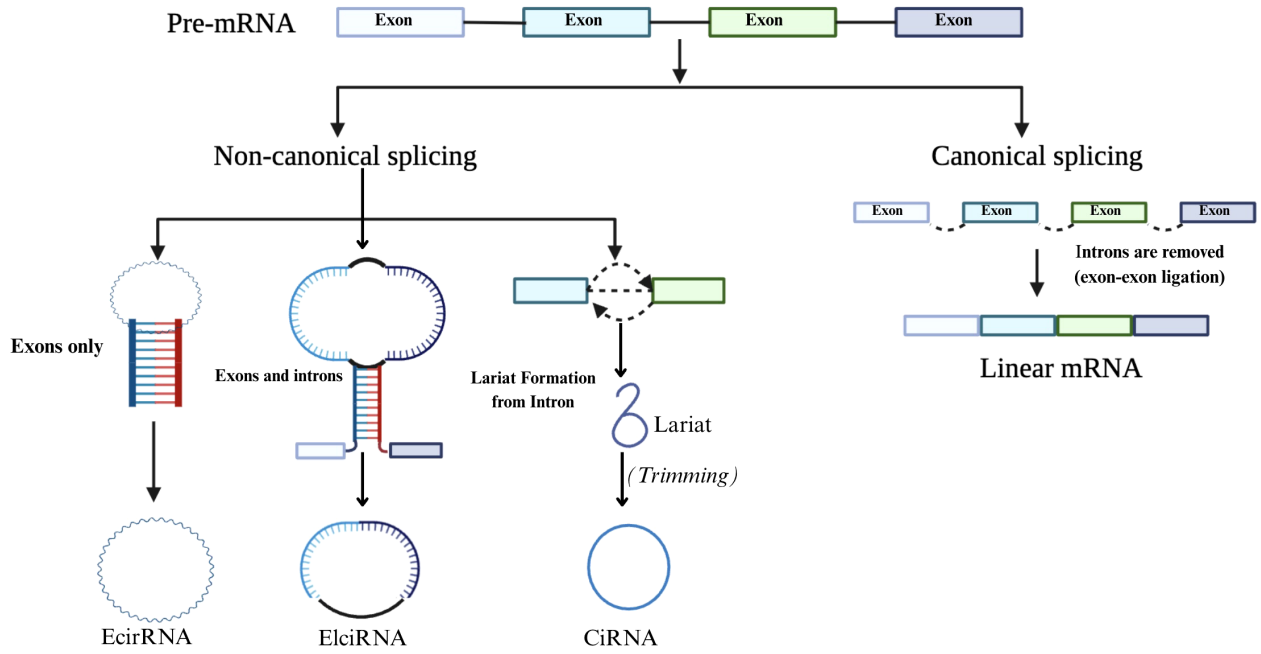


FIGURE 3
Canonical and non-canonical splicing pathways. Pre-mRNA undergoes canonical splicing to form linear mRNA, or non-canonical splicing to generate circRNAs such as EciRNA, ElciRNA, and CiRNA via different circularization mechanisms.

biomarker. Its potential use in liquid biopsies offers opportunities for early diagnosis, real-time disease monitoring, and personalized therapeutic interventions (66). Additionally, circ-000166 exhibits elevated expression levels in human CRC tissues and colon cancer cell lines (67). This circRNA has been implicated in aggressive cancer behaviors, including enhanced cell migration and invasion, making it a potential target for therapeutic intervention (67). Given its association with advanced CRC stages, targeting circ-000166 could be particularly beneficial for managing aggressive and treatment-resistant cases (67). Collectively, circRNAs demonstrate multifaceted roles in CRC pathogenesis, acting as oncogenic regulators and potential diagnostic or therapeutic targets. Their interactions with miRNAs and proteins, coupled with their detectability in tissues and bodily fluids, establish circRNAs as integral components in the molecular aspect of CRC. Future research focusing on the therapeutic targeting and diagnostic utility of circRNAs, such as Circ-0053277, hsa_circ_0026416, and circ-000166, could pave the way for innovative approaches to CRC management (68).

4 Therapeutic uses of circRNAs in CRC

CircRNAs are emerging as critical regulators in oncogenic molecular pathways, interacting with diverse molecules such as miRNAs and lncRNAs (69). Their ability to influence gene expression and cellular behaviors positions them as significant contributors to tumorigenesis and as potential biomarkers for cancer diagnosis and prognosis (54). Specific circRNAs such as circCCDC66 and ciRS-7 have been identified as prognostic biomarkers in CRC. CircCCDC66 is significantly overexpressed in CRC samples and is closely linked to poor patient prognosis (69). Functional analyses reveal that circCCDC66 modulates key oncogenic processes, including cell proliferation, anchorage-independent growth, invasion, and migration, underscoring its pivotal role in CRC progression (69).

A novel diagnostic biomarker for CRC is serum exosomal circRNA, specifically hsa_circ_0004771, which has been detected in CRC patients. Comparative analysis has revealed 39 differentially expressed circRNAs in CRC tissues, with 28 downregulated and 11 upregulated (70). Such distinct expression patterns highlight the potential utility of circRNAs in differentiating CRC from normal tissue. Another circRNA, CircFADS2, derived from the human FADS2 gene, has been strongly correlated with clinicopathological features in CRC. CircFADS2 is highly expressed in over 187 CRC tissue samples, making it a promising candidate for prognostic research (71). Conversely, hsa_circ_0026344 exhibits significantly reduced expression in CRC tissues compared to adjacent non-tumorous tissues (72). It regulates miR-21 and miR-31, suppressing CRC cell growth and adherence while inducing apoptosis. These findings suggest hsa_circ-0026344's potential as a tumor suppressor and a therapeutic agent in CRC (72).

CircRNAs also influence chemoresistance in CRC through miRNA sponging. For example, ciRS-7 (circular RNA sponge for miR-7) has been associated with advanced T-stage, lymph node involvement, and distant metastases (73). Its overexpression activates the EGFR/RAF1/MAPK pathway by inhibiting miR-7 activity, highlighting its oncogenic role and potential as a therapeutic target (73). Another circRNA, CircPTK2, promotes EMT and metastasis in CRC cells by binding to vimentin, a key

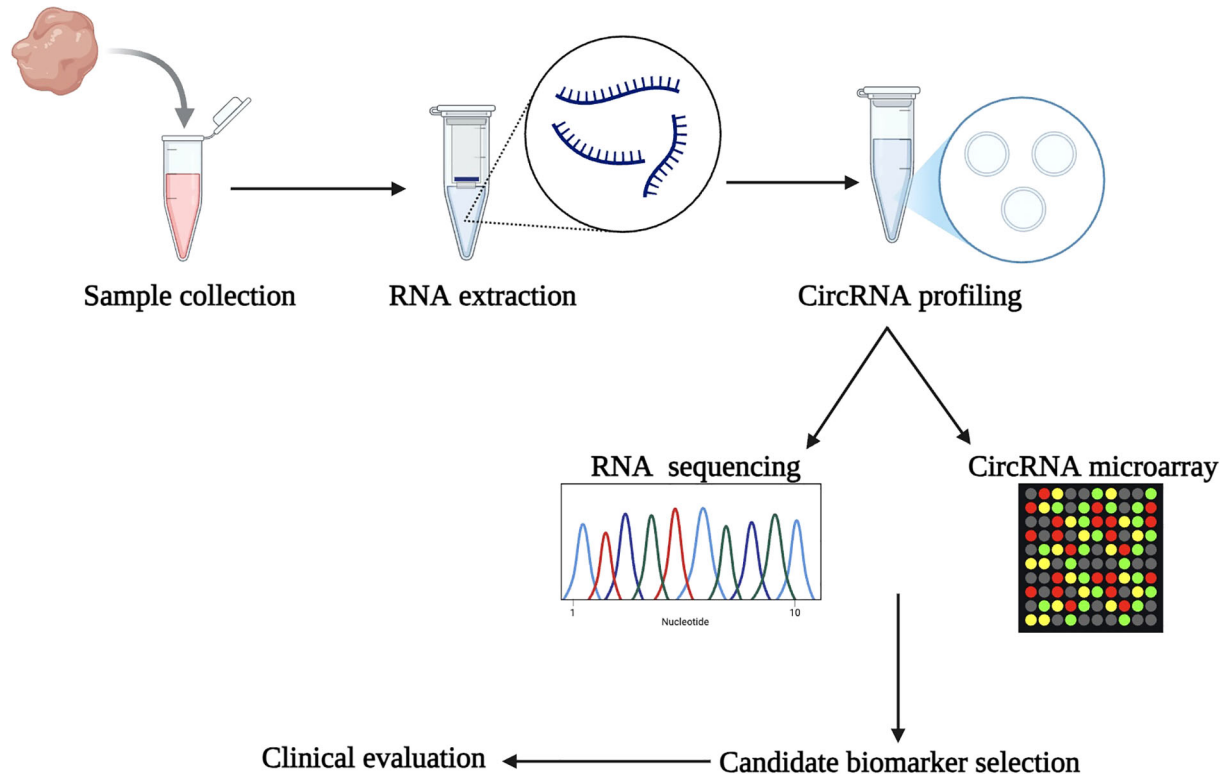


FIGURE 4
Workflow for circRNA biomarker discovery. The process begins with sample collection and RNA extraction, followed by circRNA profiling using RNA-Seq or circRNA microarrays. Candidate biomarkers are identified and evaluated clinically, leading to the development of diagnostic tools.

EMT regulator. Elevated CircPTK2 levels correlate with shorter survival rates, as Yang et al. (2020) reported, making it a potential target for metastasis control in CRC (74). Additionally, hsa_circ_0001649 has demonstrated oncogenic activity across various cancers, including liver, ovarian, and prostate cancers, underscoring its broader significance in malignancies (75). These circRNAs represent a multifaceted network of regulatory molecules that drive CRC progression and offer opportunities for innovative diagnostic, prognostic, and therapeutic strategies. Their involvement in EMT, drug resistance, and apoptosis regulation processes further strengthens their potential as crucial targets in CRC management (74, 75).

CircRNAs, known for their potential as microRNA sponges and competitive endogenous RNAs, are emerging as important factors in cancer biology (59). Despite their typically unstable expression in tumor cells, circRNAs have shown significant connections to cancer progression, particularly through interactions with miRNAs and proteins. Increased expression of CiRS-7 in CRC cells allows it to function as a microRNA sponge, sequestering miR-7 and upregulating its targets (76). This regulation affects the expression of epidermal growth factor receptors, which are pivotal in controlling cancer cell proliferation, differentiation, and signaling pathways (76). Additionally, a study by Chen et al. (2019) revealed that circNSUN2 with m6A mutation exhibited enhanced cytoplasmic export through YTHDC1 (41). Further findings demonstrated that the circNSUN2/IGF2BP2/HMGA2 RNA-protein ternary complex stabilized HMGA2 mRNA, facilitating CRC metastatic growth. These results highlight potential clinical and therapeutic implications of m6A modifications in circRNA biology (41).

Chang et al. (2023) demonstrated that introducing artificial circRNAs into mammalian cells promoted the expression of innate immunity-related genes, which protected the Venezuelan equine encephalitis virus (77). Similarly, many circRNAs with oncogenic miRNA and protein-binding sites have shown potential in restoring regulated cancer cell growth or inducing apoptosis (78). For example, circRNA0003906 exhibited diagnostic potential in CRC, with a study using an ROC curve to differentiate 122 CRC tissues from 40 healthy controls (79). In exosomal circRNAs, circPACRGL was significantly elevated in CRC cells, promoting proliferation, migration, and invasion. Meanwhile, circSLC7A6 acted as an apoptosis inhibitor and a regulator of CRC cell invasion and growth (80, 81).

Given the challenges of traditional screening methods, such as stool-based assays' low sensitivity and specificity, high colonoscopy costs, and limited global compliance, circRNAs represent a valuable alternative (82, 83). Numerous circRNAs have shown strong associations with clinicopathological features, underscoring their potential for guiding CRC prognosis and treatment decisions (84). CircRNAs like hsa_circ_0000504 have shown therapeutic promise in clinical practice, targeting miR-885-3p via the AKT signaling pathway (85). Collectively, circRNAs provide a multifaceted platform for advancing CRC diagnostics, prognostics, and

therapeutic interventions, offering hope for more effective and accessible patient care worldwide (64, 85).

Some circRNAs can discriminate between early and advanced CRC stages, indicating potential utility for staging cases and offering prognostic value (86). As a less invasive diagnostic tool, circRNAs may provide an alternative approach to CEA and better performance, e.g., CEA-sensitivity plus circRNA-specificity (87). Specific circRNAs have been associated with early and advanced disease, and circRNAs have roles in tumor growth, progression, and metastases (63). CircRNAs play roles in chemotherapy resistance and may modify a patient's response to treatment decisions and targeted therapies. They also have the potential to be a biomarker of predicting therapy response and monitoring disease progression (54). For example, circ-0084615 and circ-0006174 have influenced tumor growth and metastasis by sequestering microRNAs, while other circRNAs such as CDR1as and circHIPK3 influence CRC progression through sponging tumor-suppressing miRNAs, and promoting oncogenic signaling pathways (53). These research findings demonstrate the roles of circRNAs in CRC as a whole, but also find the potential application of circRNAs in CRC as a diagnostic, prognostic and therapeutic target (53, 54).

Oxaliplatin is a standard chemotherapeutic treatment for colon cancer, but there have been instances of therapeutic resistance, whose potential can be mediated by circRNAs (88). CircRNA hsa_circ_0076691 is overexpressed in oxaliplatin resistant colon cancer cells. It contributes to oxaliplatin resistance by acting as a molecular sponge for miR-589-3p, decreasing its available concentrations while upregulating its downstream target FGF9 (89). For instance, by sequestering miRNAs, circRNAs such as hsa_circ_0076691 adapt miRNA roles in normal regulatory networks controlling cell survival and apoptosis, which is vital for oxaliplatin-induced cytotoxicity. Consequently, circRNAs such as hsa_circ_0076691 can mitigate drug-induced apoptosis, allowing tumor cells to survive and promote chemoresistance (89). This further emphasizes their potential as therapeutic targets; e.g., by inhibiting circRNAs like hsa_circ_0076691, the sensitivity to oxaliplatin can be improved (89).

This is a similar scenario for circRNAs when it comes to 5-FU. 5-FU is an essential chemotherapeutic agent for colon cancer. The development of 5-FU resistance highly reduces its clinical utility, and circRNAs drive 5-FU resistance through direct or indirect mechanisms, particularly through regulating signaling pathways, sponging miRNA, or drug efflux (90). For example, overexpression of circNRIP1 promoted the progression of CRC, while its silencing sensitized CRC cells to 5-FU by sponging miR-532-3p (91). An additional circRNA, circACC1, was linked to increased AMPK activity (92). Increased AMPK activity contributes to increased resistance by promoting pro-survival signaling. Overall, circRNA have a significant involvement of circRNAs in chemotherapy drug resistance (92). Table 1 demonstrates various circRNAs identified in CRC, their sample types (e.g., blood, plasma, tissue) and their reported sensitivity and specificity as diagnostic biomarkers (93–100).

The ncRNAs, which include circRNAs, miRNAs, and lncRNAs, have become important candidates for diagnostic and prognostic biomarkers for CRC (101). CircRNAs are an exciting subclass of ncRNA that can be considered primarily due to their structure. CircRNAs form discrete covalently closed-loop structures, allowing increased stability and insensitivity to exonuclease digestion. Their half-life can be extremely long in circulation and is abundant compared to other RNA types (102). miRNAs can have distinct advantages for non-invasive cancer diagnostics, even though they are less stable than circRNAs. miRNAs are small, endogenous ncRNAs that regulate gene expression post-transcriptionally, and they are commonly dysregulated in colon cancer (103). Many miRNAs can be studied from body fluids like blood, stool, and urine to promote minimally invasive diagnostic screening and monitoring approaches. miRNAs can be considered tumor suppressors or oncogenes, where their expression levels have been shown to alter throughout stages of CRC development and disease progression (104). The long sequence and complex secondary structures of lncRNAs allows them to bind and interact with DNA, RNA, and proteins, influencing gene expression at the epigenetic, transcriptional, and post-transcriptional levels (105). Dysregulated lncRNAs are involved in tumor proliferation, invasion, metastasis, and treatment resistance in colon cancer. Similarly, both lncRNAs and circRNAs can act as miRNA molecular sponges that can modulate the activities of miRNA-mRNA networks, thereby regulating oncogenic signaling pathways (106).

CircRNAs are stable and more resistant to degradation than linear RNAs, which aids in their use as robust biomarkers; miRNAs are detectable in a non-invasive manner and represent dynamic changes in-state of disease; lncRNAs potentially offer more information than miRNAs due to their considerable range of functional roles in CRC and can give a better understanding of the highly connected regulations of transcription and translation in CRC (107, 108). In addition, the interactions between each class of ncRNAs could add to regulatory pathways and may allow for combinatorial biomarkers (109). Targeting these on developing diagnostic tests that will be sensitive and specific to ncRNAs and CRC may help improve the cancer diagnosis, prediction of disease progression, and treatment regimens based on patients' specific needs (110).

5 Challenges in using circRNAs for CRC diagnosis

Despite the promising potential of circRNAs as diagnostic biomarkers for CRC, several limitations exist in clinical applications. The detection and quantification of circRNAs remains challenging, with many techniques still being developed (111). While next-generation sequencing allows for transcriptome-wide circRNA identification, the reliability of these methods requires meticulous study design and execution (112). Validating circRNAs, particularly demonstrating their circularity and confirming the back-splice junction, presents technical hurdles. The variable abundance of circRNAs, with some highly expressed and others present in low quantities, may affect their consistency as biomarkers (113). Furthermore, the stability and conservation of circRNAs can vary

TABLE 1 Diagnostic performance of circRNAs in CRC.

circRNA	Sample Type	Sensitivity	Specificity	Reference
circ_0013958	Tissue	High	Moderate	(93)
circ_0001445	Plasma	Moderate	Moderate	(94)
circ_0001178	Plasma	High	High	(95)
circ_0000826	Tissue	High	High	(96)
circ_0001313	Tissue	High	Moderate	(97)
circ_0026344	Tissue	High	Moderate	(72)
circ_0035445	Plasma	High	Moderate	(98)
circ_0082182	Tissue	High	High	(99)
circ_0001313	Tissue	High	Moderate	(100)

depending on specific conditions, potentially impacting their effectiveness across diverse patient populations. Our understanding of the regulatory mechanisms controlling circRNA synthesis remains limited, thus complicating the efforts to predict or manipulate their expression (113). For instance, the role of environmental factors and microbiota in circRNA expression regulation remains underexplored, posing challenges in developing circRNA-based personalized diagnostics (114).

Integrating circRNA analysis into standard clinical workflows is a significant challenge, as current detection methods are often expensive and technically demanding (115). Ensuring cost-effectiveness and scalability will be critical for the widespread use of circRNA as a biomarker for CRC. Additionally, invasive tissue sampling methods for circRNA detection limit their applicability, underscoring the need for further research into non-invasive approaches, such as liquid biopsies (115, 116). Another critical gap is the lack of robust computational tools for large-scale circRNA analysis. Though promising, AI and machine learning techniques are not yet fully optimized to handle the complexity of circRNA datasets, which may impede their integration into clinical practice (117). Moreover, many circRNAs have been identified, and the functional and clinical significance of most remains unclear, necessitating further research, especially clinical studies, to establish their relevance in CRC diagnosis and therapeutics. Targeted circRNA delivery mechanisms, such as nanoparticle-based systems, are still under development, and their safety and efficacy require validation in preclinical and clinical settings. Addressing these constraints is critical for advancing circRNA-based CRC diagnostics and therapies (118).

6 CircRNAs in CRC: future perspectives and concluding insights

Early detection of CRC is crucial for its prevention and significantly impacts long-term patient survival. Numerous dysregulated circRNAs have been identified as potential targets for addressing chemoradiation resistance in CRC treatment. In summary, circRNAs offer potential for the early detection, prognosis, and treatment of CRC. Their utility as non-invasive biomarkers, combined with their involvement in key oncogenic pathways like the AKT signaling pathway, underscores their value in overcoming chemoradiation resistance. CircRNA-based therapeutics, particularly combined with treatments such as 5-FU, hold significant potential. Additionally, advancements in nucleic acid-editing technologies, such as CRISPR, further enhance their therapeutic relevance. Integrating multi-omics approaches and AI-driven models in future research could lead to personalized, more effective diagnostic strategies, ultimately improving long-term outcomes for CRC patients.

Our understanding of circRNAs has been further enhanced by insights from other cancers, revealing conserved oncogenic mechanisms. Cross-cancer studies underscore the potential of circRNAs as universal diagnostic and therapeutic targets, paving the way for multi-cancer diagnostic platforms. Additionally, the influence of environmental and lifestyle factors on circRNA expression opens new avenues for integrating personalized prevention strategies into CRC management. Furthermore, circRNAs have shown promise in predicting treatment response and monitoring therapy potential in CRC. However, despite these findings, significant challenges remain in translating circRNA research into clinical practice, including the need for standardized detection methods, validation in larger patient cohorts, and a deeper understanding of circRNA's role. Future integration of multi-omics approaches and advanced computational tools, such as AI-based predictive models, could improve circRNA-based diagnostics and enhance personalized CRC treatment.

In conclusion, circRNAs represent a promising frontier in CRC research, offering potential solutions for early detection, personalized treatment, and improved patient outcomes. The synergy between circRNA research and cutting-edge technologies holds the potential of CRC management, ultimately reducing the global burden of this disease. CircRNAs such as ciRS-7, circCCDC66, and hsa_circ_0026416 appear to be effective diagnostic and prognostic factors in CRC given their stability and expression. Their ability to mediate critical pathways and resistance to chemotherapy extensions indicates that circRNAs could be novel targets for CRC. Detection of hsa_circ_0026416 via liquid biopsy will help to develop a non-invasive detection method for early CRC diagnosis and monitoring. Thus circRNAs could serve as a potential way for RNA-based therapeutics and personalized treatment in CRC.

Author contributions

SN: Methodology, Visualization, Writing – original draft. KS: Methodology, Writing – original draft, Investigation. SPK: Investigation, Writing – original draft, Visualization. AB: Visualization, Methodology, Supervision, Writing – review & editing. SK: Writing – review & editing. AD: Writing – review & editing. SP: Conceptualization, Data curation, Investigation, Resources, Software, Visualization, Writing – original draft, Writing – review & editing.

Funding

The author(s) declare that no financial support was received for the research and/or publication of this article.

Acknowledgments

We want to thank the Chettinad Academy of Research and Education, Chettinad Hospital, and Research Institute for providing the facilities.

Conflict of interest

The authors declare that the research was conducted in the absence of any commercial or financial relationships that could be construed as a potential conflict of interest.

Generative AI statement

The author(s) declare that no Generative AI was used in the creation of this manuscript.

Publisher's note

All claims expressed in this article are solely those of the authors and do not necessarily represent those of their affiliated organizations, or those of the publisher, the editors and the reviewers. Any product that may be evaluated in this article, or claim that may be made by its manufacturer, is not guaranteed or endorsed by the publisher.

References

1. Al-Joufi F, Setia A, Salem-Bekhit M, Sahu R, Alqahtani F, Widyowati R, et al. Molecular pathogenesis of colorectal cancer with an emphasis on recent advances in biomarkers, as well as nanotechnology-based diagnostic and therapeutic approaches. *Nanomaterials*. (2022) 12:169. doi: 10.3390/nano12010169

2. Xi Y, Xu P. Global colorectal cancer burden in 2020 and projections to 2040. *Trans Oncol*. (2021) 14:101174. doi: 10.1016/j.tranon.2021.101174

3. Saha B, Adhikary S, Banerjee A, Radhakrishnan AK, Duttaroy AK, Pathak S. Exploring the relationship between diet, lifestyle and gut microbiome in colorectal cancer development: A recent update. *Nutr Cancer*. (2024) 76:1–26. doi: 10.1080/01635581.2024.2367266. T, R. A.

4. Underhill ML, Germansky KA, Yurgelun MB. Advances in hereditary colorectal and pancreatic cancers. *Clin Ther*. (2016) 38:1600–21. doi: 10.1016/j.clinthera.2016.03.017

5. Jasperson KW, Tuohy TM, Neklason DW, Burt RW. Hereditary and familial colon cancer. *Gastroenterology*. (2010) 138:2044–58. doi: 10.1053/j.gastro.2010.01.054

6. Jayasekara H, English DR, Haydon A, Hodge AM, Lynch BM, Rosty C, et al. Associations of alcohol intake, smoking, physical activity and obesity with survival following colorectal cancer diagnosis by stage, anatomic site and tumor molecular subtype. *Int J Cancer*. (2017) 142:238–50. doi: 10.1002/ijc.31049

7. Johnson CM, Wei C, Ensor JE, Smolenski DJ, Amos CI, Levin B, et al. Meta-analyses of colorectal cancer risk factors. *Cancer Causes Control*. (2013) 24:1207–22. doi: 10.1007/s10552-013-0201-5

8. Andrew AS, Parker S, Anderson JC, Rees JR, Robinson C, Riddle B, et al. Risk factors for diagnosis of colorectal cancer at a late stage: a population-based study. *J Gen Internal Med*. (2018) 33:2100–5. doi: 10.1007/s11606-018-4648-7

9. Roshandel G, Ghasemi-Kebria F, Malekzadeh R. Colorectal cancer: epidemiology, risk factors, and prevention. *Cancers*. (2024) 16:1530. doi: 10.3390/cancers16081530

10. Bailey CE, Hu C-Y, You YN, Bednarski BK, Rodriguez-Bigas MA, Skibber JM, et al. Increasing disparities in the age-related incidences of colon and rectal cancers in the United States, 1975-2010. *JAMA Surg*. (2015) 150:17–22. doi: 10.1001/jamasurg.2014.1756

11. Ferlizza E, Solmi R, Sgarzi M, Ricciardiello L, Lauriola M. The roadmap of colorectal cancer screening. *Cancers*. (2021) 13:1101. doi: 10.3390/cancers13051101

12. Cheng L, Eng C, Nieman LZ, Kapadia AS, Du XL. Trends in colorectal cancer incidence by anatomic site and disease stage in the United States from 1976 to 2005. *Am J Clin Oncol*. (2011) 34:573–80. doi: 10.1097/coc.0b013e3181fe41ed

13. Siegel RL, Miller KD, Fedewa SA, Ahnen DJ, Meester RGS, Barzi A, et al. Colorectal cancer statistics, 2017. *CA: A Cancer J Clin*. (2017) 67:177–93. doi: 10.3322/caac.21395

14. Petre-Mandache C-B, Margaritescu DN, Mitrut R, Kamal A-M, Padureanu V, Cucu M-G, et al. Risk factors and genetic predisposition in colorectal cancer: A study on young and old adults. *Curr Health Sci J*. (2021) 47:84–8. doi: 10.12865/CHSJ.47.01.13

15. Siegel R, Ward E, Brawley O, Jemal A. Cancer statistics, 2011: the impact of eliminating socioeconomic and racial disparities on premature cancer deaths. *CA: A Cancer J Clin*. (2011) 61:212–36. doi: 10.3322/caac.20121

16. Edwards BK, Ward E, Kohler BA, Eheman C, Zauber AG, Anderson RN, et al. Annual report to the nation on the status of cancer, 1975-2006, featuring colorectal cancer trends and impact of interventions (risk factors, screening, and treatment) to reduce future rates. *Cancer*. (2010) 116:544–73. doi: 10.1002/cncr.24760

17. Berrino F, De Angelis R, Sant M, Rosso S, Lasota MB, Coebergh JW, et al. Survival for eight major cancers and all cancers combined for European adults diagnosed in 1995–99: results of the EUROCARE-4 study. *Lancet Oncol*. (2007) 8:773–83. doi: 10.1016/s1470-2045(07)70245-0

18. Coleman MP, Gatta G, Verdecchia A, Estève J, Sant M, Storm H, et al. EUROCARE-3 summary: cancer survival in Europe at the end of the 20th century. *Ann Oncol*. (2003) 14:v128–49. doi: 10.1093/annonc/mdg756

19. Engholm G, Mette A, Brewster DH, Gaard M, Holmberg L, Hartley R, et al. Colorectal cancer survival in the Nordic countries and the United Kingdom: Excess mortality risk analysis of 5 year relative period survival in the period 1999 to 2000. *Int J Cancer*. (2007) 121:1115–22. doi: 10.1002/ijc.22737

20. Verdecchia A, Francisci S, Brenner H, Gatta G, Micheli A, Mangone L, et al. Recent cancer survival in Europe: a 2000–02 period analysis of EUROCARE-4 data. *Lancet Oncol*. (2007) 8:784–96. doi: 10.1016/s1470-2045(07)70246-2

21. Labianca R, Beretta GD, Kildani B, Milesi L, Merlin F, Mosconi S, et al. Colon cancer. *Crit Rev Oncology/Hematology*. (2010) 74:106–33. doi: 10.1016/j.critrevonc.2010.01.010

22. Cappell MS. Pathophysiology, clinical presentation, and management of colon cancer. *Gastroenterol Clinics North America*. (2008) 37:1–24. doi: 10.1016/j.gtc.2007.12.002

23. Leufkens AM, Leeuwen, van M, Siersema PD. Diagnostic accuracy of computed tomography for colon cancer staging: A systematic review. *Scandinavian J Gastroenterol*. (2011) 46:887–94. doi: 10.3109/00365521.2011.574732. A.A.J.

24. Veit-Haibach P, Kuehle CA, Beyer T, Stergar H, Kuehl H, Schmidt J, et al. Diagnostic accuracy of colorectal cancer staging with whole-body PET/CT colonography. *JAMA*. (2006) 296:2590–0. doi: 10.1001/jama.296.21.2590

25. Ravichandran SN, Kumar MM, Das A, Banerjee A, Veronica S, Sun-Zhang A, et al. An updated review on molecular biomarkers in diagnosis and therapy of

colorectal cancer. *Curr Cancer Drug Targets*. (2023) 24(6):595–611. doi: 10.2174/0115680096270555231113074003

26. Bhoopathy J, Vedakumari SW, Pravin YR, Prabhu AD. Radiopaque silk sericin nanoparticles for computed tomography imaging of solid tumors. *ACS Appl Bio Materials*. (2025) 8(6):5007–14. doi: 10.1021/acsabm.5c00230

27. Pin-Vieito N, Puga M, Fernández-de-Castro D, Cubiella J. Faecal immunochemical test outside colorectal cancer screening? *World J Gastroenterol*. (2021) 27:6415–29. doi: 10.3748/wjg.v27.i38.6415

28. Daly JM, Levy BT, Merchant ML, Wilbur J. Mailed fecal-immunochemical test for colon cancer screening. *J Community Health*. (2010) 35:235–9. doi: 10.1007/s10900-010-9227-8

29. Navarro M, Nicolas A, Ferrandez A, Lanas A. Colorectal cancer population screening programs worldwide in 2016: An update. *World J Gastroenterol*. (2017) 23:3632. doi: 10.3748/wjg.v23.i20.3632

30. Issa IA, Noureddine M. Colorectal cancer screening: An updated review of the available options. *World J Gastroenterol*. (2017) 23:5086. doi: 10.3748/wjg.v23.i28.5086

31. Pox C. Colon cancer screening: which non-invasive filter tests? *Digestive Dis*. (2011) 29:56–9. doi: 10.1159/000331127

32. Knezevic CE, Clarke W. Cancer chemotherapy. *Ther Drug Monit*. (2020) 42:6–19. doi: 10.1097/ftd.0000000000000701

33. Banerjee A, Pathak S, Subramanium VD, G. D, Murugesan R, Verma RS. Strategies for targeted drug delivery in treatment of colon cancer: current trends and future perspectives. *Drug Discov Today*. (2017) 22:1224–32. doi: 10.1016/j.drudis.2017.05.006

34. Zhang Q, Zhang C, Ma J-X, Ren H, Sun Y, Xu J-Z. Circular RNA PIP5K1A promotes colon cancer development through inhibiting miR-1273a. *World J Gastroenterol*. (2019) 25:5300–9. doi: 10.3748/wjg.v25.i35.5300

35. Hsu M-T, Coca-Prados M. Electron microscopic evidence for the circular form of RNA in the cytoplasm of eukaryotic cells. *Nature*. (1979) 280:339–40. doi: 10.1038/280339a0

36. Chen L, Huang C, Wang X, Shan G. Circular RNAs in eukaryotic cells. *Curr Genomics*. (2015) 16:312–8. doi: 10.2174/1389202916666150707161554

37. Kos A, Dijkema R, Arnberg AC, van der Meide PH, Schellekens H. The hepatitis delta (δ) virus possesses a circular RNA. *Nature*. (1986) 323:558–60. doi: 10.1038/323558a0

38. Ford E, Ares M. Synthesis of circular RNA in bacteria and yeast using RNA cyclase ribozymes derived from a group I intron of phage T4. *Proc Natl Acad Sci*. (1994) 91:3117–21. doi: 10.1073/pnas.91.8.3117

39. Li A, Wang WC, McAlister V, Zhou Q, Zheng X. Circular RNA in colorectal cancer. *J Cell Mol Med*. (2021) 25:3667–79. doi: 10.1111/jcmm.16380

40. Salzman J, Gawad C, Wang PL, Lacayo N, Brown PO. Circular RNAs are the predominant transcript isoform from hundreds of human genes in diverse cell types. *PloS One*. (2012) 7:e30733. doi: 10.1371/journal.pone.0030733

41. Chen R, Chen X, Xia L, Zhang JX, Pan Z, Ma X, et al. N6-methyladenosine modification of circNSUN2 facilitates cytoplasmic export and stabilizes HMGA2 to promote colorectal liver metastasis. *Nat Commun*. (2019) 10. doi: 10.1038/s41467-019-12651-2

42. Hou L-D, Zhang J. Circular RNAs: An emerging type of RNA in cancer. *Int J Immunopathology Pharmacol*. (2017) 30:1–6. doi: 10.1177/0394632016686985

43. Li J, Xu Q, Huang Z, Mao N, Lin Z, Cheng L, et al. CircRNAs: a new target for the diagnosis and treatment of digestive system neoplasms. *Cell Death Dis*. (2021) 12:1–13. doi: 10.1038/s41419-021-03495-0

44. Long F, Li L, Xie C, Ma M, Wu Z, Lu Z, et al. Intergenic circRNA *circ_0007379* inhibits colorectal cancer progression by modulating *miR-320a* biogenesis in a KSRP-dependent manner. *Int J Biol Sci*. (2023) 19:3781–803. doi: 10.7150/ijbs.85063

45. Yang L, Fu J, Zhou Y. Circular RNAs and their emerging roles in immune regulation. *Front Immunol*. (2018) 9:2977. doi: 10.3389/fimmu.2018.02977

46. Liu K-S, Pan F, Mao X-D, Liu C, Chen Y-J. Biological functions of circular RNAs and their roles in occurrence of reproduction and gynecological diseases. *Am J Trans Res*. (2019) 11:1.

47. Huang A, Zheng H, Wu Z, Chen M, Huang Y. Circular RNA-protein interactions: functions, mechanisms, and identification. *Theranostics*. (2020) 10:3503–17. doi: 10.7150/thno.42174

48. Ikeda Y, Morikawa S, Nakashima M, Yoshikawa S, Taniguchi K, Sawamura H, et al. CircRNAs and RNA-binding proteins involved in the pathogenesis of cancers or central nervous system disorders. *Non-coding RNA*. (2023) 9:23. doi: 10.3390/ncrna9020023

49. Louis C, Leclerc D, Coulouarn C. Emerging roles of circular RNAs in liver cancer. *JHEP Rep*. (2022) 4:100424. doi: 10.1016/j.jhepr.2021.100413

50. Li Q, Yang G, Ren B, Liu X, Tang L-Q, Shi Q, et al. ZC3H14 facilitates backsplicing by binding to exon-intron boundary and 3′ UTR. *Mol Cell*. (2024) 84 (22):4314–33. doi: 10.1016/j.molcel.2024.10.001

51. Zhou W-Y, Cai Z-R, Liu J, Wang D-S, Ju H-Q, Xu R-H. Circular RNA: metabolism, functions and interactions with proteins. *Mol Cancer*. (2020) 19. doi: 10.1186/s12943-020-01286-3

52. Margvelani G, Maquera KAA, Welden J, Rodgers D, Stamm S. Translation of circular RNAs. *Nucleic Acids Res*. (2024) 53(1). doi: 10.1093/nar/gkae1167

53. Cao Y, He Y, Liao L, Xu L. Circular RNAs perspective: exploring the direction of immunotherapy for colorectal cancer. *Front Oncol*. (2025) 15:1554179. doi: 10.3389/fonc.2025.1554179

54. Hashemi M, Khosroshahi EM, Daneii P, Hassanpoor A, Eslami M, Koohpar ZK, et al. Emerging roles of circRNA-miRNA networks in cancer development and therapeutic response. *Non-Coding RNA Res*. (2024) 10:98–115. doi: 10.1016/j.ncrna.2024.09.006

55. Yang Y, Meng W-J, Wang Z-Q. MicroRNAs (miRNAs): Novel potential therapeutic targets in colorectal cancer. *Front Oncol*. (2022) 12:1054846. doi: 10.3389/fonc.2022.1054846

56. Garlapati P, Ling J, Chiao PJ, Fu J. Circular RNAs regulate cancer-related signaling pathways and serve as potential diagnostic biomarkers for human cancers. *Cancer Cell Int*. (2021) 21. doi: 10.1186/s12935-021-02017-4

57. Verduci L, Strano S, Yarden Y, Blandino G. The circ RNA -micro RNA code: emerging implications for cancer diagnosis and treatment. *Mol Oncol*. (2019) 13 (4):669–80. doi: 10.1002/1878-0261.12468

58. Xu T, Wang M, Jiang L, Ma L, Wan L, Chen Q, et al. CircRNAs in anticancer drug resistance: recent advances and future potential. *Mol Cancer*. (2020) 19. doi: 10.1186/s12943-020-01240-3

59. Tang X, Ren H, Guo M, Qian J, Yang Y, Gu C. Review on circular RNAs and new insights into their roles in cancer. *Comput Struct Biotechnol J*. (2021) 19:910–28. doi: 10.1016/j.csbj.2021.01.018

60. Hussen BM, Abdullah SR, Jaafar RM, Rasul MF, Aroutiounian R, Harutyunyan T, et al. Circular RNAs as key regulators in cancer hallmarks: New progress and therapeutic opportunities. *Crit Rev Oncology/Hematology*. (2025) 207:104612. doi: 10.1016/j.critrevonc.2024.104612

61. Zhang Y, Luo J, Yang W, Ye W-C. CircRNAs in colorectal cancer: potential biomarkers and therapeutic targets. *Cell Death Dis*. (2023) 14:1–13. doi: 10.1038/s41419-023-05881-2

62. Zheng X, Chen L, Zhou Y, Wang Q, Zheng Z, Xu B, et al. A novel protein encoded by a circular RNA circPPP1R12A promotes tumor pathogenesis and metastasis of colon cancer via Hippo-YAP signaling. *Mol Cancer*. (2019) 18. doi: 10.1186/s12943-019-1010-6

63. Yang J, Fan Q, Wang Y, Liu Y, Xu X, Liang Y, et al. CircRNAs in colorectal cancer: potential roles, clinical applications, and natural product-based regulation. *Front Oncol*. (2025) 15:1525779. doi: 10.3389/fonc.2025.1525779

64. Ameli-Mojarad M, Ameli-Mojarad M, Hadizadeh M, Young C, Babini H, Nazemalhosseini-Mojarad E, et al. The effective function of circular RNA in colorectal cancer. *Cancer Cell Int*. (2021) 21. doi: 10.1186/s12935-021-02196-0

65. Ghafouri-Fard S, Taheri M, Hussen BM, Vafaeimanesh J, Abak A, Vafaee R. Function of circular RNAs in the pathogenesis of colorectal cancer. *Biomedicine Pharmacotherapy*. (2021) 140:111721. doi: 10.1016/j.biopha.2021.111721

66. Liang Y, Shi J, He Q, Sun G, Gao L, Ye J, et al. Hsa_circ_0026416 promotes proliferation and migration in colorectal cancer via miR-346/NFIB axis. *Cancer Cell Int*. (2020) 20. doi: 10.1186/s12935-020-01593-1

67. Hao Q, Zhang Z. hsa_circRNA_000166 Facilitated Cell Growth and Limited Apoptosis through Targeting miR-326/LASP1 Axis in Colorectal Cancer. *Gastroenterol Res Pract*. (2020) 2020:1–9. doi: 10.1155/2020/8834359

68. Malviya A, Bhuyan R. Circular RNAs in cancer: roles, mechanisms, and therapeutic potential across colorectal, gastric, liver, and lung carcinomas. *Discover Oncol*. (2025) 16. doi: 10.1007/s12672-025-01743-9

69. Chen J, Yang J, Fei X, Wang X, Wang K. CircRNA ciRS-7: a novel oncogene in multiple cancers. *Int J Biol Sci*. (2021) 17:379–89. doi: 10.7150/ijbs.54292

70. Artemaki PI, Scorilas A, Kontos CK. Circular RNAs: A new piece in the colorectal cancer puzzle. *Cancers*. (2020) 12:2464. doi: 10.3390/cancers12092464

71. Xiao Y-S, Tong H-Z, Yuan X-H, Xiong C-H, Xu X-Y, Zeng Y-F. *CircFADS2*: A potential prognostic biomarker of colorectal cancer. *Exp Biol Med*. (2020) 245:1233–41. doi: 10.1177/1535370220929965

72. Yuan Y, Liu W, Zhang Y, Zhang Y, Sun S. CircRNA circ_0026344 as a prognostic biomarker suppresses colorectal cancer progression via microRNA-21 and microRNA-31. *Biochem Biophys Res Commun*. (2018) 503:870–5. doi: 10.1016/j.bbrc.2018.06.089

73. Liu L, Liu F-B, Huang M, Xie K, Xie Q-S, Liu C-H, et al. Circular RNA ciRS-7 promotes the proliferation and metastasis of pancreatic cancer by regulating miR-7-mediated EGFR/STAT3 signaling pathway. *Hepatobiliary Pancreatic Dis Int*. (2019) 18:580–6. doi: 10.1016/j.hbpd.2019.03.003

74. Yang H, Li X, Meng Q, Sun H, Wu S, Hu W, et al. CircPTK2 (hsa_circ_0005273) as a novel therapeutic target for metastatic colorectal cancer. *Mol Cancer*. (2020) 19. doi: 10.1186/s12943-020-1139-3

75. Li W, Song Y, Zhang H, Zhou Z, Xie X, Zeng Q, et al. Decreased expression of hsa_circ_00001649 in gastric cancer and its clinical significance. *Dis Markers*. (2017) 2017:1–6. doi: 10.1155/2017/4587698

76. Weng W, Wei Q, Toden S, Yoshida K, Nagasaka T, Fujiwara T, et al. Circular RNA ciRS-7—A promising prognostic biomarker and a potential therapeutic target in colorectal cancer. *Clin Cancer Res*. (2017) 23:3918–28. doi: 10.1158/1078-0432.ccr-16-2541

77. Louis C, Leclerc D, Coulouarn C. Emerging roles of circular RNAs in liver cancer. *JHEP Rep*. (2021) 4:100413. doi: 10.1016/j.jhepr.2021.100413

78. Zhao W, Dong M, Pan J, Wang Y, Zhou J, Ma J, et al. Circular RNAs: A novel target among non-coding RNAs with potential roles in Malignant tumors (Review). *Mol Med Rep*. (2019) 20(4):3463–74. doi: 10.3892/mmr.2019.10637

79. Zhuo F, Lin H, Chen Z, Huang Z, Hu J. The expression profile and clinical significance of circRNA0003906 in colorectal cancer. *OncoTargets and Therapy. Volume*. (2017) 10:5187–93. doi: 10.2147/ott.s147378

80. Chang L-C, Chiu H-M, Wu M-S, Shen T-L. The role of small extracellular vesicles in the progression of colorectal cancer and its clinical applications. *Int J Mol Sci*. (2022) 23:1379. doi: 10.3390/ijms23031379

81. Molibeli KM, Hu R, Liu Y, Xiong D, Tang L. Potential clinical applications of exosomal circular RNAs: more than diagnosis. *Front Mol Biosci*. (2021) 8:769832. doi: 10.3389/fmolb.2021.769832

82. AmeliMojarad M, AmeliMojarad M, Wang J. The function of novel small non-coding RNAs (piRNAs, tRFs) and PIWI protein in colorectal cancer. *Cancer Treat Res Commun*. (2022) 31:100542. doi: 10.1016/j.ctarc.2022.100542

83. Long F, Lin Z, Li L, Ma M, Lu Z, Jing L, et al. Comprehensive landscape and future perspectives of circular RNAs in colorectal cancer. *Mol Cancer*. (2021) 20. doi: 10.1186/s12943-021-01318-6

84. He Z, Zhu Q. Circular RNAs: Emerging roles and new insights in human cancers. *Biomedicine Pharmacotherapy*. (2023) 165:115217–7. doi: 10.1016/j.biopha.2023.115217

85. Gao Y, Wang J, Zhao F. CIRI: an efficient and unbiased algorithm for *de novo* circular RNA identification. *Genome Biol*. (2015) 16. doi: 10.1186/s13059-014-0571-3

86. Li R-D, Guan M, Zhou Z, Dong S-X, Liu Q. The role of circRNAs in the diagnosis of colorectal cancer: A meta-analysis. *Front Med*. (2021) 8:766208. doi: 10.3389/fmed.2021.766208

87. Zhang S, Sun J, Gu M, Wang G, Wang X. Circular RNA: A promising new star for the diagnosis and treatment of colorectal cancer. *Cancer Med*. (2021) 10:8725–40. doi: 10.1002/cam4.4398

88. Luo Z-D, Wang Y-F, Zhao Y-X, Yu L-C, Li T, Fan Y-J, et al. Emerging roles of non-coding RNAs in colorectal cancer oxaliplatin resistance and liquid biopsy potential. *World J Gastroenterol*. (2023) 29:1–18. doi: 10.3748/wjg.v29.i1.1

89. Tang L, Deng X, Guan M, Zhong L. USF1-activated hsa_circ_0076691 induces oxaliplatin resistance via facilitating FGF9 expression in miR-589-3p-dependent manners. *Non-Coding RNA Res*. (2025) 13:15–28. doi: 10.1016/j.ncrna.2025.04.003

90. Blondy S, David V, Verdier M, Mathonnet M, Perraud A, Christou N. 5-Fluorouracil resistance mechanisms in colorectal cancer: From classical pathways to promising processes. *Cancer Sci*. (2020) 111:3142–54. doi: 10.1111/cas.14532

91. Liu F, Li R, Zhang R, He M, Zhang Y. Knockdown of circNRIP1 sensitizes colorectal cancer to 5-FU via sponging miR-532-3p. *Oncol Rep*. (2021) 46. doi: 10.3892/or.2021.8169

92. Li Q, Wang Y, Wu S, Zhou Z, Ding X, Shi R, et al. CircACC1 regulates assembly and activation of AMPK complex under metabolic stress. *Cell Metab*. (2019) 30:157–173.e7. doi: 10.1016/j.cmet.2019.05.009

93. Ding H-X, Zhi LV, Yuan Y, Xu Q. The expression of circRNAs as a promising biomarker in the diagnosis and prognosis of human cancers: a systematic review and meta-analysis. *Oncotarget*. (2017) 9:11824–36. doi: 10.18632/oncotarget.23484

94. Radanova M, Mihaylova G, Tasinov O, Ivanova DP, Stoyanov GS, Nazifova-Tasinova N, et al. New circulating circular RNAs with diagnostic and prognostic potential in advanced colorectal cancer. *Int J Mol Sci*. (2021) 22:13283–3. doi: 10.3390/ijms222413283

95. Zhou Q, Ju L-L, Ji X, Cao Y-L, Shao J-G, Chen L. Plasma circRNAs as biomarkers in cancer. *Cancer Manage Res*. (2021) 13:7325–37. doi: 10.2147/cmar.s330228

96. Zhang Z, Fan W, Gao Q, Han Y, Ma J, Gao W, et al. Hsa_Circ_0000826 inhibits the proliferation of colorectal cancer by targeting AUF1. *J Genet Genomics = Yi Chuan Xue Bao*. (2023) 50:192–203. doi: 10.1016/j.jgg.2022.07.006

97. Ye D, Wang S, Huang Y, Chi P. A 3-circular RNA signature as a noninvasive biomarker for diagnosis of colorectal cancer. *Cancer Cell Int*. (2019) 19. doi: 10.1186/s12935-019-0995-7

98. Liu R, Deng P, Zhang Y, Wang Y, Peng C. Circ_0082182 promotes oncogenesis and metastasis of colorectal cancer *in vitro* and *in vivo* by sponging miR-411 and miR-1205 to activate the Wnt/β-catenin pathway. *World J Surg Oncol*. (2021) 19. doi: 10.1186/s12957-021-02164-y

99. Wang L, Peng X, Lu X, Wei Q, Chen M, Liu L. Inhibition of hsa_circ_0001313 (circCCDC66) induction enhances the radio-sensitivity of colon cancer cells via tumor suppressor miR-338-3p. *Pathology Res Pract*. (2019) 215:689–96. doi: 10.1016/j.prp.2018.12.032

100. Zhoulideh Y. Non-coding RNAs and exosomal ncRNAs in colorectal cancer. *Egyptian J Med Hum Genet*. (2025) 26. doi: 10.1186/s43042-025-00646-2

101. Zhang P, Wu W, Chen Q, Chen M. Non-coding RNAs and their integrated networks. *J Integr Bioinf*. (2019) 16. doi: 10.1515/jib-2019-0027

102. Liu X, Zhang Y, Zhou S, Dain L, Mei L, Zhu G. Circular RNA: An emerging frontier in RNA therapeutic targets, RNA therapeutics, and mRNA vaccines. *J Controlled Release: Off J Controlled Release Soc*. (2022) 348:84–94. doi: 10.1016/j.jconrel.2022.05.043

103. Longo F, Gattuso G, Spoto G, Ricci D, Vitale ACV, Lavoro A, et al. The multifaceted role of microRNAs in colorectal cancer: pathogenesis and therapeutic implications. *Non-Coding RNA Res*. (2025) 14:65–95. doi: 10.1016/j.ncrna.2025.05.012

104. Chattopadhaya A, Kural S, Verma A, Gupta P, Tiwari H, Singh S, et al. Urinary miRNAs in bladder cancer. *Clinica Chimica Acta*. (2025) 567:120113. doi: 10.1016/j.cca.2024.120113

105. Statello L, Guo C-J, Chen L-L, Huarte M. Gene regulation by long non-coding RNAs and its biological functions. *Nat Rev Mol Cell Biol*. (2021) 22:96–118. doi: 10.1038/s41580-020-00315-9

106. Chen S, Shen X. Long noncoding RNAs: functions and mechanisms in colon cancer. *Mol Cancer*. (2020) 19. doi: 10.1186/s12943-020-01287-2

107. Yang L-X, Li H, Cheng Z-H, Sun H-Y, Huang J-P, Li Z-P, et al. The application of non-coding RNAs as biomarkers, therapies, and novel vaccines in diseases. *Int J Mol Sci*. (2025) 26:3055–5. doi: 10.3390/ijms26073055

108. Farzam OR, Najafi S, Amini M, Rahimi Z, Dabbaghipour R, Zohdi O, et al. Interplay of miRNAs and lncRNAs in STAT3 signaling pathway in colorectal cancer progression. *Cancer Cell Int*. (2024) 24. doi: 10.1186/s12935-023-03202-3

109. Eldakhakhny B, Sutaih AM, Siddiqui MA, Aqeeli YM, Awan AZ, Alsayegh MY, et al. Exploring the role of noncoding RNAs in cancer diagnosis, prognosis, and precision medicine. *Non-Coding RNA Res*. (2024) 9:1315–23. doi: 10.1016/j.ncrna.2024.06.015

110. Uppaluri KR, Challa HJ, Gaur A, Jain R, Krishna Vardhani K, Geddam A, et al. Unlocking the potential of non-coding RNAs in cancer research and therapy. *Trans Oncol*. (2023) 35:101730. doi: 10.1016/j.tranon.2023.101730. K, S. M.

111. Zhang J, Chen S, Yang J, Zhao F. Accurate quantification of circular RNAs identifies extensive circular isoform switching events. *Nat Commun*. (2020) 11. doi: 10.1038/s41467-019-13840-9

112. Guria A, Sharma P, Srikakulam N, Baby A, Natesan S, Pandi G. Cost-effective transcriptome-wide profiling of circular RNAs by the improved-tdMDA-NGS method. *Front Mol Biosci*. (2022) 9:886366. doi: 10.3389/fmolb.2022.886366

113. Zhang Z, Yang T, Xiao J. Circular RNAs: promising biomarkers for human diseases. *EBioMedicine*. (2018) 34:267–74. doi: 10.1016/j.ebiom.2018.07.036

114. Zhu Z, Huang J, Li X, Xing J, Chen Q, Liu R, et al. Gut microbiota regulate tumor metastasis via circRNA/miRNA networks. *Gut Microbes*. (2020) 12:1788891. doi: 10.1080/19490976.2020.1788891

115. Mi Z, Zhongqiang C, Caiyun J, Yanan L, Jianhua W, Liang L. Circular RNA detection methods: A minireview. *Talanta*. (2022) 238:123066. doi: 10.1016/j.talanta.2021.123066

116. Zhou C, Balmer L, Song M, Mahara G, Wu K, Wang W, et al. Identification of circRNA biomarkers in osteosarcoma: An updated systematic review and meta-analysis. *Non-Coding RNA Res*. (2024) 9:341–9. doi: 10.1016/j.ncrna.2024.01.007

117. Vromman M, Anckaert J, Bortoluzzi S, Buratin A, Chen C-Y, Chu Q, et al. Large-scale benchmarking of circRNA detection tools reveals large differences in sensitivity but not in precision. *Nat Methods*. (2023) 20:1159–69. doi: 10.1038/s41592-023-01944-6

118. Das U, Banerjee S, Sarkar M, Fathah Muhammad L, Soni TK, Saha M, et al. Circular RNA vaccines: Pioneering the next-gen cancer immunotherapy. *Cancer Pathogenesis Ther*. (2024). doi: 10.1016/j.cpt.2024.11.003

Glossary

CRC	Colorectal Cancer
CircRNA	Circular RNA
ncRNA	Non-coding RNA
miRNA	MicroRNA
lncRNA	Long Non-coding RNA
ceRNA	Competing Endogenous RNA
RBP	RNA-Binding Protein
RT-qPCR	Reverse Transcription Quantitative Polymerase Chain Reaction
RNA-seq	RNA Sequencing
EMT	Epithelial-Mesenchymal Transition
FIT	Fecal Immunochemical Test
g-FOBT	Guaiac Fecal Occult Blood Test
CEA	Carcinoembryonic Antigen
EGFR	Epidermal Growth Factor Receptor
CDR1as	Cerebellar Degeneration-Related Protein 1 Antisense
PET/CT	Positron Emission Tomography/Computed Tomography
CT	Computed Tomography
ROC	Receiver Operating Characteristic
AUC	Area Under the Curve
EV	Extracellular Vesicle
BSS	Back-Splice Site
EIB	Exon-Intron Boundary
UTR	Untranslated Region
m6A	N6-Methyladenosine
HMGA2	High Mobility Group AT-Hook 2
IGF2BP2	Insulin-like Growth Factor 2 mRNA Binding Protein 2
YTHDC1	YTH Domain Containing 1
HNPCC	Hereditary Non-Polyposis Colorectal Cancer
FAP	Familial Adenomatous Polyposis
IBD	Inflammatory Bowel Disease
5-FU	5-Fluorouracil
AMPK	AMP-Activated Protein Kinase
snRNA	Small Nuclear RNA
CTIC1	Colorectal Tumor Initiating Cell-1 (circCTIC1)
AKT	Protein Kinase B (PKB/AKT pathway)
MAPK	Mitogen-Activated Protein Kinase
RAF1	Proto-oncogene serine/threonine-protein kinase
CRISPR	Clustered Regularly Interspaced Short Palindromic Repeats
DNA	Deoxyribonucleic Acid
RNA	Ribonucleic Acid
snRNP	Small Nuclear Ribonucleoprotein
UTRs	Untranslated Regions
OS	Overall Survival
CI	Confidence Interval
NCT	National Clinical Trial.

frontiers | Frontiers in Pharmacology

TYPE Original Research
PUBLISHED 06 August 2025
DOI 10.3389/fphar.2025.1581122

Check for updates

OPEN ACCESS

EDITED BY
Chiara De Santi,
Royal College of Surgeons in Ireland, Ireland

REVIEWED BY
Chen Xue,
Zhejiang University, China
Pengcheng Zhou,
Southeast University, China

*CORRESPONDENCE
Jun Yang,
ayjayj_44@163.com
Qi Yang,
yangqi198903@126.com
Jian Weng,
jweng@pku.edu.cn

RECEIVED 21 February 2025
ACCEPTED 21 July 2025
PUBLISHED 06 August 2025

CITATION
Qin H, Qi T, Liu M, Sheng W, Qian J, Weng J, Yang Q and Yang J (2025) A migrasome-related lncRNA signature predicts prognosis and immune response in hepatocellular carcinoma: Implications for biomarker discovery and therapeutic targeting.
Front. Pharmacol. 16:1581122.
doi: 10.3389/fphar.2025.1581122

COPYRIGHT
© 2025 Qin, Qi, Liu, Sheng, Qian, Weng, Yang and Yang. This is an open-access article distributed under the terms of the Creative Commons Attribution License (CC BY). The use, distribution or reproduction in other forums is permitted, provided the original author(s) and the copyright owner(s) are credited and that the original publication in this journal is cited, in accordance with accepted academic practice. No use, distribution or reproduction is permitted which does not comply with these terms.

A migrasome-related lncRNA signature predicts prognosis and immune response in hepatocellular carcinoma: Implications for biomarker discovery and therapeutic targeting

Haotian Qin[1,2], Tiantian Qi[1,2], Min Liu[3], Weibei Sheng[1,2], Junyu Qian[1,2], Jian Weng[1,2]*, Qi Yang[4]* and Jun Yang[5]*

[1]Department of Bone & Joint Surgery, Peking University Shenzhen Hospital, Shenzhen Peking University-The Hong Kong University of Science and Technology Medical Center, Shenzhen, Guangdong, China, [2]National & Local Joint Engineering Research Center of Orthopaedic Biomaterials, Peking University Shenzhen Hospital, Shenzhen, China, [3]Emergency Department, Peking University Shenzhen Hospital, Shenzhen, China, [4]Department of Ultrasound Medicine, Peking University Shenzhen Hospital, Shenzhen, China, [5]Department of Radiology, Peking University Shenzhen Hospital, Shenzhen, China

Background: Hepatocellular carcinoma (HCC) remains a leading cause of cancer-related death, with limited response rates to immunotherapy. Identifying novel biomarkers to predict prognosis and guide treatment is urgently needed.

Methods: Using TCGA-LIHC data, we identified migrasome-related long non-coding RNAs (MRlncRNAs) associated with HCC prognosis and constructed a two-lncRNA signature (LINC00839 and MIR4435-2HG) through LASSO-Cox regression. The model was validated in an independent cohort (n = 100). Multi-omics analyses were conducted to explore correlations with immune infiltration, immune checkpoints, TMB, MSI, and therapeutic sensitivity. Clinical sample validation and functional assays were performed to verify biological relevance. We knocked down MIR4435-2HG in HCC cells to assess its impact on proliferation, migration, EMT phenotype, and PD-L1 expression.

Results: The MRlncRNA signature effectively stratified HCC patients by prognosis and immunotherapy responsiveness. High-risk patients exhibited elevated immunosuppressive cell infiltration and immune checkpoint expression. Functional validation revealed that MIR4435-2HG promotes malignant behaviors and immune evasion by regulating EMT and PD-L1. Single-cell analysis showed its enrichment in cancer-associated fibroblasts, suggesting a role in tumor-stroma crosstalk and immune suppression.

Conclusion: MRlncRNAs, particularly MIR4435-2HG, contribute to HCC progression and an immunosuppressive tumor microenvironment. This study establishes a robust prognostic model and identifies potential targets for precision immunotherapy in HCC.

KEYWORDS

hepatocellular carcinoma, migrasome-related long non-coding RNAs, immune microenvironment, prognostic signature, immunotherapy

Introduction

Hepatocellular carcinoma (HCC) is one of the most common and lethal malignancies worldwide, ranking as the sixth most prevalent cancer and the third leading cause of cancer-related deaths globally (Bray et al., 2018). The development of HCC is closely associated with chronic liver diseases, including hepatitis B and C virus infections, alcoholic liver disease, and non-alcoholic fatty liver disease, which induce persistent liver inflammation and fibrosis, ultimately leading to carcinogenesis (Gilles et al., 2022; Sung et al., 2021). Despite advances in diagnostic techniques, HCC is often asymptomatic in its early stages, and by the time clinical symptoms manifest, the disease is typically at an advanced stage with a high risk of local recurrence and distant metastasis. This poses significant challenges for early diagnosis and effective treatment (Yang et al., 2023). Current therapeutic options for HCC, including surgical resection, local therapies, and systemic chemotherapy, offer limited benefits for advanced-stage patients, highlighting the urgent need for novel targeted therapies and immunotherapeutic strategies to improve patient outcomes (Liu et al., 2023; Sadagopan and He, 2024).

In recent years, the discovery of migrasomes, a novel cellular structure formed during cell migration, has shed new light on tumor biology. Migrasomes are extracellular vesicles released by migrating cells, enriched with proteins and signaling molecules that play critical roles in regulating the tumor microenvironment (TME). These structures facilitate intercellular communication and influence tumor progression by promoting cancer cell invasion, metastasis, and drug resistance (Jiang et al., 2023; Deng et al., 2024). In HCC, migrasome-related genes (MRGs) have been implicated in tumor progression, where they enhance cell migration, invasion, and metastasis by modulating cell signaling and the dynamic interactions within the TME (Zhang K. et al., 2024). Furthermore, MRGs may also regulate immune cell infiltration, thereby influencing immune evasion mechanisms and contributing to tumor growth and metastasis (Zhang R. et al., 2024).

Long non-coding RNAs (lncRNAs), once considered "junk DNA," have emerged as crucial regulators of gene expression, chromatin remodeling, and post-transcriptional modifications. They play pivotal roles in various cellular processes, including proliferation, migration, and invasion, and are increasingly recognized for their involvement in cancer progression (Gupta et al., 2010; Han et al., 2022; Li et al., 2023). In HCC, specific lncRNAs, such as HOTAIR and MALAT1, have been shown to drive tumor progression and metastasis (Kadian et al., 2024; Jia et al., 2024). Moreover, lncRNAs modulate the tumor immune microenvironment by influencing the function and distribution of immune cells, such as tumor-associated macrophages, thereby playing a role in immune evasion and response to immunotherapy (Tomczak et al., 2015; Yu et al., 2012). Given their regulatory roles, lncRNAs hold great promise as diagnostic, prognostic, and therapeutic biomarkers in HCC.

In this study, we systematically analyzed migrasome-related long non-coding RNAs (MRlncRNAs) in hepatocellular carcinoma (HCC) and developed a robust 2-lncRNA prognostic signature (LINC00839 and MIR4435-2HG) using TCGA data and LASSO–Cox regression. This signature was validated in clinical tissues and HCC cell lines, and was significantly associated with overall survival and immune-related features. Functional assays confirmed that MIR4435-2HG promotes proliferation, EMT, and PD-L1–mediated immune evasion. Moreover, MRlncRNA expression correlated with immune cell infiltration, immune checkpoint activation, and response to immune checkpoint inhibitors (ICIs), as evaluated by the TIDE algorithm.

Collectively, our findings reveal that MRlncRNAs contribute to HCC progression and immunosuppressive remodeling of the tumor microenvironment. This work identifies novel biomarkers for prognosis and immunotherapy prediction and offers mechanistic insights into the migrasome–lncRNA–immunity axis, paving the way for personalized therapeutic strategies in HCC.

Materials and methods

Data sources and preprocessing

Twelve migrasome-related genes (MRGs) were initially retrieved from the GeneCards database (https://www.genecards.org/) using the keyword *"migrasome"*. These genes were further filtered and confirmed based on prior published studies that experimentally validated their roles in migrasome biogenesis and function, including *TSPAN4*, *NDST1*, *CPQ*, and *ITGAV* (Supplementary Table S1). Gene expression profiles and corresponding clinical information for liver hepatocellular carcinoma (LIHC) patients were downloaded from The Cancer Genome Atlas (TCGA) database (https://portal.gdc.cancer.gov/) (Tomczak et al., 2015), including data from 372 LIHC tumors and 50 normal liver tissues. Clinical variables included age, sex, stage, grade, TNM classification, and overall survival (OS) time and status (Supplementary Table S2). Expression data were normalized to transcripts per million (TPM). All data preprocessing and visualization were conducted in R software (v4.4.1) using the "ggplot2" package. The Wilcoxon test was applied for comparisons of gene expression between tumor and normal samples.

Identification of migrasome-related lncRNAs (MRlncRNAs)

To identify MRlncRNAs, we extracted lncRNA and mRNA expression profiles from the TCGA-LIHC dataset. Pearson correlation analysis was conducted between the expression of the 12 MRGs and all lncRNAs using the "limma" package. LncRNAs were considered migrasome-related if they met the threshold of |correlation coefficient| > 0.55 and $P < 0.001$. In total, 191 MRlncRNAs were identified based on this criterion. Co-expression relationships were visualized using the "ggplot2" and "ggalluvial" packages in R.

Construction of prognostic model based on MRlncRNAs

Univariate Cox regression analysis was performed on the 191 MRlncRNAs to identify candidates significantly associated with overall survival ($P < 0.05$), yielding 16 prognosis-related MRlncRNAs. To further optimize the model and avoid overfitting, LASSO (Least Absolute Shrinkage and Selection Operator) Cox regression with 10-fold cross-validation was conducted and repeated 1000 times. This process ultimately selected two MRlncRNAs—LINC00839 and MIR4435-2HG—as the most stable predictors with the highest prognostic contribution and minimal AIC value. These two lncRNAs were used to construct the final risk model. All model-building procedures were performed using R packages including *survival*, *caret*, *glmnet*, and *timeROC*, and visualized with *ggplot2*.

Construction and Validation of prognostic model

Risk scores for each patient were calculated using a multivariate Cox regression model based on the expression levels and coefficients of the prognostic MRlncRNAs, following the formula:

$$\text{Riskscore} = \sum \text{i Coefficient (MRlncRNAsi)} \times \text{Expression (MRlncRNAsi)}$$

The TCGA-LIHC cohort was randomly divided into a training set and a testing set in a 1:1 ratio. Patients were then stratified into high-risk and low-risk groups using the median risk score as the cutoff. Kaplan–Meier survival analysis and time-dependent ROC curve analysis were performed to evaluate the model's predictive ability, using the survival, survminer, and timeROC packages in R. To further validate the robustness and generalizability of the model, we applied the same risk score formula to an independent clinical tissue cohort (n = 100) collected from our institution. This external cohort was randomly split into validation set 1 (n = 50) and validation set 2 (n = 50). Patients in each validation set were classified into high- and low-risk groups based on the median risk score, and survival analyses were conducted accordingly. Univariate and multivariate Cox regression analyses were also performed to determine the independent prognostic value of the risk score, with results presented using forest plots (generated by the forestplot package). The predictive performance of the MRlncRNA-based model was further assessed by comparing 1-, 3-, and 5-year ROC AUCs across the TCGA and clinical validation cohorts. Additional subgroup analyses were performed based on clinical parameters such as age, gender, grade, and stage. The R packages rms, pec, and dplyr were utilized for these evaluations.

Establishment and calibration of prognostic nomogram

Based on the results of multivariate Cox proportional hazards analysis, a nomogram was developed to predict the 1-, 3-, and 5-year overall survival. Calibration curves for 1-year, 3-year, and 5-year survival were plotted to assess the consistency between the predicted and observed outcomes. Furthermore, a C-index curve was generated to confirm the predictive accuracy of the nomogram. The R packages used for these analyses include survival, regplot, rms, and survcomp.

Functional enrichment analysis

Differentially expressed genes (DEGs) between high- and low-risk groups were obtained using the Limma package in R. The adjusted P-values were used to control for false positives in the TCGA database analysis, with "Adjusted $P < 0.05$ and $|\log2FC| \geq 1$" set as the cutoff for selecting differentially expressed genes. The clusterProfiler package was used to analyze the Gene Ontology (GO) functional enrichment of DEGs and their pathways in the Kyoto Encyclopedia of Genes and Genomes (KEGG). The GO analysis focused on three aspects: Biological Process (BP), Cellular Component (CC), and Molecular Function (MF). Additionally, Gene Set Enrichment Analysis (GSEA) was used to identify potential biological pathways (http://software.broadinstitute.org/gsea/index.jsp) (Powers et al., 2018).

Genetic variations

The cBioPortal database (http://www.cbioportal.org/) (Gao et al., 2013) provides visualization tools for cancer genomic data analysis. Using TCGA data, the genomic landscape of MRlncRNAs was explored, and their mutation frequency in LIHC was assessed. The impact of MRlncRNAs mutations on LIHC patient survival was also studied. Additionally, we analyzed the effect of MRlncRNAs mutations on clinical variables, including the Buffa Hypoxia Score, Winter Hypoxia Score, Aneuploidy Score, Ragnum Hypoxia Score, Fraction Genome Altered, Last Communication Contact from Initial Pathologic Diagnosis Date, and Neoplasm Histologic Grade.

Immune cell infiltration analysis

The correlation between MRlncRNAs and immune cell infiltration was calculated using ssGSEA and CIBERSORT algorithms. Results were visualized using R software's ggplot2 package. For immune scoring, the immunedeconv package in R and CIBERSORT algorithms (Newman et al., 2015) were used to compare the degree of immune cell infiltration

between high- and low-risk groups via the Wilcoxon test. Additionally, single-sample gene set enrichment analysis (ssGSEA) (Hänzelmann et al., 2013) in the GSVA package [1.46.0] helped quantify the infiltration levels of immune cell types and the accumulation of 24 common immune cells. The Wilcoxon rank sum test was used to compare immune cell infiltration levels between high- and low-risk groups. The estimate package [1.0.13] in R was used to calculate immune cell abundance (immune score), stromal cell infiltration level (stromal score), and the combined score (ESTIMATE score).

Immunotherapy response analysis

Risk scores and the correlation with immune checkpoint-related genes were visualized using the R packages "ggplot2" and "pheatmap". Expression differences of immune checkpoint-related genes between high and low-risk score groups were analyzed, alongside the correlation between the expression of two prognostic MRlncRNAs and three clinically important immune checkpoint genes (CD274, CTLA4, PDCD1). Additionally, the prognostic significance of combining risk scores with these three immune checkpoints (CD274, CTLA4, PDCD1) in LIHC patients was assessed. Key immune checkpoint-related genes in this study included CD274, CTLA4, HAVCR2, LAG3, PDCD1, PDCD1LG2, TIGIT, and SIGLEC15. The Tumor Immune Dysfunction and Exclusion (TIDE) algorithm was used to predict potential immune checkpoint-blocking responses, with the results visualized using "ggplot2". Distributions of TIDE data were compared between high and low-risk score groups. Finally, clinical tissue samples were used to predict the response of risk scores to immunotherapy.

Single-cell sequencing data analysis

The Tumor Immune Single Cell Center (TISCH) (http://tisch.comp-genomics.org/) is a database for single-cell RNA sequencing (scRNA-seq) focused on the tumor microenvironment (TME) (Sun et al., 2021). The t-distributed stochastic neighborhood embedding (t-SNE) and heatmap of GSE125449 were generated using the TISCH database to explore the impact of MRlncRNA expression on the TME in LIHC. Furthermore, Spearman's correlation method was applied to examine the relationship between MRlncRNAs and markers of cancer-associated fibroblasts (CAFs) and epithelial-mesenchymal transition (EMT).

TMB, MSI, and potential drug screening analysis

To evaluate the clinical applicability of our risk model, we visualized the distribution of TMB and MSI scores across high and low-risk groups using stacked bar charts. Wilcoxon rank-sum tests were employed to compare TMB and MSI scores between these groups in the TCGA cohort, with results visualized using "ggplot2". The "survminer" R package was used to calculate the optimal TMB cutoff, and patients with SARC in the TCGA cohort were classified into high and low TMB/MSI groups. Kaplan-Meier survival curves were used to assess prognostic differences. Additionally, drug sensitivity differences between high- and low-risk groups were analyzed using the limma, ggpubr, and pRRophetic R packages for prospective drug screening (Geeleher et al., 2014).

TABLE 1 The primers sequences utilized in RT-qPCR.

Real-time quantitative PCR primer sequence	
Gene	Sequence (5′- 3′ on minus strand)
GAPDH	Fwd: GAGTCCACTGGCGTCTTCAC
	Rev: ATGACGAACATGGGGGCA
LINC00839	Fwd: GAACCTGTGGCATCCATCTC
	Rev: CTCCAGCAACCCCTCAACC
MIR4435-2HG	Fwd: CGGAGCATGGAACTCGACAG
	Rev: CAAGTCTCACACATCCGGGC

Human sample collection

Tissue samples were provided by Peking University Shenzhen Hospital, including 100 pairs of liver cancer and adjacent non-tumor tissues, along with corresponding clinical and follow-up data. All patients underwent pathological diagnosis, and tissue samples were embedded in 10% formalin and stored under standard conditions. Archived samples collected between 2017 and 2019 and stored in the institutional biobank were used in this study. Comprehensive clinical information, including 5-year overall survival data, was retrieved from the hospital's longitudinal medical records. The use of these archived samples for additional molecular validation experiments was approved by the Ethics Committee of Peking University Shenzhen Hospital (Approval No. 2024–116). Written informed consent was obtained from all patients prior to initial sample collection. All procedures complied with relevant ethical guidelines and institutional regulations.

Cell culture conditions

The human normal hepatocyte cell line THLE-2 (CL-0833) was purchased from Procell Life Science & Technology Co., Ltd (Wuhan, China) and cultured in Procell's specialized medium (CM-0833), a complete formulation designed for THLE-2 growth, containing basal medium supplemented with growth factors and hormones including epidermal growth factor (EGF) and insulin. Liver cancer cell lines HepG2, Huh7, and Hep3B were obtained from the American Type Culture Collection (ATCC, Manassas, VA, USA) and maintained in RPMI-1640 medium (Gibco) supplemented with 10% fetal bovine serum (FBS; Gibco) and 1% penicillin-streptomycin. All cells were incubated at 37 °C with 5% CO_2 in a humidified atmosphere.

RNA extraction and RT-qPCR

Total RNA was extracted using the Quick-RNA MiniPrep Kit (Zymo Research, Catalog No. R1054) according to the manufacturer's instructions. RNA concentration and purity were assessed spectrophotometrically using a NanoDrop 2000 (Thermo Fisher Scientific). Reverse transcription was performed with 1 μg of

total RNA using the miScript SYBR Green PCR Kit (Qiagen, Germany) on a LightCycler 96 real-time PCR system (Roche Diagnostics GmbH, Mannheim, Germany). PCR conditions were as follows: 95°C for 10 min, followed by 40 cycles of 95°C for 15 s and 60°C for 1 min. Gene expression levels were normalized to GAPDH and calculated using the $2^{-\triangle\triangle}$CT method. Primer sequences are listed in Table 1.

Cell transfection and knockdown of MIR4435-2HG

Short hairpin RNAs targeting MIR4435-2HG (sh-MIR4435-2HG) and corresponding negative control (sh-NC) were designed and synthesized by GeneRulor Biotechnology Co., Ltd. (Zhuhai, China). HepG2 and Huh7 cells were transfected using Lipofectamine™ 3000 (Invitrogen, USA) according to the manufacturer's protocol. After 48 h, knockdown efficiency was evaluated by quantitative real-time PCR (qRT-PCR), and the most efficient sequence (sh-MIR4435-2HG#2) was selected for subsequent functional experiments.

Cell proliferation assay

Cell proliferation was assessed using the Cell Counting Kit-8 (CCK-8) (Dojindo, Japan). Transfected cells were seeded in 96-well plates (3×10^3 cells/well) and incubated for 0, 24, 48, and 72 h. At each time point, 10 μL of CCK-8 solution was added per well, followed by 2 h incubation at 37 °C. Absorbance at 450 nm was measured using a microplate reader (Bio-Rad, USA).

Wound healing assay

After transfection, cells were grown to near confluence in 6-well plates, and a scratch was made using a 200 μL pipette tip. Detached cells were removed with PBS, and serum-free medium was added. Wound closure was imaged at 0 h and 24 h using a phase-contrast microscope. Migration rate was analyzed using ImageJ.

Transwell migration and invasion assays

Cell migration and invasion abilities were evaluated using Transwell chambers (8 μm pore size, Corning, USA). For migration assays, 2×10^4 cells in serum-free medium were seeded in the upper chamber. For invasion assays, chambers were precoated with Matrigel (BD Biosciences), and 5×10^4 cells were seeded. The lower chamber contained 10% FBS as a chemoattractant. After 24 h incubation, cells on the upper membrane were removed, and migrated or invaded cells were fixed with 4% paraformaldehyde, stained with 0.1% crystal violet, and counted under a microscope.

Western blot analysis

Total protein was extracted using RIPA buffer supplemented with protease inhibitors, and concentrations were determined using the BCA assay. Equal amounts of protein (30 μg) were separated by SDS-PAGE and transferred to PVDF membranes (Millipore, USA). After blocking with 5% BSA, membranes were incubated overnight at 4 °C with primary antibodies: Anti-E-Cadherin (ab40772, Abcam, United Kingdom, 1:1000), Anti-Vimentin (ab92547, Abcam, United Kingdom, 1:1000), Anti-PD-L1 recombinant antibody (ab205921, Abcam, United Kingdom, 1:1000), and Anti-GAPDH (ab8245, Abcam, 1:5000) as an internal control. After washing, membranes were incubated with HRP-conjugated secondary antibodies (1:5000, Abcam) for 1 h at room temperature. Protein bands were visualized using an ECL chemiluminescence substrate (Thermo Fisher Scientific) and imaged with a Tanon 5200 Multi chemiluminescence imaging system. Band intensities were quantified using ImageJ software and normalized to GAPDH.

Statistical analysis

All statistical analyses were conducted using R (v4.2.1) (https://www.r-project.org/). The Student's t-test was applied for normally distributed data, while the Wilcoxon test was used for non-normally distributed variables. Spearman's correlation analysis was conducted to explore the relationships between variables. Chi-square or Fisher's exact test was used for clinical feature analysis. Kaplan-Meier survival analysis, along with univariate and multivariate Cox regression analyses, were employed for prognostic assessment. P-values <0.05 were considered statistically significant (*$p < 0.05$, **$p < 0.01$, ***$p < 0.001$). All sections of the study were analyzed using specific datasets, R packages, and databases.

Results

Identification of Prognostic MRlncRNAs and Construction of Prognostic Features

The study flowchart is depicted in Figure 1. Expression levels of 12 MRGs were analyzed in 372 LIHC patients and 50 normal liver tissue samples from the TCGA-LIHC dataset. Co-expression analysis identified 191 lncRNAs significantly associated with migrasomes (Supplementary Table S3). Univariate Cox regression analysis revealed 16 MRG-lncRNAs significantly correlated with the survival prognosis of LIHC patients ($P < 0.05$) (Figure 2B). A prognostic model was developed using LASSO Cox regression based on these MRlncRNAs (Figures 2C,D). Multivariate Cox regression analysis further assessed the correlation of two MRlncRNAs, resulting in a risk score formula: RiskScore = LINC00839 × 0.299+MIR4435-2HG×0.818.

Expression and prognostic value of MRlncRNAs

The expression and prognostic performance of candidate MRlncRNAs were further evaluated within the TCGA discovery cohort. Compared to normal tissues, LINC00839 and MIR4435-2HG were significantly upregulated in liver cancer tissues (Figure 3A). ROC curve analysis showed that both lncRNAs had high diagnostic accuracy, with AUC values exceeding 0.7 (Figure 3B). Kaplan-Meier survival curves

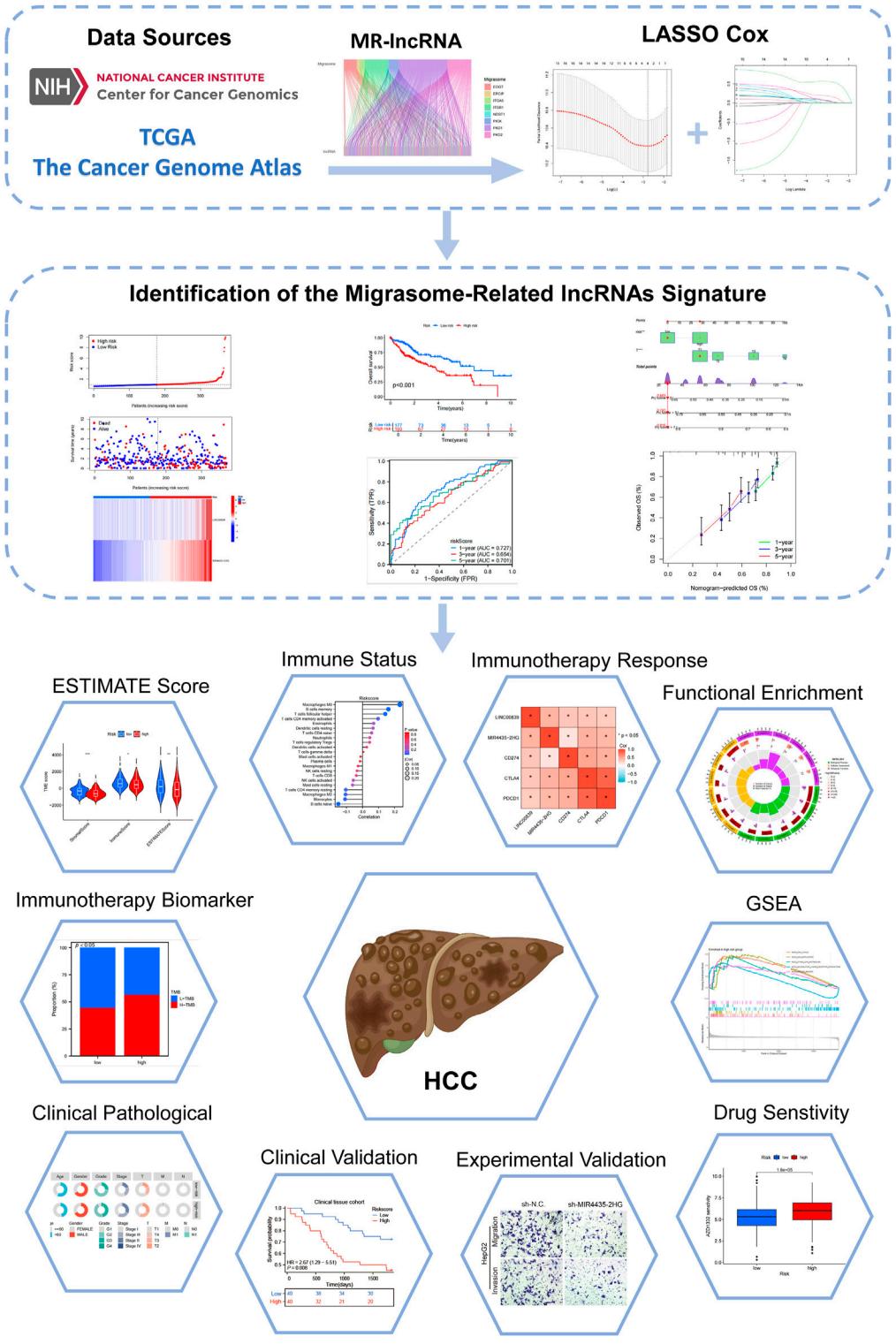


FIGURE 1
Flowchart of the present study.

demonstrated that high LINC00839 expression was associated with poorer overall survival (OS; P = 0.033, HR = 1.45 [1.03–2.05]) and disease-specific survival (DSS; P = 0.073, HR = 1.50 [0.96–2.33]) (Figure 3C). Conversely, high MIR4435-2HG expression correlated with significantly worse OS (P < 0.001, HR = 2.15 [1.50–3.08]) and progression-free interval (PFI; P = 0.005, HR = 1.53 [1.14–2.05]) (Figure 3D). These findings suggest that MRlncRNAs are promising biomarkers for LIHC diagnosis and prognosis. Univariate and multivariate Cox regression analyses further identified MIR4435-2HG as an independent prognostic factor for LIHC (Table 2).

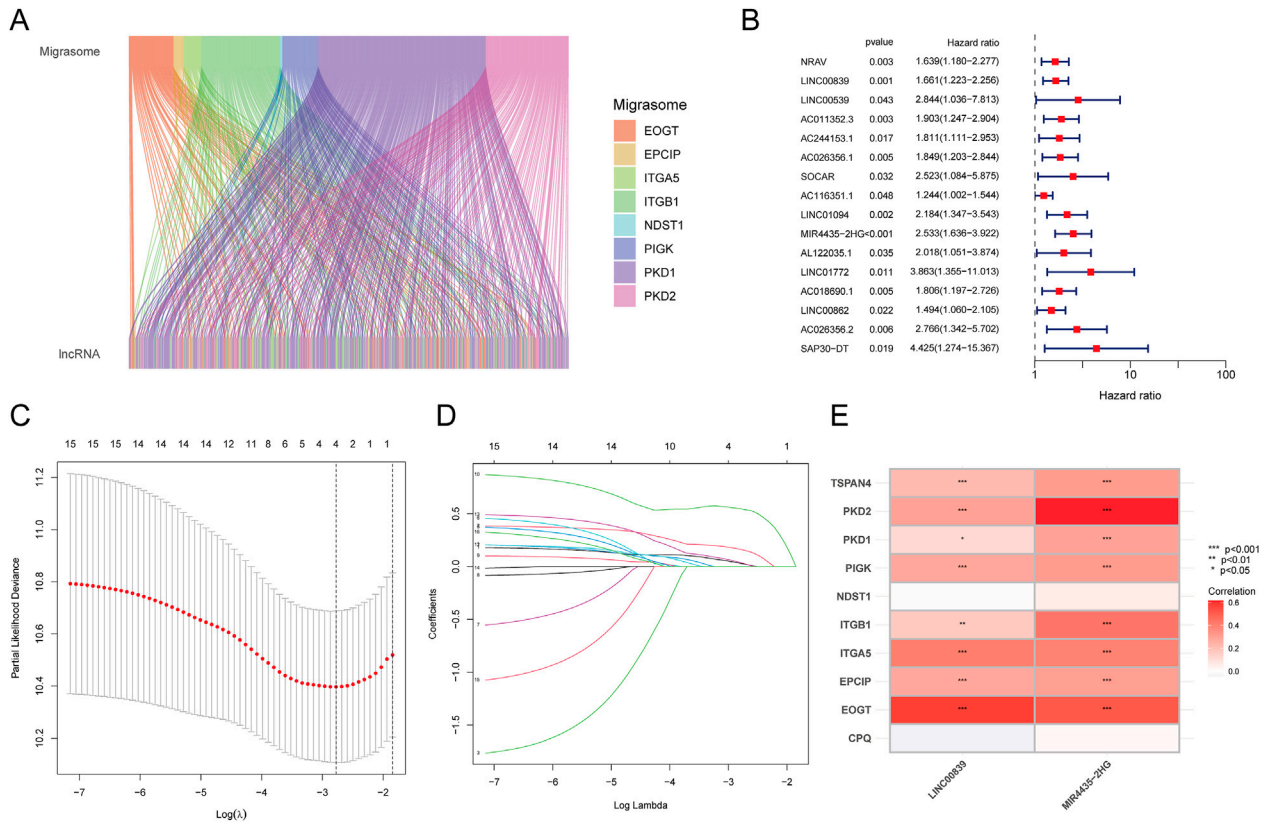


FIGURE 2
Identification of Prognostic MRlncRNAs and Construction of Prognostic Features. **(A)** Co-expression analysis of MRGs and lncRNAs; **(B)** Prognostic value of MRlncRNAs based on univariate Cox regression analysis (P < 0.05); **(C)** LASSO coefficient plot of prognostic MRlncRNAs; **(D)** Plot of the 10-fold cross-validation error rate; **(E)** Heatmap displaying the correlation between MRlncRNAs and MRGs.

Establishment and validation of the prognostic MRlncRNA model

The 370 TCGA-LIHC samples were randomly divided into training and validation sets. Patients were categorized into high-risk and low-risk groups based on median risk scores. As risk scores increased, mortality risk also increased, and survival time decreased (Figures 4A–F). Heatmaps illustrated the differential expression patterns of lncRNAs between risk groups (Figures 4G–I). Kaplan-Meier curves showed that high-risk patients exhibited significantly lower OS across all sample groups (P < 0.05, Figures 4J–L). The AUCs for 1-, 3-, and 5-year OS predictions in the entire cohort were 0.727, 0.654, and 0.701, respectively (Figure 4M). Similar results were observed in the training set (Figure 4N) and test set (Figure 4O), validating the predictive accuracy of our risk model.

Correlation with clinicopathological features

The association between risk scores and clinicopathological features was analyzed in the TCGA-LIHC cohort. Significant correlations were observed between risk scores and tumor grade, stage, and T status (Figure 5A; Supplementary Table S4). Subgroup survival analysis revealed that the high-risk group had significantly poorer survival across various clinical subgroups, suggesting that these factors play a critical role in LIHC prognosis (Figure 5B).

Development and validation of a prognostic nomogram

Univariate and multivariate Cox regression analyses identified T status (HR = 2.625, P < 0.001), N status (HR = 1.473, P = 0.043), M status (HR = 1.676, P = 0.007), and risk score (HR = 1.219, P < 0.001) as prognostic factors for OS in LIHC. The nomogram integrating risk score and T status was constructed to predict 1-, 3-, and 5-year OS in LIHC patients. ROC analysis of the nomogram demonstrated good predictive accuracy, with AUC values of 0.636 for the risk score model and 0.654 for the T status model (Figure 6C). The nomogram's calibration curve confirmed a strong concordance between predicted and observed OS (Figure 6G), with AUCs of 0.721, 0.727, and 0.781 for 1-, 3-, and 5-year OS predictions, respectively (Figure 6H).

Functional enrichment analysis of high- and low-risk MRlncRNAs

A total of 755 DEGs were identified between high- and low-risk MRlncRNA groups. GO analysis indicated that these DEGs were

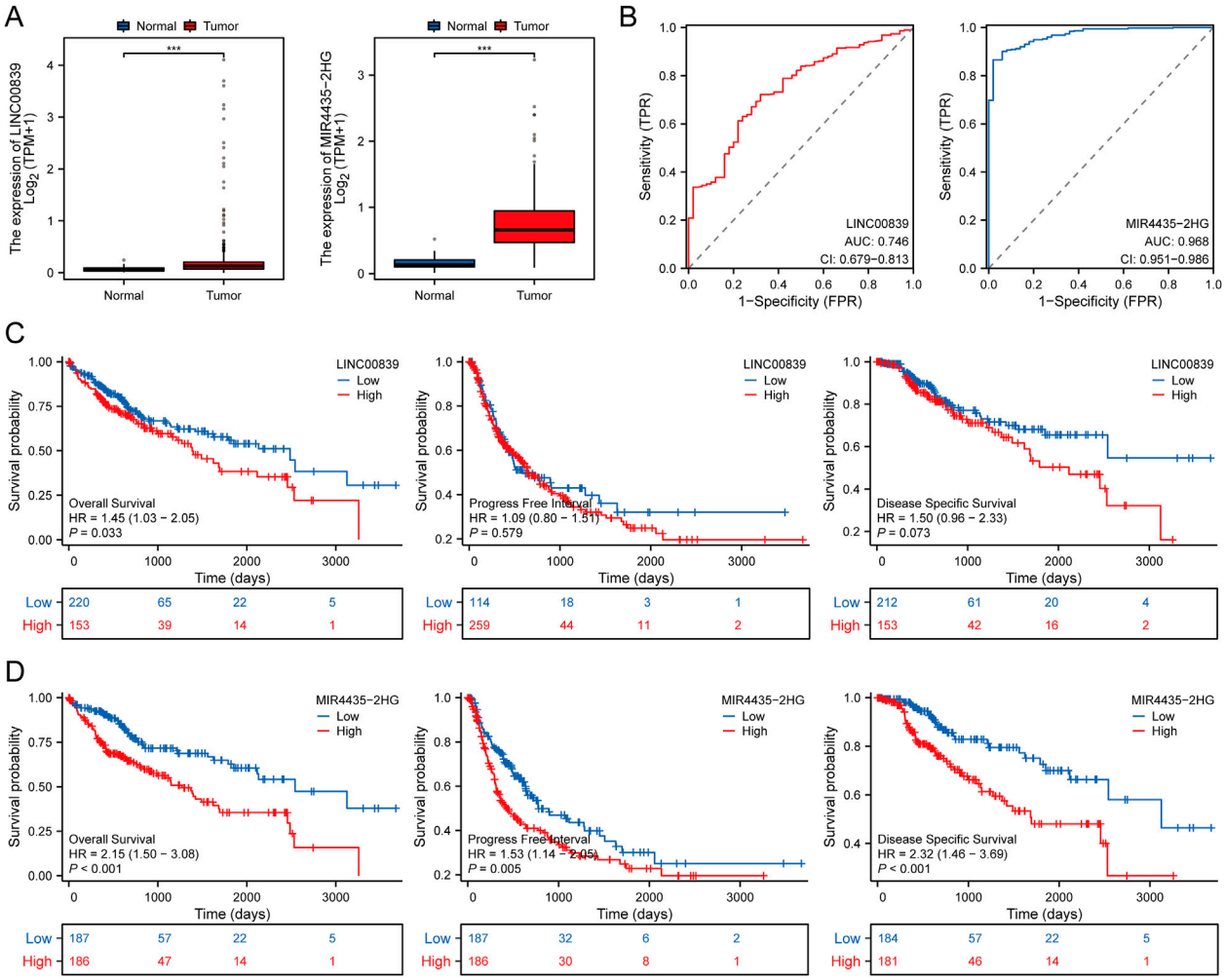


FIGURE 3
Expression and Prognostic Value Analysis of Prognostic MRlncRNAs in LIHC Patients. **(A)** Comparison of prognostic MRlncRNAs expression in liver tumors and normal tissues in TCGA databases; **(B)** ROC curves assessing the diagnostic potential of MRlncRNAs expression in LIHC; **(C)** Survival curves of OS, PFI, and DSS comparing high and low expression of LINC00839 in LIHC; **(D)** Survival curves of OS, PFI, and DSS comparing high and low expression of MIR4435-2HG in LIHC. *P < 0.05; **P < 0.01; ***P < 0.001.

enriched in biological processes such as nuclear division, chromosome segregation, and mitotic division (Figure 7A). Cellular components included chromosomal regions and kinetochores, while molecular functions were enriched in microtubule binding and ATP-dependent DNA helicase activity. KEGG pathways were mainly associated with the cell cycle, microRNAs in cancer, and p53 signaling (Figure 7B). GSEA showed that genes in the high-risk group were primarily involved in the cell cycle, DNA replication, and neuroactive ligand-receptor interactions, while genes in the low-risk group were enriched in complement and coagulation cascades, fatty acid metabolism, and bile acid biosynthesis (Figure 7C).

Genetic alteration analysis of MRlncRNAs

Genetic alterations of MRlncRNAs were analyzed using the cBioPortal database. Mutations in LINC00839 and MIR4435-2HG were detected in 175 of 348 sequenced LIHC samples (Figure 8A). Clinical analysis revealed significant differences between the mutation and non-mutation groups in Buffa Hypoxia Score, Winter Hypoxia Score, Aneuploidy Score, Ragnum Hypoxia Score, Fraction Genome Altered, Last Communication Contact, and Neoplasm Histologic Grade (Figure 8B). Survival analysis showed that genetic alterations of prognostic MRlncRNAs were significantly associated with shorter overall survival (OS, P = 0.0390), but not with progression-free survival (PFS, P = 0.250) or disease-free survival (DFS, P = 0.174) (Figure 8C). Compared to low-expression patients, high-expression patients had higher proportions of Tumor Mutational Burden (TMB) and Microsatellite Instability (MSI) (Figure 8D). TMB, MSI, and mRNAsi scores were significantly higher in the high-risk group (Figure 8E). Survival analysis indicated that high TMB and MSI scores were associated with poorer OS (Figure 8F). Additionally, survival analysis combining risk score with TMB and MSI revealed that patients in the low TMB + low-risk score group had better OS than those in the high TMB + high-risk score group (P < 0.001), and the low MSI + low-risk score group had better

TABLE 2 Cox regression analysis of MRlncRNAs in prognosis prediction.

Characteristics	Total (N)	Univariate analysis		Multivariate analysis	
		Hazard ratio (95% CI)	P Value	Hazard ratio (95% CI)	P Value
Age	373				
≤ 60	177	Reference			
>60	196	1.205 (0.850–1.708)	0.295		
Gender	373				
Female	121	Reference			
Male	252	0.793 (0.557–1.130)	0.200		
Histologic grade	368				
G1&G2	233	Reference			
G3&G4	135	1.091 (0.761–1.564)	0.636		
Pathologic stage	349				
Stage I&Stage II	259	Reference		Reference	
Stage III&Stage IV	90	2.504 (1.727–3.631)	< **0.001**	1.299 (0.177–9.518)	0.797
Pathologic T stage	370				
T1&T2	277	Reference		Reference	
T3&T4	93	2.598 (1.826–3.697)	< **0.001**	2.241 (0.304–16.546)	0.429
Pathologic N stage	258				
N0	254	Reference			
N1	4	2.029 (0.497–8.281)	0.324		
Pathologic M stage	272				
M0	268	Reference		Reference	
M1	4	4.077 (1.281–12.973)	**0.017**	1.965 (0.602–6.412)	0.263
LINC00839	373				
Low	187	Reference			
High	186	1.306 (0.923–1.848)	0.132		
MIR4435-2HG	373				
Low	187	Reference		Reference	
High	186	2.147 (1.497–3.079)	< **0.001**	2.189 (1.395–3.433)	< **0.001**

OS than the high MSI + high-risk score group ($P < 0.001$) (Figure 8G).

Immune cell infiltration analysis

Using CIBERSORT, ssGSEA, and ESTIMATE algorithms, the correlation between risk score and immune cell infiltration was analyzed. Immune infiltration scores showed marked differences between high- and low-risk MRlncRNA groups (Figure 9A). The stacked bar chart depicted the immune cell infiltration proportions between high and low expression groups (Figure 9B). The CIBERSORT algorithm revealed that naive B cells, memory B cells, and resting mast cells were more abundant in the low-risk group, while follicular helper T cells and M0 macrophages were more abundant in the high-risk group. Risk score was positively correlated with eosinophils, activated CD4 T cells, follicular helper T cells, memory B cells, and M0 macrophages, and negatively correlated with naive B cells, monocytes, M2 macrophages, resting CD4 T cells, resting mast cells, activated NK cells, CD8 T cells, resting NK cells, and M1 macrophages. Additionally, ssGSEA analysis showed higher expression of B cells, CD8 T cells, cytotoxic cells, dendritic cells (DC), eosinophils, immature DC, mast cells, neutrophils, NK CD56dim cells, NK cells, plasmacytoid DC (pDC), Tγδ cells, and regulatory T cells (TReg) in the low-risk group, while T helper cells and Th2 cells were more expressed in the high-risk group (Figures 9C,D). Correlation analysis also

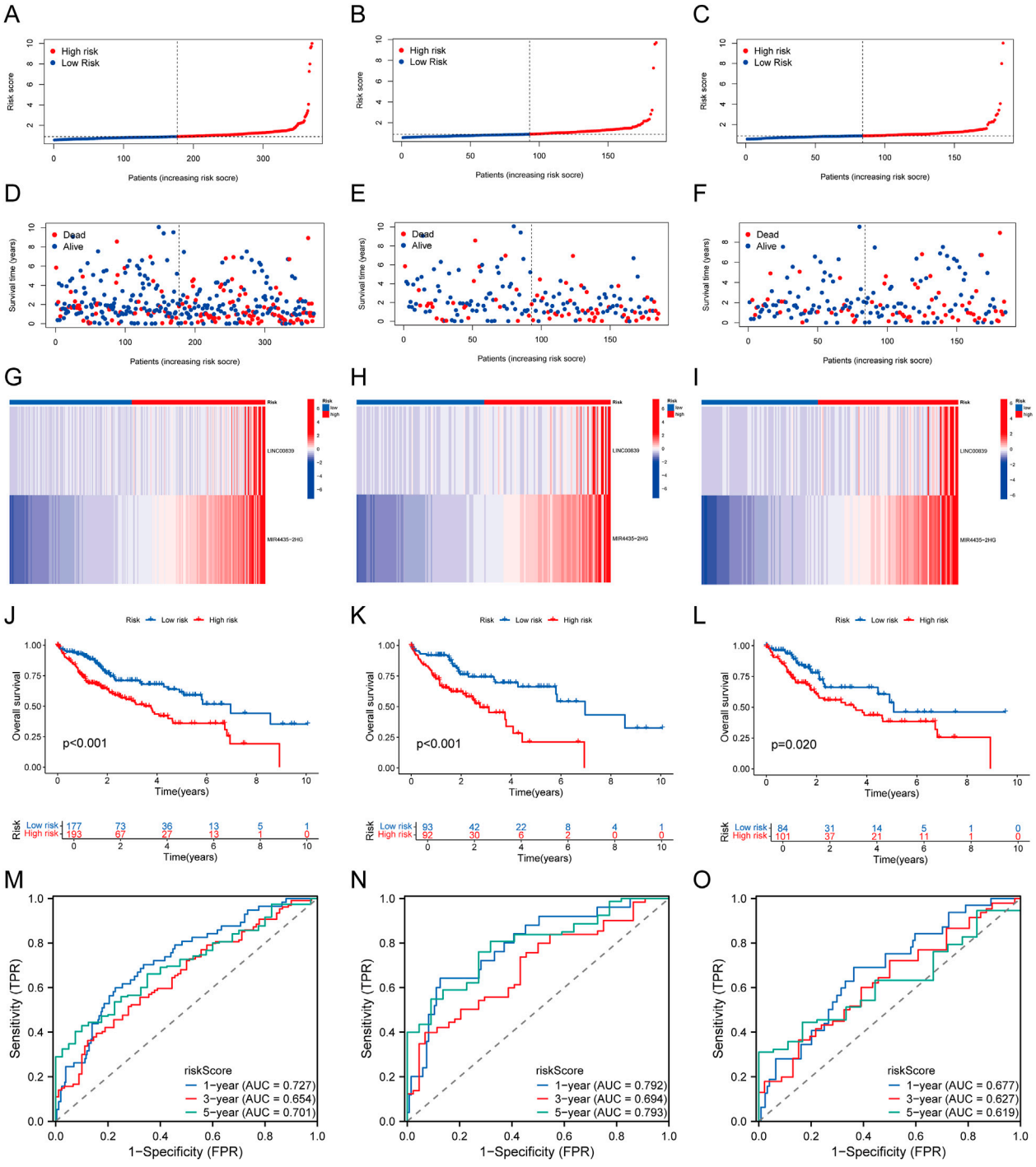


FIGURE 4
Establishment and Validation of Prognostic MRlncRNAs Features. **(A–C)** Distribution of risk scores for each patient in the TCGA-LIHC cohort, training cohort, and test cohort; **(D–F)** Distribution of overall survival status for each patient in the TCGA-LIHC cohort, training cohort, and test cohort; **(G–I)** Heatmap showing the expression of two prognostic MRlncRNAs in the TCGA-LIHC cohort, training cohort, and test cohort; **(J–L)** Kaplan-Meier survival curves for high-risk and low-risk groups comparing overall survival in the TCGA-LIHC cohort, training cohort, and test cohort; **(M–O)** Time-dependent ROC curves for 1-, 3-, and 5-year OS in the TCGA-LIHC cohort, training cohort, and test cohort.

indicated that risk score was negatively correlated with immune scores (Figure 9E). Prognostic analysis revealed that patients in the low ESTIMATE + high-risk score group had worse OS than those in the high ESTIMATE + low-risk score group ($P < 0.001$) (Figure 9F).

Single-cell RNA sequencing (ScRNA-seq) data analysis

Analysis of ScRNA-seq data from the LIHC_GSE125449 dataset in the TISCH database identified 14 cell clusters and eight cell types,

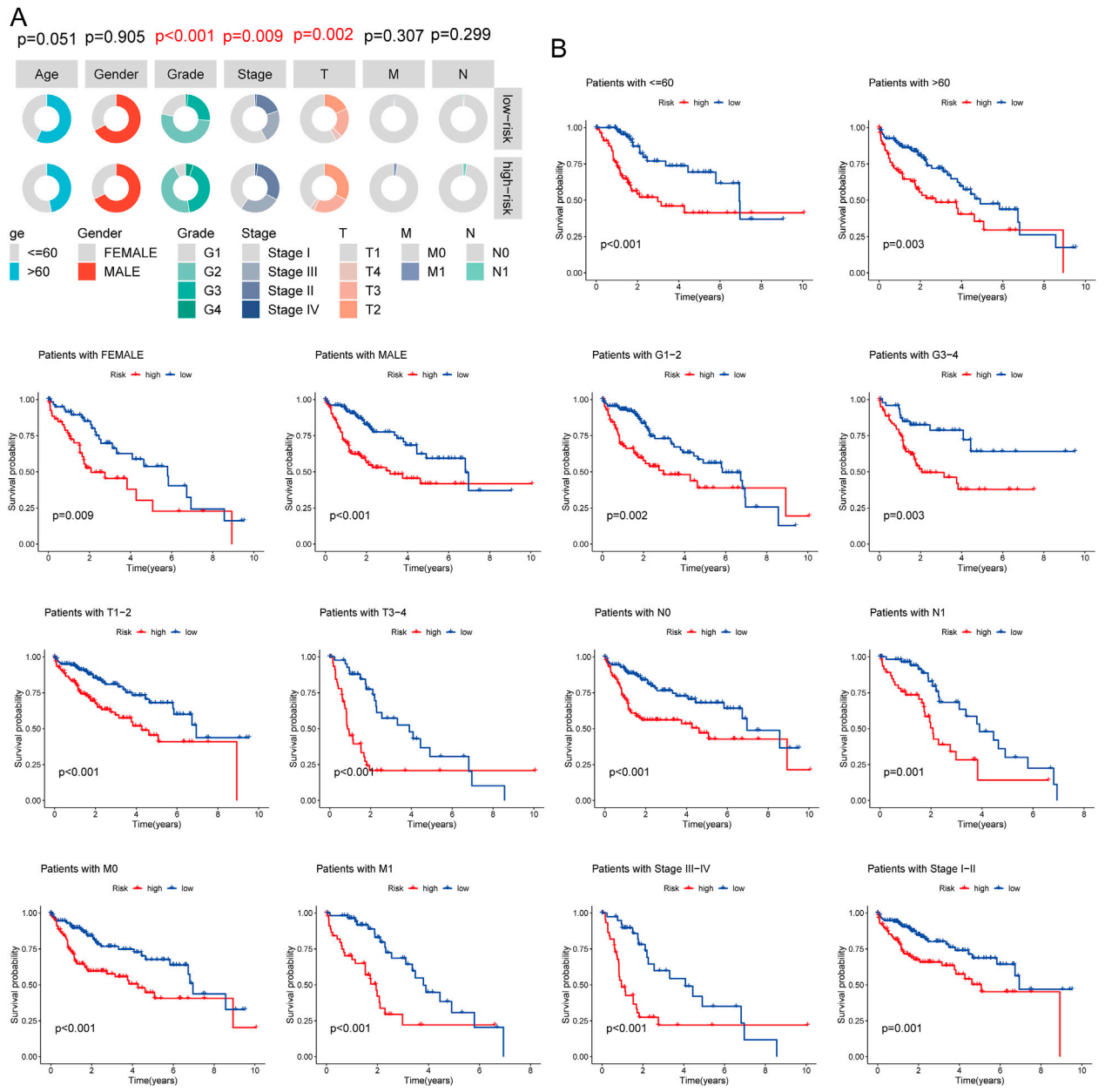


FIGURE 5
Association Between Risk Score and Clinicopathological Characteristics. **(A)** Circos plot showing the clinical factors between high and low-risk score groups; **(B)** Survival curve comparing high and low-risk score groups in different LIHC subgroups.

highlighting the distribution and abundance of various TME-related cells (Figures 10A,B). A bubble plot visualized the expression of key marker genes across different cell types (Figure 10C). The pie chart showed higher expression in malignant cells, fibroblasts, and endothelial cells (Figure 10D). The distribution of LINC00839 and MIR4435-2HG expression in different cell types revealed that MIR4435-2HG had higher infiltration in TME-related cells than LINC00839 (Figures 10F,G). Further analysis showed that LINC00839 and MIR4435-2HG were significantly associated with cancer-associated fibroblasts (CAFs) and epithelial-mesenchymal transition (EMT) markers (Figures 10H,I). These results suggest that MRlncRNAs may promote fibrosis activation and contribute to LIHC metastasis via EMT.

Immunotherapy response analysis

Heatmap analysis showed significant differences in the distribution of immune checkpoint genes and TIDE scores between high- and low-risk groups (Figure 11A). Expression analysis of eight immune checkpoint-related genes revealed higher expression of CTLA4, HAVCR2, PDCD1, TIGIT, and ITPRIPL1 in the high-risk group (Figure 11B). The relationship between risk score and three key immune checkpoints (CD274, PDCD1, CTLA4) showed positive correlations ($P < 0.05$) (Figure 11C). Survival analysis indicated that patients with high immune checkpoint expression in the high-risk group had poorer OS compared to those with low checkpoint expression in the low-

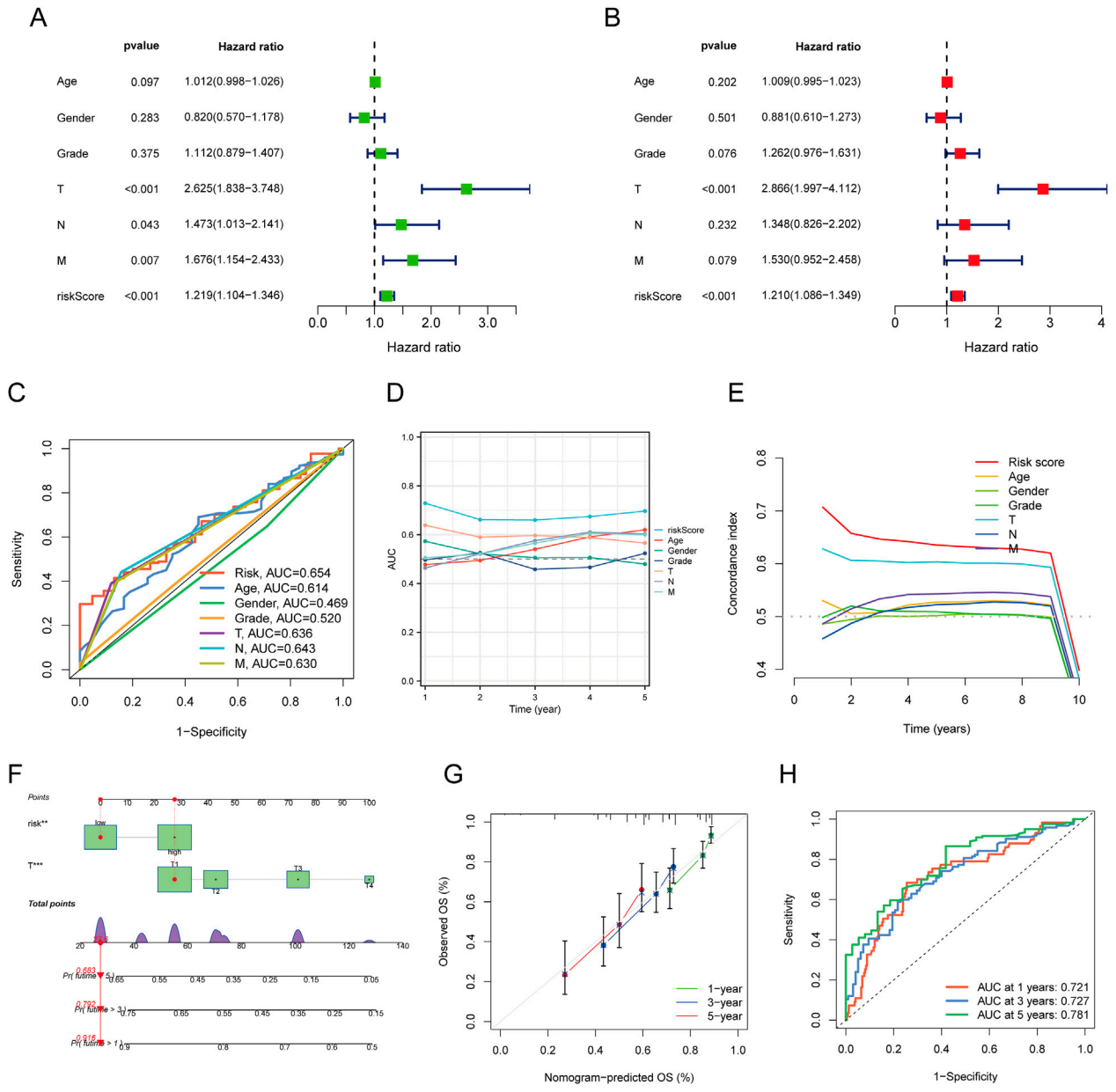
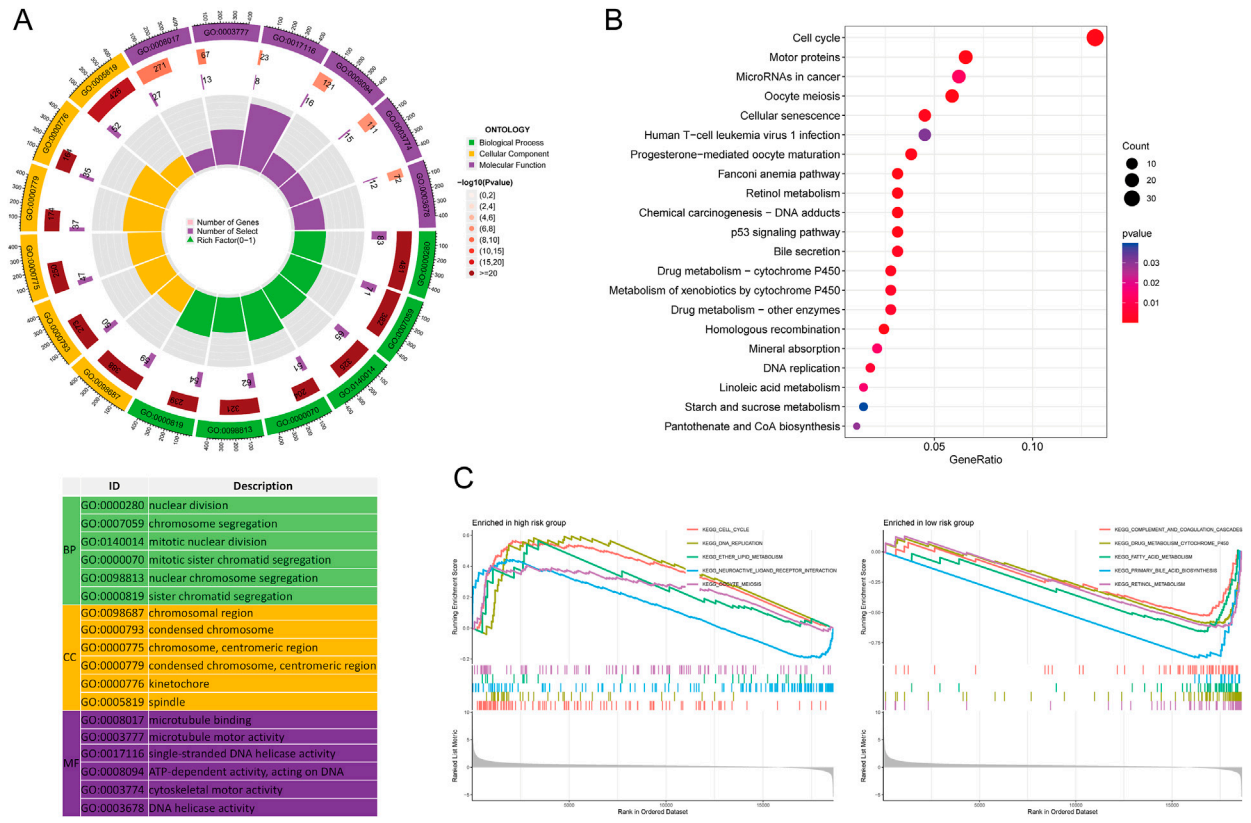


FIGURE 6
Construction and Validation of a Predictive Nomogram. **(A,B)** Univariate and multivariate Cox regression analysis of clinical variables in LIHC; **(C)** ROC curves for risk scores and various clinical pathological parameters (age, gender, Grade, T, N, M); **(D)** Time-dependent AUC curve showing the risk score's performance in predicting OS; **(E)** Consistency index of the risk score and other clinical pathological variables; **(F)** Nomogram for predicting 1-, 3-, and 5-year OS of LIHC patients; **(G)** Calibration curve of the OS nomogram model in the discovery group, with the diagonal dotted line representing the ideal nomogram; **(H)** ROC curves for predicting 1-, 3-, and 5-year OS.

risk group (Figure 11D). To predict immune treatment response, TIDE scores and clinical sample data were used. Compared to the low-risk group, the high-risk group showed higher TIDE and Exclusion scores, and lower Dysfunction scores (Figure 11E). Kaplan-Meier analysis showed that the high-risk and high-TIDE group had the worst prognosis (Figure 11F). In an external clinical cohort of 80 liver cancer samples, patients in the low-risk group had higher rates of complete or partial remission (CR/PR) with immune checkpoint inhibitors (AUC >0.7) (Figures 11G,H). These findings suggest that low-risk patients are more likely to benefit from immune checkpoint inhibitor (ICI) therapy, showing better post-treatment survival rates.

Chemotherapy drug sensitivity

Chemotherapy drug sensitivity analysis for low-risk and high-risk groups revealed that the high-risk group had significantly lower IC50 values for multiple drugs, including 5-Fluorouracil, Doxorubicin, and Paclitaxel (Supplementary Figure S1). These



ID	Description
GO:0000280	nuclear division
GO:0007059	chromosome segregation
GO:0140014	mitotic nuclear division
GO:0000070	mitotic sister chromatid segregation
GO:0098813	nuclear chromosome segregation
GO:0000819	sister chromatid segregation
GO:0098687	chromosomal region
GO:0000793	condensed chromosome
GO:0000775	chromosome, centromeric region
GO:0000779	condensed chromosome, centromeric region
GO:0000776	kinetochore
GO:0005819	spindle
GO:0008017	microtubule binding
GO:0003777	microtubule motor activity
GO:0017116	single-stranded DNA helicase activity
GO:0008094	ATP-dependent activity, acting on DNA
GO:0003774	cytoskeletal motor activity
GO:0003678	DNA helicase activity

FIGURE 7
Functional Enrichment Analysis Between High and Low-Risk Groups. **(A)** GO enrichment results; **(B)** KEGG pathways; **(C)** GSEA analysis.

results suggest that these drugs may be effective for treating high-risk LIHC patients.

Cell and clinical sample validation

To validate the expression and prognostic value of MRlncRNAs, we first performed RT-qPCR analysis in 100 paired hepatocellular carcinoma (HCC) and adjacent normal tissue samples. Both LINC00839 and MIR4435-2HG were significantly upregulated in tumor tissues (Figure 12A). Using the same cohort, patients were stratified into high- and low-risk groups based on the MRlncRNA-based risk score. Kaplan-Meier analysis revealed that high-risk patients had significantly poorer overall survival (OS) compared to low-risk patients (HR = 2.66, 95% CI: 1.47–4.79, P = 0.001; Figure 12B). Time-dependent ROC analysis showed strong predictive performance, with AUCs of 0.824, 0.851, and 0.878 for 1-, 3-, and 5-year OS, respectively (Figure 12C), and consistent accuracy over time (Figure 12D). Decision curve analysis (DCA) further demonstrated the clinical utility of the risk model for survival prediction (Figure 12E). To assess the robustness of the model, we randomly divided the 100-sample cohort into two equal subsets (Validation Set one and Validation Set two; each n = 50). In both subsets, the risk score effectively distinguished high-risk patients with significantly shorter OS (Supplementary Figure S2A, D). ROC curves yielded high AUCs in both sets: 0.833, 0.860, and 0.872 for Validation Set 1 (Supplementary Figure S2B); and 0.844, 0.855, and 0.856 for Validation Set 2 (Supplementary Figure S2E). DCA confirmed the model's predictive benefit across both subsets (Supplementary Figure S2C, F, H). Moreover, RT-qPCR analysis in HCC cell lines (Hep3B, Huh7, and HepG2) and the normal hepatocyte line (THLE-2) confirmed significant overexpression of both MRlncRNAs in tumor cells, consistent with the clinical findings (Figure 12F). Together, these results validate the MRlncRNA-based risk model across bulk tissue samples and cell lines, underscoring its translational potential for clinical prognostication in HCC.

MIR4435-2HG knockdown suppresses proliferation, migration, invasion, EMT, and PD-L1 expression in HCC cells

To validate the oncogenic function of MIR4435-2HG in hepatocellular carcinoma, we conducted a series of *in vitro* experiments in HepG2 and Huh7 cells. qRT-PCR confirmed efficient knockdown of MIR4435-2HG using three independent shRNAs, among which sh-MIR4435-2HG one exhibited the highest silencing efficiency and was selected for subsequent functional assays (Figure 13A). Cell proliferation was significantly inhibited upon MIR4435-2HG knockdown, as demonstrated by CCK-8 assays at 24, 48, and 72 h (Figures 13B,C). Wound healing assays revealed that MIR4435-2HG silencing impaired cell migration capacity at 24 h (Figures 13D,F). In addition, Transwell assays showed a marked reduction in both migratory and invasive abilities of HepG2 and Huh7 cells (Figures 13E,G,H). At the molecular level, Western blot analysis showed that MIR4435-

10.3389/fphar.2025.1581122

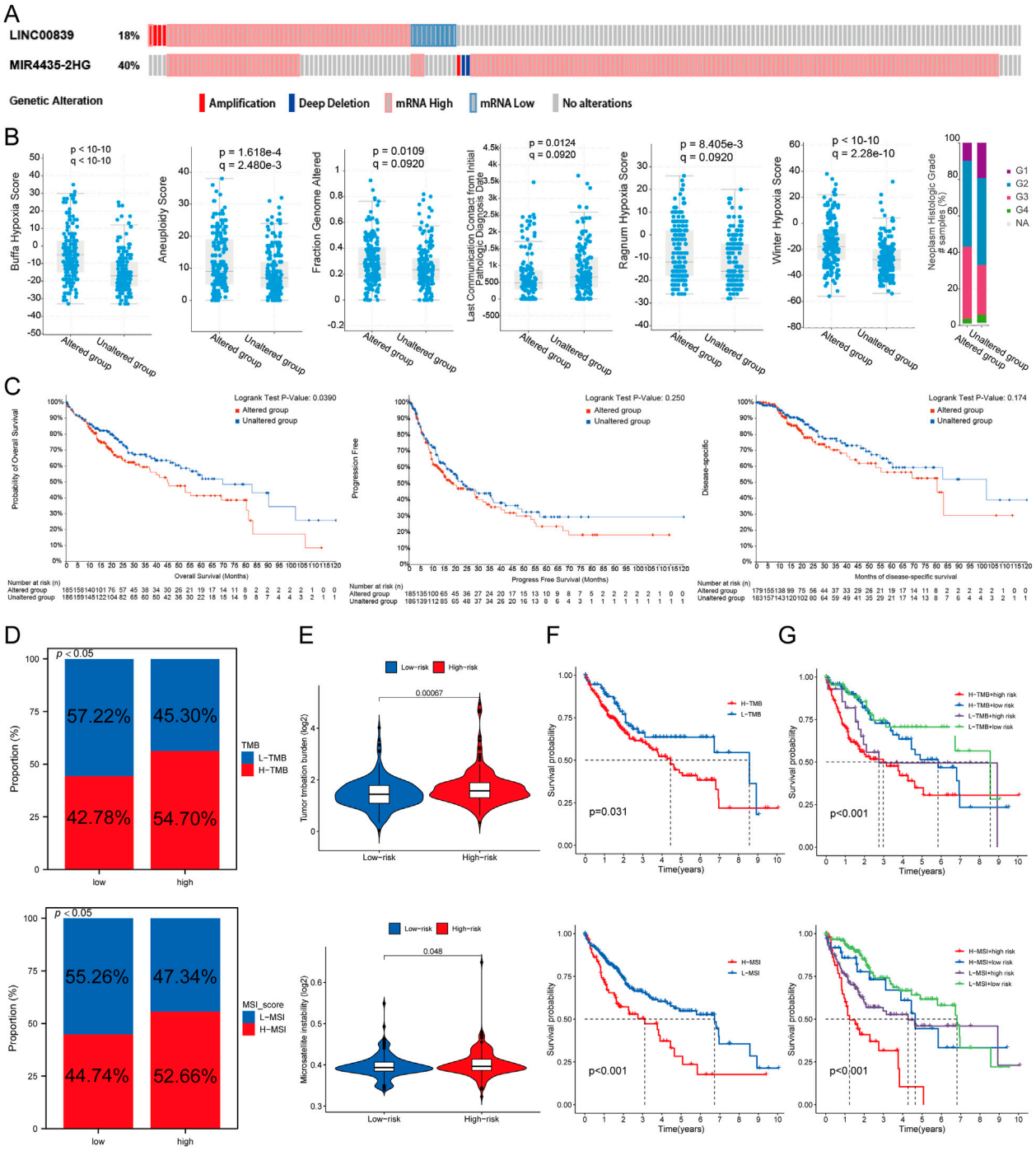


FIGURE 8
Genetic Alterations Associated with MRlncRNAs. **(A)** Oncoprint displaying somatic mutations in the LIHC tumor cohort; **(B)** Correlation between MRlncRNA alterations and various clinicopathological factors in LIHC, including Buffa Hypoxia Score, Winter Hypoxia Score, Aneuploidy Score, Ragnum Hypoxia Score, Fraction Genome Altered, Neoplasm Histologic Grade, and Last Communication Contact from Initial Pathologic Diagnosis Date; **(C)** Genetic alterations of MRlncRNAs in LIHC tissues correlated with shorter OS, PFS, and DFS in patients; **(D)** Distribution of TMB and MSI scores in high-expression and low-expression groups; **(E)** Differences in TMB and MSI between high and low-risk score groups in LIHC; **(F)** Kaplan-Meier survival curves for high and low TMB, MSI groups in LIHC; **(G)** Kaplan-Meier survival curves of four groups classified by risk score and TMB, MSI in LIHC.

2HG knockdown induced a mesenchymal–epithelial transition (MET)-like phenotype, as evidenced by upregulation of E-cadherin and downregulation of Vimentin (Figures 13I,J). Notably, the immune checkpoint molecule PD-L1 was also significantly downregulated in MIR4435-2HG–silenced cells, suggesting a potential role of this lncRNA in immune evasion. Together, these findings demonstrate that MIR4435-2HG promotes malignant phenotypes and immune escape in HCC, supporting its functional relevance in the migrasome-related lncRNA signature.

10.3389/fphar.2025.1581122

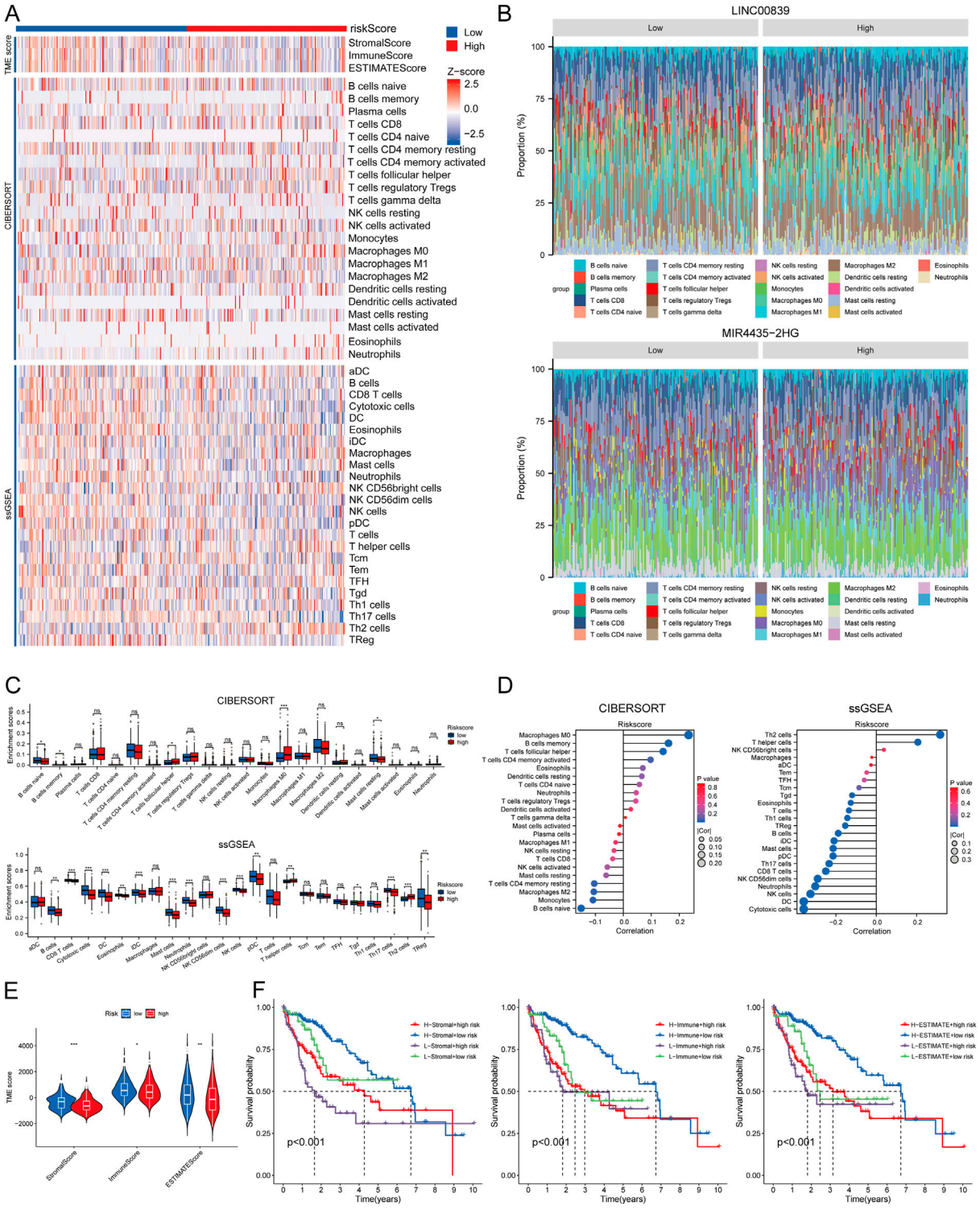


FIGURE 9
Relationship Between Risk Score and Immune Infiltration in the Tumor Microenvironment. **(A)** Heatmap of immune cell scores between high and low-risk score groups using CIBERSORT, ssGSEA, and ESTIMATE algorithms; **(B)** Percent abundance of tumor-infiltrating immune cells between high and low expression groups of two prognostic MRlncRNAs, with different colors representing various immune cell types; **(C)** Comparison of immune scores between high and low-risk score groups using CIBERSORT and ssGSEA; **(D)** Correlation analysis between risk score and immune infiltration using CIBERSORT and ssGSEA; **(E)** Differences in ESTIMATE between high and low-risk score groups; **(F)** Kaplan-Meier curves of four groups classified by risk score and three ESTIMATE scores in LIHC.

10.3389/fphar.2025.1581122

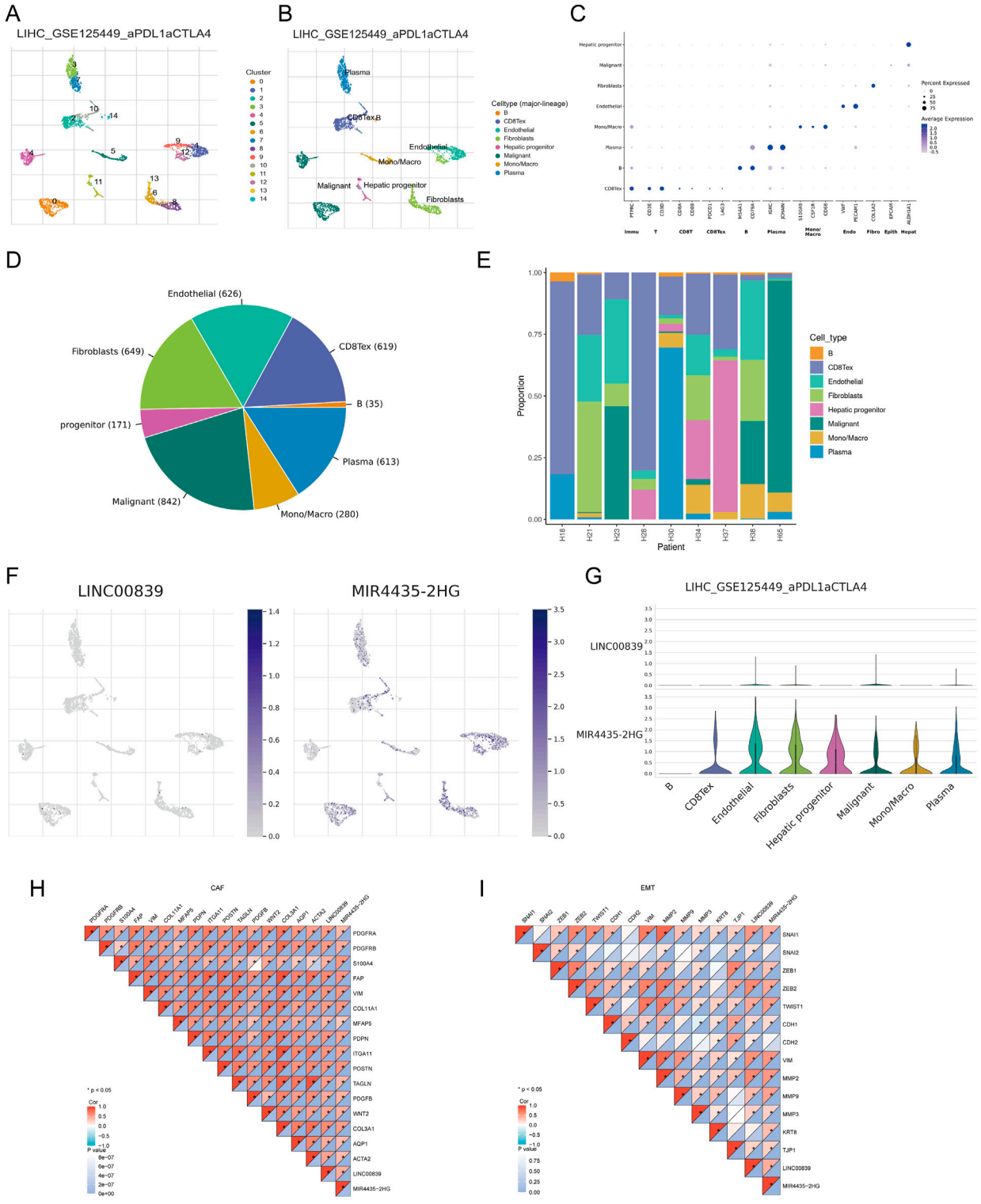


FIGURE 10
Expression of MRlncRNAs in Different Immune Cell Types in LIHC. **(A)** Clustering of cell types from scRNA-seq data; **(B)** Annotation of different immune cell types in LIHC tissues (LIHC_GSE125449); **(C)** Expression levels of marker genes in each cell cluster; **(D)** Pie chart showing the percentage of each cell type; **(E)** Percentage of each cell subtype in different patients; **(F)** Expression distribution of LINC00839, MIR4435-2HG in various cell types using single-cell resolution from the LIHC_GSE125449 dataset; **(G)** Violin plots showing the expression of LINC00839 and MIR4435-2HG in LIHC cells; **(H,I)** Correlation between LINC00839, MIR4435-2HG and CAFs or EMT-related markers.

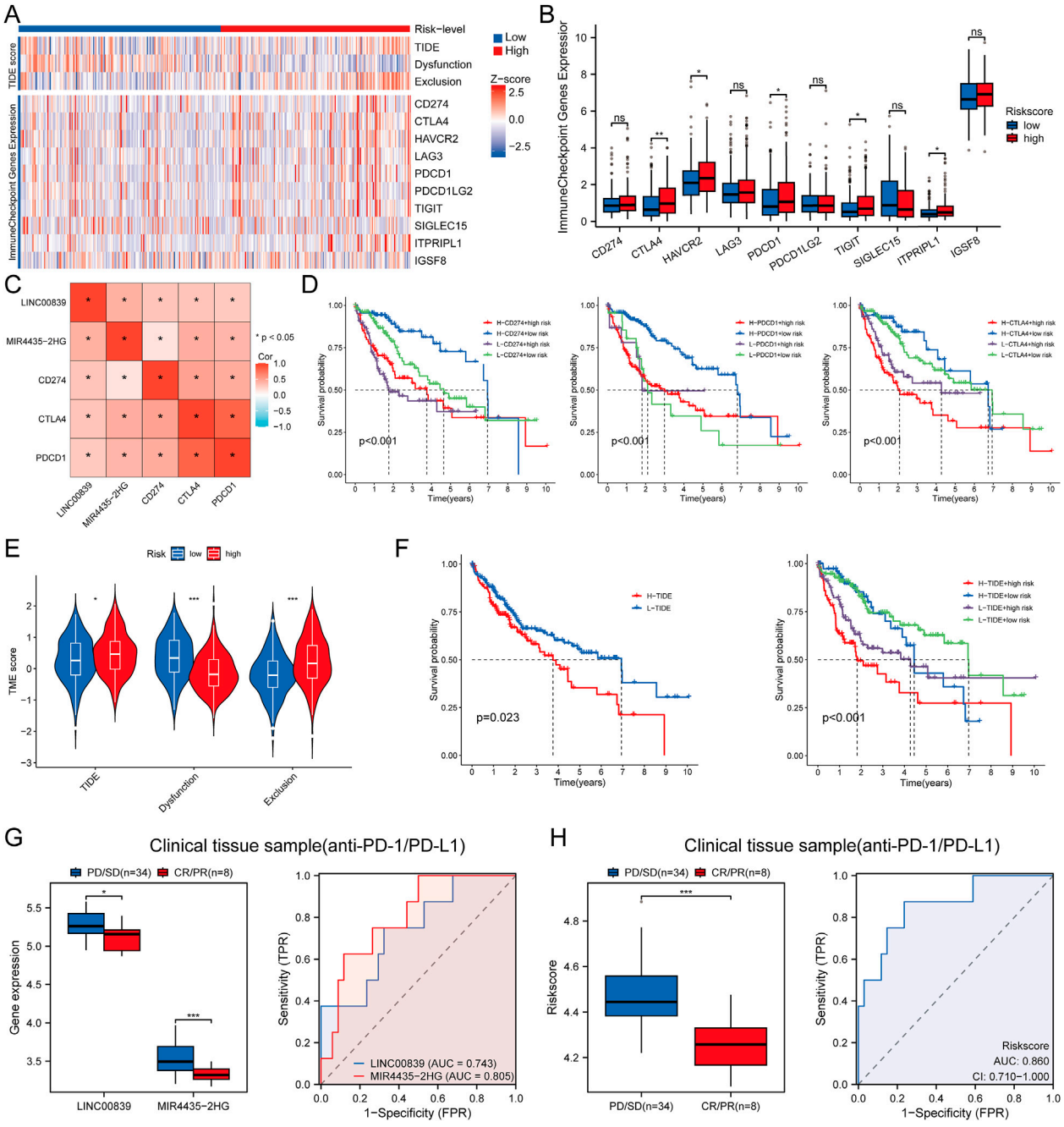


FIGURE 11
Immune Response Analysis. **(A)** Heatmap of immune checkpoint gene expression and TIDE scores between high and low-risk score groups, with different colors representing expression trends across different samples; **(B)** Expression distributions of eight immune checkpoint-associated genes between high and low-risk score groups in LIHC; **(C)** Correlation between risk score and clinical immune checkpoint-related genes in LIHC; **(D)** Kaplan-Meier survival curves for four groups classified by risk score and CD274, PDCD1, CTLA expression; **(E)** TIDE score evaluation of risk scores in response to immunotherapy in LIHC; **(F)** Kaplan-Meier survival plots of overall survival for high and low TIDE scores; **(G,H)** Differences in MRlncRNAs expression and risk score between patients with SD/PD and CR/PR in clinical tissue samples; ROC analysis of MRlncRNAs expression and risk score for predicting ICI responsiveness in clinical tissue samples (NR: non-responders; R: responders to immunotherapy).

Discussion

HCC remains a highly aggressive malignancy with poor prognosis, largely due to its molecular heterogeneity and immunosuppressive TME, which limit the efficacy of conventional and immune-based therapies. Migrasomes—recently identified as migration-dependent extracellular vesicles—have been implicated in tumor progression and immune modulation by transporting factors such as PD-L1 and TGF-β (Jiang et al., 2023; Deng et al., 2024). However, their interaction with lncRNAs, especially in the context of HCC, remains poorly understood. To address this gap, we conducted a systematic analysis of MRlncRNAs,

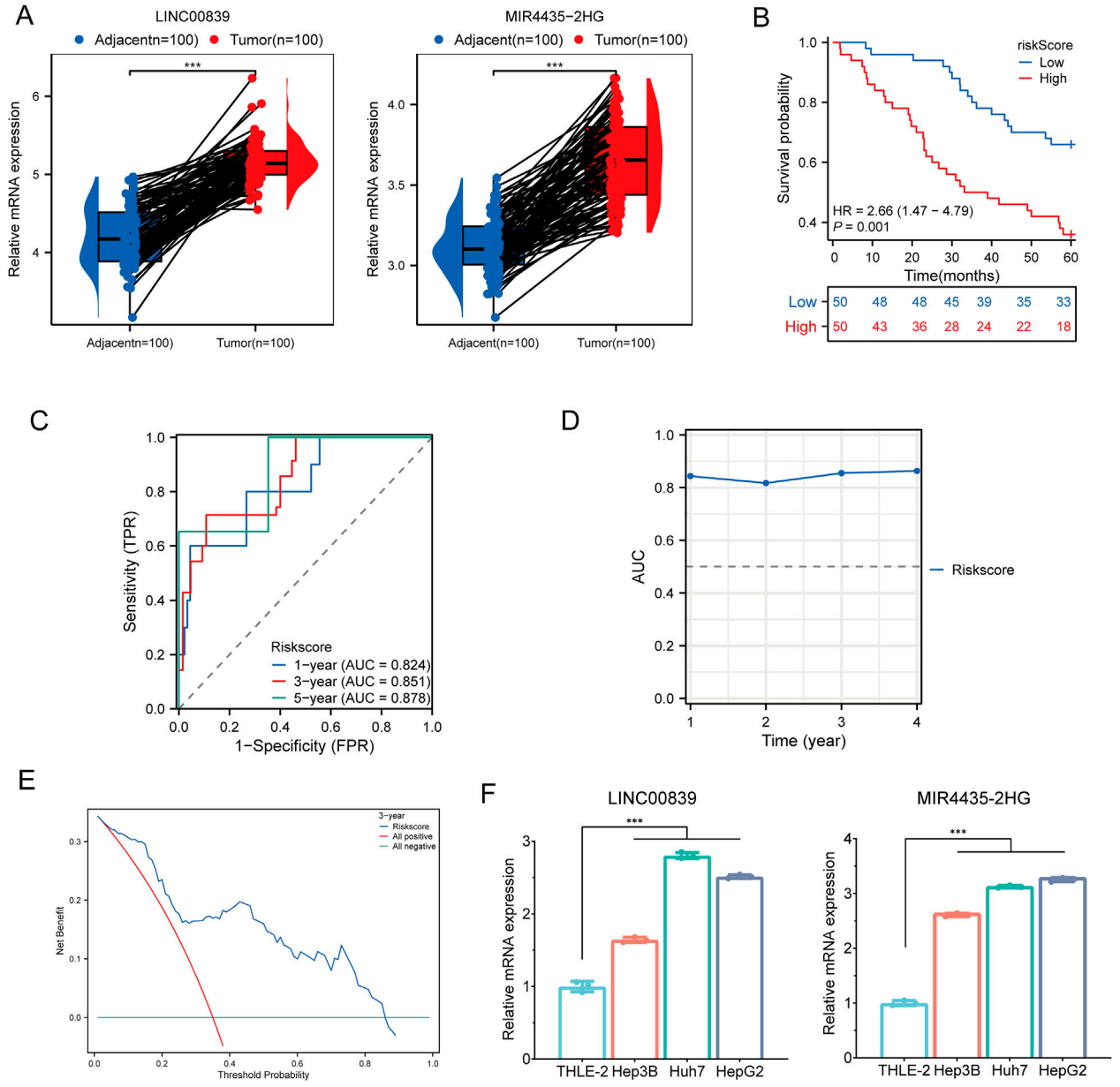


FIGURE 12
Clinical Sample and Cell Experiment Validation. **(A)** Relative expression of MRlncRNAs in normal and glioma tissues; **(B)** Overall survival curve for high- and low-risk HCC patients; **(C)** Time-dependent ROC curves for MRlncRNAs at 1, 3, and 5 years; **(D)** Time-dependent AUC curves; **(E)** Decision curve analysis for 3-year OS in clinical samples; **(F)** Differential expression of MRlncRNAs in HCC cell lines and normal cell lines.

aiming to uncover novel prognostic biomarkers and immune modulators.

By integrating transcriptomic and clinical data from TCGA-LIHC, we identified 191 candidate MRlncRNAs via Pearson correlation with 12 curated migrasome-related genes ($|R| > 0.55$, $P < 0.001$), of which 16 were associated with survival. LASSO Cox regression revealed a robust 2-lncRNA prognostic signature—LINC00839 and MIR4435-2HG—that minimized cross-validation error. This signature showed strong predictive accuracy (5-year AUC = 0.701 in TCGA, 0.872 in external cohort), indicating its broad applicability. RT-qPCR confirmed upregulation of both lncRNAs in HCC tissues and cell lines, using THLE-2 as the control, supporting the clinical relevance of our model. To elucidate functional relevance, we performed knockdown experiments targeting MIR4435-2HG in HepG2 and Huh7 cells. Silencing significantly suppressed proliferation, migration, and invasion, while increasing E-cadherin and decreasing Vimentin and PD-L1 expression, suggesting EMT reversal and reduced immune escape. These findings establish MIR4435-2HG as a key driver of both tumor aggressiveness and immunosuppressive remodeling. Additionally, LINC00839 is known to promote migration via hypoxia-induced FMNL2 activation (Xie et al., 2022), further linking MRlncRNAs to migrasome biogenesis and adaptive TME regulation. Collectively,

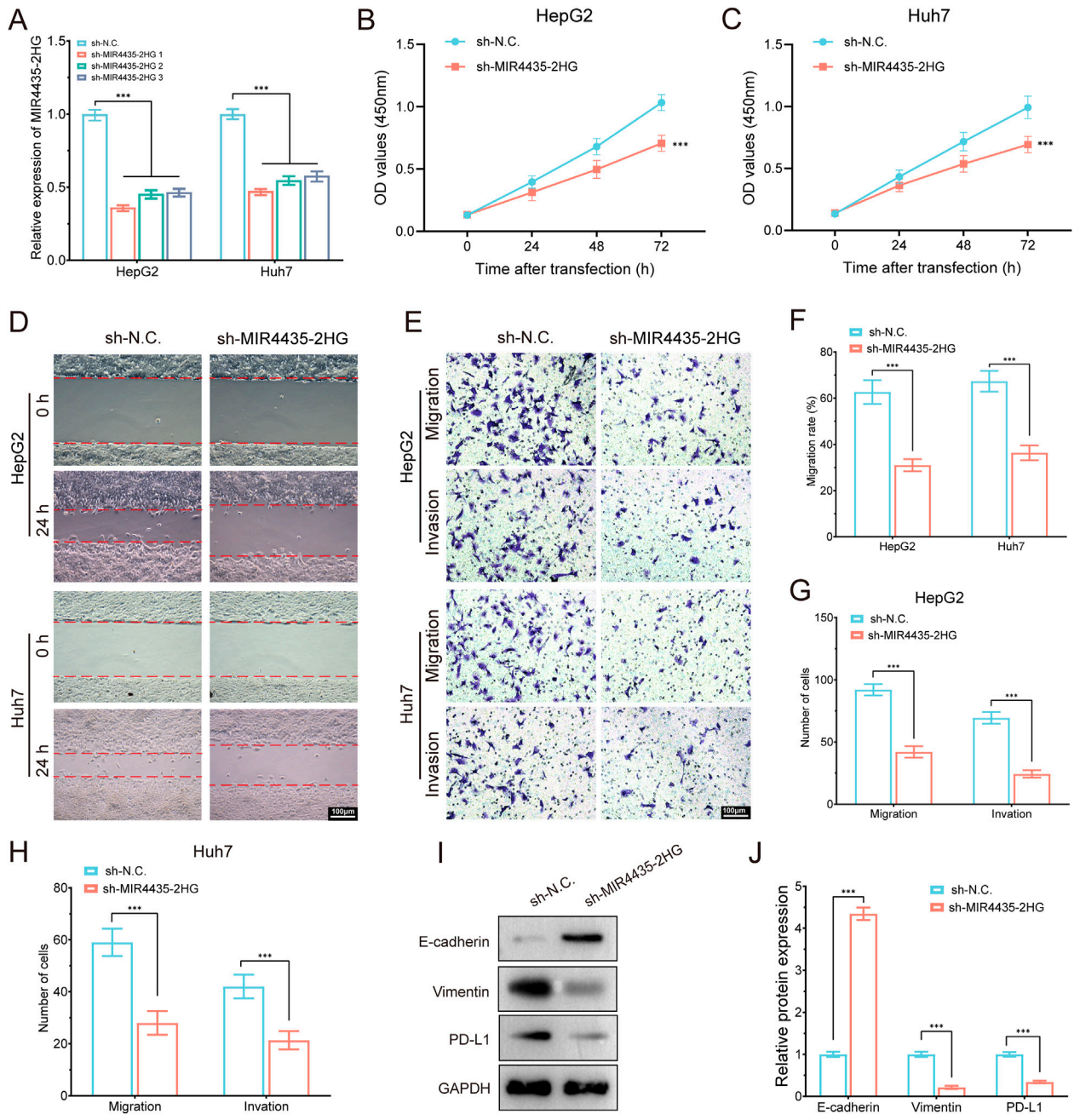


FIGURE 13
MIR4435-2HG knockdown suppresses proliferation, migration, invasion, EMT, and PD-L1 expression in HCC cells. **(A)** qRT-PCR showing knockdown efficiency of MIR4435-2HG in HepG2 and Huh7 cells using three shRNAs. **(B,C)** CCK-8 assays showing that MIR4435-2HG knockdown significantly inhibited cell proliferation in HepG2 **(B)** and Huh7 **(C)** cells at 24, 48, and 72 h. **(D)** Wound healing assay revealed impaired migration at 24 h in sh-MIR4435-2HG cells. **(E)** Transwell assays showed decreased migration and invasion. **(F–H)** Quantification of migration rates and cell numbers in HepG2 and Huh7. **(I)** Western blot showed increased E-cadherin and decreased Vimentin and PD-L1 upon MIR4435-2HG knockdown. GAPDH served as internal control. **(J)** Densitometric analysis of protein expression. Data are presented as mean ± SD; ***P < 0.001.

our data support a model in which MRlncRNAs orchestrate EMT, immune checkpoint expression, and migrasome-related communication to drive HCC progression and immune evasion.

Our study revealed a strong association between high MRlncRNA expression and an immunosuppressive TME in HCC. Specifically, patients in the high-risk group exhibited elevated infiltration of M2 macrophages and regulatory T cells (Tregs), whereas low-risk patients showed enrichment of cytotoxic T lymphocytes and dendritic cells, indicating more active anti-tumor immunity (Guo et al., 2021; Song et al., 2025). These shifts suggest that MRlncRNAs contribute to immune evasion by shaping the immune landscape. Mechanistically, knockdown of MIR4435-2HG significantly reduced PD-L1 expression and suppressed EMT markers, directly linking MRlncRNAs to both

immune checkpoint activation and tumor cell plasticity. M2 macrophages and Tregs—abundant in high-risk patients—are known to secrete IL-10 and TGF-β, which promote immune suppression and EMT (Kalluri, 2016). This supports a CAF–EMT–MRlncRNA regulatory axis that orchestrates immune exclusion, stromal remodeling, and PD-L1–mediated T cell inhibition (Wu et al., 2021). Further analysis revealed significantly higher expression of immune checkpoints (PDCD1, CTLA4, TIGIT, CD274) in high-risk patients. Integration of the MRlncRNA risk score with the TIDE algorithm markedly improved prediction of immunotherapy responsiveness, surpassing existing lncRNA-based models (Qin et al., 2023a). As immune checkpoint inhibitors (ICIs) become the frontline treatment for advanced HCC, accurate biomarkers such as MRlncRNA signatures are urgently needed to stratify patients and predict immunotherapy response, particularly given the complex clinical contexts such as liver transplantation, where ICIs pose potential risks of graft rejection (Sensi et al., 2024). While elevated TMB and MSI typically predict ICI benefit, high-risk patients in our cohort—despite high TMB/MSI—had poor outcomes, suggesting that MRlncRNA-driven immune suppression may offset these immunogenic features (Holder et al., 2024; Qi et al., 2024). This paradox highlights the complexity of the HCC microenvironment: heightened tumor immunogenicity may be neutralized by MRlncRNA-enhanced immune evasion. Collectively, our findings underscore the utility of MRlncRNAs as biomarkers of immune escape and resistance to immunotherapy in HCC.

Beyond their prognostic relevance, MRlncRNAs are functionally linked to the migrasome–CAF axis, a novel pathway contributing to tumor–stromal crosstalk and immune evasion in HCC. Migrasomes are recently identified migration-dependent extracellular vesicles involved in intercellular communication and immune regulation (Qiao et al., 2023). Several MRGs used in our co-expression analysis—TSPAN4, NDST1, and ITGAV—have been experimentally validated as essential for migrasome biogenesis and matrix interactions. Emerging studies show that HCC-derived migrasomes can carry immunosuppressive factors such as PD-L1 and TGF-β, fostering Treg differentiation and immune escape (Qin et al., 2023b). Although we did not directly localize MRlncRNAs within migrasomes, bioinformatic co-expression and functional associations strongly suggest a mechanistic interplay. MIR4435-2HG, for instance, is highly enriched in CAFs, as revealed by our scRNA-seq analysis (Cui et al., 2023). CAFs are key stromal components known to secrete TGF-β and IL-6, remodel the ECM, and promote immune suppression and tumor invasion (Qin et al., 2025). Moreover, MIR4435-2HG has been shown to regulate B3GNT5, a glycosyltransferase implicated in vesicle-mediated invasiveness (Qin et al., 2024). These findings support the hypothesis that MRlncRNAs—especially MIR4435-2HG—may influence migrasome biogenesis or cargo selection and potentiate CAF-driven immunosuppressive remodeling of the tumor microenvironment. This highlights a unique stromal regulatory circuit in HCC and suggests that MRlncRNAs may serve not only as prognostic biomarkers but also as therapeutic targets for disrupting the CAF–migrasome–immunity axis.

In addition to immune modulation, MRlncRNAs appear to orchestrate several tumor-promoting processes including EMT, metabolic reprogramming, and hypoxia adaptation. Our study revealed that MRlncRNAs are closely associated with EMT markers, supporting their role in promoting tumor invasiveness and metastasis in HCC. LINC00839 has been reported to upregulate SNAI2 and ZEB1, while MIR4435-2HG enhances expression of mesenchymal markers like Vimentin and N-cadherin, contributing to EMT activation (Xie et al., 2022; Guo et al., 2021). Notably, EMT also facilitates immune escape through PD-L1 upregulation, further implicating MRlncRNAs in immunosuppressive remodeling (Zhang et al., 2023). Moreover, MRlncRNAs may participate in cancer metabolic rewiring (Sun et al., 2022; Ghosh et al., 2021). Our enrichment analysis revealed associations with lipid metabolism and bile acid biosynthesis pathways, which are known to support tumor growth and immune evasion (Watterson and Coelho, 2023). Notably, many of the pathways associated with MRlncRNAs—including Wnt/β-catenin, mTOR, and MAPK—are well-established drivers of HCC progression and therapeutic resistance, as highlighted in recent reviews (Altaf et al., 2022). In particular, MIR4435-2HG may promote lipid metabolism, enabling HCC cells to thrive in nutrient- or oxygen-deprived conditions (Guo et al., 2021). This metabolic advantage may synergize with immune escape mechanisms to foster a more aggressive tumor phenotype. Hypoxia, a hallmark of advanced HCC, further amplifies these effects. We found that LINC00839 is upregulated under hypoxic conditions, promoting migration and invasion (Xie et al., 2022). This is consistent with earlier studies indicating that hypoxia-induced lncRNAs facilitate tumor adaptation and therapy resistance (Giraud et al., 2021; Pu et al., 2024). Therefore, MRlncRNAs may integrate hypoxia signaling, EMT progression, and metabolic alterations into a unified network that sustains tumor aggressiveness and immune evasion.

Our findings have several important clinical implications. First, the MRlncRNA-based risk score model provides a robust tool for prognostic stratification in HCC patients, enabling more personalized treatment strategies. Second, the association between MRlncRNAs and immune cell infiltration suggests that these lncRNAs may serve as therapeutic targets for enhancing anti-tumor immunity. For example, targeting MRlncRNAs with RNA interference (RNAi) or antisense oligonucleotides (ASOs) could potentially reverse the immunosuppressive TME and improve responses to ICIs. Future studies should focus on validating these findings in larger, multi-center cohorts and exploring the therapeutic potential of targeting MRlncRNAs in preclinical models. Additionally, the role of MRlncRNAs in other cancer types should be investigated to determine whether their functions are conserved across different malignancies. Finally, the development of MRlncRNA-targeted therapies will require careful consideration of delivery methods to ensure specificity and minimize off-target effects.

Despite the promising findings, this study has several limitations. First, both the TCGA-LIHC dataset and our external validation cohort (n = 100) were retrospectively collected, which may introduce selection bias. To address this, we expanded the clinical cohort and performed internal validation by dividing it into two independent subsets, each demonstrating robust and consistent prognostic performance. Nonetheless, future studies using

prospectively collected, multi-center cohorts are essential to validate the generalizability of our MRlncRNA-based model. Second, while previous studies on lncRNAs in HCC have focused on canonical oncogenic molecules like HOTAIR or MALAT1, our work is the first to systematically characterize MRlncRNAs in this context. Through integrated multi-omics approaches—encompassing transcriptomic screening, prognostic modeling, clinical validation, and scRNA-seq—we uncovered a novel CAF–EMT–immune checkpoint regulatory axis potentially modulated by migrasome signaling. Importantly, we provided direct experimental support: silencing MIR4435-2HG impaired tumor proliferation, migration, invasion, and reversed EMT and immune evasion phenotypes (upregulation of E-cadherin; downregulation of Vimentin and PD-L1). Finally, our 2-lncRNA signature (LINC00839 and MIR4435-2HG) demonstrated strong prognostic power and mechanistic relevance. Its integration with the TIDE algorithm significantly enhanced the prediction of immunotherapy response, outperforming existing lncRNA-based models. In contrast to models focused solely on tumor-intrinsic features, our signature reflects both metabolic reprogramming and immune exclusion. These findings highlight the translational potential of MRlncRNAs—and by extension, the migrasome–CAF–immune checkpoint axis—as promising therapeutic targets in HCC.

Conclusion

In summary, we developed and validated a novel 2-lncRNA signature (LINC00839 and MIR4435-2HG) associated with tumor progression and immune suppression in HCC. Using 100 clinical samples and functional assays, we confirmed that MIR4435-2HG promotes EMT and PD-L1–mediated immune evasion. Our integrative model, combining MRlncRNA expression with the TIDE algorithm, enhances immunotherapy response prediction beyond existing signatures. Moreover, scRNA-seq and *in vitro* data support a potential CAF–EMT–immune checkpoint axis driven by MRlncRNAs. These findings highlight the translational potential of targeting migrasome-related lncRNAs for improving prognostic assessment and immunotherapy outcomes in HCC.

Data availability statement

The datasets are available in TCGA database (https://portal.gdc.cancer.gov/), GeneCards 586 (https://www.genecards.org/). Further inquiries can be directed to the corresponding authors.

Ethics statement

The studies involving humans were approved by the Ethics Committee of Peking University Shenzhen Hospital. The studies were conducted in accordance with the local legislation and institutional requirements. The participants provided their written informed consent to participate in this study.

Author contributions

HQ: Conceptualization, Data curation, Funding acquisition, Investigation, Software, Writing – original draft, Writing – review and editing. TQ: Conceptualization, Formal Analysis, Investigation, Project administration, Writing – original draft. ML: Methodology, Project administration, Resources, Writing – original draft. WS: Resources, Supervision, Validation, Writing – original draft. JQ: Data curation, Investigation, Validation, Visualization, Writing – original draft. JW: Conceptualization, Data curation, Formal Analysis, Investigation, Methodology, Project administration, Writing – review and editing. QY: Formal Analysis, Funding acquisition, Project administration, Resources, Visualization, Writing – review and editing. JY: Conceptualization, Data curation, Investigation, Methodology, Software, Supervision, Writing – review and editing.

Funding

The author(s) declare that financial support was received for the research and/or publication of this article. This research was supported by grants from The Shenzhen Science and Technology Program (Nos. JCYJ20240813120109013, JCYJ20240813180905008), SanMing Project of Medicine in Shenzhen (No. SZSM202211038) and Shenzhen Medical Research Fund (No. A2402040).

Conflict of interest

The authors declare that the research was conducted in the absence of any commercial or financial relationships that could be construed as a potential conflict of interest.

Generative AI statement

The author(s) declare that no Generative AI was used in the creation of this manuscript.

Publisher's note

All claims expressed in this article are solely those of the authors and do not necessarily represent those of their affiliated organizations, or those of the publisher, the editors and the reviewers. Any product that may be evaluated in this article, or claim that may be made by its manufacturer, is not guaranteed or endorsed by the publisher.

Supplementary material

The Supplementary Material for this article can be found online at: https://www.frontiersin.org/articles/10.3389/fphar.2025.1581122/full#supplementary-material

References

Altaf, S., Saleem, F., Sher, A. A., Ali, A., Sensi, B., Angelico, R., et al. (2022). Potential therapeutic strategies to combat HCC. *Curr. Mol. Pharmacol.* 15, 929–942. doi:10.2174/1874467215666220103111009

Bray, F., Ferlay, J., Soerjomataram, I., Siegel, R. L., Torre, L. A., and Jemal, A. (2018). Global cancer statistics 2018: GLOBOCAN estimates of incidence and mortality worldwide for 36 cancers in 185 countries. *CA Cancer J. Clin.* 68, 394–424. doi:10.3322/caac.21492

Cui, S., Chen, Y., Guo, Y., Wang, X., and Chen, D. (2023). Hsa-miR-22-3p inhibits liver cancer cell EMT and cell migration/invasion by indirectly regulating SPRY2. *PLoS One* 18, e0281536. doi:10.1371/journal.pone.0281536

Deng, S., Wu, Y., Huang, S., and Yang, X. (2024). Novel insights into the roles of migrasome in cancer. *Discov. Oncol.* 15, 166. doi:10.1007/s12672-024-00942-0

Gao, J., Aksoy, B. A., Dogrusoz, U., Dresdner, G., Gross, B., Sumer, S. O., et al. (2013). Integrative analysis of complex cancer genomics and clinical profiles using the cBioPortal. *Sci. Signal* 6, l1. doi:10.1126/scisignal.2004088

Geeleher, P., Cox, N., and Huang, R. S. (2014). pRRophetic: an R package for prediction of clinical chemotherapeutic response from tumor gene expression levels. *PLOS One* 9, e107468. doi:10.1371/journal.pone.0107468

Ghosh, M., Saha, S., Bettke, J., Nagar, R., Parrales, A., Iwakuma, T., et al. (2021). Mutant p53 suppresses innate immune signaling to promote tumorigenesis. *Cancer Cell* 39, 494–508.e5. doi:10.1016/j.ccell.2021.01.003

Gilles, H., Garbutt, T., and Landrum, J. (2022). Hepatocellular carcinoma. *Crit. Care Nurs. Clin. North Am.* 34, 289–301. doi:10.1016/j.cnc.2022.04.004

Giraud, J., Chalopin, D., Blanc, J. F., and Saleh, M. (2021). Hepatocellular carcinoma immune landscape and the potential of immunotherapies. *Front. Immunol.* 12, 655697. doi:10.3389/fimmu.2021.655697

Guo, Y., Wang, J., Benedict, B., Yang, C., van Gemert, F., Ma, X., et al. (2021). Targeting CDC7 potentiates ATR-CHK1 signaling inhibition through induction of DNA replication stress in liver cancer. *Genome Med.* 13, 166. doi:10.1186/s13073-021-00981-0

Gupta, R. A., Shah, N., Wang, K. C., Kim, J., Horlings, H. M., Wong, D. J., et al. (2010). Long non-coding RNA HOTAIR reprograms chromatin state to promote cancer metastasis. *Nature* 464, 1071–1076. doi:10.1038/nature08975

Han, C., Yang, Y., Guo, L., Guan, Q., and Ruan, S. (2022). The expression of long non-coding RNA HOTAIR in advanced hepatocellular carcinoma and its prognostic correlation with sunitinib therapy. *Arch. Med. Sci.* 18, 71–78. doi:10.5114/aoms/100480

Hänzelmann, S., Castelo, R., and Guinney, J. (2013). GSVA: gene set variation analysis for microarray and RNA-seq data. *BMC Bioinforma.* 14, 7. doi:10.1186/1471-2105-14-7

Holder, A. M., Dedeilia, A., Sierra-Davidson, K., Cohen, S., Liu, D., Parikh, A., et al. (2024). Defining clinically useful biomarkers of immune checkpoint inhibitors in solid tumours. *Nat. Rev. Cancer* 24, 498–512. doi:10.1038/s41568-024-00705-7

Jia, D., He, Y., and Zhang, Y. (2024). Long non-coding RNAs regulating macrophage polarization in liver cancer. *Curr. Pharm. Des.* 30, 2120–2128. doi:10.2174/0113816128311861240523075218

Jiang, Y., Liu, X., Ye, J., Ma, Y., Mao, J., Feng, D., et al. (2023). Migrasomes, a new mode of intercellular communication. *Cell Commun. Signal* 21, 105. doi:10.1186/s12964-023-01121-4

Kadian, L. K., Verma, D., Lohani, N., Yadav, R., Ranga, S., Gulshan, G., et al. (2024). Long non-coding RNAs in cancer: multifaceted roles and potential targets for immunotherapy. *Mol. Cell. Biochem.* 479, 3229–3254. doi:10.1007/s11010-024-04933-1

Kalluri, R. (2016). The biology and function of fibroblasts in cancer. *Nat. Rev. Cancer* 16, 582–598. doi:10.1038/nrc.2016.73

Li, G. Z., Meng, G. X., Pan, G. Q., Zhang, X., Yan, L. J., Li, R. Z., et al. (2023). MALAT1/mir-1-3p mediated BRF2 expression promotes HCC progression via inhibiting the LKB1/AMPK signaling pathway. *Cancer Cell Int.* 23, 188. doi:10.1186/s12935-023-03034-1

Liu, J., Park, K., Shen, Z., Lee, H., Geetha, P., Pakyari, M., et al. (2023). Immunotherapy, targeted therapy, and their cross talks in hepatocellular carcinoma. *Front. Immunol.* 14, 1285370. doi:10.3389/fimmu.2023.1285370

Newman, A. M., Liu, C. L., Green, M. R., Gentles, A. J., Feng, W., Xu, Y., et al. (2015). Robust enumeration of cell subsets from tissue expression profiles. *Nat. Methods* 12, 453–457. doi:10.1038/nmeth.3337

Powers, R. K., Goodspeed, A., Pielke-Lombardo, H., Tan, A. C., and Costello, J. C. (2018). GSEA-InContext: identifying novel and common patterns in expression experiments. *Bioinformatics* 34, i555–i564. doi:10.1093/bioinformatics/bty271

Pu, Y., Yang, G., Zhou, Y., Pan, X., Guo, T., and Chai, X. (2024). The Macrophage migration inhibitory factor is a vital player in Pan-Cancer by functioning as a M0 Macrophage biomarker. *Int. Immunopharmacol.* 134, 112198. doi:10.1016/j.intimp.2024.112198

Qiao, X., Lin, J., Shen, J., Chen, Y., Zheng, L., Ren, H., et al. (2023). FBXO28 suppresses liver cancer invasion and metastasis by promoting PKA-dependent SNAI2 degradation. *Oncogene* 42, 2878–2891. doi:10.1038/s41388-023-02809-0

Qin, H., Qi, T., Xu, J., Wang, T., Zeng, H., Yang, J., et al. (2024). Integration of ubiquitination-related genes in predictive signatures for prognosis and immunotherapy response in sarcoma. *Front. Oncol.* 14, 1446522. doi:10.3389/fonc.2024.1446522

Qin, H., Sheng, W., Weng, J., Li, G., Chen, Y., Zhu, Y., et al. (2023b). Identification and verification of m7G-Related genes as biomarkers for prognosis of sarcoma. *Front. Genet.* 14, 1101683. doi:10.3389/fgene.2023.1101683

Qin, H., Sheng, W., Zhang, G., Yang, Q., Yao, S., Yue, Y., et al. (2023a). Comprehensive analysis of cuproptosis-related prognostic gene signature and tumor immune microenvironment in HCC. *Front. Genet.* 14, 1094793. doi:10.3389/fgene.2023.1094793

Qin, H., Wang, Q., Xu, J., Zeng, H., Liu, J., Yu, F., et al. (2024). Integrative analysis of anoikis-related genes prognostic signature with immunotherapy and identification of CDKN3 as a key oncogene in lung adenocarcinoma. *Int. Immunopharmacol.* 143, 113282. doi:10.1016/j.intimp.2024.113282

Qin, H., Xu, J., Yue, Y., Chen, M., Zhang, Z., Xu, P., et al. (2025). Disulfidptosis-related gene signatures as prognostic biomarkers and predictors of immunotherapy response in HNSCC. *Front. Immunol.* 15, 1456649. doi:10.3389/fimmu.2024.1456649

Sadagopan, N., and He, A. R. (2024). Recent progress in systemic therapy for advanced hepatocellular carcinoma. *Int. J. Mol. Sci.* 25, 1259. doi:10.3390/ijms25021259

Sensi, B., Angelico, R., Toti, L., Conte, L., Coppola, A., Tisone, G., et al. (2024). Mechanism, potential, and concerns of immunotherapy for hepatocellular carcinoma and liver transplantation. *Curr. Mol. Pharmacol.* 17, e18761429310703. doi:10.2174/0118761429310703240823045808

Song, M., Xu, J., Gui, Z., Wu, Y., Wang, F., Sheng, H., et al. (2025). Characterization of lysine crotonylation-related lncRNAs for prognostic assessment and immune response in glioma. *Front. Pharmacol.* 16, 1573694. doi:10.3389/fphar.2025.1573694

Sun, D., Wang, J., Han, Y., Dong, X., Ge, J., Zheng, R., et al. (2021). TISCH: a comprehensive web resource enabling interactive single-cell transcriptome visualization of tumor microenvironment. *Nucleic Acids Res.* 49, D1420–D1430. doi:10.1093/nar/gkaa1020

Sun, R., Zhang, Z., Bao, R., Guo, X., Gu, Y., Yang, W., et al. (2022). Loss of SIRT5 promotes bile acid-induced immunosuppressive microenvironment and hepatocarcinogenesis. *J. Hepatol.* 77, 453–466. doi:10.1016/j.jhep.2022.02.030

Sung, H., Ferlay, J., Siegel, R. L., Laversanne, M., Soerjomataram, I., Jemal, A., et al. (2021). Global cancer statistics 2020: GLOBOCAN estimates of incidence and mortality worldwide for 36 cancers in 185 countries. *CA Cancer J. Clin.* 71, 209–249. doi:10.3322/caac.21660

Tomczak, K., Czerwińska, P., and Wiznerowicz, M. (2015). The Cancer Genome Atlas (TCGA): an immeasurable source of knowledge. *Contemp. Oncol. Pozn.* 19, A68–A77. doi:10.5114/wo.2014.47136

Watterson, A., and Coelho, M. A. (2023). Cancer immune evasion through KRAS and PD-L1 and potential therapeutic interventions. *Cell Commun. Signal* 21, 45. doi:10.1186/s12964-023-01063-x

Wu, F., Yang, J., Liu, J., Wang, Y., Mu, J., Zeng, Q., et al. (2021). Signaling pathways in cancer-associated fibroblasts and targeted therapy for cancer. *Signal Transduct. Target Ther.* 6, 218. doi:10.1038/s41392-021-00641-0

Xie, Y., Lin, H., Wei, W., Kong, Y., Fang, Q., Chen, E., et al. (2022). LINC00839 promotes malignancy of liver cancer via binding FMNL2 under hypoxia. *Sci. Rep.* 12, 18757. doi:10.1038/s41598-022-16972-z

Yang, C., Zhang, H., Zhang, L., Zhu, A. X., Bernards, R., Qin, W., et al. (2023). Evolving therapeutic landscape of advanced hepatocellular carcinoma. *Nat. Rev. Gastroenterol. Hepatol.* 20, 203–222. doi:10.1038/s41575-022-00704-9

Yu, G., Wang, L. G., Han, Y., and He, Q. Y. (2012). clusterProfiler: an R package for comparing biological themes among gene clusters. *OMICS: A Journal of Integrative Biology*. 16 (5), 284–287. doi:10.1089/omi.2011.0118

Zhang, H. B., Pan, J. Y., and Zhu, T. (2023). A disulfidptosis-related lncRNA prognostic model to predict survival and response to immunotherapy in lung adenocarcinoma. *Front. Pharmacol.* 14, 1254119. doi:10.3389/fphar.2023.1254119

Zhang, K., Zhu, Z., Jia, R., Wang, N. A., Shi, M., Wang, Y., et al. (2024a). CD151-enriched migrasomes mediate hepatocellular carcinoma invasion by conditioning cancer cells and promoting angiogenesis. *J. Exp. Clin. Cancer Res.* 43, 160. doi:10.1186/s13046-024-03082-z

Zhang, R., Peng, J., Zhang, Y., Zheng, K., Chen, Y., Liu, L., et al. (2024b). Pancreatic cancer cell-derived migrasomes promote cancer progression by fostering an immunosuppressive tumor microenvironment. *Cancer Lett.* 605, 217289. doi:10.1016/j.canlet.2024.217289

Frontiers in Pharmacology

Explores the interactions between chemicals and living beings

The most cited journal in its field, which advances access to pharmacological discoveries to prevent and treat human disease.

Discover the latest Research Topics

See more →



Frontiers

Avenue du Tribunal-Fédéral 34
1005 Lausanne, Switzerland
frontiersin.org

Contact us

+41 (0)21 510 17 00
frontiersin.org/about/contact